



# Evaluation of Uncertainty Treatment in the Technical Documents Supporting TSPA-SR



Management and Technical Support Services

*A Yucca Mountain Site Characterization Office Support Organization*

---

# **Evaluation of Uncertainty Treatment in the Technical Documents Supporting TSPA-SR**

**MAY 2001**

## **Uncertainties Review Team:**

R. Rogers, Lead

H. Greenberg  
R. Linden

M. Nutt  
R. Salness

D. Sassani  
J. Savino

F. Wong  
E. Zwahlen

## **DISCLAIMER**

This report was prepared as an account of work sponsored by an agency of the United States Government. Neither the United States Government nor any agency thereof, nor any of their employees, nor any of their contractors, subcontractors or their employees, makes any warranty, express or implied, or assumes any legal liability or responsibility for the accuracy, completeness, or any third party's use or the results of such use of any information, apparatus, product, or process disclosed, or represents that its use would not infringe privately owned rights. Reference herein to any specific commercial product, process, or service by trade name, trademark, manufacturer, or otherwise, does not necessarily constitute or imply its endorsement, recommendation, or favoring by the United States Government or any agency thereof or its contractors or subcontractors. The views and opinions of authors expressed herein do not necessarily state or reflect those of the United States Government or any agency thereof.

## Acknowledgments

The authors and contributors of the Evaluation of Uncertainty Treatment in the Technical Documents Supporting TSPA-SR appreciate very valuable assistance from the following: Tom Doe, Levy Kroitoru, Paul LaPointe, Travis McGrath, Ian Miller, Bill Roberds, Bill Thompson, Dave Hoekstra, and Charlie Voss of Golder Associates; Joe Barron, George Bushnell, Art Stein, Erik Kirstein, Wayne Lewis, and Jeff Johns of Stone & Webster; and Steve Passman of Booz-Allen & Hamilton for assistance with AMR reviews.

Roseanne Perman, Bob Youngs, and Karen Jenni of Geomatrix Consultants; Ian Miller, Bill Thompson, Charlie Voss, and Levi Kroitoru of Golder Associates; Ernie Hardin of BSc; Dwight Hoxie of the USGS; Bob Bradbury of Stone & Webster; Bimal Mukhopadhyay, Bob Fish, Brenda Bowlby, Bob Murray, Mike Cline, and Barbara McKinnon of Booz-Allen & Hamilton for valuable reviews of various drafts sections of this report.

The report would never have seen the light of day without the invaluable help of Toni Caselli, Cheryl Gygi, Tammy Nakashima, Karen Nesbitt, and Scott Nesbitt of the MTS.

Much of our report is summarizing and restating information contained in the AMRs and PMRs that support the TSPA-SR. In some cases we have quoted text directly from these documents. In other cases we have used text from these documents with light editing to fit our report format. This lightly edited text is not identified with quotation marks. For those who would like to “catch” us at this we encourage you to read the AMRs and PMRs discussed in this report. In addition to having the fun of catching us, you will also have the opportunity to learn a lot from a suite of generally well written and informative documents.

INTENTIONALLY LEFT BLANK

# Evaluation of Uncertainty Treatment in the Technical Documents Supporting TSPA-SR

## Table of Contents

<u>Chapter</u>	<u>Title</u>	<u>Page</u>
	List of Figures .....	ix
	List of Tables .....	xiii
	Acronyms and Abbreviations.....	xv
	Executive Summary .....	ES-1
	Introduction .....	1
<b>1.0</b>	<b>Igneous Disruption Model – Volcanic Eruption.....</b>	<b>1-1</b>
1.1	Purpose of the Model .....	1-1
1.2	Model Component Documentation .....	1-1
1.3	Volcanic Eruption Model Structure .....	1-2
1.4	Discussion of Uncertainty Treatment.....	1-6
1.5	Uncertainty Propagation.....	1-10
1.6	Conclusions .....	1-11
<b>2.0</b>	<b>Igneous Disruption Model – Igneous Intrusion Groundwater Release Model.....</b>	<b>2-1</b>
2.1	Purpose of the Model .....	2-1
2.2	Model Component Documentation .....	2-1
2.3	Igneous Intrusion Model Structure.....	2-2
2.4	Discussion of Uncertainty Treatment.....	2-6
2.5	Uncertainty Propagation and Conclusions .....	2-9
<b>3.0</b>	<b>Probabilistic Seismic Hazard Model .....</b>	<b>3-1</b>
3.1	Purpose of the Model .....	3-1
3.2	Model Component Documentation .....	3-1
3.3	Seismic Hazard Model Structure.....	3-4
3.4	Discussion of Uncertainty Treatment.....	3-8
3.5	Conclusions .....	3-13
<b>4.0</b>	<b>Future Climate and Infiltration .....</b>	<b>4-1</b>
4.1	Purpose of Model/Intended Use.....	4-1
4.2	Model Relations .....	4-1
4.3	Model Structure.....	4-3
4.4	Discussion of Uncertainty/Variability Treatment .....	4-6
4.5	Uncertainty Propagation.....	4-10

# Evaluation of Uncertainty Treatment in the Technical Documents Supporting TSPA-SR

## Table of Contents (Continued)

<u>Chapter</u>	<u>Title</u>	<u>Page</u>
<b>5.0</b>	<b>Unsaturated Zone Flow Model and Submodels .....</b>	<b>5-1</b>
5.1	Purpose of Model/Intended Use.....	5-1
5.2	Model Relations .....	5-1
5.3	Model Structure.....	5-3
5.4	Discussion of Uncertainty/Variability Treatment .....	5-7
5.5	Uncertainty Propagation.....	5-11
5.6	Conclusions .....	5-13
<b>6.0</b>	<b>Drift Seepage Models .....</b>	<b>6-1</b>
6.1	Purpose of Model/Intended Use.....	6-1
6.2	Model Relations .....	6-1
6.3	Model Structure.....	6-3
6.4	Discussion of Uncertainty/Variability Treatment .....	6-9
6.5	Uncertainty Propagation.....	6-13
6.6	Conclusions .....	6-14
<b>7.0</b>	<b>Near Field Environment Process Models and Abstractions.....</b>	<b>7-1</b>
7.1	Purpose and Intended Use of the Model .....	7-1
7.2	Uncertainty Treatment within the Near Field Environment Models.....	7-8
7.3	Uncertainty Propagation/Capture/Integration into the Total System Performance Assessment.....	7-25
7.4	Conclusions .....	7-28
<b>8.0</b>	<b>Engineered Barrier System Models.....</b>	<b>8-1</b>
8.1	Introduction .....	8-1
8.2	Discussion of the EBS Models Uncertainty Treatment .....	8-5
<b>9.0</b>	<b>General and Localized Corrosion.....</b>	<b>9-1</b>
9.1	Purpose of the Model .....	9-1
9.2	Model Component Relations.....	9-1
9.3	General and Localized Corrosion Model Structure.....	9-2
9.4	Discussion of Uncertainty Treatment.....	9-11
9.5	Uncertainty Propagation.....	9-13
<b>10.0</b>	<b>Stress Corrosion Cracking .....</b>	<b>10-1</b>
10.1	Purpose of the Model .....	10-1
10.2	Model Component Relations.....	10-1
10.3	SCC Model Structure .....	10-2
10.4	Discussion of Uncertainty Treatment.....	10-9

# Evaluation of Uncertainty Treatment in the Technical Documents Supporting TSPA-SR

## Table of Contents (Continued)

<u>Chapter</u>	<u>Title</u>	<u>Page</u>
10.5	Uncertainty Propagation.....	10-10
<b>11.0</b>	<b>Integrated Waste Package Degradation Model.....</b>	<b>11-1</b>
11.1	Purpose of Model/Intended Use.....	11-1
11.2	Model Relations .....	11-1
11.3	Model Structure.....	11-3
11.4	Discussion of Uncertainty/Variability Treatment .....	11-18
11.5	Propagation of Uncertainty .....	11-20
<b>12.0</b>	<b>Waste Form Degradation Model .....</b>	<b>12-1</b>
12.1	Purpose of the Model .....	12-1
12.2	Model Component Relations.....	12-3
12.3	Waste Form Degradation Model Structure .....	12-7
12.4	Discussion of Uncertainty Treatment.....	12-27
12.5	Uncertainty Propagation.....	12-40
<b>13.0</b>	<b>Unsaturated Zone Transport Model .....</b>	<b>13-1</b>
13.1	Purpose of Model/Intended Use.....	13-1
13.2	Model Relations .....	13-1
13.3	Model Structure.....	13-5
13.4	Discussion of Uncertainty/Variability Treatment .....	13-12
13.5	Propagation of Uncertainty .....	13-15
<b>14.0</b>	<b>Saturated Zone Groundwater Flow Model.....</b>	<b>14-1</b>
14.1	Model Purpose.....	14-1
14.2	Model Relations .....	14-1
14.3	SZ Flow Model Structure.....	14-3
14.4	Discussion of Uncertainty and Variability Treatment.....	14-6
14.5	Uncertainty Propagation and Conclusions .....	14-11
<b>15.0</b>	<b>Saturated Zone Radionuclide Transport Model .....</b>	<b>15-1</b>
15.1	Model Purpose.....	15-1
15.2	Model Relations .....	15-1
15.3	Saturated Zone Transport Model Structure.....	15-3
15.4	Discussion of Uncertainty and Variability Treatment.....	15-7
15.5	Uncertainty Propagation.....	15-10
15.6	Conclusions .....	15-11

# Evaluation of Uncertainty Treatment in the Technical Documents Supporting TSPA-SR

## Table of Contents (Continued)

<u>Chapter</u>	<u>Title</u>	<u>Page</u>
<b>16.0</b>	<b>Biosphere Model.....</b>	<b>16-1</b>
16.1	Purpose of the Model and Intended Use .....	16-1
16.2	Model Relations .....	16-1
16.3	Model Structure.....	16-3
16.4	Discussion of Uncertainty/Variability Treatment .....	16-9
16.5	Uncertainty Propagation.....	16-14
<b>17.0</b>	<b>Integrated Site Model (ISM) .....</b>	<b>17-1</b>
17.1	Purpose.....	17-1
17.2	Model Component Relations.....	17-1
17.3	Uncertainty Treatment in the ISM .....	17-2
17.4	Conclusions .....	17-7
<b>18.0</b>	<b>Summary, Conclusions, and Recommendations .....</b>	<b>18-1</b>
<b>19.0</b>	<b>List of References .....</b>	<b>19-1</b>

# Evaluation of Uncertainty Treatment in the Technical Documents Supporting TSPA-SR

## List of Figures

<u>Figure</u>	<u>Title</u>	<u>Page</u>
1	Example of Model Structure Diagram .....	7
1-1	Volcanic Eruption Model Information Flow.....	1-3
1-2	Volcanic Eruption Model Structure Diagram .....	1-4
2-1	Igneous Intrusion Model Information Flow .....	2-3
2-2	Igneous Intrusion Groundwater Release Model Structure .....	2-4
3-1	Seismic Hazard Model Information Flow.....	3-3
3-2	Seismic Hazard Model Structure Diagram.....	3-5
4-1	Climate and Infiltration Model Relations.....	4-2
4-2	Climate and Infiltration Model Structure .....	4-4
5-1	UZ Flow (Ambient and TH) Model Relation Diagram.....	5-2
5-2	Model Structure for Unsaturated Zone Flow .....	5-4
6-1	Seepage Model Relation Diagram.....	6-2
6-2	Seepage Model Structure .....	6-4
7-1	Relations Among Near Field Environment Process Model Report Models .....	7-3
7-2	Description of the Model Aspects for the Drift Scale Test Thermohydrochemical Model .....	7-9
7-3	Description of the Model Aspects for the Ambient Thermohydrochemical Model .....	7-10
7-4	Description of the Model Aspects for the Thermohydrochemical Seepage Model .....	7-11
7-5	Description of the Model Aspects for the Multiscale Thermohydrologic Percolation Flux Model.....	7-12

# Evaluation of Uncertainty Treatment in the Technical Documents Supporting TSPA-SR

## List of Figures

<b><u>Figure</u></b>	<b><u>Title</u></b>	<b><u>Page</u></b>
8-1a	Engineered Barrier System PMR Process Models.....	8-2
8-1b	Engineered Barrier System PMR Abstraction Models .....	8-3
8-1c	Total System Performance Assessment Models for Engineered Barriers .....	8-4
8-2	Engineered Barrier System PMR Model Structure – Flow Into Drift .....	8-7
8-3	Engineered Barrier System PMR Model Structure – In-Drift Chemistry/ Chemical Processes.....	8-9
8-4	Engineered Barrier System PMR Model Structure – In-Drift Physical/ Degradation Processes .....	8-11
8-5	Engineered Barrier System PMR Model Structure – Thermal/Hydrologic Processes .....	8-14
8-6	Engineered Barrier System PMR Model Structure – EBS Transport Processes .....	8-16
9-1	General and Localized Corrosion Model AMR Relations.....	9-3
9-2	General and Localized Corrosion Model Structure .....	9-4
10-1	Stress Corrosion Cracking AMR Relationships .....	10-3
10-2	Stress Corrosion Cracking Model Structure .....	10-4
11-1	Model Relations for the Waste Package Degradation Model (WAPDEG) .....	11-2
11-2	Waste Package Degradation Model (WAPDEG) Structure.....	11-4
11-3	Logic Flow Diagram for the WAPDEG Model.....	11-7
12-1	Waste Form Degradation AMR Relationships .....	12-4
12-2	Waste Form Degradation Model Structure .....	12-8

# Evaluation of Uncertainty Treatment in the Technical Documents Supporting TSPA-SR

## List of Figures

<b><u>Figure</u></b>	<b><u>Title</u></b>	<b><u>Page</u></b>
13-1a	Model Relations for the Unsaturated Zone Radionuclide Transport Process Model .....	13-3
13-1b	Model Relations for the Unsaturated Zone Radionuclide Transport Abstracted Model .....	13-4
13-2	Unsaturated Zone Transport Model Structure.....	13-6
14-1	Saturated Zone Flow and Transport Model Relation Diagram.....	14-2
14-2	Saturated Zone Flow Model Structure Diagram .....	14-4
15-1	Saturated Zone Flow and Transport Logic Diagram.....	15-2
15-2	Saturated Zone Transport Model Diagram.....	15-4
16-1	Biosphere Model Relations .....	16-4
16-2	Biosphere Model Structure.....	16-5
17-1	Integrated Site Model Relation Diagram .....	17-3
17-2	Integrated Site Model Structure Diagram .....	17-4

INTENTIONALLY LEFT BLANK

# Evaluation of Uncertainty Treatment in the Technical Documents Supporting TSPA-SR

## List of Tables

<u>Table</u>	<u>Title</u>	<u>Page</u>
1-1	Volcanic Eruption Release Model .....	1-13
2-1	Igneous Intrusion Model .....	2-10
3-1	Seismic Hazard Model .....	3-14
4-1	Future Climate and Infiltration Model .....	4-12
5-1	Unsaturated Zone Flow Model .....	5-15
6-1	Seepage Model .....	6-15
7-1	Treatment of Uncertainties and Variability within the Thermohydrochemical Seepage (THC) Model .....	7-3
7-2	Description of the Model Aspects for the Drift Scale Test Thermohydrochemical Model .....	7-9
8-1	Models Associated with the EBS Degradation, Flow and Transport PMR .....	8-18
8-2	AMR Document Identifiers and Shorthand Notation Crosswalk .....	8-21
9-1	General and Localized Corrosion .....	9-15
10-1	Stress Corrosion Cracking .....	10-12
11-1	Waste Package Degradation Analysis: Integrated Model for Waste Package and Drip Shield Degradation .....	11-22
12-1	Waste Form Degradation Model .....	12-43
13-1	Unsaturated Zone Radionuclide Transport .....	13-18
14-1	Saturated Zone Flow Model .....	14-13
15-1	Saturated Zone Transport Model .....	15-12
16-1	Biosphere Model Uncertainty Treatment .....	16-17
17-1	Integrated Site Model .....	17-8

INTENTIONALLY LEFT BLANK

## Acronyms And Abbreviations

1D	One-dimensional
2D	Two-dimensional
3D	Three-dimensional
AD	advective-dispersive
AF	active fracture
AFM	Active Fracture Model
AMR	Analysis and Model Report
ANL	Argonne National Laboratory
BDCF	biosphere dose conversion factor
BWR	boiling water reactor
CCDF	cumulative complimentary distribution function
CDF	cumulative distribution function
CDSP	codisposal waste packages
CFR	Code of Federal Regulations
CHn	Calico Hills nonwelded hydrogeological unit
CMB	chloride mass balance
CSNF	commercial spent nuclear fuel
DCF	dose conversion factor
DCPT	Dual Continuum Particle Tracker
DDT	Discrete-heat source Drift-scale Thermal-conduction
DEM	Discret Element Model
DFN	discret fracture network
DKM	dual-permeability model
DOE	U.S. Department of Energy
DRKBA	Discrete Region Key Block Analysis
DS	Drift Scale
DSNF	U.S. Department of Energy Spent Nuclear Fuel
EBS	Engineered Barrier System
EIS	Environmental Impact Statement
EPA	U.S. Environmental Protection Agency
ESF	Exploratory Studies Facility
F&T	Flow and Transport
FEHM	Finite Element Heat and Mass
FEPs	features, events, and processes
GM	ground motion
GVP	Gaussian Variance Partitioning

## Acronyms And Abbreviations

HFM	Hydrogeological Framework Model
HLW	high-level waste
ISM	Integrated Site Model
LDTH	Line-average-heat source Drift-scale Thermo/Hydrologic
LRO	Long-Range Ordering
MIC	Microbiologically Influenced Corrosion
MM	Mineralogical Model
MSTH	Multiscale Thermohydrologic
MSTHM	Multiscale Thermohydrologic Model
MSTHM PFM	Multiscale Thermohydrologic Model Percolation Flux Model
NFE	near-field environment
NRC	U.S. Nuclear Regulatory Commission
NSNFP	U.S. Department of Energy National Spent Nuclear Fuel Program
NTS	Nevada Test Site
NWTRB	Nuclear Waste Technical Review Board
PA	Performance Assessment
PDF	probability distribution function
PMR	Process Model Report
PSHA	Probabilistic Seismic Hazard Analysis
PT	particle tracking
PTn	Paintbrush Tuff nonwelded hydrogeological unit
PVHA	Probabilistic Volcanic Hazard Analysis
PWR	pressurized water reactor
QARD	<i>Quality Assurance Requirements and Description, DOE/RW-0333P</i>
RH	relative humidity
RPM	Rock Properties Model
RTTF	Residence-Time Transfer Function
SCC	stress corrosion cracking
SCM	Seepage Calibration Model
SDT	Smeared-heat source Drift-scale Thermal conduction
SHT	Single Heater Test
SMT	Smeared-heat-source Mountain-scale Thermal-conduction
SNF	spent nuclear fuel
SR	Site Recommendation
SSC	structure, system, or component

## Acronyms And Abbreviations

SSFD	seismic source and fault displacement
SSSM	stainless steel structure material
SZ	saturated zone
TBV	to be verified
TH	thermal-hydrological
THC	thermal-hydrological-chemical
THCM	thermal-hydrological-chemical-mechanical
TSPA	Total System Performance Assessment
TSPA-SR	Total System Performance Assessment-Site Recommendation
TSPA-VA	Total System Performance Assessment-Viability Assessment
TSw	Topopah Spring welded hydrogeological unit
TSwmn	Topopah Spring welded middle non-lithophysal
UZ	unsaturated zone
UZEE	Unsaturated Zone Expert Elicitation
V&V	verification and validation
VA	Viability Assessment
WAPDEG	Waste Package Degradation
WP	Waste Package
YMP	Yucca Mountain Site Characterization Project
YMR	Yucca Mountain region

INTENTIONALLY LEFT BLANK

## Executive Summary

Estimates of risk to the public as a result of geologic disposal of high-level nuclear waste will always be uncertain. The approach used for modeling repository performance is called Total System Performance Assessment (TSPA). A TSPA model evaluates the entire repository system, including all natural and engineered barriers. Uncertainties are due to many factors resulting from the complexities of predicting the behavior of the natural and engineered barriers and the long time frames over which projections must be made. Data collection and analysis efforts of the Yucca Mountain Site Characterization Project (YMP) have led to greatly improved understanding of the site, but areas of uncertainty remain. Efforts continue to reduce uncertainties, but many will remain at the time that a decision is made on a Site Recommendation (SR). If the site is recommended, uncertainties will remain when the License Application is submitted. This is the fundamental reason that the TSPA model is constructed as a stochastic representation of the system and includes quantitative assessments of uncertainty. The treatment of these uncertainties and the discussion of that treatment in technical documents produced by the YMP are widely recognized as fundamentally important.

The potential repository design, data collection, analyses, detailed process-level modeling, and evaluation of repository performance using TSPA has been an iterative process. The results of each iteration were used to focus site characterization activities on those areas where critical information was still needed. Many of these activities were aimed at reducing or mitigating uncertainties in the many models needed to evaluate overall system performance.

In addition, the TSPA models and analyses have become more robust and sophisticated with each iteration. One of the major conceptual steps that was taken to achieve these advancements was to improve the linkage of TSPA to process level models through an enhanced abstraction process. The abstraction process allows the insights and quantitative results of the process models developed for the site, including the uncertainties, to be incorporated into the TSPA analyses. This hierarchy of data collection, modeling, and TSPA analyses leads to a more robust and defensible evaluation of the potential performance of the site, but also makes issues related to transparency and traceability even more challenging.

The YMP must be able to pass ever more stringent scientific scrutiny as significant regulatory decisions approach. The YMP has conducted this critical internal assessment to evaluate uncertainty treatment in the technical documents supporting the TSPA-SR. This assessment has been purposely critical and, as such reviews tend to do, has emphasized the negative aspects regarding the treatment of uncertainties in the technical work. However, these negative aspects were used to develop recommendations for improvement. One objective of the assessment is to point out areas where there has been exemplary treatment of uncertainty, exemplary clarity in description and illustration, and exemplary traceability. Fortunately, such positive examples were available in the hierarchy of documents supporting the TSPA-SR, and their methods and treatments are

recommended to be followed by authors of other parts of the scientific document hierarchy.

## **Uncertainty Review**

This internal assessment was conducted by a team of YMP technical specialists who were generally not involved in the work reported in the documents. The primary objective of the assessment was to review and evaluate the adequacy of the uncertainty treatment in the suite of TSPA-SR technical documents, including the TSPA-SR document, the Process Model Reports (PMRs), and the Analysis and Model Reports (AMRs). The process used in the review consisted of several steps.

- 1) Initially a suite of process models was identified and the relations of these models to the AMRs and to each other were determined. These relations are presented in the Model Relation Diagrams contained in the individual chapters of the report.
- 2) Next the internal structure of key models was identified.
  - Conceptual models were identified that describe the process.
  - Parameters/inputs that support the model were identified.
  - Representational models that implement the conceptual model were identified.
  - Model results for downstream use, particularly in the TSPA, were identified.

This information is summarized on the Model Structure Diagrams that are included in each chapter of this report.

- 3) The identification and evaluation of uncertainty treatment and incorporation of variability, which is the main objective of this study, was summarized in uncertainty/variability tables that are organized around the elements of the Model Structure Diagrams. These tables are also included in the individual model chapters of this report.
- 4) The final step in the review involved evaluating the propagation of uncertainty through the suite of process models and into performance assessment.

Uncertainty enters technical analysis for a number of reasons and at a number of locations. In order to understand how uncertainty has been treated in the YMP process models it is important to have a framework for the discussion. The model structure diagrams provide this framework. Each of the elements shown on the model structure diagrams is crucial to the development of the model, and each has associated uncertainties. The elements are not independent but are interrelated through the model. Consequently, transparency and traceability are crucial to the understanding and treatment of uncertainty. Use of the elements identified on the model structure diagrams allows for a more systematic discussion and evaluation of uncertainties and allows for the evaluation of the impacts of the uncertainties on other parts of the model.

The review of uncertainty treatment included:

- Summarizing the uncertainty
- Identifying the source of the uncertainty
- Summarizing the manner in which the uncertainty was treated
- Summarizing the basis for the treatment
- Reviewing any discussion of the potential impact of the uncertainty

This information was developed for uncertainties related to each element of the model. The results of the review are discussed in each chapter and summarized in tables developed for each model.

### **Conceptual Model Uncertainty**

All models are simplifications of the real system being modeled, and simplifications introduce uncertainties. Conceptual model uncertainties arise from incomplete understanding of the processes being modeled. There may be more than one equally plausible way to model a specific process. Alternative conceptual models may be considered equally likely or be considered equally capable of explaining the available data.

Conceptual model uncertainty is one of the most difficult issues that the YMP is dealing with in the realm of uncertainty. The principal way of addressing this type of uncertainty is to develop and evaluate alternative models that include a spectrum of viable conceptualizations. The analysis of stress corrosion cracking (SCC) in the waste package (WP) area is a good example of this approach. Two models for SCC are formulated and the most conservative (i.e., most pessimistic with respect to performance) is propagated forward for use with the TSPA. In the probabilistic seismic hazard analysis, alternative tectonic models are developed and they are incorporated directly into the hazard analysis. Only rarely on the YMP are alternative conceptual models incorporated directly into a probabilistic analysis.

In most areas, a clear description of the overall conceptual model(s), its bases, and the uncertainties, is lacking. In some areas, short descriptions are provided in the PMR. In other areas, limited discussions are presented in the AMRs. However, several AMRs lack a discussion of conceptual model(s) addressed in that AMR. This is believed to be partly due to the way that work is organized within a PMR area. For instance, the discussion of conceptual models for unsaturated zone (UZ) flow are contained in a separate AMR, while in the saturated zone (SZ) the conceptual model is discussed in the PMR and subcomponents are discussed in the AMRs.

### **Representational Model Uncertainty**

Translation of a conceptual model into a representational, or mathematical, model produces additional uncertainties because of simplifications and approximations that generally must be employed to make the problem tractable. Also, representational

models are implemented in computer programs, which introduces another set of uncertainties related to numerical representation of the representational/mathematical model.

There are examples where representational model uncertainty has been treated well, including evaluation of different computer codes, like NUFT and TOUGH2, using test data to evaluate how well a model represents a process, and evaluating submodels embedded within larger models. In other cases significant improvements can be made.

### **Parameter Uncertainty**

Uncertainty in model parameters arises from imperfect knowledge or limited data. The uncertainty may be related to measurement error, imperfect knowledge of spatial variability, or other sources. For parameters that are based on data that can be measured directly, at the appropriate scale, the uncertainty treatment could include discussions of measurement errors, representativeness, and related issues. These uncertainties should be adequately treated by the use of standard procedures, such as American Society for Testing and Materials procedures or YMP technical procedures, and reference to those procedures should be all that is required in YMP documentation. Standard error analysis of measured parameter values is important to document, and parameter distributions should be developed and analyzed whenever possible. The YMP has numerous good examples of this type of treatment.

Developed parameters have their values derived via some interpretive or analytical process involving scaling to appropriate dimensions, such as laboratory measurements of hydrologic properties, or conceptualization in terms of a model, such as incorporating lithophysal cavities into values for thermal conductivity. Error analysis of the values used for developed parameters is important, but it is also important to evaluate and discuss the uncertainties associated with the model and/or analysis bases for the parameter value. In order to fully characterize and evaluate uncertainties associated with developed parameters it is important to provide a clear discussion of the technical activities involved in deriving the parameter values.

There are a number of cases in the AMRs where parameter uncertainty is not characterized and a parameter value is chosen which is thought to be a bounding value. In some cases there is a good explanation provided for the choice of the bounding value, but in many cases the explanation for the grounds for the choice and/or the impact of the introduced uncertainty is weaker. Similarly, some parameter values are chosen as being representative. As above, in some instances the explanations of the bases are sound and in others, weaker. Lastly, some parameters are represented by probability distributions. Again, the explanations of the bases supporting some of the chosen distributions are sound, others are weaker.

### **Uncertainty in Model Results**

The main purpose for models is to simulate the future consequences of processes that cannot be directly observed. Model results serve either as input to subsequent models or

as direct input to the TSPA through abstraction. The results of modeling are uncertain because the model components (i.e., the conceptual models, representational models, and parameters) are themselves uncertain.

The AMRs differ in the manner in which they portray how uncertainties in the model components affect the results. Some AMRs explicitly show how such uncertainties affect the results. Good examples exist in the WP degradation, SZ transport, and biosphere areas. Other areas are less developed, for example SZ flow. In most areas, it was felt that additional sensitivity analyses would help demonstrate what uncertainties, at the process level, affect the model results.

Modeling of a particular process typically culminates with the development of abstraction models. These abstracted models are then implemented into the overall TSPA model. In most instances, the development of the abstracted models and their links to supporting process model results are clear. Examples of this are the abstracted models for WP degradation, waste form degradation, and dissolved concentration limits.

### **Propagation of Uncertainty**

Uncertainties propagate from field data, laboratory data, and literature information, through process-level modeling, into abstracted models, and ultimately into the TSPA. The clear propagation of uncertainty is essential in demonstrating that the TSPA itself is complete and robust.

All identified uncertainties appear to have been propagated into the TSPA. However, it was found that the manner in which this has been done is not always clear. For example, it is quite difficult for a reviewer of the TSPA to understand that all the uncertainties associated with UZ flow are contained within three calibrated sets of flow fields. It is sometimes also not revealed at the TSPA level that alternative conceptual models have been evaluated at the process-level with the most conservative one chosen. An example of this is SCC of the WP outer barrier. In addition, it was found that the TSPA-SR document sometimes neglects to comprehensively discuss the bases supporting the treatment of important uncertainties within the abstracted models. An example of this is matrix diffusion in the UZ.

### **Principal Conclusions**

- The YMP could benefit from a systematic process for identifying, documenting, categorizing, evaluating, and quantifying uncertainties.
- Conceptual model, representational model, parameter/inputs, and results provide categories that are effective for evaluating and discussing uncertainty treatment.
- Distinguishing between parameter values derived from acquired and developed data could improve parameter uncertainty treatment.

- Representational model uncertainty is addressed well in several YMP documents, and these should serve as examples for others to follow.
- The YMP could benefit from a consistent approach to the propagation of uncertainty through the TSPA model hierarchy.

### **Principal Recommendations**

- Consider developing a systematic process for identifying, documenting, categorizing, evaluating, and quantifying uncertainties.
- Provide better discussions of the bases for determining parameter values and probability distributions.
- Provide more robust and consistent justification for parameter and model bounds.
- Develop an overall conceptual model AMR for large, complex models. Improve the conceptual model discussions within AMRs.
- Describe how uncertainties from upstream models have been incorporated into AMRs for the downstream models.

# Introduction

## Objective

Meaningful quantification of the uncertainties associated with performance of the potential repository, clearly and understandably presented, is essential to provide decision makers with the information needed for judging the overall risks of disposing high level nuclear waste at Yucca Mountain. Stakeholders and oversight bodies to the Yucca Mountain Site Characterization Project (YMP)—namely, the Nuclear Waste Technical Review Board (NWTRB)—have stated that the quantification, analysis, integration, and communication of uncertainty needs to be addressed in a more rigorous manner. The NWTRB<sup>1</sup> has expressed a position that projections of repository postclosure performance will be incomplete unless a meaningful quantification of uncertainty is also provided. Internal YMP reviews of the Total System Performance Assessment—Site Recommendation (TSPA-SR, Rev. 0, ICN 1) and its basis documents also indicate that a more rigorous, quantitative treatment of uncertainty is warranted<sup>2</sup>.

The YMP recognizes the importance of quantifying, managing, and communicating uncertainties, and initiated the effort documented in this report<sup>3</sup>. The objectives of this internal-assessment were to critically review and assess the treatment and discussion of uncertainties in the technical documents supporting the TSPA-SR and develop guidance for future treatment of uncertainties and the documentation of that treatment.

## Background and Regulatory Requirements Regarding Uncertainty Treatment

The appropriate treatment of uncertainty is one of the key issues, and key difficulties, in policy analysis and risk management. Although uncertainty is often seen as a purely technical issue, one that can potentially be sufficiently resolved with more time and study, societal and policy decisions typically cannot be postponed until all technical uncertainties are resolved. Indeed, resolution of all uncertainties relevant to a complex decision is most often not feasible. Evaluating the long-term performance of a repository is no exception.

It has been known since identifying geologic disposal as the preferred means for the disposition of spent nuclear fuel (SNF) and high-level waste (HLW) that there would be a considerable amount of uncertainty associated with the projection of long-term repository performance. These uncertainties are due to many factors resulting from the complexities of the repository system and the long time frames over which projections must be made. Uncertainties arise from incomplete understanding, limited information, lack of data, and the fact that the models used are only approximations of reality. It has also been recognized that the effective treatment of these uncertainties is an integral part of the

---

<sup>1</sup> Letter, J. Cohon (NWTRB) to I. Itkin (DOE), September 20, 2000

<sup>2</sup> Specific Examples Include Deficiency Reports LVMO-01-D-028; LVMO-00-D-118; LVMO-00-D-119; BSC-01-D-0051

<sup>3</sup> Project Operations Review Board Action No. 000531-01, May 31, 2000

decision processes involved in site selection, site characterization, site designation, and issuing a license.

Effective treatment of uncertainty includes identification of the various uncertainties, their source, the manner in which they are treated, the basis for the treatment, and the overall impacts of uncertainties on the results (in the end, a projection of repository system performance). It is also necessary to communicate this treatment in a traceable and transparent manner throughout all documentation that supports the decision being made. The treatment of uncertainty and how it is communicated will differ depending on the decision being made and who is making the decision. However, a thorough, traceable, and transparent treatment is needed at all stages.

A less than complete uncertainty treatment results in the decision maker not having all of the needed information and could result in poor decisions or delay of the overall decision-making process. The presence of uncertainties complicates decision making in a number of ways: it makes it difficult to distinguish between a “good decision” and a “good outcome,” particularly when the uncertainties have not been explicitly quantified in the analysis; and it can cause delay of decisions in favor of uncertainty reduction, beyond the point at which further uncertainty reduction is valuable (Finkel 1990).

Both the U.S. Environmental Protection Agency (EPA) and the U.S. Nuclear Regulatory Commission (NRC) are in the process of promulgating regulations regarding repository safety. Both agencies fully recognize that post-closure safety assessments are inherently uncertain. Because of this, they invoke the concepts of “reasonable expectation” (EPA draft 40 Code of Federal Regulations [CFR] 197) and “reasonable assurance” (NRC draft 10 CFR 63) in what they regard as sufficient information and analyses needed to determine whether the repository system will protect the public.

In its release of draft 40 CFR 197<sup>4</sup>, the EPA states:

“Reasonable expectation means that the Commission is satisfied that compliance will be achieved based upon the full record before it. Reasonable expectation:

- a) Requires less than absolute proof because absolute proof is impossible to attain for disposal due to the uncertainty of projecting long-term performance;
- b) Is less stringent than the reasonable assurance concept that NRC uses to license nuclear power plants;
- c) Takes into account the inherently greater uncertainties in making long-term projections of the performance of the Yucca Mountain disposal system;
- d) Does not exclude important parameters from assessments and analyses simply because they are difficult to precisely quantify to a high degree of confidence; and

---

<sup>4</sup> Federal Register, Vol. 64, No. 166, August 27, 1999, § 197.14

- e) Focuses performance assessments and analyses upon the full range of defensible and reasonable parameter distributions rather than only upon extreme physical situations and parameter values.”

In its release of draft 10 CFR 63<sup>5</sup>, the NRC states:

“Proof that the geologic repository will be in conformance with the objective for postclosure performance is not to be had in the ordinary sense of the word because of the uncertainties inherent in the understanding of the evolution of the geologic setting, biosphere, and engineered barrier system. For such long-term performance, what is required is reasonable assurance, making allowance for the time period, hazards, and uncertainties involved, that the outcome will be in conformance with the objective for postclosure performance of the geologic repository. Demonstrating compliance, by necessity, will involve the use of complex predictive models that are supported by limited data from field and laboratory tests, site-specific monitoring, and natural analog studies that may be supplemented with prevalent expert judgment.”

### **Performance Assessment (PA) Modeling**

Recognizing that evaluating the long-term performance of the repository is uncertain, both agencies are proposing requirements related to the methodology that will be used to assess repository safety. This methodology is termed performance assessment. The EPA (40 CFR 197.12) defines PA as an “analysis that:

- 1) Identifies the processes, events, and sequences of processes and events (except human intrusion), and their probabilities of occurring over 10,000 years after disposal, that might affect the Yucca Mountain disposal system;
- 2) Examines the effects of those processes, events, and sequences of processes and events upon the performance of the disposal system; and
- 3) Estimates the annual committed effective dose equivalent received by the reasonably maximally exposed individual, including the associated uncertainties, as a result of releases caused by all significant processes, events, and sequences of processes and events.”

The NRC states (10 CFR 63.114) that the PA must “account for uncertainties and variabilities in parameter values and provide the technical basis for parameter ranges, probability distributions, or bounding values used in the performance assessment.”

---

<sup>5</sup> Federal Register, Vol. 64, No. 34, February 22, 1999, IX–Performance Assessment

The proposed “General Guidelines for the Recommendation of Sites for Nuclear Waste Repositories; Yucca Mountain Site Suitability Guidelines<sup>6</sup>,” state (10 CFR 963.16(a)) that “DOE will evaluate postclosure suitability using the total system PA method. DOE will conduct a total system performance assessment to evaluate the ability of the geologic repository to meet the applicable radiation protection standard...” In addition, the guidelines state (10 CFR 963.16(b)) that “In conducting a total system performance assessment under this section, DOE will...”:

- Account for uncertainties and variabilities in parameter values and provide the technical basis for parameter ranges, probability distributions, and bounding values (Item 2)
- Consider alternative models of features and processes that are consistent with available data and current scientific understanding, and evaluate the effects that alternative models would have on the estimated performance of the geologic repository (Item 3)

PA analyses consider all plausible features, events, and processes (FEPs) that could impact performance of the repository system. A PA model consists of a linked series of models, each representing a different part of the entire repository system. These models are based on site characterization data, complex process-level modeling of the various FEPs, and expert scientific judgement.

The first step in the development of a PA model involves the identification and classification of the FEPs that may affect how well the repository will isolate waste over time. These FEPs are further evaluated to determine if they will indeed affect performance. Those that are unlikely to occur or those that will result in insignificant impacts to repository performance are not considered in further analyses (excluded). Scenarios (and scenario classes) are then defined as a subset of the set of all possible future states, that accommodate the included FEPs. Scenario screening is then used to identify scenarios that contain a combination of FEPs for which the joint probability of occurrence, or the combined consequence to performance, is small enough to permit exclusion from further analysis even though the probability or consequence for individual FEPs indicates that they should be retained.

To further evaluate the remaining (included) FEPs following this screening process, detailed process-level models of the various components of the repository system are developed. Developing these detailed process models involves three steps:

- Developing conceptual models based on existing information
- Developing representational (mathematical) models that describe the conceptual models

---

<sup>6</sup> 64 FR 67054, November 30, 1999

- Defining the possible values for the input parameters

These individual process models can be quite complex. Integration of complex process models into an overall total system framework would result in a very complicated, non-transparent, and computationally inefficient model. As such, the results of detailed process modeling efforts are used to develop more simplified, or abstracted, models that are ultimately used in the overall repository system model. These abstracted models represent the most critical aspects necessary to model the entire repository system. The abstracted models are then combined into a single, overall representation of the repository system. This effectively integrates all included FEPs and scenarios into the PA model.

Each step involved in developing the overall PA model must treat uncertainty. Critical uncertainties must be propagated through the abstracted models and into the PA model. Transparent and traceable treatment of uncertainties, from the development of the complex process level models, through development of the abstracted models, and into the overall system-level model is essential.

### **Types of Uncertainty**

Classically in PAs uncertainties have been classified into three categories: scenario uncertainty, conceptual model uncertainty, and parameter uncertainty<sup>7,8,9</sup>. This classification scheme works well at the PA level. At the process model level these categories are too coarse to provide a framework for detailed uncertainty evaluation. A framework can be developed by identifying elements of a process model and evaluating how uncertainty is treated for each of the elements. For instance, the *Standard Guide for Application of a Ground-Water Flow Model to a Site-Specific Problem* (ASTM D 5447-93<sup>10</sup>) identifies model elements including conceptual model, mathematical model, boundary conditions, and parameters. Tsang<sup>11</sup> (1991) identifies a similar categorization and defines the steps taken in the development of a model.

For this study a set of process model elements was identified to serve as the framework for uncertainty review and evaluation (see Figure 1, Example of Model Structure Diagram). These components are the conceptual model, the representational or mathematical model, parameters, and results. A conceptual model is a fundamental description of a process, which is generally qualitative but may be expressed mathematically. Conceptual models are developed based on descriptions of physical processes (e.g., Newton's laws), understanding developed from laboratory and field

---

<sup>7</sup> Disposal of Radioactive Wastes: Review of Safety Assessment Methods, OECD Nuclear Energy Agency, Paris, 1991.

<sup>8</sup> Lessons Learnt From Ten Performance Assessments, OECD Nuclear Energy Agency, Paris, 1997.

<sup>9</sup> Andersson, Johan, SR 97 - Data and Data Uncertainties, Swedish Nuclear Fuel and Waste Management Co., 1999

<sup>10</sup> ASTM D 5447-93, Standard Guide for Application of a Ground-Water Flow Model to a Site-Specific Problem, 2000

<sup>11</sup> Tsang, Chin-Fu, The Modeling Process and Model Validation, Ground Water, Volume 29, No. 6, November-December, 1991, pp. 825-831

measurements, and observations of similar natural or man-made systems. Representational models are translations of conceptual models into mathematical equations that can be used to produce quantitative estimates of performance. Parameters are the data or values that are input into the mathematical equations. Results are those properties, values, trends, and observations made from executing the representational models.

Classifying and estimating the importance of uncertainties is a critical part of modeling any complex system. Uncertainties of several different types exist and can be incorporated into evaluations of repository performance in several different ways. Within the context of this report, uncertainties have been classified into five categories that are consistent with the components of a model: scenario uncertainty, conceptual model uncertainty, representational model uncertainty, parameter uncertainty, and uncertainty in the results.

### **Scenario Uncertainty**

Scenario uncertainty stems from the fact that the evolution of geologic and environmental conditions surrounding the disposal facility over tens of thousands of years cannot be predicted precisely. Scenario uncertainty includes the uncertainty associated with the FEPs that may impact the various components of the repository system. Scenarios of plausible future states imposed on the repository system, as well as their likelihood of occurrence, must be inferred from direct and indirect field evidence, or fundamental understanding of the physical, chemical and geologic processes operating on the repository system. Those scenarios that cannot be excluded through the screening process must be incorporated into assessments of performance.

Scenario uncertainty is addressed in the screening of FEPs and scenarios to identify those that may ultimately impact long-term repository performance. If a scenario cannot be excluded based on either low probability or consequence, then it must be considered in the PA. The screening decisions themselves may be uncertain. For example, the probability of a scenario occurring may be uncertain. Such uncertainties need to be included in screening decisions.

One example of a plausible but unlikely future scenario at Yucca Mountain is the occurrence of igneous activity that has the potential to affect the long-term performance of the potential repository. Yucca Mountain is in a region that has experienced repeated volcanic activity in the geologic past. The results of site-characterization studies, supported by an expert elicitation panel, indicate that although the mean value of the probability distribution function for the occurrence of igneous activity at Yucca Mountain during the next 10,000 years is small, it is greater than the criterion defined by the NRC in proposed 10 CFR 63 for inclusion in the PA (1 chance in 10,000 over 10,000 years). Volcanic activity therefore is included in the assessment of repository performance.

# Schematic of Model Structure

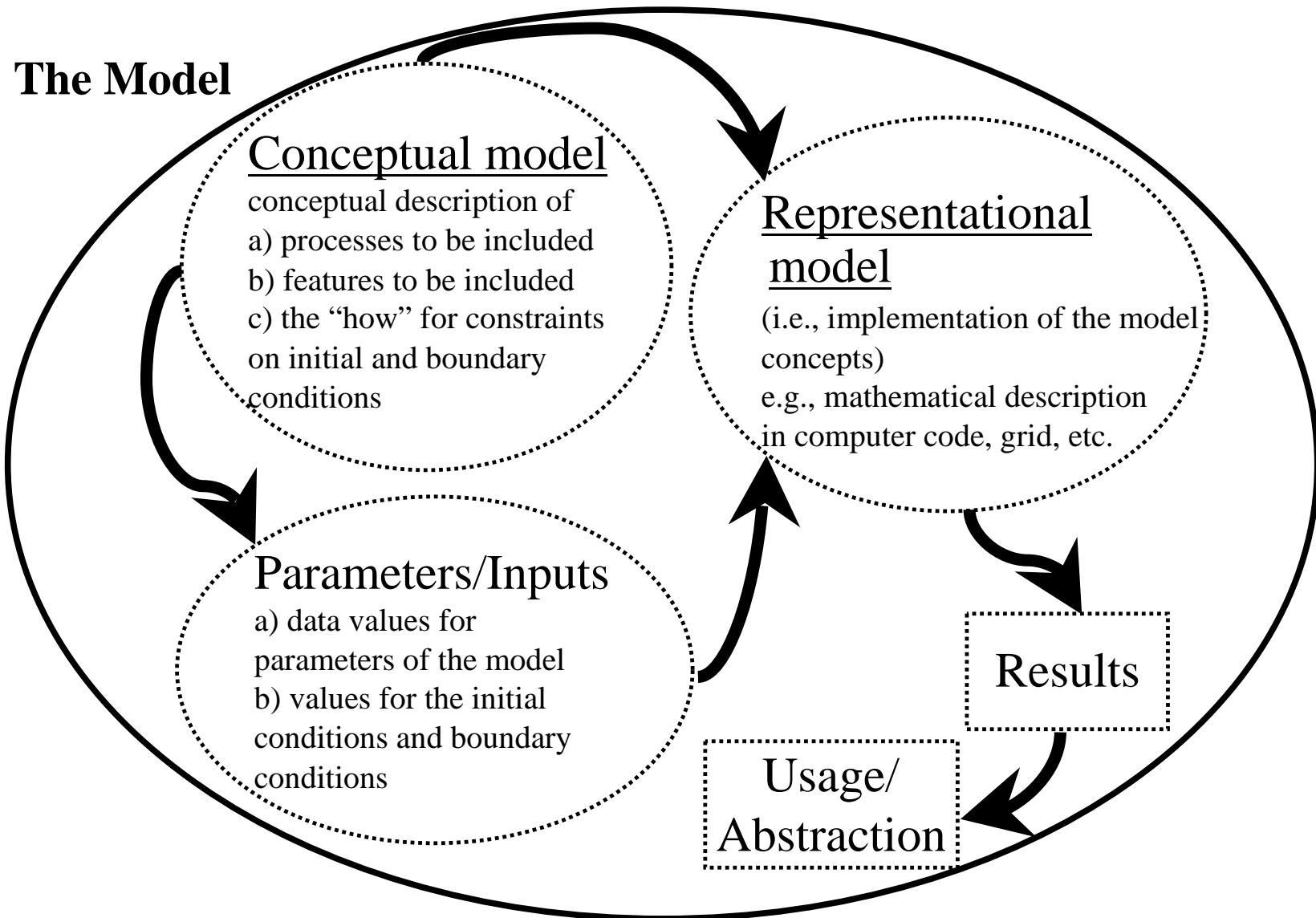


Figure 1: Example of Model Structure Diagram

An example of a plausible but likely future scenario at Yucca Mountain is that the climate will change from present-day conditions to a wetter climate. Predictions of the performance of a potential repository must take into account the likelihood and the consequences of these various plausible scenarios. Because of its high likelihood, climate change is incorporated as a specific feature that is explicitly accounted for in the TSPA model.

The focus of the review reported here was on the models ultimately included in TSPA-SR, and not on the decisions and arguments used to screen FEPs and scenarios from further analysis. As such, documents related to FEPs screening were not evaluated and scenario uncertainty has not been explicitly evaluated in this report.

### **Conceptual Model Uncertainty**

All models are simplifications of the real system being modeled, and simplifications introduce uncertainties. Model uncertainties include several types: uncertainty in conceptual models, uncertainty in mathematical descriptions of these conceptual models, and uncertainty in numerical implementations of those models.

Conceptual model uncertainty arises from incomplete understanding or characterization of FEPs that will affect the repository. There may be several equally plausible ways to conceptualize a specific process being modeled: that is, multiple alternative conceptual models may be considered equally likely or considered to explain the current data equally well. Conceptual model uncertainty is particularly important if those alternative models lead to significantly different predictions of future performance.

Communicating how uncertainties are treated includes identifying the basis for choosing one conceptual model over the other. For instance, a “conservative” model or simplifying assumption may be developed and implemented. In some cases, specific data sets are available that differentiate between conceptual models based on outcomes and/or predictions. In other cases, theoretical arguments support selection from among alternative conceptual models. Technical limitations such as the lack of definitive data may influence decisions about alternative conceptual models and may require the inclusion of more than one model in the analysis to test the significance of the models to the results of the analysis.

An example of conceptual model uncertainty is the representation of unsaturated zone (UZ) flow at Yucca Mountain using the active fracture model (Liu et al. 1998). The conceptual model simplifies the characterization of water flow through a complex fractured rock mass by using a dual-continuum fracture-matrix model, which introduces conceptual model uncertainty.

### **Representational Model Uncertainty**

Translation of a conceptual model into a mathematical model produces additional uncertainties because of simplifications and approximations that generally must be

employed to make the problem tractable. Also, mathematical models are implemented in computer programs, which introduces another set of uncertainties related to numerical representation of the mathematical model.

Continuing the example above regarding UZ flow, additional uncertainty is introduced with the mathematical representation of fracture-matrix interaction and the numerical solution of the governing equations. The model is calibrated to field conditions, but only a limited amount of data are available for the calibration, so the ability to reduce the model uncertainty by comparison with field conditions is limited.

### **Parameter Uncertainty**

The parameters of the mathematical models used to predict the performance of the repository system are subject to both uncertainty and variability. Uncertainty in model parameters arises from imperfect knowledge or limited data. In principle, uncertainty can be reduced with additional measurements; an example is the solubility of neptunium in groundwater. Variability arises from the randomness or heterogeneity of physical or behavioral characteristics in the engineered system, natural system, or biosphere. Variability and its treatment are discussed later in this section. If variability is not fully characterized, then another type of uncertainty is introduced. Variability and uncertainty are often combined in the description of a single parameter because the available information does not suffice to discriminate between them. An example is the seepage flux that can contact the waste package (WP), which depends on heterogeneity in hydrologic properties of the host rock, and is also associated with conceptual and model uncertainties, and with parameter uncertainty because of limited characterization of the natural system.

### **Uncertainty in Results**

The main purpose for models is to simulate the future consequences of processes that cannot be directly observed. For example, it is not possible to observe WP degradation over the life of the repository, or to observe the details of how water flows in the UZ at Yucca Mountain. Models produce results, or measures, of the various processes. In the example, modeling of WP performance produces estimates of when the WPs will first become breached and estimates for the size and number of such breaches over time. Modeling of UZ flow produces estimates of groundwater percolation rates in the fracture and matrix continua.

The results of modeling are uncertain because the model components, (i.e. the conceptual models, representational models, and parameters) are themselves uncertain.

### **Potential Treatments of Uncertainty**

For each of these types of uncertainty, and especially for parameter uncertainty, a range of approaches has been used for characterization. Brief descriptions of the approaches are provided below.

- *No Impact/Ignore* – An uncertainty is identified as having no impact on subsequent results and can be ignored. One example is the need to include parameters as input to a computer program when it is known that any changes in these parameters would not affect the results (e.g., the parameters are needed for a calculation but do not affect results in the vicinity of the repository). This approach has been taken in modeling radionuclide transport within the saturated zone (SZ) at Yucca Mountain where some hydrogeologic properties that do not affect the results are defined as single values such that uncertainty on these parameters is ignored.

Another example is when previous analyses indicate that uncertainty in a given model or parameter does not impact the results. An example of this is uncertainty regarding the timing of climate change. The timing of future changes in climate is not known precisely. However, analyses<sup>12</sup> indicate that repository performance (in particular, receptor dose) is not sensitive to uncertainty in timing of climate change. Accordingly, this uncertainty is ignored and a point value for the time of climate change is used.

- *Conservatively Treat/Estimate or Bound* – Available information is used to provide a conservative or bounding treatment/estimate of a model/parameter. This approach is typically taken when there is little information available to define a model or parameter. In these instances, the available information (site-specific or surrogate) is used to define a conservative or bounding estimate of the parameter/model. For example, data on stress corrosion cracking of stainless steel are used to develop a model and the parameter distributions for stress corrosion cracking of Alloy 22. Specifically, the range of threshold stress for initiation of stress corrosion cracking of Alloy 22 was estimated at 20 to 30 percent of the material yield stress. This distribution was based on literature reporting stress corrosion cracking test results for certain stainless steels in aggressive environments. It is used as a conservative, bounding distribution for Alloy 22 which is known to be less susceptible to stress corrosion cracking than stainless steels, but for which extensive data are not yet available.

For the natural system, it is a widely accepted concept that radionuclides traveling in water flowing within fractures will tend to sorb to fracture surfaces. However, little information is available to quantitatively support this conceptualization. As such, it has been decided to ignore the potential beneficial effects of sorption of radionuclides to fracture surfaces.

- *Distribution* – Sufficient data are available to support the development of a probability distribution for model input parameters. In some cases, those data were acquired from relatively short-term tests but are used to model the long-term performance of the components of the repository system. This is justified if the short-term data are used appropriately in process models developed from valid conceptual models incorporating physical and chemical principles.

---

<sup>12</sup> See *Total System Performance Assessment (TSPA) Model for Site Recommendation*, MDL-WIS-PA-000002, Rev. 0 (Section 6.3.1.1)

Data from site characterization tests have been used to develop models and parameter distributions for much of the natural system. For example, in the SZ flow model, porosity and permeability in fractured and porous media are parameters with distributions developed from field and laboratory experiments and tests. Another example is sorption coefficients for interaction of radionuclides with the rock matrix along potential transport pathways. Laboratory experiments using samples of rock from the affected units produced data which were used to develop sorption-coefficient distributions for the SZ transport model.

- *Assume* – An uncertainty has been addressed by assumption. In these instances, relevant information is used to develop and support the assumption. Assumptions can be either conceptual (e.g., application of a linear model for radionuclide sorption) or specific to a parameter value (e.g., neptunium concentration was assumed to be controlled by  $\text{Np}_2\text{O}_5$ ). Assumptions can be either conservative/bounding or representative.
- *Subsume* – Uncertainty is subsumed within a modeling approach. This does not mean that the uncertainty is ignored, but rather the effects of the uncertainty are propagated somewhat indirectly into a model. Examples where uncertainties are subsumed include the areas of model calibration, development of abstracted models, and corroboration.

An example subsuming uncertainty via calibration and corroboration is in the modeling of ground water flow in the UZ. In this case, uncertainty in hydrologic properties is treated through calibration of the model to measured parameters (e.g., matrix saturation and water potential) when imposing different surface infiltration rate boundary conditions. With a surface infiltration rate boundary condition prescribed, the calibration process determines values for uncertain hydrologic parameters such that the measured parameters are reproduced. Other information (e.g., geochemistry modeling results) is used to support or corroborate the calibrations. The calibrated model is then used to produce three-dimensional (3D) flow fields, one for each of the prescribed surface infiltration rate boundary conditions, that are used directly in the PA model (the abstraction). In this case, uncertainties in the UZ hydrologic properties are subsumed in the calibration of the model and the flow fields that are used directly by TSPA.

Another example of subsuming is the treatment of uncertainties regarding the manner in which microbes and aging/phase instability affect the corrosion of the Alloy-22 WP outer barrier. Little information and analytical support exists to define a detailed treatment within TSPA. Rather, the approach taken was to subsume all uncertainties into enhancement factors used to increase corrosion rates. These enhancement factors are represented by a range of values, believed to capture the uncertainty associated with the processes.

- *No Treatment* – uncertainty in a scenario, model, or parameter is ignored.

## Spatial and Temporal Variability

For large-scale processes variability over time and over the area of the repository may have an important impact on performance. Since variability is an intrinsic property of a system, it cannot be reduced with additional information. Four approaches can be taken for treating variability.

- *Ignore* – This approach is appropriate when the variability is small and expected to have minimal impact on the results or when regulatory requirements and/or guidance prescribe such a treatment. A specific example where variability has been ignored is in the area of solubility limits for some radionuclides. Solubility limits are characterized for certain combinations of geochemical conditions; however, these conditions are spatially variable. Quantifying solubility limits over the full range of extant geochemical conditions is currently infeasible, so a range of solubility limits is used to represent uncertainty.

As another example, the definition of the receptor in draft 10 CFR 63 prescribes the receptor as the “average member of the critical group,” eliminating the need to consider variability in the characteristics of the receptor.

- *Dissaggregate* – Explicitly represent the variability, typically through mathematical modeling techniques. The process modeling and the TSPA-SR explicitly include such treatment of variability (both temporal and spatial) at several levels. For example, precipitation in the Yucca Mountain region will be a function of long-term climate, and climate is expected to change over time. This temporal variability is explicitly captured in the models by the hypothesized (instantaneous) change from the present-day climate to wetter climates in the future.

As another example, the flow of water in the UZ from the ground surface to the water table is also expected to vary over both time and space. The UZ flow model integrates site characterization data into a calibrated 3D model that captures both temporal and spatial variation. It uses infiltration at the ground surface as a boundary condition (itself spatially and temporally variable) and estimates the distribution of percolating water in the UZ. Temporal variability in infiltration may be short term due to seasonal weather variations, or long term due to climate changes. Seasonal variations may result in episodic flow, but such episodic flow is believed to be dampened in the upper regions of the UZ to such a degree that the flow is steady in the lower regions. As such, short-term variation in infiltration is ignored. However, long-term variation is captured through the long-term climate model.

- *Use the Average Value* – This approach is appropriate when the variability is small and is expected to have minimal impact on the results. This approach may appear similar to ignoring the variability, but it is appropriate when the average value can be estimated more readily than the full distribution, and the other conditions apply. For example, spatial variability in the rock in the UZ affects the percolation flux at the repository horizon. Vertical spatial variability has been captured by defining different hydrogeologic units with different properties. However, lateral spatial variability

within a hydrogeologic unit has not been captured in the current site-scale model of the geology. The UZ flow model uses uniform rock property data for each hydrogeologic unit. Geologic variation, however, such as thickness or major mineralogic changes, is explicitly modeled.

- *Use the Maximum or Minimum Value* – In this approach, a generally conservative model or estimate is used to represent the variability. In these cases “conservative” means models or estimates such that any variability not explicitly modeled would lead to lower dose estimates than that produced by the chosen model. An example where this approach has been utilized is in the area of biosphere modeling where parameters are chosen to maximize the receptor dose for a given level of contaminant concentration in groundwater.
- *Treat as Uncertain* – In this approach, the variability is treated as an uncertainty range, with the average value representing the expected value of a probability distribution while the maximum and minimum values are used to define the extremes. This approach has been taken to define a number of modeling parameters used in TSPA. It is similar to the use of the average value or use of the maximum/minimum value discussed above except that the entire range of variability is treated solely as uncertainty.

### **Analysis and Model Report (AMR)/Process Model Report (PMR)/TSPA Construct**

Several TSPA analyses have been completed by the YMP<sup>13,14,15</sup>. Evolution of these TSPA models has resulted in more sophisticated, transparent, and traceable linkages between the abstracted models implemented into TSPA and the supporting process level models. The first TSPA models were developed primarily by PA modelers, relying on information developed in other areas of the YMP. As the YMP moved closer to a phase involving regulatory decisions, better integration between PA and process modelers was needed to develop clear documentation of the model bases and the associated uncertainties.

The TSPA-Viability Assessment (VA)<sup>10</sup> model involved the development of a technical basis document<sup>16</sup> that was the first attempt to fully integrate PA and process modelers in order to clearly document the bases for the abstracted models and the uncertainties inherent in them. An integrated approach between the different modeling groups was established. However, this technical basis document construct itself was not sufficient in terms of traceability and transparency to support a site recommendation (SR) decision. This was pointed out by YMP participants, oversight bodies, and stakeholders. A

---

<sup>13</sup> Total System Performance Assessment–1993: An Evaluation of the Potential Yucca Mountain Repository, B00000000-01717-2200-00099, Rev. 1, 1994, ACC: NNA.19940406.0158

<sup>14</sup> Total System Performance Assessment–1995: An Evaluation of the Potential Yucca Mountain Repository, B00000000-01717-2200-00136, Rev. 1, 1995, ACC: MOL.19960724.0188

<sup>15</sup> Total System Performance Assessment-Viability Assessment

<sup>16</sup> Total System Performance Assessment–Viability Assessment (TSPA-VA) Analysis and Technical Basis Document, B00000000-01717-4301-000[01-11], 1998, ACC: MOL.19981008.00[01-11]

document hierarchy structure, benefiting from the development of the TSPA-VA, has been developed to further improve traceability and transparency.

Because of the complexity of the natural and engineered systems that would interact in the potential Yucca Mountain repository, a broad suite of technical documents has been developed to support TSPA. These documents create a hierarchy that describes everything from basic data collection and analysis, through process model development and testing, to process model abstraction for TSPA, to the development and execution of the PA itself. At the base of this document hierarchy are the AMRs developed under AP-3.10Q, *Analyses and Models*, and calculations developed under AP-3.12Q, *Calculations*. A very broad range of technical activities has been documented in AMRs, including the basic data and process model results needed to support TSPA. This information forms the technical foundation of the YMP's understanding of the processes operating in the system, and this understanding is summarized in PMRs developed under AP-3.11Q, *Technical Reports*. The development of process model abstractions that are directly incorporated into TSPA are also documented in AMRs. In order to understand how uncertainty has been treated and the treatment documented for the work that supports the TSPA, it is necessary to focus on the AMRs. Most of this report is focused on these documents.

### **Approach to Uncertainty Evaluation**

As discussed above, this report documents a critical internal-assessment of the treatment of uncertainty in TSPA-SR and the documentation that supports it. This internal assessment was conducted by a team of YMP technical specialist who were generally not part of the work reported in the documents. The team is best characterized as semi-independent. This section discusses the evaluation process used.

The first step in understanding the treatment of uncertainty and variability in the technical work supporting the TSPA is to map out the relationships of the basic technical documents that report that work. For the YMP these basic documents are the AMRs. The AMRs have such diverse purposes and cover such a broad range of technical areas that it was necessary for this review to establish a logical framework to organize the information. The organization in this report is provided by the identification of a suite of models that describe the YMP's understanding of processes operating in the natural and engineered systems. The processes identified here can be mapped to the YMP's PMRs, but in most cases the PMRs include more than one process model.

For each process model discussed in this report a Model Relation Diagram has been developed that illustrates the relationships among AMRs that support the model. These diagrams show the documentation of the data feeds to the model, the elements of the model, and the outputs of the model that feed TSPA. Because of variations in approaches to scoping the AMRs, the details of the diagrams are quite different depending on the model being reviewed. Nevertheless, the diagrams provide a general map to illustrate the way that the AMRs are interrelated and how they support the TSPA.

The second step involved developing the internal structure of the key models identified. The conceptual model(s) that describe the process, the parameters/inputs that support the model, the representational model that implements the conceptual model, and the model results for downstream use, particularly TSPA, were identified. This information was used to develop the Model Structure diagrams, with Figure 1 being an example. These diagrams show the documentation of the data feeds to the model, the elements of the model, and the outputs of the model that feed TSPA. Because of variations in approaches to scoping the AMRs, the details of the diagrams are quite different depending on the model being reviewed. Nevertheless, the diagrams provide a general map to illustrate the way that the AMRs are interrelated and how they support the TSPA.

The third step in understanding the treatment of uncertainty and variability is to review and document the uncertainty treatment for each model. As discussed above, uncertainties are typically classified into five categories: scenario, conceptual model, representational model, parameter, and results. Again, the focus of the review was on the models ultimately included in the TSPA-SR, and not on the decisions and arguments used to screen FEPs and scenarios from further analysis. As such, AMRs related to FEPs screening were not evaluated and scenario uncertainty has not been explicitly evaluated in this report. The treatment of uncertainties associated with each model was evaluated for the parameter, conceptual model, representational model, and results categories. The treatment of both spatial and temporal variability has also been reviewed for each model.

Both quantified and unquantified uncertainties and spatial/temporal variability within each AMR were evaluated by a team of reviewers, independent of the developers of the documents. The focus of the evaluation was on the completeness of the treatment and transparency/ traceability of the treatment within the AMR. The communication of treatment, not the technical adequacy of the treatment, was assessed. Some of the specific characteristics of the treatment reviewed include documentation of critical assumptions; technical bases for distributions, ranges, and bounding values; and discussions of data limitations.

The treatment of uncertainty and variability within each AMR was evaluated in a structured approach. For each uncertainty evaluated, the following information was provided:

**Summary:** A brief summary discussion of the uncertainty/variability being evaluated.

**Source:** Identification of the source of the uncertainty/variability. The source could be from such items as limited data to support an assumption or uncertain inputs provided from a supporting AMR. Reviewers were instructed to clearly indicate if no such source can be determined and to provide appropriate reference citations to document sections where such sources are discussed.

**Treatment:** A summary of the manner in which the uncertainty/variability was treated. Reviewers were instructed to provide, when possible, the actual parameter values or

ranges, (or the conceptual model) and to provide appropriate reference citations to document sections where the treatment is discussed.

**Basis:** A summary of the basis for the treatment selected, as documented in the report. If the basis is data, the reviewers were instructed to indicate the source of that data. In addition, the reviewers were instructed to clearly indicate if no basis is provided and to provide appropriate reference citations to AMR sections.

**Impact:** A discussion of the potential impact of the uncertainty/variability and its treatment, and a clear indication as to whether the impact is discussed in the AMR or if this is the subjective opinion of the reviewer. Again, the reviewers were instructed to provide appropriate reference citations to AMR sections are to be provided.

As discussed above, several AMRs can comprise an overall model. For example, five AMRs comprise the overall model of SZ groundwater flow. Evaluating the treatment of uncertainty within an AMR is an important step, but evaluating the overall treatment of uncertainty within a model is needed to determine whether it is complete. This was accomplished by utilizing all the information provided in the review of the individual AMRs in conjunction with review of the PMRs and the TSPA-SR itself. A different team of reviewers was utilized, with each participant responsible for review of the models covered in a single PMR area (e.g., groundwater flow and radionuclide transport in the UZ, WP degradation, engineered barrier system[EBS]).

The fourth step in the review of uncertainty treatment was evaluation of the propagation of uncertainty. Ultimately, a PA model must integrate several abstracted models into an overall system model. As discussed above, these abstracted models are developed from the results of more detailed process models. In order to assure traceability of information and data, a hierarchy of AMRs, all developed under AP-3.10Q, was put in place. This hierarchy shows how a series of AMRs typically constitutes a single detailed process model (for example, water movement in the UZ). In some instances, a single AMR presents all aspects of a process model (for example, infiltration of water into the UZ). Many AMRs are linked together, with output information from one becoming input to another (an example of this is the results of the infiltration model providing boundary conditions for the modeling of water movement in the UZ). Some of these linkages cross disciplines and organizations within the YMP (e.g., groundwater chemistry information needed to model the degradation of WPs).

The results of process modeling efforts are then utilized as input in model abstraction AMRs that document the development of the models that will ultimately be incorporated into the overall PA model. Lastly, there is the AMR that documents the development of the PA model<sup>17</sup>. The propagation of uncertainty through this chain of models, and documents, is also discussed in this report.

---

<sup>17</sup> *Total System Performance Assessment (TSPA) Model for Site Recommendation*, MDL-WIS-PA-000002, Rev. 0

## Uncertainty Identification and Review of Treatment

The development of models within the YMP is governed by AP-3.10Q. The purpose of this procedure states: “This procedure establishes the responsibilities and process for performing and documenting activities that constitute scientific, engineering, and performance assessment analyses that are subject of the requirements of *Quality Assurance Requirements and Description* (QARD), DOE/RW-0333P. These activities include the development, documentation, checking, review, approval, and revision of analyses or models, and the calibration, validation, or use of models to support scientific, engineering or performance assessment work activities.”

The procedure discusses uncertainty treatment in very general terms. Uncertainty is defined in Section 3.22 as “a statistical measure of how well a parameter, model (including conceptual model), or analysis represents a system, process, or phenomenon.” Variability is not defined. When developing and documenting a model (Section 5.2(c)), the analyst is instructed to follow the outline in Appendix 1. Item 6 of Appendix 1 instructs the analyst to “identify the principal lines of investigation considered, include appropriate scientific literature, parameter input, assumptions, idealizations, simplifications, initial and/or boundary conditions, equations, explanations of how the software and/or routines are used (if used), and the mathematical model(s) and expected sources of uncertainty”. The checker is instructed to check that “the implications of uncertainties and restrictions discussed are evaluated within the analysis or model documentation” (Section 5.6.3(a)(7)).

The review discussed in this report started with these procedural requirements. However, the identification of uncertainties for review requires further constraints. It is well beyond the scope of this review to report on the treatment of each and every uncertainty related to the work that supports the TSPA. The following criteria were developed to focus the team’s efforts on “important” uncertainties within a model:

- **Perceived importance to TSPA (dose).** This evaluation was based on the judgment of the reviewer and the results presented in TSPA-SR, because no additional TSPA calculations were performed for this review.
- **Quality/appropriateness of the treatment.** For all of the models an attempt was made to identify both good and bad examples of uncertainty treatment.
- **Visibility in the technical community.** If a particular uncertainty is an important issue for the technical community working in this area we have tried to include it.
- **Completeness of analysis.** The team has tried to discuss uncertainty treatment in all areas identified in our model structure diagrams.

This information is documented in tables developed for each model. The tables are presented in the chapters for the individual models.

## Report Outline

The individual model chapters discuss the uncertainty treatment for each model. These chapters discuss the purpose of each model, its intended use, and its limitations as identified in the documentation. The AMRs that constitute each model and an AMR relation diagram are then provided. A model structure diagram and a discussion of the documentation of the various parts of the model (conceptual model, representational model, parameters, and results) are presented. The treatment of uncertainty and variability within the model are then presented. This discussion focuses on major trends identified in the treatment of conceptual model, representational model, and parameter uncertainty and their impact on model results. A discussion of the trends observed regarding the propagation of uncertainty within the model through the results, development of abstracted models, and ultimate inclusion in the PA model and the TSPA-SR document is also provided. Additionally, supporting information is included in tabular form that discusses observations regarding the treatment of important uncertainties identified.

Recall, the ultimate objective of this task was to develop guidance for future treatment of uncertainties and the documentation of that treatment. Meeting this objective did not require an exhaustive review and subsequent documentation of every source of uncertainty in the models and how they are propagated through subsequent models and into TSPA-SR. Rather, the criteria identified above were used to focus the review on those uncertainties judged to be “important.” As such, the discussions in each of the chapters differ somewhat.

For example, the structure of the Engineered Barrier System Flow and Transport chapter differs somewhat from the others. The majority of models developed in this area are comparatively new, being developed since completion of the Viability Assessment. In addition, there are several models within this area, some being very complex. Most are somewhat coupled. As such, the YMP documentation structure regarding the engineered barrier system models differs somewhat from the other areas. The document structure for the engineered barrier system models and resource limitations precluded a review to the level conducted in the other areas. However, sufficient information regarding how uncertainty has been treated for this model area and the entire suite of models supporting TSPA-SR was gathered to support the conclusions and recommendations made.

The last chapter of the report presents the summary of the review findings and provides the recommendations for improved treatment of uncertainty in future development of process-level, abstraction, and system-level models.

## 1.0 Igneous Disruption Model–Volcanic Eruption

### 1.1 Purpose of the Model

The purpose of the conceptual model for volcanic eruptive release at Yucca Mountain is to provide a basis for both the characterization of uncertainty in the probability of igneous disruption (volcanic eruption) of the potential repository and the consequences of a disruption for use in TSPA. The volcanic eruption modeling approach is state-of-the-art, incorporating available data from volcanoes in the Yucca Mountain Region (YMR) and data from volcanoes (modern analogs) in other parts of the world. Information about the probability of eruptive conduits forming within the repository, the characteristics of an eruption, the repository response to an eruption, and the atmospheric transport of waste-entraining ash to a critical group is logically developed and documented in the AMRs that support development of the eruption model.

The information feeds from upstream AMRs to downstream AMRs; the *Disruptive Events* PMR and the TSPA-SR are clearly identified in each of the documents. While conservative assumptions were made because of sparse data available for eruptive processes and repository interaction (e.g., the mechanics of conduit formation, WP behavior in a conduit), these assumptions are clearly identified in the AMRs and tracked into the TSPA-SR. In cases where information exists, distributions, which capture the uncertainty in model parameters, are defined in the AMRs and are clearly traceable to the TSPA-SR.

### 1.2 Model Component Documentation

The *Disruptive Events* PMR (TDR-NBS-MD-000002) and its associated AMRs and one calculation comprise the documentation of the volcanic eruption model. A brief description of the purposes of the PMR, AMRs, and calculation follow:

- *Disruptive Events* PMR (TDR-NBS-MD-000002) – Summarizes the conceptual model and the technical product output that form part of the technical basis for the TSPA.
- *Characterize Framework for Igneous Activity at Yucca Mountain, Nevada* (ANL-MGR-GS-000001) – 1) Presents a conceptual framework of igneous activity in the YMP consistent with the volcanic and tectonic history of the region and the assessment of this history by experts who participated in the PVHA (CRWMS M&O 1996); and 2) develops probability distributions needed for TSPA based on PVHA inputs applied to the current repository design; included are probability distributions for the length and orientation of volcanic dikes within the repository footprint and for the number of eruptive centers (conduits) located within the footprint, conditional on a dike intersection.
- *Characterize Eruptive Processes at Yucca Mountain, Nevada* (ANL-MGR-GS-000002) – Presents information about volcanic systems and the parameters that can be used to model their behavior. The AMR presents parameter distributions for subsequent use in downstream AMRs and TSPA-SR. Some key distributions for use in the volcanic eruption model are

conduit diameter, duration and volume of individual explosive phases during formation of a volcano, and mean ash particle size erupted during violent strombolian phases.

- *Number of Waste Packages [WPs] Hit by Igneous Intrusion (CAL-WIS-PA-000001)* – Develops a probabilistic measure for the number of WPs contained within an eruptive conduit of a specified diameter, given that a dike has intersected the drift and that the conduit(s) is located at a drift(s).
- *Miscellaneous Waste-Form FEPs (ANL-WIS-MD-000009)* – Provides estimates of particle-size (waste particle diameter) distributions for unaltered SNF exposed to a potential magmatic event through the repository. The estimates are based on investigations and data generated at the Argonne National Laboratory.
- *Igneous Consequence Modeling for the TSPA-SR (ANL-WIS-MD-000017)* – Summarizes the conceptual model and model parameters taken from the AMRs and calculation referred to above for use in TSPA modeling of a volcanic eruption. Volcanic eruptive release is described as an event that results in waste-entraining ash being ejected from Yucca Mountain and transported by an eruptive plume to a critical group downwind of the repository. A major task of this AMR is the preparation, through parameter development, of inputs to the ASHPLUME code that runs within the TSPA to model the dispersal and fallout characteristics of ash and radionuclides entrained in an eruptive plume from a volcano.

Figure 1-1, Volcanic Eruption Model Information Flow, shows how the AMRs and the calculation interact in defining the overall volcanic eruption model and the subsequent feed to the TSPA. This figure emphasizes the logical flow of information from the results of the expert elicitation reported in the PVHA and the scientific literature to the AMRs and the calculation, and finally to the development of appropriate distributions for inclusion in the TSPA-SR. Documents inside the dashed rectangles are not part of the disruptive events set of supporting AMRs. The biosphere elements shown inside the double-dashed rectangles are addressed in the companion white paper on the Biosphere Model.

### **1.3 Volcanic Eruption Model Structure**

Figure 1-2, Volcanic Eruption Model Structure Diagram, depicts the various elements that comprise the volcanic eruption model. The relationships of the elements of the conceptual and representational models, the different model parameters, and the modeling results are indicated in the figure. Figure 1-2 includes the TSPA abstraction of results as the end product of the model development in the AMRs. The analysis of volcanism in the TSPA is a fully probabilistic treatment of consequences with the volcanic eruption release analysis included in the GoldSim code, the integrating code for TSPA analysis. The dose from releases due to volcanism is treated as part of the expected annual dose by combining the probability-weighted sum of the dose due to volcanic sources and the nominal dose.

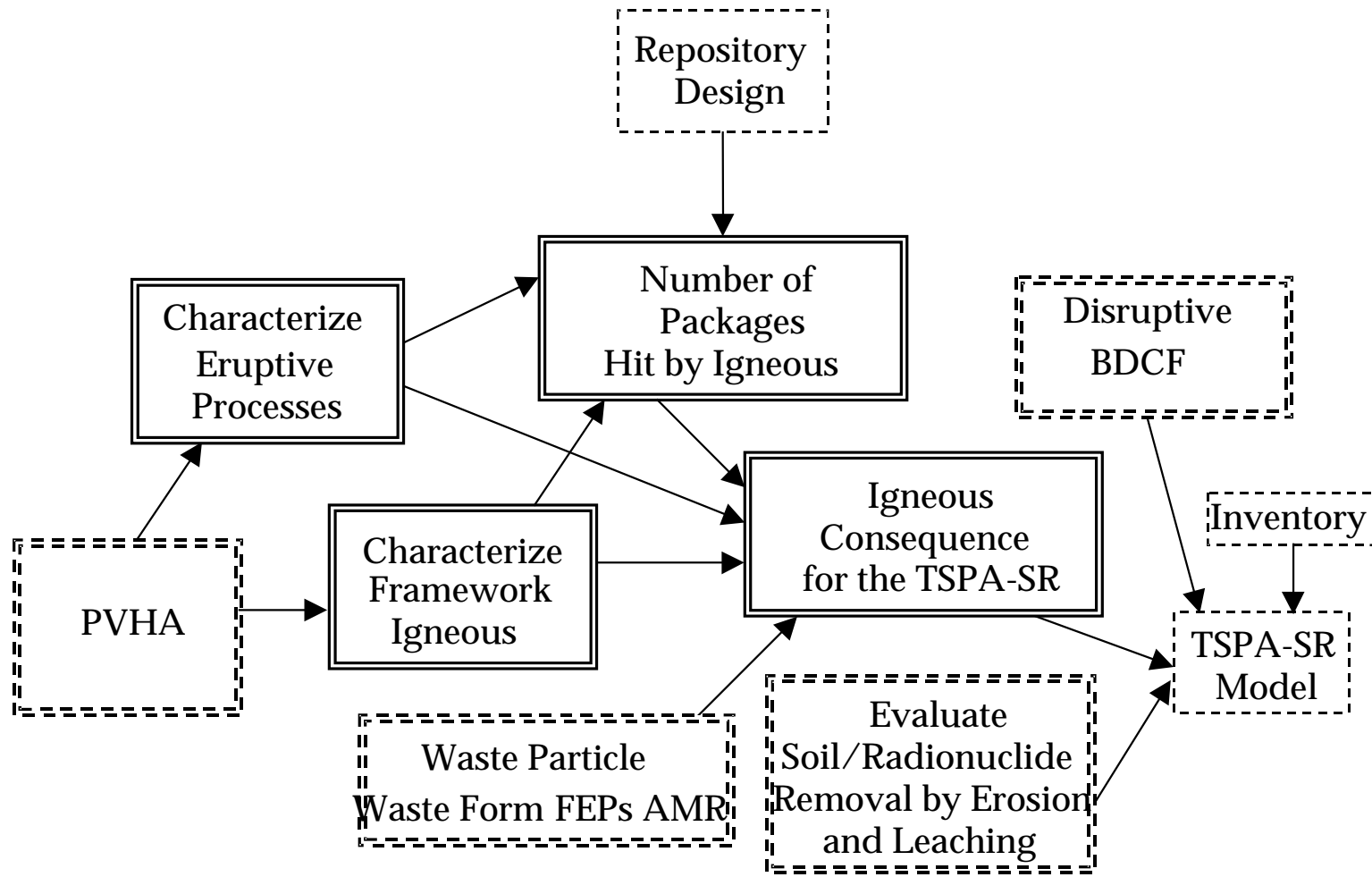


Figure 1-1: Volcanic Eruption Model Information Flow

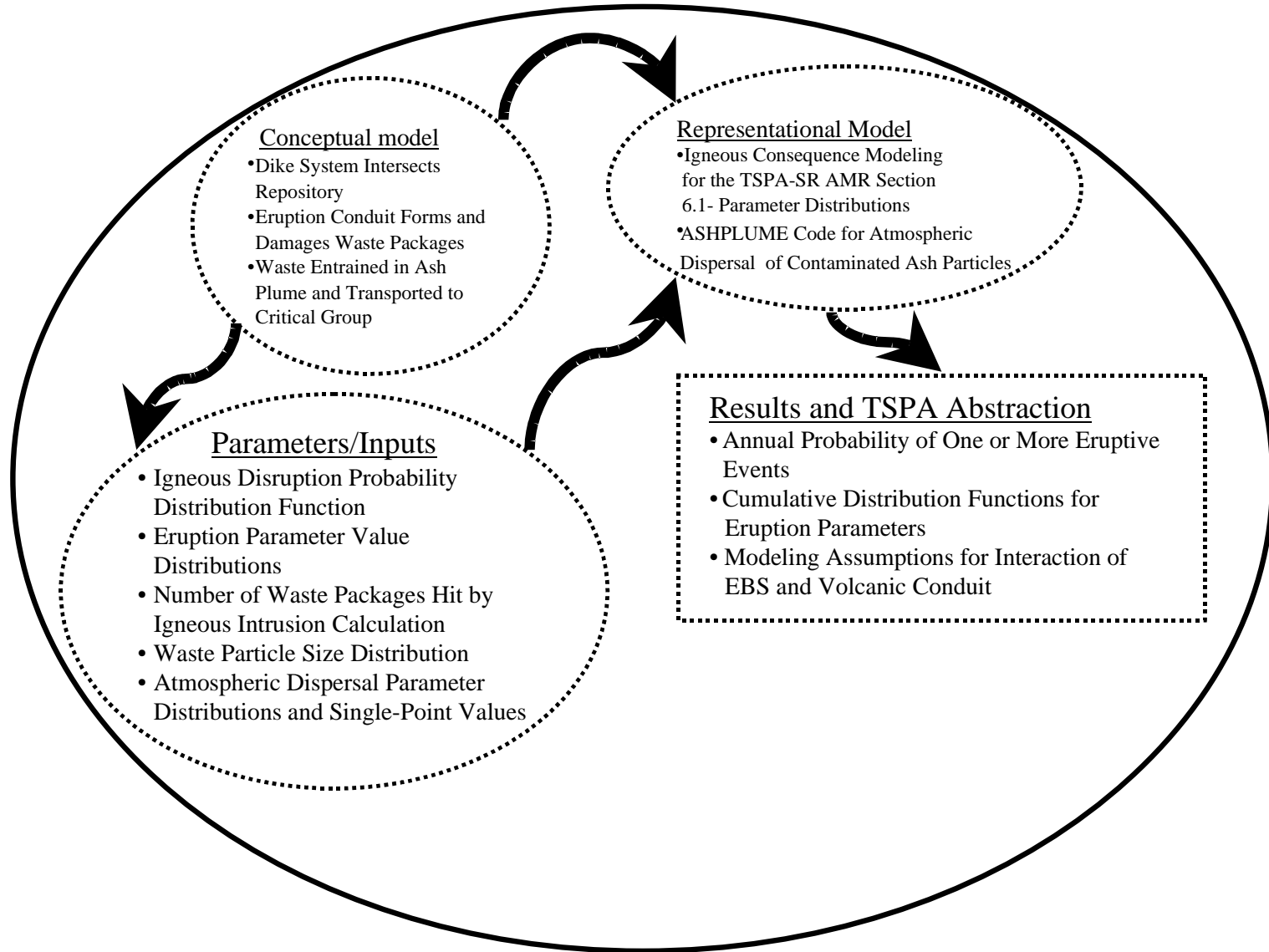


Figure 1-2: Volcanic Eruption Model Structure Diagram

## **A. Conceptual Model**

The components of the volcanic eruption model are summarized in Section 3.1 of the *Disruptive Events* PMR. In the conceptual model for volcanic eruption an igneous dike rises to the repository level and intersects one or more drifts in the repository. An eruptive conduit forms somewhere along the dike as it nears the surface, feeding a volcanic vent at the surface. WPs in the path of the conduit are assumed to be sufficiently damaged that they provide no further protection, and the waste is available to be entrained in the eruptive plume. Volcanic ash is contaminated, erupted, and then transported by wind toward the critical group. Ash settles out of the plume as it is transported downwind, resulting in an ash layer on the land surface. Members of the critical group receive a radiation dose from various pathways associated with the contaminated ash layer, including inhalation and ingestion.

The subsurface components of the volcanic eruption model are treated in the AMRs *Characterize Framework for Igneous Activity at Yucca Mountain, Nevada*, and *Characterize Eruptive Processes at Yucca Mountain, Nevada* and the calculation *Number of Waste Packages Hit by Igneous Intrusion*. Information about the probability of eruptive conduits forming within the potential repository, eruption characteristics, and the response of components of the engineered barrier system to an eruption are used to develop a distribution of parameter values characterizing uncertainty in the extent of damage to WPs and the amount of waste available to be entrained in the eruption. The AMR *Characterize Framework for Igneous Activity at Yucca Mountain, Nevada* includes a comprehensive summary of alternative spatial and temporal models of igneous activity in the Yucca Mountain region and how these models were incorporated (weighted) in the PVHA expert elicitation. This AMR also includes a detailed description of the methods used to develop probability distributions for the length and orientation of volcanic dikes within the repository footprint and for the number of eruptive centers (conduits) located within the footprint, conditional on a dike intersection.

## **B. Representational Model**

Entrainment of waste particles in the volcanic eruption (ash) and the atmospheric transport and settling of the combined waste-ash particles downwind are modeled using the ASHPLUME code. This code is a mathematical implementation of an atmospheric dispersal model first proposed in the early 1980s and subsequently modified by the Center for Nuclear Waste Regulatory Analyses to allow for coupling of waste particles to ash particles. The ASHPLUME code is discussed in Section 6.1 of the *Igneous Consequence Modeling for the TSPA-SR* AMR. Two models, PUFF and a gas-thrust model, were evaluated as possible alternatives to ASHPLUME in this AMR. These alternative models were not pursued because of the lack of a working code in the case of PUFF and certain key similarities to ASHPLUME in the case of the gas-thrust model. The gas-thrust model is discussed in the NRC Issue Resolution Status Report Key Technical Issue: Igneous Activity, Rev. 2, July 1999.

## **C. Parameters**

Parameters necessary for the volcanic eruption model in the TSPA are developed in the disruptive events AMRs and the calculation and summarized in Section 3.1 of the *Disruptive*

*Events* PMR. The AMRs and the calculation document the bases of the parameter values (single-point and distributions), in particular noting when conservative single values are used and where conservative assumptions form the basis for probabilistic inputs. The parameters used in the PA are listed in Table 3.10-4 of the TSPA-SR. As noted in this table, the parameters cover several modeling areas including the probability of a volcanic eruption, the eruption characteristics, the response of the repository components to an eruption, and the downwind atmospheric transport of contaminated ash particles in an ash plume.

## **D. Results**

The AMR *Igneous Consequence Modeling for the TSPA-SR* integrates information from the supporting AMRs and the calculation and develops parameter values, single-point and distributions, for subsequent consequence analyses in TSPA. Section 5 of this AMR identifies assumptions that are necessary for the formulation of the conceptual model and the associated parameters. The parameter values are addressed in Section 6.1 of the AMR. Information on high altitude winds in the Yucca Mountain region taken from project reports and waste particle-size (diameter) distributions from the *Miscellaneous Waste Form FEPs* AMR are introduced. Section 3.1 of the *Disruptive Events* PMR documents the parameter information from all the supporting AMRs and the calculation that are used for consequence modeling of the volcanic eruption in the TSPA-SR.

### **1.4 Discussion of Uncertainty Treatment**

The uncertainties associated with the volcanic eruption model fall into three general categories: uncertainties associated with the volcanic framework of the Yucca Mountain region; uncertainties associated with the effects of the interaction of magmatic activity with repository components; and uncertainties associated with the entrainment of waste in an eruptive plume and atmospheric transport to a critical group.

#### **A. Conceptual Model for the Volcanic Framework**

The AMR *Characterize Framework for Igneous Activity at Yucca Mountain, Nevada* describes the conceptual framework for igneous activity in the Yucca Mountain region based on the volcanic and tectonic history of the region as assessed by the experts who participated in the PVHA. Conceptual models presented in the PVHA are summarized and extended in areas in which new information has been obtained. A key objective of this AMR was the development of revised probability distributions, starting with the results of the PVHA, for the length and orientation of volcanic dikes within the repository footprint and for the number of eruptive centers located within the current repository footprint (conditional on the dike intersecting the repository). A large section of the AMR (i.e., 6.5.2.2) is devoted to a rigorous treatment of the number of eruptive conduits located within the repository footprint, conditional on a dike intersection. Table 13 in Section 7 of the AMR (Rev. 00 ICN 00) summarizes the mean and the 5<sup>th</sup> and 95<sup>th</sup> percentile values of the distribution for the annual frequency of occurrence of one or more eruptive centers within the repository footprint

The results of the PVHA expert elicitation were a set of alternative spatial and temporal models for assessing the volcanic hazard at Yucca Mountain, probabilities that each model is the appropriate model, and probability distribution functions for the parameters of the models. As such, the PVHA defines the scientific uncertainty in applying models to assess the volcanic hazard. The bases for the experts' assessments of the validity of the alternative models are documented in the PVHA (CRWMS M&O 1996). The PVHA results indicated that the statistical uncertainty in estimating the event rate was the largest component of intra-expert uncertainty (i.e., about 40 percent of the total intra-expert uncertainty). The next largest uncertainty was uncertainty in the appropriate spatial model. Other important spatial uncertainties included the spatial smoothing distance, Gaussian field parameters, zonation models, and event lengths. The temporal issues of importance included the time period of interest, event counts at a particular center, and the number of hidden events.

An important point that is noted in the PVHA report is that the experts were asked to consider the future 10,000-year period as the time period of interest for the hazard assessment. During the course of the PVHA, consideration was given to the manner in which changes might occur in the estimates of the annual frequency (probability) of intersection if they were assessed for a longer time period (e.g., 1,000,000 years). However, no formal assessments of occurrence rates or frequencies were conducted for time periods longer than 10,000 years as part of the PVHA. Results of an igneous disruption, presented in Sections 4 (e.g., Figure 4.2-1) and 5 (Figure 5.2-17 through 5.2-23) of TSPA-SR refer to time periods up to 50,000 years or more. Uncertainty that may be introduced by extrapolating results of the PVHA assessed by assuming a 10,000-year period of interest is not discussed.

## **B. Magmatic Interaction with Repository–Parameter Uncertainty**

Conditional joint probability distributions for the length and azimuth of an intersecting dike and the number of eruptive centers within the potential repository footprint for the repository configurations of Enhanced Design Alternatives II (Primary Block and Primary + Contingency Block) are derived in Sections 6.5.1.2 and 6.5.1.3, respectively, of the AMR *Characterize Framework for Igneous Activity at Yucca Mountain, Nevada*. The probability distributions are based on the results (outputs) from the PVHA expert elicitations and include rigorous uncertainty analyses. The probability distributions are input to the calculation *Number of Waste Packages Hit by Igneous Intrusion* and the AMR *Igneous Consequence Modeling for the TSPA-SR*.

The AMR *Characterize Eruptive Processes at Yucca Mountain, Nevada* discusses information about volcanic systems (Lathrop Wells and modern analogs) and the parameters that can be used to model their behavior. This information is used to develop parameter-value distributions, based on associated uncertainties, appropriate for analysis of the consequences of a volcanic eruption through the repository. Where possible, parameter distributions are based on data, typically from analog volcanoes as in the case of ash particle properties, or models available in the scientific literature. In cases for which there are relatively sparse published data, parameter distributions are suggested that conservatively capture the expected range.

One of the key assumptions in this AMR is that data from analog sites (volcanoes) are appropriate for providing a basis for estimating probability distributions related to the

dimensions (e.g., conduit diameter) and geometry (e.g., dike widths and number of dikes) of volcanic plumbing for the formation of a new volcano in the Yucca Mountain region. The basis for this assumption is that direct data on the plumbing of Quaternary basaltic volcanoes in the Yucca Mountain region are extremely limited, so either theoretical estimates or data from analog sites must be used. Theoretical estimates are not as reliable as analog data because there are no generally accepted theories that account for all the complexities of magma intrusion at shallow depth.

The objective of the calculation *Number of Waste Packages Hit by Igneous Intrusion* is to develop a probabilistic measure of the number of WPs that could be affected by a volcanic eruption. In this scenario, the number of WPs destroyed by a volcanic eruption is the calculated number of WPs contained within an eruptive conduit of a specified diameter. Several simplifications, which are noted as such in the text, concern the intersection of a drift or drifts by one or more conduits. The first simplification is that when one conduit intersects a drift, in whole or in part, the conduit is assumed to be centered within the drift and all WPs within the conduits are assumed to be destroyed. A second simplification is that when the diameter of one conduit is greater than 75 m and it intersects two drifts, the number of WPs destroyed is twice the number of packages destroyed in the first drift. When multiple conduits occur within the repository footprint, all conduits are assumed to have the same diameter and to be centered on drifts. The text of the calculation points out that these simplifications lead to conservative estimates of the number of WPs affected by an eruption.

As for the behavior of WPs, it is assumed that only those WPs located partially or entirely within the area of the eruptive conduit contribute to the radionuclide source term for the volcanic release scenario. The number of WPs within an eruptive conduit is a function of conduit diameter, WP length, and inter-package spacing.

### **C. Uncertainty Associated with Waste Entrainment and Atmospheric Transport**

The conceptual model for a volcanic eruption through the repository is developed and documented in the *Igneous Consequence Modeling for the TSPA-SR* AMR. This AMR summarizes either single-point values or uncertainty distributions for the parameters of the volcanic eruption model as feeds to the TSPA-SR.

There are several assumptions regarding the nature of an igneous event, the behavior of WPs and other components of the EBS in an eruptive conduit, and the input parameters to the ASHPLUME code that introduce conservatism to the model. The AMR authors state that the assumptions are conservative because they represent the worst possible consequences. It is recognized as conservative to assume the complete failure of the WPs, drip shields, and waste form in an eruptive conduit.

The same argument is invoked to justify the conservative assumptions involving the nature of the volcanic event (i.e., all eruptions include a violent strombolian phase). Observations of both modern and past analog volcanoes indicate that the violent phases account for only a portion of the total eruption, but available data do not support quantification of the ratio of violent to nonviolent phases in potential future eruptions at Yucca Mountain. This leads to a follow-on

assumption that the entire volume of erupted material in analog volcanoes is ejected during a violent phase, which is spelled out more explicitly in Section 3.10.2.2.1 of the TSPA-SR. The analog volcanoes considered include some volcanoes that are considerably larger than any of the Quaternary volcanoes in the Yucca Mountain region. The volume distribution assumed includes values up to 0.44 km<sup>3</sup>, approximately the entire estimated eruption volume for all the Quaternary volcanoes in the Yucca Mountain region (see Section 6.2, Page 34, of the AMR *Characterize Framework for Igneous Activity at Yucca Mountain, Nevada*). There is no discussion of the potential impact of such a conservative assumption on the consequence modeling in the *Igneous Consequence Modeling for the TSPA-SR* AMR.

A separate issue with the large eruptive volumes has to do with the wind speed information used in the ASHPLUME code. In the current version of ASHPLUME, the heights of the ash plume columns are calculated using the estimates of total eruption volume. In Section 5.2.9.5 of the TSPA-SR, the 95<sup>th</sup> percentile value for the volume of material erupted corresponds to a volume of approximately 0.34 km<sup>3</sup>, with a corresponding eruption column height of about 5 km above the ground surface. The wind speed and direction data introduced in the *Igneous Consequence Modeling for the TSPA-SR* AMR are for the Yucca Flat station and only go up to an altitude of approximately 3.7 km above the ground surface. Thus, while the sensitivity analysis reported in Section 5.2.9.5 of the TSPA-SR indicates that the total annual igneous dose rate is insensitive to the range of values for the eruptive volume, it remains to be seen what the results would be if higher altitude wind data (e.g., possibly from the Desert Rock Airstrip) are incorporated in the modeling.

Section 6.1 of this AMR discusses the atmospheric dispersal model implemented in the ASHPLUME code and describes the input parameters to the code. Two of the parameters used in ASHPLUME are assumed to take on single-point values with minimal discussion about the appropriateness of the assumed values. The parameters are: the incorporation ratio and the constant relating eddy diffusivity and particle fall time. The incorporation ratio, defined as the common logarithm of the ratio of the minimum ash particle size to the waste particle size, controls the extent to which waste particles are entrained in the eruptive column of ash. The single-point value assumed, 0.3, results in waste particles with diameters up to one-half the size of ash particle diameters being entrained in the eruption. Information on waste particle diameters is taken from the AMR *Miscellaneous Waste-Form FEPs*. While there is no discussion about the uncertainty in the value of the incorporation ratio, the results of a sensitivity analysis reported in Section 5.2.9.11 of the TSPA-SR indicate that the annual eruptive dose rate is relatively insensitive to uncertainty in this parameter. The annual eruptive dose rate increased by a negligible factor for an incorporation ratio of 0.1 and decreased by less than a factor of 2 for an incorporation ratio of 1.0.

Section 3.10.4 of the TSPA-SR discusses the role that conservative assumptions about transition-phase biosphere dose conversion factors (BDCFs) and fixed wind direction to the south play in compensating for uncertainty regarding surficial processes that might move contaminated ash from its initial point of deposition to the location of the receptor. Surficial processes include resuspension in wind or sediment transport in Forty-Mile Wash. The *Igneous Consequence Modeling for the TSPA-SR* AMR should discuss how the conservative assumption regarding

fixed wind direction to the south addresses these processes and take credit for consideration of alternative transport mechanisms.

## **D. Results**

As discussed in Section III.D, the AMR *Igneous Consequence Modeling for the TSPA-SR* integrates and develops model parameter distributions and single point values for subsequent use in TSPA. Discussions on the incorporation of uncertainty in the majority of parameter distributions are, in general, well documented. One area of possible concern, however, is that the cumulative, or compounding, effect of conservative assumptions and distributions adopted in the consequence model development and the impact of uncertainty associated with certain single point parameter values on the resultant TSPA calculations of releases associated with a volcanic eruption are not discussed. Referring to the fact that sensitivity studies will be performed in the TSPA for some of the more important assumptions and parameters could mitigate some of these concerns.

### **1.5 Uncertainty Propagation**

#### **A. Process Model**

As discussed in Section III.D, the AMR *Igneous Consequence Modeling for the TSPA-SR* summarizes information on the conceptual model and model parameters developed in the upstream AMRs. Attachment I to the *Igneous Consequence Modeling for the TSPA-SR* AMR lists a complete tabulation of the parameter distributions to be used in TSPA. As noted in the AMR, the distributions are intended to capture the range of values (e.g., volcanic conduit diameter, eruptive volume) based on data from volcanoes in the Yucca Mountain region or modern analogs. In the absence of data, conservative modeling assumptions about the behavior of the engineered barrier components are employed. The *Disruptive Events Process Model Report* summarizes conceptual models and the technical product output that form part of the technical basis for the TSPA. Traceability of model components and of model parameters is completely addressed in a series of tables in Section 3 of the PMR.

#### **B. Abstraction Model and Use in TSPA**

Table 3.10-4 in Section 3.10.2.2 of the TSPA-SR lists the abstracted parameters and parameter distributions that are incorporated in the volcanic eruption model. The parameter values (distributions or point values) are grouped according to the process model factors: probability of a volcanic eruption; eruption characteristics; repository response to an eruption; and atmospheric transport of contaminated ash.

Section 3.10.4 of the TSPA-SR discusses the treatment of uncertainty in TSPA for the volcanic eruption model. Uncertainty regarding the probability and consequences of future igneous events at Yucca Mountain is incorporated into the TSPA through several approaches. In many cases, uncertainty is included through the use of parameter distributions that allow a range of values to be used in the simulations. In several cases involving the consequence modeling, where data are insufficient to support realistic models or a defensible distribution of parameter values about a

best-estimate value, the TSPA-SR relies on conservative assumptions that provide a measure of confidence that the analysis does not underestimate the impact of the phenomenon being modeled. As noted in Section 3.10.4 of the TSPA-SR, it is generally not possible to quantify the impacts of the conservatisms. Examples of bounding assumptions occur in the treatment of the response of the WPs to igneous disruption. The assumption that all WPs in the direct path of an eruptive conduit are sufficiently damaged that they provide no further protection for the waste is an example of an assumption that is surely bounding (damage to these packages can be no greater than this), but data are not available to support a more realistic model. Were such data hypothetically available, they might show that uncertainty regarding actual conditions should include a range of WP responses, perhaps including some continued protection for the waste form. In the absence of such data, the TSPA-SR simply adopts the bounding endpoint of the unknown distribution. These bounding assumptions are consistent with the model validation philosophy adopted in Section 6.3.3 of the *Igneous Consequence Modeling for the TSPA-SR* AMR. One of the criteria used to evaluate the validity of a conceptual model is that a conceptual model is valid if it is shown to be conservative with respect to the overall performance of the system in response to igneous disruption.

## **1.6 Conclusions**

The volcanic eruption model comprises model elements with varying amounts of available information. This accounts for the different approaches that are adopted in the treatment of uncertainty in the AMRs and, subsequently, in the TSPA simulations.

Three general categories of uncertainty were outlined in Section IV. The first of these has to do with uncertainty in the conceptual model for the volcanic framework in the Yucca Mountain region. The PVHA expert elicitation provided a rigorously defined probability distribution function for the annual frequency of intersection of the repository footprint by a dike. The experts explicitly considered uncertainty in current understanding of volcanic processes and regional geology in making their estimates. The analysis took into account both spatial and temporal variability, and the resulting distribution of event probabilities reflects the full range of uncertainty expressed by the experts. The AMR *Characterize Framework for Igneous Activity at Yucca Mountain, Nevada* developed revised probability distributions, starting with the results of the PVHA, for the length and orientation of volcanic dikes within the repository footprint and for the number of eruptive centers located within the repository footprint, conditional on the dike intersecting the repository. The handoff of these results to downstream AMRs is fully documented in Section 3.1 of the *Disruptive Events* PMR. A summary discussion of the uncertainty in the probability of igneous disruption of the repository is given in Section 3.10.4 of the TSPA-SR.

The second general category of uncertainty involves the volcanic eruption characteristics and the response of the repository to a volcanic eruption. Parameter distributions were derived for eruption characteristics (e.g., conduit diameter, dike width, number of dikes associated with the formation of a volcano, water content of magmas, magma temperatures, and mean particle size erupted during the violent strombolian phase) based on observations of volcanoes in the Yucca Mountain region and, in large part, information in the literature on modern analogs. The

information researched represents the best available and is well documented in the appropriate AMR, PMR, and the TSPA.

Conservative assumptions and simplifications were employed to model the interaction of the repository contents and an eruptive conduit. Conduits intersecting a drift in whole or in part were assumed to be centered on the drift thereby maximizing the number of WPs hit. All WPs hit were assumed to be sufficiently damaged so that the contents were available for entrainment in the eruptive column. While the simplifications and assumptions made in this part of the model are discussed in the appropriate AMRs, the PMR, and the TSPA-SR, there is no discussion of the possible cumulative effect of the simplifications and assumptions on the resultant dose rates calculated for the eruptive release model.

The final category of uncertainty has to do with the modeling of waste entrainment and atmospheric transport downwind to the critical group. While distributions are developed for most of the key parameters (e.g., waste particle size, ash dispersion controlling constant), single-point values are assumed for other key parameters, with little or no discussion regarding the uncertainty in these parameters. Some of these concerns could be mitigated by referring to the fact that sensitivity studies will be performed in the TSPA for some of the apparently more important parameters.

A summary discussion of uncertainties associated with the conceptual model, representational model, and model parameters is given in the attached table. The discussion includes how, where, and why particular uncertainties are treated within the set of Disruptive Events documents and the potential impact of the uncertainties in the TSPA.

**Table 1-1: Volcanic Eruption Release Model**

Model Purpose: The purpose of the Volcanic Eruption Release Model is to provide a basis for both the characterization of uncertainty in the probability of a volcanic eruption in the potential repository and the consequences of an eruption for use in TSPA.				
Summary	Source	Treatment	Basis	Impact
<b>Conceptual Model Uncertainty</b>				
Repository footprint Intersected by a basaltic dike.	Section 6.3 of the AMR Characterize <i>Framework for Igneous Activity at Yucca Mountain, Nevada (ANL-MGR-GS 000001, Rev 00)</i> discusses the Expert elicitation process that was Conducted in the PVHA. Emphasis in the PVHA was Placed on identifying and Understanding the uncertainty Introduced by the consideration of Alternative spatial and temporal Models of volcanism.	As discussed in Section 6.5.1.1 of the AMR Characterize Framework for Igneous Activity at Yucca Mountain, Nevada, each of the 10 PVHA experts quantified the uncertainties in their estimates of the disruption Probability by developing a set of alternative probability models and model parameters for the hazard calculation. Each of the experts' models was developed in a logic tree format that explicitly incorporates the uncertainty in selecting appropriate probabilistic models and model parameters to describe the spatial and temporal occurrence of future volcanic events in the vicinity of the potential Yucca Mountain repository site and to describe the geometry (length and azimuth) of basaltic dikes associated with these events. A combined or aggregate distribution for the annual frequency of intersection of the repository footprint by a dike was developed using equal weighting of the hazard model results of each expert.	The PVHA hazard model represents the randomness inherent in the occurrence of volcanic events. In the hazard assessment, the experts were confronted with considerable uncertainty in selecting the appropriate models and model parameters arising from limited data and/or alternative interpretations of the available data. This is best exemplified by the observation that most of the aggregate hazard arises from the uncertainty that an individual expert has in interpreting the available data rather than from differences between the experts' interpretations.	The aggregate probability distribution function, revised for changes in the repository footprint, is summarized in Section 7 of the AMR Characterize <i>Framework for Igneous Activity at Yucca Mountain, Nevada</i> . The probability function captures the modeling uncertainty introduced by the experts and this uncertainty is included in the probability-weighted consequences calculated in the TSPA.

<p>Conditional distribution for the number of eruptive centers within the potential repository footprint.</p>	<p>Sections 6.2 and 6.3.2 of the AMR <i>Characterize Framework for Igneous Activity at Yucca Mountain, Nevada</i>, discuss the characteristics of vulcanism in the YMR and the evidence from analog volcanoes pertaining to intrusive versus extrusive events.</p>	<p>The consequences of volcanic eruption within the repository footprint requires an evaluation of the conditional distribution for the number of eruptive centers that occur within the potential repository footprint given that there is an intersection by a dike associated with a volcanic event. Evaluation of this distribution requires an assessment of the number of eruptive centers along the length of the dike. An assessment of the number of eruptive centers was made by the experts as part of the PVHA. These assessments, together with the characteristics of Quaternary volcanoes in the YMR and a limited number of conservative assumptions (Section 5 of the AMR <i>Characterize Framework for Igneous Activity at Yucca Mountain, Nevada</i>), are used to derive empirical distributions for the number of eruptive centers per volcanic event. A very detailed description of the derivation, implementation, and results of the calculations are given in Section 6.5 of the AMR <i>Characterize Framework for Igneous Activity at Yucca Mountain, Nevada</i>.</p>	<p>The PVHA hazard model represents the randomness inherent in the occurrence of volcanic events. In the hazard assessment, the experts were confronted with considerable uncertainty in selecting the appropriate models and model parameters arising from limited data and/or alternative interpretations of the available data. Additional uncertainty arises from conservative modeling assumptions regarding the number and locations of eruptive centers along an intrusive dike.</p>	<p>The probability distribution function for the annual frequency of occurrence of one or more eruptive centers within the potential repository incorporates the modeling uncertainty quantified in the PVHA and the conservatisms introduced as a result of modeling assumptions about the number and locations of eruptive centers along an intrusive dike. The combined uncertainties are included in the probability-weighted consequences of a volcanic eruption calculated in the TSPA.</p>
<p>Behavior of components of the EBS in an eruptive conduit.</p>	<p>Assumptions regarding the behavior of WPs, waste form, and drip shields in an eruptive conduit are discussed in Section 5.3 of the AMR <i>Igneous Consequence Modeling for the TSPA-SR</i>.</p>	<p>Any components of the EBS that are partially or completely intersected by an eruptive conduit are conservatively assumed to be fully destroyed and any waste within WPs is assumed to be available to be entrained in the eruption.</p>	<p>The discussion in Section 5.3 of the <i>Igneous Consequence</i> AMR notes that alternative, and less bounding, conceptual models for the behavior of EBS components could be proposed but data are not available to support such models.</p>	<p>The potential impact of the conservative assumptions on the TSPA is not discussed in the AMR <i>Igneous Consequence Modeling for the TSPA-SR</i>, but is addressed in a sensitivity study described in Section 5.2.9.6 of the TSPA-SR.</p>

<b>Representational Model Uncertainty</b>				
ASHPLUME code for atmospheric dispersal of contaminated ash particles.	Sections 5.4 and 6.1 of the AMR <i>Igneous Consequence Modeling for the TSPA-SR</i> discusses the ASHPLUME code, some of its limitations, and input parameters. Section 6.1 also includes a brief discussion of possible alternative models, PUFF described in the literature and a gas-thrust model proposed in the Igneous Activity Issues Resolution Status Report Rev. 2.	Single-point values and distributions for the <i>input</i> parameters are introduced in Section 6.1.1 of the AMR <i>Igneous Consequence Modeling for the TSPA-SR</i> . There is little, or no, discussion about the uncertainty regarding several of the single-point parameter values.	The basis for the uncertainty in some of the parameter distributions (e.g., waste particle diameter, ash mean particle diameter) is discussed in Section 6.1.1 of the <i>Igneous Consequence AMR</i> . However, no basis is provided for single-point parameter values that on first read appear to be key to the model (e.g., incorporation ratio).	The sampling of parameter distributions in the TSPA is mentioned in the <i>Igneous Consequence AMR</i> . There is no discussion of the how the impact of single-point parameter values will be addressed.
<b>Parameter Uncertainty</b>				
Conduit Diameter	AMR <i>Characterize Eruptive Processes at Yucca Mountain, Nevada (ANL-MGR-GS-000002, Rev 00)</i> - Source of information on conduit diameter is analog volcanoes as described in Section 6.1 of the AMR.	A log normal distribution with a minimum <i>diameter</i> equal to dike width, a median diameter of 50 meters, and a maximum value of 150 meters is recommended to conservatively capture possible range of conduit diameters for a potential volcanic event at Yucca Mountain.	Data on conduit diameters based on indirect evidence (i.e., volume of shallow wall-rock xenoliths erupted) from Lathrop Wells and analog volcanoes. No direct measurements available for volcanoes in the immediate vicinity of Yucca Mountain.	The impact of the larger conduit diameters is discussed in the calculation <i>Number of Waste Packages Hit by Igneous Intrusion</i> , Sections 3.11, 312, 3.13, and 6.1.
Event eruptive volume	The range for the event eruptive Volume is based on information from Section 6.2 of the AMR <i>Characterize Framework for Igneous Activity at Yucca Mountain, Nevada</i> , and the Igneous Activity IRSR, Rev 2, Table 3, Page 129.	A log-uniform distribution that spans the range 0.002 - 0.44 cubic km is adopted in Section 6.1.2.1 of the AMR <i>Igneous Consequence Modeling for the TSPA-SR</i> .	Eruptive volume estimates for volcanoes in the YMR based on USGS 75topographic maps and estimates of tephra fall:cone and cone:lava volume-ratios based on comparison with ratios determined for relatively young, well-preserved, basaltic analog volcanoes. Cone volumes for several of the Quaternary volcanoes in the YMR are adjusted for estimates of erosion.	No discussion in the AMR <i>Igneous Consequence Modeling for the TSPA-SR</i> , sensitivity study performed in the TSPA-SR, Section 5.2.9.5 - need appropriate high altitude wind data before drawing conclusions about the impact of the uncertainty expressed in the volume distribution range.

Ash particle mean diameter	Section 6.5.1 of the AMR <i>Characterize Eruptive Processes at Yucca Mountain, Nevada</i> .	A log triangular distribution is defined for the ash mean particle diameter with a minimum value of 0.001 cm, a mode of 0.01 cm, and a maximum of 0.1 cm in the <i>Eruptive Processes</i> AMR.	The suggested distribution is based on available information from modern analog volcanoes. The fact that there is very little data available is discussed in the AMR <i>Characterize Eruptive Processes at Yucca Mountain, Nevada</i> .	Indirectly addressed in the discussion on the incorporatio ratio in Section 5.4.1 of the <i>Igneous Consequence Modeling for the TSPA-SR</i> AMR and in the sensitivity study in Section 5.2.9,11 of the TSPA-SR.
Waste particle diameter	Attachment I to the AMR <i>Miscellaneous Waste-Form FEPs</i> and Section 6.1.1.13 of the <i>Igneous Consequence Modeling for the TSPA-SR</i> AMR.	A log triangular distribution is defined for the waste particle diameter with a minimum value of 0.0001 cm, a mode of 0.002 cm, and a maximum of 0.05 cm in Section 6.1.1,13 of the <i>Igneous Consequence</i> AMR.	The distribution is based on laboratory observations of particle sizes of unaltered spent nuclear fuel following mechanical grinding. The data were collected at the Argonne National Laboratory.	Indirectly addressed in the discussion on the incorporatio ratio in Section 5.4.1 of the <i>Igneous Consequence Modeling for the TSPA-SR</i> AMR and in the sensitivity study in Section 5.2.9.11 of the TSPA-SR.

## 2.0 Igneous Disruption Model–Igneous Intrusion Groundwater Release Model

### 2.1 Purpose of the Model

The purpose of the igneous intrusion groundwater release model is to estimate the amount of waste that would be available for groundwater transport through the UZ and SZ as a result of a dike or system of dikes intersecting the repository footprint and magma interacting with the WPs and other components of the EBS in the repository drifts. An important aspect of this model is that groundwater and radionuclide transport away from WPs damaged by igneous intrusion is calculated within the TSPA model using the nominal UZ/SZ models, and doses to humans from contaminated groundwater are determined in TSPA using nominal BDCFs. The use of the nominal models and BDCFs implies that the uncertainties associated with these models as described in the companion white papers will apply here, as well.

The information feeds from upstream AMRs to downstream AMRs; the *Disruptive Events* PMR and the TSPA-SR are clearly identified and tracked in each of the documents. In particular, conservative (bounding) assumptions regarding the interaction of magma and repository components are identified and discussed in detail. In cases where more information is available, distributions, which capture the uncertainty in model parameters, are developed in the AMRs and are clearly traceable to the TSPA-SR.

The AMRs reviewed are for the backfill design. While modeling assumptions for the no backfill design may differ from the backfill design, the uncertainty treatment is expected to be similar to the treatment in the AMRs referred to in the following.

### 2.2 Model Component Documentation

The *Disruptive Events* PMR (TDR-NBS-MD-000002) and its associated AMRs comprise the documentation of the igneous intrusion model. There are also two calculations that support the intrusion model. The purpose of the PMR, AMRs, and the calculations are:

- *Disruptive Events* PMR (TDR-NBS-MD-000002) – Summarizes the conceptual model and the technical product output that form part of the technical basis for the TSPA.
- *Characterize Framework for Igneous Activity at Yucca Mountain, Nevada* (ANL-MGR-GS-000001) – 1) Presents a conceptual framework of igneous activity in the YMR consistent with the volcanic and tectonic history of the region and the assessment of this history by experts who participated in the PVHA (CRWMS M&O 1996); and 2) develops probability calculations needed for TSPA based on PVHA inputs and revised to be consistent with the current repository design; included are probability distributions for the length and orientation of volcanic dikes within the repository footprint and for the number of eruptive centers (conduits) located within the footprint, conditional on a dike intersection.

- *Characterize Eruptive Processes at Yucca Mountain, Nevada* (ANL-MGR-GS-000002) – Presents information about natural volcanic systems and the parameters that can be used to model their behavior. This information is used to develop parameter-value distributions appropriate for analysis of the consequences of an igneous disruption of the repository.
- *Dike Propagation Near Drifts* (ANL-WIS-MD-000015) – Develops elementary analyses of the interactions and consequences of a hypothetical dike with a repository drift and with the drift contents including: WPs, drip shields, and backfill. A subsequent ICN to this AMR considers the no backfill case.
- *Number of Waste Packages Hit by Igneous Intrusion* (CAL-WIS-PA-000001) – Calculates the number of WPs damaged by an igneous intrusion (dike) that intersects the repository but does not necessarily result in an eruption. This number reflects the number of WPs in the drifts that have been damaged in situ by magma.
- *Waste Package Behavior in Magma* (CAL-EBS-ME-000002) – Determines the structural performance of WPs (containing commercial SNF [CSNF]) due to internal pressurization as a consequence of increased WP temperature resulting from direct contact with magma flow during igneous events.
- *Igneous Consequence Modeling for the TSPA-SR* (ANL-WIS-MD-000017) – Develops a conceptual model and model parameters taken from the AMRs and calculations referred to above for use in TSPA modeling of an igneous intrusion.

Figure 2-1, *Igneous Intrusion Model Information Flow*, shows how the AMRs and the two calculations interact in defining the overall igneous intrusion model and the feed to the TSPA. Documents inside the dashed rectangles are not part of the disruptive events set of supporting AMRs. This figure emphasizes the logical flow of information from the AMRs and the calculations to the development of appropriate distributions for inclusion in the TSPA-SR. As noted in Section I, but not indicated on this figure, the nominal UZ/SZ flow and transport models are employed in TSPA to model the groundwater transport of radionuclides from the WPs damaged by an igneous intrusion. Additionally, doses to humans from contaminated groundwater are determined in TSPA using nominal BDCFs.

### **2.3 Igneous Intrusion Model Structure**

Figure 2-2, *Igneous Intrusion Groundwater Release Model Structure*, depicts the various elements that comprise the igneous intrusion groundwater release model. The relationships of the elements of the conceptual model, the model parameters, and the modeling results are indicated in the figure. Figure 2-2 includes the TSPA abstraction of results as the end product of the model development in the AMRs.

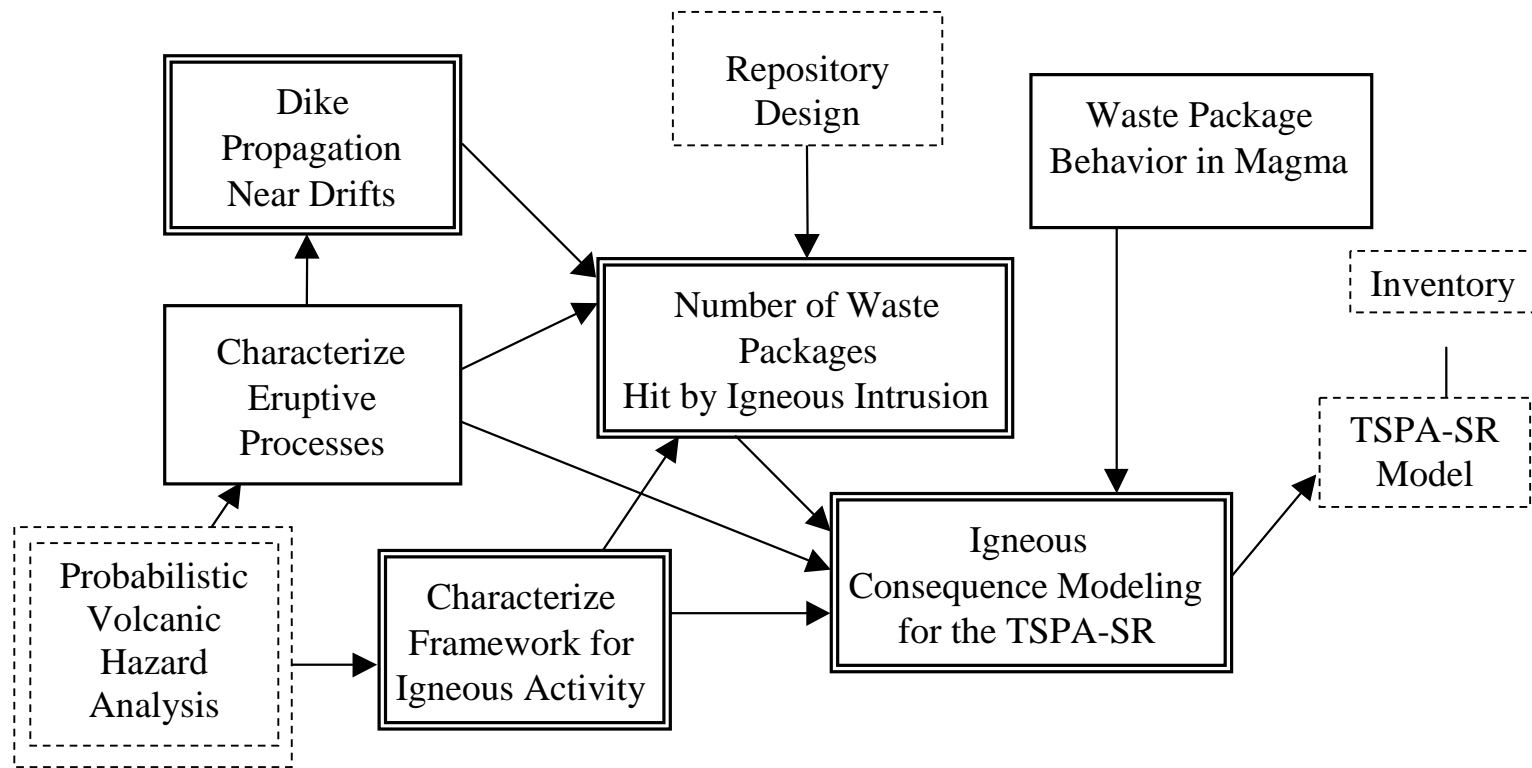


Figure 2-1: Igneous Intrusion Model Information Flow

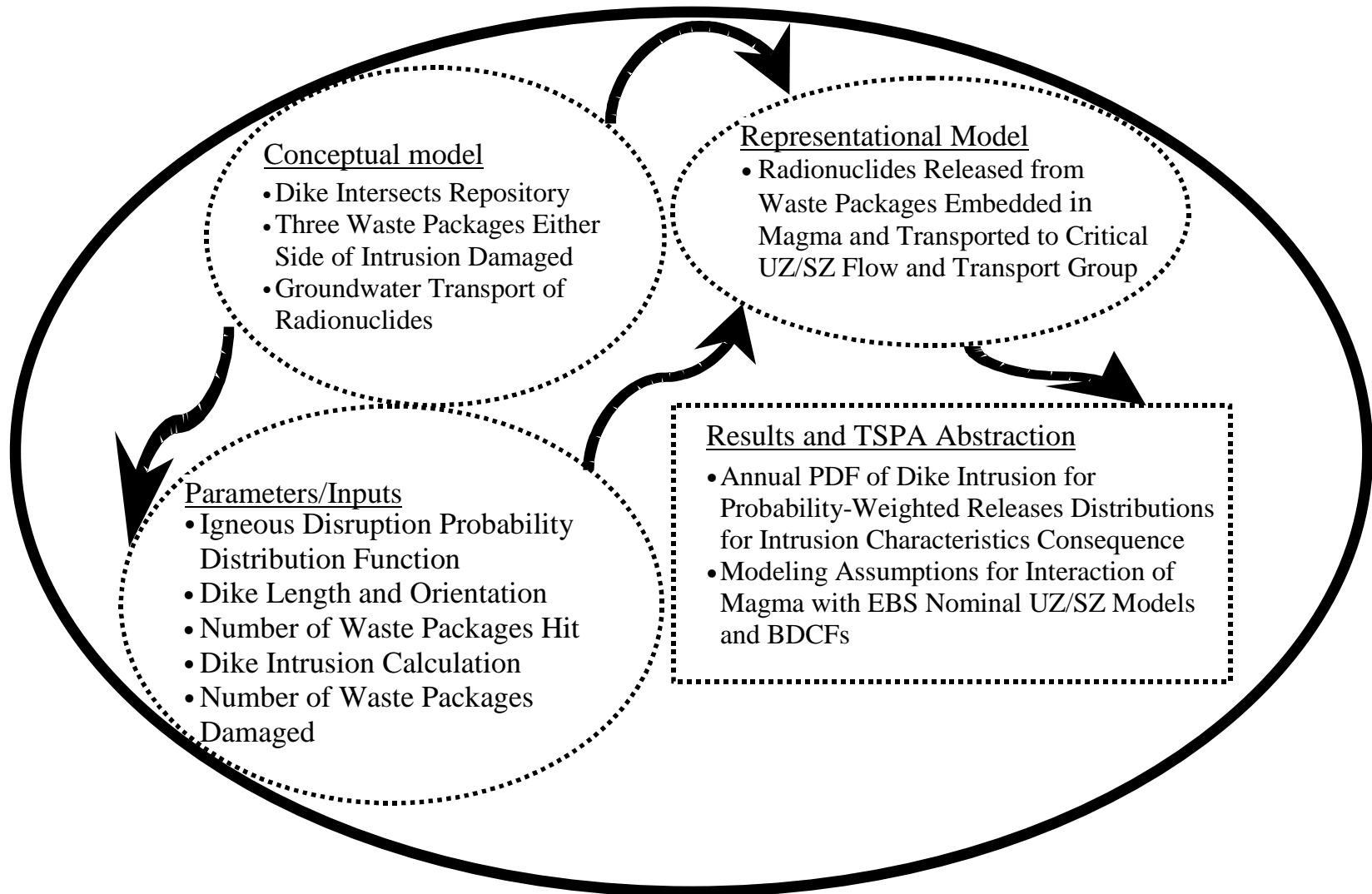


Figure 2-2: Igneous Intrusion Groundwater Release Model Structure

## **A. Conceptual Model**

The igneous intrusion groundwater release model is summarized in Section 3.1 of the *Disruptive Events* PMR. In the conceptual model, a dike, or dike system, rises to the repository level and intersects one or more drifts in the repository. As the magma enters the drifts it undergoes explosive fragmentation into pyroclasts. Damage to the WPs immediately adjacent to the point of intrusion is likely to be extensive. Magma flow down any given drift is limited to a few WP lengths by plugging from crumpled drip shields and displaced backfill. Thus, several WPs on either side of the point of intrusion are engulfed in magma, initially at a temperature in the range 1100 to 1200 degrees centigrade. Groundwater transport away from damaged WPs is calculated using the nominal scenario performance models and model parameters for UZ/SZ flow and transport of radionuclides. Doses to humans from contaminated groundwater are determined using nominal BDCFs. Recent changes in the design (i.e., the removal of backfill) have resulted in changes to some of the *Disruptive Events* AMRs. These changes will be addressed in future updates to the AMRs.

There are three main components to the igneous intrusion model. The first component consists of the assumptions regarding the behavior of WPs and other elements of the EBS that have been damaged as a result of proximity to an igneous intrusion. The second component is the calculation of the number of WPs damaged. The third component of the model is the set of assumptions regarding the use of nominal models for groundwater flow and radionuclide transport away from the WPs to the biosphere.

## **B. Parameters**

There is no separate set of computational models used in the TSPA to simulate the consequences of igneous intrusion. Instead, the igneous intrusion groundwater release model consists of a set of process model factors and associated input parameters used to define a modified source term for input to the nominal flow and transport models. The process model factors include the probability of igneous intrusion, the intrusion characteristics, and the repository response to igneous intrusion. The input probability distribution function (PDF) and parameter distributions include:

- The annual probability of igneous intrusion
- The number of dikes per event and dike width distribution
- The number of packages damaged on either side of a dike in each intersected drift, the percent of damaged packages that fail, and the total number of packages damaged depending on how many drifts are intersected

These inputs are developed in the four AMRs and two calculations introduced in Section II.

## C. Results

Section 6.2 of the *Igneous Consequence Modeling for the TSPA-SR* AMR pulls together the information on the input parameters for the igneous intrusion modeling and develops distributions (e.g., the cumulative distribution function for event probability) for subsequent use in the TSPA. No consequence calculations are performed in this AMR. Table 3.10-5 in TSPA-SR summarizes the parameters, the type of distribution for each parameter, and the actual distributions or single point values.

### 2.4 Discussion of Uncertainty Treatment

The uncertainties associated with the igneous intrusion groundwater release model fall into two general categories: uncertainties associated with the probability and characteristics of a dike intrusion in the YMR; and uncertainties associated with the response of the EBS to intrusion of magma. In general, uncertainty in the former category is based on data and described in the appropriate AMRs. Uncertainties in the latter category, however, are not quantified. Conservative assumptions are made in the absence of information that might support a less conservative (i.e., more representative) case.

As noted in Section III.A, the TSPA-SR model for radionuclide mobilization and transport away from WPs that have been damaged by igneous intrusion uses the nominal UZ/SZ flow and transport models, and doses to humans from contaminated groundwater are determined using nominal BDCFs. The uncertainties associated with these nominal models are discussed in the companion white papers on the UZ/SZ flow and transport and biosphere models.

#### A. Uncertainties Associated with Volcanic Processes

The AMR *Characterize Framework for Igneous Activity at Yucca Mountain, Nevada* describes the conceptual framework for igneous activity in the YMR based on the volcanic and tectonic history of the region as assessed by experts who participated in the PVHA. Conceptual models presented in the PVHA are summarized and extended in areas in which new information has been obtained. A key objective of this AMR was the development of revised probability distributions, starting with the results of the PVHA, for the length and orientation of volcanic dikes within the repository footprint and for the number of eruptive centers located within the current repository footprint (conditional on the dike intersecting the repository).

The results of the PVHA expert elicitation were a set of alternative spatial and temporal models for assessing the volcanic hazard at Yucca Mountain, probabilities that each model is the appropriate model, and probability distribution functions for the parameters of the models. As such, the PVHA defines the scientific uncertainty in applying models to assess the volcanic hazard. The bases for the experts' assessments of the validity of the alternative models are documented in the PVHA (CRWMS M&O 1996). The PVHA results indicated that the statistical uncertainty in estimating the event rate was the largest component of intra-expert uncertainty (i.e., about 40% of the total intra-expert uncertainty). The next largest uncertainty was uncertainty in the appropriate spatial model. Other important spatial uncertainties included the spatial smoothing distance, Gaussian field parameters, zonation models, and event lengths.

The temporal issues of importance included the time period of interest, event counts at a particular center, and the number of hidden events.

An important point that is noted in the PVHA report is that the experts were asked to consider the future 10,000-year period as the time period of interest for the hazard assessment. During the course of the PVHA, consideration was given to the manner in which changes might occur in the estimates of the annual frequency (probability) of intersection if they were assessed for a longer time period (e.g., 1,000,000 years). However, no formal assessments of occurrence rates or frequencies were conducted for time periods longer than 10,000 years as part of the PVHA. Results of an igneous disruption, presented in Sections 4 (e.g., Figure 4.2-1) and 5 (Figure 5.2-17 through 5.2-23) of TSPA-SR refer to time periods up to 50,000 years or more. Uncertainty that may be introduced by extrapolating results of the PVHA assessed by assuming a 10,000-year period of interest is not discussed.

The AMR *Characterize Eruptive Processes at Yucca Mountain, Nevada* discusses information about volcanic systems (Lathrop Wells and modern analogs) and the parameters that can be used to model their behavior. This information is used to develop parameter-value distributions, based on associated uncertainties, appropriate for analysis of the consequences of an igneous intrusion into the repository. Where possible, parameter distributions are based on data or models available in the scientific literature. In cases for which there are insufficient published data, AMR authors use parameter distributions that they believe conservatively capture the expected range of parameter values. Of particular importance to the igneous intrusion model are the distributions developed for the number of dikes associated with the formation of a volcano and the dike width(s), magma temperature and temperature data summarized in this AMR for basaltic intrusions.

One of the key assumptions in this AMR is that data from analog sites (volcanoes) are appropriate for providing a basis for estimating probability distributions related to the dimensions and geometry (e.g., dike widths and orientation of dikes) of volcanic plumbing for the formation of a new volcano in the YMR. The basis for this assumption is that direct data on the plumbing of Quaternary basaltic volcanoes in the YMR are extremely limited, so either theoretical estimates or data from analog sites must be used. Theoretical estimates are not as reliable as analog data because there are no generally accepted theories that account for all the complexities of magma intrusion at shallow depth.

## **B. Uncertainties Associated with Repository Response to Intrusion**

The purpose of the AMR *Dike Propagation Near Drifts* was to develop analyses for the interactions of a hypothetical igneous dike with a repository drift and with the drift contents. This analysis addresses a long-standing problem in understanding the nature of possible volcanic disruption of a drift, or set of drifts, in a repository. The scope of the analysis for the AMR was to conceptualize the problems and to provide bounding concepts and parameter values from literature research for some of the processes involved. The problem is approached piecemeal by examining end members or limiting cases of processes that can be modeled. The results are simplified because the fundamental processes producing the volcanic intrusion and the

subsequent interaction of the intrusive dike with the repository and the repository contents are not well understood.

The objective of the calculation *Number of Waste Packages Hit by Igneous Intrusion* is to develop a probabilistic measure of the number of WPs that could be affected by an igneous intrusion. The calculations are based on results from the PVHA, as presented in the AMR *Characterize Framework for Igneous Activity at Yucca Mountain, Nevada*, and include information on the geometry of a dike system relative to the current footprint of the repository.

The temperatures of WPs that could be engulfed in magma were analyzed to improve the conceptual model of the behavior of WPs in a magmatic environment. Comparison of the WP temperatures to results of the calculation *Waste Package Behavior in Magma* indicates that the WPs would be very near failure condition if temperature and internal pressure due to fuel rod rupture were considered. The scope of the document is limited to reporting the calculation results in terms of maximum stresses in WP shells as a function of remaining wall thickness. The authors of the AMR note that information on the tensile strengths of the WP materials are only available up to temperatures of 871 °C for the inner shell material and 760 °C for the outer shell material. Expected magma temperatures of 1100 to 1200 °C require extrapolation of the available information and introduce uncertainty in the results of the calculation. A conclusion from the calculation (Section 6, Page 8) is that the WP design can barely withstand an internal pressure load at 1200 °C even in its original configuration (i.e., no degradation of wall thickness).

The conceptual model for an igneous intrusive groundwater transport release is developed and documented in the *Igneous Consequence Modeling for the TSPA-SR* AMR. The input parameters for the igneous intrusion model are obtained from the AMRs and calculations discussed above.

There are several assumptions regarding the nature of an igneous event and the behavior of WPs and other components of the engineered barrier system that are considered conservative. For example, any WPs, drip shields, and other components of the EBS that are partially or completely intersected by an intrusive dike are assumed to be fully destroyed. In this AMR, it is pointed out that the conservative model is used because there is no technical basis for choosing any other model. However, further analyses of the behavior of the WP in a magmatic environment and modeling of water flow and radionuclide transport in the drift following magmatic disruption have the potential to support less conservative and more representative assumptions.

Another assumption concerns the behavior of the waste in proximity to an igneous intrusion. It is assumed that all waste material in WPs (three packages on either side of the intrusion) will be available for incorporation in the UZ transport model, dependent on the solubility limits and the availability of water. No credit is taken for possible water diversion by remnants of the drip shield or WP, and cladding is assumed to be fully degraded. This conservative assumption was chosen to bound the uncertainty associated with conditions in a drift in the magmatic environment.

## 2.5 Uncertainty Propagation and Conclusions

The AMRs and calculations discussed in the previous section clearly define the model component (i.e., parameter distributions) feeds from upstream documents to downstream documents and finally to the TSPA-SR. Additionally, conservative modeling assumptions are clearly defined in Section 6.2 of the AMR *Igneous Consequence Modeling for the TSPA-SR* and summarized in the *Disruptive Events* PMR and in Sections 3.10.2 and 3.10.4 of the TSPA-SR. The modeling approach adopted is to use conservative assumptions in the consequence analysis where data are unavailable or insufficient to support implementation of more realistic models.

An example of a bounding assumption concerns the response of WPs to an igneous intrusion. The assumption that the three WPs on either side of an intrusive dike and the one package intersected by the dike are sufficiently damaged that they provide no further protection to the waste provides a bound to the performance of those packages. In this case, damage is unlikely to be as severe as that suffered by the packages directly in the path of an eruption, and a more realistic distribution would likely include some continued protection of the waste form. The assumption made in the TSPA-SR provides a bound for the performance of these packages.

In general, it is not possible to quantify the degree of the conservatism; if data were available to quantify the impact, a more realistic assumption would have been used. One approach employed in the TSPA-SR to gain insight into the sensitivity of overall performance to uncertainty about the potential repository response to igneous intrusion is through sensitivity studies. The results of the sensitivity analysis in Section 5.2.9.1 of the TSPA-SR indicate that overall repository performance is most sensitive to the annual probability of igneous intrusion. A comparison of the probability-weighted mean annual igneous intrusion dose rates calculated using the revised PDF discussed in Section IV.A of this report with a fixed value of  $10^{-7}$  indicates that the peak mean dose is increased by approximately a factor of 10 using the higher  $10^{-7}$  fixed value. The highest peak mean dose rate (0.9 mrem/yr) occurs at the end of the TSPA simulation, 20,000 years after closure and remains well below the regulatory limit.

A summary discussion of uncertainties associated with the conceptual model and model parameters is given in the attached table. The discussion includes how, where, and why particular uncertainties are treated within the set of Disruptive Events documents and the potential impact of the uncertainties in the TSPA.

**Table 2-1: Igneous Intrusion Model**

Model Purpose: The purpose of the igneous intrusion model is to estimate the amount of waste that would be available for groundwater transport through the UZ and SZ as a result of a dike or dike system intersecting the repository and interacting with the drift and components of the engineered barrier system.				
Summary	Source	Treatment	Basis	Impact
<b>Conceptual Model Uncertainty</b>				
Repository footprint intersected by a basaltic dike.	Section 6.3 of the AMR <i>Characterize Framework for Igneous Activity at Yucca Mountain, Nevada</i> (ANL-MGR-GS-000001, Rev 00) discusses the expert elicitation process that was conducted in the PVHA. Emphasis in the PVHA was placed on identifying and understanding the uncertainty introduced by the consideration of alternative spatial and temporal models of volcanism.	As discussed in Section 6.5.1.1 of the AMR <i>Characterize Framework for Igneous Activity at Yucca Mountain, Nevada</i> , each of the 10 PVHA experts quantified the uncertainties in their estimates of the disruption probability by developing a set of alternative probability models and model parameters for the hazard calculation. Each of the experts' models was developed in a logic tree format that explicitly incorporates the uncertainty in selecting appropriate probabilistic models and model parameters to describe the spatial and temporal occurrence of future volcanic events in the vicinity of the potential Yucca Mountain repository site and to describe the geometry (length and azimuth) of basaltic dikes associated with these events. A combined or aggregate distribution for the annual frequency of intersection of the repository footprint by a dike was developed using equal weighting of the hazard model results of each expert.	The PVHA hazard model represents the randomness inherent in the occurrence of volcanic events. In the hazard assessment, the experts were confronted with considerable uncertainty in selecting the appropriate models and model parameters arising from limited data and/or alternative interpretations of the available data. This is best exemplified by the observation that most of the uncertainty in the aggregate hazard arises from the uncertainty that an individual expert has in interpreting the available data rather than from differences between the experts' interpretations.	The aggregate probability distribution function, revised for changes in the repository footprint, is summarized in Section 7 of the AMR <i>Characterize Framework for Igneous Activity at Yucca Mountain, Nevada</i> . The probability function captures the modeling uncertainty introduced by the experts and this uncertainty is included in the probability-weighted consequences calculated in the TSPA.

<p>Dike interaction with repository drift and drift components</p>	<p>Summarized in Section 3.1.3 of the <i>Disruptive Events</i> PMR; discussed in detail in the <i>Dike Propagation Near Drifts</i> AMR; additional modeling assumptions in Sections 5.3.2 and 5.3.4 of the <i>Igneous Consequence Modeling for the TSPA-SR</i> AMR.</p>	<p>As noted in Section 6.1 of the <i>Dike Propagation Near Drifts</i> AMR, the problem of a dike interacting with a repository drift is not amenable to direct calculations of the interactions. Rather the problem is attacked piecemeal by examining end members or limiting cases of processes which can be modeled. End members (or bounding cases) are chosen by analysts because they provide an expeditious way to identify physically possible dike/drift interactions and the consequences of those interactions. A result of the modeling is the estimate that disruption of WPs caused by flow of magma from a dike intersection extends down the drift from the dike edge to 3 or possible 4 WPs. Additional modeling assumptions in the <i>Igneous Consequence</i> AMR, about the extent of damage to WPs (fully destroyed), are noted as being conservative.</p>	<p>Analyses of dike interaction with drifts based on extension of analyses and interpretations provided in the literature. Conservative assumptions regarding fully damaged WPs are based, in part, on the calculation <i>Waste Package Behavior in Magma</i>.</p>	<p>The assumption that all WPs affected by an igneous intrusion fail and provide no further protection for the waste results in an over-estimate of the amount of waste available for groundwater transport is acknowledged in the PMR and <i>Igneous Consequence</i> AMR. However, there is no discussion regarding quantification of the over-estimation in these documents. The impact on dose results is addressed in a sensitivity study in Section 5.2.9.7 of the TSPA-SR.</p>
<p><b>Representational Model Uncertainty</b></p>				
<p>As noted in Section 3.10.2.3 of the TSPA-SR, strictly speaking there is no separate set of computational models used in the TSPA to simulate the consequences of a dike intrusion into the repository. Instead, the igneous intrusion groundwater transport model consists of a set process model factors and associated input parameters used to define a modified source term for calculations using nominal flow and transport models.</p>				

<b>Parameter Uncertainty</b>				
Magmatic temperatures	Section 6.2.4 of the <i>Characterize Eruptive Processes at Yucca Mountain, Nevada</i> .	Range of temperatures as a function of water content for Lathrop Wells magmas developed in Table 4 of the <i>Characterize Eruptive Processes AMR</i> .	Temperature range based on a combination of direct field measurements and experimental values.	The high end of the temperature range (i.e., 1169 degrees centigrade) is close to the temperature range for failure of the WP noted in the calculation <i>Waste Package Behavior in Magma</i> . This observation is invoked to support the bounding assumption that all WPs engulfed in magma fail and the waste is available for subsequent groundwater transport.
Number of WPs hit by igneous intrusion.	Summarized in Section 3.1.4 of the <i>Disruptive Events PMR</i> and developed in detail in the calculation <i>Number of Waste Packages Hit by Igneous Intrusion</i> .	The calculation <i>Number of Waste Packages Hit by Igneous Intrusion</i> develops a probabilistic measure for the number of WPs in the drifts that have been contacted by magma, given that a dike has intersected the drifts. The probability of occurrence for the igneous intrusion scenario is expressed in terms of its component probabilities: the probability that a dike of some length and orientation occurs in the repository, and the probability that a dike intersects the repository footprint. Log normal distributions for dike widths and number of dikes associated with the formation of a new volcano are taken from the <i>AMR Characterize Eruptive Processes at Yucca Mountain, Nevada</i> . The number of packages hit for the dike width/number of dikes combination is then calculated as the weighted average over all the azimuth angles and dike lengths.	The component probabilities for dike length and orientation and for dike intersection are developed in the <i>AMR Characterize Framework for Igneous Activity at Yucca Mountain, Nevada</i> . The development is based on the results of the expert elicitation in the PVHA. The log normal distributions for the dike widths and number of dikes are based on observations of volcanoes in the YMR (e.g., Lathrop Wells and Paiute Ridge for number of dikes associated with a new volcano).	A cumulative distribution function for the number of packages hit by an intrusive event is developed in Section 6.2.4 of the <i>AMR Igneous Consequence Modeling for the TSPA-SR</i> . A sensitivity study in Section 5.2.9.7 of the <i>TSPA-SR</i> indicates that performance is only moderately sensitive to the total number of WPs damaged by intrusion.

## 3.0 Probabilistic Seismic Hazard Model

### 3.1 Purpose of the Model

The Probabilistic Seismic Hazard Analysis (PSHA) (Wong and Stepp 1998) model is summarized in Section 2.1.3 of the *Disruptive Events* PMR and Section 6 of the *Characterize Framework for Seismicity and Structural Deformation at Yucca Mountain, Nevada* AMR. Seismic hazards potentially affecting the Yucca Mountain site consist of vibratory ground motion (GM) and fault displacement. For the postclosure period, the PSHA provides the basis for seismic probability analyses to be used in the TSPA. The seismic hazard results obtained from the PSHA are used to evaluate whether future GMs or fault displacements contribute to any repository events that 1) occur with a probability greater than 1 in 10,000 in 10,000 years; and 2) have significant effects on overall performance. A repository event is considered to be the failure of a structure, system, or component (SSC) to perform its functional goal. In this context, a seismic event is the failure of an SSC to perform its functional goal under ground shaking or fault displacement loading during the postclosure period.

PSHA GM results also form the basis for identifying seismic design inputs for SSCs important to preclosure safety and waste isolation. Preclosure seismic issues, however, are not part of the scope of the *Disruptive Events* PMR and are not addressed in the following.

The PSHA results are based on evaluations of seismic source characteristics, fault displacement, and earthquake GMs that reflect interpretations of different scientific hypotheses and models using all the available data for the YMR. These interpretations include uncertainties because the available data are insufficient to resolve the different hypotheses and models. The approach adopted in the PSHA to evaluate scientific uncertainty was expert elicitation. Two panels of experts, a seismic source characterization and fault displacement panel of 18 experts, and a GM panel of seven experts, provided the assessments. Uncertainties are quantified using a logic tree approach in which different interpretations form different branches of a logic tree. Branches are given a weight depending on an expert's, or expert team's, evaluation that each branch is the correct interpretation based on all available information. Using this approach and a widely accepted probabilistic formulation of the hazard calculation, the uncertainties are propagated through the analysis. The final hazard results are presented as mean, median, and fractile hazard curves representing the total uncertainty in the input interpretations.

### 3.2 Model Component Documentation

Sections 2.2.3 and 3.2 of the *Disruptive Events* PMR summarize the flow of information from the disruptive events AMRs to output for the TSPA-SR or as input to support screening decisions for seismicity and structural deformation FEPs. A brief description of the PMR and AMRs follows.

- *Disruptive Events* PMR (TDR-NBS-MD-000002) – Summarizes the objectives and methodology used in the PSHA to assess both GM and fault displacement hazards for the potential repository at Yucca Mountain. The PMR gives an overview of the primary activities involved in the PSHA including: 1) characterization of seismic sources; 2)

characterization of GM attenuation; and 3) probabilistic hazard curves for GM and fault displacement. The PMR also discusses the relationships of the supporting AMRs and the feeds to the TSPA-SR.

- *Characterize Framework for Seismicity and Structural Deformation at Yucca Mountain, Nevada* (ANL-CRW-GS-000003) – Summarizes the processes and results of the PSHA expert elicitation project that produced hazard curves for vibratory GM and fault displacement at the potential repository. The AMR also summarizes aspects of the geologic framework significant to the seismotectonics of the YMR. The role of this report is to provide summary level information to support understanding of the tectonic framework supporting disruptive events analyses and to provide a roadmap to the PSHA.
- *Effects of Fault Displacement on Emplacement Drifts* (ANL-EBS-GE-000004) – Evaluates the potential effects of fault displacement on emplacement drifts, including drip shields and WPs. The magnitude of fault displacement analyzed corresponds to an annual frequency of exceedance of  $10^{-5}$  – computed in the PSHA. Results of this analysis are used to support screening arguments for the AMR *Disruptive Events FEPs* for faulting FEPs.
- *Fault Displacement Effects on Transport in the Unsaturated Zone* (ANL-NBS-HS-000020) – Evaluates the potential for changes to the hydrogeologic system caused by fault displacement to affect radionuclide transport in the UZ at Yucca Mountain. The focus is on two possible bounding cases: 1) uniform changes in fracture properties throughout the UZ flow model domain (fault zones and fractured rock); and 2) change in fracture properties limited to fault zones. This evaluation used the bounding case estimates to determine if fault displacement.
- FEPs can be excluded from consideration with respect to UZ transport in TSPA modeling.
- *Features, Events, and Processes: Disruptive Events* (ANL-WIS-MD-000005) – Documents screening analyses for each of 21 primary FEPs relating to disruptive events. Many of the screening analyses depend on results from the PSHA for vibratory GM and fault displacements and on analyses carried out in the two AMRs dealing with fault displacement effects on emplacement drifts and on transport in the UZ. Fuel-rod cladding failure due to vibratory GM is the only seismic FEP included in the TSPA nominal scenario.

Figure 3-1, Seismic Hazard Model Information Flow, shows the feeds from the PSHA to the FEPs database and the disruptive events AMRs. The PSHA results play a key role in screening analyses for FEPs dealing with the interaction of seismic GM and fault displacement with components of the EBS. Support from AMRs performed outside of the disruptive events group is illustrated within the dashed boxes.

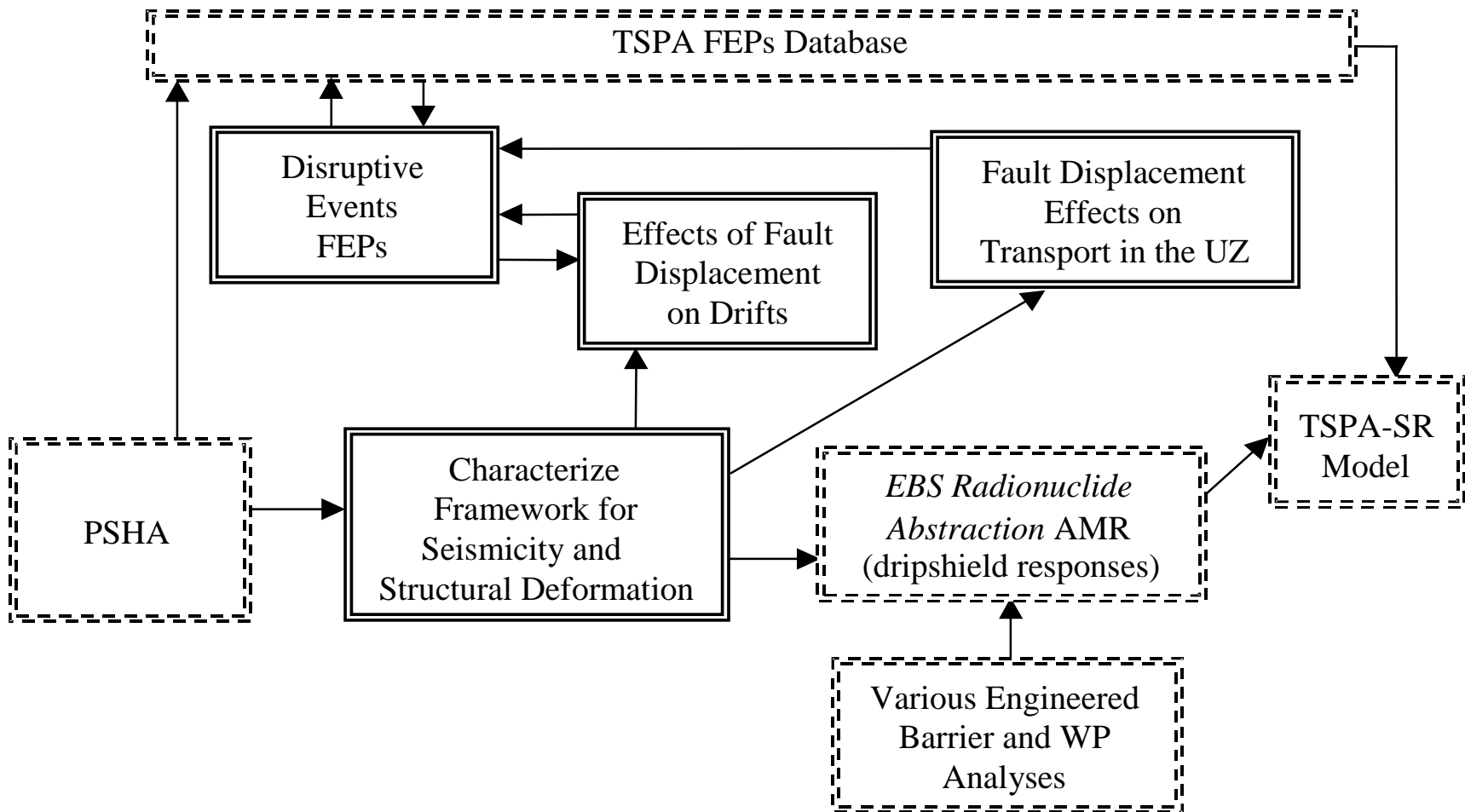


Figure 3-1: Seismic Hazard Model Information Flow

### **3.3 Seismic Hazard Model Structure**

Figure 3-2, Seismic Hazard Model Structure Diagram, depicts the various elements that comprise the seismic hazard model. The relationship of the elements of the conceptual and representational models, the model parameters, and the modeling results are indicated in the figure. Figure 3-2 indicates the abstraction of results in the TSPA as 1) screening analyses for seismic related FEPs; and 2) cladding failure resulting from seismic GM included in the nominal TSPA scenario.

#### **A. Conceptual Model**

##### **Vibratory GM**

The components of the seismic hazard model are discussed in detail in Section 6 of the AMR *Characterize Framework for Seismicity and Structural Deformation at Yucca Mountain, Nevada*. The panel of 18 experts that addressed the GM conceptual model was divided into six teams of three members per team. Each of the three-member teams was chosen to include expertise in the geology, seismology, tectonics, and paleoseismology of Yucca Mountain and the Basin and Range Province. This expert panel is referred to as the seismic source and fault displacement (SSFD) panel.

In the case of vibratory GM there are two components of the model that the SSFD panel of experts considered:

- The geometry of seismic sources (faults and areal zones) that can produce earthquakes significant to GM hazard at the site of interest
- The mean annual rate of occurrence and magnitude distribution of earthquakes occurring on each source

Two basic types of seismic sources were evaluated and characterized by the SSFD experts: fault specific sources and areal seismic zones. Both local faults (within about 10 km) and regional faults were evaluated. Areal source zones were generally defined to represent zones of distributed seismicity not apparently associated with known specific surface faults. Table 5 in the AMR *Characterize Framework for Seismicity and Structural Deformation at Yucca Mountain, Nevada* provides an excellent summary of the key components of each of the six SSFD team's seismic source characterization model, including issues regarding alternative tectonic models and potential seismic sources.

Although tectonic models are not seismic sources per se in the PSHA, they are included because their evaluation was integral to the development of seismic source characterization models. Tectonic models provide the framework that can help define or constrain some seismic source parameters (discussed in a later section). Thus, alternative tectonic models and the uncertainty associated with the applicability of each model were an integral part of the seismic source characterization and the resulting uncertainty was fully captured in the PSHA results.

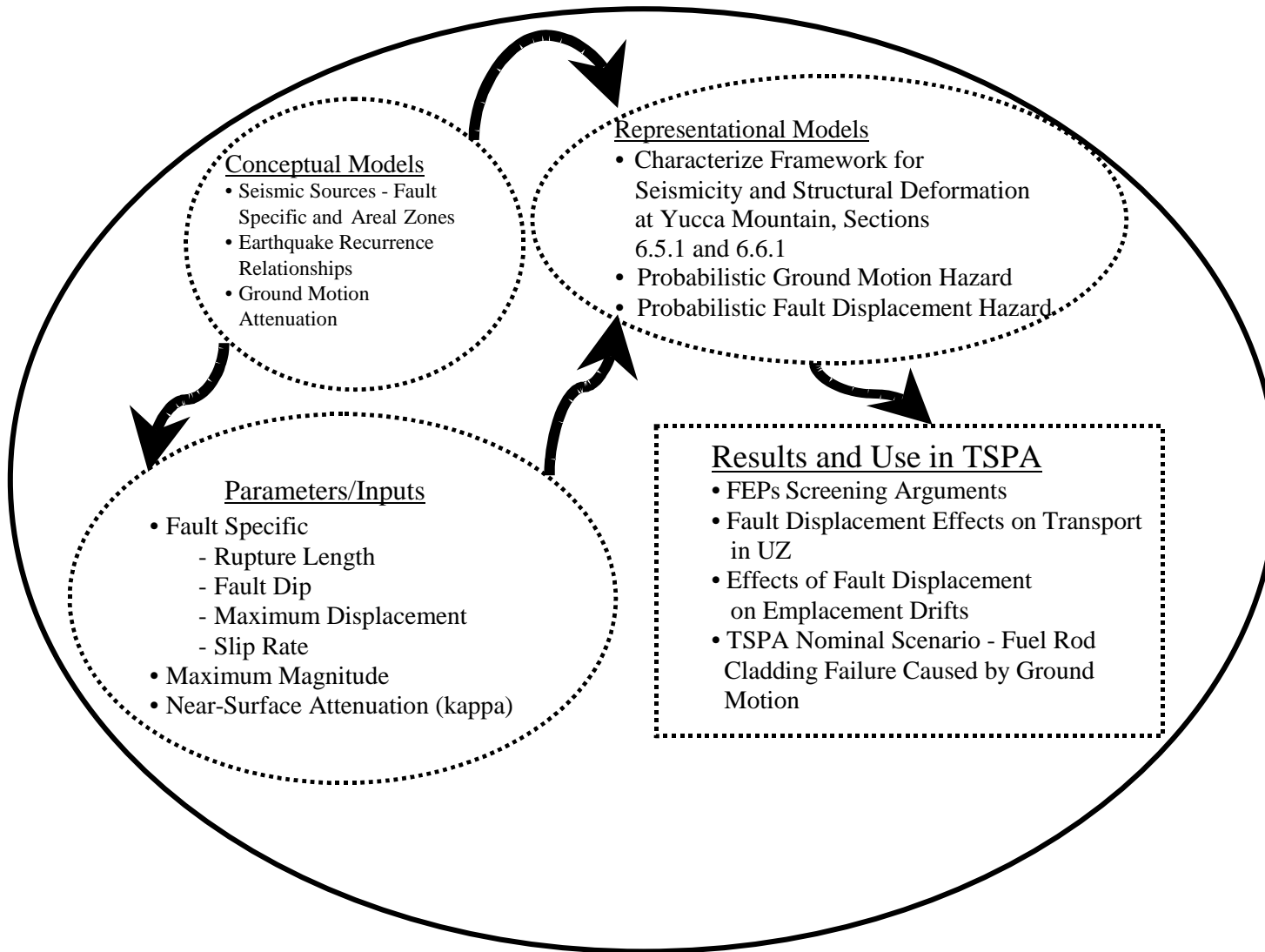


Figure 3-2: Seismic Hazard Model Structure Diagram

As noted in Section 6.3.2.4 of the *Characterize Framework* AMR, earthquake recurrence (including both recurrence models and assigned rates of activity) is one of the most significant elements of seismic source characterization for PSHA because it greatly influences what contributes most to the hazard. Earthquake recurrence relationships for a seismic source describe the frequency at which earthquakes of various magnitudes occur.

The experts used different approaches to determine the recurrence relationships for areal source zones and fault sources. In general, relationships for areal zones were determined based on the historical record of seismicity, while relationships for fault-specific sources were based on paleoseismic information. Within this general framework the SSFD teams considered several additional approaches to determine recurrence relationships for the different seismic sources (e.g., in the case of fault-specific sources, one approach involved estimating the frequency of large-magnitude surface-rupturing earthquakes on a fault of interest by dating of paleoearthquakes).

The approach to the characterization of GM attenuation, the third model component in Figure 3-2, employed by the seven members of the GM panel of experts is described in Section 6.3.3 of the AMR *Characterize Framework for Seismicity and Structural Deformation at Yucca Mountain, Nevada*. Predicting strong GMs at a site of interest is complicated by the dependence of GM on several factors for which there are very limited data for the YMR. The factors can be grouped into source, propagation path, and local site effects. A key issue with respect to characterizing GM attenuation in the YMR was the applicability of western U.S. (mainly California) attenuation models that are based on relatively large data sets, to the Basin and Range province. In their evaluations, the GM experts considered the possibility that significant differences may exist in the seismic source, regional crustal path, and shallow site properties for Yucca Mountain as compared to average source, path, and site properties represented in the western U.S. strong motion data set. Specifically, the GM experts examined whether, or to what degree, possible differences affect median GM estimates or variability in GMs expected at Yucca Mountain.

## **Fault Displacement**

Section 6.6 of the AMR *Characterize Framework for Seismicity and Structural Deformation at Yucca Mountain, Nevada* describes the methodology used to perform the PSHA calculations for fault displacement at Yucca Mountain. Table 9 in the AMR contains an excellent summary of the approaches adopted by the individual SSFD teams.

PSHA results for fault displacement are expressed in terms of the probability that the tectonically induced fault displacement at a given site will exceed a specified value. The site of interest may or may not be on an active fault. Results are in the form of fault displacement hazard curves, which show annual exceedance probability for different values of displacement.

Two approaches were employed in the PSHA for evaluation of the fault displacement hazard: an earthquake approach and a displacement approach. These two approaches are addressed in Sections 6.6.1.1–6.6.1.4 of the *Characterize Framework* AMR. The earthquake and displacement approaches developed by the SSFD experts represent original methodologies and are based primarily on empirical observations of faulting characteristics at Yucca Mountain and

in the Basin and Range province during past earthquakes (both historic and prehistoric). The empirical data were fit by statistical methods to quantify faulting parameters and their variability. The SSFD teams used these results to develop their approaches and to characterize the fault displacement potential at nine demonstration sites within the proposed repository area. These demonstration points ranged from locations on block-bounding faults to intact rock and allow for the possibility of principal faulting (e.g., on the Solitario Canyon, Bow Ridge, or possibly some of the intrablock faults) and distributed faulting at other points within the repository area.

## **B. Representational Models**

The methodologies used to calculate the probabilistic GM hazard and the fault displacement hazard are described in Sections 6.5.1 and 6.6.1 of the *Characterize Framework* AMR, respectively. The calculation for the GM hazard incorporates the model components discussed under Section A above. For each SSFD expert team the GM hazard calculation was performed for each seismic source for each combination of attenuation and seismic source parameters, resulting in an appropriately weighted hazard curve for each combination of input variables. The total hazard across sources was then aggregated for each team to obtain the team's mean and fractile hazard curves. The integrated hazard across all SSFD teams was then obtained by combining the expert teams' mean and fractile curves giving each team equal weight. The hazard was calculated for GM measures: peak ground acceleration, peak ground velocity (PGV), and spectral accelerations over a frequency range of interest in estimating the response of SSCs to GM. The results are presented in the form of summary hazard curves, which depict the mean, median, and 15<sup>th</sup> and 85<sup>th</sup> fractiles.

In the case of fault displacement, the formulation for the earthquake approach considers earthquake magnitudes and locations as intermediate variables in the calculation of fault displacement and uses the same seismic source models (i.e., source geometries and magnitude-recurrence models, and their associated uncertainties) that are used in the GM PSHA. The only substantive difference between the earthquake approach for fault displacement PSHA and the GM analysis relates to 1) attenuation considerations related to principal and distributed faulting; and 2) the dependence of fault displacement on other parameters in addition to magnitude and distance.

The displacement approach uses a direct characterization of the occurrence rate of displacement events at the site and the probability distribution of displacement per event, without using earthquake magnitude and location as intermediate variables. The occurrence rate information may be provided as direct values of the occurrence rate or in the form of slip rate divided by an average displacement per event. Although calculation of the hazard curve for this approach does not require integration over magnitudes and distances or summation over seismic sources, a logic tree analysis is required because the expert teams specified multiple alternatives for the various elements of the model and for the characteristics of the site.

Analogous to the GM results, the fault displacement hazard results are given in terms of curves representing the mean, median, and 15<sup>th</sup> and 85<sup>th</sup> fractiles for the annual frequency of exceedance of displacement at the repository demonstration points.

## C. Parameters

The characterization of local and regional faults in the PSHA was based, in part, on data from field investigations and the SSFD experts' evaluations of the tectonic models. An example of the former is given in Table 6 of the AMR *Characterize Framework for Seismicity and Structural Deformation at Yucca Mountain, Nevada*. Table 6 lists key parameters for a subset (nine) of the local faults considered in the PSHA. The parameters include rupture length, shortest distance to the repository, sense of slip, fault dip, slip rate, and probability of activity. Except for the distance to the repository, all parameters are assigned a range of values or interpretations (i.e., sense of slip). Rupture lengths and slip rates are based on field evidence obtained from surface geologic mapping and trenching investigations. Fault dip and probability of activity are estimates based, in part, on the experts' interpretations of relevant tectonic models. The range of parameter values represents the total uncertainty in the parameters determined by the experts' assessment of the available data.

A similar table of parameters is given in the AMR (Table 7) for a subset of the regional faults considered in the PSHA. Again, the experts specified parameter ranges based on the uncertainty associated with the available information. The number of regional faults interpreted to be fault-specific seismic sources by the expert teams ranged from 11 to 36, reflecting the range of interpretations based on a common data set regarding regional fault activity. All teams modeled the regional faults as planar faults to maximum seismogenic depths primarily with dips depending on the style of faulting; preferred values of 90° for strike-slip faults and generally 60° or 65° for normal-slip faults. The selection of maximum seismogenic depths relied on observations of contemporary seismicity including some of the better-studied large surface-faulting earthquakes in the Basin and Range province. Alternative fault lengths were included to express the experts' assessment of the uncertainty in the mapped lengths.

Another important parameter used in the PSHA was maximum magnitude  $M_{\max}$ . The maximum magnitude is a derived parameter based on any one of several empirical relationships between magnitude and surface-rupture length, rupture area, and/or maximum displacement and average displacement. The experts weighted the use of the different relationships according to their assessments of the reliability of the input data.

Earthquake recurrence rates for the faults were described using either recurrence intervals and/or slip rates, with most teams using the latter due to the lack of recurrence interval information. Four recurrence models were used depending on the teams' evaluations.

### 3.4 Discussion of Uncertainty Treatment

There are two aspects to the uncertainty involved in the *Disruptive Events* AMRs. The first has to do with the formal treatment of model and model parameter uncertainty in the PSHA for both the GM hazard and fault displacement hazard. The second involves the application of the PSHA results to the interaction of vibratory GM and fault displacement with the proposed repository for the postclosure period.

## A. PSHA Conceptual Model and Parameter Uncertainty

### Vibratory GM

As described in Section 6.5.2 of the AMR *Characterize Framework for Seismicity and Structural Deformation at Yucca Mountain, Nevada*, the PSHA methodology is formulated to represent the randomness inherent in the natural phenomena of earthquake generation and seismic wave propagation. The randomness in a physical process has come to be called *aleatory* uncertainty. Furthermore, in all assessments of the effects of rare phenomena, one faces uncertainty in selecting appropriate models and model parameters because the data are limited and/or there are alternative interpretations of the available data. This uncertainty in knowledge is referred to as *epistemic* uncertainty. During the course of the PSHA, the SSFD experts placed a major emphasis on developing a quantitative description of the epistemic uncertainty.

The two types of uncertainty were treated differently in the PSHA. Integration is carried out over aleatory uncertainties to get a single hazard curve. The size, location, and time of the next earthquake on a fault and the details of the resultant GM at a site of interest are examples of quantities considered aleatory. In current practice, these quantities cannot be predicted, even with the collection of additional data. Epistemic uncertainties, on the other hand, are expressed in the PSHA by incorporating multiple assumptions, hypotheses, models, or parameter values. These multiple interpretations are propagated through the analysis, resulting in a suite of hazard curves and their associated weights. Results are presented as curves showing statistical summaries (e.g., mean, median, fractiles) of the exceedance probability for each GM amplitude. The mean and median hazard curves convey the central tendency of the calculated exceedance probabilities. The separation among fractile curves conveys the net effect of epistemic uncertainty about the source characteristics and GM prediction on the calculated exceedance probabilities.

The epistemic uncertainty assessment in the PSHA was performed using a logic tree methodology. The logic tree formulation for seismic hazard analysis involves setting out the sequence of assessments that must be made in order to perform the analysis and then addressing the uncertainties in each assessment sequentially. This formulation provides an effective approach for dividing a large, complex assessment into a sequence of smaller, simpler components that can be more easily addressed.

Epistemic uncertainties are associated with each of the three components of the seismic hazard model discussed in Section III. A. The seismogenic potential of faults and other geologic features is uncertain, as a result of 1) uncertainty about the tectonic regime operating in the YMR; and 2) incomplete knowledge of these geological features. Uncertainty in the rate of seismicity is generally divided into uncertainty in the maximum magnitude, uncertainty in the type of magnitude distribution, and uncertainty in the rate parameter (i.e., activity rate, rate of large events, or slip rate). Finally, the GM attenuation functions are uncertain, which arises from uncertainty about the dynamic characteristics (earthquake source, propagation path, and site effects) of earthquake GMs in the Yucca Mountain vicinity. This uncertainty is large because few strong motions have been recorded from events in the region.

A parameter of importance in the PSHA is kappa—a measure of the near-surface attenuation of seismic waves. While analysis of data from California sites yields kappa values of approximately 0.04 seconds, the average kappa for the Yucca Mountain was taken to be 0.02 seconds based on a study of shear-wave propagation to a limited number of stations in the site area. It is expected that kappa will vary over the site area due to variations in rock properties and this variability was accounted for by the GM experts in their estimates of uncertainty in their GM attenuation relationships. If ongoing studies in the YMR indicate a different value for kappa than that used in the PSHA, then the median attenuation models provided by the experts can be adjusted by scale factors for the revised kappa value versus the current kappa value.

Uncertainties in seismic source characterization and GM attenuation relations were quantified by considering inputs from the six SSFD expert teams and the seven GM experts, and by each SSFD team's and each GM expert's assessment of uncertainty. Each SSFD team formulated multiple alternative interpretations about the characteristics of potential seismic sources and assigned weights to these interpretations according to the credibility given the current state of knowledge and the degree they are supported by the available data. Each GM expert applied a similar procedure to alternative interpretations about the source, path, and site characteristics affecting GMs.

### **Fault Displacement**

As with the GM PSHA methodology, the mathematical formulations for the earthquake and displacement approaches for the fault displacement PSHA represent the aleatory uncertainty in the natural phenomena of tectonically induced fault displacement. Epistemic uncertainty is associated with imperfect knowledge about these phenomena. In the earthquake approach, epistemic uncertainty is in the seismic source characterization, the attenuation equations, and the characteristics of the site that affect fault displacement. In the displacement approach, epistemic uncertainty is in the two elements of the model, namely the rate information and the parameters of the displacement per event distribution, as well as in the characteristics of the site that affect fault displacement.

Epistemic uncertainties in seismic source characterization and fault displacement attenuation relations were quantified by considering inputs from the six SSFD expert teams, and by each team's own assessment of epistemic uncertainty. Each expert team selected an approach for the fault displacement PSHA (earthquake, displacement, or a weighted combination of both), then formulated multiple alternative interpretations for the fault displacement attenuation relations (if using the earthquake approach) or for the rate and the distribution of displacement per event (if using the displacement approach). Calculations for the earthquake approach consider each expert team's fault displacement attenuation relations in conjunction with that team's source characterization.

### **B. Postclosure Applications of PSHA**

The results of the GM and fault displacement PSHA are used in the AMR *Features, Events, and Processes: Disruptive Events* to provide screening discussions for seismic GM and fault-related FEPs. Two key assumptions are introduced in Section 5 of the AMR. Assumption 5.4 reads that “for postclosure seismic-related and fault-related FEPs, it is assumed that the probability

criterion of one chance in 10,000 in 10,000 years ( $10^{-4}/10^4$  yr) is equivalent to a  $10^{-8}$  annual-exceedance probability.” The justification for this assumption is based on the definition of an event as a natural or anthropogenic phenomenon that has a potential to affect repository performance and that occurs during an interval that is short compared to the period of performance. The assumption of equivalence of  $10^{-4}/10^4$  yr to the  $10^{-8}$  annual-exceedance probability is justified if the possibility of an event is equal for any given year. For geologic processes that occur over long time spans, assuming annual equivalence over a 10,000-year period (a relatively short time span) for geologic-related events is reasonable.

The assumption discussed in the preceding paragraph leads to an additional assumption regarding the particular use of the hazard results with annual-exceedance probabilities in the range  $10^{-6}$  to  $10^{-8}$ . Assumption 5.5 in the *Features, Events, and Processes: Disruptive Events* AMR notes that for postclosure evaluation of fault- and seismic-related (GM) FEPs, the postclosure fault-displacement and GM hazards are better represented by the median value, rather than the mean value or 85<sup>th</sup> fractile value, due to the large uncertainties associated with  $10^{-6}$  to  $10^{-8}$  annual-exceedance probabilities. The median value is assumed in the FEPs AMR to be representative for postclosure analyses and FEPs screening.

Epistemic uncertainty in the PSHA results is highly skewed and the degree of skewness increases with decreasing annual probability. At annual-exceedance probabilities in the range  $10^{-6}$  to  $10^{-8}$  used for postclosure fault-displacement evaluations, the mean fault-displacement hazard curve approaches the 85<sup>th</sup> fractile, then crosses it. At  $10^{-8}$  annual-exceedance probabilities, the mean displacement approximately coincides with the 99<sup>th</sup> fractile. For fault displacements, this indicates that the mean displacement is being determined at these very low probabilities by the tails of the uncertainty distributions, which are modeled in the PSHA as unbounded. These values do reflect the current state of scientific and modeling uncertainty, but in considering the hazard results, the mean values of fault displacement associated with the low annual-exceedance probabilities are too large when compared to field observations of maximum single-event fault displacements observed in trenches along block-bounding faults, such as the Solitario Canyon and Bow Ridge faults.

Although the effects of the upper tails of the uncertainty distributions are not as significant for GM hazard as they are for fault-displacement hazard, they nevertheless dominate the hazard at low annual probabilities. The behavior of the hazard curves in the PSHA suggests, that at low annual-exceedance probabilities, the GM hazards are dominantly from the upper tails of the experts' uncertainty distributions on seismic sources, earthquake recurrence, and maximum magnitude.

The two assumptions discussed in the paragraphs above are used in screening arguments for fault-related and seismic-related FEPs discussed in Section 6.2 of the *Features, Events, and Processes: Disruptive Events* AMR. While many of the arguments are used to exclude possible FEPs, there is one case that is included in the TSPA nominal scenario: fuel-rod cladding failure due to vibratory GM.

The analysis for failure of the fuel-rod cladding due to GM used a simplified seismic-fragility approach. The seismic-fragility approach involves the convolving of the GM hazard probabilities with probability of damage to a system component (the seismic fragility curve or

component fragility). The result of the analysis is the risk, expressed as a probability, of damage to the component during the repository performance period of 10,000 years. Based on the analysis, the probability (risk) of damage to fuel-rod cladding was  $1.1 \times 10^{-6}$ . The fragility curve was treated as a step function (i.e., damage either did or did not occur) and the damage was associated with GM having a  $10^{-6}$  to  $10^{-7}$  annual-exceedance probability. The use of a step function, while apparently conservative, is consistent with the assumption that all locations in the repository will experience the same GM.

### **C. Downstream Disruptive Events AMRs**

FEPs pertaining to the generation of new fractures and reactivation of pre-existing fractures in the YMR and the possible effects on flow and transport paths are addressed in Section 6.2.2 of the FEPs AMR. The discussion incorporates results from the PSHA and the AMR *Fault Displacement Effects on Transport in the Unsaturated Zone*, as well as observations on fractures and fault zones made in the Exploratory Studies Facility (ESF) and the Enhanced Characterization of the Repository Block Cross Drift.

The reactivation of fractures and the development of new fractures were addressed in the PSHA (fault-displacement hazard) and shown to be low probability events. Strain is more likely to affect existing features rather than create new fractures as evidenced by field observation of reactivation features and the geologic history of Yucca Mountain.

The effects of changes to fracture systems in the UZ due to geologic effects on mountain-scale flow and radionuclide transport were investigated in the AMR *Fault Displacement Effects on Transport in the Unsaturated Zone* using a sensitivity approach. As discussed in the FEPs AMR, the sensitivity analyses included two bounding cases: 1) the change in fracture properties occurs over the entire UZ domain (fault zones and fractured rocks); or 2) a more realistic case, the effect of fault displacement is limited to fracture-property changes in fault zones. These modeling cases were chosen to bound a presumed range of fracture-aperture changes resulting from fault movement. There are no direct observations for Yucca Mountain that relate stress caused by fault displacement and induced strains to resultant changes in fracture aperture. The bounding (conservative) cases are adopted to simulate a response beyond that of the expected

The analyses presented in the AMR *Effects of Fault Displacement on Emplacement Drifts* presume worse-case orientations for fault-drift spatial relationships and examine varying fault-rupture lengths, rock-mass qualities, and distances from the fault. Because the effects of fault displacement are shown to be negligible and, additionally, are addressed by the repository design which calls for set-backs from the WPs to the surrounding drift wall, faulting does not provide a mechanism sufficient to shear a WP. The differential displacements for points within the waste-emplacement area were shown in the PSHA to be less than 2 m, which is the vertical distance from the WP/drip shield to the drift wall. At least 2m of displacement must occur for shearing conditions to occur. For the block-bounding faults, at a set-back of 60 m, the differential displacements are only on the order of a few centimeters and are insufficient to result in shearing.

### **3.5 Conclusions**

The discussions of the PSHA methodology in the *Disruptive Events* PMR and the supporting AMR *Characterize Framework for Seismicity and Structural Deformation at Yucca Mountain, Nevada* give a concise description of the logical development of the hazard models for vibratory GM and fault displacement. The treatment of uncertainty is complete and well documented, particularly in the flow of results to downstream AMRs.

As described in the AMR *Characterize Framework for Seismicity and Structural Deformation at Yucca Mountain, Nevada* the PSHA was carried out according to a highly structured process, starting with the compilation and dissemination to the participating experts of all available data in the published and unpublished literature relevant to the geology and seismotectonics of the YMR. A series of workshops, field trips, and elicitation ensured that the final seismic hazard results captured the knowledge and uncertainties about the seismic source and fault displacement characterizations expressed by the experts.

The screening arguments for many of the seismic-related and fault-related FEPs in the AMR *Features, Events, and Processes: Disruptive Events* are particularly informative and bring the results of the upstream AMRs together in a very logical and convincing manner. The FEPs screening arguments are, in many cases, based on some combination of PSHA results, data from field studies at Yucca Mountain, and calculations made in other disruptive events AMRs. The discussion involving the extension of the hazard curves to the very low exceedance probabilities points up the problem in applying the hazard results to the postclosure period and how that is best treated in terms of mean versus median hazard estimates.

A summary discussion of uncertainties associated with the conceptual model, the representational model, and model parameters is given in the attached Table 3-1. The discussion addresses how, where, and why particular uncertainties are introduced and treated within the set of Disruptive Events documents and the potential impact of the uncertainties on TSPA.

**Table 3-1: Seismic Hazard Model**

<b>Model Purpose:</b> The purpose of the Seismic Hazard Model is to provide probabilistic GM and fault displacement hazard assessments for use in TSPA.				
<b>Summary</b>	<b>Source</b>	<b>Treatment</b>	<b>Basis</b>	<b>Impact</b>
<b>Conceptual Model</b>				
Seismic source models	Section 6.3.2 of the AMR <i>Characterize Framework for Seismicity and Structural Deformation at Yucca Mountain, Nevada</i> and Section 2.1.3.2.1 of the <i>Disruptive Events PMR</i> discuss <b>the types</b> of tectonic and seismic source models (fault-specific and areal) that the PSHA SSFD experts evaluated. Table 5 in the AMR provides a complete description of the alternative models.	The uncertainty associated with the experts' evaluation of the appropriateness, or applicability, of each of the models was addressed by means of the logic tree methodology. The experts weighted alternative tectonic models and seismic source zones depending on the degree of uncertainty in the appropriateness of the different models.	The uncertainty associated with this component of the seismic hazard model arises because of an incomplete understanding of the geologic and tectonic processes operating in the YMR. Various models have been proposed in the literature and the available data are not sufficient to discriminate between the alternative models. This uncertainty is an example of epistemic uncertainty and could be reduced with the acquisition of additional information.	The degree of epistemic uncertainty arising from the treatment of alternative source models drives the tails of the distribution of hazard curves at low annual-exceedance probabilities (i.e., 1 U' to 1 U). As discussed in Section 6.2 of the AMR <i>Features, Events, and Processes: Disruptive Events</i> , mean values of the GM and fault displacement hazards at these low annual-exceedance probabilities are inconsistent (too high) with field observations. The use of median values, rather than mean values, is recommended for postclosure applications in TSPA.

<p>Rate of earthquake occurrence and magnitude distributions</p>	<p>The recurrence relationships and models evaluated in the PSHA are discussed in Section 2.1.3.2.4 of the <i>Disruptive Events PMR</i> and in Section 6.3.2 of the <i>AMR Characterize Framework for Seismicity and Structural Deformation at Yucca Mountain, Nevada</i>.</p>	<p>Different approaches were used to estimate recurrence relationships for fault-specific sources and for areal source zones. The uncertainty associated with the experts' evaluation of each approach was addressed by the logic tree methodology.</p>	<p>The recurrence relationships for fault-specific sources depend on field measurements from geologic mapping (fault lengths) and trenching (displacements and dating of paleoearthquakes). The uncertainty in these field measurements and in the empirical relationships used to define maximum magnitudes were evaluated by the experts and incorporated in their assessment (weighting) of the different approaches. In the case of areal source zones, the limited historical record of seismicity in the YMR, the extent of the zones, and the maximum magnitudes in each zones contributed to the uncertainty in recurrence relationships.</p>	<p>A sensitivity study of the hazard results indicates that, with respect to seismic source characterization, the different earthquake recurrence approaches and alternative recurrence models considered by the experts in the PSHA contribute the most to uncertainty in the GM hazard. The impact of this epistemic uncertainty on TSPA is similar to the impact described for seismic source models.</p>
<p>GM attenuation characterization</p>	<p>The GM attenuation characterization is discussed in Section 6.3.3 of the <i>AMR Characterize Framework for Seismicity and Structural Deformation at Yucca Mountain, Nevada</i>.</p>	<p>The GM experts used logic trees to characterize uncertainty in their GM evaluations. In a typical logic tree, alternative attenuation models make up the branches of the tree. a model consists of estimates of both the median GM and the aleatory variability (standard deviation). The expert-to-expert differences in the median GMs and in the standard deviations of the alternative models constitute the epistemic uncertainty. Each expert evaluated the alternative models and developed his/her own composite model for their best estimates of the median and standard deviation for a given earthquake magnitude and source-site geometry (distance). In addition, each expert quantified the epistemic uncertainty associated with their estimates of the median and standard deviation.</p>	<p>Limited strong motion data for earthquakes in the YMR and uncertainty associated with using data primarily from California.</p>	<p>A sensitivity study indicated that the uncertainty in GM attenuation was the largest contributor to uncertainty for the GM hazard. The impact of the epistemic uncertainty on TSPA is similar to that described for the seismic source models.</p>

<b>Representational Model Uncertainty</b>				
GM and fault displacement models	The representational models are described in Sections 6.5.1 and 6.6.1 of the AMR <i>Characterize Framework for Seismicity and Structural Deformation at Yucca Mountain, Nevada.</i>	In the formulation of the hazard curves, integration is carried out over aleatory uncertainties to get a single hazard curve. Epistemic uncertainties are expressed by incorporating multiple assumptions, hypotheses, models, or parameter values. These multiple interpretations are propagated through the analysis, resulting in a suite of hazard curves and their associated weights. Results are presented as curves showing statistical summaries (e.g., mean, median, fractiles) of the annual-exceedance probability for the amplitude of a GM parameter or fault displacement.	The bases for the uncertainties included in the formulations are described in the sections of this table on the basis of uncertainty in the conceptual models and parameters.	Similar discussion as under conceptual models and parameters.
<b>Parameter Uncertainty</b>				
Fault-specific parameters	Local and regional fault-specific parameters are described in Tables 6 and 7, respectively, of the AMR <i>Characterize Framework for Seismicity and Structural Deformation at Yucca Mountain, Nevada.</i>	The fault-specific parameters are expressed in terms of ranges of values in Tables 6 and 7 of the AMR referred to in the source column. The experts assigned weights to values within a range for a particular parameter according to their estimates of the epistemic uncertainties associated with the parameter values.	Limited field observations and uncertainties associated with paleoearthquake measurements (i.e., maximum fault displacement, dating of earthquakes).	Similar discussion as under conceptual models and parameters.

<p>Kappa -a measure of near surface attenuation.</p>	<p>Kappa is discussed in Section 6.3.3.1.1 of the AMR <i>Characterize Framework for Seismicity and Structural Deformation at Yucca Mountain, Nevada.</i></p>	<p>Kappa is introduced in the PSHA as a single-value parameter (i.e., median value) for use over the Yucca Mountain site area.</p>	<p>The median value of kappa is based on studies of seismic shear-wave propagation to a limited number of stations. Recordings from aftershocks of the Little Skull Mountain earthquake were used in the study. The effect of variability in kappa on the variability of the GM was accounted for since experts used estimates of the GM variability based on empirical data evaluated from either standard deviations for empirical attenuation relations or modeling uncertainty from numerical simulations. The empirical estimates of GM variability account for kappa variability within the broad site categories (e.g., rock or deep soil).</p>	<p>If ongoing studies in the YMR find that the median kappa value is different from that used in the PSHA (possibly a conservative value as indicated by preliminary results from ongoing studies), the median attenuation models provided by the experts could be adjusted using scale factors for kappa. Only the median GM would be modified. The preliminary results from the ongoing studies point to a larger value of kappa. If these preliminary results hold up then the hazard curve would be scaled down, where the amount of scaling would depend on the difference between the kappa value currently used in the PSHA and the new value.</p>
--	--	--	--	---

INTENTIONALLY LEFT BLANK

## 4.0 Future Climate and Infiltration

### 4.1 Purpose of Model/Intended Use

The purpose of the *Future Climate Analysis* (ANL-NBS-GS-000008) is to estimate the timing and nature of climate change in the YMR over the next 10,000 years, the time interval required for regulatory compliance as stated in the NRC's proposed 10 CFR 63<sup>1</sup>. The approach involved defining the climate states expected to occur over the first 10,000 years following closure of the repository and establishing the mean annual value and upper/lower bounds for precipitation and air temperature for each of the identified climate states.

The *Simulation of Net Infiltration for Modern and Potential Future Climates* (ANL-NBS-HS-000032), in turn, uses the precipitation and air temperature estimates (for the three climate states) from the *Future Climate Analysis* to provide spatially distributed time-averaged estimates of net infiltration for defining the upper boundary condition for modeling UZ water flow and radionuclide transport. Net infiltration is the component of infiltrated precipitation, snowmelt, or surface water run-on that has percolated below the zone of evapotranspiration defined by the depth of the effective root zone.

The climate model approach (i.e., examining paleoclimate records to find a past climate series that is expected to be repeated in the future) is one that can be considered routine in that it has been employed before by numerous other investigators in the field of climate study and is not unique to the YMP. Similarly, the use of neutron log data to develop models of infiltration/water movement is an established technique. The variability of site conditions (spatial dimensions, topographic relief, soil coverage and development, data locations, infrequent and often localized rainfall) have been addressed in the infiltration model. The complexities inherent in the natural system have led to large uncertainties in the final model.

### 4.2 Model Relations

The climate model and all the inputs to the model are documented entirely within the *Future Climate Analysis* AMR (ANL-NBS-GS-000008). The infiltration model is documented entirely within the *Simulation of Net Infiltration for Modern and Potential Future Climates* AMR (ANL-NBS-HS-000032). Inputs to the infiltration model are documented in the *Future Climate Analysis* AMR; no other AMRs provide input. The AMR entitled *Analysis of Infiltration Uncertainty* (ANL-NBS-HS-000027) presents sensitivity analyses using the infiltration model to identify those parameters that affect the resultant infiltration rate. This analysis is then used to determine the frequency at which the various infiltration scenarios are sampled for use in TSPA. Figure 4-1, Climate and Infiltration Model Relations, shows the linkages between the AMRs.

---

<sup>1</sup> This AMR is being revised to include projections of future climate states after the 10,000 year proposed NRC compliance period in order to support the Final Environmental Impact Statement. However, since the revision was underway (not yet complete) during the time this review was ongoing, Rev. 00 of the AMR was reviewed.

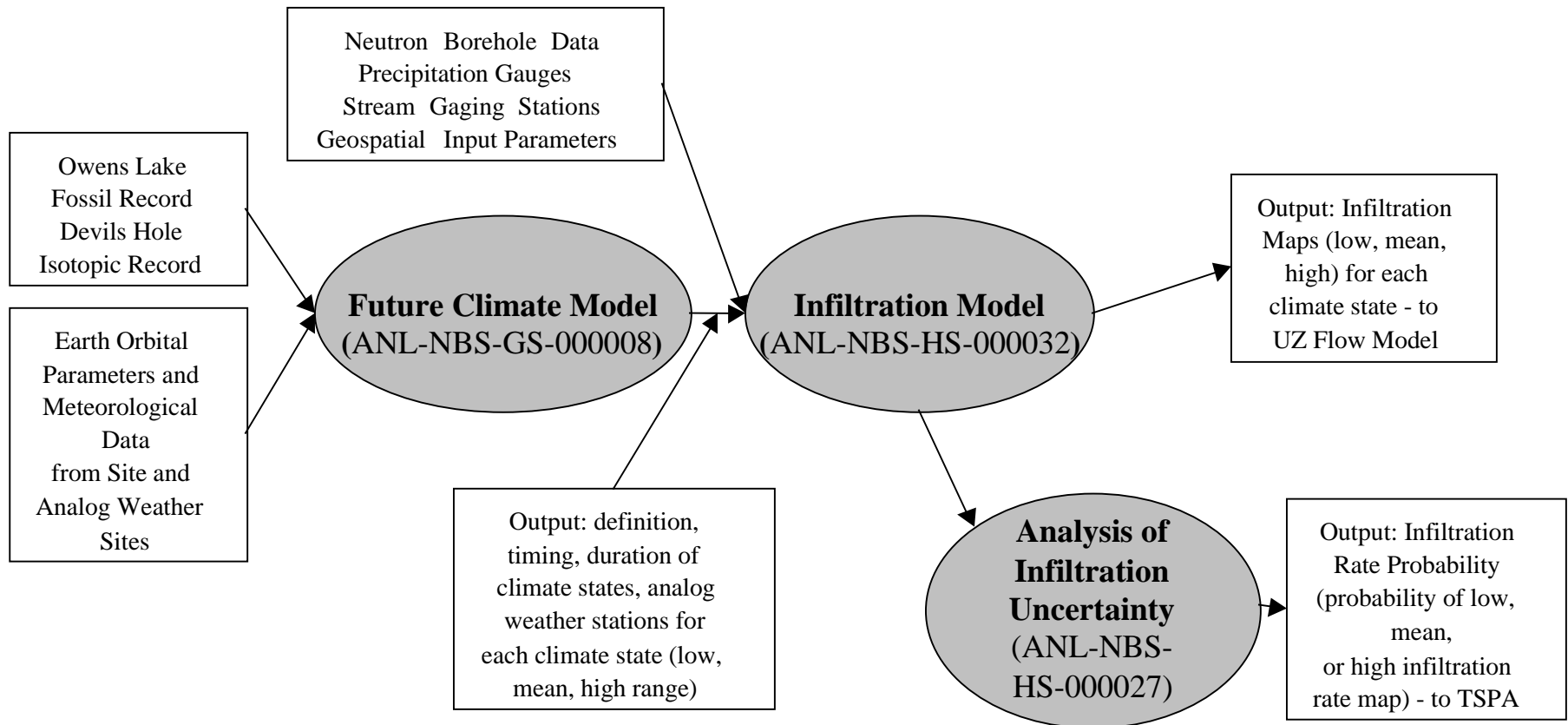


Figure 4-1: Climate and Infiltration Model Relations

### 4.3 Model Structure

Figure 4-2, Climate and Infiltration Model Structure, depicts the various elements that comprise the climate and infiltration models. Shown are those elements that comprise the conceptual and representational models, the various parameters needed, and the modeling results. Each is discussed in more detail below.

#### A. Conceptual Model

##### Climate

Four assumptions are central to the conceptual basis of the climate model:

- Climate is cyclical with several sequences of alternating glacial and interglacial periods within a timeframe of about 400,000 years. Future climates may repeat, or at least approximate, past climates.
- A relationship exists between the timing of long-term past climates and the timing of earth-orbital parameters.
- There is a relationship between the character of past climates and the sequence of those climates. Past climates are assumed to repeat in a systematic order.
- Long-term climate forcing effect (tectonic change) has been fairly constant over the last half million years and will likely remain so for the next 10,000 years.

##### Infiltration

The conceptual model for infiltration is discussed briefly in the *Simulation of Net Infiltration for Modern and Potential Future Climates* AMR (Section 6.1), focusing on general topics. In general, the development of the technical and conceptual basis for the infiltration model is discussed in another document<sup>2</sup>. This draft 1996 model provides the best available process model description of infiltration. The AMR states that the model “developed by Flint et al, 1996 adequately described and simulated the natural hydrologic system. The assumption (i.e., that the identified document described and simulated the natural hydrologic environment) is justified because both models (conceptual/numerical) were based on thorough analysis of extensive field data collected during 1984 through 1995.”

---

<sup>2</sup> Flint, et.al., 1996 Draft Conceptual and Numerical Model of Infiltration of the Yucca Mountain Area, Nevada, MOL.19970409.0087

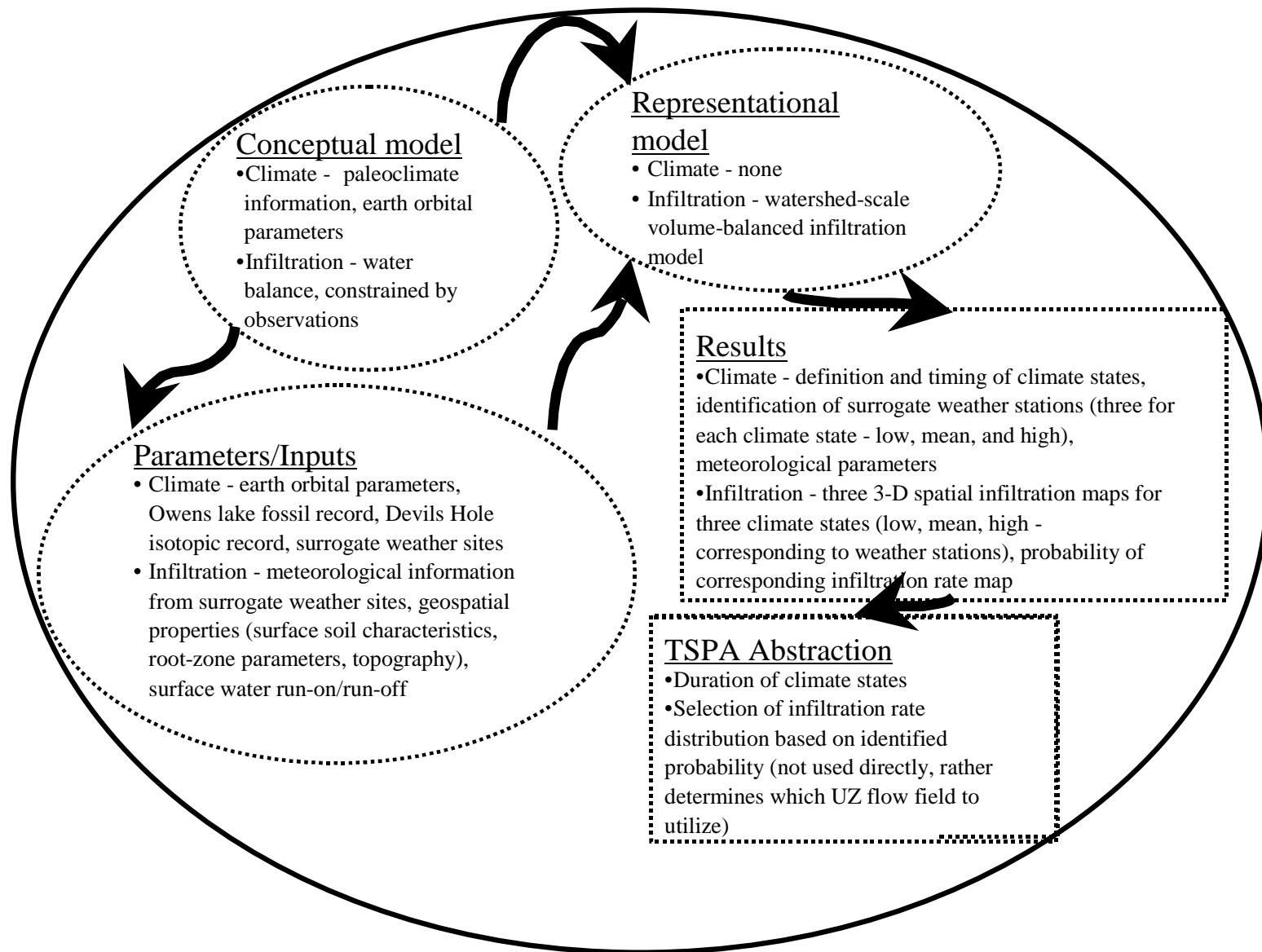


Figure 4-2: Climate and Infiltration Model Structure

## **B. Parameters**

### **Climate**

Estimation of future climate conditions is accomplished by paleoclimate reconstruction from applicable data sources. The timing and nature of climate change in the YMR is primarily based on the Devils Hole, Nevada, delta O-18 record and the microfossil data from Owens Lake, California. Past climates interpreted from this data were used to select representative meteorological stations from other states/locations to serve as future climate analogs. The precipitation and temperature data from those stations then serves as input to the *Simulation of Net Infiltration for Modern and Potential Future Climates* AMR.

### **Infiltration**

The primary source of data upon which both the conceptual and numerical models for infiltration are based comes from a network of neutron boreholes located in/on stream channels, terraces, sideslopes, and ridgetops in the immediate vicinity of the potential repository. Model parameters and their associated data input sources include precipitation rate (from site and analog meteorologic stations), evapotranspiration (from bare-soil evaporation and vegetative transpiration; also influenced by net radiation, air temperature, ground heat flux, the saturation-specific humidity curve, and wind conditions), and surface run-on (stream gages).

## **C. Representational Model**

### **Climate**

No specific representational model is employed. The term climate model is something of a misnomer, because essentially, what was accomplished in the *Future Climate Analysis* AMR is climate forecasting, rather than modeling future climate, because modeling would require that future boundary conditions be known. This analysis describes the rationale for its climate analysis methods, then applies those methods to define and forecast possible future climate scenarios.

### **Infiltration**

The representational infiltration model, discussed in Section 5.2 of the *Simulation of Net Infiltration for Modern and Potential Future Climates* AMR, involves a water-balance calculation using Darcy's law and the application of the conservation of mass principle, with all water-balance calculations being performed as volume-balances. Model calculations are performed using double-precision variables and the standard FORTRAN77 programming language. The modeling process utilizes a combination of GIS applications, field measurements, parameter estimation, and visualization and analysis techniques.

## **D. Results**

Results obtained from the climate model include forecasts of the timing and duration for the three identified future climate states: modern, monsoon, and glacial transition. Analog meteorological stations are also identified, and estimates of precipitation and temperature are also provided from these stations. Maps of expected infiltration for a range of conditions (low, mean, and high) are provided for each of the climate states.

Climate state durations and the infiltration rate probability for the low, medium, and high cases, are input directly to TSPA. Nine infiltration rate maps (three for each climate state) are incorporated into the UZ flow model as the upper boundary condition in the computation of moisture flow fields. These flow fields are then used to simulate radionuclide transport in TSPA using particle tracking techniques. Both UZ flow and radionuclide transport are discussed in companion papers included in this report (Chapters 5.0 and 13.0, respectively).

### **4.4 Discussion of Uncertainty/Variability Treatment**

An evaluation of uncertainty and variability treatment of the future climate analysis and infiltration model was performed for this exercise. For each AMR covering these subjects, the uncertainties/variabilities were identified and the thoroughness of the treatment was evaluated. Thorough treatment was considered to be: identification, treatment, impact assessment, and clear presentation of the analysis and the propagation of uncertainty in the AMR. Table 4-1 is a synopsis of some of the uncertainties and variabilities identified in this exercise.

#### **A. Conceptual Model**

##### **Climate**

Climate model uncertainties/limitations stem from several sources:

- Timing/duration of the three identified future climate states, based on uncertainties associated with data such as the rate of sediment accumulation in the Owens Lake record
- Age dating of Devils Hole calcite core and the Owens Lake sediment/fossil assemblage
- Difficulties intrinsic to identifying particular climatic sequences given the chaotic nature of climate and limited applicable data

The climate model has been developed based on the results of numerous climate studies that form the basis upon which the theory of climate modeling is founded. However, uncertainties associated with the assumptions or the conceptual climate model itself are not addressed in the *Future Climate Analysis* AMR. Uncertainties from possible changes in the climate cycle resulting from human activity are not addressed.

## **Infiltration**

The discussion in Section 5.2 of the *Simulation of Net Infiltration for Modern and Potential Future Climates* AMR does not address conceptual model uncertainty. In particular, alternative conceptual models are not identified. This is notable since several panel members of the Unsaturated Zone Expert Elicitation (UZEE<sup>3</sup>) disagreed with one aspect of the conceptual/numerical model of infiltration. YMP scientists contend that zero infiltration is expected in areas where the depth of alluvium is > 6 meters, thicknesses commonly exceeded in washes at Yucca Mountain. The opinion of the panel was that this conclusion was counter-intuitive to field observations and their collective experience. This topic is not addressed in the AMR.

Only one conceptual model is developed for the infiltration model. Model verification is treated through comparison of the infiltration model predictions to predictions of other possible conceptual models of local/regional recharge employed by other researchers (Maxey-Eaken, Winograd, Kwicklis, etc.). Site-scale net-infiltration estimates obtained for the nine identified future climate scenarios were plotted against the corresponding average annual precipitation rates and compared to net-infiltration and recharge estimates obtained from these independent methods. An assumption is made that the spatially averaged net-infiltration estimates are approximately equivalent to recharge at Yucca Mountain for a given climate scenario. Reasonable (i.e., order of magnitude) agreement regarding site infiltration and recharge is achieved this way.

## **B. Parameters**

### **Climate**

Uncertainty within the Climate AMR/Model is addressed by identifying meteorological stations that are expected to represent the extreme upper and lower bounds of weather conditions for each of the three climate states. This approach provides a range of precipitation and temperature to the subsequent infiltration calculations.

The orbital cycles are compared to the Devils Hole climate change record because the data from Devils Hole represents the best available independent and accurately dated climate record on Earth. Other long, dated climate records exist, but typically the chronology from those records relies on extensive interpolation between dates. In this analysis, the Devils Hole record forms the basis for the timing of climate change in the region of Yucca Mountain. The published Devils Hole data are taken as accurate by the AMRs author, with no additional assessment of uncertainty beyond what was described by the authors of the Devils Hole analysis.

Uncertainty in the sedimentation-accumulation rate for the Owens Lake record is incorporated in the analysis by using a range of duration for each defined future climate state (modern 400-600 yrs., monsoon 900-1,400 yrs., with the remainder of the 10,000-year period for the glacial transition).

---

<sup>3</sup> Unsaturated Zone Flow Model Expert Elicitation Project, 1997. MOL.19971009.0582

## **Infiltration**

A rigorous sensitivity analysis regarding net infiltration was addressed in the AMR entitled *Analysis of Infiltration Uncertainty* for a selected set of 12 uncertain parameters. Uncertainty in net-infiltration stems from imperfect knowledge of input parameters, such as precipitation, bedrock and soil hydrologic parameters, and evapotranspiration. Upper and lower bounds for the 12 uncertain parameters were defined by either physical limits of the parameter or by reasonable limits based on existing data and process understanding. Latin Hypercube Sampling (i.e., a form of stratified sampling whereby the sampling interval is subdivided into a number of intervals of equal probability) was used to sample values from the 12 uncertainty distributions. An equal number of samples is drawn from each of these intervals. Greater confidence in the output distribution is achieved than would be obtained using the classical random-sampling approach. For a few additional cases, the distribution of parameter values was stochastically sampled; these include lognormal distributions for conductivity parameters, uniform distribution for snow-cover parameters, and normal distributions for other unidentified parameters.

The infiltration model was run with 100 sampling realizations for each of the 12 uncertain input parameters. The glacial-transition climate was chosen for this analysis because this is the climate state in effect 8,000 years of the 10,000-year period and is in effect during the latter portion of this period when release of radionuclides is more likely. Weighting factors of 0.17, 0.48, and 0.35 were derived to determine the sampling frequency for the low, medium, and high infiltration scenarios, respectively, for use in TSPA simulations.

The basis for the selection of uncertain parameters and definition of their probability distributions for use in this uncertainty analysis is limited and not transparent, as is illustrated in the discussion below.

- Section 5 of the *Simulation of Net Infiltration for Modern and Potential Future Climates* AMR refers to the *Analysis of Infiltration Uncertainty* AMR for "complete documentation of the assumptions and their bases." That AMR (Section 4.1.1.1) then refers back to Section 6.10.2 of the *Simulation of Net Infiltration for Modern and Potential Future Climates* AMR for "details on the justification of the uncertainty distributions and their associated ranges." A limited discussion of the bases for the distributions and their range is provided in Section 6.10.2. of the *Simulation of Net Infiltration for Modern and Potential Future Climates* AMR.
- Section 5 of the *Simulation of Net Infiltration for Modern and Potential Future Climates* AMR states that 12 potentially significant parameters were selected for uncertainty analysis. Section 1 of the *Analysis of Infiltration Uncertainty* AMR supports this, but further states that the selection of these 12 parameters was constrained by schedule limitations. A future analysis might include some parameters not considered here, and exclude some that were considered.
- Further, Section 7 of the *Analysis of Infiltration Uncertainty* provides recommendations for future work, including: 1) performing a rigorous determination of uncertain input parameter correlation—no correlation is currently assumed; 2) implementation of an analysis to determine which input parameters to the infiltration code may significantly and adversely

impact the criteria for compliance and licensing; and 3) the determination of a mean uncertainty distribution of the infiltration rates for the middle analog for climate reported in Table 7-1. This would be in the form of a cumulative complimentary distribution function (CCDF). By performing multiple sets of uncertainty analyses for a climate regime, an estimate of confidence in the resulting CCDF may be obtained.

Regarding the accuracy of the input parameters, section 5.2.2 of the *Simulation of Net Infiltration for Modern and Potential Future Climates* AMR states, “Model accuracy is dependent on the accuracy of the input parameters. A thorough evaluation of the accuracy of all model input parameters has not been conducted. Analysis of model sensitivity to the accuracy of input parameters was not complete at the time of this analysis/model activity. For the purpose of this analysis/modeling activity, all input parameters are assumed to be accurate.” Uncertainty concerning the geospatial and infiltration rate input parameters, such as slope, aspect, soil classes/depth, bedrock geology, and root zone parameters (depth, layering, density) are not addressed in the AMR.

It appears that all uncertainty in the infiltration model described in the *Simulation of Net Infiltration for Modern and Potential Future Climates* AMR is taken into account by defining upper, lower, and mean values for the key parameters (i.e., precipitation and air temperature) within each climate stage, and calculating net infiltration for these combinations. The methods by which the bounds for the various climate scenarios were established are given below.

Mean infiltration estimates for the upper bound modern climate scenario were calculated using the 1980-95 model calibration period and results obtained using a 100-year stochastic simulation of daily precipitation modeled using the Nevada Test Site (NTS) Area 12 precipitation station record through 1993. Net infiltration estimates for the lower bound were obtained through sampling the 1980-95 simulations, the 100-year stochastic simulation and the driest (in terms of net infiltration) 10-year period within the 100-year simulation for the lowest net infiltration rate at each grid cell.

The lower bound for the monsoon climate scenario is defined as being equivalent to the mean modern climate scenario, and the upper bound for the monsoon climate scenario is calculated using daily climate records from two analog sites, Hobbs, NM, and Nogales, AZ. Net infiltration for the upper bound monsoon climate is calculated as the arithmetic mean of the separate infiltration simulations for Hobbs and Nogales, with mean infiltration for the monsoon climate being the arithmetic mean of the lower and upper bound net infiltration results.

The lower bound glacial-transition climate is represented using daily records from two analog sites, Beowawe, NV, and Delta, UT. The lower bound net infiltration for the glacial-transition climate state is calculated as the arithmetic mean of the separate Beowawe and Delta net infiltration simulations. The upper glacial-transition climate is represented using climate records from three analog sites located in Washington: Rosalia, Spokane, and St. John. The upper bound glacial transition net infiltration result is calculated as the arithmetic mean of the separate Rosalia, Spokane, and St. John net infiltration simulations. The mean glacial-transition climate is calculated as the arithmetic mean of the lower and upper bound net infiltration results.

The distribution of neutron borehole locations is skewed toward those sites where drilling could be most easily and safely accomplished, so stream channels and ridgetops account for the bulk of data locations, with only a small number of sites being located on sideslopes or terraces. Uncertainty introduced due to the distribution of neutron borehole locations is not addressed in the *Simulation of Net Infiltration for Modern and Potential Future Climates* AMR.

## **C. Representational Model**

### **Climate**

Since the climate model essentially has no representational model, there is no associated uncertainty. However, further use of the climate model in TSPA uses the assumption of instantaneous, discrete changes in climate. Section 3.2.1.3 of the TSPA-SR document<sup>4</sup> discusses the effect of this assumption, which is negligible.

### **Infiltration**

Accuracy and precision of the model calculations are discussed in Section 6.2.1 of the *Simulation of Net Infiltration for Modern and Potential Future Climates* AMR. In this section, it is stated that “at the time of this analysis/model activity, a quantitative analysis of model accuracy was not complete.” As such, it can be concluded that representational model uncertainty has been acknowledged, but has not yet been addressed quantitatively.

## **D. Results**

Uncertainty in the results is addressed through the determination of three infiltration rate maps for each of the three identified climate states. These maps represent low, medium, and high infiltration rates resulting from uncertainty in future climate conditions and from uncertainty in infiltration model parameters.

### **4.5 Uncertainty Propagation**

Documented uncertainties are clearly propagated between the *Future Climate* and *Simulation of Net Infiltration for Modern and Potential Future Climates* AMRs. Meteorological information from the analog stations identified in the *Future Climate* AMR is used as input to the infiltration model. In addition, the three climate states and their duration are input directly into TSPA.

---

<sup>4</sup> “Total System Performance Assessment for the Site Recommendation,” TDR-WIS-PA-000001, Rev. 00, ICN 1. MOL.20001220.0045

The infiltration rate maps computed in the *Simulation of Net Infiltration for Modern and Potential Future Climates* AMR are used as to represent uncertain upper boundary conditions in the UZ flow model. As such, all uncertainty explicitly treated in the computation of these infiltration rate maps is input directly into computation of the UZ flow fields. The probability of each infiltration rate map (low, medium, high) as determined in the *Analysis of Infiltration Uncertainty* AMR is input directly into TSPA.

**Table 4-1: Future Climate and Infiltration Model**

<b>Model Purpose:</b> The purpose of the infiltration model is estimate net infiltration at Yucca Mountain for use as the upper boundary condition for the UZ flow model. Note - from Simulation of Net for Modern and Potential Future Climates (ANL-NBS-HS-000032), except where noted.				
<b>Summary</b>	<b>Source</b>	<b>Treatment</b>	<b>Basis</b>	<b>Impact</b>
<b>Conceptual Model</b>				
Conceptual model of infiltration at Yucca Mountain	Conceptual model is described but no possible alternatives (or treatment of uncertainty in chosen conceptual model) are discussed ( <i>Simulation of Net Infiltration for Modern and Potential Future Climates</i> , ANL-NBS-HS-000032).	The conceptual model is described and the three most important components, effective precipitation, soil depth, and bedrock permeability, are identified. No alternatives are discussed.	The model has been developed based on interpretation of available data (neutron logs, soil depth estimates, lithologic logs, site meteorological data). However, no attempt to entertain alternative conceptual models has been made. Consideration of possible alternative conceptual models is only treated through an after-the-fact comparison of the model predictions to predictions of other conceptual models of local/regional recharge employed by other researchers (Maxey-Eakin, Kwicklis, etc.) as a partial validation exercise.	Calculated infiltration rates at the surface of Yucca Mountain
The chosen conceptual model has received criticism from the UZEE for its conclusion that in areas where soil depth is > 6m, depths commonly exceeded in washes at Yucca Mountain, zero infiltration is predicted.	The opinion of the panel was that this conclusion was counter-intuitive to field observations and their collective experience.	No specific treatment or discussion of this potential source of uncertainty is provided in AMR/model.	The conceptual model on which the AMR/model is based is taken as being the best available conceptual model of infiltration at Yucca Mountain and most strongly supported by analysis of the available data.	If this conclusion is in error, it could result in underestimating the amount of infiltration over the repository area.
<b>Representational Model Uncertainty</b>				
Distributed Parameter Water-Balance Model	No discussion of uncertainty in chosen approach or possible alternatives ( <i>Simulation of Net Infiltration for Modern and Potential Future Climates</i> , ANL-NBS-HS-000032).	Mathematical implementation of this model is well-described, but alternative formulations and implications are not discussed.  Items such as the 30x30 meter grid size for assessing total root zone water storage capacity may introduce considerable uncertainty in infiltration estimates. Most grid cells have no neutron boreholes to provide data for model output constraint.	It is stated that “at the time of this analysis/model activity, a quantitative analysis of model accuracy was not complete.” As such, it can be concluded that representational model uncertainty has been acknowledged, but has not yet been addressed quantitatively.	Computed infiltration rates

Parameter Uncertainty				
Present-day topography from Digital Elevation Model and temporal evolution of surface topography	No data on future geomorphological development <i>Simulation of Net Infiltration for Modern and Potential Future Climates</i> , ANL-NBS-HS-000032).	DEM data applied "as is." Uses present-day topography for the next 10,000 years.	None given.	Not discussed. Precision of maps and impacts on results not discussed. Importance and sensitivity of defining divides and channel networks mentioned. Forms basis for defining watershed domains that remain constant throughout the modeling timeframe.
Geospatial input parameters - topographic parameter subset (slope, aspect, and blocking ridges)	Single surface is used for the entire time span of modeling, apparently with no uncertainty (see above comment). If topography changes with time, so will the parameters <i>(Simulation of Net Infiltration for Modern and Potential Future Climates</i> , ANL-NBS-HS-000032).	Calibrated from present-day topographic surface; each location in the model has a unique value assigned to it.	None given.	Although not discussed, given the sensitivity of the calculation to topography, it may be significant. Model could show greater/lesser infiltration at given location.
Geospatial input parameters - soil depth classes and soil type	Geospatial input – interpolated from borehole data ( <i>Simulation of Net Infiltration for Modern and Potential Future Climates</i> , ANL-NBS-HS-000032)..	No uncertainty in soil depth classes is included; each location has a unique value assigned to it. Similarly, the parameters derived from soil type and porosity are assigned a unique value at each location.	None given. However, there should be some uncertainty in soil depth since most of the input has been extrapolated from borehole locations. Soil types were defined on the basis of field measurements of texture. Texture and porosity are used to estimate soil porosity, field capacity, residual water content, and saturated hydraulic conductivity. There is uncertainty due to limited field samples, so there should also be uncertainty associated with this parameter, porosity, and all other derived model input parameters.	Although not discussed, given sensitivity to porosity, effects could be significant.
Geospatial input parameters - bedrock geology	Bedrock geology was inferred from many different map sources. There are evidently many gaps and inconsistencies among these various maps, indicating uncertainty. <i>(Simulation of Net Infiltration for Modern and Potential Future Climates</i> , ANL-NBS-HS-000032).	The maps were rationalized, and gaps filled, according to well-described procedures. However, once this was done, the bedrock type was fixed for each local area of the model. No uncertainty in the bedrock type was incorporated. Since bedrock type is used to estimate saturated hydraulic conductivity, there should be some uncertainty in this model input parameter.	None given.	Possible impact on computed infiltration rates

Estimated soil depth	Parameter is calculated from the local slope and the local soil class, both of which are uncertain ( <i>Simulation of Net Infiltration for Modern and Potential Future Climates</i> , ANL-NBS-HS-000032)..	Uncertainty is ignored; local parts of the numerical model have unique input.	None given.	Possible impact on computed infiltration rates
Estimated root zone depth and root zone layering and density	Depth parameter is calculated from soil depth and two empirically-calculated coefficients, all of which have inherent uncertainty. Layering and density are based on soil depth and other factors, all of which are uncertain, so these two factors also have uncertainty ( <i>Simulation of Net Infiltration for Modern and Potential Future Climates</i> , ANL-NBS-HS-000032).	Uncertainty is ignored; local parts of the numerical model have unique input.	None given.	Possible impact on computed infiltration rates
1999 Infiltration Model Calibration.	Calibration was based on comparing model predictions of daily mean discharge at 5 stream gages to actual data, as well as some preliminary calibration calculations leading up to this final one. AMR describes how much of the calibration is based either on local values, or is interpolated from a few known values. This is clearly a non-unique criterion, as there are undoubtedly different combinations of input parameters that can match the 5 data points. In fact, the AMR (sec. 6.8) alludes to the non-uniqueness and imperfect knowledge of some of the calibration data ( <i>Simulation of Net Infiltration for Modern and Potential Future Climates</i> , ANL-NBS-HS-000032).	Non-uniqueness and calibration not discussed. "Satisfactory fit" was a manual trial-and-error process and not based on model predictions matching measured data within some specified numerical tolerance.	None given.	Possible impact on computed infiltration rates

<p>Uncertainty analysis - <i>Analysis of Infiltration Uncertainty</i> (ANL-NBS-HS-000027). Input distributions developed for 12 selected parameters from those included in overall infiltration model file. 100 realizations (Latin Hypercube) used to determine weighting factors to apply to low, medium, and high infiltration rate maps determined in the <i>Simulation of Net for Modern and Potential Future Climates</i> AMR.</p>	<p>Source is uncertainty in 12 selected parameters.</p> <ul style="list-style-type: none"> <li>- Bedrock bulk saturated hydraulic conductivity multiplier</li> <li>- Bedrock effective root-zone porosity</li> <li>- Bedrock root-zone thickness multiplier</li> <li>- Coefficients (two) in expression for evapotranspiration</li> <li>- Surface flow runoff area</li> <li>- Daily evapotranspiration multiplier</li> <li>- Daily precipitation multiplier</li> <li>- Snow-melt parameter</li> <li>- Soil zone thickness multiplier</li> <li>- Soil saturated hydraulic conductivity multiplier</li> <li>- First term in snow loss (sublimation) equation for temperature regime below freezing</li> </ul> <p>(<i>Simulation of Net Infiltration for Modern and Potential Future Climates</i>, ANL-NBS-HS-000032).</p>	<p>Probability distributions assigned (normal, log-normal, and uniform). Bounds were defined by either physical limits of the parameter, or by reasonable limits based on existing data and process understanding. Sampled using Latin Hypercube Sampling to compute resultant infiltration rate for a given realization.</p>	<p>Section 5 of the <i>Simulation of Net for Modern and Potential Future Climates</i> AMR refers to the <i>Analysis of Infiltration Uncertainty</i> AMR for "complete documentation of the assumptions and their bases." That AMR (Section 4.1.1.1) then refers back to Section 6.10.2 of the <i>Simulation of Net for Modern and Potential Future Climates</i> AMR for "details on the justification of the uncertainty distributions and their associated ranges." A limited discussion of the bases for the distributions and their range is provided here.</p> <p>Section 5 of the <i>Simulation of Net for Modern and Potential Future Climates</i> AMR states that 12 parameters were selected (estimated a-priori as being potentially significant). Section 1 of the <i>Analysis of Infiltration Uncertainty</i> AMR support this, but further states that the selection was constrained by schedule limitations.</p> <p>Further, Section 7 of the <i>Analysis of Infiltration Uncertainty</i> AMR provides recommendations for future work, including: performing a rigorous determination of uncertain input parameter correlation (no correlation assumed, implementation of an analysis to determine which parameters input to the infiltration code may significantly and adversely impact the criteria for compliance and licensing).</p>	<p>Range of infiltration rates for use in subsequent analyses and models (e.g., unsaturated zone flow)</p>
--	---	---	---	--

<b>Results</b>				
Uncertainty analysis - <i>Analysis of Infiltration Uncertainty</i> (ANL-NBS-HS-000027)	Various – discussed above	Upper and lower bounds were generated for 12 sensitive parameters. Bounds were described by either physical limits of the parameter, or by reasonable limits based on existing data and process understanding. In a few cases, a full distribution of parameter	See treatment.	Uncertainty analysis used to set probability of low, mean, and high infiltration rates subsequently used in TSPA.
Net Infiltration Results	Derived from input uncertainty ( <i>Simulation of Net Infiltration for Modern and Potential Future Climates</i> , ANL-NBS-HS-000032).	Spatially variable infiltration maps are produced - three for each climate state (low, medium, and high).	Bounds chosen to capture uncertainty in infiltration rate modeling.	Upper boundary condition for UZ flow model.
Uncertainty distribution for infiltration model bedrock bulk saturated hydraulic conductivity multiplier for the glacial transition climate. Section 4.1.	ANL-NBS-HS-000032 Rev. 00	Assumed lognormal distribution with a mean of 1.000 with 1.0 and 99.0 percentile low and high range values of 0.05 and 20.0, respectively (Section 4.1, p. 14, Table 4-1)	Distribution parameters obtained from Section 6.10.2 in ANL-NBS-HS-000032, <i>Simulation of Net Infiltration for Modern and Potential Future Climate</i> .	Hydraulic conductivity of the bedrock has a direct effect on infiltration to the UZ; higher conductivity results in higher infiltration.
Uncertainty distribution for infiltration model bedrock effective root-zone porosity for the glacial transition climate. Section 4.1.	ANL-NBS-HS-000032 Rev. 00	Assumed normal distribution with a mean of 10.030 with 1.0 and 99.0 percentile low and high range values of 0.0000 and 0.040, respectively (Section 4.1, p. 14, Table 4-1)	Distribution parameters obtained from Section 6.10.2 in ANL-NBS-HS-000032, <i>Simulation of Net Infiltration for Modern and Potential Future Climate</i> .	Effective root-zone porosity controls the amount of water in temporary storage in that zone. If the volume of water that can be held in temporary storage is exceeded in the model, the excess water becomes runoff (ANL-NBS-HS-000032, Section 6.4.5, p. 40).
Uncertainty distribution for infiltration model bedrock root-zone thickness multiplier for the glacial transition climate. Section 4.1.	ANL-NBS-HS-000032 Rev. 00	Assumed normal distribution with a mean of 3.000 meters with 1.0 and 99.0 percentile low and high range values of 1.0000 and 5.000 meters, respectively (Section 4.1, p. 14, Table 4-1)	Distribution parameters obtained from Section 6.10.2 in ANL-NBS-HS-000032, <i>Simulation of Net Infiltration for Modern and Potential Future Climate</i> .	Bedrock root-zone thickness controls the amount of water in temporary storage in this zone. If the volume of water that can be held in temporary storage is exceeded in the model, the excess water becomes runoff (ANL-NBS-HS-000032, Section 6.4.5, p. 40).
Uncertainty distribution for the first coefficient in the expression for evapotranspiration for the infiltration model for the glacial transition climate. Section 4.1.	ANL-NBS-HS-000032 Rev. 00	Assumed normal distribution with a mean of 1.040 with 1.0 and 99.0 percentile low and high range values of 0.540 and 1.540, respectively (Section 4.1, p. 14, Table 4-1)	Distribution parameters obtained from Section 6.10.2 in ANL-NBS-HS-000032, <i>Simulation of Net Infiltration for Modern and Potential Future Climate</i> .	This coefficient has a direct effect on the evapotranspiration. Evapotranspiration has an inverse effect on infiltration; higher evapotranspiration results in less infiltration (ANL-NBS-HS-000032, Section 6.4.6, p. 41).

Uncertainty distribution for the second coefficient in the expression for evapotranspiration for the infiltration model for the glacial transition climate. Section 4.1.	ANL-NBS-HS-000032 Rev. 00	Assumed normal distribution with a mean of 1.040 with 1.0 and 99.0 percentile low and high range values of 0.540 and 1.540, respectively (Section 4.1, p. 14, Table 4-1)	Distribution parameters obtained from Section 6.10.2 in ANL-NBS-HS-000032, <i>Simulation of Net Infiltration for Modern and Potential Future Climate</i> .	This coefficient has an inverse effect on evapotranspiration. Evapotranspiration in turn has an inverse effect on infiltration; higher evapotranspiration results in less infiltration (ANL-NBS-HS-000032, Section 6.4.6, p. 41).
Uncertainty distribution for the surface flow runoff area for the infiltration model for the glacial transition climate. Section 4.1.	ANL-NBS-HS-000032 Rev. 00	Assumed normal distribution with a mean of 100 with 1.0 and 99.0 percentile low and high range values of 0.01 and 0.490, respectively (Section 4.1, p. 14, Table 4-1)	Distribution parameters obtained from Section 6.10.2 in ANL-NBS-HS-000032, <i>Simulation of Net Infiltration for Modern and Potential Future Climate</i> .	Surface runoff has an inverse effect on infiltration. Water which contributes to runoff is unavailable for infiltration at that location (water routed to other areas of the watershed may still infiltrate) (ANL-NBS-HS-000032, Section 6.4.7, p. 41-43).
Uncertainty distribution for the daily evapotranspiration multiplier for the infiltration model for the glacial transition climate. Section 4.1.	ANL-NBS-HS-000032 Rev. 00	Assumed normal distribution with a mean of -10.000 with 1.0 and 99.0 percentile low and high range values of 0.6000 and 1.400, respectively (Section 4.1, p. 14, Table 4-1)	Distribution parameters obtained from Section 6.10.2 in ANL-NBS-HS-000032, <i>Simulation of Net Infiltration for Modern and Potential Future Climate</i> .	Evapotranspiration has an inverse effect on infiltration; higher evapotranspiration results in less infiltration (ANL-NBS-HS-000032, Section 6.4.6, p. 41).
Uncertainty distribution for the daily precipitation multiplier for the infiltration model for the glacial transition climate. Section 4.1.	Precipitation records provided by the USGS (DTN: GS000308311221.010)	Assumed normal distribution with a mean of -10.000 with 1.0 and 99.0 percentile low and high range values of 0.6000 and 1.400, respectively (Section 4.1, p. 14, Table 4-1)	Distribution parameters obtained from Section 6.10.2 in ANL-NBS-HS-000032, <i>Simulation of Net Infiltration for Modern and Potential Future Climate</i> . Only the glacial-transition climate was considered as this climate is forecast to dominate the duration of	Precipitation has a direct effect on infiltration; higher precipitation results in higher infiltration. However, high daily precipitation values will exceed the soils capacity to absorb water and a portion will report to runoff. This then results in less of the annual precipitation contributing to infiltration.
Uncertainty distribution for the snow-melt parameter for the infiltration model for the glacial transition climate. Section 4.1.	ANL-NBS-HS-000032 Rev. 00	Assumed uniform distribution with a mean of 1.78 with low and high range values of 0.78 and 2.78, respectively (Section 4.1, p. 14, Table 4-1)	Distribution parameters obtained from Section 6.10.2 in ANL-NBS-HS-000032, <i>Simulation of Net Infiltration for Modern and Potential Future Climate</i> .	Amount of snow melt incorporated in the infiltration simulations. The amount of snow melt has a direct effect on infiltration as water from snow melt enters the root-zone water balance and is subsequently available for infiltration (ANL-NBS-HS-000032, Section 6.4.3, p. 38.)
Uncertainty distribution for the soil zone thickness multiplier for the infiltration model for the glacial transition climate. Section 4.1.	ANL-NBS-HS-000032 Rev. 00	Assumed normal distribution with a mean of 3.000 with 1.0 and 99.0 percentile low and high range values of 0.05 and 1.500, respectively (Section 4.1, p. 14, Table 4-1)	Distribution parameters obtained from Section 6.10.2 in ANL-NBS-HS-000032, <i>Simulation of Net Infiltration for Modern and Potential Future Climate</i> .	Soil zone thickness controls the amount of water in temporary storage in this zone. If the volume of water that can be held in temporary storage is exceeded in the model, the excess water becomes runoff (ANL-NBS-HS-000032, Section 6.4.5, p. 40).

Uncertainty distribution for the soil saturated hydraulic conductivity multiplier for the infiltration model for the glacial transition climate. Section 4.1.	ANL-NBS-HS-000032 Rev. 00	Assumed lognormal distribution with a mean of 1.000 with 1.0 and 99.0 percentile low and high range values of 0.05 and 20.0, respectively (Section 4.1, p. 14, Table 4-1)	Distribution parameters obtained from Section 6.10.2 in ANL-NBS-HS-000032, <i>Simulation of Net Infiltration for Modern and Potential Future Climate</i> .	Potential infiltration which exceeds the saturated hydraulic conductivity for the soil layer is held in temporary storage in the overlying layer or contributes to runoff if the soil layer is the uppermost layer (ANL-NBS-HS-000032, Section 6.3.1, p.26 and 27).
Uncertainty distribution for the first term in the snow loss (sublimation) equation for temperature regime below freezing for the infiltration model for the glacial transition climate. Section 4.1.	ANL-NBS-HS-000032 Rev. 00	Assumed uniform distribution with a mean of 0.1 with low and high range values of 0 and 0.2, respectively (Section 4.1, p. 14, Table 4-1).	Distribution parameters obtained from Section 6.10.2 in ANL-NBS-HS-000032, <i>Simulation of Net Infiltration for Modern and Potential Future Climate</i> .	Amount of sublimation incorporated in the infiltration simulations. Greater amounts of sublimation reduce the amount of moisture available for infiltration (ANL-NBS-HS-000032, Section 6.4.3, p. 37 and 38).
Results of the uncertainty calculations for the lower, upper, and middle infiltration simulations. Section 6.2.	Analog infiltration simulation results presented in U.S. Geological Survey, 2000, <i>Simulation of Net Infiltration for Modern and Potential Future Climate</i> .	Since scaling factors were sampled for input parameter properties, assumed each watershed comprising the assumed rectangular footprint region has the same relative variability in their climatic, geologic, and hydrological properties. Each input parameter was assumed to vary independently.	Watershed delineations obtained from DTN: GS000308311221.004. Basis for the assumption of a rectangular area was that the INFIL program code used to perform the infiltration analysis and construct infiltration rate maps only considers rectangular regions	The rectangular area used in this AMR is slightly larger than the potential repository area and includes areas with relatively higher estimates of net infiltration. This results in slightly higher mean infiltration rates for the rectangular area relative to the repository area.
<b>Variability</b>				
Not applicable.				
<b>Results</b>				
Infiltration maps (low, mean, and high) for three climate states.	<i>Simulation of Net Infiltration for Modern and Potential Future Climates</i> , ANL-NBS-HS-000032.	Each of the identified future climate states is evaluated to produce three infiltration maps for low, mean, and high infiltration scenarios.	Infiltration maps are based on the best available conceptual model, relevant information, and process modeling.	Infiltration maps provide estimates of the upper boundary condition for UZ flow modeling. However, surface input is believed to be subsequently modified in volume and spatial distribution as it percolates deeper into the mountain. No major impacts presently identified.

## 5.0 Unsaturated Zone Flow Model and Submodels

### 5.1 Purpose of Model/Intended Use

The UZ Flow Model and its submodels have been developed to simulate past, present, and future hydrological, geochemical, and geothermal conditions in the UZ at Yucca Mountain. Its primary objective is to integrate the data/modeling results available from a wide variety of sources/AMRs into a single, comprehensive, and calibrated 3D model. Development of submodels for perched water, flow through the Paintbrush Tuff nonwelded hydrogeological unit (PTn) and Calico Hills nonwelded hydrogeological unit (CHn), and thermal effects from repository operations with representative initial and boundary conditions is also a major objective of the UZ Flow Model effort. The flow model provides parameters and conditions for models developed for predicting seepage into drifts and the evolution of the near-field environment (NFE), items critical to PA and Repository Design. The UZ flow model also provides PA with 3D flow fields for use by the Finite Element Heat and Mass Transfer (FEHM) particle tracker in the TSPA abstraction.

Many interrelated physical processes combine to determine the nature of the UZ flow field. These processes are intimately linked to hydrogeologic processes and features of the variously welded, heterogeneous volcanic rocks that comprise the UZ at Yucca Mountain. The conceptual model of flow and transport provides a framework to explain and understand these processes in the UZ at Yucca Mountain. The current conceptual model is largely based on ideas originally formulated by Montazar and Wilson (1984) and has been subsequently developed through evaluation of data collected from numerous YMP field and laboratory studies and modeling exercises.

Generally speaking, the welded units typically have low matrix porosities and high fracture densities, whereas the nonwelded units have relatively high matrix porosities and low fracture densities. Water infiltrating/percolating downward through these units is partitioned between fractures and matrix components. It is the objective of the UZ Flow Model to describe the flow field that results from this fracture vs. matrix partitioning within the individual hydrogeologic units for a given set of initial and/or boundary conditions.

The modeling approaches employed in the development of the UZ Flow Model are a mixture of both state-of-the-art techniques and more generally accepted methods of using data to interpret aspects of UZ hydrologic systems in arid environments.

### 5.2 Model Relations

As illustrated in Figure 5-1, UZ Flow (Ambient and TH) Model Relation Diagram the following AMRs provide input to the UZ Flow Model and Submodels AMR:

*Development of Numerical Grids for UZ Flow and Transport Modeling* (ANL-NBS-HS-000015)  
– Provides geologic framework (from Integrated Site Model) and numerical grid for the assignment of physical properties (geologic, hydrologic, calibrated/uncalibrated) to the various lithologic units.

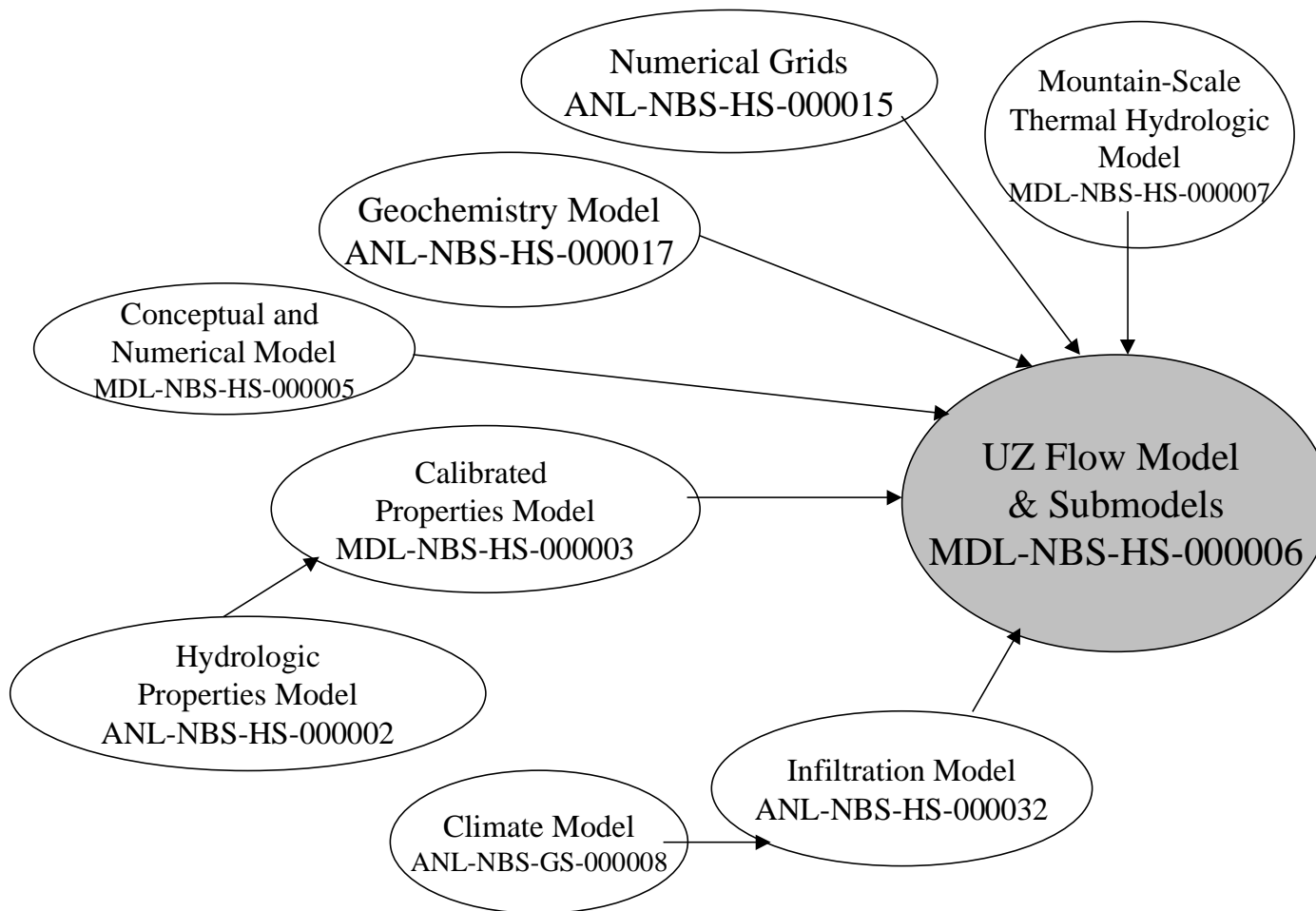


Figure 5-1: UZ Flow (Ambient and TH) Model Relation Diagram

*Future Climate Analysis* (ANL-NBS-GS-000008) – Provides prediction of precipitation and temperature ranges expected for three possible future climate scenarios (modern, monsoon, glacial transition).

*Simulation of Net Infiltration for Modern and Potential Future Climate States* (ANL-NBS-HS-000032) – Takes input from the Climate model and provides estimates of infiltration (low, mean, and high) for the three climate states. This output is the upper boundary condition for the UZ Flow Model.

*Conceptual and Numerical Model of UZ Flow and Transport* (MDL-NBS-HS-000005) – Provides a conceptual framework to explain the overall interrelationship of various physical parameters, field observations, and UZ processes.

*Calibrated Properties Model* (MDL-NBS-HS-000003) – Provides calibrated properties (fracture and matrix saturations, van Genuchten parameters for fracture and matrix components, active fracture parameter) to UZ flow model. These calibrated properties are derived from one-dimensional (1D) and two-dimensional (2D) mathematical inversions made to portions of the available UZ data sets.

*UZ Flow Model and Submodels* (MDL-NBS-HS-000006) – Provides boundary conditions for temperature, gas pressure, and liquid saturations for upper and lower model boundaries (surface and water table, respectively). All other AMRs listed in this section provide input to this AMR.

*Analysis of Geochemical Data for the Unsaturated Zone* (ANL-NBS-HS-000017) – Uses geochemical data to provide flow field with constraints on expected infiltration, percolation flux, and degree of fracture/matrix interaction.

*Analysis of Hydrologic Properties Data* (ANL-NBS-HS-000002) – Develops hydrologic property estimates and provides this data to UZ Flow Model and Calibrated Properties Model.

*Mountain-Scale UZ Thermal-Hydrological Model* (MDL-NBS-HS-000007) – Provides conceptual basis and model simulations of coupled heat and fluid flow in the UZ resulting from heat released by the decay of radioactive waste in emplacement drifts of the potential repository.

### **5.3 Model Structure**

Figure 5-2, Model Structure for Unsaturated Zone Flow, shows the general structure of the UZ Flow Model, with emphasis on the principal areas addressed by the model. Specifically, these general groupings include the Conceptual Model, the Parameters/Inputs, the Representational Model, Results, and TSPA Abstraction.

#### **Conceptual Model**

Four major assumptions underlie the development of the conceptual model of UZ flow:

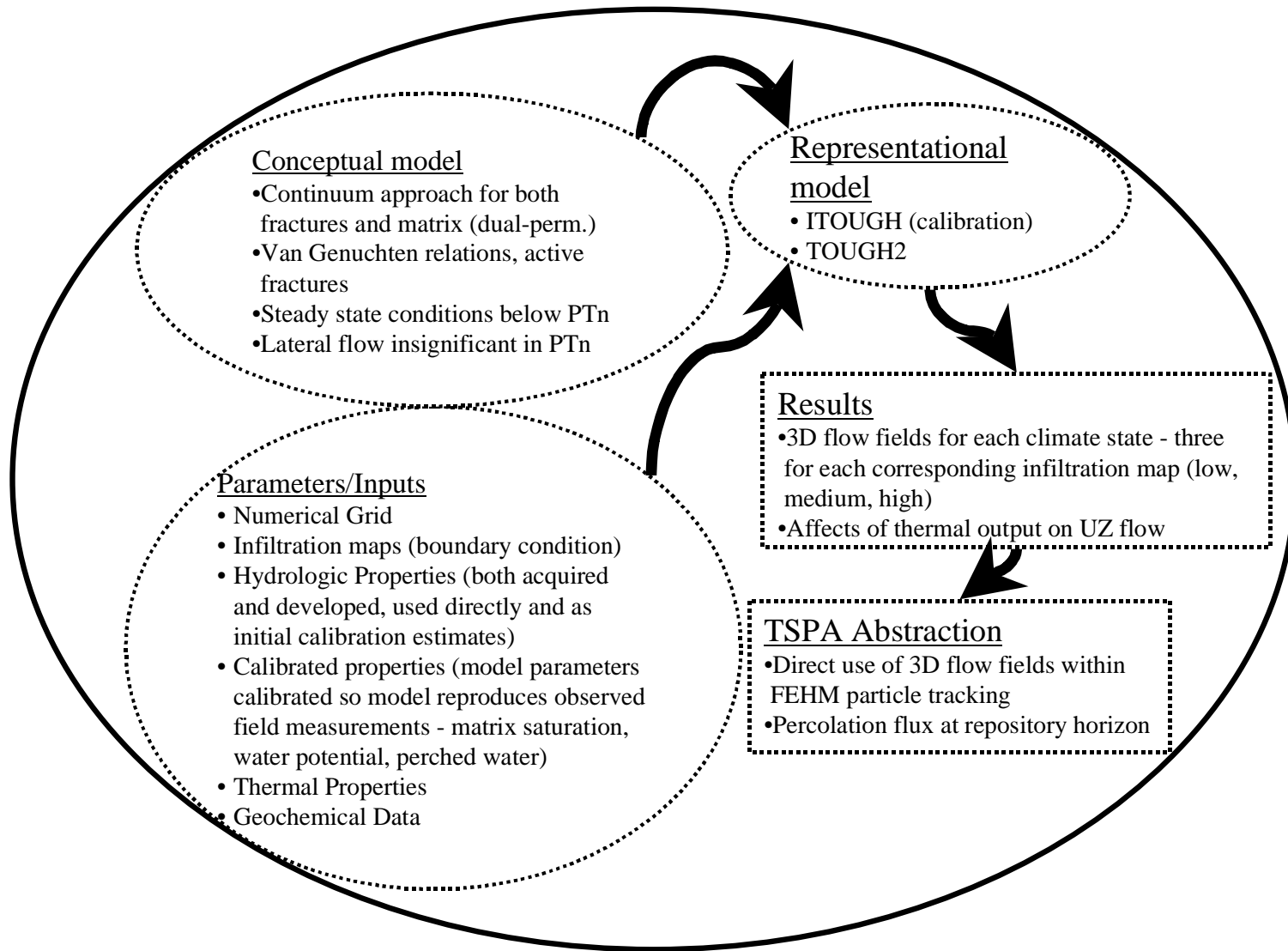


Figure 5-2: Model Structure for Unsaturated Zone Flow

1. Fracture networks can be represented by a continuum. The appropriateness of this assumption is mainly supported by the existence of dispersed fractures that actively conduct water.
2. Van Genuchten relations, originally developed for porous media, can be used as constitutive relations for liquid flow in the active fracture continuum. This assumption results from use of porous-medium equivalence for describing flow and transport in fractures.
3. Liquid flow in the UZ (specifically in the repository horizon) at Yucca Mountain is in steady-state due to dampening of transient flow by the PTn.
4. Lateral flow within the PTn is insignificant. Recent modeling studies have indicated that lateral flow within the PTn is reduced with an increase in infiltration rate, and only becomes significant (in terms of fraction of flow) when infiltration is far lower than current estimates.

In addition to unsaturated flow under ambient conditions, the effects of heat on the ambient flow field must be studied. The Mountain-Scale Thermal-Hydrological (MSTH) Model evaluates the effects of heat on UZ flow and the distribution of liquid and temperature over a period of 100,000 years. This model provides the necessary framework to test conceptual hypotheses of coupled heat and fluid flow in the UZ in response to the heat released by the decay of radioactive waste in emplacement drifts of the potential Yucca Mountain repository under a variety of thermal loading conditions.

**Parameters/Inputs** – UZ Flow Model parameters and inputs include both developed data and acquired data sources as listed below:

**Developed Data** – numerical grids, infiltration maps, calibrated fracture and matrix properties (active fracture parameter, van Genuchten parameters, permeability), estimates of percolation flux, and estimates of property uncertainty for use in initial estimates and/or to constrain the calibration exercise.

**Acquired Data** – uncalibrated fracture and matrix properties (liquid saturation, porosity, aperture, interface area), water potential data, pneumatic pressure data, stratigraphy, perched water data (locations, elevations), infiltration data, hydrologic property data, geothermal measurements, geochemical data, thermal properties (conductivity, specific heat, tortuosity), and transport properties.

**Numerical Grid** – Model domain was selected to facilitate studies at or near the potential repository area and to investigate effects of varying infiltration on fluid flow, heat flow, and radionuclide transport. A 3D numerical grid designed for simulations of 3D flow fields uses refined meshes in the vicinity of the repository horizon. Geologic formations within the UZ have been reorganized into layered hydrogeologic units primarily based on the degree of welding of the rocks.

**Infiltration Maps** – Nine infiltration maps are supplied to the UZ Flow Model. These consist of maps for low, mean, and high infiltration scenarios for each of the three climate stages, modern, monsoon, and glacial transition. These serve as input for the upper boundary condition.

The Calibrated Properties Model incorporates many different types of data from analyses and models (notably the Hydrologic Properties Model) into one model to develop calibrated properties (through the process of mathematical 1D and 2D inversion) for the UZ Flow Model. Properties derived in this manner are considered to be more “globally” representative and therefore more useful for the scale of interest. The model provides calibrated properties for saturation values, fracture and matrix permeability, fracture and matrix van Genuchten parameters, and the active fracture parameter. Due to the scale-dependent behavior of fracture permeability, model calibrations were performed on two scales, the mountain-scale and the drift-scale. The use of mathematical inversion methods to determine effective parameters/properties of data has been employed in many scientific and technical studies and can be considered an established technique.

The Ambient Geochemistry Model incorporates geochemical conceptual models and analyses to quantitatively describe geochemical processes relevant to establishing bounds on infiltration fluxes and percolation rates. The data contained in the AMR come from numerous sources including surface and subsurface core, gas, and water samples, in situ testing, and both field and laboratory measurements. Three main approaches/data sets are used to provide chemical constraints on infiltration and percolation flux: 1) chloride chemistry data; 2) Cl-36/Cl ratio data; and 3) calcite abundances. Many other chemical species are discussed in the AMR/Model (H-3, stable isotopes of H, O, and C, Sr, U, C-14, etc.), but due to limited data or sampling/analytical uncertainty, they are only considered as supporting information for the larger, less ambiguous data sets. Input on water chemistry is also provided to the near field, coupled process, and transport models.

### **Representational Model**

The numerical modeling approach for the UZ Flow Model is based on the TOUGH2 code, V1.4, for coupled multiphase, multicomponent liquid/heat flow in porous and/or fractured media. Based on the integrated finite-difference method, TOUGH2 applies mass conservation equations for air, water, and chemical constituents, and thermal energy equations, to perform dual-permeability simulations of multiphase flow in fractured porous media.

For the calibration exercise, iTOUGH2, V3.2 was used to minimize the misfit between observed and ambient conditions and differences between prior information and calibrated values for input parameters.

### **Results**

The UZ Flow Model produces 3D flow fields for each climate state (present-day, monsoon, and glacial transition) for three different infiltration scenarios (low, mean, and high).

Specific results of the MSTH model include qualitative and quantitative evaluation of the following issues:

- Extent of the two-phase (liquid and vapor water) zone and the boiling zone
- Liquid and gas flux in both the near-field and far-field
- Moisture redistribution in the UZ
- Temperature at drift walls and in pillars between drifts
- Potential for property changes in nonwelded units (PTn, CHn)
- Effects on water table and perched water bodies
- Influence of climate and ventilation

### **TSPA Abstraction**

The UZ Flow Model provides 3D flow field for use by the FEHM particle tracking in TSPA abstraction. Specification of percolation flux at the repository horizon is the most important parameter abstracted.

### **5.4 Discussion of Uncertainty/Variability Treatment**

This section presents the major findings from the review of the AMRs that contribute to the UZ Flow Model. The complete set of review comments is provided in Table 5-1.

### **Conceptual Models**

The assumption of steady-state conditions below the PTn is supported by comparison of field/laboratory data and modeling results. Flow model dual-permeability calculations can, as stated in the *UZ Flow Model and Submodels* AMR, “reasonably reproduce observed liquid saturations and water potentials” and thus provide support for the assumptions of steady-state conditions. Transient effects have not yet been incorporated into the flow model and steady-state results for layers above the PTn neglect the effects of episodic infiltration.

Overall flow and transport behavior within the UZ may be characterized by two important features:

- The coexistence of a few isolated, transient, fast flow paths and relatively uniform flow and transport within the fractures. These isolated flow paths are believed to carry only a small amount of water and do not significantly contribute to the overall flow and transport patterns in the UZ. Therefore, the dispersed nature of fracture flow should be the critical basis for evaluating numerical approaches for UZ modeling of flow and transport, and thus supports the choice of continuum methods for Yucca Mountain.
- The coexistence of matrix-dominated flow and transport in the nonwelded units and fracture-dominated flow and transport in the welded units. This second feature can be easily handled by continuum approaches, but not by other methods such as a fracture-network model, which rarely consider fracture-matrix interaction. Also, the enormous number of fractures present at Yucca Mountain (estimated at  $10^9$ ) precludes a fracture-network approach.

The use of the dual-continuum model for representation of the fractured unsaturated system treats the fracture network as a porous continuum. Such an approach assumes that the details of the fracture system are not significant to overall flow behavior. No treatment or discussion of uncertainty regarding this assumption is given in the model; however, the assumption is consistent with standard practice in the hydrologic modeling community (i.e., National Research Council). A related source of uncertainty is whether the active fracture model effectively captures the relevant details of flow within the fractures. The active fracture model was developed in recognition that only a portion of the fracture network participates in fluid flow. The inversion process produces the active fracture coefficient as an output variable. No measured data currently exists to corroborate this parameter estimate, so considerable uncertainty remains.

Based on assigned properties, faults are considered the primary conduit for radionuclide migration in the UZ Flow Model. Percolation fluxes in the UZ are predicted to converge into faults as water moves downward through the geologic units. Lateral diversion of water in the CHn and PTn units eventually encounters high angle faults that serve as flow focusing conduits for downward flow. Under glacial conditions, up to 54 percent of flow is predicted to pass through the faults to the water table. Uncertainty with this prediction arises due to:

- Lack of data from areas where perched water is in contact with a fault.
- Limited measurements of fault zone properties, particularly the influence of the CHn at fault locations (i.e., effects of change in hydraulic properties due to juxtaposition of contrasting lithologies in faulted areas, and effects of faulting on the relative components of fracture vs. matrix flow). This limitation is the major source of the uncertainty.

Modeling scenarios indicate significant lateral diversion at the CHn, and eastward into the Ghost Dance fault, resulting from the presence of perched water and/or thick low-permeability zeolitic layers. This portion of the conceptual model has not been tested and therefore is still highly uncertain.

In its present state of development, the UZ flow model does not incorporate the entire range of chemical data available for the UZ water/gaseous system as documented in the ambient geochemistry AMR. With the exception of chloride chemistry (total Cl and Cl-36/Cl) submodels and the calcite submodel, individual data sets (U-data, Sr-data, O-data, etc.) have typically been analyzed independently. Although these other data sets have not been developed into submodels or directly input to the flow model, they are still used to support/corroborate the model.

Results of chloride and calcite modeling help decrease uncertainty in UZ infiltration and percolation flux by establishing chemical constraints (i.e., what range of infiltration or percolation can be supported based on the observed chemical indicators). Greater confidence in the UZ flow model and further reduction in uncertainty could be achieved if the number of chemical species and data sets considered were enlarged.

## **Representational Model**

The hydrologic system is distinctively heterogeneous on all model scales and there are orders-of-magnitude contrasts in properties across geological layers and between fractures and rock matrix. No explicit analysis of uncertainty introduced due to the numerical grid (block size) and effects of volume-averaging is provided.

## **Parameters**

Uncertainty in input from the infiltration model is addressed by calibrating properties using a range of infiltration rates (low, mean, high). For both the mountain- and drift-scale, calibrated properties are produced for three different present-day infiltration scenarios. By providing calibrated property sets for each of these scenarios, potential future climate impacts on flow/transport can be evaluated with respect to uncertainty in present-day infiltration. Variability of input from the *Analysis of Hydrologic Properties Data* AMR is incorporated into weighting factors for calibrated property inversions.

Much of the uncertainty in the calibrated properties model comes from the underconstrained nature of inverting matrix saturation data to assign material properties to fractures based on a limited data set with many assumptions. Lack of measurements pertaining to fracture saturations in the individual rock units is the most critical. Because the calibrated properties model uses a dual continuum formulation, one should be calibrating to both fracture *and* matrix conditions. Although pneumatic testing indicates that the fracture permeability values are reliable (i.e., good agreement between test results and inversion results), the van Genuchten fracture parameters and fracture moisture parameters (water potential and saturation) are poorly constrained. If fracture-matrix interactions are highly impeded, property calibrations made for fractures based on matrix saturations may be erroneous. No discussion of uncertainty due to lack of fracture saturation data is provided.

Uncertainties are difficult to quantify for the fracture moisture-data parameter sets (saturation, water potential) because of data limitations. In addition, many of the parameters are cross-correlated and varying two or more of them simultaneously can produce the same effect on the predicted response of the system. Lack of a well-defined global minimum, and the existence of numerous, equivalent, local minima, can cause any of these local minima to produce an equally good parameter set (i.e., one that when input to the flow model may still reasonably reproduce the observed matrix saturations). Unlike the moisture data (calibrated fracture saturation), calibrated fracture permeability uncertainty estimated by the inversion of pneumatic data is low, because the data are plentiful.

Data limitations are the basic cause for poor-constraint of the calibrated properties model, where 233 data points are used to provide calibrations for 163 parameters. The final calibrated properties model, however, is taken as being acceptable because there is only a relatively small change from initial to final property estimates.

The issue of scaling was addressed through the calibration process by performing these calibrations directly on the scales of interest (mountain-scale vs. drift-scale). Subsequently, uncertainty effects due to using parameters determined on an inappropriate scale are not

expected to present a major concern because the calibration was performed on the scale intended for the particular process being modeled.

Percolation flux, probably the most critical factor for characterizing UZ flow and transport, depends strongly on infiltration rate and spatial distribution of infiltration. Percolation flux in the UZ cannot be measured directly in the field, so indirect data and model results, much of which are subject to considerable uncertainty, are used to estimate the flux. Although some uncertainty still exists, by using a variety of physical, hydrologic, and chemical indicators, the range of supportable present-day percolation flux appears to be reasonably well-constrained in the range of about 3 to 8 mm/yr.

In general, and for most chemical species, the *Analysis of Geochemical Data for the Unsaturated Zone* AMR does a good job of identifying the sources of uncertainty for the various chemical species considered in the model. In circumstances where the conditions under which samples were collected is suspect, clear indication of what portions of the data set were used, and what was not used, is given. Uncertainties are given in terms of sampling procedures and conditions, analytic/measurement precision, and statistical analysis to identify data population outliers (i.e., data points that should be excluded from consideration).

**Chloride chemistry:** Precision and accuracy have been monitored through the analysis of blind duplicate samples and standards, and background levels of contamination have been monitored through the analysis of blanks and sample duplicates. What is more uncertain is the chloride deposition rate determined from precipitation and eolian sources (wet/dry components, respectively). Only a small data set is available for analysis and conceptual/numerical model development. These records are of relatively short duration (7-12 years) and locations at which the data were gathered (Red Rock and Three Springs Valley) are between 100-125 km from Yucca Mountain. An additional source of uncertainty stems from spatial variability associated with precipitation. Because the measurements of total chloride constitute the principal data set that is used to constrain estimates of infiltration and percolation flux, such limitations can introduce considerable uncertainty. This uncertainty is not analyzed other than to assume that the available record is sufficiently representative of conditions at Yucca Mountain.

**Determination of bomb-pulse Cl-36 component:** The threshold value of the Cl-36/Cl ratio (values  $>1250 \times 10^{-15}$  indicating unambiguous bomb-pulse water) is evaluated through statistical analysis. Background levels of the Cl-36/Cl ratio have been determined to be  $550 \times 10^{-15}$ , so measurements indicating values between these two limits are interpreted to represent mixing of older and bomb-pulse waters. Analyses of samples collected from the ESF show that bomb-pulse waters are associated with samples collected from known faults and/or fracture zones. The Cl-36 model constructed for Yucca Mountain is a very specialized version of more routine procedures described in the published literature that employ Cl-36 as an indicator of hydrologic processes. No treatment/mention of concern underlying the ongoing Cl-36 validation exercise to determine whether the apparent Cl-36 signal is real or is an artifact of sample preparation and/or analytical procedures.

**Calcite abundance:** The calcite deposition model incorporates UZ processes that are believed to be important in the control of calcite precipitation. The hydrologic/chemical environment of

precipitation is treated as steady-state; evidence supporting this position comes from the opal-calcite dating of fracture/lithophysal coatings which indicates continuous deposition. Uncertainties regarding controls on the calcite deposition rate include effective reactive surface area, thermodynamic and kinetic input data, and unknown water chemistry as a function of time. Reasonable (i.e., within limits supportable by observations or experience) modifications to initial estimates of surface-reaction area captured both trends and absolute calcite abundances observed from boreholes and ESF mapping and fracture coating studies. This modeling approach provides an independent geochemical means of estimating infiltration rates and percolation flux in the UZ. Application of this technique is unique to Yucca Mountain.

**Mountain-Scale Thermal-Hydrology Model:** The MSTH model is based on the UZ Flow Model and uses climate variation, spatially varying infiltration, and mountain-scale calibrated properties to assess effects due to heat loading. Because no data on actual thermal perturbation on the mountain-scale exist, any uncertainty must be evaluated on the basis of the property data, flow fields, and boundary conditions applied to the theoretical model. Accuracy and validity of model results were evaluated based on the current understanding of fracture-matrix interactions, heat transfer, and two-phase flow in unsaturated fractured media. Modeled temperature distributions were compared to temperature profiles measured in boreholes to assess the ability of the model to replicate the ambient, mountain-scale temperature distribution. As assessed by Project scientists, the MSTH model predicted heat transfer near the drifts agrees with the observations from the Single Heater Test (SHT) and the Drift Scale Test (DST). Additional support for liquid redistribution is provided from DST data on condensation in fractures, air-injection tests, neutron logs, and electrical resistivity logs.

## **5.5 Uncertainty Propagation**

The calibrated properties model produces calibrated values for fracture and matrix saturations, fracture and matrix permeabilities, fracture and matrix van Genuchten parameters, and the active fracture parameter. Limitations, and resultant uncertainty, of the calibrated properties model are inherent in the lack of measured fracture saturation data and data applicable to testing/verifying the active fracture parameter. Results of the calibration process are fed directly into the UZ Flow Model which, in turn, provides flow fields to TSPA. No explicit input or abstraction of the calibrated properties model to TSPA is provided.

Partial validation of the Calibrated Properties Model is achieved in the following areas:

- The model is calibrated within experimental data sets.
- Comparison of predictions using the calibrated properties and the UZ Flow and Transport (F&T) Model to other data not used for calibrations. (Reasonable agreement achieved.)
- Reasonableness of calibrated values in relation to all relevant data. No major departures from expected values (i.e., measured data) are observed for the calibrated properties.
- Technical review through publication.

The Geochemistry Model serves to provide constraint for estimates of infiltration and percolation flux used in the UZ Flow Model. No actual chemistry data is fed to the UZ Flow Model or TSPA. Geochemical data is used to evaluate the ranges of infiltration or percolation flux to see if the infiltration/percolation ranges are capable of producing the observed abundance of a particular chemical species or explaining the observed characteristics of features such as fracture coatings. These findings, in turn, can be compared to estimates of infiltration and percolation obtained from other UZ studies to develop confidence in parameter estimates.

In addition, certain chemical relationships found within the UZ (the U-234/U-238 ratio, in particular) not only provide insight to what conditions prevail in the UZ, but also provide information as to what processes/controls may be operating within the SZ. For example, the high U-isotope ratios (up to 8) found within UZ waters can *only* be produced under conditions of low percolation flux. Survival of these anomalously high U-isotope ratios in recharge to the upper SZ *requires* low recharge flux from the UZ and sluggish circulation within the SZ beneath Yucca Mountain. If significant SZ through-flow were taking place, the high U-234/U-238 ratio found in waters beneath Yucca Mountain would be diluted to lower values more representative of SZ conditions observed throughout the region (commonly 2-4). Hence, chemical data from the UZ can help constrain SZ flow parameters and reduce uncertainty in UZ/SZ transport.

Because pore water, gas-phase, and fracture-coating chemistry record long-term behavior of the UZ system, their composition should, in principle, reflect the time-integrated product of the various chemical inputs and physical processes. At this stage of development, however, there is no overall model that incorporates all chemical/isotopic data sets into one integrated geochemical model capable of explaining the observed distribution and abundances of the various hydrochemical indicators.

The MSTH Model has no direct feeds to TSPA. All thermal input to TSPA comes from the EBS/Near Field studies. Limitations on the accuracy and potential applications of results of the MSTH simulations are largely due to uncertainty resulting from an as yet unspecified final repository design (i.e., heat load, drift spacing, etc.) and the scarcity of thermal property data, particularly from the Topopah Spring welded hydrogeological unit (TSw) lower lithophysal unit. Although thermal modeling techniques have been used before on various geothermal projects, the scale, complexity, and timeframe of interest of this modeling effort make it state-of-the-art.

**Model Calibrations:** As part of developing confidence in model predictions, the UZ Flow Model has been calibrated to water potentials, saturations measured in the field, and occurrences of perched water using two conceptual models. The calibrated properties (both mountain- and drift-scale) produced by the inversion method represent the best estimates available. Accurate estimation of such a large number of parameters, however, is a difficult and complex problem given data limitations and grid resolution of the numerical model, and significant uncertainties remain.

Scarcity of data on ambient flow within fractures is a major source of uncertainty, and finer discretization of the numerical models would facilitate more accurate comparison of model predictions to available data. For lack of a better means of assessing uncertainty with the calibrated properties, a “ball-park” estimate of uncertainty associated with the output (calibrated

properties) is provided by comparison with the uncertainty (principally standard deviation) assigned to the uncalibrated input parameters. After performing the inversion process, most properties experienced only modest change from initial estimates (input) obtained from site data. Such comparisons suggest that the calibrated properties are reasonably accurate.

An evaluation of this conclusion is found in the degree of agreement between predictions and field measurements of hydrologic properties made before the Cross Drift and several surface-based boreholes were completed. Modeling results are partially to generally consistent with field measurements.

Considerable uncertainty exists within the geochemistry model due to limited data and the complexity of chemical processes and interactions of the aqueous- and gaseous-phase components in the unsaturated zone. Those data sets for which there exists sufficient data/understanding to provide estimates of infiltration and percolation flux compare reasonably-well with estimates made from other sources such as geothermal heat flow.

Natural variability and heterogeneity in the geologic, hydrologic, chemical, and mechanical systems make such systems difficult to characterize and are the source of parameter uncertainty. In cases where insufficient data exists to yield a defensible range of values for a given parameter, either bounding values for the physical behavior of the system or conservative estimates of the range of physical behavior are used.

The flow fields produced by the UZ Flow Model and used in TSPA calculations have addressed remaining uncertainties through probabilistic simulations and appropriate conservative bounding where necessary. Given the inherent uncertainties in natural systems, the intent of such conservative approaches is to increase the defensibility of the models used in TSPA calculations.

## **5.6 Conclusions**

Model development and the calibrated properties on which the results are based are variably limited by the available site characterization data. In circumstances where parameter data sets are well-populated (i.e., pneumatic data), efforts to assess uncertainty have been thorough and quantitative estimates are reported.

Uncertainties in the results due to parameter input and model gridding are evaluated by generating a number of flow fields with various parameter sets, infiltration maps, and conceptual models (i.e., perched water). All reasonably supportable variants in conceptual models have been included in the evaluations to address uncertainty.

Blind test predictions and simulations of test results were performed to provide validation of the UZ flow model for its applicability, accuracy, and reliability to predict flow in the UZ at Yucca Mountain. Comparison of the matches between simulated and measured values for different data types, such as saturation, water potentials, seepage rate, pneumatic response, and tracer breakthrough, indicate a reasonable match for all cases studied. Such exercises may provide the best means of assessing impacts due to unaddressed uncertainties.

In general, the efforts to produce a viable, scientifically supportable flow model for the UZ appear to have been conducted in a conscientious manner, taking care to address uncertainty whenever sufficient data was available or testing of alternative approaches or conceptual models was possible. Model limitations and major sources of uncertainty will continue to result from imperfect knowledge of: 1) future climate and its effect on infiltration; 2) heterogeneity of rock and flow properties and their spatial distribution; 3) fracture and fault properties; and 4) lateral diversion within the CHn. Uncertainties with these items have been addressed by modeling studies to the extent possible.

**Table 5-1: Unsaturated Zone Flow Model**

**Model Purpose:** The purpose of the UZ Flow Models and Submodels is to simulate past, present, and future hydrological, geochemical, and geothermal conditions in the UZ at Yucca Mountain.

Summary	Source	Treatment	Basis	Impact
<b>Conceptual Model Uncertainty</b>				
<p>The largest uncertainty in the calibrated properties model is the underconstrained nature of inverting saturations to material properties on a limited data set with many assumptions. Perhaps the single largest gap is that the inversion is done on matrix saturations only, as there are no fracture saturation data.</p>	<p>Page 57, "discussion of results uncertainties" notes that "quantifiable uncertainties are difficult if not impossible to establish". The underconstraint results from using 233 data points to calibrate 163 parameters (in addition to the lack of fracture saturation data).</p>	<p>The small size of changes from initial estimates to final calibrated properties is taken as an indication that that inversion is not too bad. Monte Carlo or linear error analysis is suggested as a possible fix for better addressing the uncertainty issue.</p>		<p>The calibrated properties AMR uses a dual continuum model, hence one should be calibrating to both fracture and matrix conditions. The pneumatic testing does indicate that the fracture permeability parameters are reliable, but the van Genuchten parameters are highly unconstrained because there are no fracture saturation data. If the fracture-matrix interactions are highly impeded, any property calibrations of the fractures to the matrix saturation data could be uncertain.</p>
<p>The calibrated properties model depends on uncertain infiltration rates.</p>	<p>Future infiltration rates are estimated based on climate model.</p>	<p>Properties are calibrated using upper-bound, lower-bound, and base-case infiltration values.</p>	<p>Bounded based on ranges of precipitation experienced at analog meteorological sites</p>	<p>Bounding probably covers the range adequately, so impacts may not be major.</p>
<p>Fracture networks are assumed to be represented by a continuum for describing flow and transport processes. Questions concerning validity of the dual-continuum model for representing fractured unsaturated system.</p>	<p>The dual-continuum model treats the fracture network as a porous continuum. This approach assumes that details of fracture geometry are not significant to the flow behaviors.</p>	<p>Evaluation of alternative approaches (ECM, discrete fracture model) was performed for comparison.</p>	<p>The appropriateness of this assumption is mainly supported by the existence of dispersed fractures that actively conduct water.</p>	<p>Phenomena that can be shown to rely on discrete features or fractures (seepage into drifts, CI-36, H-3, etc.) may not be adequately investigated. Impacts may be limited, as the long as the model used for developing the calibrated properties uses the same assumptions as the 3D model that uses these properties</p>

The active fracture model may not adequately capture the internal details of flow within fractures (fracture-matrix interaction).	The active fracture model was developed in recognition that only a portion of the fracture network is conducting water for various reasons.	The active fracture coefficient is included as an output variable in the inversion process.		Although the active fracture concept may be approximate or lack detail, it may be effective as long as the calibrated properties are used in model that carry similar properties as the model used for developing the calibrated properties.
It is assumed that van Genuchten relations, originally developed for porous media can be used as constitutive relations for liquid flow in the active fracture continuum.	Interpretation from soil physics literature.	Alternative conceptual models are available but are not discussed.	The assumption results from the use of porous-medium equivalence for describing flow and transport in fractures.	Van Genuchten parameters will affect calculated saturation values, and fracture saturations influence fracture-matrix interaction area. This would affect diffusion and ground water travel time.
It is assumed that the observed state of saturation within the individual rock layers represents steady-state conditions resulting from the relevant hydrologic processes (infiltration, percolation, gas flow, etc.).	Low annual precipitation and infrequent storms may not have established consistent subsurface hydrologic state.	System is considered to be in steady-state due to time-integration effects of climate/hydrologic processes.	Both hydraulic and pneumatic testing support this position. Attenuation and time-lag of the surface barometric pressure signal is observed within the PTn. Transient behavior of infiltration from the ground surface of the mountain is filtered out because of damping effects of the near-surface PTn unit. Consistency of saturation values within individual rock units also support the assessment of steady-state conditions.	Although the assumption appears valid, if it were to be unsupported, UZ flow model would require major modification.
It is assumed that lateral flow is insignificant within the PTn unit. Early conceptual model hypothesized that significant lateral flow (due to capillary barrier effects) occurs within the PTn.	Variations in mineralogy and permeability have been observed within the PTn.	Recent modeling studies indicate that lateral flow is significant only when infiltration rates are far lower than current estimated values.	Improvements in PTn microstratigraphy data have been incorporated into modeling approaches.	Increased lateral flow within the PTn and diversion into the Ghost Dance fault would decrease the amount of water delivered to the repository horizon and help create more benign conditions within the potential repository.
Present conceptual model does not incorporate any treatment of the lithophysal cavities. Omission of such features imposes much uncertainty on thermal, hydrologic, chemical and mechanical models.	No data presently available on the thermal-hydrological-chemical-mechanical (THCM) behavior of lithophysal unit.	Lithophysae alter the flow of water and gas through the rock. The net effect on heat and mass transfer is unknown.	Preliminary results from systematic drilling in the Cross Drift suggest that unit is about one order of magnitude more permeable.	Predictions and modeling of heat and mass transfer in these units may be subject to as yet undetermined amounts of uncertainty.

<b>Representational Model Uncertainty</b>				
Resolution of the numerical grid	Large size of some grid blocks may introduce unwanted effects or misrepresent processes or properties.	Refined resolution within repository horizon (5 meter vert. Discret.). Lateral dimensions can be quite large outside repository boundary.		
<b>Parameter Uncertainty</b>				
Fracture permeability data are largely lacking from the base of the TSw and deeper units.	Lack of data in deeper units	Extrapolation from overlying units with similar lithology	Mapping data from boreholes and ESF	The fracture permeability of the CHn units is a major control on travel time and affects the matrix interactions required for retardation.
Fracture Frequency and Intensity in lower TSw, CHn, and deeper units are lacking and based on extrapolation.	Data from few boreholes	Extrapolation from similar overlying units	Mapping data from boreholes and ESF	The lack of data from deeper units, especially the CHn leaves room for alternate models; intensity values affect calculations of fracture interface area for matrix interactions.
Van Genuchten parameters for fractures are not measured directly.	No direct measurements	Calculation from aperture-capillary pressure relationships using apertures calculated using cubic laws, which may underestimate actual openings. Also assumes zero contact angle.	Calculation using theoretical aperture derived from packer test flows. For deeper units there are few packer tests, so calculated apertures are derived from similar overlying units.	As there are no direct measurements of fracture saturation, van Genuchten parameters that are assumed for the fractures will influence the model-calculated saturation values. Fracture saturation in turn influences wetted area for diffusion as well as groundwater travel time.
Fracture interface area difficult to measure directly.	Derived from intensity and frequency data in boreholes and ESF in units with exposures.		Mapping data cut off measurements at 30-cm, so some fracture area may have been neglected; on the other hand, not all fracture are potentially water bearing, so interfacial areas may be overestimated.	
Fracture porosity values based on very few data points	Only a few tests from one unit area available; not clear if gas-derived porosity will be similar to effective porosity of water in UZ transport (i.e. different types of dead-end pore space).	Test values extrapolated from one unit with modification to reflect assessments of differences with reference unit.	Gas tracer data	Fracture porosity is very important for groundwater travel time; however, in the UZ, the key is saturated porosity, and there are no fracture saturation data available for Yucca Mountain.

Matrix Hydraulic Properties (permeability, residual saturation, porosity, van Genuchten parameters) not available from all units.	Few tests available from lowest TSw, CHn, and deeper units.	Extrapolation of values to unsampled units from units with similar geology	Laboratory tests on cores and ESF samples	Not major
Distribution of vitric vs zeolitic portions of CHn is only poorly known. This hydrogeologic unit has a profound effect on transport issues. Small % of flow is believed to pass through zeolitized tuffs. Values of Ksat used to identify areas where CHn is vitric vs. zeolitic is based on limited data and an assumed correlation between porosity and Ksat.	UZ boreholes (total of approximately 20, with 7 in repository area)	Use of Ksat (from RPM (ISM 3.0)) as surrogate for distribution of vitric and/or zeolitic portions of CHn	Limited mineralogic analysis available to provide identification of vitric/zeol. Many more lab determinations of porosity and Ksat are available.	Uncertainty in distribution of zeolitic portion will affect groundwater flow and transport results (both numerical and conceptual aspects). Small scale heterogeneities can affect F&T calc. True mineralogic alteration and rock properties variation may not follow a layered model.
Fault properties are very important to flow and transport. These features presently convey a large % (up to 54%) of UZ flow below repository horizon. Few data exist to support these suspected properties.	Few boreholes penetrate faults (exceptions being in Alcoves 2 and 6, and UZ-7a). No fault information exists for faults below repository horizon, where transport impacts are most critical.	Fault properties are assumed to easily convey water. Treatment in Model: Vertical discretization is set equal in all three fault columns; interfaces of hydrogeological units (HGU) correspond to interfaces between gridblocks. Properties lumped by major HGU as weighted harmonic mean of non-fault properties of the constituent layers.	No measured fault properties below repository horizon available. Properties assigned based on limited measurements made at locations in upper UZ.	Faults are presumed to be major pathways for water transport. The lack of data, and even understanding of the differences of hydraulic structure between faulted and non-faulted rock, introduce major uncertainties.
<sup>36</sup> Cl/Cl ratios elevated above a threshold of about 1250 x 10 <sup>-15</sup> are attributable to the presence of bomb pulse fallout.	Assumption from the literature. Section 6.6.3; Tables 9, 13, 14. Assumption.	Statistical analyses (not shown in the AMR)	This threshold value is evaluated through statistical analysis. The interpretation of these data is not very sensitive to the precise threshold value that is calculated.	Water travel time estimates Infiltration rates. Flow mechanism.
Lower limits on pore-water and gas ages can be calculated based on the assumption that the initial <sup>14</sup> C activity is 100 pmc, and that decreases relative to the initial atmospheric activity are solely the result of radioactive decay.	Assumption. Section 6.6.4; Tables 9, 15, 16, 18, 19, 20	The high <sup>14</sup> C activities measured in the shallow boreholes are a result of global fallout and shows no indication of dilution by processes in shallow soil and bedrock. Because of various unresolved issues regarding sample representativeness apparent <sup>14</sup> C ages will be used to make preliminary interpretation. "However, a possible range of ages with some uncertainty can be assigned in the future when more data become available" (section 6.6.4.3).	The assumption for an initial <sup>14</sup> C activity of 100 pmc is supported by the high <sup>14</sup> C activities measured in the annulus of shallow boreholes (Tables 17 and 19).	Water travel time estimates. Flow mechanism.

<p>The chloride mass balance (CMB) method is assumed to be applicable to the estimation of infiltration rates at Yucca Mountain, for samples obtained above the CHn. The CMB method assumes one-dimensional, downward piston flow, constant average annual precipitation rate, constant average annual Cl deposition rate, no run-on or run-off, no Cl source other than precipitation and no Cl sink.</p>	<p>Section 6.9.2, 7; Tables 26,27. Assumption. Assumption. Of particular concern is the apparent discrepancy between infiltration estimates obtained by the CMB method and those obtained by the numerical infiltration model.</p>	<p>Well-established method for estimating recharge rates on a watershed scale and for estimating infiltration rates in deep soil profiles. Still need to show that it is applicable to Yucca Mountain conditions. The method appears to be valid for a first - approximation of infiltration at Yucca Mountain.</p>	<p>The CMB method is well-established for estimating recharge rates on a watershed scale and for estimating infiltration rates in deep soil profiles in which one-dimensional porous media flow can be assumed to apply. What has not been clearly established, however, is the validity of applying this method to an intermediate scale in which runoff and runoff may not be negligible, and in an environment where water is known to percolate through fractured rock.</p>	<p>Estimates of infiltration rates</p>
<p>Reported uncorrected <math>^{14}\text{C}</math> ages for fracture minerals are based on the law of radioactive decay and on the assumption that carbon initially incorporated into the mineral during its deposition contained 100 percent modern carbon.</p>	<p>Section 6.10.1.3, Figure 54. Assumption.</p>	<p>Calculated ages are maximum ages. <math>^{14}\text{C}</math> ages are used mainly for comparison purposes.</p>	<p>Although this assumption is not strictly true, it allows comparisons of <math>^{14}\text{C}</math> data in a geochronological framework that can be compared to <math>^{230}\text{Th}/\text{U}</math> and <math>\text{U}/\text{Pb}</math> ages; and this simplification is considered acceptable for the limited purpose of such comparisons. Calculated <math>^{14}\text{C}</math> ages are likely to be maximum ages due to incorporation of dead carbon at the surface and decay of <math>^{14}\text{C}</math> in the percolating water during travel time to site of calcite formation.</p>	<p>Seepage/percolation mechanism.</p>
<p>Reported ages calculated from <math>^{230}\text{Th}/\text{U}</math> and <math>^{207}\text{Pb}/^{235}\text{U}</math> ratios are based on the law of radioactive decay and on the assumption that studied minerals behaved as closed systems with regard to uranium and its decay products.</p>	<p>Section 6.10.1.3, 6.10.3, Table 28, Figures 54, 55, 56, 65, 67, 70 and 72. Assumption.</p>	<p>The studied minerals behaved as closed systems with regard to uranium and its decay products.</p>	<p><math>\text{U}-\text{Th}-\text{Pb}</math> isotope ratios rarely show disruption of the systematic evolution that allows ages to be calculated. Calculated <math>^{230}\text{Th}/\text{U}</math> ages are particularly sensitive to <math>\text{U}</math> leaching resulting in <math>^{230}\text{Th}/^{238}\text{U}</math> ratios greater than those allowed through closed-system decay. Lack of disturbed ratios supports the closed-system behavior of the <math>\text{U}</math> decay systems in calcite and opal.</p>	<p>Dating layers with mineral coatings. Flow/seepage mechanism. Thermal evolution of the UZ.</p>

<p>The estimated range of annual deposition rates for chloride at Yucca Mountain encompasses the present-day rate as well as the rates that prevailed when the sampled pore waters infiltrated below the soil zone. Variability.</p>	<p>Section 6.9.1, 7; Tables 26, 27. Assumption. To Be Verified (TBV) because chloride deposition rate is directly used in the CMB method for determining infiltration boundary conditions for the flow and transport model.</p>	<p>The assumption is supported by independent lines of evidence. Still needed is an estimate of uncertainties in the deposition rates.</p>	<p>This assumption is supported by several independent lines of evidence. However, what is still needed is an estimate of the uncertainties in the deposition rates, and propagation of that uncertainty through the resulting estimates of infiltration obtained by the CMB method.</p>	<p>Estimates of infiltration rates</p>
<p>Pore-water samples that have been analyzed for chloride are representative of the full spectrum of significant flow paths in the UZ at Yucca Mountain. Variability.</p>	<p>Section 6.9.2, 7; Tables 26, 27. Assumption.</p>	<p>Preferential flow allowing a portion of dilute infiltrating water to bypass root channels or fractures is negligible. Transport of Cl in soil can be approximated as piston flow.</p>	<p>It is possible that relatively dilute water that has infiltrated rapidly through fracture pathways may be inadequately represented by matrix pore water extracted for analysis because of incomplete mixing. If this is the case, matrix pore-water samples might be biased toward the slower moving, more concentrated matrix component of flow; and percolation estimates based on these samples would constitute lower bounds on the actual percolation rates. In the PTn, some component of the flux can bypass the matrix as fracture or fault flow, as evidenced by the presence of bomb-pulse tracers in the ESF.</p>	<p>Percolation/flux estimates</p>
<p>Reported calcite concentrations for cuttings from borehole WT-24 are based on the assumption that the secondary calcite is the only source for Ca released from the rock and measured CO<sub>2</sub> amounts.</p>	<p>Sections 6.10.1.1, 6.10.3.4, Figure 53. Assumption.</p>	<p>Various depositional mechanisms are evaluated. Observed textural and mineralogical features support the assumption.</p>	<p>No significant source of CO<sub>2</sub> other than calcite is present in the volcanic rock section.</p>	<p>Seepage mechanism/fracture fluxes</p>
<p>Calculated estimates of mineral formation temperatures or isotopic compositions of formation water are based on the assumption that the mineral deposition was an equilibrium process.</p>	<p>Assumption. Sections 6.10.2, 6.10.3 Mineral deposition as an equilibrium process is TBV.</p>	<p>All calculations assume that the mineral deposition was an equilibrium process.</p>	<p>Typically these assumptions are clearly stated in text when made. They are not necessarily valid, but provide a means of comparing temperature conditions between mineralization stages or between variations in the isotopic compositions of formation waters at different depositional episodes.</p>	<p>Seepage of water into emplacement drifts. Calculated release of radionuclides. Thermal evolution of the UZ.</p>

**Variability**

Fracture Permeability	Tests in vertical boreholes and ESF alcoves	Describe variability by mean and standard deviation of log values.	Lognormal variation is widely accepted in the literature.	None identified.
Fracture frequency	No variability, single values given for each unit and data lacking from deeper units.			
Van Genuchten parameters for fractures are not measured directly	No variability, single values given for each unit and data lacking from deeper units.			
Matrix hydraulic properties (permeability, residual saturation, porosity, van Genuchten parameters) are not available for all units.		Where data available, variability of permeability is expressed using mean and standard deviations of log values; porosity assumed normally distributed.		
The input data for the van Genuchten parameters and permeability are inherently variable.		Input data come from the <i>Hydrologic Properties</i> AMR. The variability measures of the input data are incorporated into the weighing factors for the property inversions. Presumably a parameter that has a large variability has more freedom to move during inversion than one that is less variable.		No clear impacts. The treatment of variability appears appropriate, except for uncertainty in the variability for those layers that have little data.

**Results**

Not applicable				
----------------	--	--	--	--

INTENTIONALLY LEFT BLANK

## 6.0 Drift Seepage Models

### 6.1 Purpose of Model/Intended Use

The objective of the Drift Seepage Models and supporting AMRs is to develop a seepage process calibration model and apply this model to the prediction of drift seepage under a variety of anticipated conditions (ambient, thermally disturbed, and future climate change). The results of this model are then abstracted for use in TSPA. Such an objective requires investigation of UZ flow processes over scales ranging from the mountain-scale distribution of percolation flux, to channeling and dispersion of flow at the intermediate-scale of the fracture network, to effects associated with the capillary-barrier (i.e., flow diversion) surrounding excavated openings, and on to micro-scale features of individual fractures. Other factors such as temperature, evaporative effects, and relative humidity of the drift environment also exert strong influence on the process.

Seepage testing, data collection, and related modeling studies are presented in four AMRs:

- *In Situ Field Testing of Processes* (AHL-NBS-HS-000005), which describes the pneumatic characterization and water-release experiments conducted in Niche 3650
- *Seepage Calibration Model and Seepage Testing Data* (MDL-NBS-HS-000004), which describes the development of a seepage process model and its calibration
- *Seepage Model for PA Including Drift Collapse* (MDL-NBS-HS-000002), which uses the seepage model to develop predictions for seepage under various conditions
- *Abstraction of Drift Seepage* (MDL-NBS-HS-000005), which describes the seepage abstraction process for use in TSPA

For the purposes of analyzing the in-situ water release tests and development of the seepage calibration model, *seepage* is defined as the flow of water into an excavated underground opening, such as a niche, alcove, or waste emplacement drift. This does not include vapor diffusion into the opening or condensation of water vapor within the opening. *Seepage flux* is defined as the rate of seepage/unit area of drift, and *seepage percentage* is defined as the ratio of seepage flux/percolation flux. **Note:** For the liquid-release tests, seepage percentage is the ratio of water seeping into the niche/total amount of water released. *Seepage threshold* is defined as the critical percolation flux beneath which there is no seepage observed. *Seepage fraction* is defined as the fraction of WPs affected by seepage, and is equivalent to the number of 5-m long sections of drift that experience nonzero seepage. *Percolation flux* is defined as the component of infiltrated precipitation that penetrates below the zone of evapotranspiration as liquid water moving downward through the unsaturated zone at some flow rate per unit area.

### 6.2 Model Relations

As illustrated in Figure 6-1, Seepage Model Relation Diagram, the following AMRs provide input and analyses to the Drift Seepage Models:

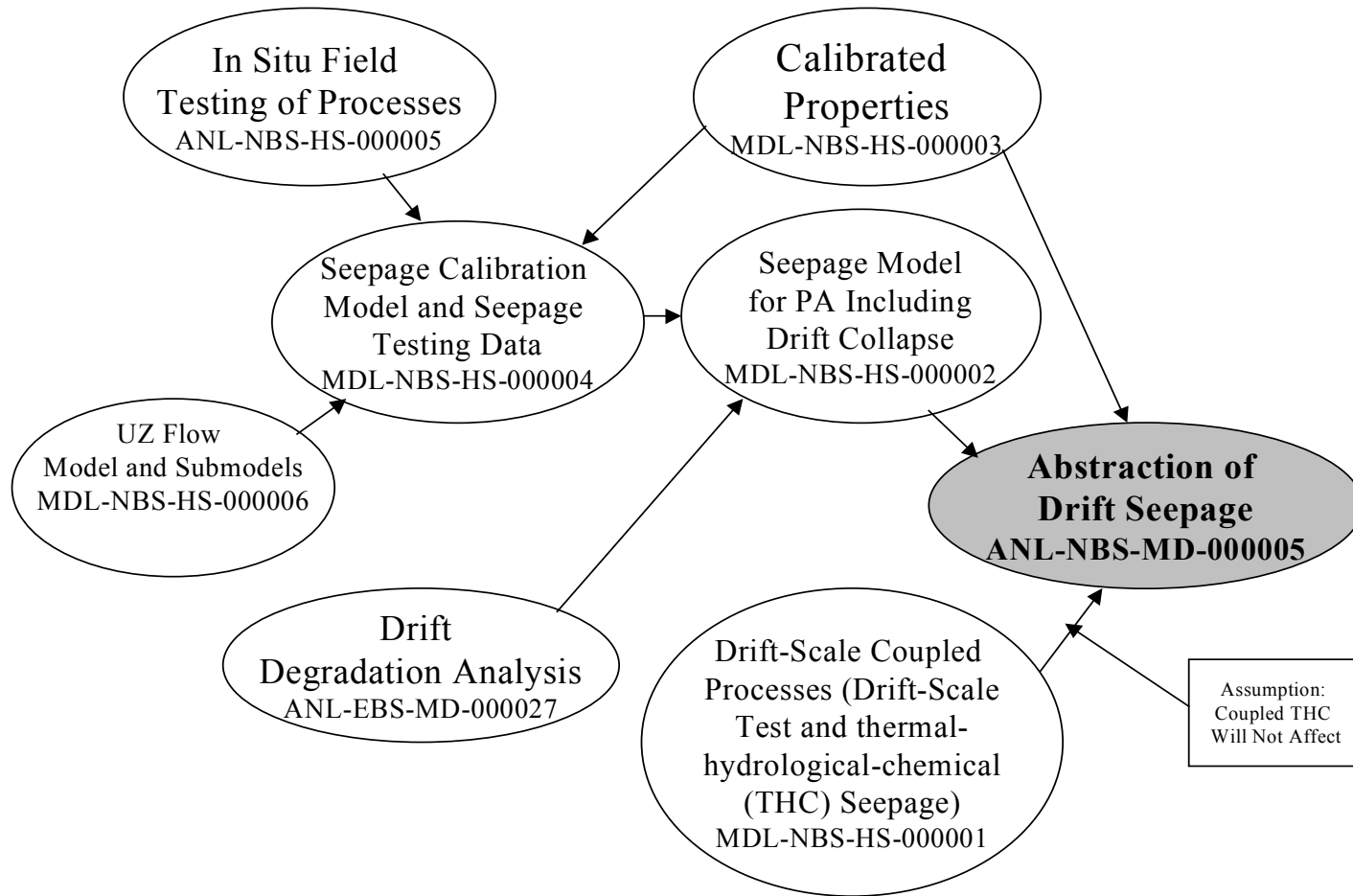


Figure 6-1: Seepage Model Relation Diagram

- *In Situ Field Testing of Processes* (ANL-NBS-HS-000005) – Provides air-permeability, water-release, and moisture monitoring data obtained from the seepage experiments performed in the ESF Niche 3650 to investigate in situ flow and transport processes. These results constitute the data upon which the Seepage Calibration Model is based. The evaluations provide a framework to refine and confirm the conceptual model of matrix and fracture processes in the UZ and to analyze the impact of excavation on UZ flow and transport.
- *Calibrated Properties Model* (MDL-NBS-HS-000003) – Provides calibrated drift-scale properties (fracture and matrix permeability, van Genuchten parameters, active fracture parameter) for use in the drift-scale seepage process models.
- *UZ Flow Model and Submodels* (MDL-NBS-HS-000006) – Provides the UZ flow fields from which large-scale distribution of percolation flux at repository horizon is obtained.
- *Drift-Scale Coupled Processes* (DST and THC Seepage) (MDL-NBS-HS-000001) – Provides THC parameters to assess potential impacts of thermal and chemical effects on seepage and to predict chemical composition of water and gas that may enter the drift environment.
- *Seepage Model for PA Including Drift Collapse* (MDL-NBS-HS-000002) – Provides seepage estimates for a variety of hydrologic properties and drift shapes resulting from rockfall and drift degradation.
- *Drift Degradation Analysis* (ANL-EBS-MD-000027) – Provides general drift shapes (four scenarios showing effects of degradation), and WP length and spacing.
- *Seepage Calibration Model and Seepage Testing Data* (MDL-NBS-HS-000004) – Template fracture continuum model based on air-k and liquid-release tests conducted in ESF Niche 3650. Provides conceptual basis and methodology for subsequent development of the seepage process models and calculates seepage thresholds and flow rates into drifts.
- *Abstraction of Drift Seepage* (ANL-NBS-MD-000005) – Provides the framework for evaluating seepage into the potential repository emplacement drifts for TSPA simulations and to generate probability distributions that represent the uncertainty and spatial variability of seepage.

### 6.3 Model Structure

Figure 6-2, Seepage Model Structure, depicts the various elements that comprise the drift seepage models. Shown are those elements that comprise the conceptual and representational models, the various parameters needed, and the modeling results. Each is discussed in more detail below.

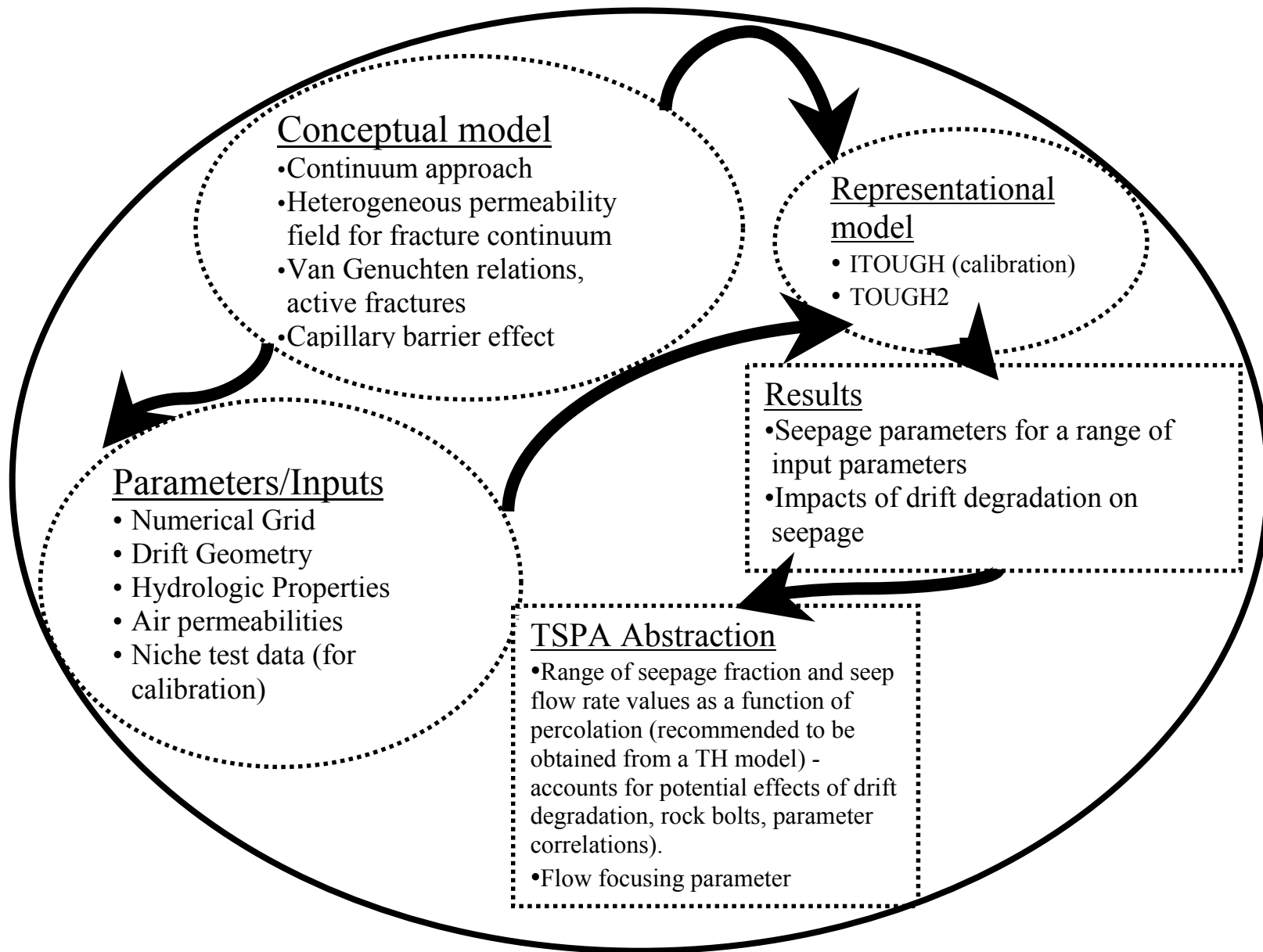


Figure 6-2: Seepage Model Structure

## A. Conceptual Model

### Seepage Calibration Model (SCM)

The SCM is a template fracture continuum model based on air-permeability and liquid-release tests conducted in ESF Niche 3650. The purpose of the SCM is to present a conceptual basis and methodology for the subsequent development of seepage process models. Specific objectives include evaluation of flow rate into drifts and determination of seepage thresholds based on the water-release test data.

### Model Assumptions–General

To assure the validity and usefulness for subsequent seepage calculations, the assumptions of the SCM are consistent with those of the UZ Flow Model and the Seepage Model for PA.

Specifically, these are:

- The continuum approach is valid to calculate percolation flux and seepage
- Flow under unsaturated conditions is governed by Richard's equation
- Permeabilities determined from air-injection tests are representative of the formation hydraulic conductivity
- Relative permeability and capillary pressure can be described as continuous functions of effective liquid saturation
- Van Genuchten alpha parameter correlates to permeability according to the Leverett scaling rule
- Water removal from the formation due to evaporation and vapor diffusion is small
- Background percolation flux is 3 mm/yr
- Matrix imbibition is small

As summarized in the UZ PMR, the conceptual model for seepage includes these principal processes and factors affecting drift seepage:

- **Capillary-Barrier Effect, Flow Diversion:** As percolating water encounters the excavated opening, relatively strong capillary forces in the rock prevent the water from seeping into the drift. Water then accumulates in the region above the drift, locally raising the saturation and causing water to be diverted laterally into adjacent areas where capillary pressures are less negative. However, if the lateral conductivity is insufficient to divert the water, the rock will become locally saturated, the capillary barrier will fail, and seepage into the drift will result.

- **Distribution of Percolation Flux, Flow Channeling:** Water percolating through the layered, unsaturated, fractured tuffs of Yucca Mountain is likely to undergo redirection and flow focusing (perhaps with subsequent dispersion at fracture intersections). Depending on the flux within an individual flow channel, the seepage threshold may or may not be exceeded. Whether seepage occurs in a given drift is determined by the distribution of such flow channels, and their frequency, width, and hydrologic properties.
- **Hierarchical Fracture Network:** Because they determine the distribution of flux and the effectiveness of the capillary barrier, seepage will be affected by the geometric and hydrologic characteristics of the fracture network. Effective anisotropy and potential compartmentalization of the flow field determine the spatial distribution of flow channels and flux within those channels. Connectivity of the fracture network and its capillary strength determine the effectiveness of the capillary-barrier.
- **Drift Geometry, Surface Roughness, Breakouts:** The likelihood of seepage occurring and the ease with which water can be diverted around the opening are determined by the geometry of the underground excavation (size, shape). Drift-wall roughness and surface characteristics (wettability, micro-roughness, dust or coatings) partially control local water accumulation, droplet formation, potential for film flow, and locations of dripping. Breakouts due to rockfall may either lead to distinct topographic lows, which promote seepage, or make drifts more cone-shaped, which results in increased flow diversion and less seepage.
- **Ventilation, Evaporation/Condensation:** Ventilation and its evaporative and condensation effects will affect temperature and relative humidity in the drift environment. Evaporation at the drift wall generally causes formation of a dry-out zone, which in turn causes a reduction in drop formation and dripping. Keeping the relative humidity below 100% by ventilation will promote decreased seepage, but increased vapor diffusion into the drift.
- **Excavation-Disturbed Zone, Dry-Out Zone:** The strength of the capillary-barrier effect is controlled by the properties of the fractured rock in the immediate vicinity of the drift. The extent of the zone of influence is approximately given by the height to which water rises due to capillarity. The zone governing seepage is likely to be smaller than the zone affected by excavation-induced stress redistribution and related rock deformations (generation of new fractures, opening/closing of pre-existing fractures).
- **Repository Design:** The design and layout of the potential repository and engineered barrier system will affect the probability of seepage entering drifts and contacting WPs.

### Abstraction of Drift Seepage

In addition to the assumptions, processes, and factors noted above for the seepage calibration model and the seepage for PA/drift degradation model, the following assumptions pertain to the abstraction of drift seepage:

- Seepage can be treated as a random process.

- The extent of flow focusing can be estimated using the active-fracture model.
- Effects of episodic flow on seepage can be neglected.
- Thermal-mechanical and THC effects on seepage can be neglected.
- Seepage can be bounded by 100 percent of the flow above the drift.
- Standard deviation of  $\log(k/\alpha)$  can be approximated by the standard deviation of  $\log(k)$ .
- Seepage is increased by 55 percent to account for drift degradation and by 10 percent for possible correlation effects of  $k$  and  $\alpha$ .

## **B. Parameters**

**Test data from Niche 3650** – In the liquid-release tests for quantifying seepage (i.e., seepage threshold and seepage fraction), the saturated conductivities are estimated from air-permeability values, capilarity of fractures are estimated from seepage threshold fluxes, and water potentials are estimated along flow paths from the liquid-release interval overlying the niche to the niche ceiling.

**Seepage Calibration Model** – Air-permeability data from air-injection testing in Niche 3650, liquid-release test data from Niche 3650, and base-case hydrologic parameter set.

**Seepage Model for PA** – The following list provides acquired and developed data that were used to characterize seepage conditions in the model:

- Proposed drift and WP configuration
- Calibrated drift-scale properties (to establish parameter ranges)
- Fracture properties (van Genuchten parameters, frequency) for Topopah Spring welded middle non-lithophysal zone (TSwmn)
- Fracture permeabilities from air- $k$  tests (to establish parameter range)
- Pneumatic pressure data (to estimate air- $k$  from SHT and DST)
- Detailed line survey of TSwmn fractures (to corroborate fracture-continuum)
- Drift geometry (from *Drift Degradation Analysis* AMR)

**Abstraction of Drift Seepage** – In addition to those parameters listed for the *Seepage Calibration Model* and the *Seepage Model for PA/Drift Collapse*, the coordinates for the repository outline,

drift and WP geometry/spacing, and flow field simulations for three glacial-transition infiltration scenarios (low, mean, high) are supplied as input.

### **C. Representational Model**

- *In Situ Field Testing of Processes* – This AMR describes and summarizes the various testing procedures and resulting data from the pneumatic testing, liquid-release testing, and moisture monitoring activities conducted in support of seepage investigations. No representational model is developed.
- Seepage Calibration Model – 2D and 3D homogeneous and heterogeneous models were developed using iTOUGH2 and various analytical software routines, mesh generators, and visual plotting software. The iTOUGH2 software provides forward and reverse modeling capabilities for unsaturated and multiphase flow in fractured-porous media and is used for calibration, validation, and prediction runs.
- Seepage Model for PA – Conceptual model is a heterogeneous permeability field for the fracture continuum generated using essentially the same software as the SCM. All cases are computed on 3D heterogeneous unsaturated systems. Three parameters were determined to be most influential in affecting drift seepage; specifically, permeability of the fracture continuum,  $k_{FC}$ , the van Genuchten alpha value, and the standard deviation of  $\ln k_{FC}$ , which provides a measure of the heterogeneity of the permeability field.
- Abstraction of Drift Seepage – Model is based on the results of the Seepage Model for PA/Drift Degradation. The seepage abstraction is an extension of the approach used for TSPA-VA.

### **D. Results**

Seepage modeling sensitivity studies have identified the following trends:

- Seepage increases with increasing correlation length ( $\gamma$ ). Analysis of post-excavation air-permeability data supports using the base-case value (i.e., the smallest correlation length).
- The van Genuchten parameters have only a minor effect on seepage.
- Seepage tends to be greater when capillary strength is correlated according to the Leverett scaling rule.
- Seepage increases as drift degradation increases.
- Episodic flow can result in higher average seepage rates than would be observed under constant percolation flux. Such events are transient and not expected to significantly affect major portions of the potential repository.

Seepage was generally observed to increase with decreasing capillary strength, decreasing lateral permeability, and increasing percolation flux. Only in cases where the capillary barrier and lateral permeability are relatively low, and the percolation flux (including flow focusing) is high, will seepage flux be high. A relatively large portion of the examined parameter space yielded a zero seepage percentage.

### **Abstraction Results**

Seepage is treated as a function of the ratio of geometric-mean fracture permeability,  $k$ , to the fracture alpha parameter,  $k/\alpha$ . The uncertainty in this ratio is taken to be one order of magnitude above and one-half order of magnitude below the best-estimate value,  $6 \times 10^{-11} \text{ m}^2 \text{ Pa}$ . The available information indicates that the uncertainty is more toward higher values of  $k/\alpha$ , so the range considered is skewed somewhat to higher values. The seepage uncertainty distribution is described by a triangular shape that appropriately represents the key features; namely, seepage values for  $k/\alpha = 6 \times 10^{-11} \text{ m}^2 \text{ Pa}$  are most likely, and  $k/\alpha$  could either be higher or lower, but those values are less likely to represent potential repository conditions.

Distributions representing the uncertainty and spatial variability of seepage into drifts as a function of percolation flux were produced. Calculations of effects due to flow focusing on seepage fraction, seepage flow rate, weep spacing, and the distance between actively flowing fractures, are provided for various infiltration scenarios.

## **6.4 Discussion of Uncertainty/Variability Treatment**

### **A. Conceptual Model**

Although included as a principal factor that may affect seepage, lateral diversion due to capillary-barrier effects of excavated drifts has not been evaluated. No measurements of lateral diversion currently exist, and no treatment of uncertainty regarding lateral diversion of water is provided in the AMR. Without such data, no rigorous mass-balance of the seepage water-release experiments is possible. **Note:** Activities planned for FY01 include constructing “bat-wing slots” in Niche 5 to obtain this data.

The model uses a stochastic continuum approach (derived from the calibration exercise effective continuum parameters) to represent the UZ fracture/matrix flow. The 95 percent confidence bands on seepage percentage as a function of seepage flux are calculated by Monte Carlo methods. Simplified validation exercises are used to evaluate the impact of “discrete” flow into a drift, and reasonable predictions are obtained, so the numerical conceptualization appears appropriate for the intended purpose.

The scope of the seepage calibration model is limited to parameters estimated from analysis of the Niche 3650 liquid-release data and is therefore only evaluated relative to an uncollapsed drift under ambient temperature. Effects from drift degradation on potential seepage are analyzed in the *Seepage Model for PA Including Drift Collapse*. Such effects include removal of rock from the roof and changes in effective processes and parameters (i.e., capillary barrier, permeability). Rock bolts are simulated as high permeability pathways. Changes in tunnel diameter and shape

are evaluated: smaller diameters should produce less seepage and the change in seepage is negligible for increases < 10%.

The active fracture flow representation is uncertain due to a lack of applicable data. No actual data on active fracture spacing or flow focusing exists, with the possible exception of CI-36 bomb-pulse data. The parameters used in this model are believed to provide bounding estimates. Percolation flux is treated as constant on the basis of the conceptual model that postulates that episodic flow is damped by the overlying lithologic units, and the assertion that episodic flow only involves small volumes of water. Although this latter point remains unproven, the degree of potential flow focusing has been estimated and it is concluded that the impact to overall percolation flux is negligible.

Coupled thermal-mechanical and thermal-chemical effects are ignored in the modeling of seepage. However, preliminary modeling of thermal-chemical effects at the drift-scale indicates that mineral deposition in fractures has only a small impact on porosity. Thermal-mechanical processes are ignored for modeling simplification.

Spacing of weeps has been calculated using dual-continuum models (i.e., such as the active fracture model) and is approximately log-normally distributed. Monte Carlo sampling of this distribution gives a flow focusing factor that is then used to adjust percolation flux.

## **B. Parameters**

In Situ Field Testing of Processes – Seepage water-release tests in ESF Niche 3650 were conducted under conditions where effects of tunnel ventilation may have influenced the test results and caused under-estimation of seepage potential. Although this subject is discussed (see General Modeling Assumptions, Seepage Calibration Model), no treatment of uncertainty is included for this in the AMR.

Out of necessity for completion of the water-release tests in a tractable timeframe, the equivalent percolation fluxes imposed are far in excess of what is expected under natural conditions. No treatment of uncertainty concerning this issue is included. However, employing these high water-release rates provides a potential benefit, namely, a mechanism for evaluating uncertainty associated with flow focusing and the enhancement of effective percolation flux in the drift environment.

Rock formation heterogeneity was systematically evaluated by air-injection tests, and borehole-scale and drift-scale distributions were produced (including excavation-induced permeability enhancements due to fracturing). Permeability variations measured in individual niches are orders of magnitude larger than the average site-to-site variations (i.e., comparison of measurements from one niche to another) along the main drift. The relatively small differences in the measured mean air-permeability from different niches suggest only moderate uncertainty in site-scale spatial heterogeneity, at least within the TSw middle nonlithophysal unit. Determination of these values for other potential repository units is presently underway.

Variations in the degree of fracturing may strongly influence “local” seepage threshold results. Uncertainty on this topic is not treated in AMR, but additional testing underway/already completed (such as in Niche 4) should provide data to assess this issue.

Capillary strength ( $1/\alpha$ ) is assumed to be heterogeneous and correlated to permeability according to the Leverett scaling rule. The parameters are estimated through numerical inversion in the calibration exercise using a spatial correlation parameter derived from air-K data. The resulting distribution is given in terms of mean and standard deviation.

Water removal from the formation and the capture system by evaporation/vapor diffusion is assumed to be small. Under isothermal conditions, potential evaporation is small compared to the relative short time of the water-release experiments, particularly for those tests in which a large rate of injection is used. This assumption may not be valid for lower water-release rates.

The accuracy of the derived parameters is estimated based on their goodness-of-fit to the observed data and the sensitivity of calculated seepage with respect to the parameter of interest. The SCM is validated against liquid-release tests (other than those used for model calibration), and linear uncertainty propagation analyses and Monte Carlo simulations were performed to evaluate prediction uncertainty.

Because different calibration exercises and data gathering activities have yielded a range of variability for parameters such as van Genuchten  $\alpha$  and  $n$ , fracture continuum permeability, and correlation length, the treatment of uncertainty has been to assume discrete values spanning a range. In general, the range is determined by reasonable minimum and maximum values obtained from the calibration exercises or from measurements made at different locations or under different experimental conditions.

Uncertainty in percolation flux is treated by a range of discrete values (5, 14.6, 73.2, 213, and 500 mm/yr). The largest value represents a possible multiplier due to concentrated precipitation (i.e., all rain falls in the first two months of the year) and flow focusing.

Calculated seepage percentages are expressed as functions of discrete parameter values and alternative scenarios. Uncertainty in  $\gamma$ , the permeability correlation length, is addressed by modifications of the parameter combinations for each realization. Calculating seepage at discrete combinations of parameters is appropriate given that input is discrete.

Uncertainty in the permeability field produces effects on the calculation of seepage percentage and seepage flow. The assumed spatial variability in permeability is based on post-excavation air-K data from the disturbed zone. A lognormal distribution is fit to the data. Uncertainty is not discussed except to note that even this data may not be representative of other important lithologic units (i.e., TSw lower lithophysal unit). Permeabilities determined from air-injection tests are assumed to be representative of the hydraulic conductivity of the tested formation. Potential inaccuracies in this assumption are compensated for through estimation of the van Genuchten  $1/\alpha$  parameter, which is correlated to permeability.

### **C. Representational Model**

Model mesh (size, geometry) can influence seepage results. Alternative mesh discretization is not systematically analyzed for potential impact or uncertainty of results.

Permeability values are simulated as stationary geostatistical fields, with input from air-K data, but no input from measured fracture data. Different types of spatial permeability models develop different degrees of channeling for a given discretization scale and could conceivably impact predicted seepage. Alternative approaches (i.e., fractal network) are not evaluated.

Development of the SCM is impacted by the small data set available for calibration. This lack of data affects various numerical and conceptual model parameters. The model is tested and evaluated relative to the location where the data was acquired, specifically, Niche 3650 in the TSw middle nonlithophysal unit. This specific test is important because it provided a test of the capillary barrier conceptual model for drift seepage. The test also helped identify parameters, boundary conditions and conceptual issues that are crucial for evaluating the applicability of the conceptual model to other areas of the potential repository. Ongoing tests are collecting data required to complete the development and evaluation of the model. No treatment of the potential uncertainty associated with the initial results is included in the AMR.

#### **Testing Status Update–Spring 2001**

Since the initial versions of the *In Situ Field Testing of Processes and Seepage Calibration Model and Seepage Testing Data* AMRs, considerable progress has been made towards acquiring more spatially and lithologically representative data applicable to assessing seepage potential. The overall seepage testing strategy is to perform experiments at selected locations within the individual formations of the potential repository horizon that can provide data for bounding predicted seepage estimates.

As discussed in the AMRs cited above, seepage testing has been conducted within the TSw middle nonlithophysal unit in a location where fracturing is low to moderate in intensity (i.e., Niche 3650). Since that time, additional seepage testing has been conducted where fracturing has been intense, such as at Niche 4 in the highly fractured zone of the ESF, also located in the TSw middle nonlithophysal unit. The range of conditions tested in the middle nonlithophysal unit is being extended further through investigations at Niche 3 in conjunction with the Alcove 8/Niche 3 infiltration test, where data regarding matrix diffusion and seepage is being collected. Note that in this case, the infiltrating water will pass from one lithologic unit to another (i.e., from the upper lithophysal unit to the middle nonlithophysal unit), so data on the effects of changes accompanying lithologic contrasts will be obtained.

Two additional studies are underway to characterize the lower lithophysal unit of the TSw: 1) a series of water-release tests similar to those conducted in Niche 3650 is being performed in Niche 5 of the Cross Drift; and 2) a systematic characterization of the lower lithophysal unit via a series of vertical, inclined, and horizontal boreholes drilled from the Cross Drift. This latter test program will provide hydrologic, pneumatic, and seepage testing data representing several

hundred meters of the lower lithophysal unit, and substantially improve the spatial representativeness of the data from this unit.

Finally, a significant portion of the TSw lower lithophysal and lower nonlithophysal units exposed in the Cross Drift has been isolated from the effects of tunnel ventilation by installing bulkheads to let the isolated section revert to ambient hydrologic conditions. This isolated section of the Cross Drift underlies an area thought to experience high infiltration, so a major objective of the activity is to see if drift seepage can be observed as the tunnel re-equilibrates (i.e., returns to original values of saturation and water potential) to ambient conditions.

When completed, the collective result of these seepage testing activities will be to have determined seepage-relevant parameters from a range of potential repository horizon environments and rock types. Such data should form a defensible basis for the prediction of drift seepage, and evaluation of the conceptual and numerical models.

## **6.5 Uncertainty Propagation**

Uncertainty associated with data limitations, testing procedures/results, and spatial representativeness as documented in the *In Situ Field Testing of Processes* AMR is propagated to the *Seepage Calibration Model and Seepage Testing Data* AMR. The *Seepage Calibration Model and Seepage Testing Data* AMR identifies additional uncertainty associated with development of the seepage threshold prediction (200 mm/yr) and notes limitations in applying these results to conditions other than those specified (i.e., ambient temperature, circular uncollapsed drift in competent rock of low fracture density in middle nonlithophysal Topopah Spring welded unit).

Resulting uncertainty is then propagated to the *Seepage Model for PA Including Drift Collapse* AMR through the use of the calibrated parameter sets developed by the *Seepage Calibration Model*. No analysis of coupled THC effects on seepage is made in the *Seepage Model for PA Including Drift Collapse* AMR due to the lack of available data.

The seepage probability distributions that constitute the seepage abstraction are based directly on the results of the *Seepage Model for PA Including Drift Collapse* AMR. Hence, the validity of the abstraction clearly derives from the approaches and site-specific data used to develop that model.

The range of seepage thresholds from the *Abstraction of Drift Seepage* AMR is well below the value indicated from the *Seepage Calibration Model*. Since a lower threshold implies increased seepage at low percolation flux, this indicates that the seepage abstraction estimate is high for low values of percolation, and should be considered appropriately conservative. The seepage abstraction recommends that fracture flux above the drifts be supplied from a thermal-hydrology model in order to account for thermal effects on seepage, such as condensate drainage.

These results are then used in TSPA to develop the probability distributions that represent the uncertainty and spatial variability of seepage into waste emplacement drifts at Yucca Mountain.

Limitations of the model include limited data available for model development. Seepage modeling is unique to the YMP; no referenceable comparative studies of ambient or thermally perturbed unsaturated zone seepage into excavated underground openings exist. All data collection and modeling efforts related to its development are “state of the art.”

## **6.6 Conclusions**

Because seepage is affected by numerous features and processes that span a broad range of scales, it cannot be adequately captured in a single model. To assure that each scale is appropriately addressed, a hierarchy of models has been developed to predict seepage threshold, seepage flow rate, and seepage fraction for the waste emplacement drifts.

The seepage models represent simplifications and abstractions of the identified seepage-relevant processes. Experiments were designed and performed to identify, understand, and characterize processes and parameters important to seepage. Seepage threshold data were evaluated and interpreted using analytical techniques originally derived for a homogeneous, unsaturated porous medium.

Seepage potential may be considered as the product of two probabilities:

- The probability of experiencing locally high percolation flux, presumably aided by flow channeling
- The probability that this focused flow will encounter a segment of a drift with a low seepage threshold

Modeling results indicate that, even under conservative assumptions of 100 percent relative humidity and no dry-out zone, seepage fluxes are smaller than percolation fluxes, and only a fraction of emplaced WPs are predicted to experience seepage.

Model uncertainty and parameter variability are addressed either by stochastic simulations and uncertainty propagation analysis, or through assuming large parameter uncertainty for TSPA calculations.

In their present, or likely future, state of development, the seepage models cannot be expected to provide accurate predictions of individual seepage events or detailed spatial distribution of seepage potential along emplacement drifts. The models can, however, provide supportable estimates of average seepage flux for 5-meter drift segments as a function of drift-scale percolation flux.

**Table 6-1: Seepage Model**

<b>Model Purpose:</b> The purpose of the Seepage Model is the development of a seepage process calibration model, the application of this model to prediction of seepage under a variety of conditions (ambient, thermal), and abstraction of seepage results for use in TSPA.				
<b>Summary</b>	<b>Source</b>	<b>Treatment</b>	<b>Basis</b>	<b>Impact</b>
<b>Conceptual Model Uncertainty</b>				
Drift degradation	Uncertainty as to whether any of the possible mechanisms of drift degradation will occur (Seepage Model for PA Including Drift Collapse, MDL-NBS-HS-0000002)	Consideration of four alternative submodels	Expert opinion on different ways drifts could collapse	Impact of treatment not discussed, other than statements suggesting that drift degradation would increase seepage.
Drift degradation	Uncertainty arises from translating the hypothesized drift degradation mechanisms into mathematical modeling cases (Seepage Model for PA Including Drift Collapse, MDL-NBS-HS-0000002)	Stress relief modeled as fracture dilation, changing kfc and 1/alpha from pre-excavation to post-excavation values; rock fall simulated by removing a 1 meter block from top and side of tunnel and using post-excavation parameter values; extended roof failure is simulated by removing blocks around roof to represent seismic failure, and using post-excavation parameter values.	Effects of drift collapse are essentially removal of rock material and change in effective parameter values.	Other mechanisms for mathematically implementing failure processes not discussed.
Temporal nature of seepage	Lack of data (Abstraction of Drift Seepage, ANL-NBS-HS-000005)	Treated as constant	Episodic flow thought to involve only very small amounts of water, and thus negligible.	Could increase seepage rates and volumes since percolation flux would be higher than if averaged over a year. AMR concludes that impact is negligible.

Active Fracture model for flow and flow focusing above drift	Lack of data regarding whether this takes place or not on intermediate scale (Abstraction of Drift Seepage, ANL-NBS-HS-000005)	Active fractures form subset of all fractures. Parameters are taken from site-scale UZ flow model. Try to estimate the degree of flow focusing that may be possible. Calculation of bounds on weep spacings, which are approximately lognormal. Monte Carlo sampling of this distribution gives flow focusing factor that is then used to adjust percolation flux.	Actual data on spacing and flow-focusing of active fractures in unknown. Some information is available from Chlorine-36 data in ESF. Parameters used are believed to provide bounding estimates.	Could increase seepage rates and volumes since percolation flux in these channels would be higher than if averaged over the entire rock cross-section. Discussion is presented in how one might approximate episodic flow effects.
Drift degradation over time	Impact of rocks bolts, physical changes around drift through time uncertain (Seepage Model for PA Including Drift Collapse, MDL-NBS-HS-000002).	Cases with altered drift shapes and with added paths to simulate impact of bolts modeled.	Drift degradation's largest unknown impact is probably shape change, and rock bolts could form preferential seepage pathways.	Decrease in performance has been estimated to be on the order of 10%.
SCM model applicability to other lithologic units or geological conditions differing from Niche 3650	Lack of testing in other units (Seepage Calibration Model and Seepage Testing Data, MDL-NBS-HS-000004)	Statement of limited applicability of calibration model results to other locations, lithologies, and conditions is provided.	Geological conditions vary throughout lithological units and structural positions in YPM; site specific values are required for model calibration and validation.	Parameter values at other locations are unknown; conclusions regarding validity of conceptual model based upon Niche 3650 may not hold elsewhere since the fundamental seepage processes may change character with different lithologies and structural positions. These issues are not discussed in the AMR.
Rock Bolts	Rock bolts provide possible pathways for enhanced seepage (Seepage Model for PA Including Drift Collapse, MDL-NBS-HS-000002).	Some very preliminary calculations undertaken in which effects are simulated as high permeability pathways.	Not Available	Inclusion of rock bolting effects could enhance seepage

<b>Representational Model Uncertainty</b>				
SCM mesh geometry	Assumption (Seepage Calibration Model and Seepage Testing Data, MDL-NBS-HS-000004)	Fixed scale and geometry of mesh used.	Numerical limitations, and the assumed geometry and scale of seepage processes around Niche were used to construct mesh.	Mesh geometry and discretization influence results; alternative mesh discretizations not systematically analyzed for impact on results.
Hydraulic permeability values for SCM model are modeled as stationary correlated fields, while fracture studies in YMP suggest other types of spatial models (for example, fractal) could be applicable.	Potential alternative representations (Seepage Calibration Model and Seepage Testing Data, MDL-NBS-HS-000004)	Permeability values are simulated as stationary geostatistical fields.	Air permeability data can be fit by stationary variograms.	Different types of spatial models develop different degrees of channeling for a given model discretization scale, and could significantly impact seepage predictions.
Use of a stochastic continuum model to represent unsaturated fracture/matrix flow (Sec. 5.3)	Assumption; difficulty in using any other type of numerical model (Seepage Calibration Model and Seepage Testing Data, MDL-NBS-HS-000004).	Calculate or derive from calibration exercises effective continuum parameters; 95% confidence bands on seepage percentage as a function of seepage flux are calculated using Monte Carlo simulation.	Simplified synthetic validation exercises are used to evaluate the impact of "discrete" flow into a drift; local flow is not predicted. Model appears to make "reasonable" prediction. Therefore numerical model conceptualization is considered appropriate for purpose intended.	Whether synthetic models bracket possible site conditions is not discussed, so comparisons may only be valid for a restricted parameter set. Synthetic DFN Model has channelized flow, but may still not reproduce actual channelized flow in drift; differences between this model and actual fracture network not discussed. Thus relevance of validation exercise not well described. Comparison with discrete fracture network models not made for valid reasons, but uncertainty remains as to how well the SCM would compare.

<b>Parameter Uncertainty</b>				
Seepage tests were conducted under conditions where the effects of tunnel ventilation may lead to under estimation of seepage potential.	Series of sixteen water release experiments conducted in Niche 2 (TSwmm) for the purposes of determining the drift seepage threshold of the TSw middle nonlithophysal unit. (In Situ Field Testing of Processes, ANL-NBS-HS-000005)	Results of water release experiments provide the basis for development of the seepage calibration model.	Data from TSwmm water release experiments represent the only measurements available for analysis of seepage potential.	Even if the effects of tunnel ventilation and evaporation are minimal (which has not been demonstrated), and the results are taken to accurately represent the seepage potential in the near vicinity of Niche 2, extrapolation of results from this location to the TSwmm in general has not been demonstrated. Also, no water release data exists on the seepage potential for the TSw lower lith. or lower nonlith, which together comprise 85% of the potential repository.
Water release rates employed in this series of tests often used equivalent percolation flux rates that are well in excess of those expected under natural conditions.	Seepage data obtained through the systematic water release experiments and the percolation flux estimates derived from various UZ natural system test programs. (In Situ Field Testing of Processes, ANL-NBS-HS-000005)	It was assumed that the high release rates may be representative of conditions where favorable fracture network geometry has operated to produce highly focused flow into the drift environment.	The impracticality of attempting to conduct the seepage experiments under conditions of ambient flux (I.e., 5 mm/yr) led to the use of the higher release rates.	Using high water release rates effectively overdrove the system to allow experimental results to be obtained in a tractable timeframe. This probably produced experimentally conservative seepage threshold results (i.e., in those cases where release rates were low, no seepage was observed).
Variations in the degree of fracturing may strongly influence "local" seepage threshold results.	Fracture characteristics were a major consideration in the selection of the location for Niche 4 (situated in the high-density fracture zone of the TSwmm in the Main Drift). This location was selected to provide a comparison to Niche 2. (In Situ Field Testing of Processes, ANL-NBS-HS-000005)	To Be Determined: Even though the testing in Niche 4 has been completed, the results obtained from Niche 4 are not yet available.	Awaiting results from activities completed in Niche 4.	Only using the existing results from Niche 2 may underestimate seepage in regions which are more fractured.

<p>The degree of lateral diversion of percolating water due to the capillary barrier effects of excavated drifts/niches needs to be addressed.</p>	<p>No means to evaluate this parameter presently exists. Installation of "bat-wing" slots cut into the sides of seepage testing niches (below the water-release horizon) would allow quantitative measurements of the amount of water diverted by the excavated opening. (In Situ Field Testing of Processes, ANL-NBS-HS-000005)</p>	<p>This parameter remains to be addressed. Until it is, no serious water-balance calculations can be made.</p>	<p>To the downward flow of water, these excavations act as extremely large pores and water tends to be shed around them. If we know the applied (or ambient) flux above the excavation, the amount taken up by the fractures and matrix, the amount collected in the collection system (seepage), the amount lost to ventilation, and the amount diverted around the opening, a complete calculation can be made.</p>	<p>The inability to determine the degree of lateral diversion due to excavation effects introduces additional uncertainty into the efforts to quantitatively model drift seepage. Under optimal conditions, lateral diversion may reduce the amount of percolation that potentially becomes drift seepage. Evaluation of this parameter is vital to accurate drift seepage modeling.</p>
<p>Thermal effects on seepage</p>	<p>Lack of field data; lack of computational capability (Abstraction of Drift Seepage, ANL-NBS-HS-000005)</p>	<p>Coupled thermal-mechanical and thermal-chemical effects are ignored.</p>	<p>Preliminary modeling of thermal-chemical processes at drift-scale shows only small impact on porosity. Thermal-mechanical processes ignored for model simplification.</p>	<p>AMR states impacts of thermal-mechanical processes are currently being addressed elsewhere.</p>
<p>Standard deviation of log (k/alpha)</p>	<p>Lack of data (Abstraction of Drift Seepage, ANL-NBS-HS-000005)</p>	<p>SD of log (k/alpha) taken to be the same as log (k).</p>	<p>Fracture alpha and permeability are poorly correlated.</p>	<p>AMR states that assumption is conservative based on the observation that "correlations tend to decrease the standard deviation of the log of their ratio" (Sect. 5). Also, perfect correlation tends to be conservative over partial correlation (the more likely scenario; see Sect. 6.3.2). Final results were adjusted by 10% to reflect correlation effects.</p>
<p>Initial calculations of seepage percentage and seepage flow rate from calculations</p>	<p>Uncertainty in permeability field (Abstraction of Drift Seepage, ANL-NBS-HS-000005)</p>	<p>Three realizations of permeability field for each set of percolation flux, permeability mean, and van Genuchten parameter (alpha)</p>	<p>Permeability heterogeneity can be varied based upon air permeability results; while a constant flux is assumed to produce negligible error; and alpha can be based on calibrations.</p>	<p>Impact not discussed; but sensitivity appears low with respect to the standard deviation and also the ratio of k/alpha</p>

Permeability	Limited amount of field data & relation of air permeability to fluid permeability (Abstraction of Drift Seepage, ANL-NBS-HS-000005)	Spatial variability of air perm data used as qualitative surrogate for fluid perm variability and functional form of probability distribution; absolute values obtained through calibration.	Assumption that air permeability varies as fluid permeability values.	Impact not discussed; but sensitivity appears low with respect to the standard deviation and also the ratio of k/alpha.
Van Genuchten alpha	Only 1 data value (Abstraction of Drift Seepage, ANL-NBS-HS-000005)	A range of values is assumed.	Mean anchored on one value; range taken arbitrarily to be one order of magnitude above and one-half order below to reflect qualitative higher uncertainty in upper values.	Not discussed
Van Genuchten alpha	Different calibration exercises have suggested a range of values (Seepage Model for PA Including Drift Collapse, MDL-NBS-HS-0000002)	4 discrete values spanning a range. Values are considered independent of kfc for most cases: $1/\alpha = 30, 100, 300, 1000$ (Pa).	Range of values corresponds to reasonable minimum and maximum values obtained from calibration exercises.	Discrete points are unweighted; final results must weight combinations involving these points to determine distribution of results. Treatment of alpha as correlated to kfc through Leverett scaling rule evaluated for subset of cases.
Final calculations of seepage percentage and flow rate	Uncertainty in input modeling parameters (Abstraction of Drift Seepage, ANL-NBS-HS-000005)	Input parameter cases used in preliminary simulations are weighted according to probabilities assigned to k/alpha. Weighting factors for k/alpha are based on fitting a lognormal probability distribution to k/alpha, and then discretizing it to cover the same ranges as in the preliminary simulations.	k/alpha is the parameter that varies; its range reflects the values of k and alpha as described in discussions of k, alpha and k/alpha above.	Binning effects discussed as being negligible; other impacts not discussed.
Fracture Continuum Permeability, Kfc	Variability in air permeability values obtained in different locations of the ESF under different conditions (Seepage Model for PA Including Drift Collapse, MDL-NBS-HS-0000002).	4 discrete values spanning a range: $0.9e-14, 0.9e-13, 0.9e-12, 0.9e-11$ (m <sup>2</sup> )	Range of values correspond to reasonable minimum and maximum values obtained from air permeability measurements in different locations and under different experimental conditions.	Discrete points are unweighted; final results must weight combinations involving these points to determine distribution of results
Standard Deviation of Kfc in ln(kfc)	Variability of value inferred from air permeability measurements (Seepage Model for PA Including Drift Collapse, MDL-NBS-HS-0000002).	3 discrete values spanning a range: 1.66, 1.93, 2.5	Range of values is anchored at the low end by the lowest value of standard deviation found. High end range is slightly greater than largest value obtained from data.	High end of range is conservative, since studies show that higher standard deviations lead to greater seepage

Van Genuchten, $n$	limited data (Seepage Model for PA Including Drift Collapse, MDL-NBS-HS-0000002)	Single constant value: 2.7	Sensitivity studies suggest differences in $n$ do not produce significantly different seepage results; single value chosen is based on fracture information in ESF.	No impact expected from treating value as constant, based on sensitivity studies.
Correlation length, $\gamma$	Apparent randomness of parameter in air permeability tests (Seepage Model for PA Including Drift Collapse, MDL-NBS-HS-0000002)	Set to grid size (creates no spatial correlation) for most simulations, and three realizations run for each case; some cases used two additional values to evaluate sensitivity (with 3 or 5 realizations for each parameter set).	Air permeability data suggests lack of spatial correlation. Values chosen for sensitivity studies reflect reported values for $\gamma$ .	Treatment presumes that the underlying permeability field conforms to a stationary geostatistical process. Other models may also be possible, but have not been evaluated.
Percolation Flux (comment from Seepage Model for PA Including Drift collapse)	Different scenarios suggest different percolation flux values (Seepage Model for PA Including Drift Collapse, MDL-NBS-HS-0000002)	5 discrete values spanning a range: 5, 14.6, 72.3, 213, 500 mm/yr	The range selected corresponds to the range expected for alternative scenarios.	Discrete points are unweighted; final results must weight the cases appropriately.
Background percolation flux (comment from Seepage Calibration Model and Seepage Testing Data)	Lack of field data. (Seepage Calibration Model and Seepage Testing Data, MDL-NBS-HS-000004)	Used as input to SCM; treated as constant, not episodic.	Consistency with UZ flow and transport modeling; small supposed impact due to high rates of seepage experiments.	Negligible. Since liquid release tests release much greater quantities and overwhelm impact of percolation. Also, percolation may be below seepage threshold.
Calculated Seepage percentages	Variability/Uncertainty of input to mathematical model (Seepage Model for PA Including Drift Collapse, MDL-NBS-HS-0000002)	Results are expressed as functions of discrete parameter values and alternative scenarios as discussed above, with the additional data reported for each realization of particular parameter values to reflect uncertainty in $\gamma$ .	Calculating seepage at discrete combinations of parameters is appropriate given input is discrete; final PA input can be calculated by weighting the combinations appropriately.	Use of discrete results not discussed in AMR
Tunnel Diameter	Final tunnel design could be different from one chosen. (Seepage Model for PA Including Drift Collapse, MDL-NBS-HS-0000002)	Diameter assumed to be 5.5 m	Current design	AMR states that smaller diameters should produce less seepage; results for larger diameters should be negligible up to 10% increase in diameter.

Liquid release test data for validation/calibration of SCM	Limited field data (Seepage Calibration Model and Seepage Testing Data, MDL-NBS-HS-000004)	The liquid release data is used for two purposes: calibration and validation. A simplified model is calibrated using the release data. Then this model is used to predict other seepage experiments not used in calibration. SCM results are considered validated if they lie within 95% confidence interval of these field results.	Liquid was released under different experimental conditions, comprising 40 tests, 16 intervals and 3 boreholes. Seepage data from 2 of 10 seeping intervals was recorded for calibration/validation. These two intervals afforded 9 tests for calibration/validation. The time for release start/end, arrival of the wetting front, the start/end of dripping were recorded. Also recorded were the release rate, the mass released, the seepage mass and the seepage percent.	Impact of uncertainty not explicitly discussed; unknown if these experimental conditions bracket the range meaningful for performance assessment.
Fracture Porosity	Limited data (Seepage Calibration Model and Seepage Testing Data, MDL-NBS-HS-000004)	Fit during calibration exercises. Resulting distributions are expressed in terms of mean and standard deviation.	No other way to develop meaningful values.	Impact not discussed
Capillary strength (1/alpha) used in SCM numerical models	Very limited data (Seepage Calibration Model and Seepage Testing Data, MDL-NBS-HS-000004)	Assumed to be heterogeneous, and correlated to permeability according to the Leverett scaling rule (Sec 6.3.2). Estimated through numerical inversion in calibration exercises, but given spatial correlation structure of air perm data. Resulting distributions are expressed in terms of mean and standard deviation.	Continuum permeability is partly related to aperture; therefore, an increase in permeability is related to a decrease in capillary strength	Impact not discussed

Hydraulic permeability values for numerical modeling of seepage.	Lack of hydraulic field data; limited amount of air permeability data. (Seepage Calibration Model and Seepage Testing Data, MDL-NBS-HS-000004)	Air permeability measurements are used to define the correlation length scale and the functional form of the semivariogram to describe spatial correlation, and are also used to specify the functional form and cumulative distribution function (CDF) of the underlying probability distribution.	Spatial pattern and probability distribution of air injection interval permeabilities are assumed to have a similar geostatistical spatial correlation pattern to the hydraulic permeability values, which are needed for modeling. Air perms used are post-excavation values in order to account for a variety of processes that might enhance seepage.	Values are used to calibrate and validate the SCM by modeling liquid release tests. It is not clear how sensitive final results of the prediction are to variability in the spatial pattern. Statement is made (Sec. 6.3.2) that due to weak spatial correlation, random, uncorrelated fields would yield similar results. Adjustment of van Genuchten parameter thought to partially compensate for inaccuracies (Sec 5.2). Some evidence is provided to suggest that a linear variogram might also be a viable semivariogram, but this alternative was not included in any calculations (Sec. 6.2.3).
<b>Variability</b>				
Spatial variability of permeability	Limited field data on air permeability in disturbed zone. (Seepage Calibration Model and Seepage Testing Data, MDL-NBS-HS-000004)	Based on geometric averages of post-excavation tests in niches. A lognormal distribution is fit to the data.	Disturbed zone around niches thought to be the best analog	Not discussed, except to note that even this data may not be representative of other lithologic units of importance.
Spatial variability of van Genuchten alpha parameter.	Only 1 data value (Abstraction of Drift Seepage, ANL-NBS-HS-000005)	Based on correlation with k (through Leverett scaling rule).		
Percolation flux - episodic vs. static representation	Possible temporal variation over year (Abstraction of Drift Seepage, ANL-NBS-HS-000005)	Sensitivity studies in which total annual rainfall occurs uniformly over first two months only.	Not provided	Not discussed
Spatial correlation structure in third dimension not analyzed due to 2D nature of the field data.	Lack of field data in three dimensions (Seepage Calibration Model and Seepage Testing Data, MDL-NBS-HS-000004)	Used to define the correlation length scale and the functional form of the semivariogram, and also the form and CDF of the underlying probability distribution.	Spatial pattern of air injection permeabilities is assumed to have a similar geostatistical spatial correlation pattern to the hydraulic permeability values, which are needed for modeling.	Fracture effects may be overemphasized. No discussion of other possible impacts.

**Results**

SCM model validation	Lack of data for validation (Seepage Calibration Model and Seepage Testing Data, MDL-NBS-HS-000004)	Predict seepage mass and percentage for experiments withheld from calibration of SCM. A 95% error band calculated from Monte Carlo simulations (2D models) or a linear uncertainty propagation analysis (3D models) of four tests is compared to field data.	Predicting seepage mass and percentage is useful for PA, and a 95% confidence band is assumed to be sufficiently accurate for PA purposes	No discussion of why 95% band is "sufficiently accurate" provided. No discussion as to how other possible measures of seepage may validate or invalidate SCM model.
----------------------	---	--	---	---

## **7.0 Near Field Environment Process Models and Abstractions**

### **7.1 Purpose and Intended Use of the Model**

This chapter describes the interrelations of the models that comprise the NFE treatment covered within the NFE PMR and the methodologies used to assess/incorporate uncertainty and variability into those process models, their associated abstractions, and ultimately into the TSPA model. The general purpose of the NFE models is to develop quantitative descriptions of the thermally perturbed processes occurring within the host rock and to provide abstractions of the relevant process effects for subsequent use in TSPA analyses. Additional processes are excluded from direct incorporation into TSPA models using FEPs screening arguments that are based on qualitative and quantitative understanding of these thermally driven, coupled processes. The two major aspects that are abstracted for use in TSPA models are thermally driven changes to 1) the percolation flux that is approaching the drifts (i.e., thermohydrologic processes); and 2) water and gas compositions that would enter the drift (i.e., THC processes). Within the category of FEP screening usage, results of the coupled THC process modeling provided the basis to exclude permanent changes to the host rock hydrologic properties from being directly incorporated into the TSPA models.

Within the NFE PMR and associated AMRs, a number of techniques were used to address uncertainties in the model results. In addition, some variability (spatial and temporal) was captured within process models. If these aspects are not incorporated explicitly into the process models, they would represent additional sources of uncertainty because the potential site is a spatially heterogeneous and evolving system. The temporal variability stems from changes in boundary conditions through time, as well as the transient thermal input associated with emplacement of the waste forms. As discussed in detail below, techniques used to assess uncertainty include cases where input parameters were evaluated explicitly over their range of uncertainty to constrain the impacts to model results, or testing of the models against independent field and laboratory observations to check their ability to reproduce those observations. In particular, results from the DST are used to test the thermohydrologic and the THC process models for their conceptual models and parameter sets. These process models are tested further by comparison to the results of additional field thermal tests and the ambient geochemical system.

The review presented below, and summarized in Tables 7-1 and 7-2, is not meant to be a comprehensive evaluation of all the sources of uncertainty within each of the models. The main objective of this work is to compile the treatment of uncertainties as documented within the AMR for the models in this NFE area, and indicate examples of good and poor treatments such that recommendations can be made for developing a strategy for consistent treatment on the YMP Project. In the course of the review and discussion below, some uncertainties that were not treated in the AMR are identified, but this should not be construed as a comprehensive listing for these models.

## **AMR, Model Relations, and Model Structure**

### **A. AMR List for NFE Models**

The NFE process models, supporting analyses, and associated model abstractions are documented in 1) the NFE PMR (TDR-NBS-MD-000001); 2) its associated AMRs; and 3) two AMRs shared with the EBS PMR (see the chapter covering the EBS). The two AMRs shared with the EBS PMR are the *Multiscale Thermohydrologic Model Analyses/Model Report* (ANL-EBS-MD-000049) and its associated abstraction AMR, *Abstraction of NFE Drift Thermodynamic Environment and Percolation Flux* (ANL-EBS-HS-000003). Descriptions of these NFE models, including their purpose, fundamental model aspects, (conceptual model, representational model, parameters, results, and usage), as well as their relation to the AMR, are provided below. In some cases a single AMR documents a number of models, whereas in other cases a single model is covered by multiple AMR.

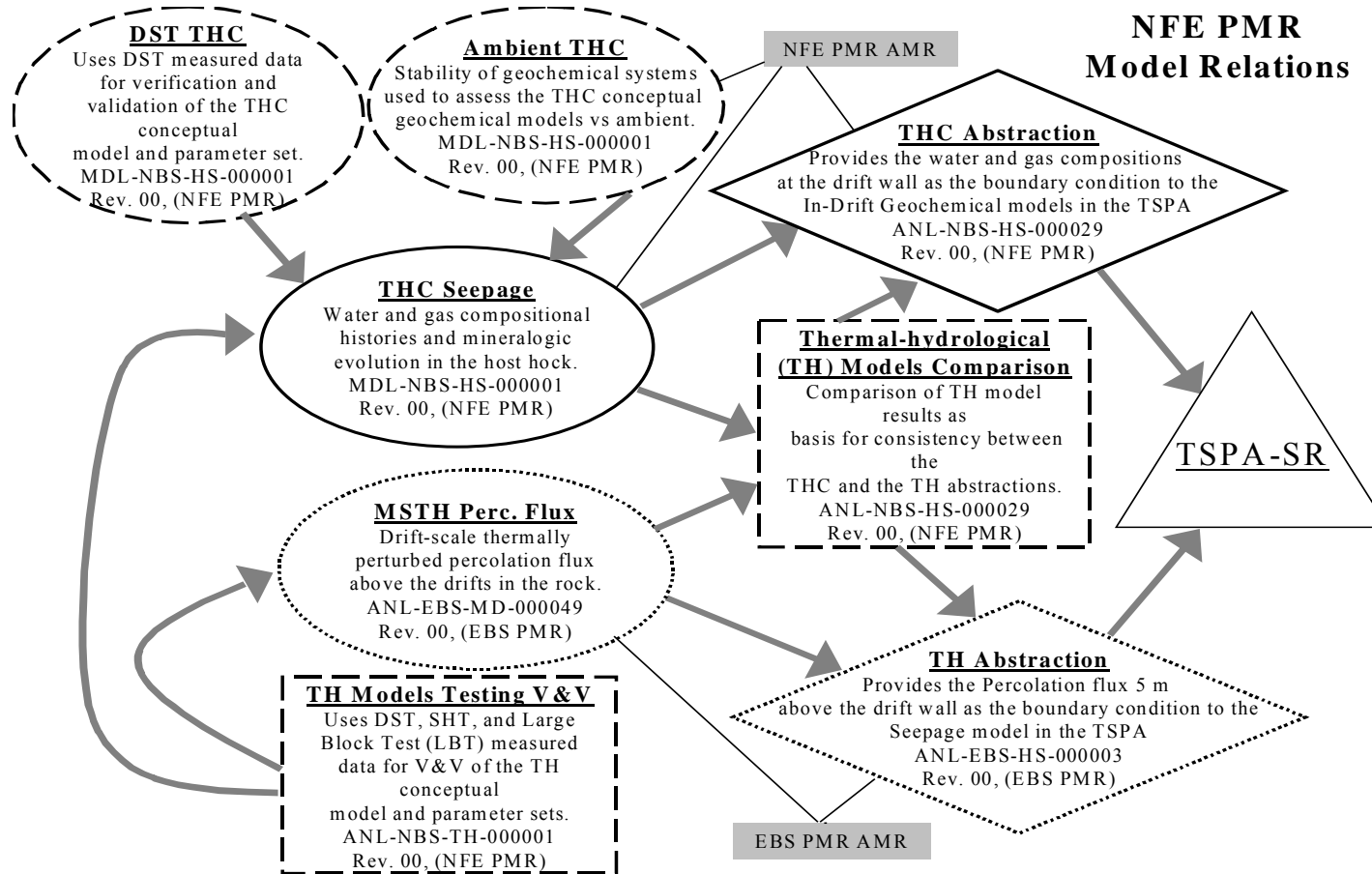
The NFE PMR (TDR-NBS-MD-000001 Rev. 00 ICN 03) summarizes the information contained in the various AMRs. The scope of the NFE PMR is limited to considerations of thermally driven coupled processes that affect seepage into drifts, water chemistry, mineralogy, and rock hydrologic properties, as well as geomechanical responses based on ambient-property inputs. In this version of the NFE PMR (TDR-NBS-MD-000001 Rev. 00 ICN 03), the coupled thermomechanical and thermohydronechanical, aspects were not covered in a model for potential post closure system behavior/evolution and are not discussed further. In addition to synthesizing the NFE models, the NFE PMR provides a high-level summary of the related work in additional PMR and the connections to the NFE PMR models.

The section below provides a short summary of each AMR in terms of its relevant model(s) that is (are) part of the NFE PMR. Specific examples for how variability and uncertainty were treated are discussed for each model that describes the behavior of the potential repository system that is abstracted for the TSPA. The discussion includes the relevant supporting models/analyses that were utilized primarily to constrain the validity of parameter sets or conceptual processes included within the models of potential repository behavior.

### **B. Summary of NFE Models in the AMR and Structure of Models**

Within this section, a short description is given of the purpose of each NFE AMR and the relevant NFE Model(s) or Analysis(es) contained in each AMR. In addition, each AMR description below contains a brief overview of the basic structure of the models (e.g., conceptual model, input parameters, representational model) documented in that AMR. Finally, the relations between each AMR and its models are discussed below, with further details of the model structures given in the next section (see also Figure 7-1, Relations Among NFE PMR Models).

*Drift-Scale Coupled Processes (DST & THC Seepage) Models* – (MDL-NBS-HS-000001, Rev. 00; also referred to here as THC AMR, N0120). This AMR provides conceptual model development, implementation, and results for THC models used for predicting spatially (vertical)



(ellipses: solid borders indicate post-closure models; dashed borders indicate supporting models), analyses (rectangles: dashed indicates model support function); abstractions (diamonds) and the TSPA-SR Model.

Figure 7-1: Relations Among Near Field Environment Process Model Report Models

and temporally varying matrix and fracture mineral alteration, water compositions, and gas compositions and fluxes. The fundamental conceptual model is that the minerals, water, and gas in the system will be driven to chemical reaction by the thermal input from a potential repository. This thermal perturbation may cause changes in water and gas compositions, transport of water (e.g., refluxing), and dissolved and gaseous species, and mineral dissolution, precipitation, and/or alteration in both the fractures and rock matrix.

Within this AMR there are three models used to validate the concepts or to represent these processes for the potential repository system. These three models are applied to 1) the ambient site (Ambient THC Model) conditions; 2) the DST (DST THC Model) observations/measurements; and 3) potential repository conditions (THC Seepage Model). The results of the THC Seepage Model are provided to other AMR as the boundary conditions to the potential emplacement drifts. In each case, two geochemical systems were analyzed: the less complex Case 2 (components are  $\text{H}_2\text{O}$ ,  $\text{CO}_2$ , pH,  $\text{Ca}^{2+}$ ,  $\text{Na}^+$ ,  $\text{SiO}_2$ ,  $\text{Cl}^-$ ,  $[\text{HCO}_3]^-$ ,  $[\text{SO}_4]^{2-}$ ); and the more complex Case 1 (extended to include the additional components  $\text{Mg}^{2+}$ ,  $\text{K}^+$ ,  $[\text{AlO}_2]^-$ ,  $[\text{HFeO}_2]^-$ , and  $\text{F}^-$ ). Further descriptions of the structural components of each of these models are provided in below in the next section covering the models. Short summaries are given below of the purpose/intended use for each of these models.

For the Ambient THC Model, THC simulations under ambient conditions (i.e., without heating) were performed for Case 1 and Case 2 using a constant infiltration rate (about 1.05 mm/year). This rate represents the base-case present-day infiltration rate at the location of Borehole SD-9, which was used to define the geology for all the THC models. These ambient simulations were run to assess the extent to which the Case 1 and Case 2 geochemical systems approached a geochemical steady state. These simulations also provide a baseline to which the results of thermally loaded simulations can be compared. This Ambient THC Model is used to assess the representation of the geochemical/hydrogeologic system (i.e., geochemical representation over geologic time frames) by assessing the stability of the geochemical system and comparing to measured ambient conditions for water and gas compositions.

For the DST THC Model, simulations were run using both of the geochemical systems to represent the processes occurring in the DST. The DST THC Model is used to evaluate the confidence in the THC representation by comparison to the measured water and gas compositions for the DST. The simulation results were compared to the  $\text{CO}_2$  concentrations observed in the DST gas samples, as well as the solution pH, and dissolved cation and anion concentrations of DST water samples. This testing of model results with independent observations provides a method for differentiation between the level of accuracy achieved using the two different geochemical systems: the less complex Case 2 system and the extended Case 1 system.

The THC Seepage Model is used to evaluate the evolution of water and gas compositions and the mineral alteration within the potential repository system through time, especially as driven by thermally coupled processes. Calculations are done for two different geochemical systems: the less complex Case 2 (components are  $\text{H}_2\text{O}$ ,  $\text{CO}_2$ , pH,  $\text{Ca}^{2+}$ ,  $\text{Na}^+$ ,  $\text{SiO}_2$ ,  $\text{Cl}^-$ ,  $[\text{HCO}_3]^-$ ,  $[\text{SO}_4]^{2-}$ ); and the more complex Case 1 (extended to include the additional components  $\text{Mg}^{2+}$ ,  $\text{K}^+$ ,  $[\text{AlO}_2]^-$ ,  $[\text{HFeO}_2]^-$ , and  $\text{F}^-$ ). The results of the THC Seepage model are provided to other AMR/models as

the boundary conditions to the potential emplacement drifts, and represent the input to the THC Abstraction.

*Abstraction of Drift-Scale Coupled Processes* – (ANL-NBS-HS-000029, Rev. 00; also referred to here as THC Abs AMR, N0125). The primary purpose of this AMR is to develop an abstracted model for input to the TSPA model from the results of the fully coupled, THC Seepage Model (MDL-NBS-HS-000001, Rev. 00) for effects on water and gas-phase composition adjacent to the drift wall (in the near-field host rock). The essential concept utilized in the abstraction is that the details of the time histories of the THC Seepage Model results can be represented by a sequence of periods with constant compositions that are meant to capture the major variations in the results. For usage within TSPA, this coarse-level representation should capture the primary aspects of the process results, with minor variations being incorporated via the uncertainty evaluated in the abstraction. This THC Abstraction Model provides the boundary conditions for input to the in-drift geochemical environment component models of TSPA. In addition within this THC Abs AMR, the thermohydrologic results of the *Multi-scale TH Model* (MSTHM) are compared quantitatively to TH results of the THC Seepage Model to evaluate the level of uncertainties introduced into TSPA by combining the abstracted results from these different models within TSPA analyses.

*Thermal Tests Thermal-Hydrological Analyses/Model Report* – (ANL-NBS-TH-000001 Rev. 00; also referred to here as TT TH AMR, N0000). The purpose of the TT TH AMR is to evaluate the drift-scale (DS) TH property set derived from the UZ flow and transport analyses for thermally perturbed conditions. Also, the secondary purpose is to conduct sensitivity studies of other TH property sets, including the MSTH property set, and to investigate modifications that would result in adequate agreement between simulated and measured TH data. Within this context, the analysis applies various TH models implemented various thermohydrologic computer codes (both TOUGH2 and NUFT) such that not only are the property sets evaluated against the field data, but the representational models are also assessed. Because some cases evaluated include parameter sets that have not been calibrated against the specific field test data to which the results are being compared, the thermal/thermohydrologic conceptual models are also being tested in this analysis.

The evaluation is based on TH measurements from the three in situ thermal tests in potential repository lithologic units at Yucca Mountain. All three thermal tests are simulated employing the dual-permeability model (DKM), including the active fracture model (AFM) to represent fracture-matrix interactions. Simulated temperatures and saturation levels are compared to the measurements from the tests. These comparative analyses form the basis for the inferences and conclusions drawn in this AMR regarding the validity of the TH models in terms of the conceptual processes, representational models, and parameter sets. These analyses provide support for the validity of the TH models and their results by quantitative comparison primarily to thermal data from DST, as well as other field thermal tests. The comparative analyses of model results against the testing data and the conclusions drawn from those are referred to in this chapter as the *TH Models Testing Verification and Validation (V&V)*.

*Multiscale Thermohydrologic Model* AMR – (ANL-EBS-MD-000049 Rev. 00; also referred to here as MSTHM AMR E0120). (This AMR is primarily a feed to the EBS PMR to which it

provides the thermodynamic environment parameters describing the conditions within the potential emplacement drifts. See EBS chapter for discussion.) The purpose of the MSTHM is to describe the thermohydrologic evolution of the NFE and EBS throughout the proposed HLNW repository at Yucca Mountain for a particular design. The basic conceptual model for this is that as the rock heats, a thermal gradient will develop driving the water in the system to evaporate (potentially by boiling), migrate as vapor down the temperature gradient, and condense potentially flowing through fractures back toward the drifts and/or between the drifts. These processes are driven by the thermal input (load) from the potential repository and result in changes to the matrix and fracture saturation, percolation flux rate, distribution of water in the host rock, thermodynamic conditions within the drift. The process-level model provides TH information (such as fracture percolation flux and saturation, in-drift temperature, relative humidity, liquid saturation in porous media matrix, etc.) for use in this and other technical products. These derived data are provided for numerous locations throughout the entire repository region as a function of time.

To address the repository and mountain scale variability while maintaining computational efficiency, the MSTHM couples the following submodels: the **S**meared-heat-source **D**rift-scale **T**hermal-conduction (SDT) model; **L**ine-average-heat-source **D**rift-scale **T**hermohydrologic (LDTH); **D**iscrete-heat-source **D**rift-scale **T**hermal-conduction (DDT) model; and **S**meared-heat-source **M**ountain-scale **T**hermal-conduction (SMT) model. The conduction-only models are run for capturing either the local heterogeneity of the design thermal load or the continuous mountain-scale heterogeneity in terms of heat transfer at this large scale. The LDTH model is developed at over 30 specific locations to capture the repository-scale heterogeneity in thermohydrology. The thermal variability constrained in these various models is then layered onto the LDTH results to produce an integrated picture of the thermohydrologic response of the system at over 600 locations in the potential repository. This is done such that the integrated model results for the flow of water and water vapor through partially-saturated fractured rock and the effects on the thermodynamic environment within the drifts reflect the variability in WP heat outputs and mountain-scale lithologic variability. Thus, the MSTHM accounts for 3D DS and mountain-scale heat flow, repository-scale variability of stratigraphy and infiltration flux, and WP-to-WP variability in heat output from WPs. All these MSTHM submodels use the NUFT thermohydrologic computer code for their implementation.

For the NFE, this MSTHM AMR provides model results for the thermally perturbed percolation flux in the near-field host rock (MSTH Percolation Flux Model [PFM]) at two locations away from the drift. The results at 5 m from the drift wall are used to represent the thermally perturbed percolation flux within the *TH Abstraction*. The values for this location are larger than the flux at the drift wall for a period of between about 300 and 600 years during the thermal peak, but are essentially the same at all other times. These values are used to account for the lack of heterogeneity in the fracture representation in the process models that may underestimate the liquid flux near the drift wall. This abstraction is documented in *Abstraction of NFE Drift Thermodynamic Environment and Percolation Flux* (ANL-EBS-HS-000003, Rev. 00). Further description of the full MSTHM implementation and abstraction of the MSTH Drift Thermodynamic Environment Model is covered within the EBS PMR Models Uncertainties chapter (the results of that model/abstraction also provide the thermodynamic conditions for the

potential in-drift environment). Additional details of the MSTH PFM structure and its abstraction usage are provided in the next section and are shown in Figure 7-1.

### C. Model Relations Diagram/Discussion

The NFE process models that provide input to the abstractions incorporated into the TSPA are 1) the THC Seepage Model; and 2) the MSTH PFM. The figures below show how these models relate to the modeling and analyses work in all the AMR that define the NFE PMR and its inputs into the TSPA (Figure 7-1). Because they are used solely as supporting work to provide confidence in these two models, the additional models and analyses shown in Figure 7-1 are discussed in the context of these two primary models.

In Figure 7-1, all the relations among the models, analyses, and abstractions relevant to the NFE Models are shown. There are two models (solid rimmed ellipses in figure) that provide descriptions of the post-closure response of the potential repository to the thermal pulse. The first of these models is the THC Seepage Model. The *TH Models Testing V&V* analysis (a supporting analysis as shown by the dashed rectangle in Figure 7-1) provides direct support to the TH aspects of this model. In addition, there are two additional supporting models that address directly some of the issues with the geochemical concepts and representation within the THC Seepage Model. These are the Ambient THC Model and the DST THC Model. These two models provide support for distinguishing between two conceptualizations of the chemical system for the THC Seepage Model.

The THC Seepage Model provides inputs to the TH Models Comparison analysis in which the output TH parameters (e.g., temperature, percolation flux) from the MSTH PFM are compared to those from the THC Seepage Model. That comparison is used to assess the consistency of combining results for TH processes from the MSTH PFM (and the in-drift results from the rest of the MSTHM as discussed in the EBS PMR models chapters) with the compositional results from the THC Seepage Model. The results from the THC Seepage Model are input to the THC Abstraction that provides the TSPA component models with the description of the water and gas compositions at the drift wall to be used as boundary conditions to the In-Drift Geochemical models (see EBS PMR models chapters).

The second model shown in Figure 7-1 that provides a description of the potential post closure behavior of the NFE is the MSTH PFM. (Note that the MSTHM in its entirety is documented within an AMR covered in the EBS PMR—see EBS chapter.) However, the NFE PMR aspects (i.e., the MSTH PFM) are those model results governing the thermally perturbed flow of water within the host rock. This MSTH PFM is supported by the *TH Models Testing V&V* analyses comparing the results of field thermal testing against the range of TH conceptual and representation models, as well as various parameter sets for those models. (This analysis is general support to all of the models that utilize TH modeling and also supports the THC Seepage Model.) The MSTH PFM provides inputs to the *TH Models Comparison* analysis (supporting analysis as shown by the dashed rectangle in Figure 7-1; ANL-NBS-HS-000029, Rev. 00). In addition, this MSTH PFM gives input to the *TH Abstraction*, which uses the thermally perturbed percolation flux conditions 5 m outside the drift to provide as input to the Seepage Model. This

abstraction is connected essentially directly to the *Seepage Abstraction* in the TSPA (the In-Drift aspects of the TH abstraction are discussed in the EBS Uncertainties chapter).

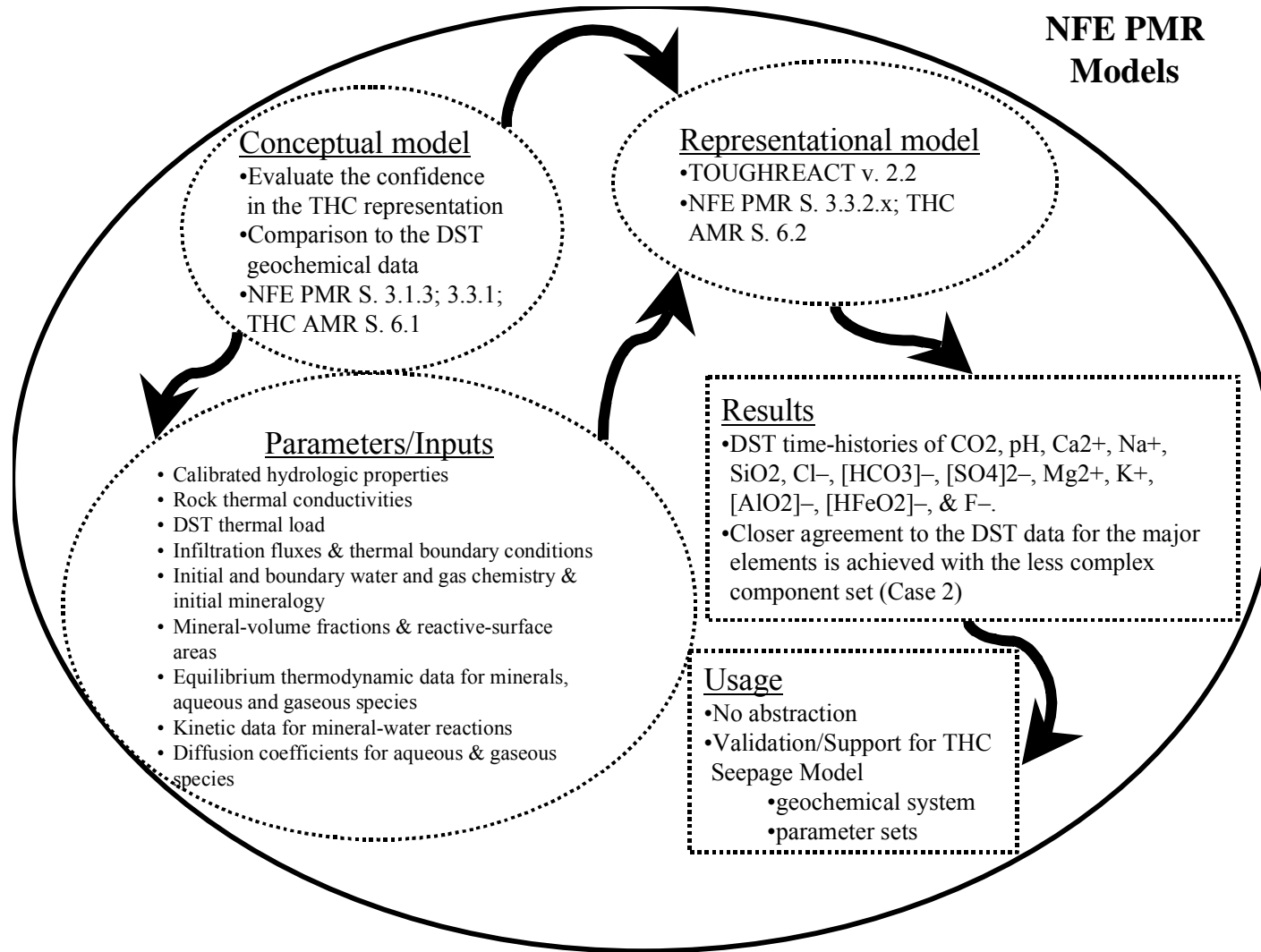
## **7.2 Uncertainty Treatment within the Near Field Environment Models**

The section below provides the discussion of the manner in which uncertainty and variability are addressed first within the THC model, and its supporting models/analyses, then for the MSTH PFM, and its supporting models/analyses. In each of these discussions, the Model uncertainties are covered within the categories shown within Figure 7-2, Description of the Model Aspects for the DST THC Model; Figure 7-3, Description of the Model Aspects for the Ambient THC Model; Figure 7-4, Description of the Model Aspects for the THC Seepage Model; and Figure 7-5, Description of the Model Aspects for the Multiscale TH Percolation Flux Model (i.e., conceptual model, the representational model, and the inputs/parameters of the model). In addition, the manner in which variability gets included in the model is covered for both spatial and temporal variability. Finally, the discussion covers the manner in which these uncertainties and variabilities are incorporated, and the degree to which they are reflected, in the final results of the model.

### **A. THC Seepage Model**

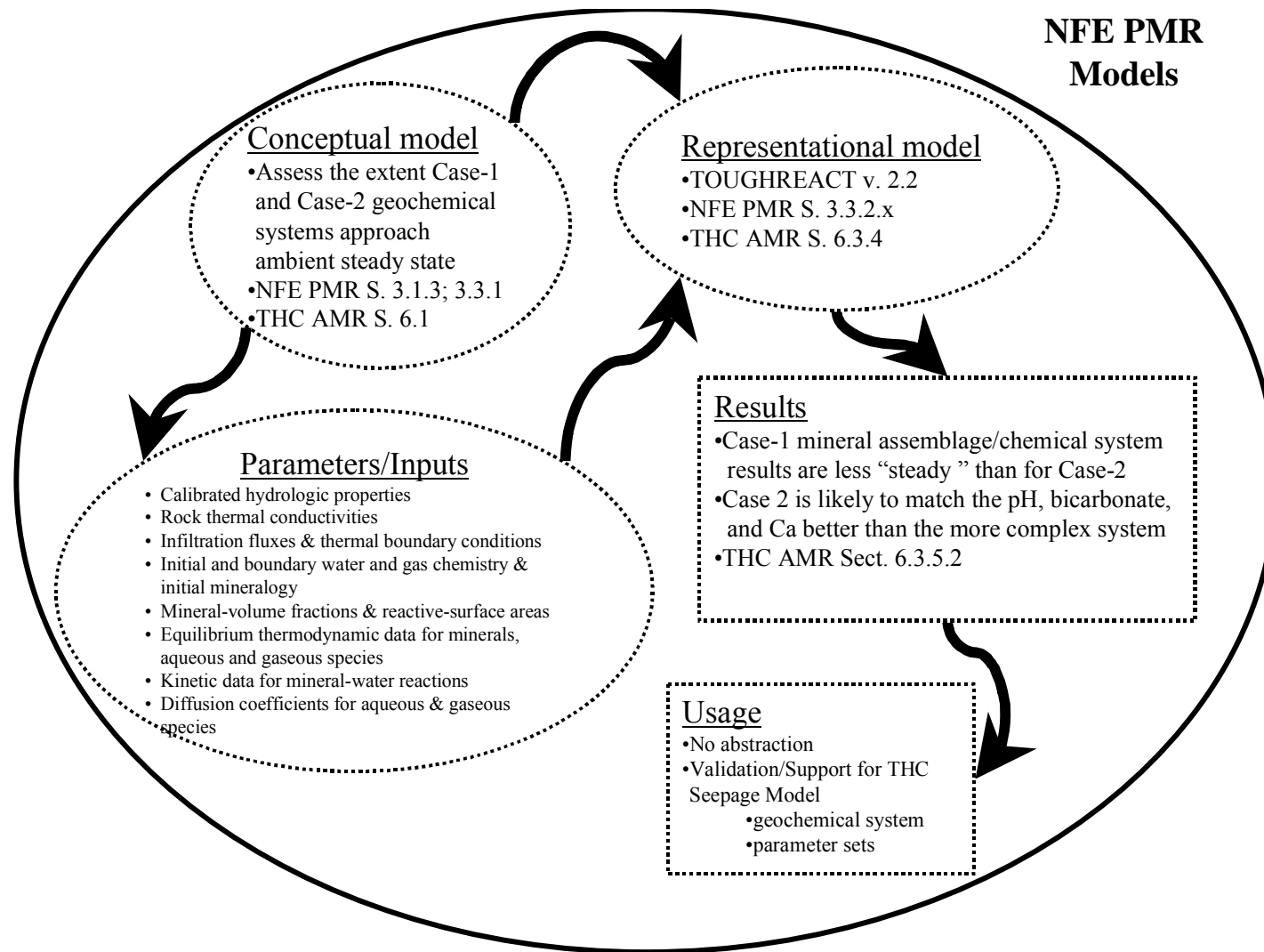
This section describes the manner in which uncertainty and variability have been incorporated into the THC Seepage Model (MDL-NBS-HS-000001, Rev. 00), and the extent to which that is reflected directly within the output/results of the model. This entails discussion of the treatment within the THC Seepage Model itself (Figure 7-2), as well as additional treatment of uncertainties via the Ambient THC and the DST THC models (Figure 7-3 and 7-4) that are developed within the same AMR (MDL-NBS-HS-000001, Rev. 00). These additional models are used for support and evaluation of the conceptual and representational models and parameter sets utilized within the THC Seepage Model (see Figure 7-1). In addition, the work done to validate the thermohydrologic models in the *TH Testing V&V* analyses provides assessment of conceptual and parameter uncertainty for the TH aspects of this THC Seepage Model and is discussed in context below.

The THC Seepage Model (MDL-NBS-HS-000001, Rev. 00) is a fully-coupled, reactive transport model for computation of the reactions among and transport of aqueous liquids, solids, and gases in a fractured porous media. This modeling approach covers hydrology, geochemistry, and transport under changing thermal conditions with explicit coupling between these areas. There are sources of uncertainties within each of these technical areas, including the manner in which the coupling is handled. Because this modeling work builds upon thermohydrologic process models, these technical areas are grouped into the following four: 1) geochemical; 2) thermohydrologic; 3) transport; and 4) coupling. The various types of uncertainties and their treatment are summarized in Table 7-1 below for each of these technical topics. The discussions below cover these in the same manner as that shown in Table 7-1, as appropriate to each subsection.



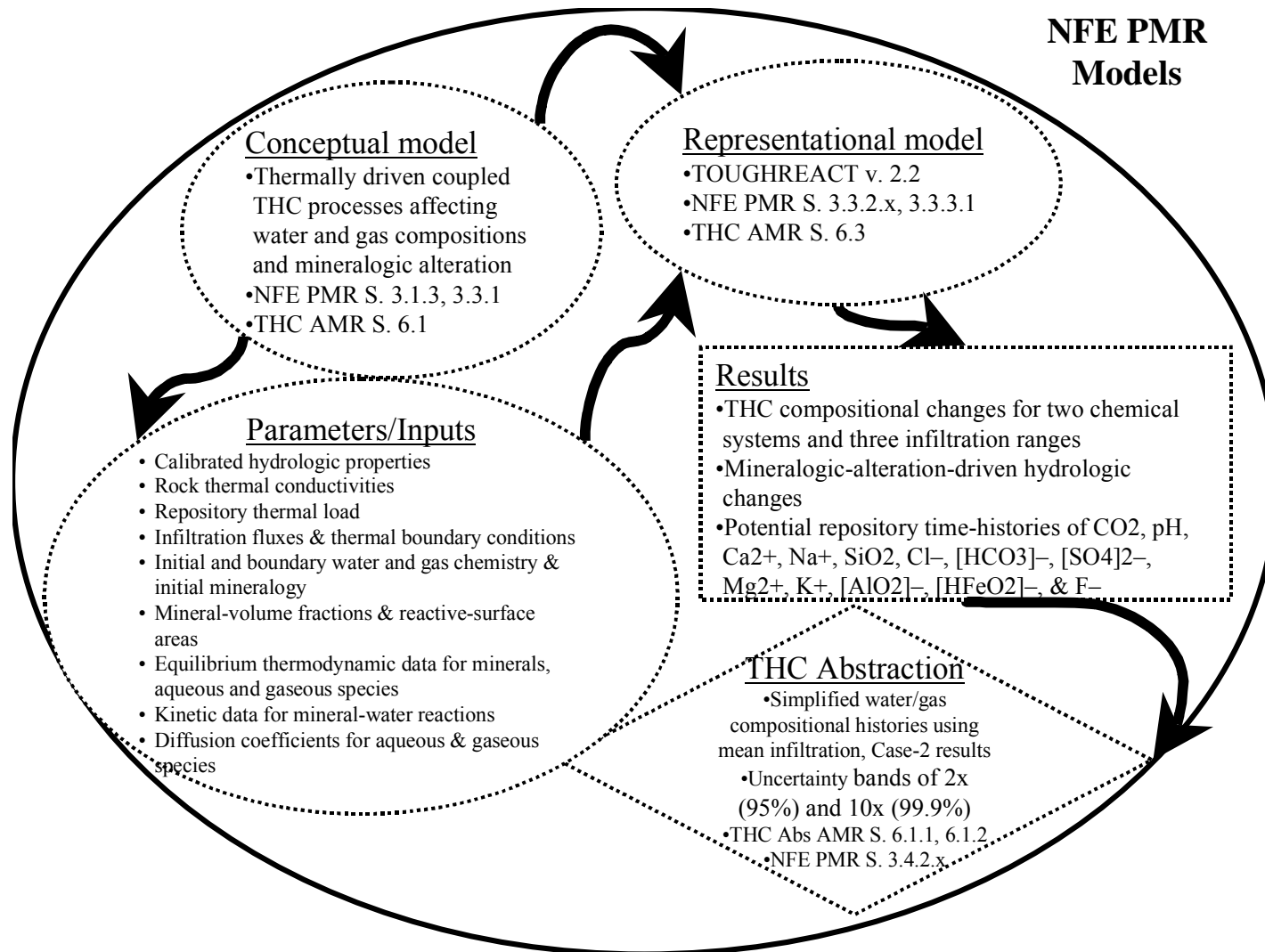
(Note: This model provides validation support to the THC Seepage Model.)

Figure 7-2: Description of the Model Aspects for the Drift Scale Test Thermohydrochemical Model



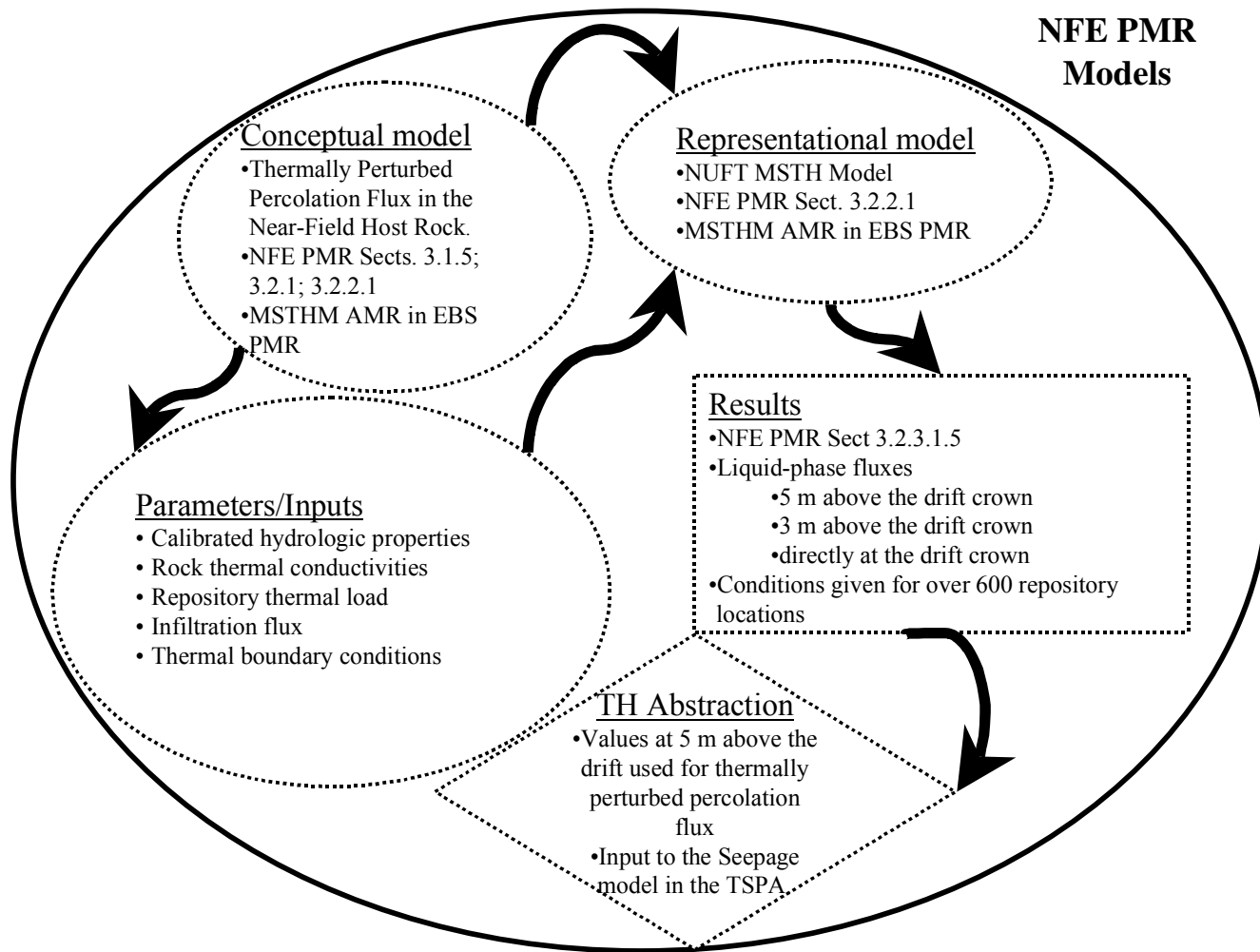
(Note: This model provides validation support to the THC Seepage Model.)

Figure 7-3: Description of the Model Aspects for the Ambient Thermohydrochemical Model



(Note: This model provides the input to the THC Seepage Abstraction.)

Figure 7-4: Description of the Model Aspects for the Thermohydrochemical Seepage Model



(Note: This model provides the input to the TH Abstraction.)

Figure 7-5: Description of the Model Aspects for the Multiscale Thermohydrologic Percolation Flux Model

## **Conceptual Uncertainties**

The THC Seepage Model (MDL-NBS-HS-000001, Rev. 00) is used within the NFE to evaluate the changes to the composition of water and gas that are moving through fractures to the drift wall. That is, this model defines the geochemical boundary conditions for the environment within the drifts. In addition, because of the fully coupled nature of this model, any changes to the thermohydrology as a result of mineral precipitation and/or dissolution or alteration of minerals would be incorporated in these calculations. If the *THC Seepage* results indicated that changes of this latter type were anticipated, the uncoupled UZ hydrology models may be revised with updated parameter values (e.g., for permeability) as predicted by the coupled models to assess the impacts to results of the UZ flow models.

Because this type of model couples geochemical reaction and transport with thermohydrologic modeling, it encompasses conceptual models in each of these areas. The THC Seepage Model is based upon the TH model implemented in TOUGH2. This TH model is conceptually similar to the thermohydrologic sub-model of the Multiscale Thermohydrology Model (MSTHM; ANL-EBS-MD-000049 Rev. 00) that is implemented using the NUFT computer code (see next section below on the MSTH PFM). In general, the thermohydrologic conceptual uncertainties are addressed by the *TH Models Testing V&V* analysis (ANL-NBS-TH-000001 Rev. 00) that provides some validation testing for the models as discussed below.

An additional conceptual uncertainty covered is the boundary condition at the surface where the infiltration flux is given as a function of changing climatic states. Three successive climate states are represented: 1) present day; 2) monsoon; and 3) glacial transition. The transitions between these are set to occur at 600 years and 2,000 years. Although this covers the inclusion of the concept of a variable climate, the uncertainty in the infiltration rate for a given climate is discussed within the parameter uncertainty below. There was no assessment of uncertainty in the timing of transition (for additional detail see the UZ PMR Uncertainties chapter section covering the Climate Model).

This THC Seepage Model implements the active fracture (AF) representation of the DKM and does not explore the potential alternate conceptual models. However, possible alternate conceptual models are discussed in the UZ PMR Uncertainties chapter covering the UZ Flow Model, for which the AF representation was derived.

*TH Models Testing V&V* – Within the TT TH AMR (ANL-NBS-TH-000001 Rev. 00), the appropriateness of the conceptual model, representational model, and parameters in various thermohydrologic models are tested by comparing simulated performance with the measured performance of relatively large-scale *in situ* tests (several meters to tens of meters). This analysis is focussed primarily on the thermal, and to a lesser extent the thermohydrologic, aspects of the test and model results. More discussion is given below in the sections covering the MSTH PFM that describes how the *TH Models Testing V&V* analysis (ANL-NBS-TH-000001 Rev. 00) addresses uncertainties of the TH modeling. The remaining uncertainties for fracture-matrix interaction within the TH models would impact directly the degree of liquid flux in the

fractures versus the matrix and, therefore, affect the amount of mineral precipitates formed in those two continua.

The geochemical conceptual model (see Table 7-1) incorporated into the THC Seepage Model covers aspects related to 1) the representativeness of the mineralogy to the potential repository horizon; 2) the comprehensiveness of the chemical system modeled; 3) the initial state of the geochemical system; 4) the initial water composition in the host rock; 5) the representativeness and functional dependency of the thermodynamic data; and 6) the representativeness and functional dependency of the kinetic data. These aspects have been discussed qualitatively, in most cases, but there was model validation evaluated within the THC AMR (MDL-NBS-HS-000001, Rev. 00) using two different geochemical systems (that directly address item (b) above, and addresses other aspects indirectly). For these two compositional systems, calculations were done for quantitative comparisons between the results of the DST and the DST THC Model (see Figure 7-3). Also, for comparison of their approach to steady state, the ambient state was evaluated for both these model geochemical systems with the Ambient THC Model (see Figure 7-4). These assessments were utilized to recommend which of the geochemical systems (i.e., conceptual models) appears to be more reasonable to use for estimates of long-term system behavior. It would seem from a theoretical point of view that the more detailed compositional system would be more appropriate. However it appears that the additional conceptual uncertainties in items (e) and (f) above, as well as additional parameter uncertainties (discussed below), for the more complex chemical system were more than enough to offset the reduction in conceptual uncertainty expected from the larger set of chemical components.

As paraphrased from the THC AMR (MDL-NBS-HS-000001, Rev. 00), the THC calculations using the Case 1 (“full”set) components include the major solid phases (minerals and glass) encountered in geologic units at Yucca Mountain, the range of possible reaction-product minerals, CO<sub>2</sub> gas, and all the aqueous species necessary to incorporate these solid phases and the DST pore-water composition into the THC model. The Case 2 (“simplified”set) is a subset of the Case 1 representation created by excluding aluminum silicate minerals, which form or dissolve much less readily than minerals such as calcite or gypsum, and for which thermodynamic and kinetic data are not as well established as for the other minerals. These aluminosilicate phases also tend to be incorporated with highly simplified representations of their complex crystal chemistry. Although this simplification is a fairly standard treatment in the literature, it results in some additional conceptual uncertainty for this aspect of the Case 1 model calculations.

It was found (MDL-NBS-HS-000001, Rev. 00) from comparison with water and gas compositions observed from the DST:

*As discussed later (Sections 6.2.7.2 and 6.3.5.2), Case- 2 THC simulations appear to predict more realistic pH and gas-phase CO<sub>2</sub> concentration trends than Case-1 simulations, because the latter may be overpredicting the reaction rates of aluminum silicate minerals, indirectly affecting these parameters. Therefore, even though Case 1 represents the near-field environment more completely than Case 2, the latter may yield more accurate THC model results than Case 1.*

In addition, for geologic time scale application, there were some analyses comparing the stability of the results based on these two compositional systems. For these Ambient THC model results it was found that:

*The large pH and carbonate concentration variations for the 1mm/yr ambient run in Case 1 (Figures 30 and 32) reflect an initially “unsteady” hydrochemical system. Obtaining an initial steady-state chemical system that is similar to the measured data for a few points is difficult because it depends on reaction rates as well as infiltration rates and rock properties. The difficulty increases with the number of reactive minerals included in the system, and with the uncertainty in reaction rates. This is the reason why calculated ambient concentration trends are less variable in Case 2 than in Case 1.*

and,

*In addition, as mentioned earlier, the simulations under ambient conditions (no thermal loading) using the Case-1 mineral assemblage reveal a chemical system that is less “steady” than for Case-2 simulations (e.g., by comparing the ambient curves for pH, bicarbonate, and CO<sub>2</sub> on Figures 28 through 33). This reflects the model uncertainty with respect to reaction rates and the difficulty in reproducing an initially balanced hydrogeochemical system, which depends on infiltration rates and rock properties as well as reaction rates. Given this observation, a reduced set of minerals with better-constrained reaction rates such as for Case 2 is likely to match the pH, bicarbonate, and Ca better than the more complex system. This is shown with simulations of the DST (Section 6.2.7), which indicate that a Case-2 mineral assemblage provides better estimates of pH and CO<sub>2</sub> concentrations than Case 1, compared to waters and gases collected in the first 20 months of heating.*

It appears that the overall uncertainty is less in the simplified case (Case 2) for the major element geochemical subsystem that is shared by both of the compositional cases. In addition though, the concentrations of the additional components that are included only within the more complex compositional case (Case 1) provide estimates for those constituents that are much less uncertain than no values at all. As such, these minor constituent values represent a reduction in conceptual uncertainty regarding those minor elements, even though they have a large relative uncertainty that results from the larger uncertainty in the major element composition of the solution. This analysis is one of the best treatments of conceptual model uncertainty through the evaluation of alternative conceptual models.

For the transport aspects of the THC Seepage Model, the main conceptual uncertainty addressed is the need for an approach that explicitly represents the fracture and matrix systems independently. This allows incorporation of the differences in initial mineralogy in these two parts of the system. Furthermore, this treatment permits evolution of different compositional conditions in the two systems. This also allows representation of disequilibrium between the fracture chemical system and the matrix chemical system as driven by differential transport processes in the two media (as well as the degree of fracture-matrix interaction). The

development of differences between these chemical systems in the fractures and the matrix will also drive differences in mineral reaction rates. The ability to include such considerations in the model addresses the conceptual issue related to attainment of equilibrium between the chemical transport system in the fractures and that in the matrix because it allows for evaluation of the disequilibrium system.

One set of processes that is unique to the coupled THC process modeling is the continuous feedback between the chemical reaction-driven changes to the system and the changes to the hydrologic properties of the system. This is represented in both the fracture and matrix media. This coupling is assumed to be negligible in the thermohydrologic process models, but is explicitly incorporated here to assess the magnitude of its affects, and thereby eliminate the large conceptual uncertainty of no representation at all. However, the conceptual uncertainties regarding how the coupling process works are not treated directly within this AMR (MDL-NBS-HS-000001, Rev. 00). Rather, the approaches used to couple mineral precipitation/dissolution to the changes in porosity and permeability within the fracture and matrix networks are taken from the standard methodologies in the literature (see Table 7-1). These are a cubic law relation for changes to fracture permeability (Section 6.1.6.2, MDL-NBS-HS-000001, Rev. 00), and a simplified Carmen-Kozeny relation (Section 6.1.6.3, MDL-NBS-HS-000001, Rev. 00). Although these relations are commonly used, they are other approaches. This is an area where conceptual uncertainty could be assessed in a more direct manner by evaluating some alternate conceptual models for how changes in porosity affect changes in permeability (e.g., see Oelkers, 1996).

### **Representational Uncertainties**

The THC Seepage Model, as implemented within the TOUGHREACT coupled reactive transport computer code, was checked to ensure that there were not computational uncertainties introduced by incorporating the geochemical aspects of the system into the thermohydrologic model representation. To do this, a comparison was made between results of the THC Seepage Model and results obtained from the code using only the thermohydrologic aspects of it. The results were found to agree closely as indicated in Section 6.3.5.2 (MDL-NBS-HS-000001, Rev. 00):

*Temperatures, liquid saturation, and air mass fractions calculated for the mean infiltration case (6/16/25 mm/year) are directly comparable to those obtained from the TH simulation (Figures 20 through 22) because the latter was carried out using the same infiltration rates. The results of the TH and THC simulations are essentially identical. As discussed later, the thermal and hydrologic behavior of the system is not significantly affected by water-gas-rock chemical interactions and, therefore, temperatures, liquid saturations, and air mass fractions calculated with THC (Case 1 and Case 2) and TH simulations are nearly the same.*

This indicates that the representational model for the chemical aspects of the system that was added to the thermohydrologic representation to build the TOUGHREACT code did not introduce any representational uncertainties within the pre-existing thermohydrologic portions.

Other representational uncertainties that were addressed in the THC AMR to some degree (see Table 7-1) are 1) the evolution of fracture permeability from mineral alteration averaged over grid block; 2) the mathematical implementation of the time step; and 3) the mathematical approach to solving the coupled equations. The third of these used standard approaches from the literature to solve simultaneously the geochemical problem for each grid block and solve sequentially the “equations for heat, liquid and gas flow, aqueous and gaseous species transport, chemical reactions, and permeability/porosity changes” (Section 6.1.3, MDL-NBS-HS-000001, Rev. 00). For these other aspects, ranges of grid sizes or time steps were used to cover in more detail those areas/times that required more detailed information, or to conduct sensitivity studies to determine values that were appropriate (see Table 7-1).

*TH Models Testing V&V* – The TOUGH2 code is the basis for the thermohydrologic representation built into the TOUGHREACT code for the THC Seepage Model. This representation was tested and found to be adequate within the TT TH AMR (ANL-NBS-TH-000001 Rev. 00) by comparing simulated performance with measured performance of relatively large scale (several to tens of meters) in situ tests. Further discussion is given below in the sections covering the MSTH PFM on how *TH Models Testing V&V* analysis (ANL-NBS-TH-000001 Rev. 00) addresses representational uncertainties of the TH modeling.

### **Parameter Uncertainties**

Within this type of coupled process model that encompasses thermally-driven hydrology and geochemical reaction and transport, there is a wide variety of parameter types that encompasses a very large number of specific parameters. Table 7-1 contains a listing of the major parameter types that are incorporated into the THC Seepage Model and a review of the manner in which they are incorporated into the model and how the uncertainties in these parameters are treated. In most cases, there is not any explicit treatment of the uncertainties involved, or there is only qualitative discussion of the uncertainties in a particular parameter type. For this AMR (MDL-NBS-HS-000001, Rev. 00), the assessment of uncertainties in this area relies mostly on the validation using comparisons of the results of the DST THC Model with the independent observations from the Drift Scale Heater test, as well as analysis of the Ambient THC Model results. This general approach is summarized in Section 7.0 (MDL-NBS-HS-000001, Rev. 00):

*There are many uncertainties in modeling coupled THC processes because of the large amount of data needed and the complexity of natural systems. These data range from the fundamental thermodynamic properties of minerals, aqueous species, and gases, the kinetic data for mineral-water reactions, to the representation of the unsaturated hydrologic system for the fractured tuffs. In addition, a wealth of site-specific thermohydrologic, geologic, and geochemical data are necessary to describe the initial and boundary conditions. For these reasons, it may not be possible to assign a model uncertainty based on the uncertainties of the data themselves, and therefore model validation gives a true test of whether the system can be described sufficiently well for the intended purposes of the model. Results of simulations of the DST captured the important changes in pH and gas-phase CO<sub>2</sub> concentrations at each location over time well within the range of variation in the measured gas and water concentrations*

*between sampling locations. This provides a sufficient validation of the model's capability for the prediction of spatial and temporal variation in water and gas chemistry.*

These specific comparative modeling analyses are discussed above in the section covering the conceptual uncertainties for the THC Seepage Model. That assessment covers the overall uncertainties and therefore the uncertainties in the parameter sets used. The major parameter sets for the geochemical portion of the model are the thermodynamic data, the intrinsic rate constants for the mineral reactions (kinetic parameters), and the reactive surface areas for both matrix and fracture minerals. In the first two cases the parameters are included based on standard approaches in the literature and published data sets, and the AMR has a qualitative discussion regarding uncertainties in the data sets.

In the case of the reactive surface areas, the THC Seepage Model uses standard published methods based on geometric approaches modified for the AF approach to the dual permeability model for the hydrologic system. However, there is no direct treatment of the uncertainty in the reactive surface area parameter values (see Section 6.1.5, MDL-NBS-HS-000001, Rev. 00). The treatment of these parameter values includes description of the mineral abundance and morphology, and the water-mineral contact areas in an unsaturated system based on the AF approach. The uncertainties in the values for these parameters could be one of the larger sources of uncertainties within this modeling work. Within a representative element volume, the estimated range of potential reactive surface area is greater than five orders of magnitude (Oelkers, 1996). This estimate represents the difference between fully saturated matrix reactive surface area and the reactive surface area of a saturated fracture, but does not include a partially saturated fracture (p. 169 Oelkers, 1996). The first aspect probably represents a method that would lead to an overestimate of the uncertainty for the THC Seepage Model because the matrix and fractures are treated explicitly separately. However, given the lack of consideration of the second aspect, the reactive surface areas may still have a range of uncertainty that is more than an order of magnitude.

The major parameters included in the THC Seepage Model covering the thermohydrologic aspects of the model are summarized in Table 7-1. The model includes the calibrated property set that encompasses a number of types of uncertainties within it (see the chapter covering the UZ flow model uncertainties treatment for details). In addition, the uncertainty in the infiltration rate is evaluated explicitly for the THC Seepage Model. As for the MSTH PFM discussed below, these uncertainties are incorporated by producing results for the three cases that encompass the low, mean and high infiltration rates that were defined based on the uncertainty in the infiltration rate (see the UZ Flow uncertainties chapter for more details). This is one of the main instances where the uncertainties were evaluated quantitatively all the way through to their explicit effect on the results of the process model. This approach was used throughout almost all of the hydrology-based models (e.g., see the UZ flow chapter).

TH Models Testing V&V – Uncertainty in the TH parameters used within the THC Seepage Model was also addressed by the validation testing done for the TH models themselves in the TT TH AMR (ANL-NBS-TH-000001 Rev. 00). Based on a review of this material, it appears that uncertainties in the heat transfer parameters are relatively small compared to other PA

parameters, but that there may be significant uncertainty in the hydrologic parameters (especially related to vapor transport and liquid refluxing in fractures). Further discussion is given below in the sections covering the MSTH PFM on how the *TH Models Testing V&V* analysis (ANL-NBS-TH-000001 Rev. 00) addresses parameter uncertainties of the TH modeling.

For the transport parameters of the THC Seepage Model, very little was done to include or assess specific uncertainties (Table 7-1). Single values were used for the tortuosity values of both the fracture pathways and the matrix pathways. In the first case, the value was based on models of in situ testing, but no uncertainty was captured in that value. The matrix value was estimated based on literature values without quantification of the uncertainty in that estimate. The uncertainty in the value used for tracer diffusion coefficients was treated using a bounding approach. This approach was to use a value for the aqueous diffusion coefficient of Cl<sup>-</sup> at infinite dilution to represent all aqueous diffusion coefficients. Semi-quantitative assessment indicated that the basis for this was in part that this value differs by at most one order of magnitude for all aqueous species (MDL-NBS-HS-000001, Rev. 00), and that most differ by less than a factor of two. Because the value chosen was the bounding value, these uncertainty estimates were not explicitly used. Finally, the gaseous diffusion coefficient for CO<sub>2</sub> was developed in this model as a temperature and pressure dependent parameter using a standard published approach, but had no explicit uncertainty treatment included.

### **Spatial Variability**

Spatial variability is captured in the THC Seepage Model (and the supporting models) in two ways (see Table 7-1). In the first, the *vertical* spatial variability of the lithologic units is included in the model through the definition of the geologic units that occur in the vertical sequence. This is the case for the fracture and matrix mineralogies included in the model, as well as the hydrologic and thermal properties of the rock. The second type of spatial variability results from some of the functional dependencies that are built into the parameter values representations. Both thermodynamic and kinetic rate constants vary spatially as a function of the variable temperatures considered within the model. In addition, the values of thermal conductivity vary as a function of the saturation, which is spatially variable across the site and in the grid blocks of the model. These functional dependencies of parameters with respect to temperature and/or saturation are also the source of some of the temporal variability found for properties within the model. The lateral variability within the lithologic units has not been captured at this point.

### **Temporal Variability**

There are only a few parameters that are defined as temporally variable inputs to the THC model. The primary one is the infiltration flux that varies through time due to potential climate changes. In addition to this, the other parameters that are temperature and saturation dependent have fully-coupled temporal variability (see Table 7-1). These include thermodynamic and kinetic rate constants, rock mass thermal conductivity, effective thermal conductivity for the *fictive* porous media that represent open air spaces in the model, and the gaseous diffusion coefficient. (**Note:** “fictive porous media” are used to represent the properties of open air spaces in porous media codes used in the THC and TH calculations. That is, an open air space is assigned the effective thermal and hydrologic properties of a non-existent porous medium in order for that region to be

treated in the model. This generally involves calibrating effective values for permeability and thermal conductivity based on analytical solutions for actual heat transfer in open air spaces via convective and radiative processes. This aspect of these models also applies to conceptual model uncertainty—see Table 7-1—but this was not covered in the document.) The gaseous diffusion coefficient is functionally dependent not just on temperature but also on pressure. The functionality of these parameters within the models allows them to capture temporal variability by evolving directly in response to the temporal changes in temperature and saturation.

### **Incorporation into the Results**

The major aspects of uncertainty that are incorporated directly into the results of the THC Seepage Model are the conceptual uncertainty of the geochemical system being modeled and the parameter uncertainty of the infiltration rate. These are captured using different simulations. Simulations were performed for both geochemical systems (Case 1 and Case 2) for each of three infiltration histories (low, mean, and high) representing the range of that uncertainty (MDL-NBS-HS-000001, Rev. 00). The uncertainty in the hydrologic properties is also captured in a less direct manner within these three infiltration scenarios because the calibrated hydrologic parameters are derived for each of the infiltration cases (Sec. 4.1.1; MDL-NBS-HS-000001, Rev. 00). Because there are a number of areas of uncertainty that have only been discussed qualitatively without any specific quantitative evaluation, there are uncertainties that have not been included quantitatively within the results of this model.

In addition, the level of uncertainty in the overall results is assessed in part within the comparison of the DST THC Model results against the observations of the drift scale test (Sec. 6.2.7; MDL-NBS-HS-000001, Rev. 00). The comparison is provided both for the modeled gas and water compositions and indicates that the results can be reproduced within an order of magnitude in most cases, and generally much better. However, the long time frame that is modeled for the post-closure system is not addressed directly by comparison with such shorter field-scale tests.

The types of variability, as discussed above, are captured directly as part of the representational model for the THC Seepage Model and no further discussion of their incorporation is needed.

### **B. MSTH Percolation Flux Model**

This section describes the manner in which uncertainty and variability have been assessed/incorporated into the MSTH PFM, and the extent to which that is reflected directly within the output/results of the model (see Table 7-2). This is provided as discussion of both the treatment within the MSTH PFM itself, and the additional treatment as documented in the TT TH AMR (ANL-NBS-TH-000001 Rev. 00). The analysis/validation of the TH models in the TT TH AMR is referred to in this document as the *TH Models Testing V&V*. Figure 7-5 shows the model components of the MSTH PFM with short descriptions of their essential elements and where they are documented. In general, the system variability is dealt with more directly within this model than is the uncertainty in the model itself. However, spatial (and temporal) variability would contribute to conceptual model and parameter uncertainty if not explicitly represented in this modeling work.

## **Conceptual Uncertainties**

The MSTH PFM is the subset of results from the MSTHM AMR (ANL-EBS-MD-000049 Rev. 00) that are applicable directly to the NFE (i.e., the thermally perturbed portion of the geosphere). This model has as its foundation the MSTHM LDTH model that is essentially a two-dimensional thermohydrologic column model. More than thirty separate columns are used to represent the repository, onto which the thermal variability defined in the conduction-only submodels (DDT, LDTH, and SMT) is layered to provide thermohydrologic conditions at over 600 locations in the potential repository. The first section of Table 7-2 covers the manner in which the conceptual uncertainties in this MSTH PFM are treated. Note that the table contains information taken from the MSTHM AMR (ANL-EBS-MD-000049 Rev. 00) as well as from the TT TH AMR (ANL-NBS-TH-000001 Rev. 00).

This approach incorporates both the processes of conductive and convective heat transfer (which includes vaporization and condensation) within the rock. These processes appear to be the primary concepts needed to represent adequately the heat transfer in the rock (see discussion below regarding the *TH Models Testing V&V*). However there remains a fairly major source of conceptual uncertainty in terms of the location and flux of liquid within the fracture system. The AFM is applied and appears to be a reasonable choice over the other conceptual models investigated (Equivalent Continuum Model and DKM). (The AFM is an extension/modification of the DKM approach that addresses the concepts that only a portion of each fracture contains the flow or that flow occurs in only a fraction of the fractures in the system. Hence the fracture-matrix interaction is reduced relative to the flux in the fractures (i.e., large portions of the matrix may be well below saturation but flow occurs in the fractures—see the chapter on the UZ Flow model for more detail). Some qualitative analysis was performed in the *TH Models Testing V&V* work (discussed below) that compared the predicted saturation with the observed hydrologic response in the DST. Quantitative analysis of the actual hydrologic data from the DST may provide an estimate of overall uncertainty within the MSTH Percolation Flux modeling approach, including uncertainty from the conceptual approach.

Another source of conceptual uncertainty within the MSTHM is the approach of combining the results of thermohydrologic column models with a series of temperature variations derived from conduction-only models. These conduction-only models are derived at various scales to capture thermal source variability and mountain-scale geologic variations. Within the conduction only portions of the SMT, one conceptual simplification that was made is that there is no lateral (horizontal) conduction (Sec. 5.3.1) at the lower boundary (1000 m below the water table). This is justified in the MSTHM AMR as bounding because basal boundary condition temperatures should be overestimated by this method.

Edge cooling is represented within the MSTHM approach because the edge locations in the LDTH submodel have thermal source histories adjusted for the edge effects (i.e., some reflect being bordered on all sides by waste, whereas others have some borders lacking waste). Because the SMT submodel allows lateral heat flow to occur, which allows the heat to spread outside of the potential repository footprint. This MSTHM approach is described in Section 6.1 of the MSTHM AMR (ANL-EBS-MD-000049 Rev. 00) as:

*It is useful to think of the LDTH submodel as the "core" submodel. These 2-D drift-scale TH submodels are run for 31 locations (Figure 5-2) spaced evenly throughout the repository area for several Areal Mass Loading (AML) values (nominal value and lower) to represent the influence of edge-cooling effects. The LDTH submodel includes the hydrologic processes and parameters (e.g., surface infiltration rates, hydrologic properties) used to describe a location, given specific coordinates within the repository. The remaining three submodels, which are conduction only, are required to account for the influence of 3-D mountain-scale heat flow and 3-D drift-scale heat flow on drift-scale TH behavior. The coupling of 3-D mountain-scale heat flow to 2-D drift-scale TH behavior is accomplished with the SMT and the SDT submodels. The SMT is 3-D and includes the influence of thermal-property variation in the mountain, lateral heat loss at the repository edges, and overburden-thickness variation with location, assuming a uniform, planar (i.e., smeared) heat source throughout the repository area. The SDT submodel is a 1-D (vertical) submodel, run at the same 31 locations and for the same AMLs as the LDTH submodels.*

It should be noted that for the comparison to the DST results (discussed below), the TT TH AMR (ANL-NBS-TH-000001 Rev. 00) only covers directly the core LDTH submodel from this suite of MSTHM sub-models.

*TH Models Testing V&V* – Within the TT TH AMR (ANL-NBS-TH-000001 Rev. 00), appropriate conceptual model, representational model, and parameters for particular near-field thermal-hydrological models are determined by comparing simulated performance with measured performance of relatively large scale (several to tens of meters) in situ tests. This analysis used several different conceptual models (including conduction only, as for ANSYS). One conceptual model (the DKM—either with the AF concept and the DS property set, or with a site specific property set for the thermal test) was confirmed by comparison of the observations from large-scale in situ thermal tests (e.g., “heat-pipe signature,” p. 54) with the model results. The other conceptual models currently considered were not as viable as determined by comparison to the observations. Based on the analysis, it appears that uncertainties in the conceptual model have been largely resolved, except perhaps for fracture-matrix interaction. Because this analysis was a highly quantitative statistical comparison for the temperature measurements, the agreement (at about the 13 percent level, ANL-NBS-TH-000001 Rev. 00) indicates that the modeling of the heat transfer processes can be viewed as fairly robust. However, the qualitative evaluation of the liquid saturation does not provide a sufficiently detailed quantitative basis for assessing similarly the detailed hydrologic processes being modeled. The remaining uncertainties for fracture-matrix interaction would impact directly the degree of liquid flux in the fractures vs. matrix.

### **Representational Uncertainties**

The second section of Table 7-2 covers the representational model uncertainties for the MSTH PFM. The MSTH PFM from the MSTHM AMR (ANL-EBS-MD-000049 Rev. 00) is generated using the thermal conduction and thermohydrologic calculations performed within NUFT. There

was little description in the document regarding the uncertainty that this representation may contain. However, the *TH Models Testing V&V* work evaluated a number of implementations of thermal models (conduction-only and TH models), including NUFT and TOUGH2, and found essentially no difference, as long as the conceptual model and model inputs were the same. The NUFT code is used for the LDTH submodel of the MSTH Modeling, and TOUGH2 is the code used for the TH module of the TOUGHREACT code that implements the THC Seepage Model (see above).

*TH Models Testing V&V* – Within the TT TH AMR (ANL-NBS-TH-000001 Rev. 00), appropriate conceptual model, representational model, and parameters for particular near-field thermal-hydrological models are determined by comparing simulated performance with measured performance of relatively large scale (several to tens of meters) in situ tests. This analysis found that either TOUGH2 or NUFT, with the appropriate parameters values, resulted in simulated performance that adequately matched measured performance of relatively large-scale in situ thermal tests. It appears that uncertainties in the mathematical model are relatively small compared to other PA uncertainties and can be ignored.

### **Parameter Uncertainties**

A number of parameter uncertainties are dealt with directly for the MSTH PFM from the MSTHM AMR (ANL-EBS-MD-000049 Rev. 00). These include 1) the infiltration/percolation flux uncertainty for each of the various climate states; 2) the saturated saturation values of both the backfill and invert materials within the potential drifts; and 3) the seepage flux (see Table 7-2). The first of these is addressed explicitly, whereas the latter two are treated in a bounding manner. For the MSTHM thermohydrologic modeling in this revision of the AMR (ANL-EBS-MD-000049 Rev. 00), no seepage flux is included directly in the model. The seepage flux is stated in Section 7.1 to be negligible compared to the amount of liquid flux entering the drift because of capillary wicking of liquid out of the fractures and into the backfill materials. Given the ubiquitous nature of this wicking flux, the limited occurrence of minor seepage flux was taken as bounded by that flux. The saturated saturation values of the backfill and invert materials are taken to be 1.0 (Section 5.2.3) and are justified as conservative because this is the upper bound for this parameter value. This tends to maximize the water content in these materials, which would maximize the potential for radionuclide transport through these materials.

*TH Models Testing V&V* – Within the TT TH AMR (ANL-NBS-TH-000001 Rev. 00), appropriate conceptual model, representational model, and parameters for particular near-field thermohydrologic models are determined by comparing simulated performance with measured performance of relatively large scale (several to tens of meters) in situ tests. For this set of comparisons, several different conceptual models, representational models, and parameter sets were used to simulate performance of large-scale in situ thermal tests. It was found that more than one parameter set provided simulated results that agreed with the monitored performance of those tests within the specified criteria when used with the DKM conceptual model. Thermal performance was evaluated statistically and hydrologic performance was evaluated only qualitatively. It was found that the DS parameter set (that is not site specific to the thermal test) was sufficiently accurate for its application to general modeling of the thermohydrologic processes at the site (see Table 7-2) when applied with the DKM and AF concept.

Uncertainties in measured test performance and in actual test boundary conditions were acknowledged and were bounded in some cases (e.g., a best estimate is used for leakage through the DST bulkhead while leakage through wing heater bore holes were ignored). A single parameter set (the DS property set) resulted in the best match between simulated and measured performance and was recommended for use in simulations of the potential repository system. It was stated in the AMR that "The assumptions, uncertainties, restrictions, and constraints used in this analysis do not appear to have a significant impact on the results and conclusions" (p. 190; ANL-NBS-TH-000001 Rev. 00). Based on a review of this material, it appears that uncertainties in the heat transfer parameters are relatively small compared to other PA parameters, but that there may be significant uncertainty in the hydrologic parameters (especially related to vapor transport and liquid refluxing in fractures).

### **Spatial Variability**

The MSTH PFM from the MSTHM AMR (ANL-EBS-MD-000049 Rev. 00) incorporates spatial variability for a number of parameters directly into the model (see Table 7-2). This model captures much of the vertical variability among the various lithologic units, but only as single, average values. For example, the average inter-unit variations of lithologic, thermal, and hydrologic properties are directly incorporated into the MSTH PFM (see Table 7-2). In addition, the MSTH PFM includes explicitly lateral variability for infiltration rates, stratigraphic thickness, and thermal loading of different WP types and within the regions of the repository.

*TH Models Testing V&V* – Within the TT TH AMR (ANL-NBS-TH-000001 Rev. 00), spatial variability in ambient conditions and properties at smaller scale than the test volume is acknowledged (because of the observed spatial variability in performance) but neglected, except for differences between different geologic units. Average conditions and parameters for each geologic unit that best reproduce performance for the entire test block were determined from a number of sets evaluated. Small-scale variability affects seepage pathways, as suggested by "fracture geometry may be a significant factor for predicting seepage into boreholes near heated regions" (p. 59). It appears that large-scale spatial variability within each geologic unit should be assessed, e.g., by assessing the spatial variability of "indicator" properties (such as average fracture densities) at that scale.

### **Temporal Variability**

The MSTH PFM from the MSTHM AMR (ANL-EBS-MD-000049 Rev. 00) has a number of time dependent results that include the major aspects of temporal variability in the system (see Table 7-2). This model includes explicit representation of climate changes (in terms of infiltration rate) and the heat transfer and hydrologic processes are functions of the thermal evolution of the system (i.e., the major dependency on the decay of the thermal source).

*TH Models Testing V&V* – Within the TT TH AMR (ANL-NBS-TH-000001 Rev. 00), seasonal variations in barometric pressure, surface temperature (e.g., Figure 13 of the TT TH AMR) and precipitation were estimated based on available records. This temporal variability was incorporated in the boundary conditions for simulating the thermal tests. Over the limited time-

scale of the thermal tests, it did not appear that any other temporal variability (e.g., degradation processes) needed to be considered to capture the transient nature of the tests. It is the reviewer's opinion that temporal variability was considered adequately in evaluating the tests. However, the effect of longer-term processes (especially chemical, including dissolution and precipitation) on thermal-hydrological behavior should also be considered in PA. This latter aspect is addressed directly by the THC Seepage Model (discussed above). Those results indicate that these processes are not expected to cause significant changes to the thermohydrologic properties of the system.

### **Incorporation into the Results**

The primary uncertainty incorporated into the MSTH PFM results is the parameter uncertainty in the infiltration rate. There are three different scenarios for infiltration for which full process-level results were generated. The uncertainty in the hydrologic properties is also captured in a less direct manner within these three infiltration scenarios because the calibrated hydrologic parameters are derived for each of the infiltration cases (ANL-EBS-MD-000049 Rev. 00—See the UZ Flow chapter for details). There are a number of areas of uncertainty that have not been quantified in this version of the work and as such could not be quantitatively included in the results. In addition, neglecting the lateral (intra-unit) variability for the rock properties (see below) was not addressed by estimation and inclusion of the resulting uncertainty in the properties values based on the range of variability that exists.

There is a large amount of variability treated within the MSTH PFM particularly related to the lateral variability of infiltration rate, thermal loading of the system, and the vertical variations in the hydrologic and thermal properties of the lithologic units (ANL-EBS-MD-000049 Rev. 00). All of these sources of variability are included within the process model results that are produced for 610 WP locations across the site. The main variability that is lacking both for thermal and hydrologic parameters is that of the within unit, lateral variation in the properties of the rock mass.

### **7.3 Uncertainty Propagation/Capture/Integration into the Total System Performance Assessment**

This section provides a discussion of the last three aspects for incorporating uncertainties into the TSPA analyses. These are 1) the description of how the uncertainties are propagated through the process models; 2) the description of how uncertainty in the process model are captured within the abstraction of those processes; and 3) the description of how uncertainty in the abstraction model are captured within the TSPA implementation of the abstraction. Because the variability is an inherent part of the process model results and therefore commonly captured directly into abstractions, this section focuses only on the propagation/capture of the uncertainties in the other modeling work.

## A. THC Seepage Model

### Propagation to Other Process Models

In the Rev. 00 set of AMR it does not appear that the results of the THC Seepage Model were used in any additional process models. Rather, the results of this model were abstracted and then the abstraction results were carried forward into other models for the in-drift geochemical environment. Some of those models utilized process-level calculations as a means for developing the abstraction that was used within the TSPA, but the intermediate process-level results were not used otherwise.

### Capture of Uncertainty in Abstraction

The two areas of uncertainty that were represented in the range of results for the THC Seepage Model were the geochemical system representation and the infiltration rate uncertainty. These are captured differently in the THC Abs AMR (ANL-NBS-HS-000029, Rev. 00). For the geochemical systems, the Case 2 results are used directly to represent that subset of the constituents that are common to both representations. In addition, to provide a rough estimate of the concentrations of the five components not represented in the Case 2 system, the values for those constituents are combined in the abstraction from the Case 1 results. This approach is discussed in the THC Abstraction AMR (ANL-NBS-HS-000029, Rev. 00, where the CRWMS 2000a citation refers to the THC AMR—MDL-NBS-HS-000001, Rev. 00):

*For the constituents included in both those chemical systems, the major differences between results (for PA purposes this is defined as a factor of 10--or one log unit--or more) are limited to  $\text{Ca}^{2+}$ ,  $\text{Na}^+$ , and  $\text{HCO}_3^-$ . These represent differences that result primarily from the more uncertain kinetic representation of the more complex chemical system (CRWMS M&O 2000a; Sections 6.1.7, 6.2.7 and 6.3.5). As discussed therein, the uncertain precipitation rates of the aluminosilicates create a feedback to the carbonate system by removing Ca from solution, impacting the carbonate system through the changes in calcite saturation state. However, estimates of the additional constituents included only within the Case 1 results should be reasonably obtained from those results. This is because the primary differences in the systems are those constituents listed above and the variations in pH, that may impact mineral equilibria in the more complex chemical system, are of lesser magnitude. The process model Case 1 results for F<sup>-</sup> are assessed to be relatively insensitive to the possible changes (CRWMS M&O 2000a; Section 6.3.5). The phase constraints applied within the Case 1 representation for these additional constituents should be largely unchanged (although more accurate kinetic parameter sets should prevent them from impacting the carbonate subsystem) and these are all trace constituents compared to the major constituents included within both Case 1 and Case 2. Given this, the values for the additional constituents from the Case 1 representation should provide at least order-of-magnitude estimates for incorporating abstracted first approximations for these constituents. In the abstraction these values are combined with the constituents from the Case 2 results to describe a more*

*comprehensive water composition (Table 3). Addition of these values to these abstracted water compositions should have only minor effects on charge balance, because these additional aqueous species are trace constituents compared to the major elements given within the Case 2 representation.*

This approach allows incorporation of the additional constituents for the extended geochemical system to reduce some of the conceptual uncertainties regarding these solution components.

Within the THC Abs AMR (ANL-NBS-HS-000029, Rev. 00), the results of the THC Seepage Model (MDL-NBS-HS-000001, Rev. 00) for the high and low infiltration cases are compared against those for the mean case to produce estimates of the uncertainties represented by this range of results for water and gas compositions. This amounts to a semi-quantitative treatment because the assessment itself is not done with statistical rigor and explicitly for each individual chemical species. (This is due, in part, to the temporal shift of the boiling period in the model results. Most major differences in compositions among these cases occur near the point the water reaches the imposed constraints for “dry” fractures in the THC model. Because the timing of this point is shifted, the comparisons at similar times are out of sync for this transient portion of the results.) The AMR provides the conclusion that (Section 6.1.2, ANL-NBS-HS-000029, Rev. 00),

*Using a factor of two to represent the standard deviation of such a distribution should encompass 95 % of the variations that are meaningful, whereas using a value of 10 would conservatively encompass all of the meaningful variations within the uncertainty bands.*

However, these values are not used to generate distributions explicitly within the THC Abstraction AMR that could then be incorporated into the TSPA (ANL-NBS-HS-000029, Rev. 00).

### **Incorporation/Integration of Abstraction into TSPA**

The THC Abstraction was incorporated into TSPA component models as the boundary conditions for the in-drift water compositions. These models utilized the values provided for the mean infiltration case directly without the associated uncertainties that were assessed. Thus these semi-quantitative estimates of the uncertainty were not applied beyond the THC Abs AMR. Therefore, only the conceptual uncertainties regarding the extended geochemical system (Case 1) are included within the TSPA in-drift water composition models.

However, the THC Abs AMR (ANL-NBS-HS-000029, Rev. 00) provides an analysis of the level of consistency between the TH results from the MSTHM (ANL-EBS-MD-000049 Rev. 00) and the TH results from the THC Seepage Model (MDL-NBS-HS-000001, Rev. 00). This *TH Models Comparison* (see Figure 7-1) was needed to assess the introduction of potential uncertainties/disconnects by combining into the TSPA the results for thermohydrologic conditions from one modeling approach (MSTHM) with the compositional results from another that has its own TH representation (the THC Seepage Model). It was found that the TH results of these two approaches were sufficiently close that combining the results of these two models

was reasonable. This assessment provides support to both the THC Abstraction and the TH Abstraction that are used by the TSPA.

## **B. MSTH Percolation Flux Model**

### **Propagation to Other Process Models**

The MSTH PFM (ANL-EBS-MD-000049 Rev. 00) does not actually feed directly into other process models. Because this is just a single element of the full MSTHM, the uncertainties are directly coupled into the rest of the TH results for the in-drift environment that are provided and abstracted for the TSPA. Within the TSPA, the results of this model are used in their abstracted form to drive the Seepage Abstraction (Figure 7-1, for more details see the UZ chapter section on the Seepage Model uncertainties).

### **Capture of Uncertainty in Abstraction**

The TH Abstraction (see Figure 1, ANL-EBS-HS-000003, Rev. 00) includes sets of results for the various infiltration scenarios that are captured directly in the MSTH PFM. The TH Abstraction also provides sets of output time histories that reflect directly the uncertainty range for infiltration rates captured in the low, high and mean cases. The TH Abstraction (ANL-EBS-HS-000003, Rev. 00) provides the values for the percolation fluxes at 5 meters above the drift crown for the 610 separate locations and the averaged values for each of the five repository bins that represent different infiltration ranges. In each of these cases this is done for the three separate infiltration conditions (low, mean, and high). The variability in the results is captured either directly using the 610 locations, or at a coarser level with the five bin-averaged values.

### **Incorporation/Integration of Abstraction into TSPA**

The abstracted values from the MSTH PFM are used within the TSPA for the Seepage Abstraction in a direct manner. The entire set of spatially variable results is used to drive the Seepage Abstraction Model results (Figure 7-1; for more details see the chapter on the Seepage Model uncertainties) with sampling across the infiltration conditions performed by the TSPA code. This approach incorporates the uncertainties in the infiltration rate directly into the Seepage Abstraction Model results, and thus into the TSPA results.

## **7.4 Conclusions**

For the NFE, the primary models that feed into the TSPA analyses are the ThermoHydroChemical Seepage Model (MDL-NBS-HS-000001, Rev. 00) and the MultiScale ThermoHydrologic Percolation Flux Model (ANL-EBS-MD-000049 Rev. 00). Each of these contains some assessment of conceptual, representational, and parameter uncertainties, and inclusion of some system variability. For the Multiscale TH modeling, an additional AMR covering the thermal testing (ANL-NBS-TH-000001 Rev. 00) provided quantitative validation of the conceptual, representational and parameter uncertainties by statistical comparison of the thermal results of the models with the observations from, in particular, the DST. This AMR also

assessed the TH modeling that forms the basis for the representation of those processes incorporated into the THC Seepage Model.

Within the THC AMR (MDL-NBS-HS-000001, Rev. 00) specific additional models (the DST THC Model and the Ambient THC Model) were used to do the quantitative validation of the geochemical modeling results in this work. These additional models were used to assess the potential trade off between two representations of the geochemical system. In one case, a more detailed conceptual representation was used (Case 1) compared to a simpler representation that included only the major components of the water compositions. The comparisons to observed data indicated that for these major constituents, the simpler compositional system provided a more accurate treatment of the chemistry. Also, the ambient state was evaluated for the model geochemical systems with the Ambient THC Model. These assessments were utilized to recommend which of the geochemical systems (i.e., conceptual models) appears to be more reasonable to use for estimates of long-term system behavior. It would seem from a theoretical point of view that the more detailed compositional system would be more appropriate. However it appears that the additional conceptual uncertainties in the treatment of the additional minerals included, as well as additional parameter uncertainties, for the more complex chemical system were more than enough to offset the reduction in conceptual uncertainty expected from the larger set of chemical components.

In both of these modeling areas, an example of strong treatment of the parameter uncertainty is in the approach used for the infiltration rate uncertainty. That uncertainty is explicitly evaluated using the low, mean, and high cases for the infiltration rates as input to both the THC Seepage Model and the MSTH PFM. In all these calculations for post-closure behavior, these cases are evaluated explicitly and process-level model results are produced that correspond to each of these cases. For the MSTH PFM (ANL-EBS-MD-000049 Rev. 00), the results for each case get explicitly and directly captured within the TH Abstraction (ANL-EBS-HS-000003, Rev. 00) as different cases and then are incorporated into the TSPA through the Seepage Abstraction. For the THC Seepage Model (MDL-NBS-HS-000001, Rev. 00), the results for these high and low infiltration cases are compared against those for the mean case to produce estimates of the uncertainties represented generally in the compositional results. This amounts to a semi-quantitative treatment because it is not done in a rigorous statistical manner and explicitly for each individual chemical species. The conclusion was that using a factor of two to represent the standard deviation of such a distribution should encompass 95 percent of the variations that are meaningful, whereas using a value of 10 would conservatively encompass all of the meaningful variations within the uncertainty bands. These semi-quantitative estimates of the uncertainty were not applied beyond the abstraction of these results

Both the THC Seepage Model and the MSTH PFM capture much of the vertical variability across the lithologic units, and have results that include the temporal variability in the system. For example, the vertical variability in terms of lithologic, thermal, and hydrologic properties is directly incorporated into the THC Seepage Model and the MSTH PFM. These two models also include explicit representation of climate changes (in terms of infiltration rate) and the thermal evolution of the system. In addition, the MSTH PFM includes explicitly lateral variability for infiltration rates, stratigraphic thickness, and thermal loading of different WP types and locations

within the regions of the repository. One of the main sources of spatial variability left untreated is the lateral heterogeneity within the lithologic units.

There are a number of areas of uncertainty that were left unquantified and were treated with some qualitative discussion or not at all. Within the THC Seepage Model, no explicit evaluation was made of uncertainties in the reactive surface areas of minerals. For the reactive surface areas, the THC Seepage Model (MDL-NBS-HS-000001, Rev. 00) uses standard published methods based on geometric approaches modified for the active fracture approach to the dual permeability model for the hydrologic system. However, there is no direct treatment of the uncertainty in the reactive surface area parameter values (see Section 6.1.5, MDL-NBS-HS-000001, Rev. 00). The discussion of these parameter values includes description of the mineral abundance and morphology, and the water-mineral contact areas in an unsaturated system based on the active fracture approach. These parameter values could be one of the larger sources of uncertainties within this modeling work—potentially there may be a range of uncertainty that is more than an order of magnitude.

Another area that is central to coupled reactive transport (THC) modeling, but also was not assessed in terms of the uncertainty, is that of the coupling between the geochemical and the hydrologic processes. For the THC Seepage Model, mineral precipitation was coupled to fracture permeability changes via a standard approach (cubic law) from the literature, but no alternatives were evaluated for their effect on the results/conclusions.

For the MSTH PFM, one of the primary areas of untreated uncertainty is that for processes constraining the liquid flux and distribution within fractures. The Thermal Testing AMR (ANL-NBS-TH-000001 Rev. 00) provides a qualitative evaluation of the liquid saturation in the models relative to that observed for the DST. This does not provide a sufficiently detailed quantitative basis for assessing the detailed hydrologic processes being modeled for the fracture continuum. The uncertainty in the results for fracture saturation and fluxes may be relatively large. Even if the fracture saturation were constrained better, the remaining uncertainties for fracture-matrix interaction would impact directly the degree of liquid flux in the fractures versus matrix.

Finally, for both of these modeling areas the lack of treatment of the intra-unit variability should be addressed as an additional uncertainty. However, neither of these areas incorporates that variability directly nor includes uncertainty to represent this untreated variability. The heterogeneity in each unit is not expected to exceed that between the units, however it could lead to local differences in results that cover a wider range of conditions with lateral variation as opposed to the homogeneous results from the average values.

Even though these models have not quantified fully their inherent uncertainties, updates to some of these documents demonstrated further progress beyond that assessed here. For example, the Thermal Testing AMR was updated (ANL-NBS-TH-000001 Rev. 00/ICN 01) to include statistical measures for comparisons of measured and simulated hydrologic responses. This provides some quantitative validation of the hydrologic results of these TH models, however the comparison was done for bulk saturation, without any explicit assessment of fracture saturation results. Another example is that the THC AMR (MDL-NBS-HS-000001, Rev. 01) was updated. This update included 1) additional data on water and gas compositions from the DST for model

validation; 2) evaluation of the first stage of a plug flow reactor experiment for validation; and 3) incorporation of more fracture system heterogeneity to the model that is centered in the Tptpmn unit (i.e., the middle non-lithophysal unit), and construction of a model for the lithology that may represent about 80 percent of the potential repository (the Tptpll unit—the lower lithophysal unit). The THC AMR update also incorporates additional sensitivity studies, including evaluations comparing results with backfill versus those without backfill. In addition to these AMR updates, another coupled-process model has been developed for thermohydromechanical coupling in the system. This work exists currently only as a draft AMR but will address some of the uncertainties in this area once completed.

**Table 7-1: Treatment of Uncertainties and Variability within the Thermohydrochemical Seepage (THC) Model**

<b>Thermohydrochemical (THC) Seepage Model</b>				
<p><b>Model Purpose:</b> The purpose of the <i>THC Seepage Model</i> (MDL-NBS-HS-000001, Rev. 00) is to evaluate the evolution of water and gas compositions and mineralogic alteration within the system through time, especially as driven by thermally coupled processes. Calculations are done for two different geochemical systems: the less complex (components are CO<sub>2</sub>, pH, Ca<sup>2+</sup>, Na<sup>+</sup>, SiO<sub>2</sub>, Cl<sup>-</sup>, [HCO<sub>3</sub>]<sup>-</sup>, [SO<sub>4</sub>]<sup>2-</sup>) and the more complex (extended to include the additional components Mg<sup>2+</sup>, K<sup>+</sup>, [AlO<sub>2</sub>]<sup>-</sup>, [HFeO<sub>2</sub>]<sup>-</sup>, and F<sup>-</sup>) geochemical systems. The results of the THC Seepage model are provided to other AMR/models as the boundary conditions to the potential emplacement drifts. The <i>THC Seepage Model</i> is supported by results for THC models evaluating spatially (vertical) and temporally varying matrix and fracture mineralogies, water compositions, and gas compositions and fluxes for the ambient site (<i>Ambient THC model</i>) and for the Drift-Scale Test (<i>DST THC model</i>), both from the same AMR (MDL-NBS-HS-000001, Rev. 00--see notes at the bottom</p>				
<b>Summary</b>	<b>Source</b>	<b>Treatment</b>	<b>Basis</b>	<b>Impact</b>
<b>Conceptual Model Uncertainty</b>				
<b>GEOCHEMICAL</b>				
<b>Repository Horizon Mineralogic Representation</b>	Lack of incorporation of data for the lower lithophysal unit. MDL-NBS-HS-000001, Rev. 00; page 13, Sec. 1.0; Sec. 6.3, page 75	Discussed Qualitatively	<i>Only part of the potential repository is planned to be located in the Tptpmn, and therefore the model may not be representative of the entire potential repository. However, most hydrogeologic data available for the potential repository are from the Tptpmn unit, including data from the Single Heater Test (SHT), DST, and many other data collected in the ESF.</i>	Water and gas chemistry may not reflect completely the major chemical aspects expected at the potential repository horizon as driven by fluid-mineral reactions. The Lower lithophysal unit potentially has higher fluoride content due to larger amounts of fluorite and other vapor phase minerals within the lithophysae.

<p><b>Chemical System Comprehensiveness</b></p>	<p>Complex system with alternate representations. MDL-NBS-HS-000001, Rev. 00; Sec. 6.1.7, pages 43-44; Tables 7 and 8; Sec. 7, p. 115</p>	<p>Two sets of chemical components and mineral assemblages were used for the simulations for the Drift Scale Test and the THC Seepage Model. The systems are denoted Case 1 and Case 2 and are presented in Tables 7 and 8, respectively.</p>	<p>Case 1 (“full”set) includes the major solid phases (minerals and glass) encountered in geologic units at Yucca Mountain, together with a range of possible reaction product minerals, CO<sub>2</sub> gas, and the aqueous species necessary to include these solid phases and the pore-water composition into the THC model. Case 2 (“simplified”set) is a subset of Case 1 excluding aluminum silicate minerals, which form or dissolve much less easily than minerals such as calcite or gypsum, and for which thermodynamic and kinetic data are not as well established as for the other minerals</p>	<p><i>As discussed later (Sections 6.2.7.2 and 6.3.5.2), Case- 2 THC simulations appear to predict more realistic pH and gas-phase CO<sub>2</sub> concentration trends than Case-1 simulations, because the latter may be overpredicting the reaction rates of aluminum silicate minerals, indirectly affecting these parameters. Therefore, even though Case 1 represents the near-field environment more completely than Case 2, the latter may yield more accurate THC model results than Case 1. In addition, as mentioned earlier, the simulations under ambient conditions (no thermal loading) using the Case-1 mineral assemblage reveal a chemical system that is less “steady” than for Case-2 simulations (e.g., by comparing the ambient curves for pH, bicarbonate, and CO<sub>2</sub> on Figures 28 through 33). This reflects the model uncertainty with respect to reaction rates and the difficulty in reproducing an initially balanced hydrogeochemical system, which depends on infiltration rates and rock properties as well as reaction rates. Given this observation, a reduced set of minerals with better- constrained reaction rates such as for Case 2 is likely to match the pH, bicarbonate, and Ca better than the more complex system. This is shown with simulations of the DST (Section 6.2.7), which indicate that a Case-2 mineral assemblage provides better estimates of pH and CO<sub>2</sub> concentrations than Case 1, compared to waters and gases collected in the first 20 months of heating.</i></p>
---	---	---	--	--

<p><b>Initial State of Geochemical System</b></p>	<p>Complex system with alternate representations MDL-NBS-HS-000001, Rev. 00; Sec. 1.0, page 13; Sec. 6.3, page 75; Sec. 6.3.4, p. 81; Sec. 6.3.5.2, p. 95; Sec. 7, p. 115</p>	<p><i>In addition, simulations under ambient conditions, without heating, were performed for Case 1 and Case 2 using a constant infiltration rate (about 1.05 mm/year). The latter represents the base-case present-day infiltration rate at the location of Borehole SD-9, which was used to define the geology of the model.</i></p>	<p><i>These ambient simulations were run to assess the extent to which the Case-1 and Case-2 geochemical systems approached a geochemical steady state. These runs also provide a baseline to which the results of thermal loading simulations can be compared.</i></p>	<p><i>The large pH and carbonate concentration variations for the 1mm/yr ambient run in Case 1 (Figures 30 and 32) reflect an initially “unsteady” hydrochemical system. Obtaining an initial steady-state chemical system that is similar to the measured data for a few points is difficult because it depends on reaction rates as well as infiltration rates and rock properties. The difficulty increases with the number of reactive minerals included in the system, and with the uncertainty in reaction rates. This is the reason why calculated ambient concentration trends are less variable in Case 2 than in Case 1. In addition, as mentioned earlier, the simulations under ambient conditions (no thermal loading) using the Case-1 mineral assemblage reveal a chemical system that is less “steady” than for Case-2 simulations (e.g., by comparing the ambient curves for pH, bicarbonate, and CO<sub>2</sub> on Figures 28 through 33). This reflects the model uncertainty with respect to reaction rates and the difficulty in reproducing an initially balanced hydrogeochemical system, which depends on infiltration rates and rock properties as well as reaction rates. Given this observation, a reduced set of minerals with better-constrained reaction rates such as for Case 2 is likely to match the pH, bicarbonate, and Ca better than the more complex system. This is shown with simulations of the DST (Section 6.2.7), which indicate that a Case-2 mineral assemblage provides better estimates of pH and CO<sub>2</sub> concentrations than Case 1, compared to waters and gases collected in the first 20 months of heating.</i></p>
---	---	--	---	---

<p><b>Initial Water Composition</b></p>	<p>Lack of data for water moving through fractures. MDL-NBS-HS-000001, Rev. 00; Sec. 4.1.3, page 22</p>	<p>qualitative discussion that this uncertainty should be relatively small</p>	<p><i>There are very few complete pore-water analyses from other units of the Topopah Spring Tuff, and none from the lower lithophysal unit (Tptpll). Data from the lower non-lithophysal unit (Tptpln) (DTN:GS950608312272.001) suggest pore waters from this unit may exhibit a slightly more sodium-carbonate character (and less calcium-chloride type) than the water composition shown in Table 3. However, the general water chemistry trends resulting from TH processes simulated in this study are not expected to vary significantly with the range of possible initial water composition. In addition, the model uncertainty with respect to initial water composition is likely to be insignificant relative to uncertainties in reaction rates, hydrologic parameters, and the variability of pore water compositions within a particular geologic unit.</i></p>	<p><i>There are many uncertainties in modeling coupled THC processes because of the large amount of data needed and the complexity of natural systems. These data range from the fundamental thermodynamic properties of minerals, aqueous species, and gases, the kinetic data for mineral-water reactions, to the representation of the unsaturated hydrologic system for the fractured tuffs. In addition, a wealth of site-specific thermohydrologic, geologic, and geochemical data are necessary to describe the initial and boundary conditions. For these reasons, it may not be possible to assign a model uncertainty based on the uncertainties of the data themselves, and therefore model validation gives a true test of whether the system can be described sufficiently well for the intended purposes of the model. Results of simulations of the DST captured the important changes in pH and gas-phase CO<sub>2</sub> concentrations at each location over time well within the range of variation in the measured gas and water concentrations between sampling locations. This provides a sufficient validation of the model's capability for the prediction of spatial and temporal variation in water and gas chemistry. (Section 7.0)</i></p>
---	---	--	--	---

<p><b>Chemical Equilibria/ Thermodynamic Data-- temperature dependent equilibrium constants</b></p>	<p>Complex system with alternate representations MDL-NBS-HS-000001, Rev. 00; Are the necessary phases included and appropriately represented? Sec. 6.2.7.2, page 57; Sec. 4.1.4, Att. IV; Sec. 6.1.7, pages 43-44; Tables 7 and 8; Sec. 7, p. 115</p>	<p>The analysis incorporated thermally-dependent equilibrium constants for mineral, gas, and aqueous species reactions; qualitative discussion that this uncertainty should be assessed through testing of the results with measured data sets. Two sets of chemical components and mineral assemblages were used for the simulations for the Drift Scale Test and the THC Seepage Model. The systems are denoted Case 1 and Case 2 and are presented in Tables 7 and 8, respectively.</p>	<p><i>Case 1 (“full ”set) includes the major solid phases (minerals and glass) encountered in geologic units at Yucca Mountain, together with a range of possible reaction product minerals, CO2 gas, and the aqueous species necessary to include these solid phases and the pore-water composition into the THC model. Case 2 (“simplified ”set) is a subset of Case 1 excluding aluminum silicate minerals, which form or dissolve much less easily than minerals such as calcite or gypsum, and for which thermodynamic and kinetic data are not as well established as for the other minerals. In addition, the uncertainties in thermodynamic data for the aluminosilicates (e.g. zeolites and clays), the unknown reaction rates for many of the minerals, and the assumption of end member mineral thermodynamic models instead of solid-solution models must play a role in the evaluation of the results. Therefore, comparison to measured data must play an important role in the evaluation of the results.</i></p>	<p><i>As discussed later (Sections 6.2.7.2 and 6.3.5.2), Case- 2 THC simulations appear to predict more realistic pH and gas-phase CO2 concentration trends than Case-1 simulations, because the latter may be overpredicting the reaction rates of aluminum silicate minerals, indirectly affecting these parameters. Therefore, even though Case 1 represents the near-field environment more completely than Case 2, the latter may yield more accurate THC model results than Case 1. In addition, as mentioned earlier, the simulations under ambient conditions (no thermal loading) using the Case-1 mineral assemblage reveal a chemical system that is less “steady” than for Case-2 simulations (e.g., by comparing the ambient curves for pH, bicarbonate, and CO2 on Figures 28 through 33). This reflects the model uncertainty with respect to reaction rates and the difficulty in reproducing an initially balanced hydrogeochemical system, which depends on infiltration rates and rock properties as well as reaction rates. Given this observation, a reduced set of minerals with better- constrained reaction rates such as for Case 2 is likely to match the pH, bicarbonate, and Ca better than the more complex system. This is shown with simulations of the DST (Section 6.2.7), which indicate that a Case-2 mineral assemblage provides better estimates of pH and CO2 concentrations than Case 1, compared to waters and gases collected in the first 20 months of heating.</i></p>
---	---	--	--	---

<b>Kinetic Reaction Rates- -temperature dependent intrinsic rate constants</b>	<p>Complex system with alternate representations MDL-NBS-HS-000001, Rev. 00; Are the necessary phases included and appropriately represented? Sec. 6.2.7.2, page 57; Sec. 4.1.5, Table 4; Sec. 6.1.7, pages 43-44; Tables 7 and 8; Sec. 7, p. 115</p>	<p>The analysis incorporated effective rates in the system that depend on the intrinsic rate constants as well as the reactive surface areas of the phases; thermally-dependent intrinsic rate constants for mineral dissolution/precipitation reactions; qualitative discussion that this uncertainty should be assessed through testing of the results with measured data sets. Two sets of chemical components and mineral assemblages were used for the simulations for the Drift Scale Test and the THC Seepage Model. The systems are denoted Case 1 and Case 2 and are presented in Tables 7 and 8, respectively.</p>	<p><i>Case 1 (“full ”set) includes the major solid phases (minerals and glass) encountered in geologic units at Yucca Mountain, together with a range of possible reaction product minerals, CO2 gas, and the aqueous species necessary to include these solid phases and the pore-water composition into the THC model. Case 2 (“simplified ”set) is a subset of Case 1 excluding aluminum silicate minerals, which form or dissolve much less easily than minerals such as calcite or gypsum, and for which thermodynamic and kinetic data are not as well established as for the other minerals. In addition, the uncertainties in thermodynamic data for the aluminosilicates (e.g. zeolites and clays),the unknown reaction rates for many of the minerals, and the assumption of end member mineral thermodynamic models instead of solid-solution models must play a role in the evaluation of the results. Therefore, comparison to measured data must play an important role in the evaluation of the results.</i></p>	<p><i>As discussed later (Sections 6.2.7.2 and 6.3.5.2), Case- 2 THC simulations appear to predict more realistic pH and gas-phase CO2 concentration trends than Case-1 simulations, because the latter may be overpredicting the reaction rates of aluminum silicate minerals, indirectly affecting these parameters. Therefore, even though Case 1 represents the near-field environment more completely than Case 2,the latter may yield more accurate THC model results than Case 1. In addition, as mentioned earlier, the simulations under ambient conditions (no thermal loading) using the Case-1 mineral assemblage reveal a chemical system that is less “steady” than for Case-2 simulations (e.g., by comparing the ambient curves for pH, bicarbonate, and CO2 on Figures 28 through 33). This reflects the model uncertainty with respect to reaction rates and the difficulty in reproducing an initially balanced hydrogeochemical system, which depends on infiltration rates and rock properties as well as reaction rates. Given this observation, a reduced set of minerals with better- constrained reaction rates such as for Case 2 is likely to match the pH, bicarbonate, and Ca better than the more complex system. This is shown with simulations of the DST (Section 6.2.7), which indicate that a Case-2 mineral assemblage provides better estimates of pH and CO2 concentrations than Case 1, compared to waters and gases collected in the first 20 months of heating.</i></p>
<b>THERMOHYDROLOGIC</b>				
<b>Climate Changes Infiltration / Percolation flux</b>	<p>Complex system with alternate and changing climatic conditions MDL-NBS-HS-000001, Rev. 00; See Table 2, Sect. 4.1.1; and Table 12 Section 6.3.2</p>	<p>three different climate states used with different precipitation and changes to infiltration/percolation fluxes. <i>Three different infiltration regimes were modeled simulating a range of future climate conditions (Table 12).</i></p>	<p>see Climate Model AMR in UZ PMR.</p>	<p>Variable climatic conditions for rate of infiltration as the boundary conditions, drives different flux through system. Different results for different climate states.</p>

<p><b>Dual Permeability Active Fracture Model for hydrologic system</b></p>	<p>Complex system with alternate possibilities that are constrained only partially by data MDL-NBS-HS-000001, Rev. 00; see Table 2, Sect. 4.1.1; and Sec. 6.1.1; see chapter on UZ Flow AMR; see MSTHM AMR Sec. 6.3</p>	<p>flow occurs in fractures and matrix as if they were separate continua with some degree of interaction between these two systems. The active fracture concept addresses the fact that not all of the fracture system and/or not the entire surface of a particular fracture, is actively flowing with water. This means that only a portion (subset) of the fracture continuum has water contacting the fracture-matrix interface. This allows for flow in fractures to occur at bulk saturations less than unity, and provides for a reduced fracture matrix interaction.</p>	<p>see chapter on UZ Flow AMR for detailed justification and basis</p>	<p>Basic conceptual representation used for all the results. Allows non-equilibrium flow for water in fracture system that is not fully saturated.</p>
<p><b>Appropriate Thermohydrologic Processes</b></p>	<p>Uncertainties in near-field coupled thermal-hydrological mechanisms (including heat-transfer, vapor transport and refluxing, and fracture-matrix interaction). ANL-NBS-TH-000001 Rev. 00:</p>	<p>Appropriate conceptual models for near-field thermal-hydrological performance are determined by comparing simulated performance with measured performance of relatively large scale (several to tens of meters) in situ tests</p>	<p>Used several different conceptual models (including conduction only, as for ANSYS). One conceptual model was essentially confirmed by performance monitoring of large scale in situ thermal tests (by "heat-pipe signature", p. 54), and there are essentially no other conceptual models currently considered viable.</p>	<p>"The assumptions, uncertainties, restrictions, and constraints used in this analysis do not appear to have a significant impact on the results and conclusions." (p. 190). It is the reviewer's opinion that uncertainties in the conceptual model have been largely resolved, except perhaps for fracture-matrix interaction.</p>
<p><b>Heat transfer by primarily by thermal conduction and convection in a dual permeability system</b></p>	<p>Complex system with competing processes of heat transfer. MDL-NBS-HS-000001, Rev. 00; Sect. 5, assumption A1; Sect. 4.1.1 Table 2</p>	<p>Conduction and convective heat transfer are included. Thermal conductivity is a property of the rock matrix, convective heat transfer occurs both through the fracture and matrix continua.</p>	<p><i>It is assumed that the rock can be described by the dual permeability model that considers separate, but interacting fracture and matrix continua. The fracture continuum is considered as separate but interacting with the matrix continuum, in terms of the flow of heat, water, and vapor through advection and conduction. Each continuum has its own well-defined initial physical and chemical properties. It is assumed that the dual-permeability approach, with appropriate material and fracture properties and an appropriate discretization of time and space, is an accurate approximation of the real world. The dual-permeability approach for modeling physical processes in fractured-porous media is discussed in detail in the UZ PMR, UZ flow AMR, (see chapter on UZ Flow models) and the MSTH AMR.</i></p>	<p>Both processes are captured in the models.</p>

<b>Saturation dependant variability in thermal conductivity</b>	Lack of full dataset. Observations of thermal conductivities at variable rock saturation, Calibrated property set, MDL-NBS-HS-000001, Rev. 00; Table 2, page 20, Sec. 4.1.1	linear interpolation between wet and dry values based on saturation in rock	wet and dry thermal conductivity (Kth) values measured on cores in the lab.	End members constrained by data, but relation for interpolating not well constrained.
<b>EBS "effective" (fictive porous media) thermal conductivities</b>	Lack of data and lack of capabilities in codes used for implementing the model. MDL-NBS-HS-000001, Rev. 00; Sec. 4.1.7.2, Att. VI	Heat transfer from the WP to the drift wall is implemented in the model by using time-varying "effective" thermal conductivities (for open spaces within the drift) that were calculated to account for radiative and convective heat-transport components. These time-varying data were input into the model as coefficients (values between 0 and 1) for each open zone within the drift. Each zone was also assigned a constant maximum thermal conductivity (Kth max), which was then multiplied by the corresponding time-varying coefficients to obtain effective conductivities as a function of time (Attachment VI). The sources of these data are listed in Table 2.	Not provided directly in the AMR. Source data indicated basis is analytical models of heat transfer via radiation and convection in open concentric cylinders that are used to calibrate the "effective" thermal conductivity of the fictive porous media. (See DTN:SN9907T0872799.002).	Details of heat and vapor transport within the potential drifts are not very well represented by this approach.
<b>TRANSPORT</b>				
<b>Dual-Permeability Approach for Transport</b>	Lack of data for site-wide characterization of this aspect. MDL-NBS-HS-000001, Rev. 00; Section 6.1.1	<i>To handle these separate yet interacting processes in fractures and matrix, we have adopted the dual permeability method. In this method, each grid block is separated into a matrix and fracture continuum, each of which is characterized by its own pressure, temperature, liquid saturation, water and gas chemistry, and mineralogy.</i>	<i>Transport rates greater than the rate of equilibration via diffusion necessarily leads to disequilibrium between waters in fractures and matrix. This can lead to differences in the stable mineral assemblage and to differences in reaction rates. Because the system is unsaturated, and undergoes boiling, the transport of gaseous species is an important consideration. The model must also capture the differences between initial mineralogy in fractures and matrix and their evolution.</i>	The fracture and matrix get treated explicitly but there is little data to constrain the various representations across the potential repository.

<b>COUPLING</b>				
<b>Evolution of Fracture Permeability from Mineral Alteration</b>	Uses Standard treatment from literature. Lack of site specific data. MDL-NBS-HS-000001, Rev. 00; sections 6.1.6.1 & 6.1.6.2	Porosity changes are related directly to changes in mineral molar volumes. <i>Fracture permeability changes are approximated using the porosity change and an assumption of plane parallel fractures of uniform aperture (cubic law —Steefel and Lasaga 1994, p. 556).</i>	Standard methodology in the Literature.	Incorporates standard representation for assessing the effects on fracture permeability in the model results.
<b>Evolution of Matrix Permeability from Mineral Alteration</b>	Uses standard treatment from literature. Lack of site specific data MDL-NBS-HS-000001, Rev. 00; Sections 6.1.6.1 & 6.1.6.3	Porosity changes are related directly to changes in mineral molar volumes. <i>Matrix permeability changes are calculated from changes in porosity using ratios of permeabilities calculated from the Carmen-Kozeny relation (Bear 1972, p. 166, eq. (5.10.18), symbolically replacing <math>n</math> by <math>\phi</math>), and ignoring changes in grain size, tortuosity and specific surface area</i>	Simplified Standard methodology in the Literature.	Incorporates standard representation for assessing the effects on fracture permeability in the model results.
<b>Representational Model Uncertainty</b>				
<b>COUPLING</b>				
<b>Evolution of Fracture Permeability from Mineral Alteration Averaged over Grid Block</b>	Distributing local effects in fractures throughout grid block fracture volume -- MDL-NBS-HS-000001, Rev. 00; Section 6.3.1	The area extending approximately 50 meters above the drift is more finely gridded than other areas to capture THC effects potentially affecting seepage into the drift. Outside the drift, the smallest grid spacing was specified at the drift wall (20 cm), and increasing outward. Because of its minor relevance to this modeling effort, the geology below the tsw38 model layer was simplified compared to the original SD-9 data, which allowed for coarser gridding in this area. The mesh has a total of 2510 gridblocks, including those representing matrix, fracture, and in-drift design elements.	The gridblock size was kept fine enough to provide enough resolution at key model locations such as at the vicinity of drift and geologic contacts, but as coarse as possible to provide the computing efficiency needed for reasonable simulation times.	Potentially averages out local effects that may serve to more completely occlude smaller sections of fractures. This may not be an issue since the plugging would have to occur continuously and ubiquitously through a horizon of the fracture system in order to actually close down permeability at the grid block scale.

<b>Mathematical Implementation of the time step</b>	Numerical dispersion MDL-NBS-HS-000001, Rev. 00; Sec. 6.3.3, page 81	<i>Maximum time-step lengths of 6 months for pre-closure simulations, 10 years for simulation times between 50 and 20,000 years, and 50 years for simulation times between 20,000 and 100,000 years provided a reasonable compromise between computing efficiency and accuracy.</i>	<i>Sensitivity analyses were performed to determine a suitable maximum time step length for THC simulations. Maximum time steps of 6 months (pre-closure only), 1, 10, and 100 years were investigated.</i>	Time changes are captured at a level that corresponds to the time stepping. Appropriate testing appears to limit the uncertainty due to this potential effect.
<b>Mathematical Approach to solving the coupled equations</b>	Numerical dispersion MDL-NBS-HS-000001, Rev. 00; Section 6.1.3	<i>The geochemical module incorporated in TOUGHREACT V2.2 solves simultaneously a set of chemical mass-action, kinetic rate expressions for mineral dissolution/precipitation, and mass-balance equations. This provides the extent of reaction and mass transfer between a set of given aqueous species, minerals, and gases at each grid block of the flow model (Xu and Pruess 1998; Xu et al.1999). Equations for heat, liquid and gas flow, aqueous and gaseous species transport, chemical reactions, and permeability/porosity changes are solved sequentially (e.g., Steefel and Lasaga 1994, p. 550).</i>	Standard methodology in the Literature.	Standard treatment used to minimize uncertainties resulting from this with reasonably efficient computational requirements.
<b>Mathematical Coupling of Chemistry to the Thermohydrology Representation</b>	Implementation of additional aspects in the code MDL-NBS-HS-000001, Rev. 00; Sec. 6.3.5.1, page 82; Sec. 6.3.5.2, pp. 85-86	<i>For comparison to the TH simulations, the THC Seepage Model was run with thermal loading and without reactive transport (i.e., considering only thermal and hydrological effects).</i>	<i>This simulation was run using the mean infiltration rates and corresponding rock property set (Table 12) and serves as a basis for interpreting the effects of water-gas-rock chemical interaction on the thermal and hydrological behavior of the system</i>	<i>Temperatures, liquid saturation, and air mass fractions calculated for the mean infiltration case (6/16/25 mm/year) are directly comparable to those obtained from the TH simulation (Figures 20 through 22) because the latter was carried out using the same infiltration rates. The results of the TH and THC simulations are essentially identical. As discussed later, the thermal and hydrologic behavior of the system is not significantly affected by water-gas-rock chemical interactions and, therefore, temperatures, liquid saturations, and air mass fractions calculated with THC (Case 1 and Case 2) and TH simulations are nearly the same.</i>

**THERMOHYDROLOGIC**

<b>Appropriate mathematical models</b>	ANL-NBS-TH-000001 Rev. 00: Approximations and simplifications in representation of conceptual model, e.g., in geometry and geology, in thermal loading, etc.	Appropriate mathematical models for near-field thermal-hydrological performance are determined by comparing simulated performance with measured performance of relatively large scale (several to tens of meters) in situ tests. Either TOUGH2 or NUFT is adequate.	Either TOUGH2 or NUFT, with the appropriate parameters values, resulted in simulated performance that adequately matched measured performance of relatively large-scale in situ thermal tests.	"The assumptions, uncertainties, restrictions, and constraints used in this analysis do not appear to have a significant impact on the results and conclusions." (p. 190). It is the reviewer's opinion that uncertainties in the mathematical model are relatively small compared to other PA uncertainties and can be ignored.
--	--	---	--	--

**Parameter Uncertainty**

**GEOCHEMICAL**

<b>Thermodynamic Data</b>	MDL-NBS-HS-000001, Rev. 00; Sec. 4.1.4, Att. IV	Thermally dependent equilibrium constants for mineral, gas, and aqueous species reactions, no uncertainty evaluated for these data	Various published data sources including SUPCRT92; standard industry approach to thermochemical database.	<i>There are many uncertainties in modeling coupled THC processes because of the large amount of data needed and the complexity of natural systems. These data range from the fundamental thermodynamic properties of minerals, aqueous species, and gases, the kinetic data for mineral-water reactions, to the representation of the unsaturated hydrologic system for the fractured tuffs. In addition, a wealth of site-specific thermohydrologic, geologic, and geochemical data are necessary to describe the initial and boundary conditions. For these reasons, it may not be possible to assign a model uncertainty based on the uncertainties of the data themselves, and therefore model validation gives a true test of whether the system can be described sufficiently well for the intended purposes of the model. Results of simulations of the DST captured the important changes in pH and gas-phase CO2 concentrations at each location over time well within the range of variation in the measured gas and water concentrations between sampling locations. This provides a sufficient validation of the model 's capability for the prediction of spatial and temporal variation in water and gas chemistry. (Section 7.0)</i>
---------------------------	---	--	---	--

<p><b>Mineral Intrinsic Reaction Rates</b></p>	<p>Lack of data for full implementation MDL-NBS-HS-000001, Rev. 00; Sec. 4.1.5, Table 4</p>	<p>Thermally-dependent intrinsic rate constants for mineral dissolution/precipitation reactions, with only qualitative discussion of the uncertainties</p>	<p>Various published data sources (see Table 4). Industry Standard approach.</p>	<p><i>There are many uncertainties in modeling coupled THC processes because of the large amount of data needed and the complexity of natural systems. These data range from the fundamental thermodynamic properties of minerals, aqueous species, and gases, the kinetic data for mineral-water reactions, to the representation of the unsaturated hydrologic system for the fractured tuffs. In addition, a wealth of site-specific thermohydrologic, geologic, and geochemical data are necessary to describe the initial and boundary conditions. For these reasons, it may not be possible to assign a model uncertainty based on the uncertainties of the data themselves, and therefore model validation gives a true test of whether the system can be described sufficiently well for the intended purposes of the model. Results of simulations of the DST captured the important changes in pH and gas-phase CO<sub>2</sub> concentrations at each location over time well within the range of variation in the measured gas and water concentrations between sampling locations. This provides a sufficient validation of the model's capability for the prediction of spatial and temporal variation in water and gas chemistry. (Section 7.0)</i></p>
--	---	--	--	---

<p><b>Matrix and Fracture Mineral Reactive Surface Areas</b></p>	<p>Lack of data MDL-NBS-HS-000001, Rev. 00; Sec. 4.1.2, Table 2; Section 7.0</p>	<p>No treatment of uncertainty for these parameters. This is one of the largest potential sources of uncertainty that has not been treated.</p>	<p><i>The two forms of the reactive surface area are used to describe minerals in the matrix of the rock (cm<sup>2</sup>/g mineral) or those on the surface of fractures (m<sup>2</sup>/m<sup>3</sup>). These data are given in Attachments II (volume fractions) and III (reactive surface areas) for minerals initially present in the model hydrological units. The DTNs for data from which these properties were derived are given in Table 2, and include Borehole SD-9 mass percent minerals as determined by X-ray diffraction (3-D Mineralogical Model: LA9908JC831321.001). The calculation of the mineral volume fractions and reactive surface areas require significant additional information, such as mineral stoichiometries, mass densities, grain size and fracture-matrix surface area. The fracture-matrix surface area is part of the mean calibrated hydrological property set and is listed by DTN in Table 2.</i></p>	<p><i>There are many uncertainties in modeling coupled THC processes because of the large amount of data needed and the complexity of natural systems. These data range from the fundamental thermodynamic properties of minerals, aqueous species, and gases, the kinetic data for mineral-water reactions, to the representation of the unsaturated hydrologic system for the fractured tuffs. In addition, a wealth of site-specific thermohydrologic, geologic, and geochemical data are necessary to describe the initial and boundary conditions. For these reasons, it may not be possible to assign a model uncertainty based on the uncertainties of the data themselves, and therefore model validation gives a true test of whether the system can be described sufficiently well for the intended purposes of the model. Results of simulations of the DST captured the important changes in pH and gas-phase CO<sub>2</sub> concentrations at each location over time well within the range of variation in the measured gas and water concentrations between sampling locations. This provides a sufficient validation of the model's capability for the prediction of spatial and temporal variation in water and gas chemistry. (Section 7.0)</i></p>
--	--	---	---	---

**THERMOHYDROLOGIC**

<p><b>Infiltration / Percolation flux</b></p>	<p>Observations made at the site as well as projections for other climates. Varying rock properties by lithostratigraphic unit, Calibrated Property Set, MDL-NBS-HS-000001, Rev. 00; Table 2, page 20, Sec. 4.1.1; Sec. 6.3.2, Table 12, page 80</p>	<p>High, medium, and low infiltration scenarios</p>	<p>Assumed cases analyzed based on UZ hydrologic model from the UZ PMR (see UZ Flow Model chapter).</p>	<p>Infiltration-flux uncertainty affects the local percolation flux, which affects the fracture saturation in the near-field host rock surrounding the drifts which in turn affects the reactive surface area of fracture minerals and the flux of dissolved constituents. Fracture saturation decreases and duration of potential fracture dryout increases with decreasing percolation flux. This uncertainty is addressed by including the mean, high, and low infiltration-flux cases in this AMR. These three cases are judged to adequately span the range of uncertainty of the infiltration flux. The low infiltration-flux cases had a longer dryout duration than either the mean or high infiltration-flux cases, water compositions were somewhat different only for a few time steps outside of the duration of dryout.</p>
<p><b>Calibrated Hydrologic Properties</b></p>	<p>Data density/coverage MDL-NBS-HS-000001, Rev. 00; Varying rock properties by lithostratigraphic unit, Calibrated Property Set, Table 2, page 20, Sec. 4.1.1</p>	<p>High, medium, and low present-day infiltration scenarios</p>	<p>Calibrations performed for low medium and high infiltration rates for present-day climate (note this uncertainty is directly correlated to the uncertainty in the infiltration/percolation flux).</p>	<p>Infiltration-flux uncertainty affects the local percolation flux, which affects the fracture saturation in the near-field host rock surrounding the drifts which in turn affects the reactive surface area of fracture minerals and the flux of dissolved constituents. Fracture saturation decreases and duration of potential fracture dryout increases with decreasing percolation flux. This uncertainty is addressed by including the mean, high, and low infiltration-flux cases in this AMR. These three cases are judged to adequately span the range of uncertainty of the infiltration flux. The low infiltration-flux cases had a longer dryout duration than either the mean or high infiltration-flux cases, water compositions were somewhat different only for a few time steps outside of the duration of dryout.</p>

<p><b>Appropriate parameters for near-field thermal-hydrological models</b></p>	<p>Uncertainties in measured test performance (especially moisture from ERT data) and in actual test boundary conditions (especially heat and moisture leakage through DST bulkhead and heater boreholes). ANL-NBS-TH-000001 Rev. 00.</p>	<p>Appropriate parameters for particular near-field thermal-hydrological models are determined by comparing simulated performance with measured performance of relatively large scale (several to tens of meters) in situ tests. Uncertainties in measured test performance and in actual test boundary conditions are acknowledged but were ignored, e.g., a best estimate was used for leakage through the DST bulkhead while leakage through heater boreholes was ignored. A single parameter set that resulted in the best match between simulated and measured performance was recommended, i.e., no parameter uncertainty.</p>	<p>No basis for ignoring parametric uncertainty was provided. However, several different parameter sets were used to simulate performance of large scale in situ thermal tests, with more than one set resulting in an adequate match of simulated and monitored performance of those tests, with thermal performance evaluated statistically and hydrologic performance evaluated only qualitatively.</p>	<p>"The assumptions, uncertainties, restrictions, and constraints used in this analysis do not appear to have a significant impact on the results and conclusions." (p. 190). It is the reviewer's opinion that uncertainties in the heat transfer parameters are relatively small compared to other PA parameters, but that there may be significant uncertainty in the hydrologic parameters (especially related to vapor transport and refluxing in fractures).</p>
<p><b>TRANSPORT</b></p>				
<p><b>Fracture Pathway Tortuosity</b></p>	<p>dearth of site specific data MDL-NBS-HS-000001, Rev. 00; Section 4.1.6</p>	<p><i>Tortuosities were set to 0.7 for fractures (DTN:LB990861233129.001) based on models of in-situ testing. No uncertainty was investigated</i></p>	<p><i>This value corresponds to the highest tortuosity given by de Marsily (1986, p. 233), with the rationale that fracture tortuosity should be high compared to matrix tortuosity (i.e., less tortuous path in fractures than in the matrix). Fracture tortuosities were further modified for fracture-fracture connections by multiplication of the tortuosity by the fracture porosity of the bulk rock to obtain the correct value for the fracture to fracture interconnection area (only for calculation of diffusive fluxes; the entire grid block connection area is used for calculating advective fluxes, because the bulk fracture permeability of the entire grid block is entered into the model).</i></p>	<p>Provides a distinction between fracture and matrix pathways without any range within those.</p>
<p><b>Matrix Pathway Totuosity</b></p>	<p>dearth of site specific data MDL-NBS-HS-000001, Rev. 00; Section 4.1.6</p>	<p><i>Matrix tortuosities are unknown, and therefore a value of 0.2 was estimated from values reported by de Marsily (1986, p. 233). No uncertainties were investigated.</i></p>	<p><i>Matrix tortuosities are unknown, and therefore a value of 0.2 was estimated from values reported by de Marsily (1986, p. 233).</i></p>	<p>Provides a distinction between fracture and matrix pathways without any range within those.</p>

<b>Aqueous Diffusion Coefficients</b>	Dearth of data for, and identification of, specific species MDL-NBS-HS-000001, Rev. 00; Section 4.1.6, Sec. 5, assumption A5	<i>Diffusion coefficients for aqueous species are considered to be identical and equal to the tracer diffusion coefficient of a single aqueous species (Cl) at infinite dilution. The aqueous diffusion coefficient of Cl at infinite dilution is <math>2.03 \times 10^{-9} \text{ m}^2/\text{s}</math> at 25 °C (Lasaga 1998, Table 4.1, p.315), which in the model input was rounded to <math>2.0 \times 10^{-9} \text{ m}^2/\text{s}</math>, essentially a bounding approach.</i>	<i>This is justified because the tracer diffusion coefficients of aqueous species differ by at most about one order of magnitude, with many differing by less than a factor of 2 (Lasaga 1998, p. 315).</i>	All species diffuse in similar manner. No differential transport due to intrinsic species differences.
<b>Gaseous Diffusion Coefficient for CO2</b>	Simplified representation of the CO2 gas diffusion behavior. MDL-NBS-HS-000001, Rev. 00; Section 4.1.6	Diffusion coefficient represented as pressure and temperature dependent relation, but no uncertainties evaluated.	<i>For an ideal gas, the tracer diffusion coefficient of a gaseous species can be expressed as a function of temperature and pressure in the following form (Lasaga 1998, p. 322). Standard technical approach.</i>	Standard approach for CO2 gas diffusion that varies as function of conditions. Does not capture uncertainty in this coefficient.
<b>Variability</b>				
<b>GEOCHEMICAL</b>				
<b>Matrix Mineralogy: Spatial - vertical variability only, related to lithologic unit</b>	'Varying mineralogy by lithostratigraphic unit, MDL-NBS-HS-000001, Rev. 00; Table 2, page 20, Sec. 4.1.2;	lithologic variability for matrix mineralogic variation in vertical direction based on the various model lithologic units.	Mineralogic analysis of SD-9 borehole (as given by the 3-D Mineralogical Model:LA9908JC831321.001), SHT lithology, and DST lithology.	Modeling does not capture mineralogic variation laterally within units. Bulk composition of tuff does not vary largely, but some minor variation for lithophysal mineralogy may be missed, particularly for lithophysal units compared to this model that is based in the middle non-lithophysal unit of the TSw2.
<b>Fracture Mineralogy: Spatial - vertical variability only, related to lithologic unit</b>	'Varying rock properties by lithostratigraphic unit, Calibrated Property set, MDL-NBS-HS-000001, Rev. 00; Table 2, page 20, Sec. 4.1.1 & 4.1.2; Section 1.0 page 13;	lithologic variability for fracture mineralogic variation in vertical direction based on the various model lithologic units.	Mineralogic analysis of SD-9 borehole (as given by the 3-D Mineralogical Model:LA9908JC831321.001), SHT lithology, and DST lithology.	Modeling does not capture mineralogic variation laterally within units. Bulk composition of tuff does not vary largely, but some minor variation for lithophysal mineralogy may be missed, particularly for lithophysal units compared to this model that is based in the middle non-lithophysal unit of the TSw2.
<b>Thermodynamic Data: Temporal Variability-- temperature deltaas drive variations in equilib. constants</b>	Thermally dependent parameters, MDL-NBS-HS-000001, Rev. 00; Sec. 4.1.4, Att. IV	The model incorporates thermally-dependent equilibrium constants for mineral, gas, and aqueous species reactions.	Various published data sources including SUPCRT92; standard industry approach to thermochemical database.	Model interactively captures the changes to thermochemical properties as a function of temperature variations.

<b>Mineral Intrinsic Reaction Rates: Temporal Variability-- temperature deltas drive variations in intrinsic rate constants</b>	Thermally dependent parameters MDL-NBS-HS-000001, Rev. 00; Sec. 4.1.5, Table 4	The analysis incorporates thermally-dependent intrinsic rate constants for mineral dissolution/precipitation reactions.	Various published data sources (see Table 4). Industry Standard approach.	Model interactively captures the changes to intrinsic kinetic rates as a function of temperature variations.
<b>THERMOHYDROLOGIC</b>				
<b>Infiltration / Percolation flux: Temporal Variability</b>	climate changes MDL-NBS-HS-000001, Rev. 00; Sec. 6.3.3, Page 80, Table 12	Variation among three climatic states through time with transitions at 600 and 2000 years	Climate model	Model captures the changes to infiltration rates as a function of climate state.
<b>Repository-scale variability in hydrologic properties: Spatial - vertical variability only, related to lithologic unit</b>	Inter-unit and intra-unit variability MDL-NBS-HS-000001, Rev. 00; *Varying rock properties by lithostratigraphic unit, Calibrated Property set, Table 2, page 20, Sec. 4.1.1; Section 1.0 page 13;	lithologic variability for calibrated hydrologic properties--variation in vertical direction based on the various model lithologic units.	Lithostratigraphic variability in measured/calibrated hydrologic properties.	Model does not captures the variability within the lithostratigraphic units.
<b>Repository-scale variability in thermal conductivity: Spatial - vertical variability only, related to lithologic unit</b>	Inter-unit and intra-unit variability MDL-NBS-HS-000001, Rev. 00; *Varying rock properties by lithostratigraphic unit, Calibrated Property Set, Table 2, page 20, Sec. 4.1.1	lithologic variability for initial thermal conductivities--variation in vertical direction based on the various model lithologic units.	Host rock unit variability in measured thermal conductivities in the lab, as well as adjustments for lithophysical porosities in appropriate units	Model captures only the variations from unit to unit.
<b>Saturation dependant variability in thermal conductivity: Spatial and temporal - related to variable saturation of rock units in model</b>	Saturation dependent parameter MDL-NBS-HS-000001, Rev. 00; Observations of thermal conductivities at variable rock saturation, Calibrated property set, Table 2, page 20, Sec. 4.1.1	linear interpolation between wet and dry values based on saturation in rock	wet and dry thermal conductivity (Kth) values measured on cores in the lab.	Model interactively captures the changes to thermal conductivity of a unit as a function of saturation variations.

<b>EBS "effective" (fictive porous media) thermal conductivities: Temporally variability-driven by temperature changes</b>	Properties used to represent air are for porous media but depend on temperature MDL-NBS-HS-000001, Rev. 00; Sec. 4.1.7.2, Att. VI	Heat transfer from the WP to the drift wall is implemented in the model by using time-varying "effective" thermal conductivities (for open spaces within the drift) that were calculated to account for radiative and convective heat-transport components. These time-varying data were input into the model as coefficients (values between 0 and 1) for each open zone within the drift. Each zone was also assigned a constant maximum thermal conductivity ( $K_{th\ max}$ ), which was then multiplied by the corresponding time-varying coefficients to obtain effective conductivities as a function of time (Attachment VI). The sources of these data are listed in Table 2.	Not provided directly in the AMR. Source data indicated basis is analytical models of heat transfer via radiation and convection in open concentric cylinders.	Model interactively captures the changes to effective thermal conductivity of fictive porous media as a function of temperature variations.
<b>TRANSPORT</b>				
<b>Gaseous Diffusion Coefficient for CO2: Spatial and Temporal Variability--variations in temperature and pressure drive variations in this parameter.</b>	Property dependent on temperature and pressure changes MDL-NBS-HS-000001, Rev. 00; Sec. 4.1.6, Eqn 1	Temperature and pressure dependent gaseous diffusion coefficient.	<i>In the gas phase, CO2 is the only transported reactive species (other than H2O vapor). For an ideal gas, the tracer diffusion coefficient of a gaseous species can be expressed as a function of temperature and pressure in the following form (Lasaga 1998, p.322):</i>	Model interactively captures the changes to gaseous diffusion coefficient as a function of temperature and pressure variations.
<b>Results</b>				
Conceptual Geochemical System	Complex system with alternate possible representations, lack of data for some phases	Separate calculations with two differing geochemical systems, one a subset of the other. Compared to the DST results, and approach to steady state for Ambient THC evaluated.	Both geochemical systems analyzed. Two sets of results generated. For major element chemistry, the Case 2 results using a subset of the Case 1 representation provides better comparison to the DST gas and water compositions, as well as a more stable long time solution for the ambient system.	Comparative analysis allows selection of more accurate results, but the additional constituents quantified in the other calculations allow estimates of trace species concentrations. These representations are combined in the abstraction.
Climate and Infiltration Rate Uncertainty	Changes to climate and shorter term and local variations	Separate calculations performed at the low, mean and high end of the uncertainty ranges for the infiltration rate for a 3-stage climate (i.e., two transitions).	Three sets of results reflecting the range of uncertainty in the infiltration rates.	Each set of these results can be used to abstract the uncertainty into the TSPA. This uncertainty is assessed in the abstraction but is not carried into the TSPA.

Spatial and Temporal variabilities are captured in the model	Number of spatially or temporally dependent parameters.	These variable aspects are directly built into the model.	The variabilities discussed are those that are built into the model.	Vertical Variability captured, but lateral (intra unit) variability lacking. The results integrate these effects directly.
<p><b>NOTE 1:</b> The purpose of the <i>Ambient THC Model</i> (MDL-NBS-HS-000001, Rev. 00) is to evaluate the representation of the geochemical/hydrogeological system (i.e., geochemical representation over geologic time frames) by assessing the stability of the geochemical system and comparing to measured ambient conditions for water and gas compositions. THC simulations under ambient conditions, i.e., without heating, were performed for Case 1 and Case 2 using a constant infiltration rate (about 1.05 mm/year). This value represents the base-case present-day infiltration rate at the location of Borehole SD-9, which was used to define the geology of the model. These ambient simulations were run to assess the extent to which the Case-1 and Case-2 geochemical systems approached a geochemical steady state. These runs also provide a baseline to which the results of thermal loading simulations can be compared. Calculations are done for two different geochemical systems: the less complex Case 2 (components are CO<sub>2</sub>, pH, Ca<sup>2+</sup>, Na<sup>+</sup>, SiO<sub>2</sub>, Cl<sup>-</sup>, [HCO<sub>3</sub>]<sup>-</sup>, [SO<sub>4</sub>]<sup>2-</sup>) and the more complex Case 1 (extended to include the additional components Mg<sup>2+</sup>, K<sup>+</sup>, [AlO<sub>2</sub>]<sup>-</sup>, [HFeO<sub>2</sub>]<sup>-</sup>, and F<sup>-</sup>) geochemical systems.</p>				
<p><b>NOTE 2:</b> The purpose of the <i>Drift-Scale Test (DST) THC Model</i> (MDL-NBS-HS-000001, Rev. 00) is to to evaluate the confidence in the THC representation by comparison to the measured water and gas compositions for the DST. This provides a differentiation between the level of accuracy achieved using two different geochemical systems: the less complex Case 2 (components are CO<sub>2</sub>, pH, Ca<sup>2+</sup>, Na<sup>+</sup>, SiO<sub>2</sub>, Cl<sup>-</sup>, [HCO<sub>3</sub>]<sup>-</sup>, [SO<sub>4</sub>]<sup>2-</sup>) and the more complex Case 1 (extended to include the additional components Mg<sup>2+</sup>, K<sup>+</sup>, [AlO<sub>2</sub>]<sup>-</sup>, [HFeO<sub>2</sub>]<sup>-</sup>, and F<sup>-</sup>) geochemical systems. Agreement with measurements for the major components of the carbonate subsystem is better using the less complex Case 2 representation. This may be due to a higher degree of parameter uncertainty for kinetic and thermodynamic properties of the phases in the aluminum bearing system (like clays and zeolites). In addition, these phases are treated as end-members, rather than as solid solutions.</p>				
<p><b>NOTE 3:</b> The purpose of the <i>Thermal Tests Thermal-hydrological (TH) Analysis/Model Report</i> (AMR; ANL-NBS-TH-000001 Rev. 00) is to evaluate the drift scale thermal-hydrologic (DS) property set derived from the unsaturated zone (UZ) flow and transport analyses for thermally perturbed conditions. Also, the secondary purpose is to conduct sensitivity studies of other TH property sets, including the mountain scale thermal-hydrologic (MS) property set, and to investigate modifications that would result in adequate agreement between simulated and measured TH data. The evaluation is based on TH measurements from the three in situ thermal tests in potential repository lithologic units at Yucca Mountain. All three thermal tests are simulated employing the dual-permeability [conceptual] model (DKM), including the active fracture model (AFM) to represent fracture-matrix interactions. Simulated temperatures and saturations are compared to the measurements from the tests. These comparative analyses form the basis for the</p>				

**Table 7-2: Treatment of Uncertainties and Variability within the Multiscale Thermohydrology Percolation Flux (MSTHPF) Model**

Multiscale Thermohydrologic Percolation Flux Model (MSTH Perc. Flux Model)				
<p><b>Model Purpose:</b> The purpose of the <i>Multiscale Thermohydrology Percolation Flux Model</i> (MSTH PFM) for the NFE is that, as a subset of the results from the <i>Multiscale Thermohydrologic Model</i> (MSTHM) AMR (ANL-EBS-MD-000049 Rev. 00 -- see description at the bottom of this table), it provides the Thermally Perturbed Percolation Flux in the Near-Field Host Rock. These results at 5 m from the drift wall are used to represent the thermally perturbed percolation flux in abstractions that feed the TSPA model. For additional specific submodel descriptions and uncertainty treatment, see the EBS PMR models and AMR uncertainty reviews. This model is supported by the <i>TH Model Testing V&amp;V</i> (ANL-NBS-TH-000001 Rev. 00) that for the NFE PMR provides V&amp;V of the TH models and their results by comparison of the models to thermal data from the field tests, including the DST.</p>				
Summary	Source	Treatment	Basis	Impact
<b>Conceptual Model Uncertainty</b>				
<b>Active fracture model</b>	Complex system with alternate possibilities that are constrained only partially by data ANL-EBS-MD-000049 Rev. 00: Section 6.3, page 78	<i>The active fracture concept accounts for the contact area between the fracture and the matrix (Table 4-2), as well as the frequency of fractures (Table 4-2). The AFC is that fracture flow only occurs through some of the fractures.</i>	This is more conservative than assuming the influx flows evenly through all fractures. This maximizes flux and results in fast pathways for flux through the mountain.	Provides for flow at much less than average fracture saturations of 1.
<b>Edge cooling effect</b>	The potential repository will have an edge ANL-EBS-MD-000049 Rev. 00: Section 6.1, p. 75; Section 6.3, p. 78	<i>It is useful to think of the LDTH submodel as the "core" submodel. These 2-D drift-scale TH submodels are run for 31 locations (Figure 5-2) spaced evenly throughout the repository area for several Areal Mass Loading (AML) values (nominal value and lower) to represent the influence of edge-cooling effects.</i>	<i>The LDTH submodels are run at the 31 drift-scale-submodel locations (Figure 5-2) and for 5 different values of Areal Mass Loading (AML = 15, 25, 36, 50, and 60 MTU/acre). Representing the influence of edge-cooling effects requires that most of the LDTH submodel runs use an AML that is less than the nominal value.</i>	Allows variable thermal evolution across the potential repository with differing timing of cooling and rewetting.
<b>Horizontal conduction</b>	Heat loss at in saturated zone could be in three directions ANL-EBS-MD-000049 Rev. 00: Section (assumption) 5.3.1	Heat transfer in the horizontal direction is negligible at the base of the model that is situated deep within the saturated zone.	This assumption is conservative from a temperature standpoint because if energy was lost in the horizontal direction the result would be lower temperatures. Used in Attachment X and Section 6.2.3.	Constrains the lower boundary condition to be adiabatic and minimizes impact on results

<b>Heat-Pipe Zone development</b>	Coupling of liquid and vapor transport to temperature of phase change ANL-EBS-MD-000049 Rev. 00: Section 6.11.1.4, p. 120	Incorporation of the conductive and convective heat transfer processes allows for zones to develop that maintain a fairly constant temperature over a finite spatial extent at about the boiling condition. This leads to refluxing of water in fractures in this fractured porous media.	<i>The increase in q<sub>liq</sub>, 5m arises from heat-driven condensate flow; which occurs in the refluxing zone (also called the heat-pipe zone), just beyond where dryout is occurring. Thirty years into the post-closure period (Figure 6-26d) the heart of the heat-pipe zone has reached at least 5 m above the drift.</i>	The model can produce the effects if the conditions are appropriate.
<b>Dimensions and properties of EBS components</b>	Thermal source term from various WPs and the various modeling scales used. ANL-EBS-MD-000049 Rev. 00: Section 6.1, p. 75	<i>The DDT submodel is a 3-D drift-scale submodel which includes individual WPs (with distinctive heat-generation histories) and accounts for thermal radiation in addition to thermal conduction between the WPs and drift surfaces.</i>	Different WP types as defined by the WP design group (see Section 4.1.4).	Accounts for thermal differences generated for the package-scale variability.
<b>Appropriate Thermohydrologic Processes</b>	Uncertainties in near-field coupled thermal-hydrological mechanisms (including heat-transfer, vapor transport and refluxing, and fracture-matrix interaction). ANL-NBS-TH-000001 Rev. 00:	Appropriate conceptual models for near-field thermal-hydrological performance are determined by comparing simulated performance with measured performance of relatively large scale (several to tens of meters) in situ tests	Used several different conceptual models (including conduction only, as for ANSYS). One conceptual model was essentially confirmed by performance monitoring of large scale in situ thermal tests (by "heat-pipe 4", p. 53), and there are essentially no other conceptual models currently considered viable.	"The assumptions, uncertainties, restrictions, and constraints used in this analysis do not appear to have a significant impact on the results and conclusions." (p. 190). It is the reviewer's opinion that uncertainties in the conceptual model have been largely resolved, except perhaps for fracture-matrix interaction.
<b>Representational Model Uncertainty</b>				
<b>Combination of Conduction Results with TH Results</b>	Indirectly coupled combination of results from TH and conduction-only models. ANL-EBS-MD-000049 Rev. 00: Section 6, p. 74	<i>The MSTHM is a computationally efficient means of determining TH conditions in the NFE and EBS as a function of location in the repository and WP type; such determination would otherwise require millions of grid blocks if a brute-force monolithic numerical model were used.</i>	<i>The MSTHM calculates 38 NFE and EBS TH variables (Table 1-1). These TH variables are calculated for 623 repository subdomains distributed throughout the repository area (Figure 6-1). Four different WP types (in the specific sequence shown Figure 4-1) are modeled. Because there are 8 different WP locations, this results in 8 different WPs that are considered at each of the 623 repository subdomains. Thus, at each of the 623 repository subdomains, 38 TH variables are calculated for 8 different WPs, resulting in 623 x 38 x 8 = 189,392 TH variables at each calculational timestep. Because there are 352 timesteps, this results in 189,392 x 352 = 66,855,376 TH data points per infiltration-flux case. Because there are three infiltration-flux cases (mean, high, and low flux) considered in this AMR, there are a total of 66,855,376 x 3 = 200,566,128 TH data points calculated by the MSTHM in this AMR.</i>	Representation is designed to efficiently account for many of the thermal variabilities and scaling aspects of the problem.

<p><b>Appropriate mathematical models</b></p>	<p>Approximations and simplifications in representation of conceptual model, e.g., in geometry and geology, in thermal loading, etc ANL-NBS-TH-000001 Rev. 00.</p>	<p>Appropriate mathematical models for near-field thermal-hydrological performance are determined by comparing simulated performance with measured performance of relatively large scale (several to tens of meters) in situ tests. Either TOUGH2 or NUFT is adequate.</p>	<p>Either TOUGH2 or NUFT, with the appropriate parameters values, resulted in simulated performance that adequately matched measured performance of relatively large-scale in situ thermal tests.</p>	<p>"The assumptions, uncertainties, restrictions, and constraints used in this analysis do not appear to have a significant impact on the results and conclusions." (p. 190). It is the reviewer's opinion that uncertainties in the mathematical model are relatively small compared to other PA uncertainties and can be ignored.</p>
<p><b>Parameter Uncertainty</b></p>				
<p><b>Infiltration / Percolation flux</b></p>	<p>Observations made at the site as well as projections for other climates. Varying rock properties by lithostratigraphic unit, Calibrated Property Set ANL-EBS-MD-000049 Rev. 00: Section 6.11.1.4</p>	<p>High, medium, and low values of infiltration used for each of three climate states.</p>	<p>Assumed cases analyzed were based on the infiltration model from the UZ PMR (see UZ Flow Model chapter).</p>	<p>Infiltration-flux uncertainty affects the local percolation flux, which affects the duration of dryout in the near-field host rock surrounding the drifts as well as rewetting the backfill and invert to ambient (humid) conditions. Dryout duration increases with decreasing percolation flux. This uncertainty is addressed by including the mean, high, and low infiltration-flux cases in this AMR. These three cases are judged to adequately span the range of uncertainty of the infiltration flux. The low infiltration-flux cases had a considerably longer dryout duration than either the mean of high infiltration-flux cases. <i>The spatial extent of dryout decreases with increasing infiltration (or percolation) flux. The lateral extent of boiling is considerably greater for the low infiltration-flux case than for the mean or high infiltration-flux cases (Figure 6-12). For the median WP location, the maximum lateral extent of boiling is 8.4 m, 9.1 m, and 10.5 m for the high, mean, and low infiltration-flux cases, respectively</i></p>
<p><b>Invert and backfill satiated saturation</b></p>	<p>Lack of data on the saturation level at which water flows in the backfill. ANL-EBS-MD-000049 Rev. 00: Section 5.2.3</p>	<p><i>The assumed value for satiated saturation of the invert and backfill materials is 1.0. This assumption is used in all NUFT input files (used throughout).</i></p>	<p><i>This is an upper bound for this parameter, and is therefore conservative. This assumption does not require confirmation.</i></p>	<p>Maximizes the potential for liquid flux and radionuclide transport through the materials.</p>

<p><b>Appropriate parameters for near-field thermal-hydrological models</b></p>	<p>Uncertainties in measured test performance (especially moisture from ERT data) and in actual test boundary conditions (especially heat and moisture leakage through DST bulkhead and heater boreholes). ANL-NBS-TH-000001 Rev. 00:</p>	<p>Appropriate parameters for particular near-field thermal-hydrological models are determined by comparing simulated performance with measured performance of relatively large scale (several to tens of meters) in situ tests. Uncertainties in measured test performance and in actual test boundary conditions are acknowledged but were ignored, e.g., a best estimate was used for leakage through the DST bulkhead while leakage through heater boreholes was ignored. A single parameter set that resulted in the best match between simulated and measured performance was recommended, i.e., no parameter uncertainty.</p>	<p>No basis for ignoring parametric uncertainty was provided. However, several different parameter sets were used to simulate performance of large scale in situ thermal tests, with more than one set resulting in an adequate match of simulated and monitored performance of those tests, with thermal performance evaluated statistically and hydrologic performance evaluated only qualitatively.</p>	<p>"The assumptions, uncertainties, restrictions, and constraints used in this analysis do not appear to have a significant impact on the results and conclusions." (p. 190). It is the reviewer's opinion that uncertainties in the heat transfer parameters are relatively small compared to other PA parameters, but that there may be significant uncertainty in the hydrologic parameters (especially related to vapor transport and refluxing in fractures).</p>
---	---	--	--	--

## Variability

<p><b>Repository-scale infiltration / percolation flux</b></p>	<p>Spatial variability of the surface infiltration ANL-EBS-MD-000049 Rev. 00: Section 6.1, p. 75; Section 6.3.1, p. 79; Section 6.3.6, p. 87 Section 7, page 302</p>	<p>The LDTH submodel includes the hydrologic processes and parameters (e.g., surface infiltration rates, hydrologic properties) used to describe a location, given specific coordinates within the repository. Infiltration rates at each submodel location in column.data (CRWMS M&amp;O 2000a) are found using a routine that interpolates, and then normalizing the results from the 31 locations. ConvertCoords prepares the input data for the interpolation routine, columnInfiltration (see Figure 3-4). The output from columnInfiltration is one large file (CRWMS M&amp;O 2000a, infiltration.tex). This file is split into the nine constituent infiltration rates with the routine infiltab. The average of the 31 infiltration rates was found to differ from the average of all the infiltration rates in the source data that were within the repository footprint. To account for this the infiltration rates are normalized with respect to the average of the source data over the repository footprint.</p>	<p>Input data for infiltration variable across the repository footprint. Goal is to have the 31 representative locations for LDTH models providing the same average infiltration as that over the whole footprint. Section 7, page 302</p>	<p>Variability of surface infiltration is captured in the LDTH submodels of the MSTH Model. This variability will flow directly into that for the thermally perturbed percolation flux.</p>
--	--	--	--	---

<p><b>Repository-scale stratigraphic variability</b></p>	<p>Varying units and unit thickness, ANL-EBS-MD-000049 Rev. 00: Table 6-1, page 79; Section 4.1.2</p>	<p>The LDTH submodel locations are shown in Figure 5-2, and represent repository-scale variability of thermal properties, hydrologic properties, infiltration flux, and overburden thickness. The stratigraphic columns corresponding to the LDTH submodel locations are output from YMESH in the file &lt;column&gt;.nft (CRWMS M&amp;O 2000a). The software used in manipulating the source data into a YMESH input file (excluding the location file, column.data) are rme6 and makeColumns. The thickness of the stratigraphic units at each location is output from readUnits (CRWMS M&amp;O 2000a, 31 files: &lt;column.col.units&gt;), and is tabulated in Table 6-1.</p>	<p>31 representative locations are distributed throughout the repository footprint with stratigraphy represented from the site-scale UZ flow model (see Section 4.1.2).</p>	<p>Stratigraphic variation of units across the potential repository site captured in the MSTH model.</p>
<p><b>Repository-scale variability in hydrologic properties</b></p>	<p>Varying rock properties by lithostratigraphic unit, Calibrated Property Set ANL-EBS-MD-000049 Rev. 00: Section 4.1.1.18;</p>	<p>Spatial - related to lithologic unit; Each stratigraphic unit has two sets of properties, one for its matrix and the other for its fractures. The matrix properties are: permeability, porosity, Van Genuchten <math>\alpha</math> parameter, Van Genuchten <math>\beta</math> parameter, residual saturation, and saturated saturation. The fracture parameters include the six categories used for the matrix of the rock (although the values for the fractures are different) and 3 additional parameters: active fracture parameter, fracture frequency, and fracture to matrix area. The thermal properties include grain density, grain specific heat, wet thermal conductivity, dry thermal conductivity, and tortuosity. There are three infiltration cases (each corresponding to an expected climate) over which the repository is being modeled. There is a set of hydrologic properties for each of these infiltration cases.</p>	<p>Matrix imbibition, diffusivity, and capillary wicking in fractures</p>	<p>Matrix-imbibition diffusivity and capillary wicking in fractures uncertainty affects the duration of dryout in the near-field host rock surrounding the emplacement drifts. The rewetting of the host rock is also strongly affected by the magnitude of the local percolation flux, which depends on the ambient infiltration flux. Dryout duration increases with decreasing local percolation flux and with decreasing capillarity of the matrix and fractures in the host rock. This AMR considered a wide range of infiltration flux, which, in effect, is equivalent to considering a wide range of matrix-imbibition diffusivity and a wide range of capillarity of fractures in the host rock.</p>

<p><b>Repository-scale variability in overburden thickness</b></p>	<p>Lithostratigraphic variability ANL-EBS-MD-000049 Rev. 00: Section 6.1, p. 75; Table 6-2, Section 6.3.1.2; Section 4.1.2</p>	<p>The SMT is 3D and includes the influence of thermal-property variation in the mountain, lateral heat loss at the repository edges, and overburden-thickness variation with location, assuming a uniform, planar (i.e., smeared) heat source throughout the repository area.</p>	<p>The ground surface is irregular, the stratigraphic data in table 6-2 indicate the geologic model units as defined in the site-scale UZ flow model (see Section 4.1.2 of ANL-EBS-MD-000049 Rev. 00 and the chapter on the UZ Flow model).</p>	<p><i>Overburden thickness (which is equal to the depth of the repository below the ground surface) affects temperatures in the repository because it determines the thickness of the (rock) insulation lying between the repository and the ground surface. Because the ground surface is a constant-temperature boundary, acts like a heat sink. The influence of overburden thickness is negligible during the first 300 to 500 yr (Hardin et. al 1998, Section 3.7.7.1). This influence is also relatively unimportant close to the repository edges and are increasingly important toward the center of the repository (Hardin et. al 1998, Section 3.7.7.1). The greatest long-term temperature rise occurs where the overburden thickness is greatest in the central region of the repository (Hardin et. al 1998, Section 3.7.7.1). Because the largest values of overburden thickness occur close to the center of the repository, it is difficult to discern the influence of the edge-cooling effect from the influence of overburden thickness (Figure 6-7h through Figure 6-7m); both influences cause higher long-term temperatures at the center and lower long-term temperatures at the edges of the repository.</i></p>
--	--	--	---	--

<b>Repository-scale variability in thermal conductivity</b>	Varying rock properties by lithostratigraphic unit, Calibrated Property Set ANL-EBS-MD-000049 Rev. 00: Table 4-3, page 62	lithologic variability; wet to dry variability (provides some within unit variability); Each stratigraphic unit has two sets of properties, one for its matrix and the other for its fractures. The matrix properties are: permeability, porosity, Van Genuchten $\alpha$ parameter, Van Genuchten $\beta$ parameter, residual saturation, and saturated saturation. The fracture parameters include the six categories used for the matrix of the rock (although the values for the fractures are different) and 3 additional parameters: active fracture parameter, fracture frequency, and fracture to matrix area. The thermal properties include grain density, grain specific heat, wet thermal conductivity, dry thermal conductivity, and tortuosity. There are three infiltration cases (each corresponding to an expected climate) over which the repository is being modeled. There is a set of hydrologic properties for each of these infiltration cases.	Host rock unit variability; the uncalibrated thermal properties of the stratigraphic units are given in Table 4-4. The source of this data is thermal_UZ.xls (LB991091233129.006).	Incorporates the major variability expected for thermal conductivities of the rock mass, which dominates heat transfer within the system.
<b>Seepage flux uncertainty and variability</b>	Liquid flux into the drifts will be spatially variable ANL-EBS-MD-000049 Rev. 00: Section 7.1, page 307	Taken as negligible	Wicking flux of the backfill overwhelms any other effects of water entering the drift	This treatment would perhaps be very different depending on the presence or absence of backfill
<b>WP-to-WP variability in heat generation rate</b>	Various thermal loading in the different waste package types. ANL-EBS-MD-000049 Rev. 00: Section 6.1, p. 75; Section 4.1.4 p. 62	<i>The DDT submodel is a 3-D drift-scale submodel which includes individual WPs (with distinctive heat-generation histories) and accounts for thermal radiation in addition to thermal conduction between the WPs and drift surfaces.</i>	Different WP types as defined by the WP design group (see Section 4.1.4).	Captures the package scale variability expected for the potential repository design

<b>Thermal Conductivity: Saturation dependant variability</b>	Data showing variation of effective thermal conductivity with saturation state ANL-EBS-MD-000049 Rev. 00: wet and dry thermal conductivity Kth values (Table 4-3)	linear interpolation between wet and dry values based on saturation in rock	experimental measures for variable saturations state of the tuff.	Model interactively captures the changes to thermal conductivity of a unit as a function of saturation variations.
<b>Infiltration / Percolation flux</b>	Changes to climate and shorter term and local variations ANL-EBS-MD-000049 Rev. 00: Section 6.3.6, p. 87	Infiltration data is in the nine files from Section 4.1.3, representing three cases (low, mean, and upper, each having three climates (present day, monsoon, and glacial).	Climate variation and spatial variation of infiltration data.	Each set of these results can be used to abstract the uncertainty into the TSPA, This uncertainty is assessed in the abstraction as separate results
<b>Spatial Heterogeneity at various scales</b>	Heterogeneities in rock matrix within and between geologic units, and heterogeneities in fractures. variability ANL-NBS-TH-000001 Rev. 00:	Appropriate parameters for particular near-field thermal-hydrological models are determined by comparing simulated performance with measured performance of relatively large scale (several to tens of meters) in situ tests. Spatial variability in ambient conditions and properties at smaller scale than the test volume is acknowledged (because of the observed spatial variability in performance) but is ignored, except for differences between different geologic units. Average conditions and parameters for each geologic unit that best reproduce performance for the entire test block are determined. It is implied that there is no spatial variability within each geologic unit at this scale.	It would be difficult to characterize and model spatial variability in ambient conditions and properties at smaller scale than the test volume, although it is also stated that "...heterogeneity of fracture properties...can be readily accommodated in the TH model." (regarding simulation of the drift scale test using NUFT, p. 86). No basis is provided for assumption of no spatial variability within geologic units.	Small-scale variability affects seepage pathways, as suggested by "fracture geometry may be a significant factor for predicting seepage into boreholes near heated regions." (p. 59). It is the reviewer's opinion that large-scale spatial variability within each geologic unit needs to be assessed, e.g., by assessing the spatial variability of "indicator" properties (such as average fracture densities) at that scale.

<b>Temporal Variability of Boundary Conditions</b>	Barometric pressures, surface temperatures and humidity/precipitation change with time naturally. variability ANL-NBS-TH-000001 Rev. 00:	Seasonal barometric changes and surface temperature/precipitation records were considered during simulation of the thermal tests. Seasonal barometric and surface temperature changes (e.g., Fig 13), and precipitation, were estimated (based on available records) and this temporal variability was incorporated in the boundary conditions for simulating the thermal tests.	Over the limited time-scale of the thermal tests, it is difficult to envision any other temporal variability (e.g., degradation processes) besides the transient nature of the tests, which were adequately considered.	It is the reviewer's opinion that temporal variability was adequately considered in evaluating the tests. However, the effect of longer-term processes (especially chemical, including dissolution and precipitation) on thermal-hydrological behavior should also be considered in PA.
<b>Temporal/Spatial Variability in Porosity</b>	Spatial variability is due to rock and fracture heterogeneities. The source of temporal variability is unknown. "...porosity, which may be spatially and temporally variable." (p.66) ANL-NBS-TH-000001 Rev. 00:	Temporal variability in porosity is ignored. Spatial variability in porosity within a geologic unit is ignored.	There is no reasonable basis for assuming temporal variability in porosity. See above regarding basis for ignoring spatial variability.	It is the reviewer's opinion that ignoring temporal variability in porosity has little impact. See above for impact of ignoring spatial variability.
<b>Results</b>				
Conceptual and representational models, and parameter uncertainties	Variety of sources as given above in the Table. Assessed in ANL-NBS-TH-000001 Rev. 00	The results of the various implementations of the TH models (TOUGH2 and NUFT) and conduction only models (ANSYS) are compared to the observations from the field thermal tests (especially the Drift-scale test). This is done in a quantitative statistical manner for thermal results, and in a semi-qualitative comparative manner for the hydrologic parameters.	The various parameter sets used with the various models were tested against the temperature data for agreement using a number of statistical measures. The criteria for agreement were defined in a variety of ways for different groups of the observations but were generally to meant to evaluate the model versus the data to about 15%.	These types of models appear to reproduce the measures to within 15% for thermal aspects. Only qualitative agreement was discussed for the hydrologic aspects of these model results.
Climate and Infiltration Rate Uncertainty	Changes to climate and shorter term and local variations	Separate calculations performed at the low, mean and high end of the uncertainty ranges for the infiltration rate for a 3-stage climate (i.e., two transitions).	Three sets of results reflecting the range of uncertainty in the infiltration rates.	Each set of these results can be used to abstract the uncertainty into the TSPA. This uncertainty is assessed in the abstraction and carried into the TSPA.
Spatial and Temporal variabilities are captured in the model	Number of spatially or temporally dependent parameters.	These variable aspects are directly built into the model.	The variabilities discussed are those that are built into the model.	Vertical Variability captured, but lateral (intra unit) variability lacking. The results integrate these effects directly.

<p>The purpose of the <i>Multiscale Thermohydrologic Analysis/Model</i> Report (MSTH AMR; ANL-EBS-MD-000049 Rev. 00) is to describe the thermohydrologic evolution of the near-field environment (NFE) and EBS throughout the high-level nuclear waste repository at Yucca Mountain for a particular engineering design. The process-level model will provide TH information and data (such as in-drift temperature, relative humidity, liquid saturation, etc.) for use in other technical products. This data is provided throughout the entire repository area as a function of time. The MSTHM couples the <i>Smearred-heat-source Drift-scale Thermal-conduction</i> (SDT), <i>Line-average-heat-source Drift-scale Thermohydrologic</i> (LDTH), <i>Discrete-heat-source Drift-scale Thermal-conduction</i> (DDT), and <i>Smearred-heat-source Mountain-scale Thermal-conduction</i> (SMT) submodels such that the flow of water and water vapor through partially-saturated fractured rock is considered. The MSTHM accounts for 3-D drift-scale and mountain-scale heat flow, repository-scale</p>				
<p>The purpose of the Thermal Tests Thermal-hydrological (TH) Analysis/Model Report (AMR; ANL-NBS-TH-000001 Rev. 00) is to evaluate the drift scale thermal-hydrologic (DS) property set derived from the unsaturated zone (UZ) flow and transport analyses for thermally perturbed conditions. Also, the secondary purpose is to conduct sensitivity studies of other TH property sets, including the mountain scale thermal-hydrologic (MS) property set, and to investigate modifications that would result in adequate agreement between simulated and measured TH data. The evaluation is based on TH measurements from the three in situ thermal tests in potential repository lithologic units at Yucca Mountain. All three thermal tests are simulated employing the dual-permeability [conceptual] model (DKM), including the active fracture model (AFM) to represent fracture-matrix interactions. Simulated temperatures and saturations are compared to the measurements from the tests. These comparative analyses form the basis for the inference</p>				

INTENTIONALLY LEFT BLANK

## 8.0 Engineered Barrier System Models

### 8.1 Introduction

The *EBS Degradation, Flow and Transport* PMR (TDR-EBS-MD-000006) and its associated AMRs comprise the documentation of the EBS models. This includes 23 Rev. 00 AMRs, divided into 17 process-level AMRs, 4 abstraction-level AMRs, and 2 FEPs AMRs. (Subsequent to Rev. 00, the two FEPs AMRs were combined into one AMR.) A number of the process level models were used for FEPs screening, rather than direct input to TSPA. Uncertainty treatments in the process-level and abstraction-level AMRs are addressed in this chapter of the report, however the FEPs AMRs are not addressed directly.

The EBS PMR summarizes the development and abstraction of models for processes that govern the evolution of conditions within the emplacement drifts, drift degradation, and transport of radionuclides out of the drift into the UZ. Figure 8-1 (Figure 8-1a, Engineered Barrier System PMR Process Models; Figure 8-1b, Engineered Barrier System PMR Abstraction Models; Figure 8-1c, Total System Performance Assessment Models for Engineered Barriers) provides a high-level overview of the models that comprise the EBS PMR. Some of these models may be developed in an individual AMR, and some are sub-models, several of which are developed in one AMR. Note that dashed ovals and arrows are used in Figure 8-1 to indicate models in other PMRs and information flow to and from the other PMRs. Table 8-1 identifies the AMRs and PMR sections that are related to the five major modeling areas that are portrayed on Figure 8-1a. Table 8-1 refers to the AMRs by AMR ID number and the short AMR identifier. A mapping of the AMR numbers/identifiers, Document Identification numbers, and AMR titles is provided in Table 8-2, and the complete references are given in Chapter 19.

This chapter summarizes the models developed in the AMRs associated with the EBS PMR, and the treatment of uncertainties as documented in Rev. 00 of those AMRs. A few of the AMRs discussed are Rev. 00, ICN 01 (typically ICN 01 of the Rev. 00 AMRs were issued to address the removal of backfill from the design at SR). The exception to this is the *Invert Diffusion* AMR Rev. 01 that includes significant changes in the model and the treatment of uncertainty. The specific document versions addressed in this review are shown in Table 8-2.

The EBS PMR and its associated AMRs discuss a large number of potentially complex, wide-ranging, and highly coupled processes, and therefore, some of the models are relatively immature compared to other PMR areas. A number of the AMRs contain only conceptualizations of the processes being evaluated (e.g., conceptual models). An example of this is the *Seepage/Invert Interaction* AMR that discusses the potential interactions between invert materials and fluids moving through the invert, but does not actually evaluate those reactions quantitatively.

The EBS PMR/AMR models cover a wide range of coupled processes using a large number of models (see Table 8-1). Some of the EBS models are abstracted into TSPA, but most are used for FEPs screening analysis. In some cases, these EBS models derive their boundary conditions from models developed in other PMR areas. In other cases the EBS AMRs develop models/estimates for the boundary conditions. This variability is also the case for the interfaces

Note: The dashed lines are used to indicate models and information flow to and from other PMRs.

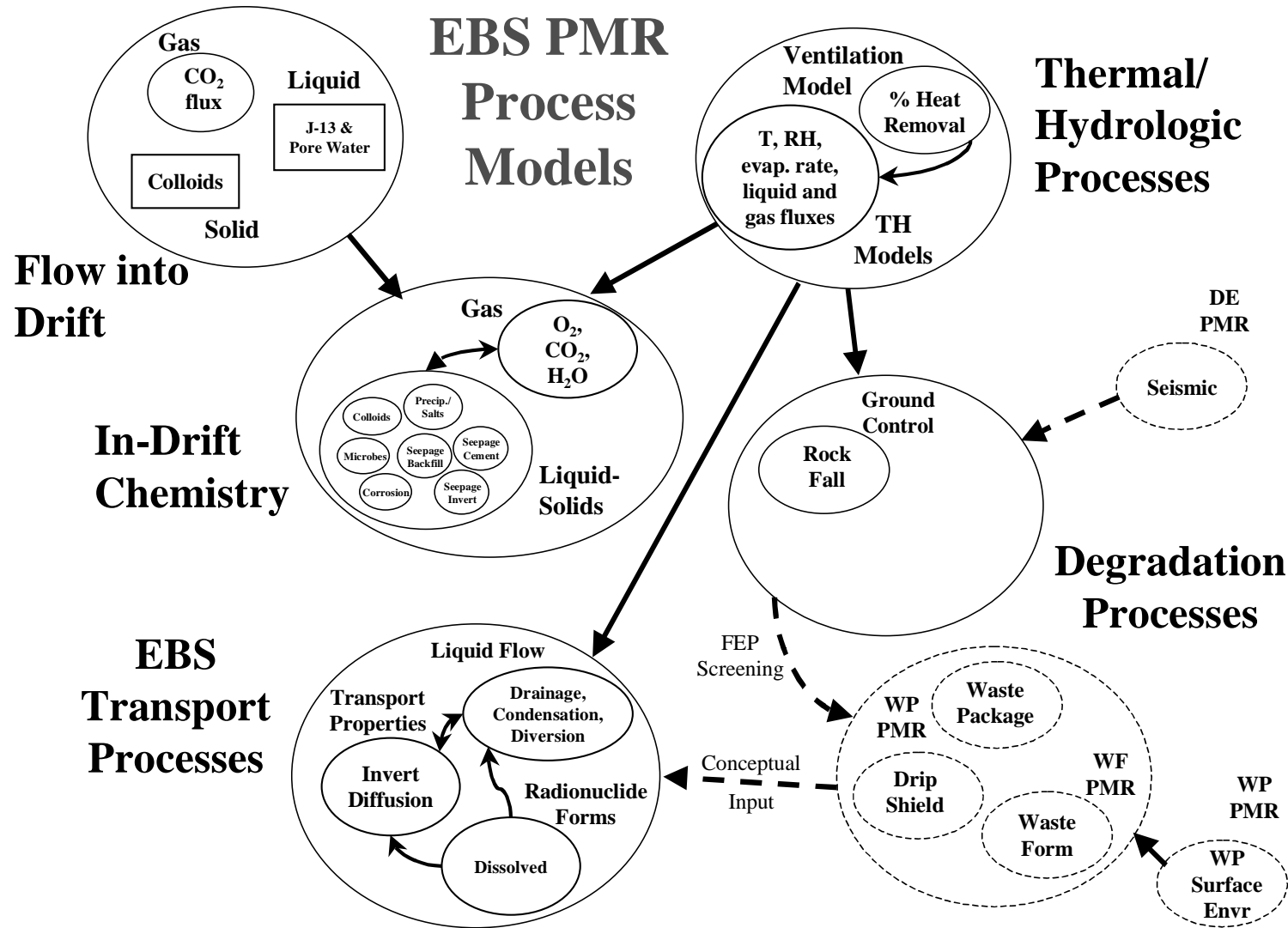


Figure 8-1a: Engineered Barrier System PMR Process Models

Note: The dashed lines are used to indicate models and information flow to and from other PMRs.

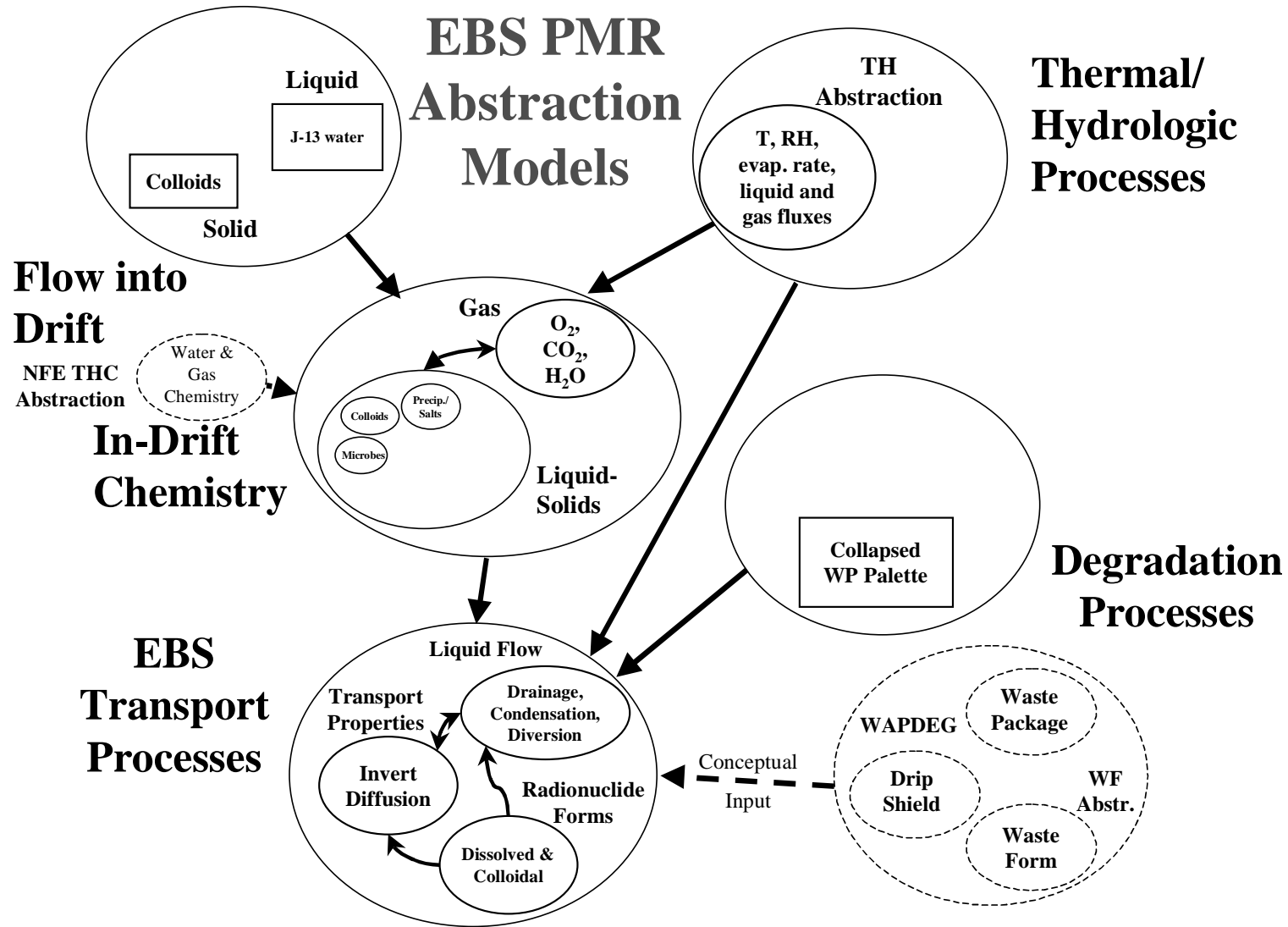


Figure 8-1b: Engineered Barrier System PMR Abstraction Models

Note: The dashed lines are used to indicate models and information flow to and from other PMRs

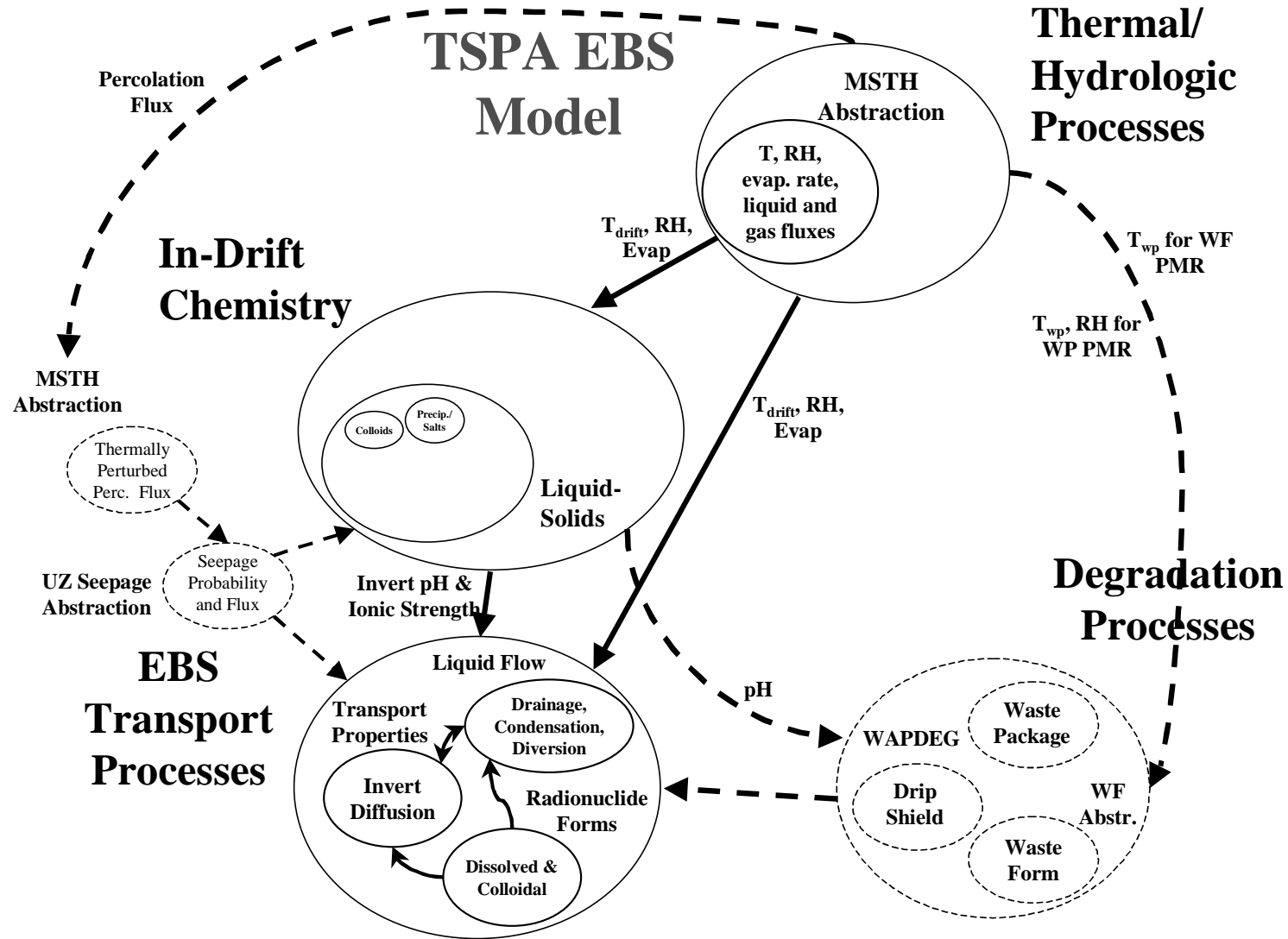


Figure 8-1c: Total System Performance Assessment Models for Engineered Barriers

defined within this suite of EBS models. Some EBS models use bounding assumptions as inputs, whereas others use the actual results from the other EBS models. This heterogeneous treatment makes it difficult to follow how these complex interrelations among internal and external models are constructed. Because of the complexity of the EBS PMR, this chapter covers the treatment of uncertainties at a relatively general level using a categorization of the modeling areas as shown in Figure 8-1. The five broad modeling areas defined for the treatment of these models (defined in Figure 8-1a and Table 8-1).

- Flow into the Drifts
- In-Drift Chemistry/Chemical Processes
- In-Drift Physical/Degradation Processes
- Thermal/Hydrologic Processes
- EBS Transport Processes

Even at this level of delineation, it can be seen in Figure 8-1a that there are at least three levels of submodels. Further complicating the picture is the fact that because only some of the process models are intended to be abstracted and integrated into the TSPA, these model interfaces change at the abstraction level (Figure 8-1b) and then again at the TSPA level (Figure 8-1c).

Both Table 8-1 and Figure 8-1 (1a, 1b, and 1c) define the relations among and between the process models, the abstraction models, the TSPA implementations, and their associated AMRs. At the abstraction level shown in Figure 8-1b, models that were used only for FEP screening analysis have been left off the figure (e.g., the ventilation model and the rock fall model). This Figure 8-1b also shows the external feeds from other PMR areas that are used with the EBS abstraction models (e.g., water and gas chemistry coming into the drift is based on the THC abstraction – see the NFE chapter).

The information flow is also different at the TSPA model level, as shown in Figure 8-1c, primarily due to the manner in which various sub-component abstraction models are implemented. For example, Figure 8-1c shows that the seepage probability and flux into the drift for TSPA comes from the *UZ Seepage Abstraction* AMR (MDL-NBS-HS-000002, as driven by the Multiscale TH Percolation Flux Model – see the Chapter on the NFE models).

## **8.2 Discussion of the EBS Models Uncertainty Treatment**

The discussion in the following subsections covers the model structure and information flow in each of the five broad modeling areas defined above.

### **A. Flow into the Drifts**

The modeling for flow into the drifts includes gas, liquid, and solids that move from the UZ into the drifts. The sub-models within this group do not appear to result in direct inputs to TSPA, but provide input to some of the in-drift chemistry and chemical process models of the EBS PMR.

The models for flow into the drift come from three AMRs:

- The gas flow model covers O<sub>2</sub> and CO<sub>2</sub> and develops a model for thermally coupled gas flux to the drift wall (ANL-EBS-MD-000033).
- The liquid flow model defines the water chemistry of J-13 water (carbonate type), and pore water (chloride-sulfate type) used as boundary conditions to the drift (ANL-EBS-MD-000033, ANL-EBS-MD-000045).
- The solid flow model defines the ambient clay colloid type and size distributions (ANL-EBS-MD-000042).

In some cases, these models are developed as boundary conditions within AMRs that also develop the downstream models that use them.

Figure 8-2, Engineered Barrier System PMR Model Structure – Flow Into Drift, depicts the various elements that comprise the model for flow into the drifts including the conceptual models, parameters/inputs, representational model, results, and usage. It can be seen in Figure 8-2 that the usage of these models to provide boundary conditions is limited to other process models covered in the EBS PMR. They do not directly provide the basis for abstractions are input into the TSPA. A more detailed discussion is not provided since these models are not directly used in TSPA-SR.

As noted in Table 8-1, the models for flow into the drift were developed in several sections of the Physical & Chemical Environment Process Model (ANL-EBS-MD-000033), and in a section of the In-Drift Colloids and Concentration Model (ANL-EBS-MD-000042). The uncertainty review of these AMRs showed that in many cases uncertainty was not directly addressed and that where it was addressed it was done primarily by the use of conservatively bounding assumptions with respect to parameter uncertainties. The *Precipitates/Salts* AMR (ANL-EBS-MD-000045) addresses the uncertainty in the abundance of CO<sub>2</sub> gas in the atmosphere impinging on the drift by providing the abstracted water composition look-up tables for water composition as functions of pCO<sub>2</sub>. For evaporative affects on the water composition, the CO<sub>2</sub> composition of the gas phase can then be varied to evaluation the effects on the solution.

There are few data on the composition of natural colloids at the potential repository site. Given this uncertainty in groundwater colloid concentration and stability, the *In-Drift Colloid* AMR (ANL-EBS-MD-000042) simply uses bounding values for the concentrations/stabilities that are defined as functions of ionic strength, and pH).

## **B. In-Drift Chemistry/Chemical Processes**

The model for in-drift chemistry and chemical processes includes gas, liquid, and solid phases and represents the physical and chemical processes that define the in-drift environment. The sub-models within this modeling area do not appear to result in direct inputs to TSPA, except for the precipitates and salts model. The model results primarily provide inputs to the EBS transport process models, or provide screening arguments for the effects of seepage interaction with other

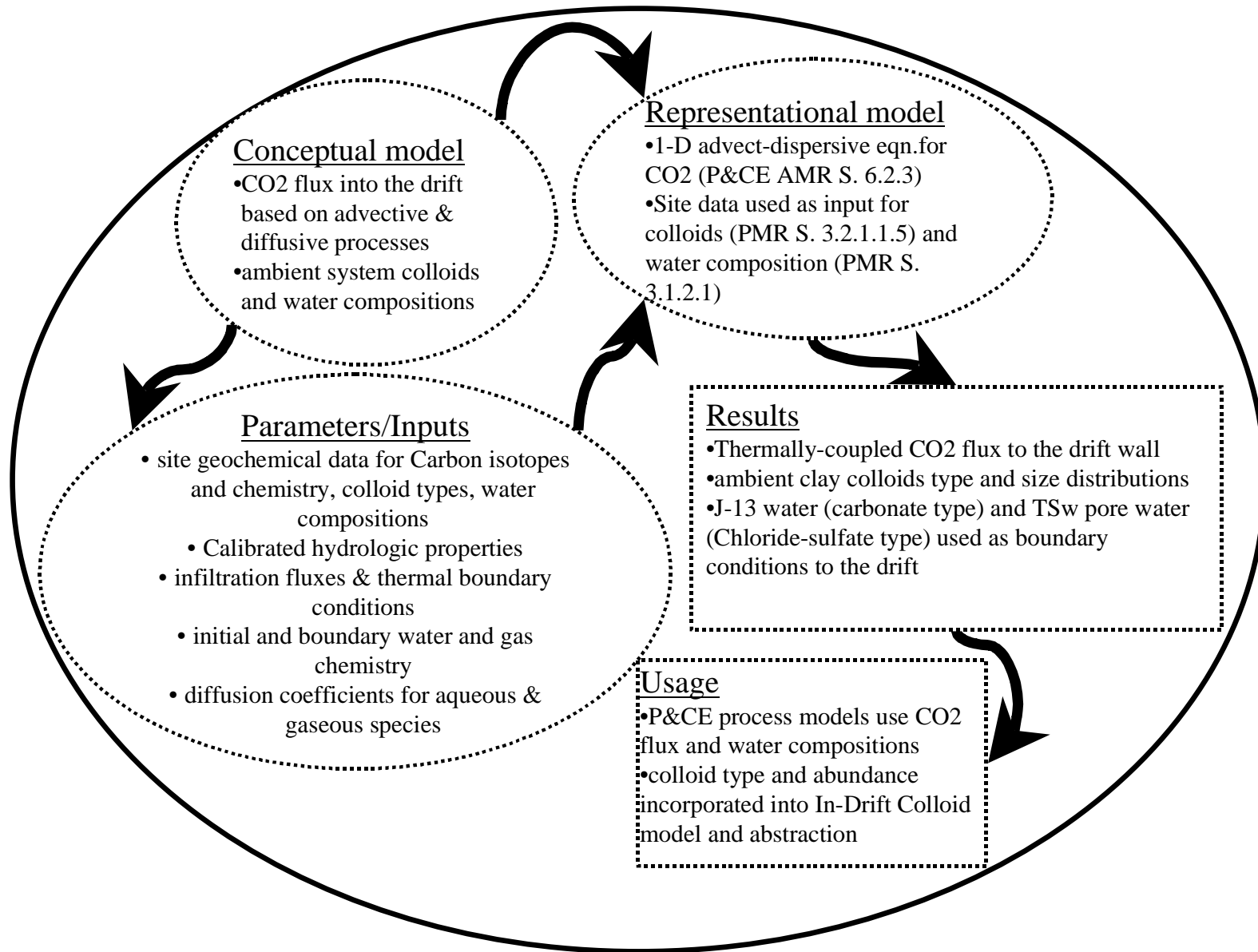


Figure 8-2: Engineered Barrier System PMR Model Structure – Flow Into Drift

in-drift materials. Bounding calculations of microbial abundance are used to screen-in microbial effects for waste package corrosion, but the quantitative results for microbial growth are not used directly. The primary results of the various in-drift chemistry models are:

- Screening arguments for chemical effects from degradation of backfill, invert, cement grout, ground support, and corrosion resistant alloys
- Bounding microbial growth conditions and abundance
- Brine compositions from low humidity (RH 50% to 85%) to high humidity (RH  $\geq$ 85%) as function of water/gas BC's, T, RH, seepage and evaporation rates
- Bounding functional relations for colloidal transport of radionuclides

Figure 8-3, Engineered Barrier System PMR Model Structure – In-Drift Chemistry/Chemical Processes, depicts the various elements that comprise the model for in-drift chemistry/chemical processes. However, the discussion below is limited to those models that have a direct or indirect affect on the models abstracted for TSPA-SR. For example, none of the in-drift seepage interaction models are discussed below, because they are only used for FEPS screening analysis.

While potential effects of microbially induced corrosion (MIC) are screened-in by the Microbial Communities AMR for localized corrosion, the potential effects of MIC are accounted for by adjusting the generalized corrosion rate in the *WP Degradation* (WAPDEG) AMR (ANL-EBS-PA-000001) and TSPA. The *General/Local Corrosion – Drip Shield* AMR (ANL-EBS-MD-000004, Section 6.0) also screens-in MIC. WAPDEG screens out localized corrosion on the Waste Package and Drip Shield, but assumes that the affect of MIC is conservatively bounded by randomly increasing the rate of generalized corrosion. The increased rate is determined by randomly sampling a uniform distribution between 1 and 2. This randomly increased factor for generalized corrosion is triggered by a threshold relative humidity of 90% or greater.

The conceptual model for the *Precipitates and Salts* AMR includes phases that are allowed to precipitate/dissolve reversibly and instantaneously (i.e., at equilibrium). Phases that are kinetically inhibited from forming are "suppressed" in the calculational model (i.e., they are not allowed to precipitate or dissolve). Chemical reactions are assumed to occur rapidly compared to anticipated seepage and evaporation rates. However, several slow-forming minerals are not allowed to precipitate. The assumption of equilibrium conditions will not affect the uncertainty in the model.

The EQ3nr and EQ6 computer codes from the EQ3/6 geochemical modeling package model are used in the *Precipitates and Salts* AMR to implement the model of evaporative concentration of potential in-drift solutions. The EQ3/6 implementation of the Pitzer model for electrolyte solutions is used to simulate solution chemistry and mineral precipitation/dissolution for relative humidity values above 85 percent. This Pitzer approach using the PT4 database constructed for the *Precipitates/Salts HRH Model* allows evaluation of solution-mineral equilibria and irreversible mass transfer to the high ionic strengths that may occur in an evaporating solution.

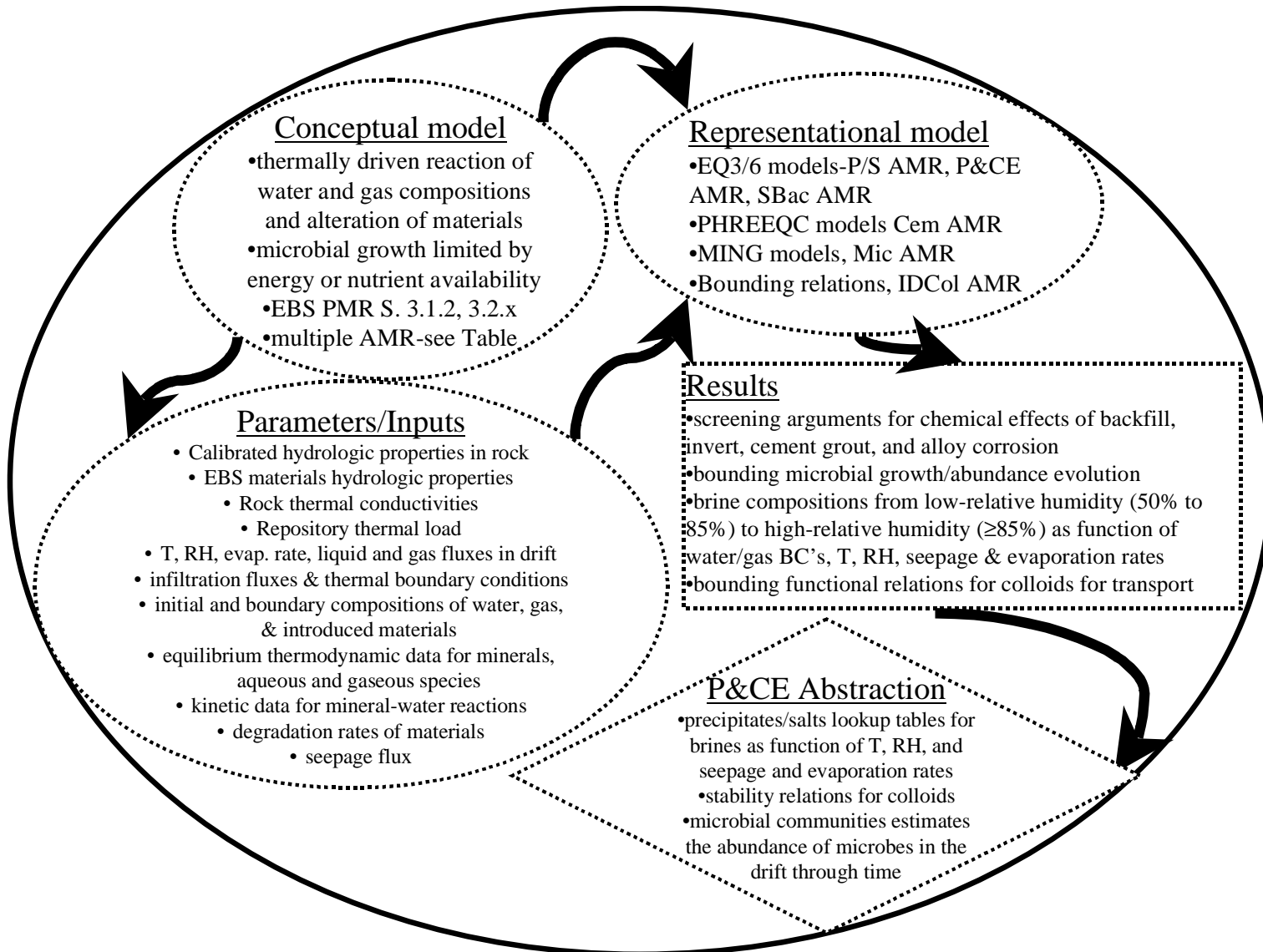


Figure 8-3: Engineered Barrier System PMR Model Structure – In-Drift Chemistry/Chemical Processes

The *Precipitates/Salts HRH Model* is used for the system  $\text{Na}^+$ ,  $\text{K}^+$ ,  $\text{Ca}^{2+}$ ,  $\text{Mg}^{2+}$ ,  $\text{Cl}^-$ ,  $\text{F}^-$ ,  $\text{CO}_3^{2-}$ ,  $\text{SO}_4^{2-}$ ,  $\text{NO}_3^-$ ,  $\text{SiO}_2$ ,  $\text{Fe}^{3+}$ ,  $\text{Al}^{3+}$ , and  $\text{H}_2\text{O}$  at temperatures ranging from 20°C to 95°C.

The results from the model consist primarily of brine compositions for low relative humidity (50% to 85%) to high relative humidity (85 to 100%) as a function of water and gas boundary conditions, temperature, relative humidity, seepage, and evaporation rates.

The results are used in TSPA in the form of lookup tables for brines that result from various boundary conditions for gas and liquid compositions and fluxes into the drift, for example as from the *Near-Field THC Abstraction AMR*. These lookup tables are used within the TSPA in conjunction with inputs for the thermohydrologic environment in the drift. The primary input parameters are from the *Multiscale TH Abstraction AMR*, including temperature, relative humidity, evaporation rate, and liquid and gas fluxes in-drift.

### C. In-Drift Physical/Degradation Processes

The model for drift degradation processes in the EBS PMR is limited to the key-block analysis which is used to develop the screening argument to eliminate rock fall induced failure of the drip shield and waste package within the first 10,000 years. The models of drip shield, waste package, and waste form degradation are developed in other PMRs (Waste Form and Waste Package). The waste pallet is assumed to have failed, with the waste package sitting directly on the invert in the *Radionuclide Transport Abstraction AMR*. The primary model results are:

- Rock fall size, distribution, and frequency for post-closure timeframe with thermal and seismic effects

Figure 8-4, Engineered Barrier System PMR Model Structure – In-Drift Physical/Degradation Processes, depicts the various elements that comprise the model for in-drift physical/degradation processes. The model for rock fall and drift degradation is discussed below even though it does not result in any specific TSPA models. The failure of the waste package pallet is not actually modeled, but it is assumed in the *Radionuclide Transport Abstraction AMR*, so it is not discussed below.

Key blocks determined by the fracture sets and patterns in the drifts are identified, and drift shape changes, thermal-mechanical effects, and seismic effects are taken into account to determine potential key block size distributions and failure probabilities during the first 10,000 years. The maximum block sizes are then compared in the WP AMRs to waste package and drip shield designs to screen out failure due to rock fall. Geometric limitations of potential block size and shape are taken into consideration in the screening process, since the largest blocks would fall on multiple drip shields, thus limiting the size that affects one drip shield.

Field data on fallen rock blocks, and mapping of joint sets in the ESF, joint geometrical data, joint frictional properties data, and rock thermal and mechanical property data are all utilized in the analysis. Thermal transients from the *Multiscale TH Model AMR* and seismic data from the *Disruptive Events Model AMR* are also used.

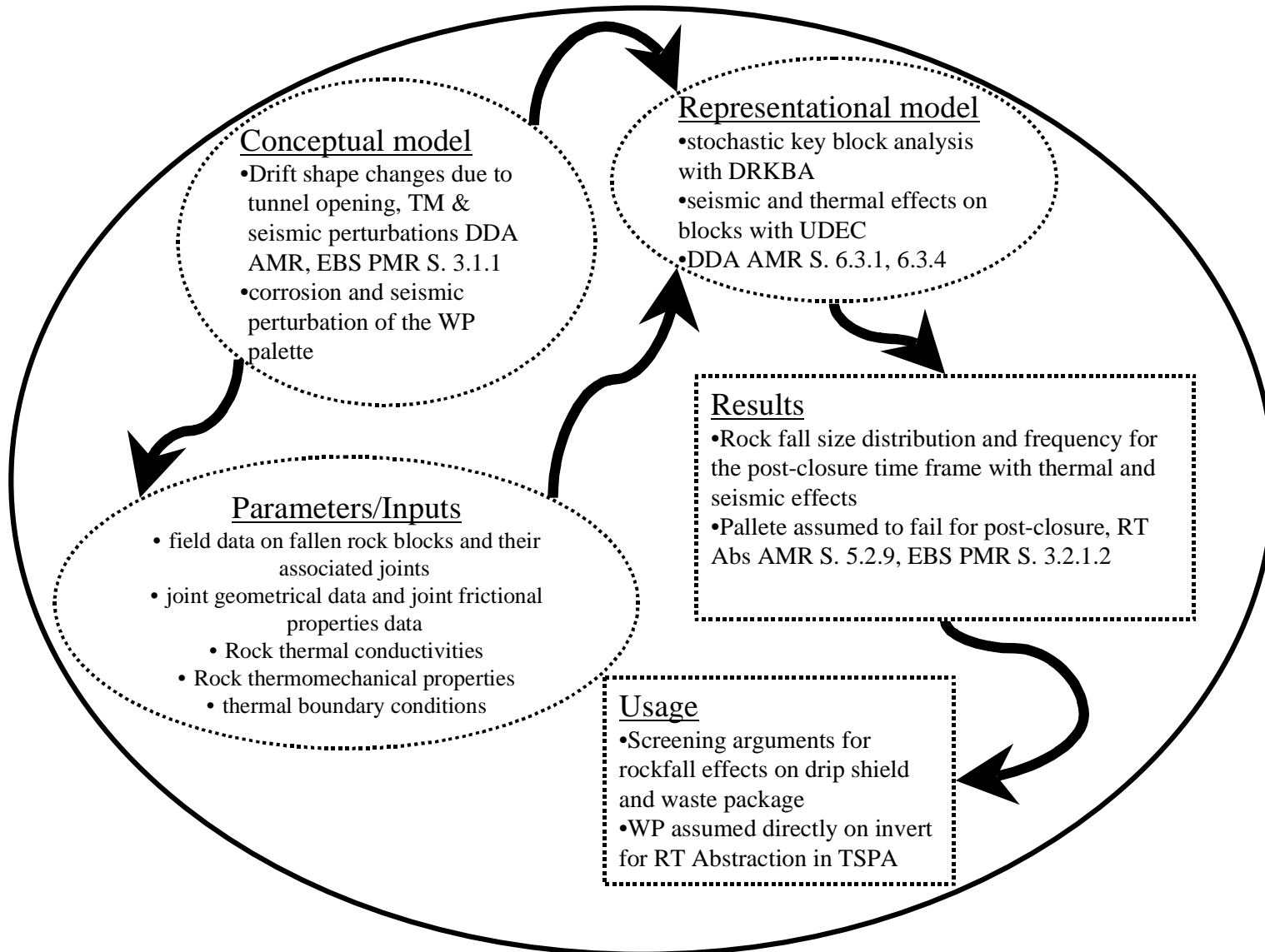


Figure 8-4: Engineered Barrier System PMR Model Structure – In-Drift Physical/Degradation Processes

As described in the Section 6.3.1 of the *Drift Degradation* AMR, the Discrete Region Key Block Analysis (DRKBA) software employs a bipolar Watson distribution for joint orientation data. The principal axis orientation and a concentration factor  $k$  are the required inputs for the bipolar Watson distribution. The concentration factor  $k$  is an index of the concentration. The larger the value of  $k$ , the more the distribution is concentrated towards the principal axis orientation. Joints are represented as circular discs in the DRKBA analysis. Joint radii, spacing, and positioning are simulated with Beta distributions. The Beta distribution is a four-parameter distribution with the parameters  $a$ ,  $b$ ,  $p$ , and  $q$ . The parameters  $a$  and  $b$  represent the ends of the closed interval upon which the Beta distribution is defined. The parameters  $p$  and  $q$  determine the shape of the distribution curve, their values were calculated from the mean and standard deviation of the transformed data. The transformed data were obtained by normalizing the data with the maximum value. The cohesion and friction angle of the joints are simulated as a bivariate normal distribution. Inputs for the mean and standard deviation of the joint strength parameters are required.

A stochastic key block analysis was performed using the DRKBA computer code. The DRKBA code is commercially available software that was purchased after a literature search determined that it was an appropriate tool for this application. The DRKBA probabilistic approach assesses the maximum size of key blocks, and also predicts the number of potential key blocks that will be formed within a referenced length of tunnel. The DRKBA approach also allows for a variety of tunnel and jointing configurations.

The software simulates structural discontinuities as circular discs placed in the rock mass according to probabilistic distributions determined from tunnel mapping data. Joint planes are simulated by a Monte Carlo technique from probability distributions representing the orientation, spacing, and trace length of the corresponding joint set. DRKBA then analyzes these blocks to determine whether they are geometrically feasible and to determine whether they are mechanically stable.

For each of four lithologic units (Ttptul, Ttptmn, Ttptll, and Ttptln) that the emplacement drifts and performance confirmation drifts will occupy, the analysis evaluated the cumulative frequencies of occurrence corresponding to 50, 75, 90, 95 and 98 percentile block volume. The Rock fall size distribution and frequency for the 10,000-year post-closure time frame are provided for screening of waste package and drip shield based on design data.

The models for rock fall and drift degradation are used for screening arguments to screen-out rock fall causing waste package and drip shield failure in the first 10,000 years.

#### **D. Thermal/Hydrologic Processes**

The model for thermal and hydrologic processes consists of a ventilation system model, and a thermal/hydrologic analysis model. The ventilation system model is used to calculate transient ventilation system heat removal effectiveness during preclosure. The model provides an analysis to confirm that the 70% preclosure heat removal efficiency of the ventilation system assumed in other TH models for TSPA is feasible. The MSTHM provides one of the primary outputs from the EBS PMR to other PMRs and AMR models and to TSPA.

- Pre-closure ventilation system temperature transients and heat removal effectiveness

- Mountain scale and DS models of postclosure thermal transients that provide transient temperature, relative humidity, evaporation rate in the invert, and gas and liquid fluxes in the drift

Figure 8-5, Engineered Barrier System PMR Model Structure – Thermal/Hydrologic Processes, depicts the various elements that comprise the model for thermal/hydrologic processes.

Uncertainty treatment in the *Ventilation* AMR is not critical, since the AMR was only used to show that a range of design options existed that could achieve the 70% pre-closure heat removal assumed by other TH models for TSPA. Therefore that model is not discussed in detail. While the *MSTHM* and *Abstraction Model* AMRs provide key inputs for TSPA and inputs for other AMRs, this model was discussed extensively in the NFE models chapter with respect to development of percolation flux. Therefore, the reader is referred to the discussion in the NFE models chapter, and the discussion below is limited to evaluation of in-drift models.

The purpose of the MSTHM is to describe the thermal/hydrologic evolution of the NFE and EBS throughout the repository for a particular design. The basic conceptual model for this is that as the rock heats, a thermal gradient will develop driving the water in the system to evaporate (potentially by boiling), migrate as vapor down the temperature gradient, and condense potentially flowing through fractures back toward the drifts and/or between the drifts. These processes are driven by the thermal input (load) from the potential repository and result in changes to the matrix and fracture saturation, percolation flux rate, distribution of water in the host rock, and thermodynamic conditions within the drift.

The process-level MSTH Model provides TH information (such as fracture percolation flux and saturation, in-drift temperature, relative humidity, liquid saturation in porous media matrix, etc.) for use in this and other technical products. These data are provided for numerous locations throughout the entire repository region as a function of time.

To address the repository and mountain scale variability while maintaining computational efficiency, the MSTHM couples the following submodels: the SDT model; LDTH; DDT model; and SMT model. The conduction-only models are developed to capture the local heterogeneity of the design thermal load and the continuous mountain-scale heterogeneity in terms of heat transfer at this large scale. The LDTH model is developed at over 30 specific locations to capture the repository-scale heterogeneity in thermohydrology. The thermal variability constrained in these various models is then layered onto the LDTH results to produce an integrated picture of the thermal/hydrologic response of the system at over 600 locations in the potential repository. This is done such that the integrated model results for the flow of water and water vapor through partially-saturated fractured rock and the effects on the thermodynamic environment within the drifts reflect the variability in waste package heat outputs and mountain-scale lithologic variability. Thus, the MSTHM accounts for 3D DS and mountain-scale heat flow, repository-scale variability of stratigraphy and infiltration flux, and WP-to-WP variability in heat output from WPs. All these MSTHM submodels use the NUFT code for their implementation.

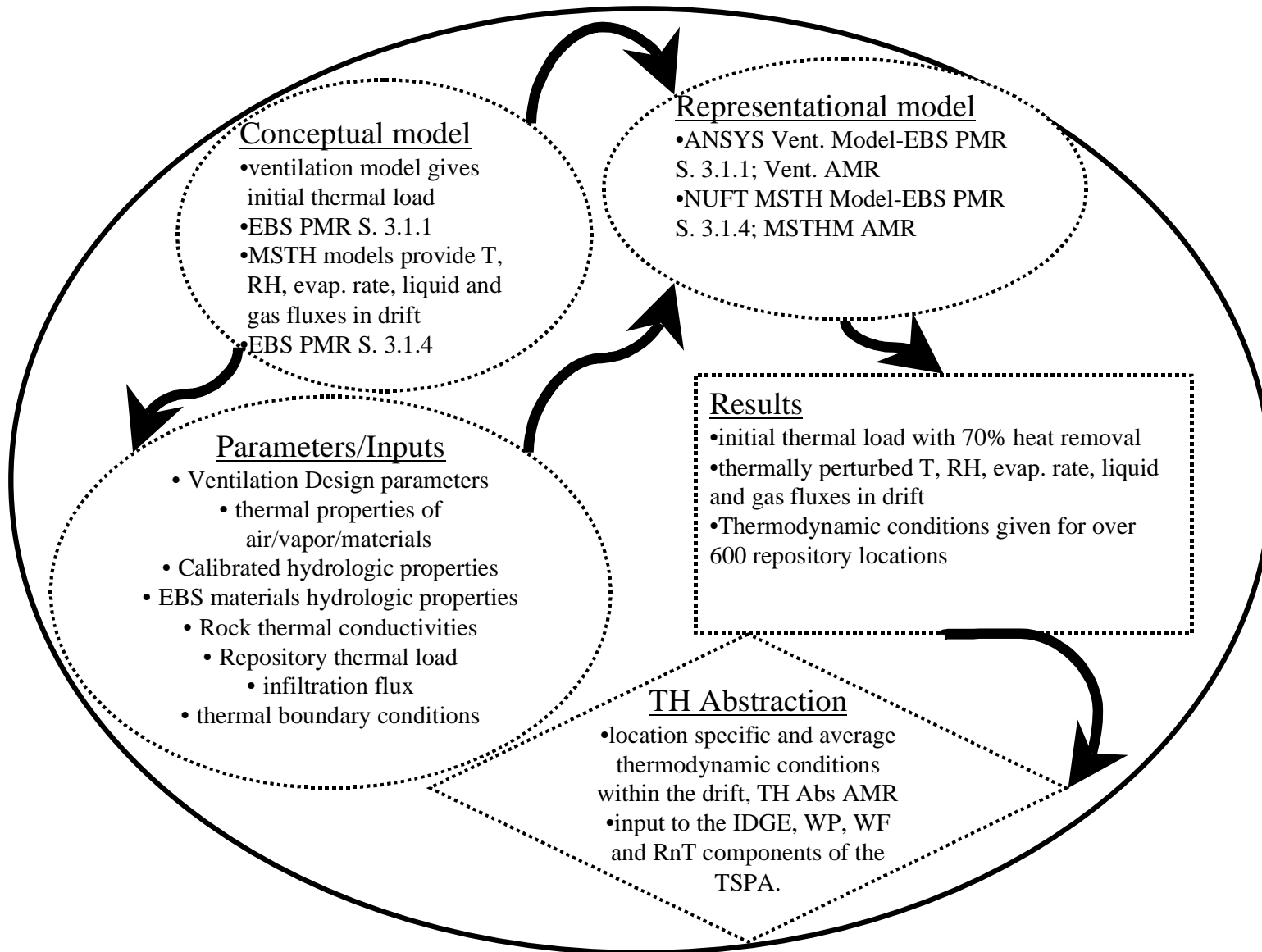


Figure 8-5: Engineered Barrier System PMR Model Structure – Thermal/Hydrologic Processes

## E. Radionuclide Transport

The model for EBS transport processes includes models to calculate movement of both dissolved and colloiddally attached radionuclides through the invert after they have left the waste package. Radionuclide source terms are provided to TSPA from the waste package and waste form PMRs, and the transport models for movement from the drift to the UZ come from EBS transport process models. The water diversion and removal models do not appear to be directly used in TSPA. However, the abstraction of the invert diffusion and transport models provides key inputs to TSPA. These models include:

- Water diversion by the drip shield and invert
- Water drainage from the invert with and without fracture plugging
- Onset conditions for condensation under the drip shield
- Invert diffusion coefficient as a function of invert water content
- 1D advective-dispersive-diffusive transport equations through the invert at high and low invert flow rates

Figure 8-6, Engineered Barrier System PMR Model Structure – EBS Transport Processes, depicts the various elements that comprise the model for EBS radionuclide transport processes. Many details of EBS flow and transport have substantial uncertainty, particularly when complex processes are represented as a one-dimensional abstraction. The EBS *Radionuclide Transport Abstraction* AMR used bounding approximations when substantial uncertainties were thought to exist. As stated in Section 7 of the EBS *Radionuclide Abstraction* AMR, areas where bounding assumptions were used included:

- Seepage through the DS always falls on a WP.
- Seepage is assumed to uniformly wet the DS and WP.
- Diffusive transport is maximized because transport is always possible through SCCs and because the WP is in contact with the invert.
- Release of radionuclides through advective transport is independent of the location of breaches on the WP.
- Evaporation within and on the WP is ignored.
- Bounding value for diffusion coefficient. The effect of porosity and liquid saturation on the free water diffusion coefficient was included in a conservative manner (thus enhancing diffusion).

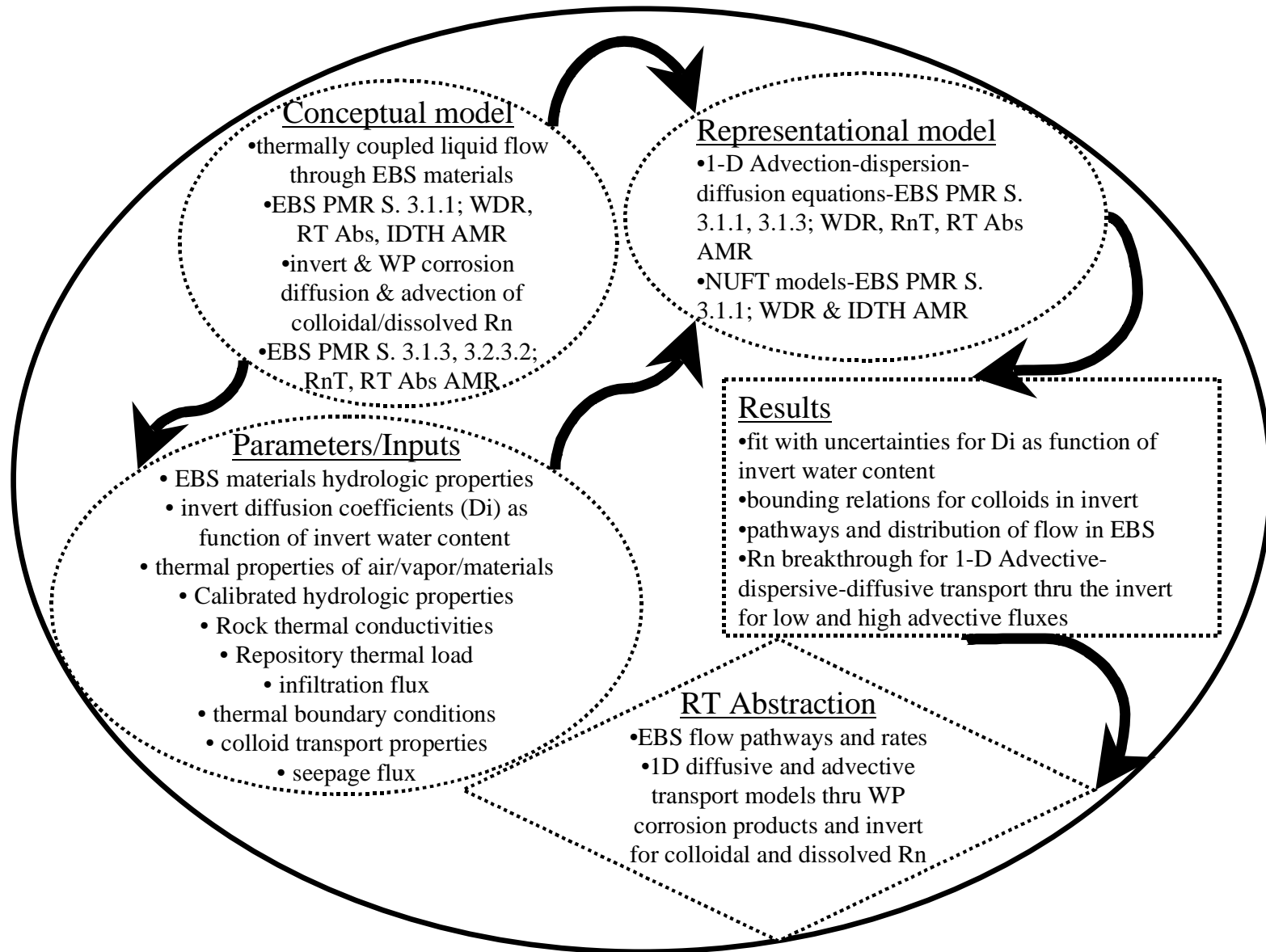


Figure 8-6: Engineered Barrier System PMR Model Structure – EBS Transport Processes

The flow paths are time dependent, in the sense that DS gaps, DS penetrations, and WP penetrations will vary with time and local conditions in the repository. For example, at very early times there may be no penetrations through the DS, so fluid can reach the WP only if evaporation from the invert and condensation on the DS is active. The conceptual model for flow through the EBS also includes two mixing cells: one for the WP (and internals) and a second for the invert. The two mixing cells are conceptualized to have a cylindrical, concentric one-dimensional geometry for volume calculations. The first cell has a diameter given by the diameter of the WP. The second cell (invert) wraps around the lower half of the WP and is 0.606 meters thick. This is the maximum thickness of the invert directly beneath the WP. This value was chosen because flow out of the WP is primarily vertically downward, centered over the thickest part of the invert.

While the EBS *Radionuclide Transport Abstraction* AMR treats uncertainty with conservative bounds for many assumptions, it does assume representative values for a number of parameters and does perform sensitivity analyses over a range of values for these parameters (see AMR Table 3-42). The parameters treated in this manner include:

- Flowpath length (m)
- Volumetric water content
- Porewater velocity (m/yr)
- Liquid water flux (m/yr)
- Porosity
- Dispersivity (m<sup>2</sup>/yr)
- Molecular diffusion coefficient (m<sup>2</sup>/yr)
- Grain density (g/cm<sup>3</sup>)
- Partition coefficient (cm<sup>3</sup>/g)

It also treats invert diffusion with a more extensive analysis. The *Invert Diffusion* AMR used a large experimental data set (125 test samples) of varying granular material types, and fit an empirical correlation to the data. It then determined upper and lower 95% confidence bands. For validation it plotted an alternative conceptual model using Archie's Law and noted that the model results using Archie's Law fell within the 95% confidence bands of the original empirical fit. The EBS *Radionuclide Transport Abstraction* AMR uses the 95% confidence band to treat uncertainty in the invert diffusion adjusted for porosity and invert saturation. It also uses a distribution function covering the confidence band.

In the 1D advective-dispersive-diffusive model analysis uncertainty in flow rates is treated by considering both low and high advective fluxes. The EBS *Radionuclide Transport Abstraction* AMR also performed a sensitivity and uncertainty analysis on the one-dimensional solute transport equation, as summarized in Table 3-43 of the AMR.

There are two new water diversion models in Rev. 01 of the *Water Diversion and Removal* AMR that may be used in the next revision of TSPA—flow through crevices in the waste package and drip shield, and flow on the outside of the drip shield and waste package in thin films adsorbed on their surfaces. Rev. 00 ICN 01 of the EBS *Radionuclide Abstraction* AMR (ANL-WIS-PA-000001)

**Table 8-1**  
**Models Associated with the *EBS Degradation, Flow and Transport* PMR**

<b>Models</b>	<b>Sub-Models</b>	<b>Conceptual Models</b>	<b>Parameters/Inputs</b>	<b>Associated AMRs</b>	<b>PMR Section</b>
Flow into the Drifts	Gas	Gas flow, Gas chemistry	CO <sub>2</sub> gas flux, and 1-D ambient diffusion/dispersion coefficient	P&CE AMR - E0100 (Section 6.2.3)	3.1.2.2
	Liquid	Seepage flow and water chemistry	Seepage flow as a fraction of percolation flux; Assumed J-13 and pore water chemistries	P&CE AMR - E0100 (TH Model - Section 6.1)	3.1.2.1
	Solid (Colloids)	Colloid formation in the rock	Colloid types (primarily clays), Size distributions	In-Drift Colloids (IDCol AMR)- E0045	3.2.1.1.5
In-Drift Chemistry/ Chemical Processes	Gas	In-Drift Gas	O <sub>2</sub> , CO <sub>2</sub> , H <sub>2</sub> O Gas flux, & composition; Diffusion/dispersion coeff for CO <sub>2</sub>	In-Drift Gas (IDG AMR) - E0035, P&CE AMR - E0100, P&CE Abstraction - E0010	3.2.1.1.1 3.1.2 3.2.3.1
	Liquid	Seepage - Cement	Diffusion of CO <sub>2</sub> in the rock; Carbonation of the rockbolt grout	Seepage - Cement – (Cem. AMR) E0055, P&CE AMR - E0100, P&CE Abstraction - E0010	3.2.1.1.2 3.1.2 3.2.3.1
		Seepage - Backfill (not used for SR)	Water-quartz interaction model; potential for backfill plugging	Seepage - Backfill – (SBac AMR) E0030, P&CE AMR - E0100, P&CE Abstraction - E0010	3.1.2.3 3.1.2 3.2.3.1
		Seepage - Invert	Flow pathways; rationale for screening out seepage-invert interactions	Seepage - Invert (SI AMR) - E0060, P&CE AMR - E0100, P&CE Abstraction - E0010	3.2.1.1.2 3.1.2 3.2.3.1
	Solid	In-Drift Colloids	Colloid types: smectite, iron oxide & clays, colloid stability/concentration relations and Size distributions	In-Drift Colloids - E0045, P&CE AMR - E0100, P&CE Abstraction - E0010	3.2.1.1.5 3.1.2 3.2.3.1
		Microbial Communities	Quantity of microbes, Temperature range & RH for biotic activity	Microbial Communities (Mic AMR) E0040 P&CE AMR - E0100, P&CE Abstraction - E0010	3.2.1.1.3 3.1.2 3.2.3.1
		Precipitates/Salts Formation	pH, chloride concentration and ionic strength vs temp, RH, Pco <sub>2</sub> , and evaporative concentration	Precipitates/Salts – (P/S AMR) E0105, P&CE AMR - E0100, P&CE Abstraction - E0010	3.2.1.1.4 3.1.2 3.2.3.1
		In-Drift Corrosion	Inventory of different corrosion products	In-Drift Corrosion Products (CorP AMR)- E0020, P&CE AMR - E0100, P&CE Abstraction - E0010	3.1.2.3 3.1.2 3.2.3.1

**Table 8-1 (Continued)**  
**Models Associated with the *EBS Degradation, Flow and Transport* PMR**

<b>Models</b>	<b>Sub-Models</b>	<b>Conceptual Models</b>	<b>Parameters/Inputs</b>	<b>Associated AMRs</b>	<b>PMR Section</b>
In-Drift Physical Processes/ Degradation	Ground Control	Drift Degradation of tunnel opening; thermal-mechanical (TM) and seismic perturbations	Rock fall size distribution and frequency	Drift Degradation Anal (DDA AMR) E0080, P&CE AMR - E0100, P&CE Abstraction – (PCE Abs AMR) E0010	3.1.1
	WP Support Pallet	WP Support failure	No credit in TSPA - assumed to fail (WP assumed to sit on the invert)	Radionuclide Transport Abstraction (RT Abs AMR) - E0095 (Section 5.2.9)	3.2.1.2
	Invert	Invert Degradation	No model developed - excluded on the basis of low consequences in FEPS AMR (FEP 2.1.06.05.00)	EBS FEPS AMR (FEP AMR) - E0110 (Section 6.2.27)	-----
Thermal/ Hydrologic Processes	Ventilation Heat Removal	ANSYS Model	Percent preclosure heat removal	Ventilation (Vent AMR) E0075	3.1.1
	Temperature/ Humidity Transients	Thermal-hydrologic flow model (NUFT Model)	Temp & RH transients for drift wall, drip shield, WP, and invert	Multiscale TH Model (MSTH AMR) E0120	3.1.4
		Thermal-hydrologic flow model abstraction for TSPA	Probabilistic data for temp & RH for drift wall, drip shield, WP, and liquid flux in host rock & invert	Near Field Env. TH Abstract. (TH Abs AMR) E0130	3.2.2.3

**Table 8-1 (Continued)**  
**Models Associated with the *EBS Degradation, Flow and Transport* PMR**

<b>Models</b>	<b>Sub-Models</b>	<b>Conceptual Models</b>	<b>Parameters/Inputs</b>	<b>Associated AMRs</b>	<b>PMR Section</b>
Radionuclide Transport	Advection/ Flow	Water Drainage	Drainage not modeled - assumed	Water Drainage (Drn AMR)- E0070, Water Dist. & Removal (WDR AMR) -E0090	3.1.1
		Water Diversion	Water flow thru drip shield failures versus RH	Water Diversion (WDiv AMR) - E0085, Water Dist. & Removal (WDR AMR) -E0090	3.1.1
		Condensation	Onset conditions for condensation under drip shield	In-Drift THC Model (IDTH AMR) E0065	3.1.1
	Diffusive Transport	Invert Diffusion	Diffusion coefficient vs water content (based on percent saturation and porosity)	Invert Diffusion (InvD AMR) E0000	3.1.3
	Radionuclide Transport	Colloidal Transport	Primarily advective transport of irreversibly and reversibly attached radionuclides on WF colloids, and reversibly attached colloids on iron oxide and natural colloids; Stability of colloids in the invert	Radionuclide Transport Abstraction AMR -(RT Abs AMR) E0095	3.2.1.2
		Dissolved Radionuclides	1-D Advection / dispersion / diffusion transport for breakthrough time thru the invert (Not used)	Radionuclide Transport AMR (RnT AMR)- E0050	3.1.3 3.2.3.2
			<u>From WP to Invert</u> : Diffusion through SCCs; Diffusion and advection through patches; Diffusion and advection through pits (if present) <u>From Invert to UZ</u> : 1-D Diffusion and advection through the invert	Radionuclide Transport Abstraction AMR -(RT Abs AMR) E0095	3.1.3 3.2.3.2

**Table 8-2**  
**AMR Document Identifiers and Shorthand Notation Crosswalk**

<b>Title</b>	<b>AMR#</b>	<b>AMR ID</b>	<b>Document Control ID</b>	<b>Rev</b>	<b>ICN</b>
EBS Degradation, Flow and Transport PMR	N/A	EBS PMR	TDR-EBS-MD-000006	00	01
AMR (Invert Diffusion Properties Model)	E0000	InvD	ANL-EBS-MD-000031	01	
AMR (Physical & Chem. Environ. Abstraction Model)	E0010	PCE Abs	ANL-EBS-MD-000046	00	
AMR (EBS FEPs Degradation.Modes Analysis)	E0015	Deg	ANL-EBS-MD-000035	00	
AMR (Corrosion Products)	E0020	CorP	ANL-EBS-MD-000041	00	
AMR (Seepage/Backfill Interaction)	E0030	Sbac	ANL-EBS-MD-000039	00	
AMR (In-Drift Gas Flux & Composition)	E0035	IDG	ANL-EBS-MD-000040	00	
AMR (Microbial Communities)	E0040	Mic	ANL-EBS-MD-000038	00	
AMR (In-Drift Colloids and Concentration)	E0045	IDCol	ANL-EBS-MD-000042	00	
AMR (EBS Radionuclide Transport Model)	E0050	RnT	ANL-EBS-MD-000034	00	01
AMR (Seepage/Cement Interaction)	E0055	Cem	ANL-EBS-MD-000043	00	
AMR (Seepage/Invert Interaction)	E0060	SI	ANL-EBS-MD-000044	00	
AMR (In-Drift THC Analysis)	E0065	IDTH	ANL-EBS-MD-000026	00	01
AMR (Water Drainage Model)	E0070	Drn	ANL-EBS-MD-000029	00	
AMR (Ventilation Model)	E0075	Vent	ANL-EBS-MD-000030	00	
AMR (Drift Degradation Analysis)	E0080	DDA	ANL-EBS-MD-000027	00	
AMR (Water Diversion Model)	E0085	Wdiv	ANL-EBS-MD-000028	00	
AMR (Water Distribution and Removal Model)	E0090	WDR	ANL-EBS-MD-000032	00	01
AMR (EBS Radionuclide Transport Abstraction)	E0095	RT Abs	ANL-WIS-PA-000001	00	01
AMR (Physical & Chemical Environment Process Model)	E0100	PCE	ANL-EBS-MD-000033	00	01
AMR (Precipitates / Salts Analysis)	E0105	P/S	ANL-EBS-MD-000045	00	
AMR (EBS Degradation Modes & FEPs Abstraction)	E0110	FEP	ANL-WIS-PA-000002	00	
AMR (Multiscale Thermal/Hydrologic Model)	E0120	MSTH	ANL-EBS-MD-000049	00	
AMR (Abstraction of NFE Thermodynamic Environment and Percolation Flux)	E0130	TH Abs	ANL-EBS-HS-000003	00	
AMR (EBS Features, Events, and Processes) (*Note: the title changed in Rev 01, and AMRs E0015 and E0110 Rev. 00 were combined into Rev. 01)	E0110	FEPS	ANL-WIS-PA-000002	01	

INTENTIONALLY LEFT BLANK

## 9.0 General and Localized Corrosion

### 9.1 Purpose of the Model

General and localized corrosion are potential corrosion modes that can result in penetration of the WP outer barrier. The purpose of the general and localized corrosion model is to evaluate the potential for such corrosion modes to affect the performance of the drip shield (Ti Grade 7) and WP outer barrier (Alloy 22) and to develop models for inclusion into the WAPDEG model.

General and localized corrosion (including such effects as aging, phase stability, and microbiologically influenced corrosion) has been studied for many years for many different types of metals. As such, the modeling approaches used are considered standard and relevant parameters can be obtained from standard corrosion experiments. However, for some parameters, the availability of data specific to the environment within the Yucca Mountain repository is limited and conservative input parameters have been selected (conservative is defined as resulting in poorer than anticipated WP performance).

### 9.2 Model Component Relations

Details of the mechanisms and models for general and localized corrosion are documented in the WAPDEG PMR (TDR-WIS-MD-000002 REV 00 ICN 01), one calculation, and the following AMRs:

- *Aging and Phase Stability of Waste Package Outer Barrier*, (ANL-EBS-MD-000002) – Details the effects of thermal aging and phase stability of the WP outer barrier material (Alloy 22).
- *Environment on the Surface of the Drip Shield and Waste Package Outer Barrier* (ANL-EBS-MD-000001) – Specifies the environments on the surface of the drip shield and WP outer barrier that are consistent with the relevant environmental conditions of the repository.
- *General Corrosion and Localized Corrosion of Waste Package Outer Barrier* (ANL-EBS-MD-000003) – Develops models for both general and localized corrosion of the WP outer barrier (Alloy 22).
- *General Corrosion and Localized Corrosion of the Drip Shield* (ANL-EBS-MD-000004) – Develops models for both general and localized corrosion of the drip shield (titanium grade 7).
- *Degradation of Stainless Steel Structural Material* (ANL-EBS-MD-000007) – Accounts for both general and localized corrosion of the WP structural support material (316NG stainless steel).
- *Calculation of General Corrosion Rate of Drip Shield and Waste Package Outer Barrier to Support WAPDEG Analyses* (CAL-EBS-PA-000002) – Produces cumulative distribution

functions representing the general corrosion rate distributions for the drip shield (titanium grade 7) and the WP outer barrier (Alloy 22).

- *Abstraction of Models for Pitting and Crevice Corrosion of Drip Shield and Waste Package Outer Barrier* (ANL-EBS-PA-000003) – Reviews and analyzes information from process-level models relevant to pitting and crevice corrosion of the drip shield and WP outer barrier in order to develop abstracted models for inclusion in the WAPDEG WP performance model.
- *Abstraction of Models for Stainless Steel Structural Material Degradation* (ANL-EBS-PA-000005) – Reviews and analyzes information from process-level models relevant to general, pitting, and crevice corrosion of the stainless steel structural material in order to develop abstracted models for inclusion in the WAPDEG WP performance model.

Figure 9-1, General and Localized Corrosion Model AMR Relations, illustrates the relationship of the general and localized corrosion AMRs within the entire set of WAPDEG AMRs.

Although analyses were developed regarding the stainless steel WP inner barrier, a later decision was made to not take credit for this barrier in modeling the overall performance of the WP.

Although the stainless steel barrier will provide some performance benefit, it is not intended to be a corrosion barrier, but rather to provide structural support. As such, the discussion in this report focuses on the drip shield and WP outer barrier.

### **9.3 General and Localized Corrosion Model Structure**

Figure 9-2, General and Localized Corrosion Model Structure, depicts the various elements that comprise the general and localized corrosion model. The relationships of the elements of the conceptual model, the model parameters, and the modeling results are indicated in the figure. Figure 9-2 includes the TSPA abstraction of results as the end product of the model development in the AMRs.

#### **A. Conceptual Model**

The performance of the WP outer barrier is affected by the following potentially important degradation processes:

- General corrosion
- Localized (pitting and crevice) corrosion
- Microbiologically influenced corrosion
- Long-term aging and phase instability of WP outer barrier and their effect on corrosion

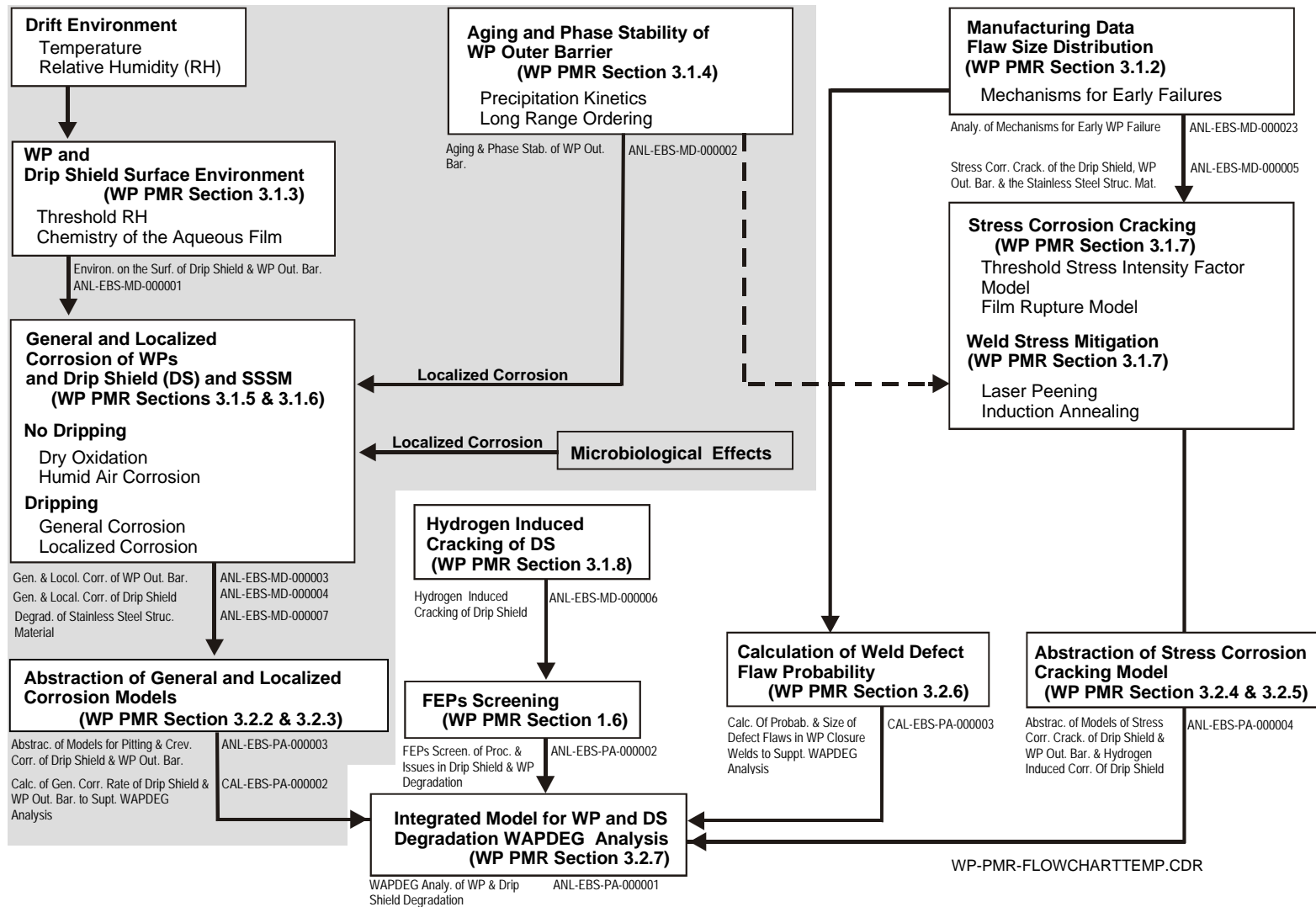


Figure 9-1: General and Localized Corrosion Model AMR Relations

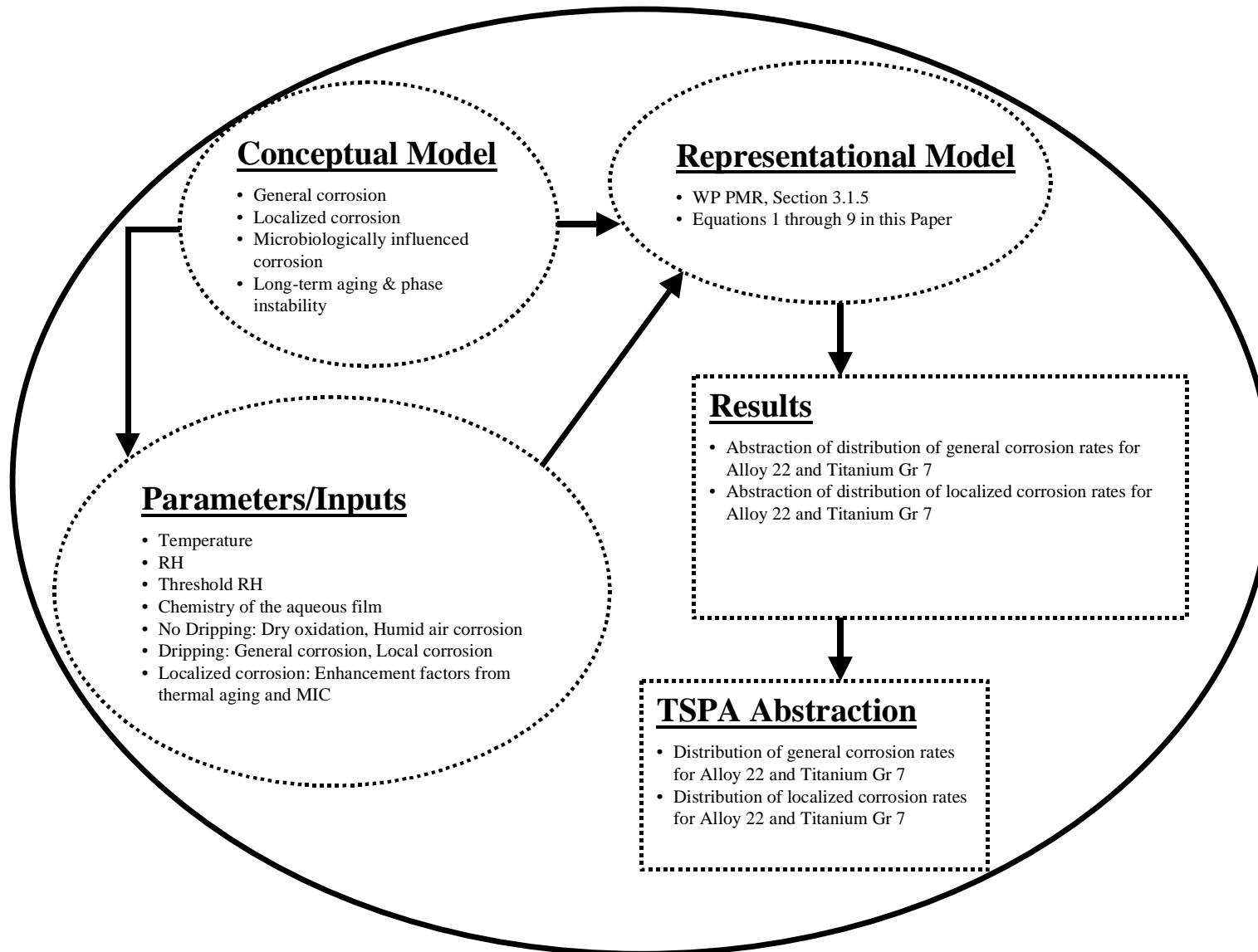


Figure 9-2: General and Localized Corrosion Model Structure

## General Corrosion

Conceptual models for general corrosion of the drip shield and WP outer barrier are discussed in the *General Corrosion and Localized Corrosion of the Drip Shield* and *General Corrosion and Localized Corrosion of Waste Package Outer Barrier* AMRs, respectively. General corrosion is manifested by the relatively uniform thinning of materials without significant localized corrosion. Depending on the local environment, the mode of general corrosion differs. The repository environment will result in three different general corrosion modes. These are dry oxidation, humid-air corrosion, and aqueous phase corrosion.

### Dry Oxidation

Dry oxidation (dry air corrosion) occurs at any RH below the threshold for humid air corrosion:

$$RH < RH_{critical} \quad (1)$$

This process results in the formation of an adherent, protective oxide film of uniform thickness. The rate of dry air corrosion may be limited by the rate of mass transport through the growing metal oxide film. In such cases, the oxide thickness is expected to obey a parabolic growth law (film thickness proportional to the square root of time). The parabolic growth law is derived from Fick's law and then from relating oxide growth to molar flux of the reacting species. This scenario has been adopted for Alloy 22 due to the availability of data at elevated temperature to support such a model. Reasonable values of the parabolic rate constant are discussed below. It must be noted that a logarithmic law may be more applicable at lower temperatures. However, there is insufficient data to support such a model for Alloy 22 and 316NG. There is sufficient data to support the application of a logarithmic law to the dry air corrosion of titanium.

The conceptual approach for dry oxidation of Alloy 22 is given mathematically below, where  $x$  is the oxide thickness,  $x_o$  is the initial oxide thickness,  $k$  is a temperature-dependent rate constant, and  $t$  is time (the parabolic growth law):

$$x = \sqrt{x_o^2 + k \times t} \quad (2)$$

The conceptual approach for dry oxidation rate of titanium grade 7 is given mathematically by the equation below:

$$\frac{dX}{dt} = ke^{-kt} \quad k = k_o e^{-E_a / RT} \quad (3)$$

where:  $X$  = the oxide thickness  
 $k$  = rate constant  
 $E_a$  = activation energy  
 $R$  = universal gas constant  
 $T$  = absolute temperature

The parabolic growth law predicts continuous growth of the oxide, which is much more conservative than a logarithmic growth law. Since such conservative estimates of the rate of dry oxidation do not appear to be life limiting and since reliable data for determining the maximum oxide thickness for Alloy 22 do not appear to be available, the parabolic growth law will be used for the WP outer barrier.

The dry oxidation model presented here assumes uniform oxidation of the WP outer barrier surface. An alternative conceptual model would include the possibility of preferential dry oxidation along grain boundaries in Alloy 22 and should be considered. Such preferential attack would ultimately be diffusion controlled, with the diffusion path being equivalent to the length of the oxidized grain boundary.

### **Humid Air Corrosion**

Humid air corrosion is assumed to occur above a threshold RH, provided that there are no impinging drips:

$$RH \geq RH_{critical} \quad (4)$$

The threshold RH for humid air corrosion ( $RH_{critical}$ ) is determined experimentally (discussed later in this report). Note that “threshold RH” and “critical RH” are synonymous terms. The existence of this threshold is due to the relationship between water adsorption and RH.

It was conservatively assumed that the rate of humid air corrosion is represented by the same corrosion rate distribution used for aqueous phase corrosion during the period where humid air corrosion is operable. It was further conservatively assumed that the corrosion rate is constant and does not decrease with time.

### **Aqueous Phase Corrosion**

At a given temperature, the existence of liquid-phase water on the surface of the WP depends upon the presence of a salt deposit. In the presence of such a deposit, a thin-film liquid phase can be established at a higher temperature than otherwise possible. In the model discussed here, it is assumed that two conditions must be met for aqueous phase corrosion: RH above the deliquescence point of the deposit at the temperature of the WP surface and drips impinging on the WP surface. The threshold RH for aqueous phase corrosion is identical to that for humid air corrosion:

$$RH \geq RH_{critical} \quad (5)$$

This threshold RH for aqueous phase corrosion ( $RH_{critical}$ ) is determined experimentally (discussed later in this report). The composition of the electrolyte formed on the WP surface was assumed to be that of simulated concentrated water below 100° C, and that of simulated saturated water above 100° C. It is conservatively assumed that the corrosion rate is constant and that it does not decrease with time. All experimental data for Alloy 22 (up to two years) exhibited a decreasing trend in the corrosion rate as a function of time (note that only 12-month data exists for Ti).

## Localized Corrosion

Conceptual models for localized corrosion of the drip shield and WP outer barrier are discussed in the *General Corrosion and Localized Corrosion of the Drip Shield* and *General Corrosion and Localized Corrosion of Waste Package Outer Barrier* AMRs, respectively.

The generic localized corrosion model for drip shield and WP materials assumes that localized attack occurs if the open circuit corrosion potential ( $E_{corr}$ ) exceeds the threshold potential for breakdown of the passive film ( $E_{critical}$ ):

$$E_{corr} \geq E_{critical} \quad (6)$$

Corrosion and threshold potentials were determined using cyclic polarization measurements in synthetic concentrated J-13 well waters. Measurements were made in four different standard test media and at different temperatures. Threshold Potential 1 from these measurements was assumed to define the critical corrosion potential in the *Abstraction of Models for Pitting and Crevice Corrosion of the Drip Shield and Waste Package Outer Barrier* AMR.

Alloys such as Alloy 22 rely on a stable, tenacious oxide film to enhance corrosion resistance. To date, limited evaluations have been conducted using atomic force microscopy to understand the nature of the passive films. A detailed understanding of the stability of passive films over very long time scales, which particularly addresses the effects of dissolution and diffusion processes, does not exist. The impact of aggressive species, mechanical damage, mechanical strength, and adhesion of the growing film on passive film behavior needs to be understood. In order to gain insight into the fundamental behavior of passive films over long time scales, a passive film stability model is being developed (as it is being developed, it was not included in Rev 00 of the AMR).

The key issues that the passive film model will address are:

- Calculation of potential-pH diagrams for the multi-component Alloy 22 system in Yucca Mountain bounding environments and temperatures
- Growth of thicker oxides at higher temperatures (90° – 170° C)
- Determination of the kinetics of film growth
- Determination of the chemical, structural, and mechanical properties of films, including thickened films, using a battery of surface analytical techniques
- Correlation of changes in corrosion potential measured in corrosion tests with the compositional changes in films over time
- Determination of changes in film structure/properties for cold-worked materials
- Compare films formed on Alloy 22 with other similar alloys that have a longer industrial experience, including Alloys C-4 and 625

Little information exists regarding the rate of localized corrosion of Ti-7 and Alloy-22 under repository-relevant conditions. Conservative estimates of the localized corrosion rate of both alloys were obtained from literature sources under more aggressive environments.

### **Microbiologically Influenced Corrosion (MIC)**

Conceptual models for MIC of the drip shield and WP outer barrier are discussed in the *General Corrosion and Localized Corrosion of the Drip Shield* and *General Corrosion and Localized Corrosion of Waste Package Outer Barrier* AMRs, respectively.

It has been observed that both titanium-7 and nickel-based materials such as Alloy 22 are relatively resistant to microbiologically influenced corrosion. Furthermore, it is believed that microbial growth in the repository will be limited by the availability of nutrients. Ultimately, the impact of microbiologically influenced corrosion can be accounted for by adjusting  $E_{corr}$ ,  $E_{critical}$ , pH and the sulfide concentration. The possible augmentation of corrosion rates over the entire surface of the material due to microbiologically influenced corrosion was accounted for by using an enhancement factor ( $G_{MIC}$ ), as shown below, for both the general and localized corrosion rates. It was also assumed that MIC influenced the corrosion rate immediately in TSPA simulations; no initiation criteria were assumed. The MIC enhancement factor is calculated as the ratio of corrosion rates (microbes to sterile).

$$\left( \frac{dp}{dt} \Big|_{effective} \right)_{corrected} = G_{MIC} \times \left( \frac{dp}{dt} \Big|_{effective} \right)_{original} \quad (7)$$

### **Phase Stability and Aging**

The conceptual models for phase stability and aging are discussed in the *Aging and Phase Stability of Waste Package Outer Barrier* AMR. The long-term aging of Alloy 22 at elevated temperature can cause the precipitation of undesirable intermetallic phases, affecting the corrosion resistance of the metal. As discussed in the *General and Localized Corrosion of the Drip Shield* AMR, the effects of phase instability on the degradation of Ti-7 is expected to be insignificant. For Alloy-22, nucleation and growth kinetics of the intermetallic phases were assumed to obey the following relation:

$$f = 1 - \exp(-kt^n) \quad k = C_1 \exp(-C_2/T) \quad (8)$$

where:  $f$  = the volume fraction of the precipitating phase  
 $k$  = constant that depends on nucleation and growth rates  
 $C_i$  = constants  
 $n$  = constant  
 $T$  = temperature  
 $t$  = time

All parameters in the above relation are determined experimentally. For TSPA-SR Rev. 00, these experiments are typically conducted at higher temperatures than are expected in the repository. This is necessary because the precipitation of intermetallic phases at lower

temperatures is extremely slow. This necessitates the extrapolation of parameters to temperatures expected in the repository environment. However, the impact of aging and phase instability on the corrosion of Alloy 22 is expected to be minimal for WP temperatures below approximately 300°C. Aging tests are being performed in a range of expected repository temperatures, but long testing times are required to obtain measurable results.

The effect of thermal aging on the corrosion rate of Alloy-22 is accounted for in an enhancement factor,  $G_{aged}$ , and is based upon a ratio of the non-equilibrium passive current densities for base metal and aged material (see Section 6.7 of the *General Corrosion and Localized Corrosion of Waste Package Outer Barrier* AMR). The enhancement factor is applied to both the general and localized corrosion rates. It was also assumed that aging and phase instability influenced the corrosion rate immediately in TSPA simulations; no initiation criteria were assumed.

$$\left( \frac{dp}{dt} \Big|_{effective} \right)_{corrected} = G_{aged} \times \left( \frac{dp}{dt} \Big|_{effective} \right)_{original} \quad (9)$$

## B. Parameters

The parameters used in the general and localized corrosion models are documented in the *General Corrosion and Localized Corrosion of the Drip Shield* and *General Corrosion and Localized Corrosion of Waste Package Outer Barrier* AMRs, respectively.

For Alloy-22, published values of the rate coefficient at high temperatures (600-900°C) were used to conservatively estimate the dry oxidation rate. For titanium grade 7, literature information was used to determine the rate coefficient as a function of temperature and the activation energy.

The threshold relative humidity, conservatively defined as the deliquescence point of  $\text{NaNO}_3$ , was determined as a function of temperature in the *Environment on the Surface of the Drip Shield and Waste Package Outer Barrier* AMR. This AMR also determined the solution composition for standard test media used in the long-term corrosion tests and the corrosion potential experiments.

General corrosion penetration rates were estimated based on weight-loss information obtained from the long-term corrosion test facility. Corrosion potential information ( $E_{corr}$  and  $E_{crit}$ ) were determined (as a function of temperature) using cyclic polarization in test media relevant to the expected repository environment. Localized corrosion rates and failure mode characteristics (e.g., number of failure sites and opening sizes) were obtained from published data.

The enhancement factors for phase stability and aging ( $G_{aged}$ ) and MIC ( $G_{MIC}$ ) of the Alloy 22 metal is discussed in the *General Corrosion and Localized Corrosion of Waste Package Outer Barrier* AMR. As discussed in the *General and Localized Corrosion of the Drip Shield* AMR, the  $G_{MIC}$  value for Alloy-22 was assumed to be applicable to Ti-7. The enhancement factor for aging is approximately one ( $G_{aged} \sim 1$ ), whereas the value of  $G_{aged}$  for fully aged material is larger ( $G_{aged} \sim 2.5$ ). Material with less precipitation than the fully aged material would have an

intermediate value of  $G_{aged}$  ( $1 \leq G_{aged} \leq 2.5$ ). Therefore, a value of 2.5 for  $G_{aged}$  was conservatively used to bound the potential aging effect. The AMR recommends that half the range be assumed to represent spatial variability and half be assumed to represent uncertainty. Hence, in TSPA there is no explicit link between the degree of aging computed from process modeling or determined from experimental information and the aging enhancement factor. For MIC, the value of  $G_{MIC}$  for Alloy 22 in sterile media is about one, whereas the value of  $G_{MIC}$  for Alloy 22 in inoculated media is larger, approximately two.

### C. Representational Model

There are no explicit representational models for general and localized corrosion of the drip shield and WP outer barrier. Rather, experimental and literature information is used to determine the parameters for the various conceptual models discussed above.

### D. Results

As discussed above, the overall purpose of the general and localized model is to evaluate the potential for such corrosion modes to affect the performance of the drip shield (Ti Grade 7) and WP outer barrier (Alloy 22) and to develop models for inclusion into the WAPDEG model. As such, the focus of the suite of the *General Corrosion and Localized Corrosion of the Drip Shield* and *General Corrosion and Localized Corrosion of Waste Package Outer Barrier* AMRs is to both identify the conceptual models and select parameter values for use in these models. The AMRs clearly discuss the conceptual models used. Selection of the parameters (either single values or probability distributions) is based on both literature and experimental information. These AMRs discuss the source of information used (experimental or literature), the selection of parameter values (and ranges), and provide the basis for this selection.

The information from these AMRs is used as input into the *Calculation of General Corrosion Rate of Drip Shield and Waste Package Outer Barrier to Support WAPDEG Analyses* and the *Abstraction of Models for Stainless Steel Structural Material Degradation* AMR. These documents present the abstracted models for general and localized corrosion that are ultimately incorporated into the WAPDEG code<sup>1</sup>. Recall that subsequent decisions were made to not take credit for the stainless steel inner barrier in TSPA analyses. Additional information from the *General Corrosion and Localized Corrosion of the Drip Shield* and *General Corrosion and Localized Corrosion of Waste Package Outer Barrier* AMRs is also provided as direct input for the development of the WAPDEG model<sup>1</sup>.

The effect of general and localized corrosion on both WP and overall repository system performance is documented in TSPA-SR (Section 4.1)<sup>2</sup>, including sensitivity studies (Section 5.2.3) that show the effects of uncertain parameters on repository system performance.

---

<sup>1</sup> Documented in “WAPDEG Analysis of Waste Package and Drip Shield Degradation,” ANL-EBS-PA-000001

<sup>2</sup> **Note:** through the development of the WAPDEG model, which is incorporated directly into the TSPA-SR model.

## 9.4 Discussion of Uncertainty Treatment

An evaluation of uncertainty and variability treatment of the AMRs was performed for this exercise. For each AMR, the uncertainties/variabilities were identified and a determination was made on the thoroughness of treatment. Thorough treatment was considered to be: identification, treatment, impact assessment, and clear presentation of the analysis and the propagation of uncertainty in the AMR. Table 9-1 is a synopsis of some of the uncertainties and variabilities identified in this exercise. The following is a discussion of the evaluation process and uncertainty/variability analysis trends within the AMR/model process.

### A. Conceptual Model

Conceptual model uncertainty is not treated explicitly. Rather, the conceptual models utilized are consistent with accepted theories of corrosion and available experimental evidence. In some instances less conservative models may be applicable, however data limitations were judged to preclude their selection (e.g., dry oxidation of Alloy-22).

### B. Parameters

The majority of the uncertainties in the general and localized corrosion models are associated with the parameter values and ranges selected for use. All parameters are presented in the form of distributions (usually uniform distributions) that are then used in WAPDEG and subsequent TSPA analyses. These distributions have been determined from the experimental results. Where experimental results are not available or sufficient, analogous data from literature have been used (e.g. crevice corrosion rates). The technical rationales for using analogous data are described. Appropriate justification is clearly provided for all values and uncertainty ranges used. The treatment of uncertainties in the generalized and localized corrosion model parameters is well documented and discussed within each AMR and between them. Integration of parameter uncertainty between the AMRs is clear.

The dry oxidation models are based upon published data, and do not include estimates of uncertainty. The rates of dry air corrosion are very small and any uncertainty in the dry air corrosion rate is not expected to have any significant impact on the performance of these materials. In addition, given the very slow rate of dry oxidation expected for both Ti-7 and Alloy-22, this corrosion mechanism is not considered in the overall WP and drip shield degradation model implemented into WAPDEG.

The RH thresholds are based on experimental information. To account for uncertainty, this threshold was conservatively defined as the measured deliquescence point of  $\text{NaNO}_3$  (function of temperature). The evaporative concentration of simulated well J-13 water, a bicarbonate water, results in a solution of  $\text{Cl}^-$ ,  $\text{NO}_3^-$ ,  $\text{CO}_3^{2-}$ ,  $\text{Na}^+$ , and  $\text{K}^+$  ions. Other ions that could form salts with lower deliquescence points, such as  $\text{Ca}^{2+}$  and  $\text{Mg}^{2+}$ , are precipitated as insoluble species in these waters. It is therefore conservatively assumed that the deliquescence point of  $\text{NaNO}_3$  determines the threshold RH. Thus, the uncertainty in the relative humidity threshold was not explicitly quantified, but rather was treated through a conservative assumption.

Detailed error analyses were conducted to determine the uncertainty in the general corrosion rates as determined from weight-loss data obtained from the long term corrosion tests. Note that these are the general corrosion rate is the only parameter used in the general corrosion model since a constant rate conceptualization was assumed. Distributions of corrosion rate are provided for both Ti Grade-7 and Alloy 22. The range of these distributions was assumed to represent uncertainty in the corrosion rate. Spatial variability in the corrosion rates was assumed to be comparable in magnitude to these ranges (defined as a triangular probability distribution). Note that a different approach was used when the general corrosion information was implemented into WAPDEG. Information regarding this approach can be found in the chapter that discusses the WAPDEG model.

The general method used in the formal error analysis is documented in Section 6.5.3 of both the *General Corrosion and Localized Corrosion of Waste Package Outer Barrier* and *General Corrosion and Localized Corrosion of the drip shield* AMRs and summarized below. The error analyses were performed on experimental weight loss data from the long term corrosion test facility using samples examined after 6, 12, and 24 months of exposure. Approximately 144 samples were examined at each time interval, and the samples were exposed at two temperatures (60 and 90 °C) and three different environments (pH range: 2.7 to 10.0). The formulations used in the weight loss data error analysis are summarized below (Equations 10 through 15).

Consider the dependent variable  $y$  defined by the following generic function:

$$y = f(x_1, x_2, x_3, x_4 \cdots x_n) \quad (10)$$

where  $x_i$  is the  $i^{th}$  independent variable. The total derivative of  $y$  is then defined as:

$$dy = \frac{\partial y}{\partial x_1} dx_1 + \frac{\partial y}{\partial x_2} dx_2 + \frac{\partial y}{\partial x_3} dx_3 + \frac{\partial y}{\partial x_4} dx_4 + \cdots + \frac{\partial y}{\partial x_n} dx_n \quad (11)$$

Based upon this definition, the maximum error in  $y$  can then be defined as:

$$\Delta y = \left| \frac{\partial y}{\partial x_1} \Delta x_1 \right| + \left| \frac{\partial y}{\partial x_2} \Delta x_2 \right| + \left| \frac{\partial y}{\partial x_3} \Delta x_3 \right| + \left| \frac{\partial y}{\partial x_4} \Delta x_4 \right| + \cdots + \left| \frac{\partial y}{\partial x_n} \Delta x_n \right| \quad (12)$$

where  $\Delta x_i$  is the error in the  $i^{th}$  independent variable. Let the dependent variable  $y$  be the general corrosion rate measured in the long term corrosion test facility:

$$y = \frac{dp}{dt} = \frac{w}{\rho \times t} \frac{1}{[2(a \times b) + 2(b \times c) + 2(a \times c)]} \quad (13)$$

where:  $w$  = measured weight loss (grams)  
 $\rho$  = density ( $\text{g/cm}^3$ )  
 $t$  = exposure time (hours)  
 $a$  = length of test coupon (inches)  
 $b$  = width of test coupon (inches)

$c$  = thickness of test coupon (inches)

The total derivative of the corrosion rate is:

$$dy = \frac{\partial y}{\partial w} dw + \frac{\partial y}{\partial \rho} d\rho + \frac{\partial y}{\partial t} dt + \frac{\partial y}{\partial a} da + \frac{\partial y}{\partial b} db + \frac{\partial y}{\partial c} dc \quad (14)$$

The maximum error in the corrosion rate is:

$$\Delta y = \left| \frac{\partial y}{\partial w} \Delta w \right| + \left| \frac{\partial y}{\partial \rho} \Delta \rho \right| + \left| \frac{\partial y}{\partial t} \Delta t \right| + \left| \frac{\partial y}{\partial a} \Delta a \right| + \left| \frac{\partial y}{\partial b} \Delta b \right| + \left| \frac{\partial y}{\partial c} \Delta c \right| \quad (15)$$

The  $\Delta$ -parameters are the corresponding error in the individual parameters. In this error analysis, errors in six independent parameters (weight loss, density, exposure time, sample length, sample width, and sample thickness) were used to determine the maximum error in the corrosion rate.

Determinations of corrosion and threshold potentials for both Alloy-22 and Ti-7 were based upon three replicate cyclic polarization measurements at each combination of environment and temperature. The uncertainty in the corrosion potential due to gamma radiolysis was (maximum positive shift in error of about 250 mV). Some uncertainty in the selection of corrosion and threshold potential is clearly shown. Numerical representations of this uncertainty have been made and were provided as input in the development of WAPDEG. The rates of localized corrosion have been bounded with the range of values found in the published literature.

Uncertainty in the effects of aging/phase stability and MIC is treated through a range of corrosion rate enhancement factors. Recall, aging/phase instability is not expected to affect the corrosion rate of the Ti-7 drip shield. For Alloy-22, the aging/phase instability enhancement factor is assumed to range from 1 to 2.5 with half the range assumed to represent spatial variability and half assumed to represent uncertainty. For both Ti-7 and Alloy-22, the MIC enhancement factor is assumed to range from 1 to 2 with half the range assumed to represent spatial variability and half assumed to represent uncertainty.

## C. Results

As discussed above, the results of this model are primarily parameter values and distributions, which are provided as input for the development of the WAPDEG model. The impact of uncertain parameters on the results (WP and repository performance) is clearly discussed in the TSPA-SR document (Chapters 4 and 5). The results shown in the TSPA-SR document demonstrate how uncertainty in parameters affects the first breach of the WPs and the number of breaches on the WPs as a function of time.

### 9.5 Uncertainty Propagation

The uncertainties related to general and localized corrosion are clearly propagated through the AMRs, up to the abstraction level. These include uncertainties in general corrosion rates, localized corrosion rates, corrosion rate enhancement factors for both MIC and aging/phase

instability, corrosion potentials, and threshold corrosion potentials. Propagation of the uncertainties into TSPA is through the AMR that presents the WAPDEG model. The chapter regarding the WAPDEG model discusses how the uncertainties regarding general and localized corrosion are implemented into the WAPDEG model. Some differences between the recommendations for uncertainty treatment in the supporting AMRs and their implementation into WAPDEG exist, as discussed in the WAPDEG model chapter.

**Table 9-1: General and Localized Corrosion**

<p><b>Model Purpose:</b> The purpose and scope of the process-level model is to account for both general and localized corrosion of the WP outer barrier, which is assumed to be Alloy 22 and TI-7. This model will include several sub-models, which will account for dry oxidation, humid air corrosion, general corrosion in the aqueous phase, and localized corrosion in the aqueous phase. This AMR serves as a feed to the WAPDEG code analyses. It also serves as a basis for the WP PMR and model abstraction for WAPDEG.</p>				
Summary	Source	Treatment	Basis	Impact
<b>Conceptual Model</b>				
Environment on the surface of drip shield and WP outer barrier	AMR No. ANL-EBS-MD-000001	This process-level model addresses the evolution of the chemistry of the water film on the drip shield and WP outer barrier as a function of temperature and RH. The concentrations of aqueous salt solutions that can form on the hot WP surface are being determined experimentally and theoretically (based upon chemical thermodynamics). These concentrations define the medium for testing WP materials under a bounding scenario. Abstracted models are developed for the evolution of environments on the exposed surfaces of the drip shield and WP outer barrier as a function of time and location within the repository.	Experimental analyses	Determines solution concentrations for conducting corrosion tests. Identifies deliquescence point of NaNO <sub>3</sub> – used as the threshold for humid air corrosion.
General corrosion and localized corrosion	ANL-EBS-MD-000003 and ANL-EBS-MD-000004; experimental and literature information	Three separate process-level models were developed to address general corrosion and localized corrosion of the drip shield, WP outer barrier and stainless steel structural support, respectively. Each of these models includes sub-models for dry air oxidation, humid air corrosion, general corrosion in the aqueous phase, and localized corrosion in the aqueous phase. Microbial corrosion is addressed in the localized corrosion model.	Literature information and experimental data	Identifies the modes of corrosion, when each is expected to occur, and the conceptual models determined for use.
Long-term aging and phase instability	ANL-EBS-MD-000003; experimental and literature information	This process-level model addresses degradation of the WP outer barrier resulting from exposure to elevated temperatures. In the case of Alloy 22 and related materials, such thermal histories can result in the formation of precipitates ( $\mu$ , P, $\sigma$ phases) and other undesirable phases. Precipitation can cause embrittlement, thereby increasing susceptibility to damage by rockfall and mechanical impact. The time-temperature-transformation curve and an expression for estimating the volume fraction of precipitates in the grain boundary have been developed for Alloy 22.	Literature information and limited experimental data	Potential to increase corrosion rates.

<b>Parameters and Inputs</b>				
Section 6.5.3 (AMR No. ANL-EBS-MD-000003) Error Analysis for Weight Loss Measurements summarizes the error analysis for the general corrosion rates based on weight loss measurements	Experimental uncertainty	Error analysis determined the maximum uncertainty in the general corrosion rate for weight loss measurements. A general corrosion rate greater than 160 nm per year (4 std dev) was deemed to be well outside the range of experimental error.	Experimental data from Long Term Corrosion Test Facility	Section 6.5.4 (AMR No. ANL-EBS-MD-000003) describes a simple and defensible representation of the observed corrosion rates based on the error analysis. See Figure 26, p. 79.
Section 6.7.3 (AMR No. ANL-EBS-MD-000003) describes the overall effect of thermal aging on the general corrosion rate	Experimental uncertainty	An enhancement factor with a uniform distribution between 1 and 2.5 is applied to the general corrosion rate. It is recommended that this distribution is half uncertainty and half variability.	Section 6.7.1 (AMR No. ANL-EBS-MD-000003) describes cyclic polarization tests on aged samples of the WP outer barrier	Potential to increase the general corrosion rate as a result of thermal aging effects (Section 6.7.3).
Section 6.8 (AMR No. ANL-EBS-MD-000003) describes the overall effect of MIC on the general corrosion rate	Experimental uncertainty	An enhancement factor with a uniform distribution between 1 and 2.0 is applied to the general corrosion rate. It is recommended that this distribution is half uncertainty and half variability.	Section 6.8 describes the experimental results of MIC on WP outer barrier	Potential to increase the general corrosion rate as a result of thermal aging effects (Section 6.8).
Section 6.4.4 (AMR No. ANL-EBS-MD-000003) describes the effect of gamma radiolysis on corrosion potential	Experimental uncertainty	Shifts in corrosion potential have been examined under various radiolytic conditions to determine effects of gamma radiolysis on corrosion rates.	Literature data of the corrosion and threshold potentials of Alloy 22 in the presence of gamma radiation	In the current process models, extremely high radiation levels would be required to achieve significant shifts in corrosion potential and since even the maximum shifts in potential would be less than those required for breakdown of the passive film, it is unlikely that gamma radiolysis will have a significant effect on the localized corrosion of Alloy 22.
Section 6.6.6 (AMR No. ANL-EBS-MD-000003) describes the estimated rate of localized corrosion	Experimental uncertainty	The logarithm of the localized corrosion rate is normally distributed as shown in Table 22.	Experimental determinations of crevice pH and current, per AP-E-20-81, Rev 1	In the current TSPA models, the threshold potential for localized attack is not exceeded, and thus, localized corrosion of the WP outer barrier model is not invoked.

Section 6.2 (AMR No. ANL-EBS-MD-000002), Figure 98 depicts the graphical extrapolation of the curves in Figure 97 to repository relevant temperatures	Aging data on base metal	Curves associated with grain boundary coverage and bulk precipitation in Figure 97 are graphically extrapolated to 10,000 years in Figure 98 (AMR No. ANL-EBS-MD-000002).	Assuming that the precipitation mechanism does not change, the lines in Figure 97 can be extrapolated to give times that can be expected for various stages of precipitation at lower temperatures. These data, however, are preliminary. The times were estimated from examination of micrographs from samples with widely spaced aging times. Extrapolation to lower temperatures is difficult because the precipitation rate is quite sensitive to temperature; small changes in slope make a very large change in the time obtained from extrapolation to lower temperatures.	Even accounting for the rather large uncertainty, bulk precipitation does not appear likely in 10,000 yr at 300 °C. Grain boundary precipitation may, however, occur. Therefore, a good bounding argument would be to assume that the precipitation covers the grain boundaries.
Section 6.5 (AMR No. ANL-EBS-MD-000002), Figure 99 depicts the graphical extrapolation of the limited kinetic data for Long Range Ordering (LRO) in Alloy 22 base metal	Aging data on base metal	The kinetics of ordering in Alloy 22 can be estimated by looking at the earliest times where LRO is seen. From the TTT diagram (Figure 96), the earliest times where LRO is observed are 1000 hours at 538 °C and 30,000 hours at 427 °C. These two points are used in Figure 99. Data were curve fit with an exponential function.	The points in Figure 99 were chosen because the amount of ordering observed after aging under those conditions was relatively small. The amount of ordering in the sample aged at 538 °C is greater than that in the sample aged at 427 °C. To get the same amount of ordering at 427 °C, a longer time would be needed. This shift would increase the slope of the curve, which would result in higher extrapolated time at 300 °C.	Given the present treatment with the limited amount of LRO kinetic data, the approach is bounding and conservative.
<b>Variability</b>				
Variability in corrosion rate enhancement due to MIC and aging/phase instability	ANL-EBS-MD-000003; experimental and literature information	Corrosion rate enhancement factors developed for both MIC and aging/phase instability – ranges. Recommend to use half the range as uncertainty, half as variability.	Limited data – assumption made in AMR.	Increases corrosion rates.

<b>Results</b>				
Distribution of general corrosion rates for Alloy 22 and Titanium Gr 7	CAL-EBS-PA-000002	Abstraction of distribution of general corrosion rates for Alloy 22 and Titanium Gr 7.	Experimental data documented in ANL-EBS-MD-000003	General corrosion of Alloy-22 and Ti-7
Distribution of localized corrosion rates for Alloy 22 and Titanium Gr 7	ANL-EBS-MD-000003 and ANL-EBS-MD-000004; literature information	Abstraction of distribution of localized corrosion rates for Alloy 22 and Titanium Gr 7. Used conservative values obtained from literature for more aggressive environments.	Choice of values based on more aggressive environments than expected	Localized corrosion rates – note that localized corrosion is not expected in the Yucca Mountain repository environment

## 10.0 Stress Corrosion Cracking

### 10.1 Purpose of the Model

Stress corrosion cracking (SCC) is a potential corrosion mode that can result in penetration of the WP outer barrier. The purpose of the SCC model is to evaluate the potential for SCC of the WP outer barrier (Alloy 22) and to develop models for inclusion into the WAPDEG model.

SCC has long been recognized as a potential failure mode for highly corrosion resistant alloys. Considerable industry experience exists regarding SCC resulting in different theoretical (conceptual) models and experimental studies have been conducted to develop material-specific parameters for inclusion in these models. As such, techniques for modeling SCC are well developed and accepted by the technical community.

Modeling SCC of the WP outer barrier, however, is a rather recent endeavor. Past WP degradation modeling efforts (e.g., TSPA-VA) did not explicitly model SCC because the expected stress in the WP materials was lower than the required stress. However, the possibility was identified that high residual stresses in the final closure weld could lead to SCC. Since SCC has only recently been identified as a potential WP failure mode, limited data exist to guide the identification of a conceptual model and the selection of parameter values for use in these models. This has resulted in the selection of both a conservative model and conservative input parameter values (conservative is defined as resulting in poorer than anticipated WP performance with respect to SCC).

### 10.2 Model Component Relations

Details of the mechanisms and models for stress corrosion cracking are documented in the WAPDEG PMR (TDR-WIS-MD-000002 REV 00 ICN 01) and the following AMRs:

- *Analysis of Mechanisms for Early Waste Package Failure*, ANL-EBS-MD-000023 – Evaluate the types of defects or imperfections that could occur and potentially lead to early failure of some WPs.
- *Stress Corrosion Cracking of the Drip Shield, the Waste Package Outer Barrier and the Stainless Steel Structural Material* (ANL-EBS-MD-000005) – Provide a detailed description of the process-level models that can be applied to assess the performance of the material (Alloy 22) used for the WP outer barrier, if it is subjected to the effects of SCC. Although the title implies that SCC is evaluated for the drip shield and stainless steel structural material, the AMR only focuses on the Alloy 22 outer barrier. The AMR states:

“For the current design of the DS and WP, however, the DS will be excluded from the SCC evaluation because stresses that are relevant to SCC are insignificant in the DS. The major sources of stresses in the DS are loadings due to backfill and earthquakes. These stresses will not induce SCC because the stress caused by backfill is generally compressive stress and the stress caused by earthquakes is temporary in nature. The 316NG stainless steel inner barrier of the WP will also be excluded from the SCC

evaluation because the SCC performance assessment will not take credit from the inner barrier.”

- *Abstraction of Models of Stress Corrosion Cracking of Drip Shield and Waste Package Outer Barrier and Hydrogen-Induced Corrosion of Drip Shield (ANL-EBS-PA-000004) – Develop abstracted models of stress corrosion cracking of the WP outer barrier and hydrogen induced cracking of the drip shield for use as input into the WAPDEG model.*

Figure 10-1, Stress Corrosion Cracking AMR Relationships, illustrates the relationship of the SCC AMRs within the entire set of WAPDEG AMRs.

### **10.3 SCC Model Structure**

Figure 10-2, Stress Corrosion Cracking Model Structure, depicts the various elements that comprise the SCC model. The relationships of the elements of the conceptual model, the model parameters, the representational model, and the modeling results are indicated in the figure. Figure 10-2 includes the TSPA abstraction of results as the end product of the model development in the AMRs.

#### **A. Conceptual Model**

SCC of materials may occur when an appropriate combination of material susceptibility, tensile stress, and environment are present. Two conceptual models are discussed in the *Stress Corrosion Cracking of the Drip Shield, the Waste Package Outer Barrier and the Stainless Steel Structural Material* AMR. The first conceptual model (termed the threshold model) is based on threshold stress intensity factor criterion for initiation of SCC ( $K_I > K_{ISCC}$ ). The second conceptual model (termed the slip dissolution model) is based upon a threshold stress and a finite rate of SCC propagation that is dependent upon the local environment and the stress intensity factor at the crack tip. The stresses for initiation and propagation of SCC are induced by residual stresses in unannealed closure welds, deformation caused by rock fall, and the weight of the WP. The conceptual models require appropriate stress analysis models and measurements for calculation of the through-wall stress distribution for representative cross sections of the WP, including unwelded base metal and unannealed welds. This stress distribution is used to calculate a corresponding stress intensity factor distribution for flaws that range in size from zero to the entire thickness of the wall including the welded region. This stress intensity factor distribution is used as input for both conceptual model.

In the threshold model, SCC initiates at pre-existing flaws that develop during fabrication of the WP, or at flaws that develop during localized corrosion. Cracks are assumed to rapidly propagate through the thickness of the metal. In the slip dissolution model, SCC is initiated if the threshold stress is exceeded on a smooth surface. Then, the SCC propagation rate is calculated as a function of local environment and stress intensity factor. The time-to-failure is determined by integrating the calculated propagation rate.

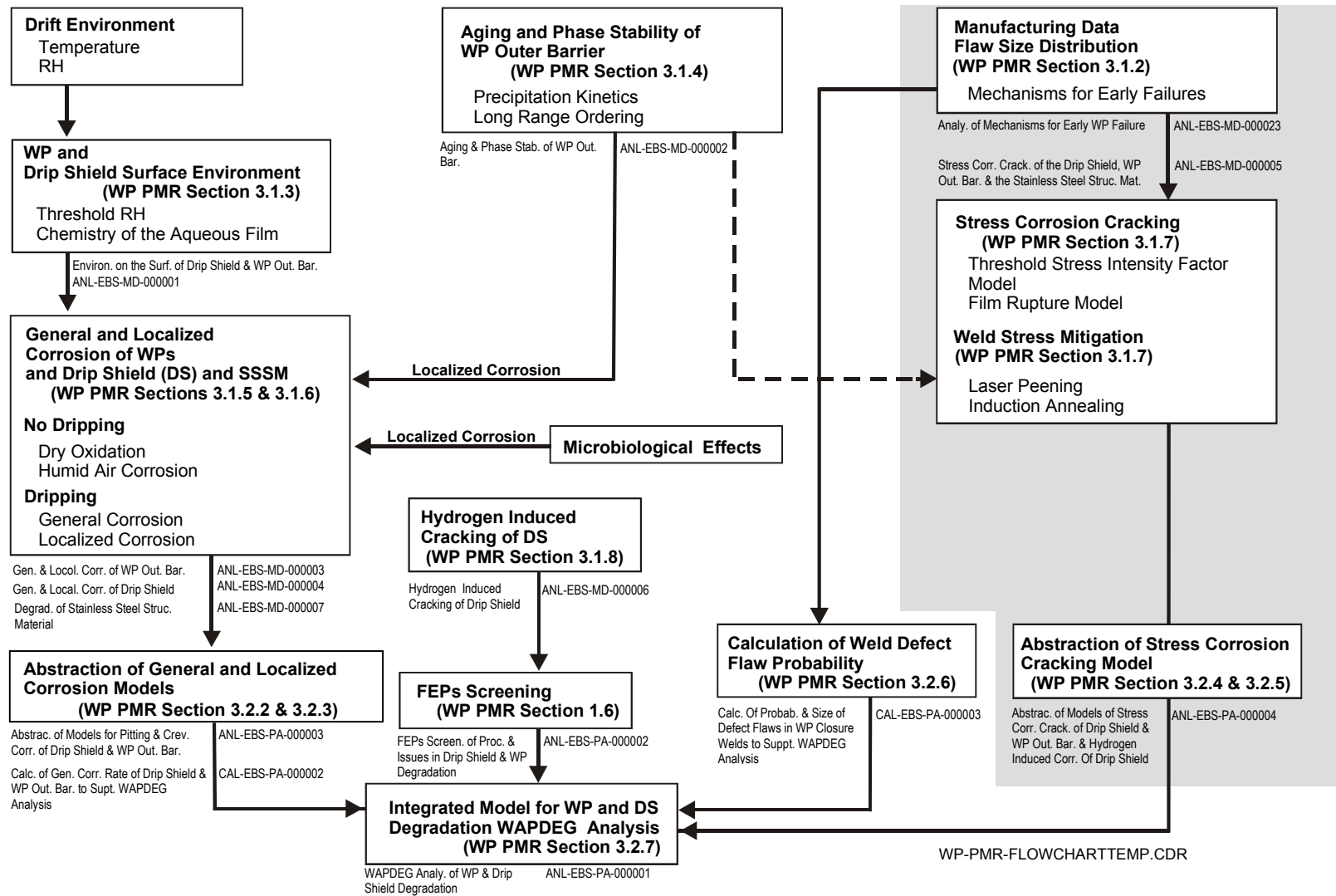


Figure 10-1: Stress Corrosion Cracking AMR Relationships

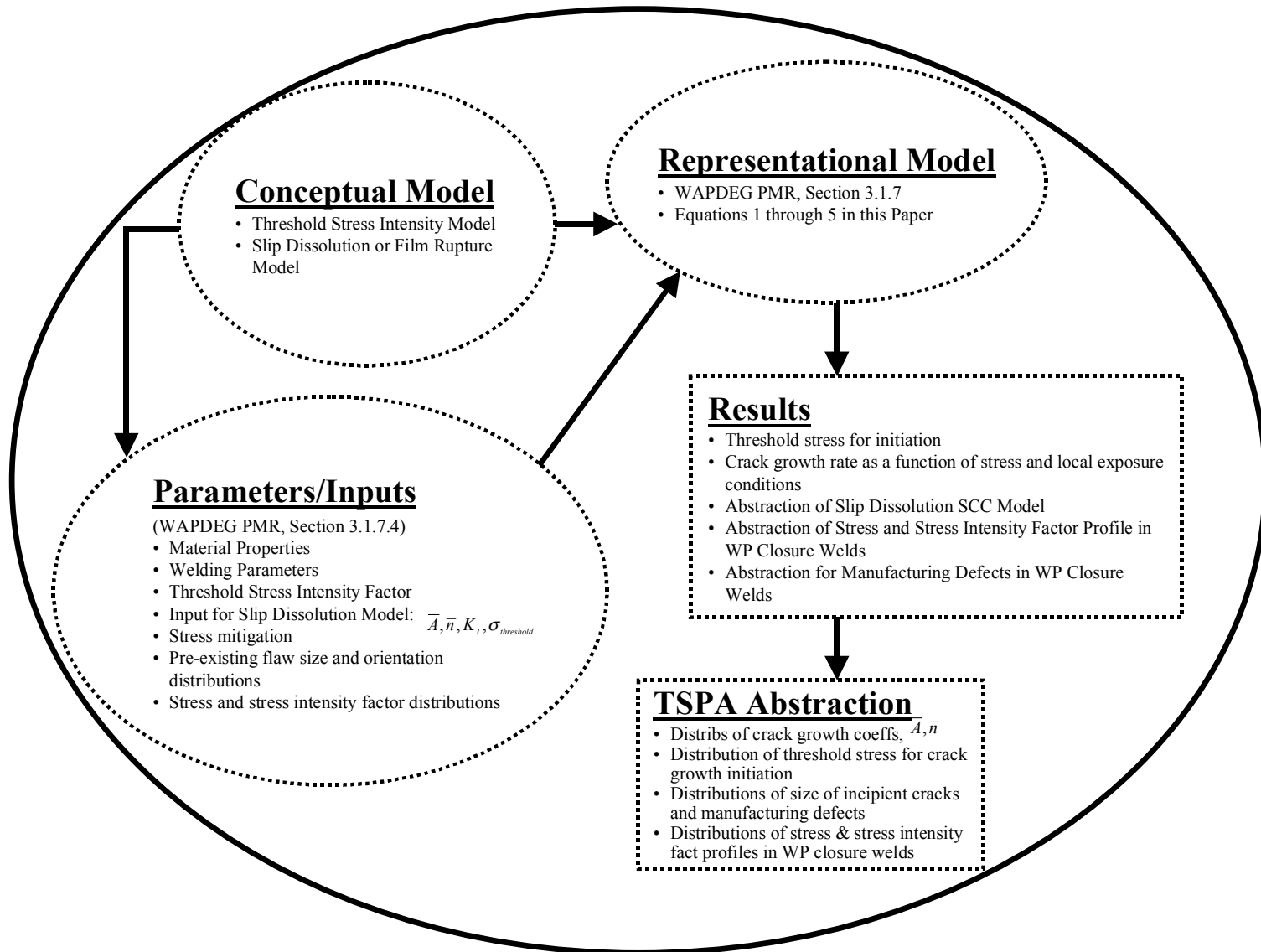


Figure 10-2: Stress Corrosion Cracking Model Structure

As discussed above, the drip shield and the stainless steel structural material were excluded from SCC evaluation because stresses in the drip shield relevant to SCC are insignificant and credit for the stainless steel inner barrier is not being taken (see Section 5 of the *Stress Corrosion Cracking of the Drip Shield, the Waste Package Outer Barrier and the Stainless Steel Structural Material* AMR). The stainless steel inner barrier is conservatively assumed to be only a structural component of the WP, and its corrosion properties are not analyzed. The SCC evaluation focused on the WP outer barrier closure weld because the residual stress in this weld cannot be relieved completely as it can be for other container welds. This region of the WP is potentially susceptible to SCC since welding will produce high-tensile residual stress in close proximity to the weld and since pre-existing flaws due to fabrication and welding have much higher distribution in the weld than in the base metal.

An effective approach to eliminate the threat of SCC and resultant through-wall cracking in the closure weld is to implement a post-weld stress mitigation process to either remove residual tensile stresses in the weld region, or reduce them below threshold values for SCC initiation and growth. The initial process selected to mitigate SCC in the WP outer barrier closure weld was single-pass laser peening. The laser peening process utilizes a rapidly pulsed, high energy density laser beam rastered across the surface region of the closure weld to induce a compressive surface layer. Testing data indicate that a compressive layer with a thickness (depth) of 2-3 mm can be produced, thus removing the potential for SCC initiation in the compressive layer. However, the rate of removal of this compressive layer by general corrosion indicated that it would be eliminated in an unacceptably short time leading to possible SCC initiation and through-wall growth. The closure design was therefore modified to include two lids (inner and outer lid) with two separate post-weld stress mitigation processes; laser peening of the inner lid and induction annealing stress relief of the outer lid weld. During the induction annealing process, the weld region is very rapidly heated to the solution annealing temperature to remove weld residual stresses and rapidly cooled to avoid precipitation of potentially deleterious intermetallic phases.

This two-lid design and stress mitigation strategy forms part of the conceptual basis for the SCC model. Conceptually, it is necessary to remove the compressive layers in both lids before SCC can initiate.

## **B. Parameters**

The parameters used in the SCC model are documented in the *Stress Corrosion Cracking of the Drip Shield, the Waste Package Outer Barrier and the Stainless Steel Structural Material* AMR.

Both conceptual models require estimates of the weld residual stress. This is determined using finite element analysis techniques to analyze the temperature history and subsequent residual stresses in the weld region resulting from the welding and stress mitigation process. Both models also require the determination of the stress intensity factor. The stress intensity factor ( $K_I$ ) is determined as a function of the residual weld stress, crack depth, size and shape of the crack and the configuration of the structural component (e.g. the WP outer barrier closure lids).

The threshold stress intensity factor approach requires the determination of the threshold stress intensity factor. Values of  $K_{ISCC}$  are based upon data published in the technical and scientific literature, or measurements made with double cantilever beam and compact tension specimens. To account for uncertainty, the parameter is represented by a normal distribution with a mean of  $33.0 \text{ Mpa(m)}^{1/2}$  and a standard deviation of  $1.77 \text{ Mpa(m)}^{1/2}$ .

The slip dissolution mechanism relies on the crack-tip strain rate (which encompasses the effects of mechanics parameters), as well as the repassivation rate, (which encompasses the effects of material characteristics and water chemistry). Because of the expected similarity in SCC behavior and mechanical response of face-centered-cubic alloys, the same crack-tip strain rate formulations that were employed for quantitative prediction of SCC in austenitic 304 or 316 stainless steels in 288°C high-purity boiling water reactor water can be used for SCC modeling of Alloy 22.

The rate of repassivation is captured by the parameter  $n$ , the repassivation slope. A characteristic of the slip dissolution or film rupture model is that SCC susceptibility decreases with increasing values of  $n$  (Section 5 of the AMR). For stainless steels, which are more susceptible to SCC than Alloy 22, test data indicates that  $n = 0.54$ . Recent test results for SCC crack growth in Alloy 22 provide the upper and lower bound values of 0.92 and 0.843, respectively, for the parameter “ $n$ ” of the slip dissolution model (Section 4.1.4 of the AMR).

Although the slip dissolution model assumes crack growth can initiate at any surface defect that can generate a stress intensity factor ( $K_I$ ), regardless of defect size and tensile stress, examination of the relevant SCC literature indicates that there is a threshold stress ( $\sigma_{threshold}$ ) below which SCC will not initiate on a “smooth” surface (free of surface breaking flaws).

An input to the SCC modeling approach is information regarding defects. Both incipient cracks and manufacturing defects are considered. Incipient crack information is documented in the *Stress Corrosion Cracking of the Drip Shield, the Waste Package Outer Barrier and the Stainless Steel Structural Material* AMR (Section 6.5.2). Information regarding manufacturing defects is documented in the *Analysis of Mechanisms for Early Waste Package Failure* AMR. In the former AMR, a probability distribution of incipient crack size and an assumption regarding crack distribution are provided. The latter AMR assesses the probability of waste fabrication defects, their uncertainty and variability, and the consequences of the defects on WP failure (e.g., number of manufacturing defects and size distribution).

### **C. Representational Model**

The two conceptual models are represented using the following equations, as discussed in the *Stress Corrosion Cracking of the Drip Shield, the Waste Package Outer Barrier and the Stainless Steel Structural Material* AMR:

#### **Threshold Stress Intensity Model**

A pre-existing crack will not grow or is in an arrest state if  $K_I(a, \sigma) < K_{ISCC}$ . The stress intensity factor,  $K_I(a, \sigma)$ , depends on the size and shape of the crack and the configuration of the structural component and is determined from the following relation:

$K_I(a,\sigma) = \beta\sigma(\pi a)^{1/2}$  where  $a$  is the crack depth and  $\sigma$  is the stress.

Closed-form solutions for the geometry factor, ( $\beta$ ), exist particularly for cases of uniaxial tensile stress and relatively simple geometry. Finite element techniques can also be used to determine ( $\beta$ ) for complex “custom” geometry, but in most fracture mechanics calculations, the closed-form solutions are widely accepted and applicable. A simplified solution utilizing fracture mechanics was used.

$$K_I = G(K_I)_{SECP} \quad (1)$$

Where:  $G$  = Geometrical correction factor  
 $(K_I)_{SECP}$  =  $K_I$  derived from a single edge cracked panel with an infinitely wide flaw

The analytic solution for  $(K_I)_{SECP}$  is

$$(K_I)_{SECP} = (\pi a)^{1/2} [A_0F_1 + (2a/\pi) A_1F_2 + (a^2/2) A_2F_3 + (4a^3/3\pi) A_3F_4] \quad (2)$$

Where:  $F_i$  = magnification factors, function of crack depth versus thickness (tabulated in literature)

$A_i$  = coefficients of a third order fit of the through-wall stress distribution

### **Slip Dissolution Model**

The slip dissolution model determines a crack growth rate as a function of the strain rate at the crack tip, given by:

$$V_t = A(\dot{\epsilon}_{ct})^n \quad (3)$$

Where:  $V_t$  = crack growth rate

$A$  = constant taken from measured repassivation response

$n$  = slope of oxidation current density (log-log scale) from repassivation response

$\dot{\epsilon}_{ct}$  = strain rate at the crack tip

The parameter  $A$  can be expressed as a function of  $n$  by the following relation:

$$A = 7.8 \times 10^{-3} n^{3.6} \quad (4)$$

The strain rate at the crack tip can be represented as a function of the stress intensity factor by the following relation, for constant load:

$$\dot{\epsilon}_{ct} = 4 \times 10^{-14} K_I^4 \quad (5)$$

## Stress Analysis

Both the threshold stress intensity factor and slip dissolution models require a determination of the residual stress in the weld, namely the hoop stress. ANSYS (version 5.3), a finite element analysis code, is used for the thermal and stress analysis (see Section 3.1.7.3).

The results of the ANSYS model are fit to a polynomial equation to determine the hoop stress as a function of depth for both the inner and outer lids. The equation is of the following form, where  $x$  is the distance from the outer surface of the lid.

$$\sigma = A_0 + A_1x + A_2x^2 + A_3x^3$$

Variability in the hoop stress along the circumference of the weld is determined using the following equation:

$$\sigma(\theta) = \sigma(0^\circ) - \nabla\sigma (1-\cos(\theta))$$

Where:  $\sigma(\theta)$  = Hoop Stress at angular location  $\theta$   
 $\sigma(0^\circ)$  = Hoop stress at arbitrarily chosen  $0^\circ$  location (equation above)  
 $\nabla\sigma$  = 2.5 ksi

The uncertainty in the stress state is introduced through a scaling factor,  $sz(z)$  of the function form shown below.

$$sz(z) = \left( \frac{z \cdot YS \cdot F}{3} \right)$$

$YS$  is the yield strength,  $F$  is the yield strength scaling factor (a constant, see the WAPDEG chapter), and  $z$  is the magnitude of the uncertainty variation from the mean profile (sampled from a distribution). The yield strength scaling factor,  $F$ , defines the maximum uncertainty variation possible (the bounds). The value  $z$  is represented by a triangular distribution between  $\pm 3$  with a mode of 0.

## **D. Results**

The models and parameters for SCC identified in the *Stress Corrosion Cracking of the Drip Shield, the Waste Package Outer Barrier and the Stainless Steel Structural Material* AMR were used as input to the *Abstraction of Models of Stress Corrosion Cracking of Drip Shield and Waste Package Outer Barrier and Hydrogen-Induced Corrosion of Drip Shield* AMR. In the latter AMR, abstracted models were developed for initial defects (probability of flaw existence and flaw size distribution), closure lid weld stress and stress intensity factor, the slip dissolution SCC model, and the threshold stress intensity factor SCC model.

Bounding analyses were conducted that demonstrate the time to failure using the slip dissolution conceptual model for various values of stress intensity ( $K_I$ ) and the repassivation factor ( $n$ ).

Additional analyses using the threshold stress intensity factor conceptual model indicate that this approach would never result in failure of either of the closure lids due to SCC.

The affect of SCC on both WP and overall repository system performance are documented in TSPA-SR (Section 4.1), including sensitivity studies (Section 5.2.3.2) that show the effects of uncertain parameters on repository system performance.

#### **10.4 Discussion of Uncertainty Treatment**

An evaluation of uncertainty and variability treatment of the AMRs was performed for this exercise. For each AMR, the uncertainties/variabilities were identified and the thoroughness of the treatment was determined. Thorough treatment was considered to be identification, treatment, impact assessment, and clear presentation of the analysis and the propagation of uncertainty in the AMR. Table 10-1 is a synopsis of some of the uncertainties and variabilities identified in this evaluation. The following is a discussion of the evaluation process and uncertainty/variability analysis trends within the AMR/model.

##### **A. Conceptual Model**

Conceptual model uncertainty is considered through the use of two alternative conceptual models, the threshold stress intensity model and the slip dissolution model. Both models are fully developed and documented, including uncertainties in parameters. Bounding analyses were conducted and the results indicated that the threshold stress intensity factor approach would never result in failure of the WPs due to SCC. As such, a decision was made to only consider and include the slip dissolution model in TSPA. These results are clearly documented and the decision supported.

##### **B. Parameters**

The majority of the uncertainties in the SCC models are parameter in nature. All parameters used in these models originate from experimental data. All parameters are presented in the form of distributions (usually uniform distributions) that are then used in WAPDEG and subsequent TSPA analyses. These distributions have been determined from the experimental results. Where experiment results are not available or sufficient, analogous data from literature have been used (e.g. threshold stress for SCC initiation in Alloy 22). The technical rationales for using analogous data are described. Appropriate justification is clearly provided for all values and uncertainty ranges used. The treatment of uncertainties in the SCC model parameters is well documented and discussed within each AMR and between them. Integration of parameter uncertainty between the AMRs is clear. However, as discussed below (in the following Sections), integration between the AMRs, the PMR, and TSPA-SR is not clear in two instances.

With respect to manufacturing defects, an uncertainty analysis was performed for probabilities estimated from event sequence trees. This analysis was used to provide confidence in the bounded limits of the event sequence tree results and is described in detail in the AMR. The AMR contains detailed treatments of the methods used in formulating the distributions of the eleven generic types of defect examined (a wide range of defects was surveyed, and eleven were

deemed to be applicable to the WP). Details of the uncertainties associated with the distributions are clearly discussed in the AMR.

### **C. Representational Model**

Representational model uncertainty is not explicitly quantified. However, the parameters for both SCC models are determined experimentally (essentially fits to experimental data). As such, the representational model uncertainty is captured as parameter uncertainty.

The ANSYS code is an industry standard tool for performing thermal and stress analyses. Uncertainty in the resultant stress is captured as parameter uncertainty, as discussed previously. It was noted that the PMR references the *Stress Corrosion Cracking of the Drip Shield, the Waste Package Outer Barrier and the Stainless Steel Structural Material* AMR for details regarding the thermal and stress analysis. However, that AMR provides a very limited discussion of the analysis (Section 6.2.2.1) and does not include ANSYS as the computer software used (see Section 3.1). As such, traceability between the stress profiles cited in this AMR and the detailed ANSYS analyses is not present.

### **D. Results**

The process model AMR, the abstracted model AMR, and TSPA-SR all show results, with those documented in TSPA-SR being the “final” SCC results. The impact of uncertain parameters on the results is clearly discussed. Results shown in the *Abstraction of Models of Stress Corrosion Cracking of Drip Shield and Waste Package Outer Barrier and Hydrogen-Induced Corrosion of Drip Shield* AMR show how uncertainty in parameters impacts the following:

- The resultant hoop stress
- Time for cracks to penetrate the Alloy-22 lids using the slip dissolution model with bounding assumptions
- $K_{ISCC}$  for the threshold model

The TSPA-SR document shows how uncertainty in SCC parameters affects the performance of the WPs in terms of first crack penetration and the density of penetrated cracks on WPs as a function of time.

### **10.5 Uncertainty Propagation**

Most of the uncertainties related to SCC are clearly propagated through the AMRs and into TSPA. Three areas of inconsistency related to transparency and traceability were identified.

- Section 3.4.1.3 of TSPA-SR does not identify that two conceptual models of SCC were evaluated with one selected for inclusion in the TSPA model (the slip dissolution model).
- Uncertainty in both the weld residual stress and the resultant stress intensity factor are discussed in several sections of the PMR. Weld residual stress uncertainty limits of  $\pm 10$

percent of yield stress are considered defensible (Section 3.1.7.12). However, two cases are considered in subsequent sections. Section 3.2.5.1 (realistic case abstraction) gives a range of  $\pm 5$  percent of yield strength while Section 3.2.5.3 (alternative conservative abstraction) gives a range of  $\pm 30$  percent of yield strength. Additionally, Section 6.2.2.5 of the *Stress Corrosion Cracking of the Drip Shield, the Waste Package Outer Barrier and the Stainless Steel Structural Material* AMR states that “for welds subjected induction heat annealing or laser peening, the range is assumed to be  $\pm 5$  percent of yield strength. Lastly, TSPA-SR considers an uncertainty range of  $\pm 30$  percent of yield stress as the base case and evaluates the ranges of  $\pm 10$  percent and  $\pm 5$  percent in sensitivity analyses. It should be noted that this is only ascertained in Section 5.2.3.2 and is not identified in Section 3.4.1.3 where the SCC input parameters are discussed.

- The PMR states that (Section 3.1.7.5) this threshold stress is conservatively estimated to be between 10 and 40 percent of the yield stress. However, Section 3.2.4.3 of the PMR and Section 6.4.3 of the AMR state that a range of 20 to 30 percent of yield stress, represented as a uniform distribution was used. Additionally, TSPA-SR, Section 3.4.1.3 provides no indication regarding which range was used.

**Table 10-1: Stress Corrosion Cracking**

<p><b>Model Purpose:</b> This process-level model accounts for the possibility of SCC of the drip shield, the WP outer barrier, and the stainless steel structural material. Abstracted models have been developed for SCC of the WP outer barrier (Alloy 22). These abstracted models include: 1) a threshold stress for initiation; 2) a crack growth rate as a function of stress and local exposure conditions; 3) crack density; and 4) crack morphology. Crack morphology includes a description of the size of openings. The abstracted models are in a form that is suitable for input to the WAPDEG analysis, and include the uncertainty and variability of the above processes.</p>				
Summary	Source	Treatment	Basis	Impact
<b>Conceptual Model</b>				
Analysis of manufacturing defects and failure modes that may lead to early failure of a WP	Literature survey	The AMR on early failure includes a literature review directed towards obtaining information on the rate of manufacturing defect-related failures in various types of welded metallic containers, the types of defects that produce these failures, and the mechanisms that cause defects to propagate to failure. Types of defects applicable to the current WP design are identified. For each applicable type of defect, the probability of its occurrence on a WP is estimated. Potential consequences to the long-term performance of the WP if the defect is present are discussed.	Results of a literature review performed to determine the rate of manufacturing defect-related failure for various types of welded metallic containers. In addition to providing examples of the rate at which defective containers occur, this information provides insight into the various types of defects that can occur and the mechanisms that cause defects to propagate to failure. In summary, eleven generic types of defects were identified.	Determines the number of possible defect locations on the WP closure weld surface.
Threshold Stress Intensity Model	One of two alternative conceptual approaches for modeling SCC.	SCC initiates at pre-existing flaws that develop during fabrication of the WP, or at flaws that develop during localized corrosion. Values of $K_{ISCC}$ are based upon data published in the technical and scientific literature, or measurements made with the double cantilever and compact tensions beam techniques.	This model is based on the theory that there exists a threshold value of the stress intensity factor ( $K_{ISCC}$ ) such that no growth occurs in a crack having a stress intensity factor ( $K_I$ ) less than the threshold value.	Not used in TSPA-SR. Analyses indicate that SCC cracks will never penetrate when using this approach. Conservatively chosen not to implement this approach.

Slip Dissolution or Film Rupture Model	One of two alternative conceptual approaches for modeling SCC.	SCC is initiated if the threshold stress is exceeded on a smooth surface. Then, the SCC propagation rate is calculated as a function of local environment and stress intensity factor. The time-to-failure is determined by integrating the calculated propagation rate.	This model relates crack advance to the metal oxidation that occurs when the protective film at the crack tip is ruptured. This slip dissolution or film rupture model is described in a subsequent section. In this case, the existence of a nominal threshold stress for SCC initiation on a smooth surface ( $\sigma_{\text{threshold}}$ ) is assumed.	This conceptual approach was implemented into TSPA and results in initial breach of the WPs.
<b>Parameters and Inputs</b>				
Uncertainty and variability of residual stresses in the WP.	Finite element structural analyses described in Section 6.2.2.5 of AMR No. ANL-EBS-MD-000005	Calculated residual stress is the mean with a normal distribution bounded by 3 std dev. For welds not subjected to stress mitigation techniques, uncertainty range is $\pm 35\%$ of the yield strength. For the inner lid of the outer barrier, uncertainty range is $\pm 20\%$ . For welds subjected to stress mitigation techniques, uncertainty range is $\pm 5\%$ .	Literature data survey results	Determines the distribution of stress along the circumference of the closure welds. Ultimately affects initiation of SCC cracks and propagation rates using the slip dissolution model.
Density and distribution of incipient crack and crack sizes for the slip dissolution model.	Section 6.5.2 (AMR No. ANL-EBS-MD-000005)	Assumed that every corrosion patch on a WP one incipient crack. An exponential distribution of incipient cracks with max possible size of 0.05 mm and a median size of 0.02 mm and the corresponding complementary cumulative probability function.	Assumptions – no definitive basis given.	Impacts the number of SCC cracks that can occur on a WP and propagation rates.
Approach for treating manufacturing defects in closure-lid welds	Section 6.2 (AMR No. ANL-EBS-PA-000004) – Literature survey of container and piping defects	Uncertainty is included for the parameters of 1) flaw detection distribution ( $b$ and $v$ ), where $b$ and $v$ are uniform distributions, and 2) the fraction of surface breaking flaws ( $\psi$ ), also a uniform distribution.	Results of literature survey	Sufficiently bounds the flaw data observed in the literature results. Identifies the number of incipient cracks on the WP surface.

Approach for treating stress and stress intensity profiles in closure-lid welds.	Section 6.3 (AMR No. ANL-EBS-PA-000004) – Non-linear elasto-plastic finite element stress analyses simulating residual stresses due to welding and stress mitigation techniques	Hoop stress and $K_I$ stress intensity factor profiles are developed as a function of angular location and depth from the surface of the closure-lid welds.	Results of non-linear elasto-plastic finite element stress analyses that define the spatial distribution of residual stresses in the closure weld due to welding and stress mitigation techniques	Sufficiently bounds the results of the finite element stress analyses of the closure-lid welds. Impacts crack initiation and crack growth rates.
Approach for including the slip dissolution model to simulate SCC crack advancement	Section 6.4 (AMR No. ANL-EBS-PA-000004) - SCC crack growth rate tests	Uncertainty with the crack growth rate is captured with the uncertainties in the model parameters, i.e., $n$ and $K_I$ . $K_I$ profiles are represented with a normal distribution bounded at three std dev from the mean profile. $n$ is coarsely defined as uniform distribution.	Results of non-linear finite element stress analyses and SCC crack growth tests. As described above, the non-linear finite element analyses set the spatial distribution of residual stresses at the closure weld, which are used in determination of the stress intensity factors, $K_I$	Sufficiently bounds experimental and analytical results for SCC. Impacts the rate of crack growth.
Threshold stress for crack growth initiation in the slip dissolution model	Section 6.4.3 (AMR No. ANL-EBS-PA-000004) - Literature data for yield strength of Alloy 22	Uncertainty in the threshold stress is represented as uniform distribution of 20 to 30 percent of the yield strength	Literature data for yield strength of Alloy 22	Impacts the initiation of SCC using the slip dissolution model.
<b>Variability</b>				
Variability in Hoop Stress	Section 6.2.2 (AMR No. ANL-EBS-MD-000005) – finite element modeling and literature information	The hoop stress is assumed to vary both through the thickness of the closure lids and around the circumference of the closure weld.	Basis is ANSYS finite element results and literature information regarding austenitic stainless steel piping.	Stress distribution in the closure welds.
<b>Results</b>				
Threshold stress for initiation	AMR No. ANL-EBS-MD-000005 and AMR No. ANL-EBS-PA-000004	Distribution of threshold stress for crack growth initiation – 20% to 30% of yield stress	Conservative estimate	Initiation of SCC using the slip dissolution model

Crack growth rate as a function of stress and local exposure conditions	AMR No. ANL-EBS-MD-000005	Distributions of crack growth coefficients, $\bar{A}, \bar{n}$	Bases provided in development of the slip dissolution model in Section 6.4 of the AMR.	Rate of SCC crack growth using the slip dissolution model.
Abstraction of Stress and Stress Intensity Factor Profile in WP Closure Welds	No. ANL-EBS-PA-000004	Distributions of stress & stress intensity factor profiles in WP closure welds	Abstraction of results presented in AMR No. ANL-EBS-MD-000005	Initiation of SCC using the slip dissolution model
Abstraction for Manufacturing Defects in WP Closure Welds	No. ANL-EBS-PA-000004	Distributions of size of incipient cracks and manufacturing defects	Abstraction of results presented in AMR No. ANL-EBS-MD-000005	Density of cracks in closure weld patches.

INTENTIONALLY LEFT BLANK

## 11.0 Integrated Waste Package Degradation Model

### 11.1 Purpose of Model/Intended Use

The purpose of developing the WAPDEG is to permit analysis of WP and drip shield corrosion degradation as a function of exposure time under exposure conditions anticipated in the repository. WAPDEG is an integrated, system-level model that includes all degradation modes expected to affect the long-term performance of the WPs and drip shields. WAPDEG is essentially an abstracted model that integrates the various abstractions of the process models for the corrosion degradation processes considered in supporting AMRs.

The output from the WAPDEG analysis is a set of profiles for the failure (i.e., initial breach) and subsequent number of penetration openings in the WP and drip shield as a function of time. WAPDEG is used directly within the TSPA-SR model. Hence, these outputs are intermediate TSPA results. In the TSPA analysis, these results are used as input for the waste form degradation model and the radionuclide release from failed WPs model.

The various corrosion processes integrated into the WAPDEG model have been studied for many years for many different types of metals. As such, modeling these corrosion modes is not considered difficult or unique. However, integrating the models of the various processes into a system-level model, applying this model to a large number of WPs, and using the model to analyze performance over very long time periods is unique.

### 11.2 Model Relations

Details regarding the WAPDEG model are documented in the *WAPDEG Analysis of Waste Package and Drip Shield Degradation* (ANL-EBS-PA-000001) AMR. As discussed above, WAPDEG integrates the abstraction models developed for the various corrosion modes. These abstractions are documented in several documents, listed below and shown schematically in Figure 11-1, Model Relations for the Waste Package Degradation Model (WAPDEG).

- *Abstraction of Models for Pitting and Crevice Corrosion of Drip Shield and Waste Package Outer Barrier* (ANL-EBS-PA-000003) – Review and analyze information from process-level models relevant to pitting and crevice corrosion of the drip shield and WP outer barrier in order to develop abstracted models for inclusion in the WAPDEG WP performance model.
- *Calculation of General Corrosion Rate of Drip Shield and Waste Package Outer Barrier to Support WAPDEG Analyses* (CAL-EBS-PA-000002) – Produce cumulative distribution functions representing the general corrosion rate distributions for the drip shield (titanium grade 7) and the WP outer barrier (Alloy 22).

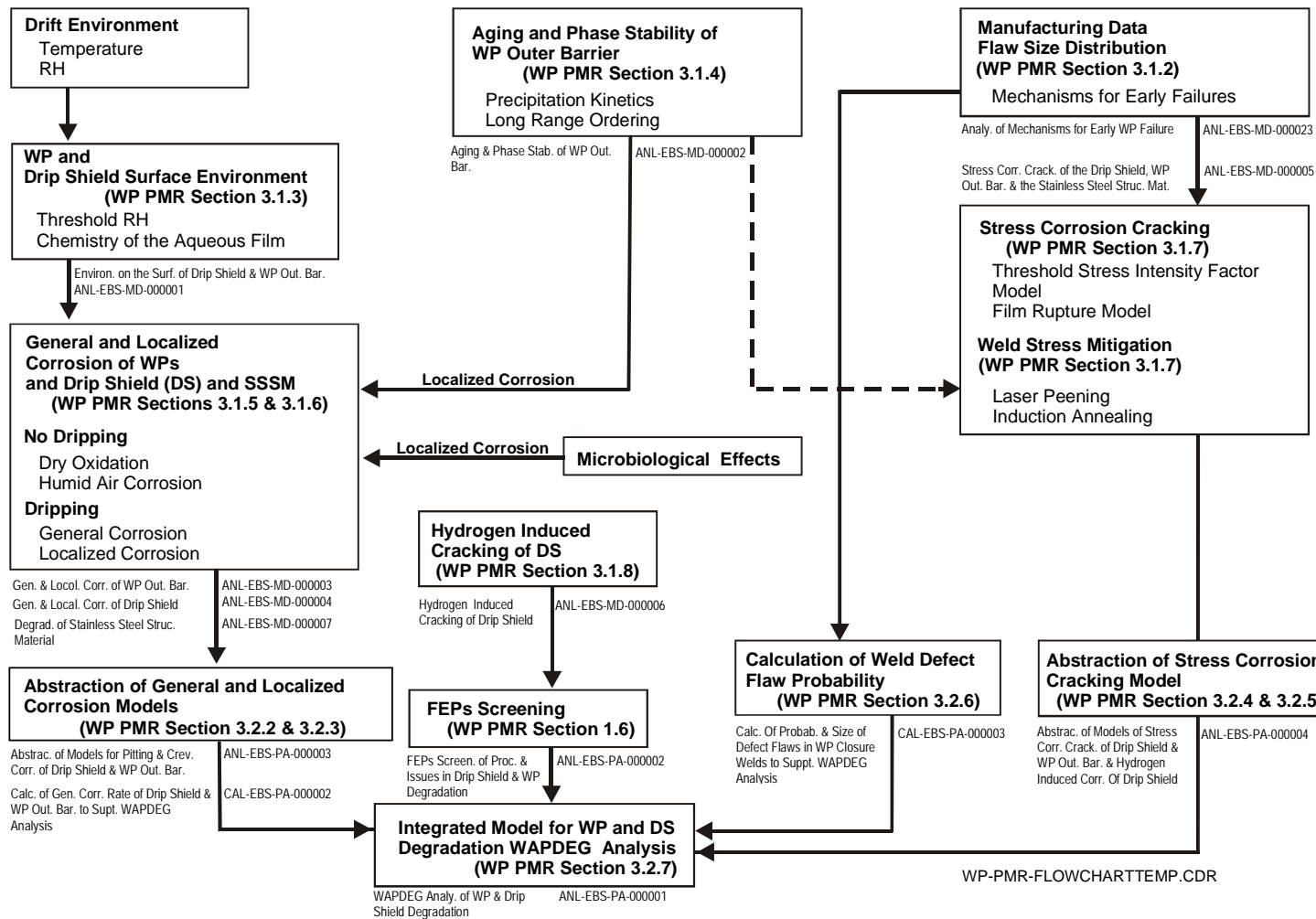


Figure 11-1: Model Relations for the Waste Package Degradation Model (WAPDEG)

- *Abstraction of Models of Stress Corrosion Cracking of Drip Shield and Waste Package Outer Barrier and Hydrogen-Induced Corrosion of Drip Shield* (ANL-EBS-PA-000004) – Develop abstracted models of SCC of the WP outer barrier and hydrogen induced cracking of the drip shield for use as input into the WAPDEG model.
- *Calculation of Probability and Size of Defect Flaws in Waste Package Closure Welds to Support WAPDEG Analysis* (CAL-EBS-PA-000003) – Develop distributions representing the frequency of occurrence and size of flaws potentially found in WP closure welds.
- *Abstraction of Models for Stainless Steel Structural Material Degradation* (ANL-EBS-PA-000005) - Review and analyze information from process-level models relevant to general, pitting, and crevice corrosion of the stainless steel structural material in order to develop abstracted models for inclusion in the WAPDEG WP performance model.

### 11.3 Model Structure

Figure 11-2, Waste Package Degradation Model (WAPDEG) Structure, depicts the various elements that comprise the WAPDEG model. Shown are those elements that comprise the conceptual and representational models, the various parameters needed, and the modeling results. Each is discussed in more detail below. These discussions are slightly edited texts obtained from the various AMRs cited and the WAPDEG PMR.

#### A. Conceptual Model

Conceptual models of each of the corrosion processes are presented in supporting AMRs and summarized in companion papers. The *WAPDEG Analysis of Waste Package and Drip Shield Degradation* AMR presents the integrated conceptual model of WP degradation.

The WAPDEG model was developed to model the current WP and drip shield design. The drip shield is comprised of titanium grade-7. The WP design consists of a double-wall WP made from an Alloy 22 outer container and a 316 nuclear grade stainless steel inner container. A dual closure-lid design has been adopted for the closure-end of WP outer barrier. That is, there is one Alloy 22 lid on one end of the outer barrier and two Alloy 22 lids on the closure end of the outer barrier. This dual closure-lid design was adopted to mitigate the potential for early failure of the closure lid weld regions by SCC. There is a physical “gap” between the two closure-lids. Thus, any SCC cracks penetrating the outer closure-lid stop at the gap between the closure-lids. The inner closure-lid welds are then subject to the environment of the emplacement drift, SCC initiation, and subsequent crack growth.

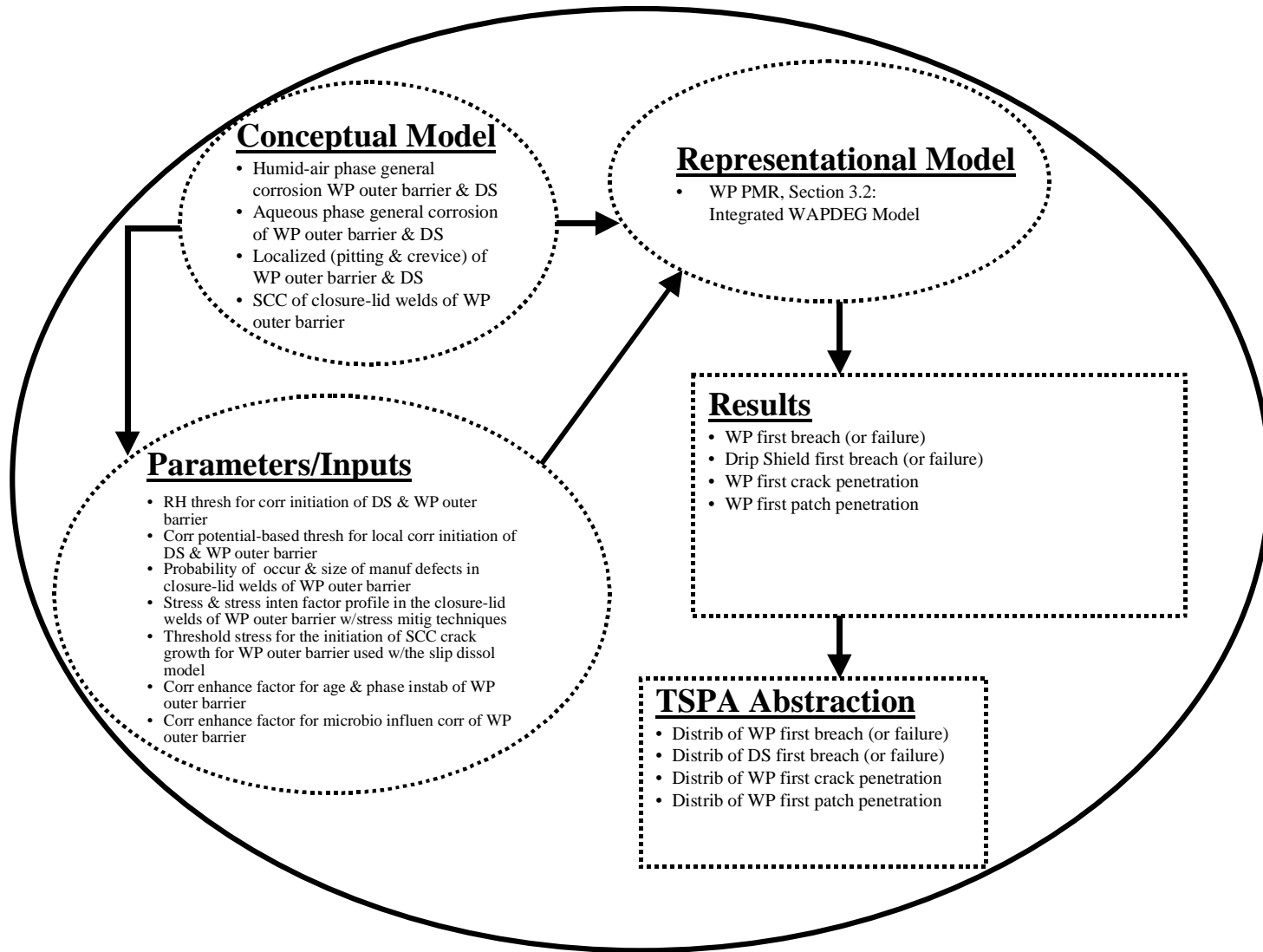


Figure 11-2: Waste Package Degradation Model (WAPDEG) Structure

WAPDEG models various types of corrosion mechanisms that may occur on a WP and drip shield as a function of the exposure time and conditions. (For convenience of discussion in this paper, the drip shield is considered an integral part of the WP. Except where it is necessary, no separate discussion is given for the drip shield). In the nominal case analysis of TSPA-SR, the WP outer barrier and drip shield were included in the WP degradation analysis. The stainless steel inner shell, whose primary purpose is to provide structural support to the WP, is not expected to provide any substantial time period of waste-containment performance after an initial breach of the WP outer barrier. Once exposed to corrosive conditions, the stainless steel inner shell is expected to fail by localized corrosion and SCC in a relatively short time period (see *Abstraction of Models for Stainless Steel Structural Material Degradation*). Because of this, no performance credit is taken for the stainless steel inner shell in the waste package degradation analyses. However, in reality the inner shell would provide “some” waste containment performance after breach of the WP outer barrier, and would also serve as a barrier to radionuclide transport after WP failure. The potential performance credit of the stainless steel inner shell is ignored in the nominal TSPA-SR analysis. This is a conservative modeling approach.

The corrosion modes that were included in the WAPDEG model are:

- Humid-air phase general corrosion of drip shield
- Aqueous phase general corrosion of drip shield
- Localized (pitting and crevice) corrosion of drip shield
- Humid-air phase general corrosion of WP outer barrier
- Aqueous phase general corrosion of WP outer barrier
- Localized (pitting and crevice) corrosion of WP outer barrier
- SCC of closure-lid welds of WP outer barrier

The exposure condition parameters that were considered were RH and temperature at the WP surface, seepage into the emplacement drift, and chemistry of the seepage water. In the WAPDEG analysis, the humid-air corrosion condition occurs when there is no dripping water contacting the WP surface and the RH at the WP surface is equal to or greater than the no-drip threshold RH (i.e., the threshold RH in the absence of drips). The aqueous corrosion condition requires the presence of dripping water and the RH at the WP surface to be equal to or greater than the drip threshold RH (i.e., the threshold RH in the presence of drips). In the current analysis, the no-drip and drip threshold RH distributions are identical.

In the WAPDEG analysis the WP (or drip shield) surface is discretized into many subareas referred to as “patches.” It is at the patch level that corrosion degradation processes are modeled (i.e., the relevant corrosion model parameter values and/or corrosion rates are sampled and applied to each patch). A schematic showing the patch conceptual modeling approach is shown below. This approach allows for representation of potentially “variable” degradation processes on the patches composing a single WP. For example, patches contacted by dripping water (those marked with “s”) could be subject to localized corrosion depending on the exposure conditions (e.g., chemistry of contacting water, primarily pH) that those patches experience. Patches with closure-lid welds (those marked with “y”) could be subject to SCC depending on the stress state

and exposure conditions. In addition, the general corrosion rate may vary over the WP surface. This potential variability is represented by populating the general corrosion rate over the patches.

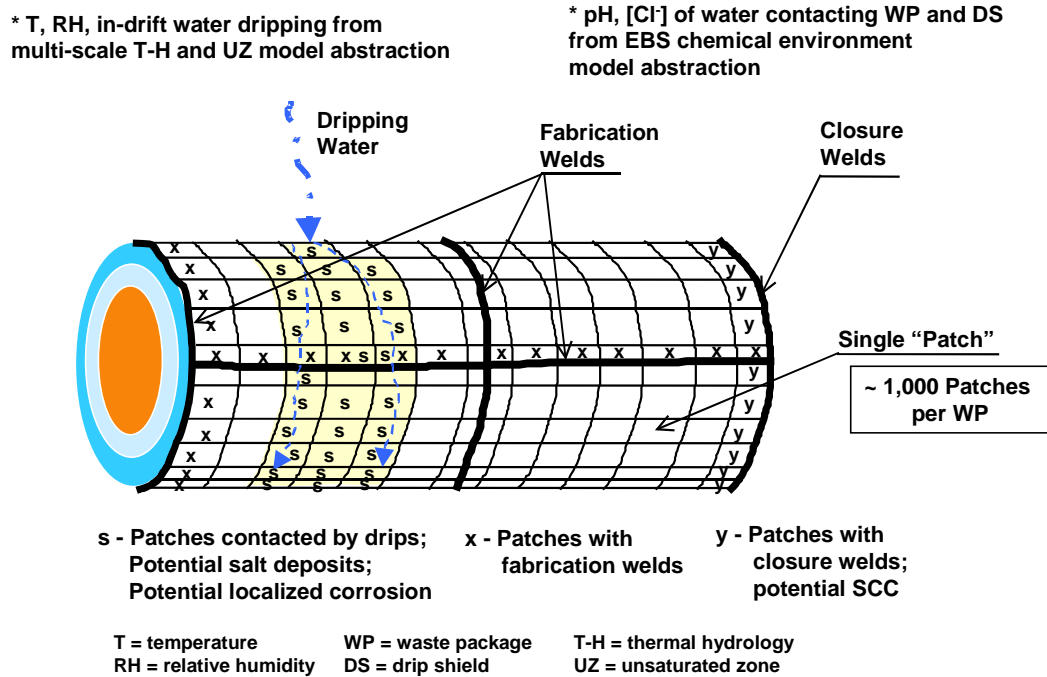


Figure 11-3, Logic Flow Diagram for the WAPDEG Model, shows a logic flow diagram for the WAPDEG model for WP (or drip shield) degradation analysis. In Figure 11-3, each of the gray boxes represents a model abstraction or model abstractions. The logic flow repeats for a drip shield, if included in the analysis, and each layer of the WP. The logic is applied to each patch.

### Exposure Conditions

Exposure conditions that are included are temperature and RH at the WP (and drip shield) surface, in-drift dripping water, and pH of the water contacting WP (and drip shield). The temperature and RH histories at the WP and drip shield surfaces are provided by the multi-scale thermal-hydrologic model abstraction. The evolution of pH of solution contacting WP is provided by the EBS chemical environment abstraction.



## **Humid Air and Aqueous General Corrosion**

In the analysis, the WP surface RH is compared to the threshold RH ( $RH_{th}$ ) for corrosion initiation. The  $RH_{th}$  is based on the deliquescence point of pure  $\text{NaNO}_3$  salt as discussed in a companion report. If the surface RH becomes greater than or equal to the threshold RH, the WP (or drip shield) undergoes corrosion. Depending on whether the WP (or drip shield) is dripped on or not, it could undergo different corrosion degradation modes. In the current analysis, the same threshold RH is used for both the dripping and no-drip conditions. Both the upper and under sides of drip shield are assumed subject to corrosion if the initiation threshold is met, that is, if the RH on the drip shield is equal to or greater than the threshold RH. This is because the both sides are exposed to the exposure conditions in the emplacement drift.

WPs that are not dripped on undergo humid-air corrosion during the entire time that the threshold RH is exceeded. Under humid-air conditions, the WPs undergo general corrosion and eventually fail by gradual thinning of the container wall. No localized corrosion occurs in the absence of dripping water.

For a WP (or a drip shield) that is dripped on, the wetted area (or patches) of the WP is assumed to undergo aqueous corrosion if the RH at the surface is greater than the threshold RH. Again, the same threshold RH is used for both the dripping and no-drip conditions. It is assumed that the entire surface of WP (or drip shield) is wetted by the drips if it is dripped on. This is a conservative assumption. While the drip shield is operative (i.e., not failed), the WP underneath the drip shield is assumed to undergo humid-air corrosion. General corrosion occurs all the time under aqueous corrosion condition.

For the WP outer barrier and drip shield, the current model assumes the same general corrosion rate distribution for both humid-air general corrosion and aqueous general corrosion (i.e., regardless of whether it is dripped on or not).

## **Localized Corrosion**

Initiation of localized (pitting and crevice corrosion) corrosion is dependent on the local exposure environment on the wetted patches. It is assumed that localized corrosion of the drip shield and WP outer barrier can initiate only under dripping conditions. This is because of the necessary presence of aggressive ions (such as chloride) in order to initiate and sustain pit and crevice growth and because the only mechanism for these species to gain ingress to the drift is through drips. Localized corrosion of a patch is assumed to initiate if the corrosion potential ( $E_{corr}$ ) of the patch is greater than or equal to the “threshold” critical corrosion potential ( $E_{crit}$ ) sampled for the patch. After initiated, localized corrosion continues while  $E_{corr} \geq E_{crit}$ . If  $E_{corr}$  becomes less than  $E_{crit}$ , or dripping ceases, localized corrosion stops.

## **SCC**

As indicated in the logic flow diagram, the inputs to the SCC analysis are: 1) the area subject to SCC, such as the closure-lid weld regions as in the current analysis; 2) stress and stress intensity factor ( $K_I$ ) versus depth of the affected area; 3) SCC crack propagation model (slip dissolution

model or threshold stress intensity factor ( $K_{ISCC}$ ) model); 4) threshold stress for crack propagation; and 5) manufacturing defect occurrence and size in the affected area.

Both the slip dissolution model and the threshold stress intensity factor model have been incorporated in the WAPDEG model. However, as recommended in supporting analysis (*Abstraction of Models of Stress Corrosion Cracking of Drip Shield and Waste Package Outer Barrier and Hydrogen-Induced Corrosion of Drip Shield*), the slip dissolution model was used to access the SCC degradation of the WP outer barrier.

For SCC analysis with the slip dissolution model, the following criteria must be met before initiating SCC on a patch: 1) the stress intensity factor ( $K_I$ ) must be positive; and 2) the stress state at the crack tip must be greater than or equal to the threshold stress. In the WAPDEG analysis, for those patches with a compressive stress zone (or layer) in their outer surface, the compressive stress zone must be removed by general corrosion before SCC can initiate. The delay time depends on the compressive zone thickness and the general corrosion rate sampled for the patch. The same SCC model and inputs are applied for both humid-air and aqueous conditions.

The drip shield is assumed to be fully annealed before it is placed in the emplacement drift. The drip shield could be subject to rockfall-induced SCC and through-wall cracks. However, those degradation processes are not considered in the current nominal case analyses as discussed below. Likewise, all the fabrication welds in the waste container, except the welds for the closure lids, are assumed fully annealed and thus not subject to SCC. Therefore, only the closure-lid welds were considered in the SCC analysis.

In addition, all pre-existing manufacturing defects in a patch are assumed all surface-breaking. The manufacturing defects considered in the current analysis include both the initially surface-breaking and embedded defects (which are conservatively assumed to be surface-breaking). The defects are assumed to grow at the general corrosion rate sampled for the patch. This is based on the modeling assumption that the same exposure condition that a patch experiences during a given time step is also applicable to the interior of the defects in the patch. Growth of the defects at the general corrosion rate of the patch is a highly conservative assumption. Patches with pre-existing defects would be subject to SCC earlier than other patches without defects.

### **Microbial Influenced Corrosion**

For microbiologically influenced corrosion, process-level models recommend the use of a threshold RH of 90 percent. However, the WAPDEG model conservatively assumes that microbiologically influenced corrosion is possible if RH at the surface is greater than the threshold RH for corrosion initiation. This conservatism was necessary due to input limitations of the WAPDEG software. The effect of microbiologically influenced corrosion is modeled with a corrosion rate multiplier (enhancement factor), which is applied to the general corrosion rate of the barrier (both humid air and aqueous). The microbiologically influenced corrosion enhancement factor is applied to the entire WP outer barrier surface whenever the RH is above the threshold RH (i.e., corrosion initiation threshold RH).

The drip shield is assumed not to be subject to microbiologically influenced corrosion under expected repository exposure conditions.

The potential for microbiologically influenced corrosion on localized corrosion is represented with the same corrosion rate enhancement factor as used for general corrosion

### **Aging and Phase Instability**

The current model assumes that the Alloy 22 WP outer barrier is subject to aging and phase instability under expected repository conditions. The effect is modeled with a corrosion rate multiplier (enhancement factor) that is applied to the general corrosion rate (both humid air and aqueous). The drip shield is assumed not subject to aging and phase instability. The potential for aging and phase instability effects on localized corrosion is represented with the same corrosion rate enhancement factor as used for general corrosion

### **Inside-Out Corrosion**

When a WP fails, the WAPDEG model also considers corrosion degradation of the WP from the inside-out corrosion. Inside-out corrosion will not occur prior to WP failure due to the inert environment inside intact WPs. The inside-out corrosion analysis includes general corrosion and localized corrosion of the WP outer barrier. The inside-out corrosion would cause penetrations by general and localized corrosion in addition to those by the outside-in corrosion only. The inside-out general corrosion is assumed to initiate at the time of the WP failure. Like the outside-in localized corrosion, initiation of the inside-out localized corrosion is based on the corrosion potential and critical corrosion potential, which are a function of the pH of water inside the failed WP (as determined by the in-package chemistry model). The in-package water chemistry results from degradation of the waste form and other internal structural materials (such as basket materials).

### **Other Considerations**

The WAPDEG model does not include the radiolysis-enhanced corrosion of WP outer barrier and drip shield because the materials are not subject to radiolysis enhanced corrosion under the repository conditions. Also the current model does not consider rockfall induced stress states, which could lead to SCC of the drip shield, or HIC of the drip shield. These processes would result in through wall cracks which will continue to corrode at very low passive corrosion rates until the gap region of the tight crack opening is “plugged” by the corrosion product particles and mineral precipitates, such as carbonate, present in the water. Any water transport through this oxide/salt filled crack area will be mainly by diffusion-type transport processes. Thus, the effective water flow rate through cracks in the drip shield would be expected to be extremely low and should not contribute significantly to the overall radionuclide release rate from the underlying failed WP.

### **Spatial Variability**

For most of the degradation models and parameters used, data and analyses are available to quantify their uncertainty and variability. Thus, uncertainty and variability were represented

explicitly in the WAPDEG analysis. Variability in the degradation of the WPs to be modeled is represented by allocating the total variability variance of the individual degradation models and their parameters to WP-to-WP variability and to patch-to-patch variability within a single WP. For general corrosion, the uncertainty and variability are not quantifiable and the variance in the general corrosion rate is considered to represent a mix of uncertainty and variability. The fraction of the total variance due to uncertainty was treated as an uncertain parameter and sampled randomly for each realization.

## **A. Parameters**

The majority of input parameters used in the WAPDEG model are developed in supporting abstraction model AMRs identified above. The key parameters are summarized below.

### **Humid-Air and Aqueous General Corrosion Rates**

A probability distribution of general corrosion rates, applicable to both humid-air and aqueous conditions, was developed in the *Calculation of General Corrosion Rate of Drip Shield and Waste Package Outer Barrier to Support WAPDEG Analyses* AMR. The distribution is considered a mix of uncertainty and spatial variability of the general corrosion rate.

The maximum general corrosion rate for Alloy 22 was set to  $7.30\text{E-}5$  mm/year. This assumed upper bound is slightly greater than the maximum penetration rate of  $7.25\text{E-}5$  mm/year observed in the Long-Term Corrosion Test Facility. The maximum general corrosion rate of Titanium Grade 7 was set to  $3.25\text{E-}4$  mm/year. This assumed upper bound is slightly greater than the maximum penetration rate of  $3.19\text{E-}4$  mm/year observed in the Long-Term Corrosion Test Facility.

The relationship between the critical threshold RH and exposure temperature is based on the assumption of the presence of a sodium nitrate ( $\text{NaNO}_3$ ) salt film on the WP and drip shield surface and the deliquescence point of the salt as documented in the Analyses and Models Report entitled *Environment on the Surfaces of the Drip Shield and Waste Package Outer Barrier* AMR.

### **Localized Corrosion**

The model parameters regarding localized corrosion are presented in the *Abstraction of Models for Pitting and Crevice Corrosion of Drip Shield and Waste Package Outer Barrier* AMR. Two localized corrosion initiation criteria are considered; one representing the localized corrosion initiation criterion for the WP outer barrier (Alloy 22) and the other for the localized corrosion initiation criterion for the drip shield (Titanium Grade 7). Cyclic polarization measurements were made in several synthetic concentrated J-13 waters. For each cyclic polarization curve obtained, the critical potential for localized corrosion initiation,  $E_{crit}$ , and the corrosion potential,  $E_{corr}$ , were determined. The potential difference between  $E_{crit}$  and  $E_{corr}$  (i.e.,  $\Delta E = E_{crit} - E_{corr}$ ) was then fit to a function of relevant exposure parameters. As discussed above, localized corrosion initiates if  $\Delta E < 0$  (i.e.,  $E_{crit} < E_{corr}$ ). The following relation was used, with coefficients obtained through data regression (coefficients  $c_i$  and  $\epsilon$  - the error term). Of interest is that the only important environmental parameter was found to be the water pH. The regression showed no dependence on other environmental parameters, such as the  $\text{Cl}^-$

concentration and temperature. In application of this model in WAPDEG, the pH is obtained from the in-drift chemistry model.

$$\Delta E = c_0 + c_1 \bullet pH + c_2 \bullet pH^2 + \epsilon$$

A set of assumptions were employed in the model abstraction. Key assumptions are described below.

- “Threshold Potential 1” was used as the critical potential above which localized corrosion can initiate. This is the lowest (most conservative) of the various critical thresholds identified in the test data.
- For both the WP outer barrier (Alloy 22) and the drip shield (Titanium Grade 7), it was assumed that  $\Delta E$  varied linearly with relevant exposure parameters. However, as noted above, the regression analyses indicated that  $\Delta E$  was only dependent on pH. Any dependence on other environmental parameters is captured in the error term  $\epsilon$ .

## SCC

The associated parameters in the slip dissolution model include two model parameters ( $A$  and  $n$ ), stress intensity factor ( $K_I$ ), threshold stress, and incipient crack density and size. The nominal-case SCC analysis also includes pre-existing manufacturing defects in the closure-lid welds. Abstractions for the manufacturing defects and the residual stress and stress intensity factor in the closure-lid welds are discussed in the *Abstraction of Models of Stress Corrosion Cracking of Drip Shield and Waste Package Outer Barrier and Hydrogen-Induced Corrosion of Drip Shield* AMR. The current abstractions for the model parameters ( $A$  and  $n$ ), threshold stress, and incipient cracks expand the process model analysis results to represent and quantify the uncertainty and variability associated with the parameters. The process model results are documented in the *Stress Corrosion Cracking of the Drip Shield, the Waste Package Outer Barrier and the Stainless Steel Structural Material* AMR. The abstraction assumes that statistical sampling of the associated model parameter values within their probable range capture the effects of the complex processes affecting the SCC crack initiation and growth rate.

As implemented in TSPA-SR, the  $n$  value is assumed to range uniformly from 0.75 to 0.84<sup>1</sup>. The  $A$  value is determined as a function of the  $n$  value. The hoop stress (the dominant stress in the closure lid welds) is represented by the following empirical relation as a function of depth:

$$\sigma_s(x) = A_0 + A_1 \bullet x + A_2 \bullet x^2 + A_3 \bullet x^3$$

The coefficients were determined through a regression fit to finite element stress analyses, as documented in the *Stress Corrosion Cracking of the Drip Shield, the Waste Package Outer Barrier and the Stainless Steel Structural Material* AMR.

---

<sup>1</sup> ICN 1 of the WAPDEG AMR considers different parameter ranges range and values than those used in TSPA-SR. For example,  $n$  is assumed to vary uniformly from 0.843 to 0.92.

The hoop stress profile varies along the circumference of the closure lid welds, and those represent the variability in the profiles on a given WP. The angular variation in the hoop stress,  $\sigma_t(x)$  (ksi), where  $x$  is the thickness (in inches), is given by,

$$\sigma_t(x, \theta) = \sigma_s(x) - (17.236892) \cdot (1 - \cos(\theta))$$

where  $\theta$  is angle around the circumference of the WP closure-lid welds ( $\theta = 0$  point arbitrarily chosen).

The uncertainty in the stress state and stress intensity factor is introduced through a scaling factor,  $sz(z)$  of the function form shown below.

$$sz(z) = \left( \frac{z \cdot YS \cdot F}{3} \right)$$

$YS$  is the yield strength,  $F$  is the yield strength scaling factor (a constant), and  $z$  is the magnitude of the uncertainty variation from the mean profile (sampled from a distribution). The yield strength scaling factor,  $F$ , defines the maximum uncertainty variation possible (the bounds). The value  $z$  is represented by a triangular distribution between  $\pm 3$  with a mode of 0. The TSPA-SR model<sup>1</sup> assumes that  $F$  equals 0.3. The *WAPDEG Analysis of Waste Package and Drip Shield Degradation* AMR considers three values for  $F$  (0.05 as optimistic, 0.10 as realistic, and 0.30 as conservative).

The stress relation, accounting for uncertainty, is given by

$$\sigma(x, \theta, z) = \sigma_t(x, \theta) + sz(z)$$

and the stress intensity factor relation is given by

$$K(x, \theta, z) = K_s(x) \frac{\sigma_t(Thck, \theta)}{\sigma_t(Thck, 0)} + 0.058534 \cdot sz(z) \cdot \sqrt{\pi \cdot x}$$

Note that this is the more conservative approach of the two alternative approaches discussed in the *Abstraction of Models of Stress Corrosion Cracking of Drip Shield and Waste Package Outer Barrier and Hydrogen-Induced Corrosion of Drip Shield* AMR.

The threshold stress is defined as the minimum stress at which cracks start growing. In the TSPA-SR model<sup>1</sup>, it is assumed to range uniformly from 20% to 30% of the yield strength of the material<sup>2</sup> (ICN 1 of the *WAPDEG Analysis of Waste Package and Drip Shield Degradation* AMR assumes a range of 10% to 40%).

Initial crack parameters were obtained from the *Calculation of Probability and Size of Defect Flaws in Waste Package Closure Welds to Support WAPDEG Analysis* AMR. For a given realization of WAPDEG within the TSPA-SR model, the model parameters are defect location parameter (uniform 1.6-5), defect scale parameter (uniform 1-3), and the fraction of defects

capable of propagation (uniform 0.3481 – 0.3622). These parameters are sampled independently to estimate the probability of a defect occurrence. Then the number of defects that appear on a patch is sampled stochastically as a Poisson random variable.

### **MIC/Aging and Phase Instability**

The WAPDEG model requires a threshold relative humidity for microbial activity and a corrosion rate multiplier to model the affect of microbial activity. The MIC corrosion enhancement factor is applied to the “effective” penetration rate (e.g., general and localized corrosion rate). The MIC enhancement factor has a uniform distribution between 1 and 2 (*General Corrosion and Localized Corrosion of Waste Package Outer Barrier* AMR). It was conservatively assumed that microbial influenced corrosion initiates at the same relative humidity threshold as general humid-air corrosion (conservative).

The WAPDEG model requires a corrosion rate multiplier to model the effect of aging and phase instability. The aging corrosion enhancement factor is applied to the “effective” penetration rate (e.g., general and localized corrosion rate). The aging/phase instability enhancement factor has a uniform distribution between 1 and 2.5 (*General Corrosion and Localized Corrosion of Waste Package Outer Barrier* AMR).

### **Spatial Variability**

As discussed above, spatial variability in the degradation of the WPs is represented by allocating the total variability of the individual degradation models and their parameters to WP-to-WP variability and to patch-to-patch variability within a single WP. For general corrosion, the uncertainty and variability are not quantifiable and the variance in the general corrosion rate is considered to represent a mix of uncertainty and variability. The fraction of the total variance due to uncertainty was treated as an uncertain parameter and sampled randomly for each realization.

The WAPDEG model makes use of a technique called Gaussian Variance Partitioning (GVP). Details regarding GVP are discussed further in this paper. For each realization of uncertainty, GVP separates the input general corrosion rate CDF, containing both uncertainty and variability, into two separate distributions, one that characterizes variability and another that characterizes uncertainty. Each distribution has only a fraction of the input CDFs total variance (i.e., if the fraction of the total variance due to uncertainty is U, then the fraction due to variability is 1-U).

The median value of the variability distribution is sampled from the uncertainty distribution. The fraction of the total variance due to uncertainty (U) is itself uncertain and is sampled from a uniform distribution between 0 and 1. The quantile at which to sample the median general corrosion rate is also uncertain and is sampled from a uniform distribution between 0 and 1. In this way the same sampling method is used for both WP materials to sample the uncertain space of possible general corrosion rate variability distributions. Although there is also no technical bases for this approach to uncertainty modeling, it does reflect that the variances of the general corrosion rate distributions are potentially due to uncertainty and variability, and the fraction of variance due to uncertainty and variability is itself uncertain.

## B. Representational Model

WAPDEG itself is a numerical model, hence it is the representational model. The abstracted representational models of the various corrosion modes are integrated into an overall system model. These representational models are discussed in the AMRs that support the *WAPDEG Analysis of Waste Package and Drip Shield Degradation* AMR. These representational models are summarized in companion papers on SCC and general/localized corrosion. The most significant numerical representation implemented into WAPDEG is the GVP technique to account for spatial variability. This discussion focuses on the GVP technique.

GVP starts with distributions that involve both uncertainty and variability. For general corrosion of the drip shield and WP outer barrier materials, these distributions are documented in the *Calculation of General Corrosion Rate of Drip Shield and Waste Package Outer Barrier* calculation. The GVP technique then works backward to obtain two separate distributions, one that characterizes variability and another that characterizes uncertainty. This is accomplished by assuming that uncertainty and variability are independent. If the mixed distribution is normally distributed, i.e.  $N(\mu, \sigma_\mu^2 + \sigma_v^2)$ , then it can be represented as a random variable  $\gamma$  having the form

$$\gamma = m + v$$

where  $m$  is a normal random variable with mean  $\mu$  and variance  $\sigma_\mu^2$ , and  $v$  is a normal random variable with mean zero and variance  $\sigma_v^2$ . Thus,  $\gamma$  is a random variable distributed around the mean  $\mu$  with a total variance given by the sum of the variances due to uncertainty and variability. If uncertainty is defined as the uncertainty in the mean value and variability as the variance about that mean, then  $\gamma$  can be alternatively parameterized as

$$\gamma \sim N(m, \sigma_v^2), \text{ where } m \sim N(\mu, \sigma_\mu^2)$$

The uncertain mean is represented by the random variable,  $m$ , which is normally distributed with mean,  $\mu$  and variance,  $\sigma_\mu^2$ . The random variable,  $\gamma$ , is then the convolution of the distributions of the random variable given by  $m$  and a random variable,  $v$ , which can be represented by the addition of two normal random variables as given above where

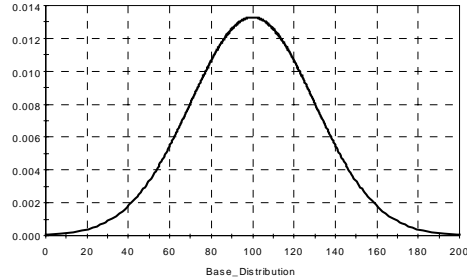
$$m \sim N(\mu, \sigma_\mu^2) \text{ and } v \sim N(0, \sigma_v^2)$$

Thus, given the distributions for  $m$  and  $v$ , a variability distribution is realized by sampling a value from the parameter uncertainty distribution and adding it to the mean zero variability distribution.

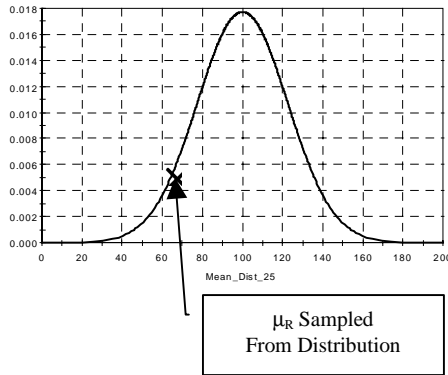
The figure below shows an example for a normal distribution with a mean of 100 and a variance of 30. In this example, 75% of the overall variance is assumed to represent uncertainty in the mean and 25% is assumed to represent spatial variability. In this example, the two distributions become:

$$m = N(100, 22.5^2) \quad v = N(0, 7.5^2)$$

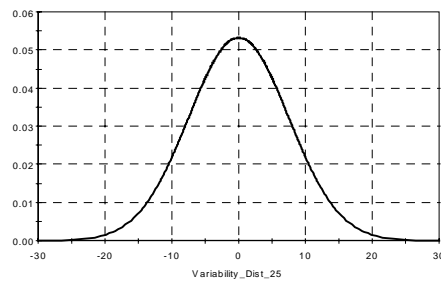
Original Distribution  
 $\mu=100, \sigma = 30$



Resulting Distribution  
 due to Uncertainty  
 $F = 25\%$



Resulting Distribution  
 of Spatial Variability  
 $F = 25\%$



Once this splitting has been completed, the next step is to sample a single value of the corrosion rate from the  $N(\mu, \sigma_u)$  distribution. As discussed above, the quantile at which to sample the median general corrosion rate is also uncertain and is sampled from a uniform distribution between 0 and 1. The resultant is shown schematically by the symbol  $\mu_R$  on the Figure above. This value is representative of the mean corrosion rate across all WPs and patches (e.g., mean of the spatially varying corrosion rate).

WAPDEG models a large number of WPs (400), each containing a large number of corrosion patches (1000). Next,  $\sigma_v$  is further split into a fraction that represents spatial variability from WP to WP ( $\sigma_{v-WP}$ ) and a fraction that represents spatial variability from corrosion patch to corrosion patch on a single WP ( $\sigma_{v-Patch}$ ). The degree of splitting is accomplished by sampling a factor,  $F_{var}$ , that is assumed to vary from zero to one.

$$N(0, \sigma_v) = N(0, \sigma_{v-WP}) + N(0, \sigma_{v-Patch})$$

$$\sigma_v = F_{var} \sigma_{v-WP} + (1 - F_{var}) \sigma_{v-Patch}$$

With this splitting accomplished, WAPDEG then determines two distributions. The first is  $N(\mu_R, \sigma_{v-WP})$  which is used to determine a mean corrosion rate ( $\mu_{WP}$ ) for each WP. A second distribution is then developed for each WP,  $N(\mu_{WP}, \sigma_{v-Patch})$ , that is used to populate each patch with its own individual corrosion rate.

The GVP technique is applied six times for different regions of the WP outer barrier to the distribution of general corrosion rates. These regions are:

- Base metal outer surface
- Base metal at half thickness (this results in re-sampling the corrosion rate after half of the material has been removed)
- Outer closure lid weld material outer surface
- Inner closure lid weld material outer surface
- Base metal inner surface (for inside-out corrosion)
- Inner closure lid weld material inner surface (for inside-out corrosion)

### C. Results

Section 6.5 of the *WAPDEG Analysis of Waste Package and Drip Shield Degradation AMR* presents analysis results. These results were generated from 100 realizations of WAPDEG to account for the uncertainty analysis of the uncertain corrosion parameters. Each WAPDEG realization corresponds to a complete WAPDEG run to represent the degradation variability for a given number of WP and drip shield pairs. Recall that WAPDEG is an integral part of the TSPA-SR model and each realization of the TSPA-SR model results in a realization of WAPDEG. Thus, the WP performance results shown in the TSPA-SR document are equivalent to the results presented in the AMR<sup>2</sup>.

The analysis results are presented for the upper and lower bounds, mean, and 95<sup>th</sup>, 75<sup>th</sup>, 25<sup>th</sup>, and 5<sup>th</sup> percentiles as a function of time. The results are summary statistics related to consideration of all 100 realizations. Results are presented for the following output parameters:

- WP first breach (or failure)
- Drip shield first breach (or failure)
- WP first crack penetration
- WP first patch penetration
- WP crack penetration numbers per failed WP
- WP patch penetration numbers per failed WP
- Drip shield patch penetration numbers per failed drip shield

---

<sup>2</sup> ICN 1 of the WAPDEG AMR considers two sets of input parameters, one for what is termed the “current WAPDEG model” and one for what is termed the “updated WAPDEG model.” The “current WAPDEG model” inputs are used in TSPA-SR.

Four sensitivities were also conducted to evaluate the impacts of parameters in the slip dissolution SCC model. The parameters investigated were the yield strength scaling factor, the stress threshold, and the flaw fraction.

Additional sensitivity studies are presented in TSPA-SR that show how various waste package degradation parameters affect the receptor dose rate (see Section 5.2.3). Parameters evaluated pertain to the SCC model and GVP.

#### **11.4 Discussion of Uncertainty/Variability Treatment**

An evaluation of uncertainty and variability treatment of the AMRs was performed for this exercise. For each AMR, the uncertainties/variabilities were identified and it was determined if a thorough treatment was performed. Thorough treatment was considered to be: identification, treatment, impact assessment, and clear presentation of the analysis and the propagation of uncertainty in the AMR. Table 1 is a synopsis of some of the uncertainties and variabilities identified in this exercise. The following discusses the treatment of uncertainty and variability within the WAPDEG model.

##### **A. Conceptual Model**

The WAPDEG model integrates the various abstracted models into an integrated model of waste package degradation. The development of the abstracted models is predicated by the conceptual models of the various corrosion modes. As such, WAPDEG inherently includes such conceptual uncertainties only if they manifest themselves in the abstracted models.

Two companion papers discuss the treatment of conceptual uncertainty for the various corrosion modes (general corrosion, localized corrosion, and SCC). The observations in these papers are reiterated below.

- For SCC, conceptual model uncertainty is considered through the use of two alternative conceptual models, a threshold stress intensity model and a slip dissolution model. Both models were fully developed and documented, including uncertainties in parameters. Bounding analyses were conducted and the results indicated that the threshold stress intensity factor approach would never result in failure of the WPs due to SCC. As such, a decision was made to only consider the slip dissolution model in TSPA. These results are clearly documented and the decision supported.
- Conceptual model uncertainty is not treated explicitly for general and localized corrosion. Rather, the conceptual models utilized are consistent with accepted theories of corrosion and available experimental evidence. In some instances less conservative theoretical models may be applicable, however data limitations preclude their selection (e.g., dry oxidation of Alloy-22).

In regard to overall WP performance, the most important conceptual uncertainty is the extrapolation of corrosion rates measured in the laboratory to many thousands of WPs over many

thousands of years. No temporal variability is assumed. No detailed process or representational models have been developed to support the extrapolation of laboratory data.

In regard to spatial extrapolation, it has been assumed that laboratory measured corrosion rates are applicable to all WPs in the repository. It is further assumed that the total variance in the measured general corrosion rates is a combination of true uncertainty and spatial variability. However, the uncertainty and variability are not quantifiable and the variance in the general corrosion rate is considered to represent a mix of uncertainty and variability. As discussed above, the fraction of the total variance due to uncertainty was treated as an uncertain parameter (ranging uniformly from 0 to 1) and sampled randomly for each realization through application of the GVP technique. Application of this technique results in an “average” WP performance result being representative of 50% variability and 50% uncertainty.

It may be argued that spatial variations in moisture, chemical conditions, surface properties, alloy composition, and stress state are among the potential sources of variability in the potential repository. These variations may occur over all length scales of interest including at the WP to WP and patch to patch levels. However, laboratory measurements to-date do not quantitatively support such variability. This may be a result of the very low corrosion rates for Ti-7 and Alloy 22 not showing any such dependencies over the period of time that the materials have been tested under Yucca Mountain relevant environmental conditions. It is recognized that efforts are underway to gather data using techniques designed to better characterize the variability in the general corrosion rate. As discussed below, the supporting *General Corrosion and Localized Corrosion of the Drip Shield* and *General Corrosion and Localized Corrosion of Waste Package Outer Barrier* AMRs suggest a different approach.

Although acknowledged as an uncertainty in the *WAPDEG Analysis of Waste Package and Drip Shield Degradation* AMR, the effects of the stainless steel inner WP material on the corrosion of Alloy-22 has not been assessed beyond application of the laboratory measured corrosion rates. For example, local water chemistry changes resulting from the corrosion of the stainless steel is not explicitly modeled.

## **A. Parameters**

All parameters used in the development of the WAPDEG model were implemented as developed in supporting AMRs, with the following exceptions (Section 6.3).

- **General Corrosion Rate Uncertainty Treatment** – The supporting AMRs (*General Corrosion and Localized Corrosion of the Drip Shield* and *General Corrosion and Localized Corrosion of Waste Package Outer Barrier*) are somewhat unclear in their recommendations for treating uncertainty in the general corrosion rate. First, these AMRs recommend that the entire distribution of measured corrosion rates for both Ti-7 and Alloy-22 be assumed as uncertainty. They then go on to recommend the use of triangular distributions for variability of each material. However, specific information regarding the implementation of these techniques is not provided in the supporting AMR. Possible approaches are discussed in the *WAPDEG Analysis of Waste Package and Drip Shield Degradation* AMR. Rather than applying these approaches, the GVP technique is used.

- The *WAPDEG Analysis of Waste Package and Drip Shield Degradation* AMR states “Although there is also no technical bases for this approach to uncertainty modeling, it does reflect that:
  - The variances of the general corrosion rate distributions are potentially due to uncertainty and variability, and
  - The fraction of variance due to uncertainty and variability is itself uncertain.”
- In addition, the AMR claims that the “GVP technique for the treatment of uncertainty is more reasonable than the approaches recommended in the process-level models.”
- Aging and Phase Instability and Microbiologically Influenced Corrosion Uncertainty Treatment – The supporting AMR recommended treating the ranges for the enhancement factors as 50% variability and 50% uncertainty. In the development of the WAPDEG model, it was assumed that the ranges represented 100% variability. This assumption was judged to be more conservative in terms of the first failure time of WP.
- The rationale for choosing different parameter values and ranges than those documented in the supporting AMRs is clearly documented in Section 6.3 of the *WAPDEG Analysis of Waste Package and Drip Shield Degradation* AMR.

### **C. Representational Model**

As discussed above, WAPDEG itself is a numerical model, hence it is the representational model. This includes the implementation of the GVP technique to model spatial variability. No representational uncertainty is quantified and all uncertainty in the model is treated through the use of uncertain input parameters. In the case of treating variability/uncertainty, the GVP technique is the only one applied. Although possible approaches for the other techniques recommended are described in the *WAPDEG Analysis of Waste Package and Drip Shield Degradation*, they were not implemented into WAPDEG as possible alternative representations.

### **D. Results**

As discussed above, results were generated from 100 realizations of WAPDEG to account for the uncertainty analysis of the uncertain corrosion parameters. Thus, documented uncertainties in the WAPDEG model are clearly evaluated through to the results, both within the *WAPDEG Analysis of Waste Package and Drip Shield Degradation* AMR and TSPA-SR.

### **11.5 Propagation of Uncertainty**

All uncertainties identified in supporting AMRs were clearly propagated into the overall WAPDEG model. A few exceptions exist where recommended parameter values were changed for use in WAPDEG. These exceptions (discussed above in Section IV.B), and their basis, are clearly documented in the *WAPDEG Analysis of Waste Package and Drip Shield Degradation* AMR.

A discrepancy exists regarding whether MIC can affect Ti-7 corrosion rates. The AMR entitled *WAPDEG Analysis of Waste Package and Drip Shield Degradation* states that the drip shield is not subject to MIC and references the *General Corrosion and Localized Corrosion of the Drip Shield* AMR as the basis for the assumption (section 5.8). However, the latter AMR clearly states that although MIC is not likely for Ti-7, the potential for it impacting corrosion rates cannot be ruled out and recommends using the MIC enhancement factors developed for Alloy-22.

The WAPDEG model, as presented in the *WAPDEG Analysis of Waste Package and Drip Shield Degradation* AMR, is an integral part of the overall TSPA-SR model. Thus, all uncertainties included in the WAPDEG model become part of the TSPA-SR model.

**Table 11-1: Waste Package Degradation Analysis:  
Integrated Model for Waste Package and Drip Shield Degradation**

<p><b>Model Purpose:</b> The WAPDEG model is the integrated model used for WAPDEG analysis. The abstractions of the process models for the corrosion degradation processes and the exposure condition parameters for the WPs and drip shields in the repository were incorporated into the WAPDEG Model. The output from the WAPDEG analysis is a set of profiles for the failure (i.e., initial breach) and subsequent number of penetration openings in the WP and drip shield as a function of time. In the TSPA analysis, these analysis results are used as input for waste form degradation analysis and radionuclide release analysis from failed WPs. The WAPDEG Model is used directly in the TSPA for WP degradation analysis.</p>				
Summary	Source	Treatment	Basis	Impact
<b>Conceptual Model</b>				
Humid-air phase general corrosion WP Outer Barrier & Drip Shield	Evaluation of standard corrosion models to determine relevant parameters.	The rates of general corrosion of the Alloy 22 and Ti Gr 7, over the range of repository-relevant exposure conditions, were determined to be insensitive to temperature, stress state, or water chemistry. In the WAPDEG conceptual model, the WP outer barrier could potentially be contacted by humid-air, dripping, and in-package (inside-out corrosion) water conditions. The general corrosion rate distribution provided for the Alloy 22 WP outer barrier applies to all these water conditions. In the WAPDEG conceptual model, the water condition above the drip shield could potentially have humid-air conditions followed by dripping water conditions followed by humid-air conditions. The general corrosion rate distribution provided for the drip shield applies to both humid-air and dripping water (aqueous) conditions. However, the variance of the general corrosion rate distribution is due to both uncertainty and variability, which differs for the two conditions. Therefore, two calls are made to the GVP DLL.	Treatment is appropriately conservative given the limited material specific data on corrosion processes.	General corrosion rates and WP failure times under humid-air conditions.
Aqueous phase general corrosion of WP Outer Barrier & Drip Shield	Evaluation of standard corrosion models to determine relevant parameters.	See discussion above.	See discussion above	General corrosion rates and WP failure times under aqueous conditions.

Localized (pitting & crevice) of WP Outer Barrier & Drip Shield	Analysis of test data to evaluate implementation of standard corrosion models.	Localized corrosion initiation for the WP Alloy 22 outer barrier can only occur when the WP surface is exposed to dripping water (see Section 5.4, AMR No. ANL-EBS-PA-000001). If $E_{crit1} < E_{corr}$ , then localized corrosion can initiate. As indicated by Figure 1 (Section 4.1.5, AMR No. ANL-EBS-PA-000001), localized corrosion of Alloy 22 cannot initiate at any pH based on the $4\sigma$ confidence interval. As discussed in Section 5.2 (AMR No. ANL-EBS-PA-000001), there is no localized corrosion initiation threshold or localized corrosion rate model for the drip shield implemented in the WAPDEG conceptual model. As shown in Figure 2 (Section 4.1.6, AMR No. ANL-EBS-PA-000001), localized corrosion of titanium grade 7 cannot initiate even at a pH of 14 based on the $3\sigma$ and $4\sigma$ confidence intervals.	Experimental test data supports conceptualization	Impact is minimal since environment is not expected to result in localized corrosion.
WP inside-out corrosion	Evaluation of standard corrosion models to determine relevant parameters.	The inside-out corrosion analysis includes general and localized corrosion of the WP outer barrier. The inside-out corrosion would cause penetrations by general and localized corrosion in addition to those by the outside-in corrosion only. The inside-out general corrosion is assumed to initiate at the time of the WP failure. Like the outside-in localized corrosion, initiation of the inside-out localized corrosion is based on the corrosion potential and critical corrosion potential, which are a function of the pH of water inside the failed WP	Conceptual assumption	Additional penetrations of the WP following first breach – influences radionuclide transport characteristics.
SCC of closure-lid welds of WP Outer Barrier	Evaluation of standard SCC models to determine relevant parameters.	Slip Dissolution Model Abstraction  Stress Intensity Factor Threshold Model (Alternative Conceptual Model)	Theory and observations regarding SCC support two conceptualizations.	Slip Dissolution Model is used in TSPA-SR. Stress Intensity Factor Threshold model is an alternative conceptual model. Stress Intensity Factor approach results in no SCC failures – conservative to consider only Slip Dissolution.
<b>Parameters and Inputs</b>				
WP outer barrier localized corrosion initiation threshold and rate abstraction model	Analysis of experimental data. AMR No. ANL-EBS-PA-000003	Localized corrosion initiation threshold is based on potentiodynamic polarization data for Alloy 22 measured in several repository-relevant solution compositions. Figure 1 (of ANL-EBS-PA-000001) is a plot of median potential difference given by Equation 1 (of ANL-EBS-PA-000001) as a function of pH. 3 and 4 std dev confidence intervals are also shown. The localized corrosion rates are represented as a log-uniform distribution (Table 2 of ANL-EBS-PA-000001)	Sufficiently bounds the experimental results on Alloy 22 localized corrosion initiation threshold and rates. Functional dependence on exposure parameters can be embodied in pH dependence.	Provides parameters and models for invoking localized corrosion of the WP outer barrier. No impact of uncertainties since current environmental conditions do not result in localized corrosion.

Drip shield localized corrosion initiation threshold and rate	Analysis of experimental data from literature. AMR No. ANL-EBS-PA-000003	Localized corrosion initiation threshold is based on potentiodynamic polarization data for Ti Gr 7 measured in several repository-relevant solution compositions. Figure 2 (of ANL-EBS-PA-000001) is a plot of median potential difference given by Equation 3 (of ANL-EBS-PA-000001) as a function of pH. The localized corrosion rates are uniformly (or rectangularly) distributed between the bounds specified in (Table 3 of ANL-EBS-PA-000001).	Sufficiently bounds the experimental results on Ti Gr 7 localized corrosion initiation threshold and rates.	Provides parameters and models for invoking localized corrosion of the drip shield. No impact of uncertainties since current environmental conditions do not result in localized corrosion.
Inputs from the manufacturing defect abstraction model	Results of literature survey of data characterizing manufacturing defects. AMR No. ANL-EBS-PA-000004	$b$ , location parameter for probability of non-detection: uniform distribution over the range of 1.6 - 5.0 mm. $V$ , the scale parameter for the non-detection probability: uniform distribution over the of 1 - 3. $\psi$ , the fraction of surface breaking flaws: uniform distribution over the range of 0.0013 - 0.0049.	Results of literature survey on manufacturing defects	Identifies probability of existence of surface breaking flaws and their size for use in the SCC model.
Stress and stress intensity factor profile abstraction model for the closure lid welds	Results of non-linear finite element analyses. AMR No. ANL-EBS-PA-000004	The stress and stress intensity factor profiles are presented here as a functions of depth in tabular (stress intensity factor) and polynomial (stress)	Bounds results of non-linear finite element analyses that specify the spatial residual stress distribution near the closure weld	Accounts for variation in hoop stress around circumference of the closure weld. Determines stress state of the weld material for use in the SCC model.
Inputs to the slip dissolution abstraction model	Results of literature survey. AMR No. ANL-EBS-PA-000004	Threshold stress: uniform distribution over the range of 0.2 - 0.3 fraction of the yield strength. $n$ , crack growth exponent: uniform distribution over the range 0.75 – 0.84.	Bounds results of literature survey	Impacts rate of crack growth using the Slip Dissolution Model.
Input for the general corrosion rate of the drip shield and WP outer barrier.	Laboratory testing – weight loss measurements. CAL-EBS-PA-000002	Corrosion Rate probability distributions for Alloy-22 and Ti-7. See discussion below regarding variability – Gaussian Variance Partitioning approach.	Laboratory measurements – weight loss tests.	General corrosion rate of Alloy-22 and Ti-7. Direct impact on WP failure time.
Input from the Drip Shield and WP outer barrier MIC abstraction model	MIC test results. AMR No. ANL-EBS-MD-000003 and AMR No. ANL-EBS-MD-000004.	General corrosion multiplier distribution: uniform distribution over the range 1.0 - 2.0. Supporting AMRs recommend treating range as half variability, half uncertainty. WAPDEG AMR considered range as all variability. See discussion below.	Range sufficiently bounds uncertainties in MIC effects on the general corrosion rate.  In addition, for the drip shield the supporting AMR (ANL-EBS-MD-000004) recommends using multiplier – WAPDEG AMR does not consider MIC for the drip shield, citing supporting AMR as basis.	Impacts general corrosion rate of the drip shield (not considered) and WP outer barrier.

Input from the WP outer barrier aging and phase instability abstraction model	Aging and phase stability test results. AMR No. ANL-EBS-MD-000003 and AMR No. ANL-EBS-MD-000004.	General corrosion multiplier distribution: uniform distribution over the range 1.0 - 2.5. Supporting AMRs recommend treating range as half variability, half uncertainty. WAPDEG AMR considered range as all variability. See discussion below.	Sufficiently bounds uncertainties in aging and phase stability effects on the general corrosion rate.	Impacts general corrosion rate of the WP outer barrier.
<b>Variability</b>				
GVP Technique	Methodology developed in WAPDEG AMR – ANL-EBS-PA-000001	GVP starts with distributions that involve both uncertainty and variability. For general corrosion of the drip shield and WP outer barrier materials, these distribution are documented in the CAL-EBS-PA-000002. The GVP technique then works backward to obtain two separate distributions, one that characterizes variability and another that characterizes uncertainty. A complete discussion of the technique is provided in the text.  Overall assumption is to assume that variance in the measured corrosion rates can be split with a fraction representing variability and the remainder uncertainty. This fraction is assumed to vary from 0 to 1 (or pure variability to pure uncertainty). Corrosion patches on the WP surface are then populated with corrosion rates that are sampled from distributions determined using the GVP technique.	Basis is that measured corrosion rates are likely to vary due to uncertainty and variability. No laboratory data to date quantitatively supports variability. However, low corrosion rates and duration of tests to-date may not be revealing any variability. Activities are ongoing in an attempt to better quantify.	The approach has a direct impact on the manner in which WPs fail over time. Impacts the distribution of first WP breach and the condition of the WPs post-breach.
MIC and aging/phase instability general corrosion enhancement factors.	MIC and aging/phase instability test results. AMR No. ANL-EBS-MD-000003 and AMR No. ANL-EBS-MD-000004.	Supporting AMRs provide ranges for enhancement factors and recommended treating range as half variability, half uncertainty. WAPDEG AMR considered range as all variability.	Basis is that assumption results in conservative WP performance – in terms of first WP breach.	Impacts the manner in which general corrosion rates are assigned to various WP patches – as discussed above, impacts the distribution of first WP breach and the condition of the WPs post-breach.
<b>Results</b>				
WP first breach (or failure)	WAPDEG AMR – ANL-EBS-PA-000001	Distribution of WP first breach (or failure). Different failure distributions as a function of time due to sampling of uncertain parameters and different GVP splits on variability/uncertainty.	WAPDEG Results using input parameters and application of GVP.	WAPDEG is directly coupled to the overall TSPA model – as such, these are direct input to the TSPA model. Impacts radionuclide releases from the waste form.
Drip Shield first breach (or failure)	WAPDEG AMR – ANL-EBS-PA-000001	Distribution of Drip Shield first breach (or failure). Different failure distributions as a function of time due to sampling of uncertain parameters and different GVP splits on variability/uncertainty.	WAPDEG Results using input parameters and application of GVP.	WAPDEG is directly coupled to the overall TSPA model – as such, these are direct input to the TSPA model. Impacts radionuclide transport through the EBS.

WP first crack penetration	WAPDEG AMR – ANL-EBS-PA-000001	Distribution of WP first crack penetration. Different failure distributions as a function of time due to sampling of uncertain parameters and different GVP splits on variability/uncertainty.	WAPDEG Results using input parameters and application of GVP.	WAPDEG is directly coupled to the overall TSPA model – as such, these are direct input to the TSPA model. Impacts radionuclide releases from the waste form.
WP first patch penetration	WAPDEG AMR – ANL-EBS-PA-000001	Distribution of WP first patch penetration. Different failure distributions as a function of time due to sampling of uncertain parameters and different GVP splits on variability/uncertainty.	WAPDEG Results using input parameters and application of GVP.	WAPDEG is directly coupled to the overall TSPA model – as such, these are direct input to the TSPA model. Impacts radionuclide transport through the EBS.

## 12.0 Waste Form Degradation Model

### 12.1 Purpose of the Model

The Waste Form Degradation Model consists of eight major modeling/analysis components: 1) Radioisotope Inventory; 2) In-Package Chemistry; 3) CSNF Degradation; 4) CSNF Cladding Degradation; 5) U.S. Department of Energy (DOE) SNF (DSNF) Degradation; 6) HLW Degradation; 7) Radioisotope Dissolved Concentration (solubility); and 8) Radioisotope Colloidal Concentration. These eight components are generally connected sequentially starting with the radioisotope inventory as input and ending with projected radioisotope dissolved and colloidal concentration.

The purpose of each of these models is discussed below.

#### 1. Radioisotope Inventory

The purpose of the radioisotope inventory abstraction component is to estimate the inventory of those radionuclides most important to human dose. The inventory abstraction component is used as input for the waste form degradation models and is developed from a series of steps that starts with radioisotope inventories of various spent nuclear fuel assemblies and HLW and then estimates the radioisotope inventory when packaged in disposal containers. Three important aspects of the radionuclide inventory are 1) selecting the most important radionuclides for human dose out of the few hundred found within the waste; 2) obtaining the radioisotope inventories of various wastes; and 3) grouping the fuels into the WPs selected for modeling in the TSPA-SR analysis.

#### 2. In-Package Chemistry

The purpose of the in-package chemistry model component is to estimate the fluid chemistry inside the WP over time after the initial breach of the disposal container. The resultant chemistry is used by several of the other waste form model components, including the rate of degradation of the matrix of waste, the dissolved concentration of radionuclides, colloid stability, and cladding degradation. The rate of degradation of the waste matrix and inner stainless steel container, in turn, influences the fluid chemistry so there is a coupling between all the chemically interacting components of the system.

#### 3. CSNF Degradation

The purpose of the CSNF degradation model is to determine the rate of degradation of the CSNF fuel as a function of temperature and water chemistry (specifically, pH, and partial pressures of O<sub>2</sub> and CO<sub>2</sub>). The CSNF degradation rate is dependent on the in-package chemistry and is used by the cladding degradation model. In addition, the CSNF degradation model examined the distribution of radionuclides within the fuel and establishes a gap fraction for the more volatile radionuclides.

#### 4. CSNF Cladding Degradation

The purpose of the cladding degradation model is to predict the rate that the CSNF matrix is exposed and altered based on the number of rods with perforated cladding at any given time. The model includes the number of failed rods that occur while in the reactor and during storage, potential creep failures because of high disposal temperatures, stress corrosion cracking from high stresses and the presence of halide ions, hypothetical physical failures from seismic loads, and hypothetical localized corrosion inside the WP.

#### 5. DSNF Degradation

The purpose of the DSNF degradation model is to predict the rate of degradation of the DSNF waste category and of the immobilized plutonium ceramic waste. Over 250 distinct types of DSNF may be disposed of in the potential repository at Yucca Mountain. The Office of Civilian Radioactive Waste Management and the National Spent Nuclear Fuel Program have collaborated in the identification of spent nuclear fuel “groups” to simplify the analysis of their effects on repository preclosure safety analyses or for postclosure TSPA. In addition, the degradation of the immobilized ceramic plutonium waste form was also evaluated. This waste form will consist of disks of a plutonium-containing, titanium dioxide-based ceramic that will be enclosed in stainless steel cans, which in turn will be encased in a borosilicate glass matrix within the HLW canisters.

#### 6. HLW Degradation

The purpose of the HLW Degradation Component is to provide a conservative model for calculating the rate of degradation of borosilicate glass for the range of conditions (immersion, humid air, and dripping water) to which it may be exposed after the WPs fail.

#### 7. Dissolved Radioisotope Concentration

The purpose of the dissolved concentration model is to evaluate the dissolved concentration of radionuclides (or parents of radionuclides) that are important to human dose as determined by the radioisotope inventory component. Doses calculated for groundwater pathways from the repository to the environment depend critically on the concentrations of radionuclides in fluids issuing from breached WPs. While dissolution of radioisotope-containing SNF rods and/or HLW glass solids into incoming fluids provides the primary source term, the formation of secondary phases often limits the amounts of radionuclides available for subsequent groundwater transport.

#### 8. Colloidal Radioisotope Concentration

The purpose of the colloidal radioisotope concentration model is to determine the concentration of colloid-associated radionuclides that may be transported from the WP. Colloid transport is potentially important for radionuclides that have low solubility and can be entrained in, or sorbed onto, waste form, engineered barrier, or geologic barrier materials that form colloidal particle substrates. Of these radionuclides, only those that are a major part of the waste inventory and

have potentially large dose conversion factors are of potential importance to the performance of the disposal system. Considering these screening criteria, plutonium is the dominant colloidal radionuclide and was previously treated in TSPA-VA. In TSPA-SR, in addition to plutonium, americium was also considered.

## **12.2 Model Component Relations**

The entire waste form degradation model is summarized in the *Waste Form Degradation Process Model Report* (TDR-WIS-MD-000001). Figure 12-1, Waste Form Degradation AMR Relationships, illustrates the relationship of the eight waste form component models and lists the AMRs and calculations that document each component model. Some of the component models consist of a single AMR while others have multiple AMRs. The purpose of each document is summarized below.

### **1. Radioisotope Inventory**

- *Inventory Abstraction* (ANL-WIS-MD-000006) – The purpose of this AMR is to evaluate a series of relative dose calculations and recommend a set of radionuclides that should be modeled in TSPA-SR, including the initial inventory of these radionuclides.
- *Relative Contribution of Individual Radionuclides to Inhalation and Ingestion Dose* (CAL-WIS-MD-000002) – Determine the relative importance of individual radionuclides when calculating inhalation and ingestion doses. Calculations address the effects of inventory abundance, radionuclide longevity, element solubility, and element transport affinity on a radionuclide's contribution to dose. Calculation applies to the period up to 10,000 years following repository closure.
- *Relative Contribution of Individual Radionuclides to Inhalation and Ingestion Dose – One Million Years* (CAL-WIS-MD-000005) – Determine the relative importance of individual radionuclides when calculating inhalation and ingestion doses. Calculations address the effects of inventory abundance, radionuclide longevity, element solubility, and element transport affinity on a radionuclide's contribution to dose. Calculation applies to the period between 10,000 years and 1,000,000 years following repository closure.
- *Radioactive Decay and In-Growth Modeling Approximations for TSPA-SR* (CAL-WIS-MD-000003) – Determine the amount of Am-241 that would be produced inside the WPs from the decay of Pu-241 over the lifetime of the proposed Yucca Mountain repository.
- *Waste Package Radionuclide Inventory Approximations for TSPA-SR* (CAL-WIS-MD-000004) – Determine the average radionuclide inventories (at 2040) for each of the WP configurations proposed for SR.
- *Per Canister Inventories for DOE SNF for TSPA-SR* (CAL-WIS-MD-000006) – Determine average and bounding radionuclide inventories in DSNF.

### Waste Form PMR/AMR Diagram

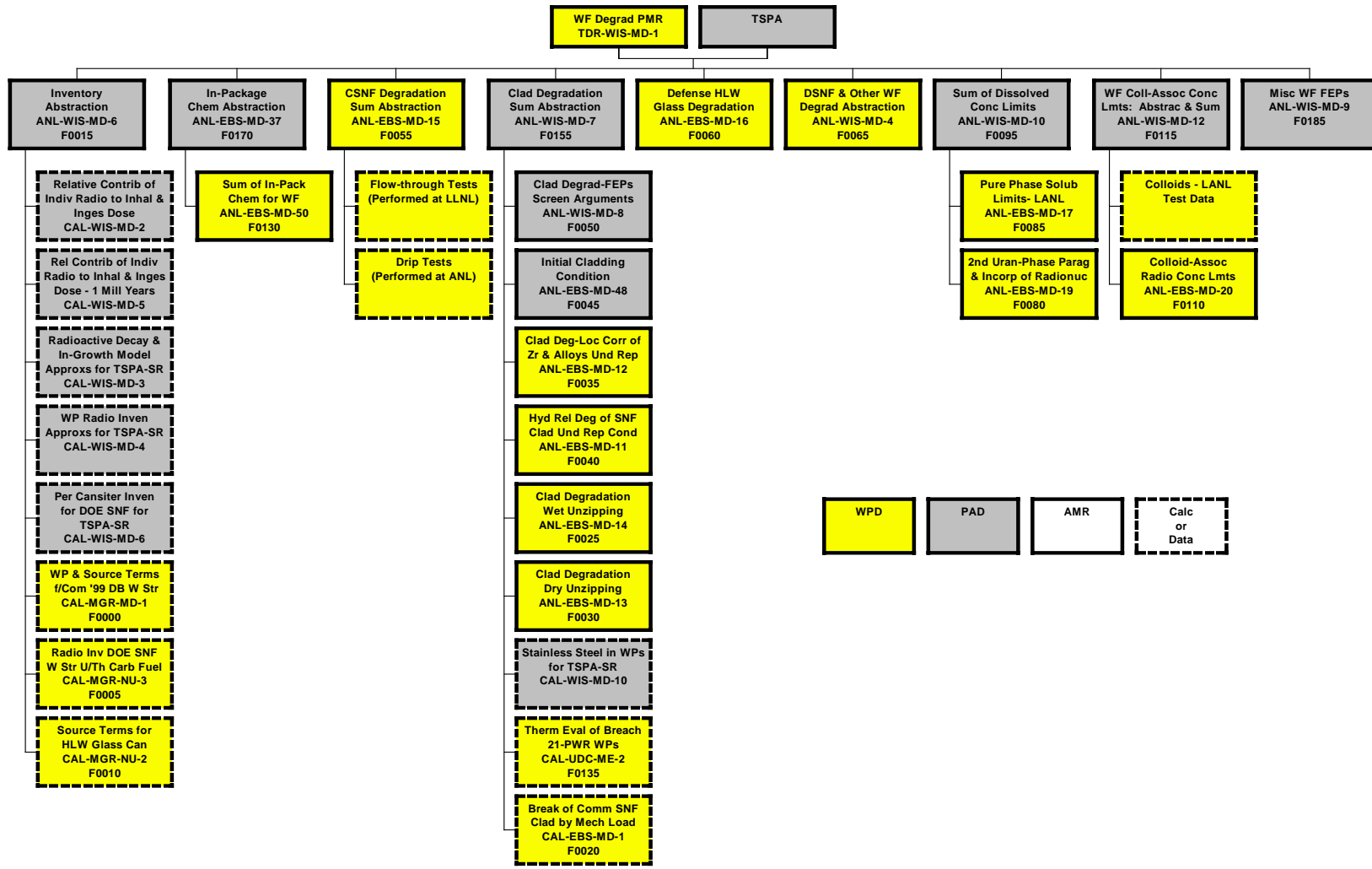


Figure 12-1: Waste Form Degradation AMR Relationships

- *Waste Packages and Source Terms for the Commercial 1999 Design Basis Waste Streams* (CAL-MGR-MD-000001) – Compile source term and commercial waste stream information for use in the analysis of WP designs for commercial fuel.
- *Radionuclide Inventories for DOE SNF Waste Stream and Uranium/Thorium Carbide Fuels* (CAL-MGR-NU-000003) – Generate radionuclide inventories for the DSNF waste stream—one for uranium/thorium carbide fuels in the waste stream and one for the entire waste stream.
- *Source Terms for HLW Glass Containers* (CAL-MGR-NU-000002) – Determine the source terms that include radionuclide inventory, decay heat, and radiation sources due to gamma rays and neutrons for the HLW from the West Valley Demonstration Project, Savannah River Site, Hanford Site, and the Idaho National Engineering and Environmental Laboratory.

## 2. In-Package Chemistry

- *Summary of In-Package Chemistry for Waste Forms* (ANL-EBS-MD-000050) – Examine the probable range of in-package fluid chemistries likely to result from the influx of ambient fluids into, and their reaction with, breached WPs containing either CSNF or co-disposed DSNF and DHLW.
- *In-Package Chemistry Abstraction* (ANL-EBS-MD-000037) – Develop the in-package chemistry abstraction model.

## 3. CSNF Degradation

- *CSNF Waste Form Degradation: Summary Abstraction* (ANL-EBS-MD-000015) – Provide a summary of data and updated models for CSNF intrinsic (forward) dissolution (high water-flow) rates. Summarize the chemical interactions of  $\text{UO}_2$  with groundwater and its components. Provide a comparison of the three types of CSNF dissolution measurements available within and outside the Yucca Mountain program. Discuss gap and grain boundary radionuclide inventories of clad spent fuel. Compare the current knowledge of uranium mineral phases that form in laboratory tests with spent fuel and  $\text{UO}_2$  with mineral assemblages found in natural uranium-bearing sites. Develop bounding models that apply to all  $\text{UO}_2$ -based spent fuel expected to be disposed in the repository.

## 4. CSNF Cladding Degradation

- *Clad Degradation – Summary and Abstraction* (ANL-WIS-MD-000007) – Develop the summary cladding degradation abstraction that describes the postulated condition of commercial Zircaloy clad fuel as a function of time after it is placed in the repository.
- *Initial Cladding Condition* (ANL-EBS-MD-000048) – Describe the condition of commercial Zircaloy clad fuel as it is postulated to be at the time it is received at the YMP site.

- *Clad Degradation – Local Corrosion of Zirconium and its Alloys Under Repository Conditions* (ANL-EBS-MD-000012) – Assess the conditions under which zirconium and its alloys might suffer accelerated or enhanced corrosion.
- *Hydride-Related Degradation of SNF Cladding Under Repository Conditions* (ANL-EBS-MD-000011) – Analyze the degradation of CSNF cladding under repository conditions by the hydride-related metallurgical processes, such as delayed hydride cracking, hydride reorientation, and hydride embrittlement.
- *Clad Degradation – Wet Unzipping* (ANL-EBS-MD-000014) – Develop the appropriate modeling concepts and algorithms for the rate of breach extension (“unzipping” of a breached spent fuel rod) for cases where the cladding has been breached and water is present and the extent for spent fuel surface exposure following the unzipping process. Make recommendations for simplified/bounding models for inclusion in TSPA.
- *Clad Degradation – Dry Unzipping* (ANL-EBS-MD-000013) – Provide a current summary of data and develop a semi-empirical model for the unzipping of cladding due to dry-air oxidation of CSNF.
- *Stainless Steel in Waste Packages for TSPA-SR* (CAL-WIS-MD-000010) – Define the number of CSNF WPs that will contain stainless-steel clad assemblies, and the average stainless steel fraction in those WPs.
- *Thermal Evaluation of Breached 21-PWR Waste Packages* (CAL-UDC-ME-000002) – Determine the radial temperature distribution in a breached WP as a function of time for a 21-pressurized water reactor spent nuclear fuel WP.
- *Breakage of Commercial Spent Nuclear Fuel Cladding by Mechanical Loading* (CAL-EBS-MD-000001) – Calculate the expected rate for breakage of CSNF cladding caused by mechanical loading.

#### 5. DSNF Degradation

- *DSNF and Other Waste Form Degradation Abstraction* (ANL-WIS-MD-000004) – Select and/or abstract conservative degradation models for DSNF and the immobilized ceramic Pu disposition waste form.

#### 6. HLW Degradation

- *Defense High Level Waste Glass Dissolution* (ANL-EBS-MD-000016) – Develop models for radionuclide release from HLW glass dissolution that can be integrated into TSPA.

#### 7. Dissolved Radioisotope Concentration

- *Summary of Dissolved Concentration Limits* (ANL-WIS-MD-000010) – Perform abstraction on solubility limits of radioactive elements based on the process-level modeling. This

analysis predicted solubility limits as functions, distributions, or constants for all transported elements selected for inclusion in the TSPA model.

- *Pure Phase Solubility Limits – LANL (ANL-EBS-MD-000017)* – Compile and evaluate available thermodynamic data on key radionuclides, namely neptunium, plutonium, technetium, and several elements of secondary priority.
- *Secondary Uranium-Phase Paragenesis and Incorporation of Radionuclides Into Secondary Phases (ANL-EBS-MD-000019)* – Assess the potential for uranium (VI) compounds, formed during the oxidative corrosion of spent UO<sub>2</sub> fuels, to sequester certain radionuclides and, thereby, limit their release.

#### 8. Colloidal Radioisotope Concentration

- *Waste Form Colloid-Associated Concentration Limits: Abstraction and Summary (ANL-WIS-MD-000012)* – Present and describe the abstraction of process models regarding the types, formation, and stability of radionuclide-bearing colloids.
- *Colloid-Associated Radionuclide Concentration Limits: ANL (ANL-EBS-MD-000020)* – Develop a useful description of the following waste form colloid characteristics: 1) composition; 2) size distribution; and 3) quantification of the rate of waste form colloid generation. Provide recommendations for colloid source term management.

Figure 12-2, Waste Form Degradation Model Structure, illustrates the modeling and analysis links for the waste form degradation models.

### **12.3 Waste Form Degradation Model Structure**

Figure 12-2 depicts the various components that comprise the Waste Form Degradation model. The relationships of the components of the conceptual model, the model parameters, and the modeling results are indicated in the figure. Figure 12-2 includes the TSPA abstraction of results as the end product of the model development in the AMRs.

#### **A. Conceptual Model**

##### 1. Radioisotope Inventory

Nuclear waste contains hundreds of radionuclides. However, it is not necessary to consider all radionuclides in TSPA analyses. The total inventory can be screened to select those that may contribute significantly to the receptor's dose. This screening process is described in detail in the *Inventory Abstraction* AMR. The screening method for the nominal case considered inventory

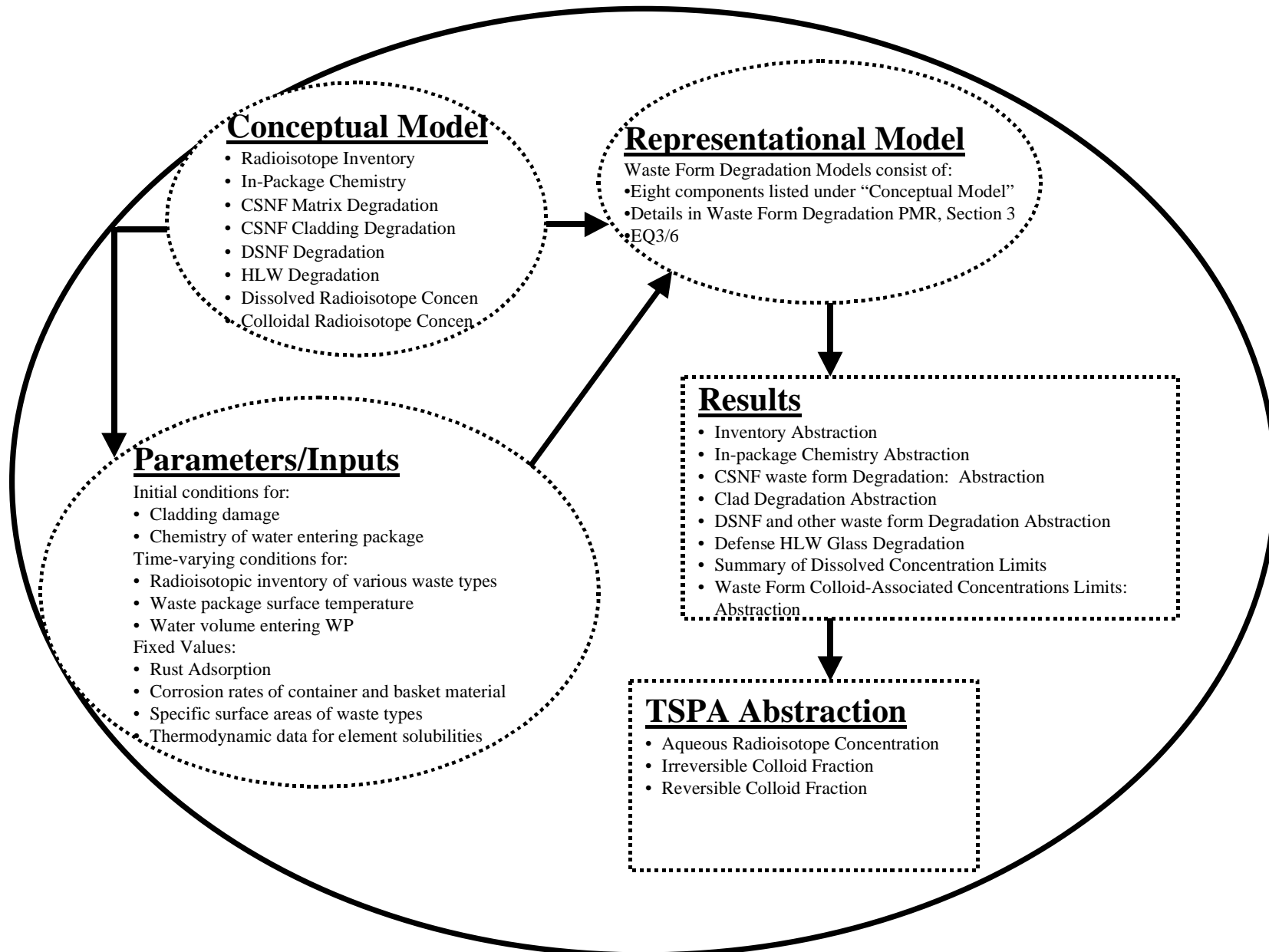


Figure 12-2: Waste Form Degradation Model Structure

abundance, radionuclide longevity, elemental solubility, and transport affinity. For the direct release via a disruptive event scenario, the screening method considered only inventory abundance and radionuclide longevity. The screening method for the human intrusion scenario considered inventory abundance, radionuclide longevity, and transport affinity.

- Information regarding inventory abundance was obtained from three sources: the commercial utilities for CSNF, the DOE National SNF Program (NSNFP) for DSNF, and the Yucca Mountain Environmental Impact Statement (EIS) program for the HLW, mixed oxide fuel, and plutonium ceramic. Eight waste forms were considered: an average pressurized water reactor (PWR) SNF fuel assembly, a bounding PWR SNF assembly, an average boiling water reactor (BWR) SNF fuel assembly, a bounding BWR SNF fuel assembly, an average DSNF canister, a bounding DSNF canister, an average DHLW canister, and a bounding DSNF canister.
- Any radionuclide with a half-life of less than 20 years was not considered since it will have decayed significantly prior to closure of the repository. The remaining radionuclides were examined at several times, ranging from 100 to 10,000 years. Radionuclides were screened separately for one million years for importance in EIS calculations.
- Radionuclides that are not soluble in the environment around the WPs may not be released to the environment via groundwater transport, even if available in high abundance. Thus, solubility is considered in the screening approach.
- Transport affinity is a global term that describes a radionuclide's potential for movement from the source to the environment. All transport mechanisms, such as matrix diffusion, fracture flow, and colloid-facilitated transport, were considered. The screening approach divided the radionuclides into three groups, with associated likely transport mechanisms: 1) highly sorbing – via colloid facilitated transport; 2) moderately sorbing – via fracture flow with sorption occurring due to matrix diffusion; and 3) slightly to non-sorbing – transport via advection and/or diffusion. Each group was examined individually. For example, the relative dose contribution from one highly sorbing radionuclide was compared to the relative dose from other highly sorbing radionuclides.

The screening approach resulted in only a sub-set of the full inventory being considered in TSPA. A cut-off was used where the radionuclides considered in the sub-set contribute to 95 percent of the relative dose (either inhalation or ingestion). The 5 percent error introduced was felt to be negligible compared to the overall uncertainties contained in the TSPA model.

Alternative screening approaches for developing the radionuclide inventory have been explored in previous TSPAs, in the draft EIS, and by the NRC.

The inventory of radionuclides identified by the screening process was determined for the different design basis WP configurations. Five configurations are considered for CSNF and six configurations are considered for the co-disposal DSNF and DHLW. A weighted average

inventory is then determined for the CSNF and co-disposal WPs. This weighted average is determined using the following relation:

$$\bar{a}_i = \frac{1}{N} \sum_{j=1}^c N_j a_{i,j} \quad N = \sum_{j=1}^c N_j$$

where:  $\bar{a}_i$  = average radionuclide inventory for radionuclide i within a waste form type, for example CSNF (grams per WP)

$a_{i,j}$  = average radionuclide inventory for WP configuration, j (grams per WP)

$N_j$  = number of WPs in WP configuration j

$N$  = total number of WPs for a waste form type (e.g., CSNF)

## 2. In-Package Chemistry Component

The in-package chemistry component model conceptualization is discussed briefly in the *Waste Form Degradation PMR* and in the *Summary of In-Package Chemistry for Waste Forms AMR*. The conceptual model considers the coupling of the seepage rate of water into the package and degradation of the steel, aluminum, DSNF, CSNF, and HLW inside the package in the evaluation of water chemistry parameters such as hydronium ion concentration ( $H_3O^+$ ), total carbonate concentration, dissolved partial pressures of carbon dioxide and oxygen, ionic strength, and fluoride and chloride ion concentrations (i.e., pH,  $p[CO_3]_T$ ,  $P_{CO_2}$ ,  $P_{O_2}$ , [I], [F], [Cl]).

The fluid chemistry inside the package (in-package chemistry) is dependent upon the initial chemistry of the water entering the breached package, the volume of water flowing through the package, the amount of water remaining within the package, and the amount of time that inflows into the WP occur. J-13 well water is used as a surrogate for the groundwaters passing through the repository and possibly into breached WPs several thousand years after the repository has closed. J-13 well water is quite dilute and its composition is not expected to significantly affect the in-package chemistry. Ongoing work is underway to verify this assumption, or provide better information.

Gases in solution within the WP were assumed to remain in equilibrium with the ambient atmosphere outside the WP. The temperature of the simulations was set at 25°C to represent the conditions that will occur several thousand years after WP emplacement, when the original thermal pulse has passed and temperatures have returned to near ambient levels. Evaporation of fluids was also neglected. Early breach of a WP would almost certainly entail chemical interaction under substantially higher temperatures. Under such a scenario, evaporative concentration of reacting fluids would be expected to result in in-package fluids that diverge substantially from the compositions calculated under the 25°C, zero-evaporation limiting case considered.

Various breach scenarios can be envisioned for the container. The current model assumes a simple degradation scenario that entails breaching the WP; filling of the WP void volume with seepage fluids from the drift; reaction within the WP materials; and releasing contaminated fluids at the same rate at which fresh fluids entered. Each breached WP was modeled as a continually stirred, fixed volume vessel.

In-drift solutions seeping into a breached WP would encounter a number of kinetically reactive solids whose reaction rates are only known within orders of magnitude. Such solids include  $\text{UO}_2$  fuel wrapped in Zircaloy cladding, Al alloy, 316 stainless steel (with and without neutron absorbers, such as boron or  $\text{GdPO}_4$ ), and A516 low carbon steel. Dissolution of the fuel, and release of radionuclides, occurs only after degradation of some of the cladding. General corrosion of cladding is likely to be insignificant under the geochemical conditions expected inside reacting WPs. The WP configuration used for the codisposal package calculations was that of the Fast Flux Test Facility DSNF with five HLW glass logs.

Calculations of the in-package chemistry utilize the EQ3/6 software, as discussed below. The conceptualizations implemented into the software are discussed in the *Waste Form Degradation PMR* and in the *Summary of In-Package Chemistry for Waste Forms AMR*. These conceptualizations are summarized below.

EQ3/6 periodically assesses the chemical equilibrium state of the solution and removes newly saturated, secondary mineral or gas phases from the fluid. In addition to kinetic inputs (e.g., rates, compositions, and masses of reactants), EQ3/6 relies on a thermodynamic database describing the chemical stability of minerals, aqueous species, and gases. When the reacting solution becomes saturated with respect to solids or gasses, EQ3/6 converts dissolved components into the respective phase and then allows the latter to act as a reservoir of the respective components for use at subsequent times. In this way, EQ3/6 tracks the elemental composition of the reacting fluid for the duration of the reaction path calculation while at the same time providing estimates of the nature and masses of secondary phases that are predicted to form. The code, however, does not provide for the kinetic inhibition for phase formation, which is, therefore, the responsibility of the analyst. Generally, the assessment of kinetic inhibition must be made on the basis of there being an absence of the particular phase in low-temperature ( $\sim 25^\circ\text{C}$ ) environments. For example, dolomite ( $\text{CaMg}(\text{CO}_3)_2$ ) is predicted to form in a number of runs due to the accumulation of Ca, Mg, and alkalinity upon reaction with WP components. Dolomite, though thermodynamically favored to grow in a number of low temperature natural solutions such as seawater, apparently must overcome severe kinetic obstacles to actually form and is actually observed growing only in highly evaporated brines. These kinetic considerations are then the basis for suppressing formation of dolomite in the reaction path calculations. Similar arguments are used to suppress the formation of a number of oxide and silicate minerals that are typically observed to form only under high temperature conditions.

### 3. CSNF Degradation Component

Most of the waste to be put in the repository is CSNF in the form of  $\text{UO}_2$ . Under oxidizing conditions in the presence of liquid or vapor water, the  $\text{UO}_2$  in CSNF is not stable and alters. Alteration of the  $\text{UO}_2$  matrix can liberate radionuclides important to human dose. The *CSNF*

*Waste Form Degradation: Summary Abstraction* AMR is the primary document supporting the CSNF Matrix Degradation Model Component (see Figure 12-1). This, in turn, depends on the data reports of the major sets of experiments conducted on CSNF. A minor document supporting this AMR is *Miscellaneous Waste-Form FEPs*.

The main function of the CSNF degradation model component is to determine the rate of degradation of the CSNF fuel as a function of temperature and water chemistry (specifically, pH, and partial pressures of O<sub>2</sub> and CO<sub>2</sub>). This degradation rate function is combined with the in-package chemistry to determine a rate, which is then directly used by the Cladding Degradation Model Component to determine the rate that the CSNF cladding splits open and exposes more of the fuel matrix. In addition, the CSNF degradation model examined the distribution of radionuclides within the fuel and established a gap fraction for the more volatile radionuclides.

The CSNF Matrix Degradation Component uses two linear regression equations based on pH, p[CO<sub>3</sub>]<sub>T</sub>, pO<sub>2</sub>, and temperature (T) to evaluate matrix degradation over time; one equation is applicable for pH less than or equal to 7 and the other is applicable for pH greater than 7. The regression variables used, pH, p[CO<sub>3</sub>]<sub>T</sub> and pO<sub>2</sub>, are coupled to in-package chemistry to account for uncertainty.

Unsaturated drip tests, batch tests, literature, and natural analogs support the CSNF degradation conceptual model.

Long-term drip testing of CSNF under hydrologically unsaturated conditions, i.e., limited water and an oxidizing atmosphere, has been done over the past six years to determine the relationship between the rate of CSNF alteration, i.e., dissolution and secondary phase formation, and the release rate of radionuclides. Small samples of two commercial PWR spent nuclear fuels, Approved Testing Material-103 and Approved Testing Material-106, are subjected to three experimental conditions: vapor injection, low-drip-rate injection, and high-drip-rate injection, all at 90°C. All drip samples were completely wetted. The nominal drip rate of J-13 water is 0.75 mL every 3.5 days in the high-drip-rate tests and 0.075 mL every 3.5 days in the low-drip-rate-tests. In the vapor tests, minimum water is available for transport, and the absence of added cations and anions limits the type of alteration products (secondary phases) that may form. A CSNF intrinsic dissolution/corrosion rate is estimated from the release of highly soluble <sup>99</sup>Tc and <sup>90</sup>Sr, which are assumed to be homogeneously distributed in the spent fuel matrix (<sup>129</sup>I and <sup>137</sup>Cs are concentrated at the fuel grain boundaries and fuel-clad gap).

The rate models can be compared against batch tests, published data cited in reviews by Grambow (1989) and McKenzie (1992) of pre-1992 literature, as well as more recent, flow-through measurements of de Pablo et al. (1997), Torrero et al. (1997), and Tait and Luht (1997). Batch dissolution rates are lower than predicted rates but within a factor of 6. The rate model above does not have as strong a carbonate dependency as that seen by de Pablo et al.'s (1997) study. The alkaline pH model predicts 0.0002 mol/L total carbonate rates that are consistently higher than Torrero et al.'s (1997) carbonate-free rates. The difference in carbonate levels though makes direct comparison impossible. Torrero's acidic data can be as low as 1/20th of the predicted value, yet Torrero's acidic data overall seem low compared to other work (see Grambow 1989). In general, the present model predicts Tait and Luht's (1997) results well at the

various sample, temperature, oxygen, and water-chemistry conditions. Moreover, the trends in the model and data with temperature, carbonate, and oxygen are the same. The models underpredict Tait and Luht's (1997) data at bounding conditions, such as 75°C, and 0.1 mol/L bicarbonate by at most 0.88 orders of magnitude, which is within the uncertainty range of the model.

To establish confidence that experimental CSNF alteration pathways effectively represent likely natural processes, it is useful to compare the alteration mineralogy observed in experiments with natural occurrences of altered uranium oxides. Uranium dioxide occurs in nature as the mineral uraninite, which is structurally similar to CSNF. Nopal I, a uranium mining site at Peña Blanca, Mexico, contains substantial quantities of uraninite and is arguably one of the best natural analogs for CSNF degradation in Yucca Mountain as it possesses geologic, geochemical, and hydrogeologic characteristics most similar to those at Yucca Mountain. The volcanic (tuffaceous) host rock at Nopal I, the youngest of the studied sites, has been relatively oxidizing for tens of thousands of years, though uraninite, containing  $U^{4+}$ , was originally formed several million years ago.

In general, uraninite has been oxidized and hydrated at Nopal I. In the presence of silicate and alkali ions, such as calcium and sodium, various alkaline uranyl silicate hydrates such as Na-boltwoodite and  $\beta$ -uranophane dominate alteration mineralogy at long times. Overall, the phase assemblage observed at Nopal I is similar to that derived experimentally in the CSNF alteration drip tests.

The general agreement between the observed alteration products in the various tests, the natural analogs, and the geochemical modeling provide confidence that the mechanisms of spent fuel corrosion are well understood, and that the forward dissolution model is bounding for long-term prediction of CSNF degradation rates.

#### 4. CSNF Cladding Degradation Component

The overall conceptual model of cladding performance in the repository is summarized in the *Waste Form Degradation PMR* (Section 3.4). Conceptualizations specific to the various processes that affect clad performance are also discussed in individual AMRs (good examples being the *Clad Degradation – Local Corrosion of Zirconium and its Alloys Under Repository Conditions* and *Initial Cladding Condition* AMRs). These conceptual models are summarized below.

Since the 1950s, most CSNF has been clad with less than 1 mm (usually between 600 through 900  $\mu\text{m}$ ) of Zircaloy, an alloy that is about 98 percent zirconium with small amounts of tin, iron, nickel, and chromium. The Zircaloy cladding is not a designed engineered barrier of the Yucca Mountain disposal system, but rather is an existing characteristic of the CSNF that is important to determining the rate of release of radionuclides once engineered barriers such as the WPs have breached. Zircaloy is very resistant to corrosion, and cladding failure is expected to be minimal in the first 10,000 years. However, while Zircaloy provides excellent protective properties, characterization of the uncertainty in its performance is important. This characterization is

possible since data have been collected on its performance over the past 40 years by the nuclear industry and by others in several different harsh environments.

The degradation of CSNF cladding is assumed to proceed through two distinct steps: 1) rod failure (perforation of the cladding); and 2) progressive exposure of UO<sub>2</sub> spent fuel matrix. The number of failed rods is based on the observed rod failures while in the reactor and during storage, potential creep failures because of high disposal temperatures, stress corrosion cracking from high stresses and the presence of halide ions, hypothetical physical failures from seismic loads, and hypothetical localized corrosion inside the WP. While other mechanisms of initiating cladding perforations such as diffusion controlled cavity growth or delayed hydride cracking were explored, they were screened out based on low consequence through the features, events, and processes screening approach. Such perforations can occur anywhere on a fuel rod. However, in the current conceptualization perforations are conservatively assumed to occur at the center of the rod because this ensures the fastest exposure of the waste matrix.

After the initial perforation, further cracking and splitting of the cladding is assumed to occur, which exposes the CSNF matrix as it progresses. The splitting of the cladding (unzipping) is calculated as a function of the CSNF matrix alteration rate. The reaction is assumed to unzip the fuel rod because the fuel volume increases during oxidation of the UO<sub>2</sub>, (i.e., the oxidation of the UO<sub>2</sub> to secondary phases of uranium is assumed to cause enough pressure by volume expansion to burst the cladding from within). This mechanism for increasing the exposed surface area of the matrix is sensitive to environmental conditions such as temperature. Based on observed behavior within storage pools at reactors, unzipping in a wet environment does not occur in observed time periods of 40 years, once the Zircaloy cladding has been perforated. However, because unzipping in a wet environment could not be entirely ruled out and because complete exposure of the matrix bounds diffusive releases of radionuclides through the pinhole perforations, the project included the possibility of the clad unzipping in a wet environment. A small percentage of the inventory of iodine, cesium, and a few other radionuclides resides in the gap between the cladding and waste matrix. The release of the gap inventory is assumed to be instantaneous when the cladding is perforated and, thus, independent of the cladding unzipping. Cladding that was initially perforated is predicted to release its gap inventory when the WP is breached.

## 5. DSNF Degradation Component

The DSNF Degradation Model Component predicts the rate of degradation of the DSNF waste category and of the immobilized plutonium ceramic waste. The component was developed using the logic shown in Figure 3 of *Standard Practice for Prediction of the Long-Term Behavior of Materials, Including Waste Forms, Used in Engineered Barrier Systems (EBS) for Geologic Disposal of High-Level Radioactive Waste* (ASTM C1174-97).

The primary document supporting the DSNF Degradation Model Component was the *DSNF and Other Waste Form Degradation Abstraction* AMR (ANL-WIS-MD-000004), which in turn was supported to a limited extent by *Miscellaneous Waste-Form FEPs* (ANL-WIS-MD-000009).

The degradation rates of all waste forms other than CSNF and HLW were analyzed in *DSNF and Other Waste Form Degradation Abstraction* (ANL-WIS-MD-000004). Over 250 distinct types

of DOE spent nuclear fuel may be disposed of in the potential repository at Yucca Mountain. The Office of Civilian Radioactive Waste Management and the National Spent Nuclear Fuel Program have collaborated in the identification of spent nuclear fuel “groups” to simplify the analysis of their effects on repository preclosure safety analyses or for postclosure TSPA.

The DOE spent nuclear fuel groups are:

- Group 1–Naval spent nuclear fuel
- Group 2–Plutonium/uranium alloy
- Group 3–Plutonium/uranium carbide
- Group 4–Mixed oxide and plutonium oxide fuels
- Group 5–Thorium/uranium carbide
- Group 6–Thorium/uranium oxide
- Group 7–Uranium metal
- Group 8–Uranium oxide
- Group 9–Aluminum-based spent nuclear fuel
- Group 10–Unknown
- Group 11–Uranium-zirconium-hydride

In addition, the immobilized ceramic plutonium waste form was also evaluated. This waste form will consist of disks of a plutonium-containing, titanium dioxide-based ceramic that will be enclosed in stainless steel cans, which in turn will be encased in a borosilicate glass matrix within the HLW canisters.

*DSNF and Other Waste Form Degradation Abstraction* (ANL-WIS-MD-000004) provided three types of degradation models for the DOE spent nuclear fuel and plutonium-ceramic waste forms: upper-limit, conservative, and best-estimate, to provide the user of the models appropriate flexibility in their application to any particular postclosure performance scenario. An upper-limit model predicts release rates that are always well in excess of actual dissolution rate data. The conservative degradation model provides an estimate of the dissolution rate that reflects the higher rate end of available dissolution data or the SNF groups or similar materials. A best-estimate model is appropriate only when sufficient dissolution data exist and the characteristics of the waste form can be shown to correspond to the characteristics of the materials that provided the dissolution database. For the conservative and best-estimate models, various surrogate spent nuclear fuels were evaluated for degradation behavior.

The AMR discusses each group and, where possible, provides an equation for the degradation rate of that group. Some of the groups have no data for degradation rate. Other groups contain such a mixture of types of waste that a single degradation rate is not representative of the group.

The bulk of the DSNF is the metallic uranium N-reactor fuel. Also, its degradation rate provides a conservative upper bound for the other types of defense waste. Therefore, as a reasonably conservative simplification, the degradation rate for Group 7 (metallic uranium) was chosen as the degradation rate for all DSNF. As noted in the inventory abstraction component, the inventory of DSNF is a weighted average of all groups.

## 6. HLW Degradation Component

The function of the HLW Degradation Component is to provide a conservative model for calculating the rate of degradation of borosilicate glass for the range of conditions (immersion, humid air, and dripping water) to which it may be exposed after the WPs fail. The HLW Degradation Component uses bounds on parameters of a phenomenological model to develop a simplified (Arrhenius-type) rate equation of degradation that is dependent only upon pH and temperature. Conservative estimates of the model parameters are based upon experimental data for the degradation of borosilicate glass.

The HLW model will be implemented in the TSPA-SR analysis to calculate the rate of glass degradation. The rate of radionuclide release from the HLW matrix will be calculated by multiplying the glass degradation rate by the mass fraction of the radionuclide in the glass. This approach for calculating the radionuclide release rate is based on the conservative assumption that the release of radionuclides is congruent with the degradation of borosilicate glass.

In the unsaturated environment of the Yucca Mountain site, it is likely that waste glass will be contacted initially by humid air. When glass is exposed to humid air, molecular water will sorb onto specific sites on the glass surface, primarily silanol sites, and alkali metal sites. The amount of liquid water that sorbs on the glass will depend on the relative humidity of the air, temperature of the glass surface, and hygroscopicity of the glass surface. The first monolayer forms at a relative humidity of only a few percent. Subsequent monolayers form as water vapor bonds with sorbed water to form beads of water on the glass surface. At relative humidities above about 80 percent, a sufficient amount of water has condensed to coalesce into a thin film covering the entire surface. The glass will react with these sorbed water layers just as it does when immersed in water. Initial reactions will likely result in the dissolution of alkali metals into the film of water. This will decrease the equilibrium vapor pressure of the film of water and cause more water to condense in the film. After the initial film of water is sorbed, the amount of water on the glass will likely be determined by the salinity of the water.

In an open system such as the disposal system, water vapor will continually condense in the film of saline water on the exposed waste glass as the glass corrodes. For the various configurations in which fractured glass may be contacted by humid air or dripping water, water may drip or flow away from the glass or may accumulate over time while contacting the glass. Once alkali metals are released into the film of water, the hygroscopicity of the film will result in continuous condensation of water vapor. Continuous exposure to water-saturated air will result in a process of vapor condensation, flow across the sample, and dripping, wherein dissolved species can be transported away from the glass as solution drips from the glass, and fresh water vapor condenses. The corrosion rate of the glass under these conditions will be affected by the rates at which water vapor condenses in the film, and solution drips from the sample. These processes will affect the glass dissolution rate through their effects on the solution chemistry of the film. The effects of the condensation, flow, and drip rates on the glass dissolution rate are taken into account in the model by the use of experimental data measured under test conditions designed to replicate the phenomena discussed above.

The model is implemented in the form of an analytical expression containing four parameters ( $\eta$ -a pH dependent coefficient,  $E_a$ -the activation energy,  $S$ -the surface area, and  $k_{eff}$ -a term dependent on the intrinsic dissolution rate and solution chemistry) and two variables (i.e., temperature and pH) and two variables (i.e., temperature and pH). A low and a high pH equation is given in the model because of a difference in dissolution mechanisms in the two regimes.

Consistent with the conceptual model for in-package chemistry, degradation of borosilicate glass is assumed to occur as if the glass were fully immersed, although it is expected that much of the glass will be exposed to humid air or dripping water conditions. This assumption is based on a comparison of the model that was developed for immersion to the model developed for glass degradation in humid air or dripping groundwater. This comparison showed that the rate of glass corrosion under humid air and dripping water conditions was conservatively bounded by the dissolution rate under immersion conditions.

The primary document supporting the HLW Degradation Model Component was the *Defense High Level Waste Glass Degradation* (ANL-EBS-MD-000016), which in turn was supported to a limited extent by *Miscellaneous Waste-Form FEPs* (ANL-WIS-MD-000009).

## 7. Dissolved Radioisotope Concentration Component

The *Waste Form Degradation PMR*, the *Pure Phase Solubility Limits – LANL AMR* and the *Summary of Dissolved Concentration Limits AMR* all discuss conceptual aspects related to radioisotope solubility. The conceptualizations are based on experimental observations and thermodynamic modeling analyses. Information generated both within and outside the Yucca Mountain Project supported the conceptualizations. Effects of chemistry, likely controlling phases, and thermodynamic/kinetic aspects are presented.

Doses calculated for groundwater pathways from the repository to the environment depend on the concentrations of radionuclides in fluids issuing from breached WPs. While dissolution of radioisotope-containing SNF rods and/or HLW glass solids into incoming fluids provides the primary source term, the formation of secondary phases often limits the amounts of radionuclides available for subsequent groundwater transport.

The primary document supporting the radioisotope concentration model component is *Summary of Dissolved Concentration Limits AMR* (ANL-WIS-MD-000010). An important component of this AMR was the analysis with EQ3NR (a component of the qualified EQ3/6 Version 7.2b package). Ultimately though, the values described in the radioisotope concentration model reflect a newly revised thermodynamic database developed. New measurements of radionuclide solubilities were combined with a critical review of recent thermodynamic parameterizations of Np, U, Pu, and Am phase stabilities that are being used by the international waste disposal community (NEA OECD) at large.

Important components of this effort included the following.

- Measurement and critical analysis of Np solubility in J-13 groundwater. This led to revision of the formation free energy of  $\text{Np}_2\text{O}_5 \cdot x\text{H}_2\text{O}$ , an important Np-limiting phase, and Np speciation data.
- Measurement and critical analysis of Pu solubility in J-13 groundwater.
- Critical analysis of technetium and uranium silicate thermodynamic data.

The dissolved concentration limit calculation builds upon three primary feeds: 1) estimates of in-package fluid major element composition (pH, Eh, ionic strength, carbonate levels); 2) measured (and estimated) thermodynamic parameters describing the stability of aqueous species and solid radioisotope phases; and 3) a determination of the likely solubility-controlling phases for the specific radionuclides of concern. The in-package chemistry is described in Section 3.2 of the *Waste Form Degradation PMR* (TDR-WIS-MD-000001 REV 00 ICN 01). The thermodynamic databases that were used are described in the supporting AMRs (see Figure 12-1).

#### 8. Colloidal Radioisotope Concentration Component

The conceptual processes related to colloid facilitated release and transport are discussed in the *Waste Form Degradation PMR*, the *Colloid-Associated Radionuclide Concentration Limits* AMR and the *Waste Form Colloid-Associated Concentration Limits: Abstraction and Summary* AMR. The conceptualizations are based on both field and experimental observations. These conceptualizations are summarized below.

Colloid transport is potentially important for radionuclides that have low solubility and can be entrained in, or sorbed onto, waste form, engineered barrier, or geologic barrier materials that form colloidal particle substrates. Of these radionuclides, only those that are a major part of the waste inventory and have potentially large dose conversion factors are of potential importance to the performance of the disposal system. Considering these screening criteria, plutonium is the dominant colloidal radionuclide and is considered in the analyses. In addition to plutonium, americium is also considered.

The radionuclide-bearing colloids are formed by radionuclide entrainment as discrete phases in, or by radionuclide sorption onto, colloidal substrates. They are, therefore, classified into “types” based on the source of the substrate material and can be further classified based on how the radionuclides are attached to the substrates. Three major types of colloids are recognized to be important for the colloidal radionuclide concentration component based on the source of the colloid substrate material:

- Waste-form colloids formed during degradation of HLW glass. (**Note:** these colloids are further classified into “reversibly attached” and “irreversibly attached” radionuclide types.)
- Corrosion-product colloids formed during corrosion of iron-containing WPs.

- Groundwater colloids present in the waste-form area.

The colloid concentration component is determined by summing the contributions of the three colloid types to the colloid radioisotope concentration for each radionuclide. The conceptualization identified the availability and the stability of three categories of colloids: 1) colloids generated during degradation of the waste; 2) colloids generated during degradation of the disposal container; and 3) existing colloids in the groundwater.

The development of the conceptual model and implementation requires consideration of colloid generation, colloid-radionuclide interaction, colloid stability behavior, and to some extent, colloid transport/retardation behavior. Information used for groundwater colloids, waste-form colloids, and corrosion-product colloids was obtained primarily from Yucca Mountain specific studies. Consequently, the colloid-concentration model is expected to be representative of Yucca Mountain behavior.

A model was developed to calculate the colloid radioisotope concentration for each of the three colloid types. The model for the waste form colloids includes the contributions of the engulfed (irreversibly attached) plutonium observed in waste glass tests. The models for all three colloid types include reversibly attached radionuclides. These models are based on the population of each colloid type (expressed in terms of mass of colloids per volume of fluid) and experimental data for the sorption of radionuclides onto the colloid substrate materials involved. The effects of pH and ionic strength on the stability of dispersions of each colloid type are considered. The location of the boundaries between pH and ionic strength regimes in which each type of colloid substrate is stable or unstable is defined together with the colloid mass concentration in each regime.

Field evidence of small concentrations of radionuclides associated with colloids migrating considerable distances provides insight into possible colloid behavior at Yucca Mountain. At the Benham nuclear test site at the NTS, rapid transport of colloid-associated Pu appears to have occurred. At a point approximately 1.3 km from the blast site,  $1 \times 10^{-14}$  mol/L colloid-associated plutonium was detected 30 years after the detonation. It is difficult to determine what fraction of the transport was due to transport on colloids, injection through fractures by the blast, or transport as dissolved Pu. However, in the cases of other detonations, fracture injections have not been observed to extend beyond a few hundred meters, and dissolved Pu would be expected to sorb strongly to the fracture surfaces. It is plausible that the Pu was transported as Pu irreversibly attached to colloids. This example underscores the potential significance of the irreversibility of radionuclide attachment to smectite colloids observed in the Argonne National Laboratory (ANL) waste form corrosion experiments.

Irreversibly attached colloids are included as a contribution to the colloid-associated radionuclide concentration. The colloids formed from CSNF and DSNF are assumed to have reversibly attached radionuclides; this assumption is potentially non-conservative and remains to be verified when results from ongoing tests become available.

## B. Parameters

### 1. Radioisotope Inventory

The calculations entitled *Relative Contribution of Individual Radionuclides to Inhalation and Ingestion Dose* and *Relative Contribution of Individual Radionuclides to Inhalation and Ingestion Dose – One Million Years* present the radionuclides that account for 95% of either the relative inhalation dose rate or the relative ingestion dose rate for the various screening factors identified above (e.g., inventory abundance, solubility, transport affinity). Information is provided for both bounding and average fuels, DSNF and HLW as well as CSNF, time periods from 100 to 1 million years, and both inhalation and ingestion doses. This information was then used in the screening approach.

The inventory of each radionuclide for the various WP configurations is documented in the calculation entitled *Waste Package Radionuclide Inventory Approximations for TSPA-SR*. This information was used to determine the average WP inventory for the CSNF and co-disposal waste types.

### 2. In-Package Chemistry Component

Several parameters are needed for the in-package chemistry component model. These parameters, discussed in detail in the *Summary of In-Package Chemistry for Waste Forms* AMR, are summarized below.

As discussed above, the temperature of the simulations was set at 25°C to represent the conditions that will occur several thousand years after WP emplacement, when the original thermal pulse has passed and temperatures have returned to near ambient levels. Evaporation of fluids was also neglected.

The in-package chemical reaction calculations used input fluid flows of 0.0015 m<sup>3</sup>/yr, 0.015 m<sup>3</sup>/yr, and 0.15 m<sup>3</sup>/yr. The *Waste Form Degradation* PMR states that the void volumes considered were a constant 4,507 L for the CSNF WP and a constant 5,811 L for the DSNF WP. However, the *Summary of In-Package Chemistry for Waste Forms* AMR provides only a void volume for CSNF (4511 L).

Uncertainties in initial clad failure, localized corrosion, mechanical damage, and other degradation mechanisms were addressed in the cladding degradation AMRs. However, this information was not available when the in-package calculations were started, so a range of clad damage and CSNF fuel exposure was investigated (100 percent, 20 percent, and 1 percent clad coverage).

Dissolution of DHLW glass was considered for two end-member rates (high and low). Regression equations as a function of pH were used, with the regression parameters differing by an order of magnitude. A similar approach was used for the dissolution of WP structural materials. The dissolution of UO<sub>2</sub> was modeled using a single regression equation, as a function of pH.

As will be discussed below, EQ3/6 software package was used as the representational model. The existing thermodynamic database for EQ3/6 was used and is contained in the YMP database (DTN: SN0001T0811199.006).

### 3. CSNF Degradation

The CSNF Matrix Degradation Component uses two linear regression equations based on pH,  $p[\text{CO}_3]_{\text{T}}$ ,  $p\text{O}_2$ , and temperature (T) to evaluate matrix degradation over time; one equation is applicable for pH less than or equal to 7 and the other is applicable for pH greater than 7. The regression variables used, pH,  $p[\text{CO}_3]_{\text{T}}$  and  $p\text{O}_2$ , are coupled to in-package chemistry to account for uncertainty.

### 4. CSNF Cladding Degradation

The overall CSNF cladding degradation model includes several sub-models and analyses. The discussion that follows focuses on three areas: initial cladding condition, localized corrosion, and wet unzipping. These model areas were ultimately propagated through abstraction and into TSPA and are the most important models regarding clad performance.

- **Initial Cladding Condition**

Input parameters used in the assessment of the initial cladding condition are clearly documented in the *Initial Cladding Condition* AMR (section 4). Key input parameters include fuel rod dimensions and fill pressures, fission gas release fractions, helium production, fuel rod failure data, fuel reliability information, dry storage temperatures, and creep failure criteria. The various sources of this information are all non-project literature. These sources are clearly identified.

- **Localized Corrosion**

Parameters, namely observed Zircaloy corrosion rates under various test environments, used in the assessment of localized corrosion of Zircaloy are clearly documented in the *Clad Degradation – Local Corrosion of Zirconium and its Alloys Under Repository Conditions* AMR. The input information used in the analysis is from laboratory measurements conducted outside the project and modeling efforts conducted at Bettis Atomic Power Laboratory.

- **Wet Unzipping**

Several parameters are needed to implement the wet unzipping model. These include fuel rod properties, Zircaloy properties (unirradiated and irradiated), anticipated breach sizes, the CSNF forward dissolution rate, reaction products, and reaction rate parameters (free energy). The parameters used and their source are clearly documented in the *Clad Degradation – Wet Unzipping* AMR (Section 4)

## 5. DSNF Degradation

The DSNF degradation component requires the bounding value of the DSNF intrinsic dissolution rate and the specific surface area. The waste composition is determined in the inventory component, and the degradation rate is product of the dissolution rate times the specific surface area.

## 6. HLW Degradation

The model is implemented in the form of an analytical expression containing four parameters ( $\eta$ -a pH dependent coefficient,  $E_a$ -the activation energy,  $S$ -the surface area, and  $k_{eff}$ -a term dependent on the intrinsic dissolution rate and solution chemistry) and two variables (i.e., temperature and pH) and two variables (temperature and pH). The model parameters account for the pH, temperature, surface area, and the combined effects of glass composition and solution composition on the rate of glass corrosion. Conservative estimates of the values for the model parameters are provided based on experimental data. Implementation of the model for the TSPA-SR analysis requires input of temperature and pH data.

## 7. Dissolved Radioisotope Concentration

Input parameters used in the *Pure Phase Solubility Limits – LANL AMR* are J-13 groundwater composition, thermodynamic data. The source of these parameters is clearly documented in the AMR.

Input parameters used in developing solubility limits for subsequent use in TSPA, as documented in the *Summary of Dissolved Concentration Limits AMR* consist of thermodynamic data and calculated solubility limits. Thermodynamic data used for Np and Pu was obtained from the *Pure Phase Solubility Limits – LANL AMR*. Thermodynamic data used for Am and U was obtained from reviews conducted by the Nuclear Energy Agency. Recommended solubility limits from the *Pure Phase Solubility Limits – LANL AMR* for Nb, Ni, Zr, Ra, Sn, Pa, and Pb were used.

## 8. Colloidal Radioisotope Concentration

Two AMRs document the development of the waste form colloid model. These are the *Colloid-Associated Radionuclide Concentration Limits: ANL* and the *Waste Form Colloid-Associated Concentration Limits: Abstraction and Summary AMRs*. The fundamental basis for the colloid model developed in these AMRs is field and laboratory information.

The sources of information used in the *Colloid-Associated Radionuclide Concentration Limits: ANL AMR* is clearly documented (Section 4). This information is laboratory data from waste form material degradation tests conducted at ANL. The data included the properties of the colloids that formed and their size distribution. Uncertainty in the data was clearly presented.

The primary technical inputs used in the *Waste Form Colloid-Associated Concentration Limits: Abstraction and Summary AMR* are observations, results, and conclusions documented in the

*Colloid-Associated Radionuclide Concentration Limits: ANL and the Waste Form Colloid-Associated Concentration Limits: Abstraction and Summary* AMR. Other sources of information were also used. These sources were clearly documented.

The modeling of reversible attachment of radionuclides to colloids involves the use of an effective distribution coefficient ( $K_{ds}$ ). The probability distributions for these parameters are not provided in the AMR, but rather are accessible only through a data tracking number (MO0004SPAKDS42.005). The information presented in the technical database presents the probability distributions, but does not provide the bases for the selected distributions and the distribution parameters. In addition, the basis for the value/source cited in the AMR (table 1) is a technical product development plan. However, this technical development plan does not provide the bases for the probability distributions either.

### **C. Representational Model**

#### 1. Radioisotope Inventory

The radioisotope screening methodology and the determination of the average WP radioisotope inventory required no representational model.

#### 2. In-Package Chemistry Component

The representational model used in the in-package chemistry component model is the geochemical equilibrium code, EQ3/6<sup>1</sup>. As described in the *Summary of In-Package Chemistry for Waste Forms* AMR simulations of WP alteration by ambient groundwater were done using the qualified reaction path code EQ3/6, which titrates masses of WP components at a rate determined by input reaction rates and fluid influxes into the breached WP.

#### 3. CSNF Degradation

The CSNF degradation component directly develops a regression equation for PA.

#### 4. CSNF Cladding Degradation

The overall CSNF cladding degradation model includes several sub-models and analyses. The discussion that follows focuses on three areas: initial cladding condition, localized corrosion, and wet unzipping. These model areas were ultimately propagated through abstraction and into TSPA and are the most important models regarding clad performance.

- **Initial Cladding Condition**

No complex representational model was developed for evaluation of the initial clad condition presented in the *Initial Cladding Condition* AMR. Rather, literature information was used. In some instances, empirical relations were used to estimate some of the initial clad condition

---

<sup>1</sup> The software package, EQ3/6, Version 7.2b, was approved for QA work by LLNL and is identified as Computer Software Configuration Item (CSCI): UCRL-MA-110662 V 7.2b.

parameters, as discussed clearly in the *Initial Cladding Condition* AMR. Some relations were developed within the AMR and others were obtained from existing literature. Empirical relations were developed within the AMR for helium production and surface corrosion. Empirical relations were obtained from literature for cladding stress, helium fill gas pressure, and fission gas pressure (the last two being application of the Ideal Gas Law).

- **Localized Corrosion**

The evaluation of localized corrosion of Zircaloy did not involve any representational models. Either single value estimates or empirical relations, both based on experimental observations, were developed.

- **Wet Unzipping**

Two sets of representational models were developed to evaluate fuel rod unzipping; one set for the unzipping velocity and one for determining the amount of fuel exposed. Both bounding and representative models were developed, based on differing conceptualizations regarding the manner in which a crack would propagate. These models are clearly documented in the *Clad Degradation – Wet Unzipping* AMR. Multiple models were used to explicitly account for uncertainty in applying simplified representations of these processes.

#### 5. DSNF Degradation

The DSNF degradation component has a simple, bounding representational model. The AMR proposes a degradation rate for each group and then shows that using the N-reactor equation is a reasonably conservative bound.

#### 6. HLW Degradation

The HLW degradation component directly develops a regression equation for PA.

#### 7. Dissolved Radioisotope Concentration

The representational model used in the in-package chemistry component model is the geochemical equilibrium code, EQ3/6, and was also used as the representational model for evaluating solubility limits in both the *Pure Phase Solubility Limits – LANL* and *Summary of Dissolved Concentration Limits* AMRs.

#### 8. Colloidal Radioisotope Concentration

The representational model for the waste form colloid model is described most clearly in Figure 3.8-2 of the *Waste Form Degradation Process Model Report* (TDR-WIS-MD-000001). The flowchart in that figure describe how the reversible and irreversible colloid concentration is calculated based on ionic strength and pH, HLW colloid generation and stability, iron oxide availability and stability, groundwater colloid availability and stability, and sorption coefficients.

## D. Results

### 1. Radioisotope Inventory

The *Inventory Abstraction* AMR provides a recommended sub-set of radionuclides for consideration in TSPA analyses. The screening approach resulted in 27 radionuclides identified as important (24 based on human dose and 3 mandated by the Groundwater Protection Requirements of the proposed EPA Standard 40 CFR 197). The AMR also provides average WP inventories (grams per WP) for two waste form types, CSNF and codisposal WPs (CDSP).

### 2. In-Package Chemistry Component

Results were generated using EQ3/6 for the different combinations of uncertain input parameters discussed above. These results are documented in the *Summary of In-Package Chemistry for Waste Forms* AMR. A sampling of the results are shown in figures, with all results contained on a CD that accompanies the AMR. In addition, the results were placed in the technical data management system.

The results from the *Summary of In-Package Chemistry for Waste Forms* AMR were used as input for developing the abstracted in-package chemistry models, as discussed in the *In-Package Chemistry Abstraction* AMR. This AMR developed response surfaces for solution pH, total carbonate concentration, and Eh. The abstracted pH response surfaces functionally include the uncertain input parameters (e.g., clad coverage, flow rate, and WP material corrosion rates) for both CSNF and CDSP waste types. Response surfaces were generated for two time periods. The first period is for times less than 1,000 years following WP breach and the second one for times greater.

The abstracted models for total carbonate and Eh are functions of the solution pH. Thus, the uncertainty in the input parameters is also considered in these abstractions through the pH.

A different approach was used to develop the abstracted model for ionic strength. For time periods less than 1,000 years following WP breach, the minimum ionic strength from all combinations of uncertain input parameters was used (for both CSNF and CDSP). For time periods greater, the average value was used.

Constant values were recommended for use in TSPA for the chloride concentration, oxygen fugacity, and carbon dioxide fugacity within the WP. A range was recommended for use in TSPA for the fluoride concentration.

### 3. CSNF Degradation

The result of the CSNF degradation component is two regression equations for the rate of spent fuel degradation as a function of pH,  $p[\text{CO}_3]_{\text{T}}$ ,  $p\text{O}_2$ , and temperature (T), one for pH less than or equal to 7 and the other is applicable for pH greater than 7.

#### 4. CSNF Cladding Degradation

The overall CSNF cladding degradation model includes several sub-models and analyses. The discussion that follows focuses on three areas: initial cladding condition, localized corrosion, and wet unzipping. These model areas were ultimately propagated through abstraction and into TSPA and are the most important models regarding clad performance.

- **Initial Cladding Condition**

The *Initial Cladding Condition* AMR clearly presents the analysis results. Ranges of parameter values are provided for the initial state of the cladding (e.g., burnup, internal pressure, oxide thickness, etc.). A probability distribution is also provided for the fraction of fuel rods failed initially within a WP. This distribution considers various fuel failure modes, including reactor operation, dry storage, and transportation.

- **Localized Corrosion**

The results of the analysis of localized corrosion are clearly presented in the *Clad Degradation – Local Corrosion of Zirconium and its Alloys Under Repository Conditions* AMR. An empirical model for the general corrosion of the Zircaloy clad is presented. Accelerated corrosion rates for different chemical compositions (pH, Cl<sup>-</sup>, F<sup>-</sup>) are also presented.

- **Wet Unzipping**

The result of the unzipping model, documented in the *Clad Degradation – Wet Unzipping* AMR, is a range of values that is multiplied by the CSNF alteration velocity to determine an unzipping rate. To account for uncertainties, the unzipping velocity is bound by 1 and 240, with a best estimate of 40 times the CSNF alteration velocity. This range was subsequently used in TSPA analyses.

The AMR also recommends a model for use in determining the amount of spent fuel exposed. This model is a simplified representation of the actual process that will occur and is deemed conservative. The most conservative model is also suggested as a possible approach for consideration in TSPA. This model was adopted.

#### 5. DSNF Degradation

The DSNF degradation component proposes a single fractional degradation rate value of  $\sim 45 \text{ yr}^{-1}$  to be used as the degradation rate. This value is large enough that the DSNF degrades within a single TSPA time-step after the WP fails.

#### 6. HLW Degradation

The result of the HLW degradation component is two expressions for the rate of borosilicate glass degradation as a function of pH and temperature (T), one for low pH and one for high pH.

These two equations form a V-shape when plotted as a function of pH. These expressions are directly used in TSPA.

## 7. Dissolved Radioisotope Concentration

The AMR entitled the *Pure Phase Solubility Limits – LANL* AMR documents thermodynamic data for several elements (Np, Pu) and provides recommended solubility limit ranges for other elements (Nb, Ni, Zr, Ra, Sn, Pa, Pb).

The AMR entitled *Summary of Dissolved Concentration Limits* AMR presents the recommended solubility limits for use in TSPA. Various different forms are recommended. Response surfaces are recommended for U, Np, Am, Pu. The AMR recommends that the Am response surface be used for Ac, Cm, and Sm, based on conclusions drawn in the *Pure Phase Solubility Limits – LANL* AMR. Several response surfaces were considered, with the most conservative one recommended for subsequent use. Probability distributions are recommended for other elements (Ni, Pa, Pb) based on the ranges recommended in the *Pure Phase Solubility Limits – LANL* AMR. Single bounding values are recommended for some elements (Nb, Zr, Ra). The values chosen are the upper extremes of the ranges recommended in the *Pure Phase Solubility Limits – LANL* AMR. A single value is also recommended for Th, supported by corroborating information. The AMR recommends that Tc, I, C, Cl, Cs, and Sr be considered as soluble.

## 8. Colloidal Radioisotope Concentration

The AMR entitled *Colloid-Associated Radionuclide Concentration Limits: ANL* clearly presents the results and observations obtained from laboratory testing. The AMR discusses the types of colloids that form (smectite clays in the case of HLW glass) and the manner in which they form. It presents the conclusion that HLW colloids become unstable above a critical ionic strength (~ 0.05 M) and presents a size distribution (log-normal with a mean size of approximately 100 – 160 nm). Empirical estimates of the rate of colloid formation for HLW glass under the test conditions are also provided. In the case of CSNF, the AMR concludes that the normalized release rate of Pu-bearing colloids is less than  $10^{-5}$  times the normalized release rate of technetium per day.

Abstracted models were developed in the *Waste Form Colloid-Associated Concentration Limits: Abstraction and Summary* AMR. Bounding empirical relations were developed based on experimental information and field observations (conducted at ANL and elsewhere). The abstractions consisted primarily as response surfaces. For example, zones of colloid instability were developed as functions of pH and ionic strength.

### **12.4 Discussion of Uncertainty Treatment**

An evaluation of uncertainty and variability treatment in the AMRs was performed for this exercise. For each AMR, the uncertainties/variabilities were identified and an evaluation was made of the treatment that was performed for each AMR. Thorough treatment was considered to be: identification, treatment, impact assessment, and clear presentation of the analysis and the propagation of uncertainty in the AMR. Table 12-1 is a synopsis of some of the uncertainties

and variabilities identified in this exercise. The following is a discussion of the evaluation process and uncertainty/variability analysis trends within the AMR/model process:

## A. Conceptual Model

### 1. Radioisotope Inventory Component

The screening approach is well documented and clearly presented in the AMR. Prior screening approaches conducted by both the YMP and the NRC are discussed.

### 2. In-Package Chemistry Component

Important conceptual model uncertainties are clearly discussed in Section 3.2.2 of the *Waste Form Degradation* PMR. This information is summarized in this section.

The in-package modeling effort in support of the SR represents the first attempt to model the chemical interactions that occur within the WP for use within the TSPA calculations. Only limited sensitivity runs have been completed to study the importance of uncertainties. Some of the conceptual model uncertainties are:

- **Feedback between chemistry and corrosion rates (built-in or iterations)** – The substantial accumulation of alteration products might “choke off” subsequent corrosion. At the same time, sharp shifts in fluid chemistry associated with WP alteration might also accelerate corrosion. At present, there is little feedback, either negative or positive, within the modeling. Iterations or more involved rate laws describing chemical corrosion would allow the more important feedbacks to be assessed. For example, for a flooded WP, the development of an alteration rind, even 1 cm thick, could prevent widespread oxidizing conditions at the sites of waste form degradation, which could substantially lower actinide solubilities. The uncertainties associated with predictions of fluid flow and solid exposure in the WP are formidable. By assuming full exposure of WP components, the calculation is conservative since it maximizes the potential for chemical degradation of the WP and for release of radionuclides.
- **Water contact scenario** – Predictions of specific degradation geometries and reduction in the uncertainty due to water contact scenario are difficult. The water contact scenario in the TSPA-SR analysis used to calculate in-package chemistries is merely the simplest of approaches. Only scoping calculations to determine the sensitivity of the system are justified at this time.
- **Hydrogen evolution** – The assumption was made that H<sub>2</sub> gas was not evolved in modeling carbon steel corrosion. This is conservative in allowing for the maximum pH reduction.
- **Radiolysis** – Radiolysis was neglected in the present analysis. The probability of WP breach is quite low before about 1,000 years, and the likelihood of significant radiolysis is much lower at later times. In theory the formation of NO<sub>2</sub> by radiolysis might conceivably cause in-package pHs to decrease by forming nitric acid. Two features that would tend to work

against such a scenario are the inherent buffer capacity of the assemblage and outgassing of NO<sub>2</sub> from the breached WP and into the drift. Radiolysis of water and off-gassing of H<sub>2</sub> may also increase the local effective Eh; however, at late times this is also not expected to be significant. Highly localized energy deposition from alpha decay might have some effect on dissolution rates, but these effects are also not expected to be significant.

The above limitations and uncertainties were considered as the modeling was performed. The range of predicted chemistry is quite large and conservative, and further work is expected to only fine-tune the scenario and time-dependent in-package chemistry. The calculated range of in-package chemistries is believed to represent the widest possible range of conditions that can confidently be expected. Indeed, a number of natural processes would tend to prevent more extreme chemistries than predicted here. Substantial reservoirs of freely exchangeable carbon dioxide would tend to prevent excursions to hyperalkaline conditions. Dissolution of solid components in the WP can buffer pH as well. The fact that free oxygen is likely to prevail in the drifts sets limits on how reduced WP fluids can become. Moreover, the accumulation of reactive corrosion products formed during WP degradation will also tend to buffer in-package solution chemistries.

### 3. CSNF Degradation Component

The conceptual model uncertainties are clearly discussed in the CSNF Degradation AMR and the Waste Form PMR. Because of the uncertainties, a regression that is reasonably conservative and bounds the experimental data was chosen. Some of the uncertainties are discussed next.

- Lack of mechanistic model – The CSNF degradation model is merely a regression of experimental data. The model is of the classical Butler-Volmer form, which has a thermodynamic basis, but is mainly empirical not mechanistic. Kinetic effects that are not predicted by thermodynamics alone can affect the degradation rate.
- Extrapolation error – Although some of the experiments have been ongoing for six years and CSNF degradation has been studied for many years, CSNF degradation in the repository will be over a much longer time than experiments. The extrapolation can lead to uncertainty, particularly because of the lack of a mechanistic model.
- Repository conditions – The experiments were conducted at a wide variety of conditions to attempt to bound repository conditions. However, uncertainty in the evolution of the in-package geochemical environment results in uncertainty.

### 4. CSNF Cladding Degradation Component

Development of the clad performance involved a formal evaluation of those FEPs related to clad performance. This approach helps to ensure completeness in the overall conceptual model of clad performance. Twenty FEPs were evaluated to determine their applicability. Those mechanisms that are not expected to affect clad performance in the repository environment have been screened out of further analyses. An example of this is localized corrosion resulting from chloride attack in pits. This failure mechanism has not been explicitly considered given the low

potential of achieving aggressive ferric chloride chemistries. The long-life of the WPs also results in a low potential for the generation of radiolytic acids. As such, radiolysis effects are not considered. However, to address the possibility of other forms of localized corrosion affecting clad performance, a conservative model has been developed.

The conceptual models of cladding degradation are based on over 40 years of experiments and observations of cladding behavior. The analysis of initial cladding conditions is based on reactor fuel performance reports that have been published since the start of the nuclear industry. Creep, SCC, and delayed hydride cracking analyses are supported by an extensive experimental base. Zirconium alloys were originally developed for use in the chemical industry to handle very corrosive fluids such as hydrochloric acid. In water environments, continuous corrosion experiments have been performed for 27.5 years. Fuel has been exposed in spent fuel pools for over 25 years and in dry storage research programs.

Constraints, caveats, and limitations to the model have been identified. The model is only applicable to commercial PWR fuel with Zircaloy cladding. Fuel reliability from reactor operation is for both PWR and BWRs. It is also limited to fuel exposed to normal operation and anticipated operational events (events which are anticipated to occur within a reactor lifetime), and not fuel that has been exposed to severe accidents. (For example, fuel from the Three Mile Island reactor accident is included in the DSNF fuel category.) Fuel burnup projections have been limited to the current licensing environment with restrictions on fuel enrichment, oxide coating thickness, and rod plenum pressures. Cladding degradation from YMP surface facility handling and operation was not considered.

##### 5. DSNF Degradation Component

The application of the DSNF and immobilized ceramic Pu degradation models involves the extrapolation of the models over long periods of time, which are orders of magnitude greater than the experimental test periods used to generate the data used to derive the models. ASTM C1174-97 (Section 24), recommends that uncertainties in the extrapolation of such models be minimized through the use of models whose mathematical forms are as mechanistic as possible. However, the lack of any directly relevant experimental dissolution/degradation data for many of the DSNF waste forms, and the small amount of data for those which have been tested, precludes the development of a mechanistic model at this time. Additionally, uncertainties in the data used to generate the models—such as in the surface area measurements used to calculate normalized dissolution rates—produce significant uncertainties even in the short-term application of the models. For this reason and because preliminary TSPA analyses have shown that the overall performance of the repository is very insensitive to the degradation rate of the DSNF, upper-limit or bounding degradation models will be used.

The initial results of TSPA sensitivity analyses for DSNF indicate that the performance of the repository is very insensitive to the DSNF degradation kinetics. That is, the use of the upper-limit model for the DSNF in the TSPA performed in that study still resulted in a calculated boundary dose well within requirements. Use of a less conservative model for the DSNF in the TSPA boundary dose calculation would not significantly lower the calculated boundary dose,

because even with the upper limit, model releases due to DSNF are significantly lower than those due to HLW and CSNF.

If, because of this insensitivity, the upper-limit model were the only one used for TSPA analyses, then validation of the other models would be unnecessary. Since the upper limit release model is that of instantaneous release of all radionuclides, i.e., the maximum rate conceivable, it does not require validation. It depends only on the total inventory of radionuclides in the DSNF. Thus, the upper limit model proposed for the DSNF and Pu disposal waste forms are impacted primarily by the total inventory of radionuclides that are present. The conservative and best estimate models for the DSNF waste forms are primarily impacted by the validity of the uranium metal-based SNF dissolution models.

For TSPA-VA, the model for the degradation of metallic uranium was a classic Arrhenius kinetic rate equation using parameters from assessments of SNF and HLW. The overall degradation rate was the Arrhenius rate times the effective surface area. In TSPA-VA, the effective surface area was five times the geometric surface area. Because the degradation rate estimated by the Arrhenius equation was so rapid, the sensitivity of the results to varying the multiplier for the geometric surface area between 0.1 and 100 (thus, the overall degradation rate) was small.

#### 6. HLW Degradation Component

The conceptual model uncertainties are clearly discussed in the Defense HLW Glass Degradation AMR and the Waste Form PMR. Because of the uncertainties, a regression that is reasonably conservative and bounds the experimental data was chosen. Some of the uncertainties, which are the same as for CSNF degradation, are discussed next.

- Lack of mechanistic model – Although the mechanism of glass dissolution has been studied extensively, the HLW degradation model is merely a regression of experimental data. Experimental results indicate that the long-term dissolution rate is controlled by the silica concentration in the water. However, the current TSPA approach does not compute the silica concentration in the water. Thus, the effect was approximately included as a coefficient in the overall regression equation.
- Extrapolation error – Although glass dissolution has been studied extensively for many years and in many countries, the extrapolation of short-term experiments can lead to uncertainty, particularly because the expression used in TSPA is not truly a mechanistic model.
- Repository conditions – As with the CSNF degradation experiments, the HLW experiments were conducted at a wide variety of conditions to attempt to bound repository conditions. However, uncertainty in the evolution of the in-package geochemical environment results in uncertainty.

#### 7. Dissolved Radioisotope Concentration Component

The primary conceptual uncertainty associated with evaluating and modeling concentration limits is the determination of the controlling mineral phase. This is clearly identified as a

conceptual uncertainty in the *Pure Phase Solubility Limits – LANL* and the *Summary of Dissolved Concentration Limits* AMRs. A conservative approach has been taken where the recommended solubility limits are based on the controlling phase that results in the highest concentration limit.

#### 8. Colloidal Radioisotope Concentration Component

The abstractions are based on laboratory results from waste form corrosion testing and testing of adsorption and desorption properties of Pu and Am on clay and iron-(hydr)oxide colloids. To the extent that the laboratory tests and test conditions represent anticipated repository conditions, the abstraction is valid for calculating the colloid-associated radionuclide concentrations and colloid mass concentrations.

The approach described herein for the colloidal radionuclide source term is consistent with what was done in the TSPA-VA but is more sophisticated in several ways. The treatment for the TSPA-SR analysis includes direct consideration of groundwater chemical conditions (pH and ionic strength) on stability of waste-form and corrosion-product colloids. The effect of ionic strength was considered in the TSPA-VA for groundwater colloids, as it is in the TSPA-SR analysis. In TSPA-VA, the concentration of colloids ( $C_c$ ) was evaluated from a linear empirical relation with ionic strength of the liquid solution. Here, the mass concentration of colloids is not assumed to be constant but varies according to groundwater chemical conditions. This approach provides more realism in the TSPA-SR analysis calculations.

In terms of radionuclide uptake, the treatment herein utilizes laboratory results that describe the irreversible uptake, or engulfing, of plutonium phases in smectitic waste-form colloids created during glass corrosion. In contrast, in the TSPA-VA, the parameter distribution for the fraction of radionuclides irreversibly sorbed on colloids was estimated using preliminary information from the Benham nuclear test area at the NTS. The Benham data showed rapid transport of colloid associated plutonium had occurred. For reversible uptake, a similar approach to what was used in the TSPA-VA is used; experimental results for Pu and Am sorption by colloidal iron-(hydr)oxides, montmorillonite, and silica were used to develop  $K_d$  values.

An alternative model for waste-form colloid generation was proposed in *Colloid-Associated Radionuclide Concentration Limits* (ANL-EBS-MD-000020) in which the rate of colloid formation was based on the amount of altered waste form as indicated by release of boron for glass and technetium for spent fuel. This model was not used because it is based on limited laboratory data. It may, however, be useful in the future.

To a large extent, the effectiveness of colloids in facilitating contaminant transport is due to their very large surface area available for sorption. Depending on the size distribution of colloids in the groundwater, the impact of choosing a mass-based  $K_d$ , or a surface-area-based  $K_a$ , may be significant. The greatest variability exists in situations in which an inordinately large number of very small colloids exist, which have a high surface-area-to-mass ratio. Based on experimental measurements and observations of colloid characteristics in Yucca Mountain groundwater, this situation does not exist at Yucca Mountain, and the use of a mass-based  $K_d$  is appropriate.

In the TSPA-VA, a slightly different approach was taken by assuming a constant steady-state mass concentration of colloids in groundwater. The steady-state mass concentration was embedded in a sorption term referred to as  $K_c$ . The approach described herein is more comprehensive in that the effect of ionic strength and pH on mass concentration is included. In the waste-form area, the  $K_d$  approach adopted here will provide more realism by accounting for the destabilizing effect of high ionic strength conditions and some pH conditions. The  $K_c$  approach, however, is well suited for far-field transport, where transients in aqueous chemical conditions are not expected.

## **B. Parameters**

### 1. Radioisotope Inventory Component

The screening analysis is reasonable because all fuel types, bounding and average, all time periods, and all transport groups were examined. Any changes that might be expected in the wastes that may be disposed at Yucca Mountain will not change the radionuclides that were screened in for modeling in TSPA.

### 2. In-Package Chemistry Component

As discussed above, important parameters in the in-package model were treated as being uncertain. The in-package chemistry was determined for all combinations of the uncertain parameters considered. The documentation contained in the *Summary of In-Package Chemistry for Waste Forms* AMR regarding the treatment of parameter uncertainty was quite clear. However, it was noted in the review that the various dissolution rate equations used is based on information from various source documents, not including other AMRs or calculations. In particular, a large amount of information is accessible only through a data tracking number that accesses a large spreadsheet calculation (DTN: SN9911T0811199.003).

A key input to the in-package chemistry analysis is the EQ3/6 thermodynamic database. However, no uncertainty in this database is considered beyond stating the following assumption.

“... the existing database supplied with the EQ3/6 computer package is sufficiently accurate for the purposes of this calculation. The justification for this is that the data have been carefully scrutinized by many experts over the course of several decades and carefully selected by Lawrence Livermore National Laboratory for incorporation in to the database. These databases are periodically updated and/or new databases added.”

### 3. CSNF Degradation Component

The CSNF degradation model is a regression of experimental data, which has some inherent error. The experimental error is discussed in the AMR and is probably small. Regression also introduces uncertainty. The coefficients are chosen to minimize the error, but the model is expected to be correct within about 1.5 orders of magnitude.

The abstracted CSNF dissolution model was based on a large set of qualified flow-through experiments. It is valid from pH 3 to 10, oxygen pressure from 0.002 to 0.2 atmospheres, and total carbon concentrations from  $2 \times 10^{-4}$  to  $2 \times 10^{-2}$  molar. At pHs less than or equal to 7, this model is valid at  $\text{CO}_2$  pressures of  $10^{-3}$  atmospheres. From an analysis of the fit of the model to the data, and from further consideration of the uncertainty of application of data from young spent fuel (< 30 years out of reactor) and unburned  $\text{UO}_2$  toward the prediction of long-term (> 1,000 year) performance of spent fuel, the model was estimated to be valid to within 1.5 orders of magnitude. This model was compared to unsaturated drip tests, batch tests, and a range of literature results. The model and uncertainty range adequately accounted for, or overestimated, all dissolution rate data. In addition, a comparison of the phases produced in the unsaturated drip tests compare well with that of natural analogs.

The surface area of the CSNF in the experiments is not known precisely. It is assumed to be  $2.1 \times 10^{-4} \text{ m}^2/\text{g}$ , based on an idealized geometry of wedge shaped pieces. If a roughness factor (the ratio of the measured surface area to the geometrically estimated surface area) of three is assumed, the high-drip-rate dissolution rates are estimated to be 17 and 38  $\text{mg}/(\text{m}^2 \cdot \text{d})$ , compared against a predicted value of 22  $\text{mg}/(\text{m}^2 \cdot \text{d})$  at pH 8, 0.001 mol/L carbonate, and  $90^\circ\text{C}$  for a fuel with a burnup of 30 MWd/kgU. Therefore, the agreement between the rate model above and  $^{99}\text{Tc}$  release rates is good. The calculations for the other isotopes show reduced release rates because the isotopes are retained in corrosion products.

#### 4. CSNF Cladding Degradation Component

The overall CSNF cladding degradation model includes several sub-models and analyses. The discussion that follows focuses on three areas: initial cladding condition, localized corrosion, and wet unzipping. These model areas were ultimately propagated through abstraction and into TSPA and are the most important models regarding clad performance.

- **Initial Cladding Condition**

The evaluation of the initial condition of CSNF cladding, documented in the *Initial Cladding Condition* AMR, considered various sources of information for key input parameters. The source information often provided ranges of values for the parameters. Thus, parameter uncertainty is treated in the analysis through the use of multiple information sources and consideration of the ranges in values provided from these sources. The AMR clearly points out that the analysis is based on PWR CSNF and provides justification that the analysis bounds the expected condition of BWR CSNF.

- **General and Localized Corrosion**

A simple empirical relation for the general corrosion of Zircaloy and its alloys is presented from the work conducted at Bettis Atomic Power Laboratory. Uncertainty in the relation is not discussed. However, the relation indicates that general corrosion of Zircaloy under repository-relevant conditions is expected to be very slow (no penetration within one million years) and any uncertainty in the general corrosion rate will not affect the performance of the clad.

The information obtained from literature was utilized in regression fits of the localized corrosion of zirconium and its alloys as a function of chemistry (pH, Cl<sup>-</sup>, F<sup>-</sup>). However, besides showing a figure that plots predicted versus actual corrosion rates, uncertainty in the resultant regression is not discussed.

- **Wet Unzipping**

The wet unzipping model, documented in the *Clad Degradation – Wet Unzipping* AMR, treated parameter uncertainty differently for various parts of the evaluation. The parameter uncertainties associated with each aspect of the analysis were clearly documented. Constant parameters were used to evaluate the unzipping potential. It was concluded that the information to date indicates that the CSNF oxidative dissolution reactions are likely to be self-sealing in a fuel rod with perforated cladding. This results in limited availability of water for the reactions and negative volume changes. Under these conditions, unzipping is not expected to occur. However, the AMR points out that “only limited experimental evidence and no quantitative mass transport calculations are available to support this point.” To account for these uncertainties, it was conservatively assumed that perforated fuel rods do unzip.

The available information was also used to determine the rate under which perforated fuel rods unzip. Uncertain parameters (spent fuel dissolution rates, reaction product solid – fractional volume increase) were used to define the time range required to fill the fuel-clad gap with reaction products. Although a range of time was identified, it was conservatively recommended that the gap be instantaneously filled with reaction products.

Different approaches were used to determine the unzipping velocity, one deemed bounding and one deemed more representative. Uncertainty in the associated parameters was treated in the determination of unzipping velocity using both approaches. To account for uncertainty, the AMR recommended using an approach where the unzipping velocity is simply a value multiplied by the spent fuel alteration velocity. The recommended unzipping value, determined from the available information, is bound by 1 and 240, with a best estimate value of 40 times the CSNF alteration velocity.

## 5. DSNF Degradation Component

No parameter uncertainty is specified in the DSNF degradation component. A single, bounding fractional degradation rate value of 45 yr<sup>-1</sup> is used for the fractional degradation rate of the matrix.

## 6. HLW Degradation Component

Based on regression of experimental data, the parameters in the glass degradation equation are all given with stochastic ranges. The ranges are used directly in TSPA.

## 7. Dissolved Radioisotope Concentration Component

Various sources of information were used to evaluate solubility limits in the *Pure Phase Solubility Limits – LANL AMR*. These information sources result in a range of solubility behavior that was considered in the analyses.

The entire range of results from the *Pure Phase Solubility Limits – LANL AMR* was considered in developing the recommended solubility limits for use in TSPA. As such, uncertainty in parameters was explicitly assessed in developing the TSPA solubility limits documented in the *Summary of Dissolved Concentration Limits AMR*.

## 8. Colloidal Radioisotope Concentration Component

As stated above, the source of information used in the *Colloid-Associated Radionuclide Concentration Limits: ANL AMR* is laboratory data from waste form material degradation tests conducted at ANL. The uncertainties associated with this experimental data are clearly discussed.

With the exception of the effective distribution coefficient used for the reversible attachment of radionuclides to colloids, uncertainty in all parameters used in the analysis is clearly discussed in the *Colloid-Associated Radionuclide Concentration Limits: ANL* and the *Waste Form Colloid-Associated Concentration Limits: Abstraction and Summary AMR*.

## **C. Representational Model**

### 1. Radioisotope Inventory

The radioisotope screening methodology and the determination of the average WP radioisotope inventory required no representational model.

### 2. In-Package Chemistry Component

The *Summary of In-Package Chemistry for Waste Forms AMR* discusses the use of the EQ3/6 software (Section 3.1). Although it is stated that “the programs have been used only within the range of validation in accordance with AP-SI.1Q,” a discussion of the uncertainty associated with the software is not provided.

### 3. CSNF Degradation

The CSNF degradation component produces a reasonably conservative regression that is used directly by PA.

### 4. CSNF Cladding Degradation

The overall CSNF cladding degradation model includes several sub-models and analyses. The discussion that follows focuses on three areas: initial cladding condition, localized corrosion, and

wet unzipping. These model areas were ultimately propagated through abstraction and into TSPA and are the most important models regarding clad performance.

- **Initial Cladding Condition**

As discussed above, no complex representational model was used to evaluate the initial cladding condition. Empirical relations were used in the development of some parameters. Representational model uncertainty was not explicitly considered in these relations. However, application of these relations using a range of uncertain parameters resulted in a range of output results, which likely captures the range of uncertainty.

- **Localized Corrosion**

The evaluation of localized corrosion of Zircaloy did not involve any representational models.

- **Wet Unzipping**

As discussed above, two different approaches were used to determine the unzipping velocity. The bounding approach used fracture mechanics and the mechanical properties of Zircaloy. In the representative approach, experimental evidence related to the shape of the breached rod is used.

Three different representational approaches are also presented that can be used to determine the amount of spent fuel exposed as a result of unzipping. These approaches differ in their degree of simplification, the simpler ones being conservative. The most conservative of these representational approaches is to assume that the spent fuel is reacted once the unzipping breach has reached the axial location of that spent fuel.

## 5. DSNF Degradation

The DSNF degradation component produces a reasonably conservative rate value for use in TSPA.

## 6. HLW Degradation

The HLW degradation component produces a reasonably conservative rate value for use in TSPA.

## 7. Dissolved Radioisotope Concentration

Both the *Pure Phase Solubility Limits – LANL* and *Summary of Dissolved Concentration Limits* AMRs discuss the use of the EQ3/6 software (Section 3 in both AMRs). Although it is stated in the *Pure Phase Solubility Limits – LANL* AMR that “the programs have been used only within the range of validation in accordance with AP-SI.1Q,” a discussion of the uncertainty associated

with the software is not provided. A similar observation is made in regard to in-package chemistry modeling.

## 8. Colloidal Radioisotope Concentration

The development of the waste form colloid model used no representational model.

### **D. Results**

#### 1. Radioisotope Inventory

The screening approach resulted in a single sub-set of radioisotopes recommended for consideration in TSPA analyses. The nominal, disruptive, and human intrusion scenarios were considered. The approach, and the resultant screened radioisotope sub-set, is felt to be conservative.

Single values of the representative radioisotope inventory for an average CSNF and CDSP WP are provided. The actual waste streams and inventories will be known only at the time of actual repository loading. The projected waste streams could differ from the actual waste streams in their fuel burnups, fuel ages, fuel enrichments, and utility efficiencies. However, changes that might be expected in the waste stream will produce only minimal (less than 20 percent) changes in the radionuclide activities in the fuels. Given this, the values chosen for initial inventories in CSNF and codisposal WPs are felt to be reasonable representations of the inventory that may be disposed at Yucca Mountain.

#### 2. In-Package Chemistry Component

As discussed above, both the process modeling results and the abstracted model appropriately represent the uncertainty explicitly treated in the in-package modeling effort.

#### 3. CSNF Degradation

The CSNF degradation component produces a reasonably conservative regression that is used directly by PA.

#### 4. CSNF Cladding Degradation

The overall CSNF cladding degradation model includes several sub-models and analyses. The discussion that follows focuses on three areas: initial cladding condition, localized corrosion, and wet unzipping. These model areas were ultimately propagated through abstraction and into TSPA and are the most important models regarding clad performance.

- **Initial Cladding Condition**

As discussed above, results presented in the *Initial Cladding Condition* AMR all include uncertainty. Ranges of parameter values are provided for the initial state of the cladding. A

probability distribution is also provided for the fraction of fuel rods failed initially within a WP. It is clearly stated in the AMR that this distribution does not consider any failures related from handling at the repository.

- **Localized Corrosion**

No uncertainty in the results is presented in the *Clad Degradation – Local Corrosion of Zirconium and its Alloys Under Repository Conditions* AMR, except for a range of accelerated corrosion rates to use when the pH is greater than 3.18, the fluoride concentration is greater than 5 ppm, and the temperature is less than 55°C.

- **Wet Unzipping**

As discussed above, the results of the unzipping model account for uncertainty through the recommendation of a broad range of unzipping velocity factors and models for use in calculating the amount of fuel exposed.

#### 5. DSNF Degradation

The DSNF degradation component produces a reasonably conservative rate expression for use in TSPA.

#### 6. HLW Degradation

The HLW degradation component produces a reasonably conservative rate expression for use in TSPA.

#### 7. Dissolved Radioisotope Concentration

As discussed above, solubility limits recommended for use in TSPA are response surfaces, probability distributions, or single values. Different response surfaces were considered for U, Np, Am, and Pu with the most conservative one recommended for subsequent use in TSPA. Explicit treatment of uncertainty in the solubility limit for these response surfaces results from uncertainty in the inputs to the response function (e.g., pH, carbon dioxide fugacity).

Probability distributions were recommended for Ni, Pa, and Pb. Thus, uncertainty in the solubility limits is inherent in the chosen distributions. Single values are chosen for the solubility limit of Nb, Zr, Ra, and Th where the value is felt to be bounding, except for Th.

#### 8. Colloidal Radioisotope Concentration

As discussed above, the AMR entitled *Colloid-Associated Radionuclide Concentration Limits: ANL* clearly presents the results. Uncertainties associated with these results are also discussed within the AMR.

As discussed above, abstracted models in the form of response surfaces were developed in the *Waste Form Colloid-Associated Concentration Limits: Abstraction and Summary* AMR. Uncertainty in the response surface itself was not explicitly considered. However, the response surfaces are deemed to be bounding. As such, uncertainty in the output of the response surface (for example radionuclide bearing colloid concentration) results solely from uncertainty in the input parameter (ionic strength in the case of the example cited). An alternative abstraction model is also presented. However, the AMR clearly states the model is “preliminary and is provided for information and as a basis for potential discussion and planning.”

## **12.5 Uncertainty Propagation**

### **1. Radioisotope Inventory Component**

The sub-set of radioisotopes obtained through the screening approach are used directly in TSPA. In addition, the average radioisotope inventory determined for the CSNF and CDSP waste forms is also used directly in TSPA.

The inventories of the main radioisotopes are accounted for in TSPA through reasonable representations that are not expected to change significantly. Any inventory changes due to future changes in fuel burnup or receipt of waste at the repository are expected to have minimal impact because the abstraction uses a reasonable average for the inventory.

### **2. In-Package Chemistry Component**

The uncertainties related to the in-package chemistry component model are clearly propagated through the AMRs up to the abstraction into TSPA. The regression used in TSPA is the same as proposed in the AMR. This regression has an uncertainty term that chooses a value for the pH between a high and low value, which is based on the potential in-package material. This accounts for uncertainty and variability in the repository.

### **3. CSNF Degradation Component**

The uncertainties related to the CSNF degradation component model are clearly propagated through the AMRs up to the abstraction into TSPA. The regression used in TSPA is the same as proposed in the AMR. The regression for degradation is based on experimental data. An uncertainty term in the regression of  $\pm$  one order of magnitude accounts for uncertainty in the experimental conditions, extrapolation of experimental data, and regression error. The regression is reasonably conservative.

### **4. CSNF Cladding Degradation Component**

The uncertainties related to the CSNF degradation component model are clearly propagated through the process-based AMRs through the abstraction AMR (*Clad Degradation – Summary and Abstraction* AMR) and into TSPA.

- **Initial Clad Failure**

The initial number of clad perforations was represented as a probability distribution. This distribution was developed in the *Initial Cladding Condition* AMR.

- **Creep Failure**

The abstraction AMR developed the entire model to assess the potential for creep failure of the cladding. The entire documentation regarding this approach is clearly presented in this AMR. Various creep correlations were compared with the one that best fit the data selected. Uncertainty associated with this correlation was also discussed. Although the correlation was developed for unirradiated cladding, it is clearly demonstrated as being bounding for irradiated clad.

In regard to uncertainty propagation, the correlation was used to define a probability distribution for the fraction of fuel rods perforated from creep as a function of WP surface temperature. This distribution was used directly in the TSPA model.

However, an apparent disconnect with supporting AMRs was noticed. No information regarding the initial state of the clad, as documented in the initial cladding condition AMR, appears to have been considered in the analysis. Namely, the probability distributions for gas pressures and the recommended correlations for computing the gas pressure as a function of temperature do not appear to have been used.

- **Localized Corrosion**

The *Clad Degradation – Summary and Abstraction* AMR develops a simplified approach to model corrosion of Zircaloy in fluoride-containing environments. However, it does not appear that any of the recommendations made in the supporting *Clad Degradation – Local Corrosion of Zirconium and its Alloys Under Repository Conditions* AMR were explicitly included. However, the model developed in the abstraction AMR is considered conservative.

- **Wet Unzipping**

The recommended range for the unzipping velocity, represented as a multiplier to the CSNF alteration velocity provided in the *Clad Degradation – Wet Unzipping* AMR, was used directly. However, neither the *Clad Degradation – Summary and Abstraction* AMR nor the TSPA document mention that current evidence, although uncertain, indicates that wet unzipping is actually unlikely. The abstraction also uses the conservative approach regarding exposed fuel surface area discussed in the *Clad Degradation – Summary and Abstraction* AMR where the entire fuel surface is assumed to be altered at the location where the unzipping is occurring.

The uncertainties related to the CSNF cladding degradation component model are clearly propagated through the AMRs up to the abstraction into TSPA. The regression used in TSPA is the same as proposed in the AMR. Each term in the model is either given as a distribution based

on experimental data or as a bounding value. The localized corrosion model (due to fluoride in the water) is a surrogate for unknown corrosion mechanisms. The unzipping uncertainty parameter (1 to 240) gives a reasonably conservative model.

#### 5. DSNF Degradation Component

The uncertainties related to the DSNF degradation component model are clearly propagated through the AMRs up to the abstraction into TSPA. The N-reactor fuel, which is the major portion of DSNF, has the highest degradation rate. Use of N-reactor as a surrogate for all DSNF is reasonably conservative. The bounding fractional degradation rate value of  $45 \text{ yr}^{-1}$  ensures that the entire matrix of DSNF degrades in a single TSPA time-step.

#### 6. HLW Degradation Component

The uncertainties related to the HLW degradation component model are clearly propagated through the AMRs up to the abstraction into TSPA. The regression used in TSPA is the same as proposed in the process model AMR. The uncertainty is implemented through uncertainty in the coefficients in the regression and uncertainty in the chemical conditions. A surface area cracking factor of approximately 20 is reasonably conservative.

#### 7. Dissolved Radioisotope Concentration Component

The uncertainties related to the dissolved radioisotope concentration component model are clearly propagated from the *Pure Phase Solubility Limits – LANL* through the abstraction, documented in the *Summary of Dissolved Concentration Limits* AMR, and into TSPA. As discussed above, the chosen representations of solubility are conservative based on bounding values, reasonable regressions of experimental data, or theoretical calculations using the most soluble controlling phase.

#### 8. Colloidal Radioisotope Concentration Component

The development of the colloidal radioisotope concentration component model is based on laboratory data specific to Yucca Mountain and literature information. The information was used to develop abstracted models (deemed to be bounding) for use in TSPA. These abstracted models were implemented as recommended in the TSPA model. Uncertainty propagation is through pH and ionic strength parameters in the colloidal concentration equations used in TSPA. These parameters are determined in the in-package chemistry component model.

**Table 12-1: Waste Form Degradation Model**

<p><b>Model Purpose:</b> The Waste Form Degradation Model predicts the dissolved or colloidal radionuclides available for transport in the TSPA for SR (TSPA-SR). The Waste Form Degradation Model consists of eight major modeling/analysis components: 1) Radioisotope Inventory; 2) In-Package Chemistry; 3) CSNF Degradation; 4) CSNF Cladding Degradation; 5) DSNF Degradation; 6) HLW Degradation; 7) Radioisotope Dissolved Concentration (solubility); and 8) Radioisotope Colloidal Concentration. These eight components are generally connected sequentially starting with the radioisotope inventory as input and ending with projected radioisotope dissolved and colloidal concentration. Unless otherwise stated, the references in this table refer to pages in the corresponding model component AMRs.</p>				
Summary	Source	Treatment	Basis	Impact
<b>Conceptual Model</b>				
Radioisotope Inventory	The sources of information are based on internal documents for CSNF, reports from the NSNFP for DSNF, and the EIS for HLW. An updated screening was conducted and resulted in 27 radionuclides identified as important (24 based on human dose and 3 mandated by the Groundwater Protection Requirements of the proposed EPA Standard 40 CFR 197 [64 FR 46976]).	The radioisotope inventory abstraction component estimates the inventory of those radionuclides most important to human dose. The inventory abstraction component is input for the waste form degradation models and is developed from a series of steps that starts with radioisotope inventories of various spent nuclear fuel assemblies and HLW then estimates the radioisotope inventory when packaged in disposal containers. Three important aspects of the radionuclide inventory are 1) selecting the most important radionuclides for human dose out of the few hundred found within the waste; 2) obtaining the radioisotope inventories of various wastes; and 3) grouping the fuels into the WPs selected for modeling in the TSPA-SR analysis.	Not discussed in AMR.	Not discussed in AMR. PMR indicates changes in the waste stream will produce only minimal (less than 20 percent) change in radionuclide activities in fuel. Impact on dose is not discussed.

<p>In-Package Chemistry</p>	<p>The analysis is performed using the EQ3/6 geochemical code. The sources of information for the EQ3/6 geochemical simulations include a chemical thermodynamics database and information on the in-package environment. These results influence degradation of the CSNF cladding and matrix, HLW degradation, radionuclide solubility, and colloid availability and stability. The degradation of the CSNF matrix and HLW, in turn, influence the In-Package Chemistry Component.</p>	<p>The in-package chemistry model component estimates the fluid chemistry inside the WP over time after the initial breach of the disposal container. This chemistry is then used by the several other model components since the rate of degradation of the matrix of waste, the resulting dissolved concentration of radionuclides, the stability of any colloids, and degradation of cladding are all dependent on the chemistry of fluids within the WP. The rate of degradation of the waste matrix and inner stainless steel container, in turn, influences the fluid chemistry and so there is a coupling between all the chemically interacting components of the system.</p>	<p>Use of EQ3/6 is a reasonable approach to bounding the in-package chemistry.</p>	<p>Not discussed in AMR.</p>
-----------------------------	---	---	--	------------------------------

<p>CSNF Matrix Degradation</p>	<p>The regression variables used, pH, <math>p[\text{CO}_3]_T</math> and <math>P_{\text{O}_2}</math>, are coupled to in-package chemistry to account for uncertainty. The sources of information include flow through, static, batch reactor, and drip tests involving the dissolution of fresh and spent reactor fuels under both saturated and unsaturated conditions.</p>	<p>The CSNF degradation model component determines the rate of degradation of the CSNF fuel as a function of temperature and water chemistry (specifically, pH, and partial pressures of <math>\text{O}_2</math> and <math>\text{CO}_2</math>). This degradation rate function is combined with the in-package chemistry to determine a rate, which is then directly used by the Cladding Degradation Model Component to determine the rate that the CSNF cladding splits open and exposes more of the fuel matrix. In addition, the CSNF degradation model examined the distribution of radionuclides within the fuel and established a gap fraction for the more volatile radionuclides.</p>	<p>Not discussed in AMR.</p>	<p>Affects the rate of CSNF dissolution and radionuclide release from waste form.</p>
--------------------------------	---	--	------------------------------	---

<p>CSNF Cladding Degradation</p>	<p>The sources of information include failure data from reactor operation, pool and dry storage, and transportation. To better evaluate the performance of the cladding, two steps of degradation are included: perforation and matrix exposure. Perforation mechanisms include cladding damage during reactor use, creep failures at high temperatures during dry storage, transportation, or initial disposal, mechanical failure from earthquakes, and localized corrosion after disposal. The process of exposing the matrix and releasing radionuclides is through potential unzipping of the cladding caused by expansion of the fuel matrix as the uranium dioxide (UO<sub>2</sub>) forms secondary minerals.</p>	<p>The cladding degradation component of the Waste Form Degradation Model predicts the rate that the CSNF matrix is exposed and altered based on the number of rods with perforated cladding at any one time.</p>	<p>Not discussed in AMR.</p>	<p>Affects the rate of CSNF dissolution and radionuclide release from waste form.</p>
----------------------------------	--	---	------------------------------	---

DSNF Degradation	<p>The <i>DSNF Degradation Component</i> developed for TSPA-SR uses a constant, bounding degradation rate based upon experimental data for N-Reactor SNF for all the DSNF waste types with the exception of naval SNF. However, the radioisotope inventory is the weighted mass average of DSNF waste types. Naval SNF degradation behavior is bounded by that of the CSNF.</p>	<p>The DSNF Degradation Model Component predicts the rate of degradation of the DSNF waste category and of the immobilized plutonium ceramic waste. The component was developed using the logic shown in Figure 3 of <i>Standard Practice for Prediction of the Long-Term Behavior of Materials, Including Waste Forms, Used in Engineered Barrier Systems (EBS) for Geologic Disposal of High-Level Radioactive Waste</i> (ASTM C1174-97).</p>	<p>Bounding approach used in the model.</p>	<p>Essentially releases DSNF as soon as the WP fails. PMR indicates that past studies have shown the dose to be insensitive to DSNF.</p>
HLW Degradation	<p>The <i>HLW Degradation Component</i> developed for TSPA-SR uses bounds on parameters of a phenomenological model to develop a simplified (Arrhenius-type) rate equation of degradation that is dependent only upon pH and temperature. Conservative estimates of the model parameters are based upon experimental data for the degradation of borosilicate glass.</p>	<p>The HLW Degradation Component provides a conservative model for calculating the rate of degradation of borosilicate glass for the range of conditions (immersion, humid air, and dripping water) to which it may be exposed after the WPs fail.</p>	<p>Not discussed in AMR.</p>	<p>Affects the rate of glass dissolution and radionuclide release from waste form.</p>

<p>Dissolved Radioisotope Concentration</p>	<p>The sources of information include EQ3/6 simulations of in-package chemistry for three categories of radionuclides. Three radioisotope solubilities were abstracted as a direct function of in-package chemistry (Np, U, Am) and three radionuclides solubilities (Ac, Cm, Sm) set equal to that of Am. Four additional radioisotope solubilities were defined by probability distributions (Pu, Pb, Pa, Ni). All other radioisotope solubilities were set at bounding values. The distributions and bounding values were based on results of the process modeling of the in-package chemistry.</p>	<p>The dissolved concentration component evaluates the dissolved concentration of radionuclides (or parents of radionuclides) that are important to human dose as determined by the radioisotope screening described in the inventory.</p> <p>Doses calculated for groundwater pathways from the repository to the environment depend critically on the concentrations of radionuclides in fluids issuing from breached WPs. While dissolution of radioisotope-containing SNF rods and/or HLW glass solids into incoming fluids provides the primary source term, the formation of secondary phases often limits the amounts of radionuclides available for subsequent groundwater transport.</p>	<p>Reasonable solubility values provided to TSPA based on experimental data and EQ3/6 calculations.</p>	<p>Affects EBS release rate and dose.</p>
---	--	---	---	---

Colloidal Radioisotope Concentration	For the <i>Colloidal Radioisotope Concentration Component</i> , the conceptualization directly used YMP-relevant experimental results from YMP-specific work and from the published literature. The conceptualization identified the availability and the stability of three categories of colloids: 1) existing colloids in the groundwater; 2) colloids generated during degradation of the waste; and 3) colloids generated during degradation of the disposal container.	The colloidal radioisotope concentration component calculates the concentration of colloid-associated radionuclides that may be transported from the WP.	Reasonably bounding model developed in AMR.	Affects EBS release rate and dose.
<b>Parameters and Inputs</b>				
<u>Inventory Abstraction</u> : The relative importance of individual radionuclides when estimating inhalation and ingestion doses was determined. The goal was to identify the radionuclides that contribute to 95% of the dose. (Section 4.1.1)	Input Transmittal for Status of the Radionuclide Screening for the Total Systems Performance Assessment - Site Recommendation (TSPA-SR), R&E-PA-99217.Tb (CRWMS M&O 1999c)	Calculating the relative importance involved multiplying its inventory abundance by the dose conversion factor. Then, the radionuclides were ranked with the highest contributor to the dose given the highest ranking. Each relative dose was then converted to a percent contribution, and a cumulative sum of the percent dose contributions was calculated for each radionuclide in its ranked order. Last, the radionuclides were chosen for the calculation to assure a reasonable estimate of the dose.	Not discussed in AMR.	Not discussed in AMR. PMR indicates changes in the waste stream will produce only minimal (less than 20 percent) change in radionuclide activities in fuel. Impact on dose is not discussed.

<p><u>Initial Cladding Condition:</u> Fission gas releases are estimated from inadequate data</p>	<p>Limited data is available in the literature. It varies greatly: sometimes the dependence on parameters is known, sometimes not.</p>	<p>Very conservative estimates are used.</p>	<p>Very conservative estimates are based on systematic overestimation of the limited data.</p>	<p>Probable effect is discussed in the AMR. It is overestimation of the number of fuel rods that will fail.</p>
<p><u>CSNF Waste Form Degradation:</u> Flow-through test dissolution data (AMR Section 4.1.2, Pages 17-20)</p>	<p>The exact water conditions and chemistry of groundwater that could eventually contact spent fuel is not well known. Based on the information provided in Table 1, the dissolution rate is seen to vary with water temperature, CO<sub>3</sub> concentration, O<sub>2</sub> concentration, and pH.</p>	<p>Dissolution tests on spent fuel were performed at several different temperatures, pHs, oxygen and carbonate concentrations, and fuel burnups in order to attempt to quantify the effects of varying these parameters on dissolution rate in the flow-through scenario. Section 4.1, Pg. 17, states "flow-through dissolution studies on spent fuel and UO<sub>2</sub> performed PNNL and LLNL, provides direct dissolution measurements over a wide range of aggressive conditions that bracket the typical Yucca Mountain groundwater and environmental conditions." Section 6.2.2.2, page 47, states "The tests that provide the data set for the model were undertaken at aggressive conditions to provide the basis for a <b>bounding dissolution model</b>. These aggressive conditions included alkaline pHs up to 10; total carbonate concentrations ten times that found in typical groundwaters, including J-13; and high water-flow rates that eliminated precipitation or reverse reactions." Thus parameter uncertainty</p>	<p>Section 1, Pg. 11, Purpose, states that "These models of CSNF degradation are bounding models that apply to all UO<sub>2</sub>-based spent fuel expected to be disposed in a repository. These models are valid within the range of qualified experimental data: pH down to 3 and up to 10, oxygen pressure from 0.002 to 0.2 atmospheres, carbonate/bicarbonate concentrations from 2x10<sup>-4</sup> to 2x10<sup>-2</sup> molar. At pHs less than or equal to 7, these models are only shown to be valid at CO<sub>2</sub> pressures of 10<sup>-3</sup> atmospheres. Corroborating data outside of these ranges indicate that the valid ranges may extend beyond those stated."</p>	<p>The impact of using test data taken over a wide range of water temperatures and water chemistry parameters is considered to be development of a mathematical model that is valid within the range of parameters that will actually occur in the Yucca Mountain groundwater. The impact of using a conservative mathematical model intended to predict dissolution rates that bound those that could actually occur is that the model could overpredict spent fuel dissolution rates by a relatively large factor, as discussed in a following item.</p>

<p><u>CSNF Waste Form Degradation: Spent Fuel Burnup</u></p>	<p>There is uncertainty with dissolution data associated with high burnup spent fuel. In runs #1 through 38 of Table 1, burnup varies from 15 to 50 MWd/kgU. Page 17 states "Runs 61-64 are new runs for a very high-burnup fuel (ATM-109, DTN: LL990901851021.084). The ATM-109 burnup measurements are still uncertain with an approximate value of 70 MWd/kgU (Wolf et al. 1999)."</p>	<p>Page 19 states "Because of this uncertainty in burnup, the newest four runs are separated in the table and were not a part of the modeling regression data set for Section 6.2. Instead, they were used for model validation."</p>	<p>Section 6.2.2.5, page 55, concludes that "the newest runs at high burn-up, 61-64, were not included in the production of the model and thus serve as validation runs. The error metrics (EM) of the abstraction model, Equation 16, and Table 16 are quite good (+0.05, +0.5, -0.32 and +0.15 for runs 61-64 respectively).</p>	<p>Since the error metrics are relatively small, it is considered that the mathematical model does a good job predicting fuel with very high burnup. Thus the impact of uncertainty due to spent fuel burnup could be characterized as small.</p>
--	---	---	--	---

<p><u>CSNF Waste Form Degradation:</u> Limited data for spent fuel dissolution rates in an acidic environment.</p>	<p>Data on the dissolution rate of spent fuel under acidic conditions in the flow-through tests is extremely limited. Whereas for alkaline conditions, there were 64 different runs performed, under acidic conditions only a single qualified measurement was made. Page 19 states that "Gray (DTN:LL990707151 021.075) reports an acidic spent fuel (ATM-103) dissolution rate of 109 mg/(m<sup>2</sup>xd) at a pH of 3. This measurement was performed at 25°C in 10<sup>-3</sup> M nitric acid sparged with CO<sub>2</sub>-free air. This is the only qualified data point at an acidic pH (Section 6.2.2.4)."</p>	<p>An abstracted acid dissolution model was constructed (Section 6.2.2.4, Page 54) using this qualified data point, the alkaline abstracted model, and the assumption that the temperature and oxygen pressure coefficients from the alkaline model could be used for the acid model. Unqualified outside data were obtained as discussed on Page 20: "Steward and Mones (1996) obtained acidic dissolution rates for UO<sub>2</sub> at room temperature. The UO<sub>2</sub> dissolution rates were 5 mg/(m<sup>2</sup>xd) at pH = 4 and 3 mg/(m<sup>2</sup>xd) at pH = 6. At 75°C the rate for pH = 4 was 23 mg/(m<sup>2</sup>xd). Table 2 contains published results (Torrero et al. 1997) of changes in UO<sub>2</sub> dissolution rate versus pH at room temperature. These data were used for confirmation purposes only in Section 6.2.2.5." Section 6.2.2.5 states "The Grambow model (Eq. 17) and the three NQ data points by Steward and Mones (1996) corroborate that the dissolution model in acid pH, Equation 18 is bounding (see Figure 12-2)... The error metrics for these three points are +0.93, +0.33, and +0.7</p>	<p>The basis for this treatment is discussed in Section 6.2.2.4, page 54. In regards to the assumption regarding coefficients, page 54 states "The basis of this assumption is the relative insensitivity of the wet dissolution rate to the relatively small range of temperature and assumed constant O<sub>2</sub> pressure in the repository. Next, the dissolution rate at pH = 7 was evaluated using the alkaline model (Eq. 16), at 25°C, atmospheric oxygen pressure, and CO<sub>2</sub> pressure of 10<sup>-3</sup> atmospheres. This calculated point was combined with the qualified data point at pH = 3 to obtain the slope and intercept terms, a<sub>4</sub> and a<sub>0</sub>, respectively. The resulting abstracted model is shown in Figure 12-2, along with several unqualified data points and the Grambow model. The resulting dissolution model (see Figure 12-2) gives reasonable or overestimated dissolution rates (see model validation, Section 6.2.2.5)."</p>	<p>The impact of the limited data upon which the acid dissolution model was based is that there is a relatively high degree of uncertainty. Section 6.2.2.4, page 54 states that "it is concluded that the uncertainty in the acid model is comparable to that in the alkaline model." The alkaline model for the spent fuel dissolution rate has an uncertainty of approximately a factor of 32, as discussed above.</p>
<p><u>HLW Glass Degradation:</u> Dissolution rate parameters: pH dependence coefficient, effective activation energy, and the intrinsic rate coefficient</p>	<p>Literature data and experimental results mainly from borosilicate glass tests.</p>	<p>Uniform distributions have been used for these parameters and are well documented in the HLW glass AMR</p>	<p>This treatment bounds the dissolution rate parameters.</p>	<p>Not discussed in AMR.</p>

<u>Dissolved Radioisotope Concentration</u> : The dissolved concentration of radionuclides (or parents of radionuclides) that are important to human dose as determined by the radioisotope screening described in the inventory.	Literature data, experimental results, and results from analyses performed with EQ3/6 and EQ3NR.	Table 3.7-5 in the WF PMR (excerpted from Table 19 in the Summary of Dissolved Concentration Limits AMR) lists and summarizes the dissolved concentration limits used in TSPA-SR for the 21 radionuclides of interest. The distribution type (function, constant, or log-uniform) is included as well as the minimum and maximum values (mol/L).	The basis for the formulation of the distribution type (function, constant, or log-uniform) for each radionuclide of interest is well documented in the corresponding section of the Summary of Dissolved Concentration Limits AMR and summarized in Section 3.7.1 of the WF PMR.	Not discussed in AMR.
<u>Colloid Source Term</u> : Parameter names, definitions, and values that are used in the colloid source term model abstraction.	Literature data and experimental results on colloids.	Table 3.8-1 in the WF PMR (Same as Table 1 in the Waste Form Colloid-Associated Concentrations Limits: Abstraction and Summary AMR) lists and describes about 35 parameters for waste-form, iron-hydr(oxide), and groundwater colloids and the colloid source term. The values and distributions as well as the basis for all parameters are included in Table 3.8-1.	Table 3.8-1 in the WF PMR (Same as Table 1 in the Waste Form Colloid-Associated Concentrations Limits: Abstraction and Summary AMR) lists the basis for all parameters used in the colloid source term abstraction model.	Not discussed in AMR.
<b>Variability</b>				
Not applicable				
<b>Results</b>				
Aqueous radioisotope concentration	Not discussed in AMR.	The dissolved concentration limits (aqueous phase) for radioisotope concentrations builds upon three pieces of information: 1) estimates of in-package water chemistry (pH, Eh or oxygen partial pressure, ionic strength, carbonate concentration or partial pressure of carbon dioxide), 2) determination of the likely solubility-controlling phases for the specific radionuclides of concern, and 3) measured (or estimated) thermodynamic parameters describing the stability of aqueous species and solid radioisotope phases. From this information, a functional relationship, a distribution, or a constant value was selected for the radionuclides of importance.	Not discussed in AMR.	Not discussed in AMR.

Irreversible Colloid Fraction	Not discussed in AMR.	The mass of irreversibly bound radionuclides is tracked using surrogate species that represent the radioisotope mass embedded in waste form colloids. The masses of the surrogate species, or irreversibly bound isotopes, are proportional to the amount of waste form exposed using the high-level radioactive waste glass dissolution rate. To start the TSPA calculations, an initial inventory of radioisotopes must be provided. For the surrogate species, an arbitrarily large value is used, so that the irreversibly bound colloid species cannot become inventory limited. Irreversible colloids are allowed to form and be released as long as radioisotopes are present in the high-level radioactive waste glass waste form cell.	Not discussed in AMR.	Not discussed in AMR.
Reversible Colloid Fraction	Not discussed in AMR.	Each combination of colloid type (waste form, corrosion product, and groundwater) and critical radionuclide has a specified $K_d$ value representing reversibly sorbed radionuclide concentrations. To calculate the reversible radionuclide concentration in each waste form environment, colloid masses are determined based on ionic strength and, in all cases except groundwater colloids, pH. Masses are then used with dissolved radionuclide concentrations and $K_d$ values to determine a concentration associated with colloids.	Not discussed in AMR.	Not discussed in AMR.

## 13.0 Unsaturated Zone Transport Model

### 13.1 Purpose of Model/Intended Use

The purpose of the UZ transport model is to evaluate possible radionuclide transport from the potential repository horizon to the SZ beneath Yucca Mountain. The modeling approach synthesizes and integrates the complex UZ flow process and accounts for the transport of aqueous and colloidal species in interacting fracture and matrix continua resulting from advective/dispersive, diffusive, and sorptive processes.

The UZ modeling effort involved the development of two models. The objective of the first model, the site-scale UZ transport model, was to analyze the major transport mechanisms operating in the various lithologies, with particular emphasis on major hydrogeologic features (perched water, faults, permeability changes). The second model, itself a site-scale model, was developed to model UZ radionuclide transport within the overall TSPA model. Both models are summarized later in this chapter.

While modeling contaminant transport within geologic environments is widely performed, their use in unsaturated media is limited. Some of the main limitations result from uncertainties associated with modeling the movement of water within the UZ. These uncertainties are discussed in the chapter regarding UZ flow. Additional limitations arise in regard to modeling transport-related processes specific to unsaturated media at Yucca Mountain (such as matrix diffusion, sorption, dispersion, and colloidal transport).

### 13.2 Model Relations

The *Unsaturated Zone Flow and Transport Process Model Report* (PMR) (TDR-NBS-HS-000002) and several associated AMRs comprise the documentation of the unsaturated transport model. The titles, document identification numbers, and objectives of these reports is discussed below:

- *Development of Numerical Grids for UZ Flow and Transport Modeling* (ANL-EBS-HS-000015) – Develop numerical grids of the UZ hydrogeologic system beneath Yucca Mountain. This is an integral part of the development of complex three-dimensional UZ flow and transport models.
- *Conceptual and Numerical Models for UZ Flow and Transport* (MDL-NBS-HS-000005) – Document the conceptual and numerical models for modeling UZ fluid flow and solute transport.
- *Analysis of Hydrologic Properties Data* (ANL-NBS-HS-000002) – Describe the methods used to determine hydrologic properties based on the available field data from the UZ. Provide representative estimates of fracture and matrix properties for use in the inversion process in the *Calibrated Properties Model* AMR and fracture spacing for generating dual-permeability grids as documented in the *Development of Numerical Grids for UZ Flow and Transport* AMR.

- *Calibrated Properties Model* (MDL-NBS-HS-000003) – Develop calibrated parameter sets for unsaturated flow and transport models (matrix and fracture parameters).
- *UZ Flow Model and Submodels* (MDL-NBS-HS-000006) – Document the UZ fluid flow and solute transport models and submodels. Present UZ flow fields for subsequent use.
- *Unsaturated Zone and Saturated Zone Transport Properties* (ANL-NBS-HS-000019) – Summarize transport properties for the lower UZ hydrogeologic units and the SZ at Yucca Mountain and provide a summary of data from the Busted Butte UZ Transport Test.
- *Unsaturated Zone Colloid Transport Model* (ANL-NBS-HS-000028) – Document the development of a model for simulating colloid transport including: 1) evaluating the potential mechanisms for colloid transport; 2) providing ranges of parameters for significant colloid transport processes; and 3) providing a basis for the development of an abstracted model.
- *Radionuclide Transport Models Under Ambient Conditions* (MDL-NBS-HS-000008) – Evaluate (by means of 2D semianalytical and 3D numerical models) the transport of radioactive solutes and colloids in the UZ under ambient conditions.
- *Abstraction of Flow Fields for RIP* (ANL-NBS-HS-000023) – Post-process UZ site scale flow fields (simulated using TOUGH) for use by the FEHM particle tracking model that is integrated directly into the TSPA model.
- *Particle Tracking Model and Abstraction of Transport Processes* (ANL-NBS-HS-000026) – Presents the numerical methods for simulating radionuclide transport and model setup for the UZ transport abstraction model (FEHM<sup>1</sup> particle tracking approach).
- *Analysis of Base-Case Particle Tracking Results of the Base-Case Flow Fields* (ANL-NBS-HS-000024) – Provide insight into the UZ performance through particle tracking analysis of the base-case flow fields. Determine how different system parameters such as matrix diffusion, sorption, water-table rise, and perched water influence the transport of radionuclides to the water table.
- *Analysis Comparing Advective-Dispersive Transport Solution to Particle Tracking* (ANL-NBS-HS-000001) – Compare transport simulations utilizing particle tracking methods (two methods: FEHM and a dual continuum particle tracker) with simulations using the more rigorous fully coupled advective-dispersive approach.

Figures 13-1a, Model Relations for the Unsaturated Zone Radionuclide Transport Process Model, and Figure 13-1b, Model Relations for the Unsaturated Zone Radionuclide Transport Abstracted Model, illustrate the linkage of the various AMRs in the development of the UZ transport models. Figure 13-1a depicts the fully coupled advective-dispersive model (termed the process model in this chapter) and Figure 13-1b depicts the FEHM particle tracking model ultimately used by TSPA (termed the abstracted model).

---

<sup>1</sup> A FEHM transfer numerical analysis tool.

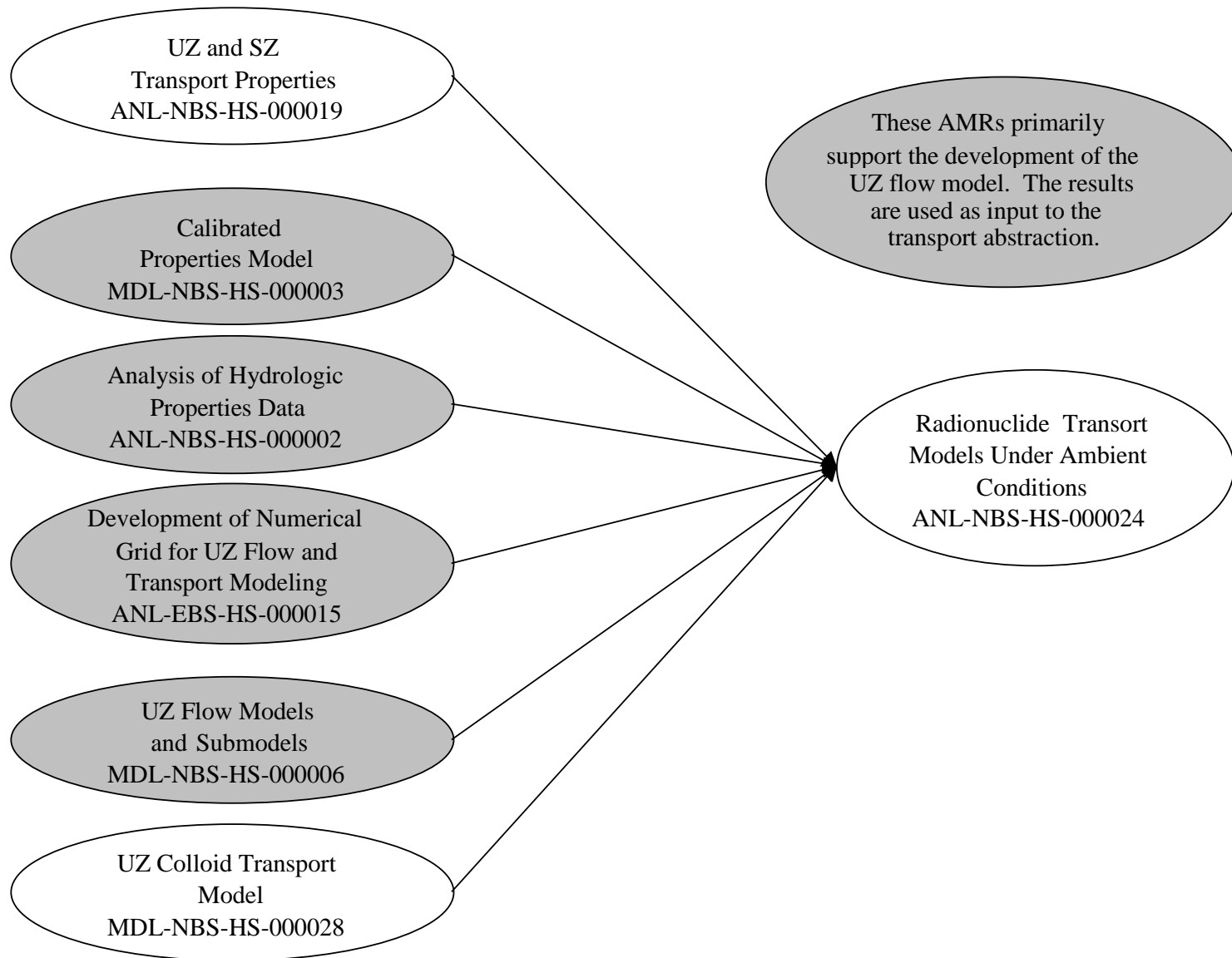


Figure 13-1a: Model Relations for the Unsaturated Zone Radionuclide Transport Process Model

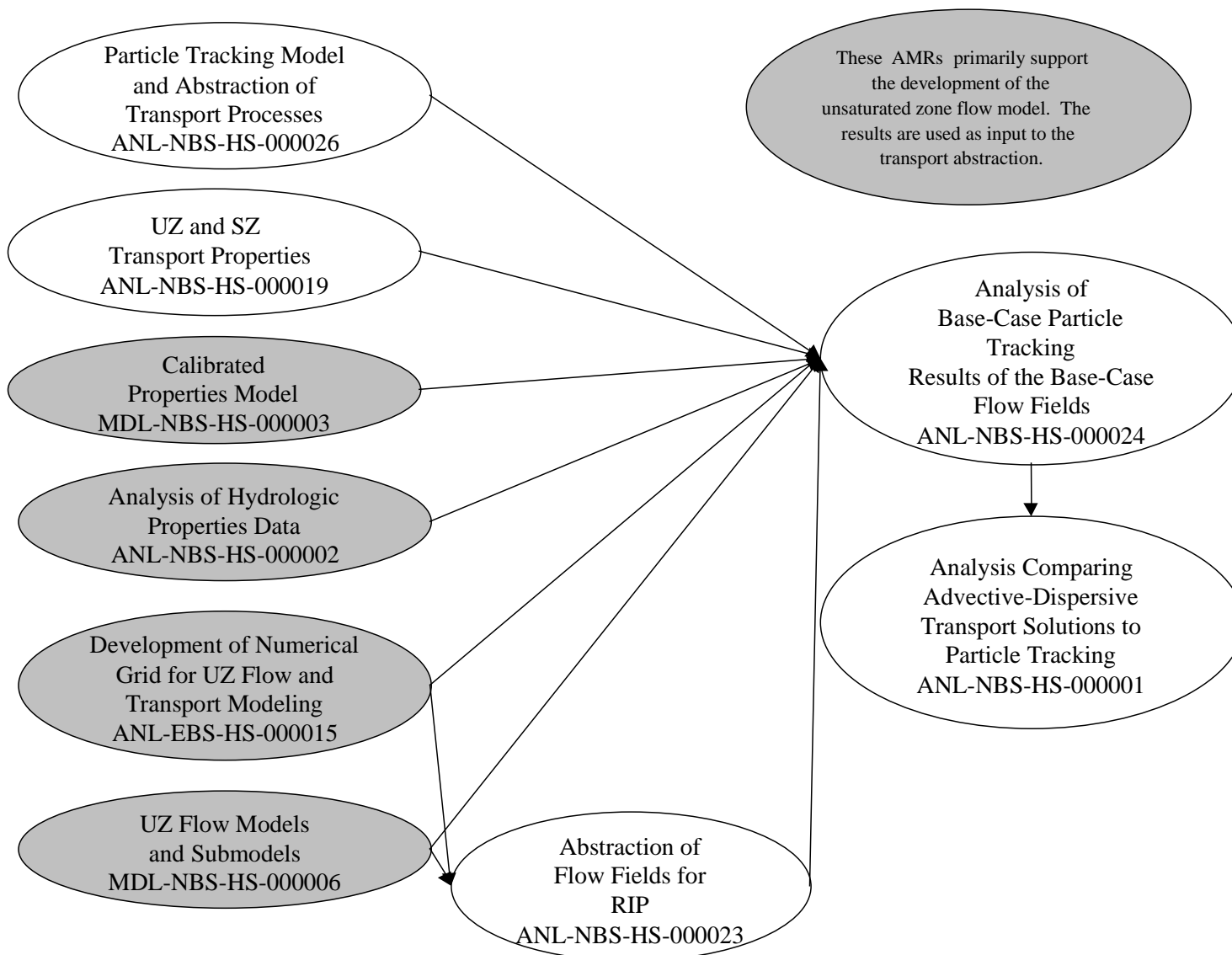


Figure 13-1b: Model Relations for the Unsaturated Zone Radionuclide Transport Abstracted Model

Figures 13-1a and 13-1b were developed by reviewing the documented linkages between the AMRs. It should be noted that this information is not presented in any of the reports, including the *UZ Flow and Transport* PMR and represents the reviewer's interpretation from the documentation as to how the various AMRs are linked. Development of the abstracted transport model does not appear to utilize any information from the process transport model. In other words, there are no identifiable linkages in the documentation between the process and abstracted UZ transport models. The *Radionuclide Transport Models Under Ambient Conditions* AMR (the process model) is not referenced by any of the AMRs used to develop the abstracted model. Thus, it appears that both the process and abstracted models were developed independently, with the process model results not informing the development of the abstracted model. In addition, the *Conceptual and Numerical Models for UZ Flow and Transport* AMR cannot be linked within any of the diagrams.

### **13.3 Model Structure**

Figure 13-2, *Unsaturated Zone Transport Model Structure*, depicts the various elements that comprise the UZ transport models. Shown are those elements that comprise the conceptual and representational models, the various parameters needed, and the modeling results. Each is discussed in more detail below.

#### **A. Conceptual Model**

Since radionuclide transport in the UZ is advective, the most important conceptual models are those related to flow, namely the dual-permeability conceptualization. The conceptual models related to flow are discussed in the *UZ Flow* chapter. This section will summarize those conceptualizations related solely to radionuclide transport.

Section 6.2 of the *Conceptual and Numerical Models for UZ Flow and Transport* AMR and Section 6.1 of the *Radionuclide Transport Models Under Ambient Conditions* AMR are the primary sources that discuss the conceptual models related to UZ transport. Additional conceptualizations related to colloid facilitated transport are discussed in the *UZ Colloid Transport Model* and the *Particle Tracking Model and Abstraction of Transport Processes* AMRs. The conceptualizations utilized in the UZ transport model are discussed below, and are applicable to both the abstraction and process models except where noted:

- Advection – Transport is strongly related to liquid water flow through advection with transport pathways coinciding with flow pathways. In welded units, advection through fractures is expected to dominate. At interfaces between welded and nonwelded units, transitions occur between dominant fracture flow and dominant matrix flow. Perched water results in lateral transport. Dominant fracture flow in the zeolitic components of the Calico Hills units result in faster travel than in the vitric components where matrix flow dominates.

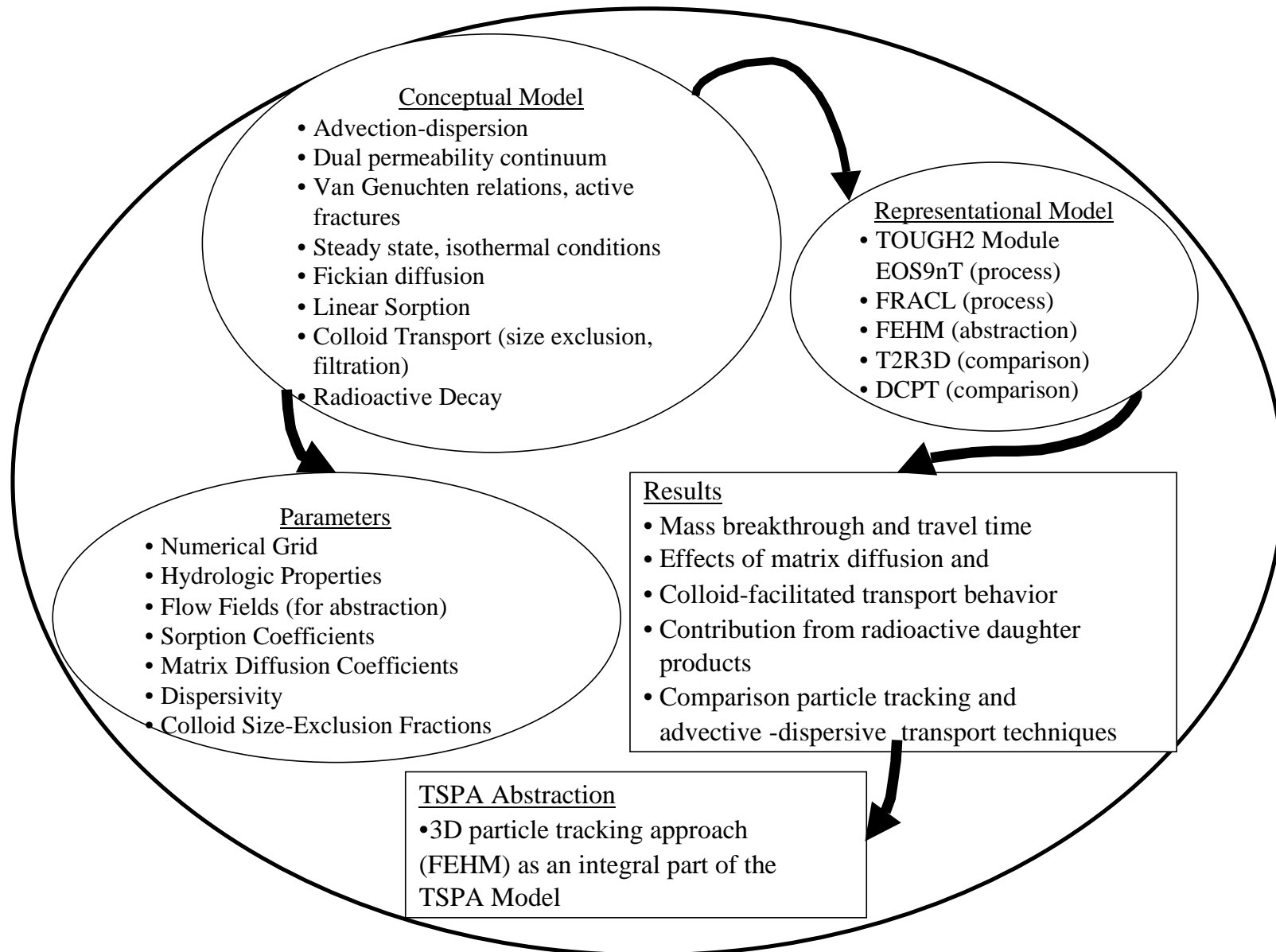


Figure 13-2: Unsaturated Zone Transport Model Structure

- Dispersion – Hydrodynamic dispersion, namely the use of a dispersivity coefficient, is not expected to play an important role in modeling radionuclide transport. The dual-permeability approach for modeling water flow explicitly models the variations in transport velocity caused by the fracture-matrix system that result in dispersivity. Dispersion within either the matrix or fracture continua will be a smaller-order effect.
- Matrix Diffusion – Mass transfer via diffusion between the fractures and tuff matrix may play an important role in transport. Since transport velocities are slower in the matrix, transfer of mass into the matrix can significantly retard the overall transport rate to the water table. Matrix diffusion depends on several factors, including the effective contact area between the fractures and matrix, the effective diffusion coefficient, and the characteristics of the fracture network.
- Fracture and Matrix Sorption – Sorption refers to a combination of chemical and physical interactions between dissolved solutes and the solid phases (e.g., rock matrix). The strength of the sorptive behavior depends on the chemical element, the rock type involved in the interaction, and the geochemical conditions of the water contacting the rock. Sorption can act to retard the movement of radionuclides in groundwater.

Minerals lining fracture surfaces may be capable of sorbing radionuclides. However, characterization of the fracture-lining minerals and sorptive interactions with these minerals has been limited and the volume and surface area of the fracture lining is relatively small. As such, it has been conservatively assumed that no sorptive interactions with fracture surfaces occur and sorption is only modeled within the rock matrix.

Sorption also depends on the degree of exposure that solutes have with the rock. For example, if little opportunity exists for mass to flow within the rock matrix (e.g., via matrix diffusion), then the effect of matrix sorption will be small even though the rock may have strong sorptive characteristics.

Sorption is modeled using a linear model, utilizing a distribution coefficient ( $K_d$ ). The distribution coefficient can vary both temporally and spatially due to variations in the chemical composition of both the aqueous and solid phases. As such, a conservative approach has been adopted using a minimum  $K_d$  approach (smallest reasonable ratio of radionuclides attached to the solid phase versus the aqueous phase).

- Colloid-Facilitated Transport – Colloids (particles small enough to become suspended and thus are transportable) may facilitate the transport of radionuclides within the UZ. Colloids interact with dissolved radionuclides through sorption mechanisms (reversible). Some radionuclides may also be an integral part of the colloid structure (irreversible). The colloids themselves may be mobile, resulting in more rapid transport of radionuclides than the aqueous phase alone. Colloid-facilitated transport depends on advection, matrix diffusion, dispersion, colloid sorptive properties, and filtration.

Details regarding the conceptualizations implemented into the abstracted model are discussed in TSPA-SR (Section 3.7) and the *Particle Tracking Model and Abstraction of Transport*

*Processes* AMR. Both reversible and irreversible colloids were modeled in the abstracted model. A linear approach for reversible sorption of radionuclides onto colloids was used in the abstracted model (FEHM particle tracking) used in TSPA. This is implemented by defining a  $K_c$  parameter, which equals the product of the concentration of colloids in the water and the effective distribution coefficient ( $K_d$ ) for sorption of radionuclides onto the colloids.

The abstraction model assumed that a fraction of the irreversible colloids traveling in the rock matrix of a hydrogeologic unit are filtered at the interface with another unit due to a size-exclusion effect. In this approach, irreversible colloids traveling in the rock matrix that are larger than the pore size of the downstream unit rock matrix are permanently filtered. This size-exclusion model is not used within the fractures nor is it applied to reversible colloids. Other mechanisms that could retard colloid transport (e.g., kinetic filtration) were not modeled (assumed to not occur).

The process models, documented in the *UZ Colloid Transport Model* and *Radionuclide Transport Models Under Ambient Conditions* AMRs, consider primarily irreversible colloids. Both AMRs model size-exclusion effects at the fracture-matrix interface. However, unlike the abstracted model, neither model size-exclusion effects within the rock matrix at unit interfaces. Filtration is also modeled within both process model AMRs.

- Radioactive Decay – For simple decay, the radionuclide concentration decreases exponentially with time during transport through the UZ. Chain-decay result in the ingrowth of new radionuclides as a result of the decay of a parent radionuclide.

## **B. Parameters**

A large number of parameters that affect radionuclide transport are needed for the dual-permeability UZ flow model. As discussed above, the advective transport of radionuclides in the UZ depends significantly on the movement of liquid water. Thus, two of the fundamental sets of parameters are the hydrologic properties and the flow fields within the UZ. These are determined via the UZ flow model for different climate states and infiltration rates. The development of these flow fields (and the uncertainty associated with them) is discussed in the UZ Flow chapter. The remainder of this section focuses on those parameters related specifically to radionuclide transport.

These parameters are discussed in several AMRs and the TSPA-SR document. All parameters used in the process model are documented in the *Radionuclide Transport Models Under Ambient Conditions* AMR. Parameters for the abstracted model are documented primarily in TSPA-SR and the *Unsaturated Zone and Saturated Zone Transport Properties* AMR.

### **Sorption Coefficients**

Sorption coefficients ( $K_d$ ) used in the abstracted model for TSPA are identified in Section 6.4.2 of the *Unsaturated Zone and Saturated Zone Transport Properties* AMR. Probability distributions are provided for several radionuclides for devitrified, vitric, and zeolitic tuffs (Table

2a of the AMR). Initial estimates of these distributions were based on an expert elicitation held in 1993. The experts from whom the values were elicited were familiar with sorption experiments that had been conducted by the YMP prior to the time of the elicitation and with literature available at that time. Subsequent changes were made to the distribution parameters based on laboratory data obtained since the time of the elicitation. In particular, of the radionuclides considered in the TSPA model, the  $K_d$  ranges for all but Am, Th, and Pa have been modified to reflect more current data.

Single values for sorption coefficients are used in the process model and are documented in the *Radionuclide Transport Models Under Ambient Conditions* AMR (accessible through a data tracking number). These values differ from the mean values that are used in the abstracted model, as shown below for a few select elements.

Element	Mean Value $K_d$ (mL/G) <i>Unsaturated Zone and Saturated Zone Transport Properties</i> (Table 2a)	$K_d$ (mL/G) <i>Radionuclide Transport Models Under Ambient Conditions</i> (DTN LB991220140160.019)
Neptunium	Devitrified 0.3 Vitrified 0.3 Zeolitic 0.5	Devitrified 1.0 Vitrified 1.0 Zeolitic 4.0
Uranium	Devitrified 0.5 Vitrified 0.5 Zeolitic 4.0	Devitrified 2.0 Vitrified 1.0 Zeolitic 4.0
Plutonium	Devitrified 37.5 Vitrified 100.0 Zeolitic 100.0	Devitrified 100.0 Vitrified 100.0 Zeolitic 100.0

### **Matrix Diffusion Coefficient**

Matrix diffusion coefficients for use in TSPA are presented in Section 6.6.3 of the *Unsaturated Zone and Saturated Zone Transport Properties* AMR. Probability distributions are defined for anionic and cationic species that are based on reviews of literature and rock-beaker experimental results (tritiated water for cations, technetium as  $\text{TCO}_4^-$  for anions). Further analysis of the rock-beaker experimental data indicates that application of the cationic diffusion coefficients is conservative for sorbing species.

Matrix Diffusion Coefficients (Beta Probability Distributions)				
	Mean ( $\text{m}^2 \text{s}^{-1}$ )	Standard Deviation ( $\text{m}^2 \text{s}^{-1}$ )	Minimum ( $\text{m}^2 \text{s}^{-1}$ )	Maximum ( $\text{m}^2 \text{s}^{-1}$ )
Anionic Species	$3.2 \times 10^{-11}$	$1.0 \times 10^{-11}$	0.0	$10^{-9}$
Cationic Species	$1.6 \times 10^{-10}$	$5.0 \times 10^{-11}$	0.0	$10^{-9}$

## **Dispersivity**

Values for dispersivity are discussed in several documents. TSPA-SR uses a value of 20 meters over the approximately 300 meters of travel distance in the UZ, citing consistency with a dispersivity versus scale correlation (~10% of path length). TSPA-SR further states that prior analyses indicate that radionuclide transport in the UZ is insensitive to dispersivity over the range of 0 to 75 meters. The AMR entitled *Radionuclide Transport Models Under Ambient Conditions* (e.g., the process model) utilizes a value of 1 meter in the fractures and 0.1 meters in the matrix, citing scientific judgment in the absence of available data.

## **Colloid Facilitated Transport**

For the abstracted model, the  $K_c$  parameter distribution used in TSPA to model reversible colloid transport is identical to that used in the saturated zone and is determined in the *Uncertainty Distribution for Stochastic Parameters* AMR<sup>2</sup>. The parameters needed to implement the size-exclusion models are presented in the *Particle Tracking Model and Abstraction of Transport Processes* AMR. Single values were used.

For the process model, documented in the *Radionuclide Transport Models Under Ambient Conditions* AMR, size exclusion parameters were obtained from the *UZ Colloid Transport Model* AMR. It appears that the two process models developed in each AMR use different ranges of kinetic filtration parameters.

## **C. Representational Model**

The mathematical equations related to radionuclide transport are discussed in Section 6.2 of the *Radionuclide Transport Models Under Ambient Conditions* AMR. The numerical and semianalytical models used in the process model of radionuclide transport in the UZ are discussed in Section 6.3 of the AMR. Three-dimensional modeling uses the EOS9nT module of the TOUGH2 family of codes. Two-dimensional modeling uses the FRACL code, and implementation of semianalytic solutions.

- EOS9nT first solves the Richards equation for flow, then sequentially solves the set of linearly independent transport equations. The transport equations account for advection, molecular diffusion, hydrodynamic dispersion, kinetic or equilibrium physical and chemical sorption, colloid filtration, and colloid-assisted solute transport. EOS9nT includes two types of Laplace transform formulations in addition to conventional timestepping.
- FRACL is an implementation of semianalytical solutions and accounts for matrix diffusion, mass transfer between mobile and immobile water fractions, sorption (linear, kinetic, or irreversible), and radioactive decay. The solutions are analytical in Laplace space and numerically inverted to provide the solution in time.

---

<sup>2</sup> Uncertainty Distribution for Stochastic Parameters, ANL-NBS-MD-000011. The information contained in this AMR is used within the TSPA-SR model. It is not used in the development of the AMRs depicted in Figures 13-1a and 13-1b.

Model validation is presented in Section 6.4.2. A two-dimensional analytic solution was compared to EOS9nT and FRACL solutions. The results indicate that FRACL exactly reproduces the analytic solution and that EOS9nT can reproduce the analytic solution with appropriate grid sizing (medium coarseness).

The abstracted model, as documented in the *Particle Tracking Model and Abstraction of Transport Processes* AMR, utilizes a particle tracking approach within the FEHM computer code. The particle tracking technique, called the residence time transfer function (RTTF), is discussed in detail in Section 6.1 of the AMR. Section 6.2 discusses implementation of the technique for modeling radionuclide transport in the UZ. Section 6.3 of the AMR discusses verification of the technique where solutions of fairly simple problems using the particle tracking algorithm are compared to analytic solutions. The results in this section indicate that the particle tracking solution is adequate provided a sufficient number of particles are used.

Section 6.4 of the *Particle Tracking Model and Abstraction of Transport Processes* AMR compares the results of particle tracking to dual-permeability and discrete fracture benchmark simulations. The AMR entitled *Analysis Comparing Advective-Dispersive Transport Solution to Particle Tracking* is dedicated to comparing the FEHM particle tracking technique with both a dual continuum particle tracking approach (DCPT) and a fully coupled advective-dispersive code (T2R3D). A discussion of the results of these comparisons is presented later in this Chapter.

## **D. Results**

Results and sensitivity analyses regarding UZ radionuclide transport are presented in several documents. The *UZ Colloid Transport Model* AMR presents simulations of colloid-facilitated transport using a two-dimensional discrete fracture model. Sensitivity analyses using different assumptions about size exclusion and filtration are presented. The *Radionuclide Transport Models Under Ambient Conditions* AMR presents results of both two- and three-dimensional analyses using the process model. Several sensitivity analyses were conducted and documented.

AMRs related to development of the abstracted model also present results, mostly for simplified one- and two-dimensional problems. As discussed above, the *Particle Tracking Model and Abstraction of Transport Processes* AMR presents results that compare the particle tracking technique to simple analytic solutions and to other numerical approaches. The AMR entitled *Analysis Comparing Advective-Dispersive Transport Solution to Particle Tracking* presents results that compare the particle tracking technique with both a DCPT approach and a fully coupled advective-dispersive code (T2R3D).

The *Analysis of Base-Case Particle Tracking Results of the Base-Case Flow Fields* AMR presents results calculated using the three-dimensional abstracted model and the base case flow fields (determined from TOUGH2). A unit source of mass was released over the repository footprint and breakthrough curves are shown. Constant transport parameters (e.g., matrix diffusion, sorption coefficients) were used.

Results that fully couple the releases from the engineered barrier system with abstracted UZ transport model (including uncertainty in transport parameters) are shown in TSPA-SR (Section 4). An analysis using this fully coupled model to evaluate the sensitivity of the receptor dose to different matrix diffusion alternatives is also shown (Section 5.2.6).

### **13.4 Discussion of Uncertainty/Variability Treatment**

An evaluation of uncertainty and variability treatment of the AMRs was performed for this exercise. For each AMR, the uncertainties/variabilities were identified and it was determined if a thorough treatment was performed. Thorough treatment was considered to be: identification, treatment, impact assessment, and clear presentation of the analysis and the propagation of uncertainty in the AMR. Table 13.1 is a synopsis of some of the uncertainties and variabilities identified in this exercise. The following is a discussion of the evaluation process and uncertainty/variability analysis trends within the AMR/model process.

#### **A. Conceptual Model**

As discussed above, since transport in the UZ is dominated by advection, the most important conceptual models are those related to flow, namely the dual-permeability conceptualization. The conceptual models related to flow and the associated uncertainties in this conceptualization are discussed in the UZ Flow Chapter. With regard to transport, the general concepts such as advection, dispersion, sorption, and matrix diffusion, are fairly well understood. Cited literature, experimental evidence, and field observations support these concepts. An exception is the modeling of colloid facilitated transport where it is acknowledged that limited data has resulted in a very uncertain conceptualization (see Section 7 of the *UZ Colloid Transport Model* AMR). The most important uncertainties lie in both the numerical representation of these processes and the development of parameters.

#### **B. Parameters**

##### **Sorption**

Several important assumptions relate to the determination of sorption coefficients ( $K_d$ ) for subsequent use in the abstracted model (and subsequently by TSPA) are documented in Section 6.4.2 of the *Unsaturated Zone and Saturated Zone Transport Properties* AMR. Confirmation of these assumptions is still required. However, it cannot be determined from the AMR whether these are being formally tracked as “to-be-verified.” These include:

- Waters from Wells J-13 and p#1 bound the major ion chemistry of the groundwaters at Yucca Mountain (this assumption requires confirmation of redox conditions for Np, Pu, Tc, U, and Se).
- Sorption parameters determined in laboratory experiments using crushed tuff are applicable to transport through solid tuff matrix in the field (requires confirmation for actinide elements).

- In-situ flow rates are sufficiently slow that sorption equilibrium is achieved during solute transport (requires confirmation for radionuclides with slow sorption kinetics).
- Sorption experiments conducted under saturated conditions yield results applicable to unsaturated conditions (requires confirmation).
- Sorption parameters in laboratory experiments have not been significantly affected by microbial activity (requires confirmation).

In the 1993 elicitation, the experts chose bounds (lower and upper) that were beyond those dictated by the available data in acknowledgement that the database was incomplete.

### **Matrix Diffusion**

The rationale for selecting the beta probability distribution for the matrix diffusion coefficient (anionic and cationic species) and the bases for the selected distribution parameters are not provided (beyond what was stated in Section II.B). In addition, it is not clear what sources of literature were used.

Although inspection of the distribution parameters implies a broad range (minimum to maximum), the beta distribution itself results in a much narrower uncertainty range. For both anionic and cationic species, the range from the 1<sup>st</sup> to the 99<sup>th</sup> percentile is less than half an order of magnitude using the defined distribution parameters. Although no error analysis was presented regarding the experimental data, it may be possible that the uncertainty in the diffusion coefficients inferred from this data is larger than a factor of five. In addition, the Busted Butte tests indicate that matrix diffusion coefficients measured in field tests are less than those measured in laboratory experiments, and generally decrease as tracer residence time increases (see Section 7 of the *Unsaturated Zone and Saturated Zone Transport Properties* AMR).

### **Colloid Facilitated Transport**

The AMR entitled *UZ Colloid Transport Model* provides parameters related to colloid-facilitated transport. Of importance is the size-exclusion model, which is used in the TSPA-SR model to model irreversible colloid transport (e.g., wasteform colloids). Size-exclusion parameters developed in this AMR were used in both the three-dimensional process and abstracted models. Although the *UZ Colloid Transport Model* AMR also develops filtration parameters, they were not used in the abstracted model or TSPA.

Colloid size-exclusion fractions were treated as constants (varying from unit to unit), both for development of the process and abstracted models and within TSPA. Sensitivity analyses conducted in the AMR demonstrate that size-exclusion effects play a significant role in the transport of colloids. However, Section 7 of the AMR states “the limitation [to representing colloid facilitated transport] is not having the data to support the implementation of the processes, which leads to assumptions made on top of assumptions, making it more difficult to defend the conservative approach taken in this analysis.” Given this statement, uncertainty regarding size exclusion effects is likely to exist and is not captured in the modeling approach.

As discussed above, the  $K_c$  value was used to model reversible colloid facilitated radionuclide transport. This model was applied to corrosion product colloids (iron oxide) and natural colloids. A distribution for  $K_c$  was used to account for uncertainty.

### C. Representational Model

Section 6.4 of the *Particle Tracking Model and Abstraction of Transport Processes* AMR compares the results of particle tracking to dual-permeability and discrete fracture benchmark simulations. The results indicate that for low diffusion, particle tracking and discrete fracture approaches yield similar results. It is claimed that dual-permeability modeling yields artificially early solute arrival times for systems with considerable fracture flow. For higher diffusion, solute arrival for particle tracking is slower than arrival for dual-permeability and discrete fracture approaches. This is due to the RTTF assumption inherent in the particle tracking approach that solute that diffuses into the matrix becomes immobile until it diffuses back out (whereas in the other two approaches the solute moves within the matrix). This deviation is larger for sorbing solutes.

The AMR entitled *Analysis Comparing Advective-Dispersive Transport Solution to Particle Tracking* is dedicated to comparing the FEHM particle tracking technique with both a DCPT approach and a fully coupled advective-dispersive code (T2R3D). The results of this analysis indicate that particle tracking and advective-dispersive approaches yield significantly different results, with particle tracking showing much earlier median transport times. The differences are also attributed to the RTTF matrix diffusion assumptions. This AMR claims that although differences exist between the different techniques, the FEHM particle tracking approach is conservative.

Of interest is the discrepancies between the particle tracking and fully coupled advective dispersive techniques. On one hand, in the *Particle Tracking Model and Abstraction of Transport Processes* AMR, particle tracking results in slower median solute transport times. On the other hand, in the *Analysis Comparing Advective-Dispersive Transport Solution to Particle Tracking* AMR, particle tracking results in more rapid transport times. Both claim that the RTTF approach for modeling matrix diffusion is the source of the discrepancy. In the *Particle Tracking Model and Abstraction of Transport Processes* AMR, it is claimed that the RTTF approach causes solute that diffuses into the matrix to remain stagnant whereas the advective-dispersive approach permits it to transport in the matrix flow field. It is claimed that this result in comparatively slower travel times for the RTTF approach (see page 68). In the *Analysis Comparing Advective-Dispersive Transport Solution to Particle Tracking* AMR, it is claimed that the RTTF approach tends to keep solute more associated with the fracture continuum, where faster velocities occur (see page 40).

A similar discrepancy was noted regarding initial arrival of solute (initial breakthrough). The *Particle Tracking Model and Abstraction of Transport Processes* AMR states that the early arrival of solute in the dual-permeability approach (as compared to particle tracking) is essentially erroneous, “because the fracture/matrix diffusion term is underestimated, and mass remains in the fracture to an unrealistic degree” (see page 68) However, in the *Analysis*

*Comparing Advective-Dispersive Transport Solution to Particle Tracking* AMR, initial arrival is also earlier for the fully-coupled advective-dispersive model. This early breakthrough is not identified in that AMR as being erroneous. In fact, it is stated that “the diffusive mass flow between the fracture and matrix model in the T2R3D allows radionuclides to diffuse into the matrix, yielding much lower initial breakthrough times via the fractures” (see page 40).

The AMR entitled *Particle Tracking and Abstraction of Transport Properties* performs several benchmark calculations using the abstracted model, concluding that a sufficient number of particles must be used. This is best done by increasing the number of particles until the results no longer show a significant change from a simulation with fewer particles. The number of particles used when the abstracted model was coupled to TSPA cannot be determined from the documentation. The *Analysis of Base-Case Particle Tracking Results of the Base-Case Flow Fields* AMR uses “nearly 100,000 particles over the repository region” (Section 4.3). However, neither TSPA-SR, nor the TSPA-SR Model<sup>3</sup> state the number of particles used in TSPA simulations.

Although some discrepancies in the comparisons were identified, the analyses discussed above present a very solid discussion of the uncertainties associated with the representational models chosen. However, besides claiming that the FEHM particle tracking method is conservative, no representational model uncertainty is propagated into the overall TSPA results.

## **D. Results**

As discussed above, several documents present results. Many of these are the results of sensitivity analyses where parameters related to transport are varied. Thus, documented uncertainties in the model are clearly evaluated through to the results, both for the abstracted and process models.

### **13.5 Propagation of Uncertainty**

Several items were identified regarding the propagation of uncertainty through the AMRs and into TSPA. These include:

- The text in TSPA-SR is not completely correct in its assertion that “sorption  $K_{ds}$  have been quantified using results of batch sorption experiments for different radionuclides and rock types” (Section 3.7.3). Although this is true for some elements, the discussion in TSPA-SR does not acknowledge that the sorption coefficients for Am, Th, and Pa are still based on the 1993 expert elicitation.
- The sorption coefficients are accessible from the *Radionuclide Transport Models Under Ambient Conditions* AMR through a data tracking number (LB991220140160.019). This DTN states that “this data submittal includes values (directly and/or calculated) from scientific literatures for AMR U0060 ‘Radionuclide Transport Models Under Ambient

---

<sup>3</sup> MDL-WIS-PA-000002, Section 6.3.6. Test runs were conducted using a maximum of 525,000 particles were conducted. However, it cannot be determined whether fewer particles were used in actual simulations (and any basis for the selected number of particles).

Conditions’.” This requires any reviewer to have access to the Project’s technical database to obtain the basis for the sorption coefficients used, rather than providing the information in the AMR. In addition, the development of the process transport model does not utilize any of the information provided in the *Unsaturated Zone and Saturated Zone Transport Properties* AMR.

- The *Radionuclide Transport Models Under Ambient Conditions* AMR (Section 6.17) presents results for an alternative model having no matrix diffusion. These results indicate that radionuclide transport through the UZ is much more rapid when matrix diffusion is neglected. The nominal TSPA-SR case (Section 3.7) considers that matrix diffusion will occur and evaluates the alternative model having no matrix diffusion as a sensitivity study. No basis is provided for not including the alternative model in the nominal case, beyond justifying the probability distribution chosen (which is based on very limited laboratory information). The results of this sensitivity study (Section 5.2.6.1) indicate that matrix diffusion also plays a strong role with respect to overall repository performance.
- For the nominal case, TSPA-SR directly utilizes the matrix diffusion coefficients distributions presented above (Section II.B) in its transport simulations, consistent with the supporting AMR. However, TSPA-SR implies that the distributions are solely based on the rock-beaker experiments and does not allude to the fact that literature information was used. In addition, TSPA-SR does not clearly discuss the basis for the distribution parameters (however, this would not have been possible at the TSPA level since the basis is not clearly articulated in the supporting AMR).
- Although radionuclide transport has been shown to be insensitive to variations in dispersivity, a clear link between the value chosen for use in TSPA and supporting AMRs does not exist. The lack of consistency between values used in TSPA and the process model (documented in the *Radionuclide Transport Models Under Ambient Conditions* AMR) also hampers transparency.
- TSPA-SR only mentions that the size-effect model for colloid transport was used. It does not acknowledge that constant parameters were used and that the *UZ Colloid Transport* AMR indicates that this model plays a key role in regards to the transport of colloids in the UZ. It should be noted that the size-exclusion fractions used by TSPA were not obtained from the *UZ Colloid Transport Model* AMR. Rather, they were obtained via a Technical Data Supplement<sup>4</sup>. As such, although the data is traceable through the Project’s databases, traceability of data from TSPA-SR, through the abstracted model AMR, into the *UZ Colloid Transport Model* AMR does not exist.

---

<sup>4</sup> Total System Performance Assessment (TSPA) Model For Site Recommendation (MDL-WIS-PA-000002) refers to the *Particle Tracking Model and Abstraction of Transport Processes* AMR. This AMR then cites DTN:LA0003MCG12213.002 as the source. The DTN then refers to the accession number MOL.2000310.0085 where the Technical Data Supplement can be found. The information contained in the database refers to MOL.20000310.0085 in the RIS database for the formulas used to calculate these data.

- The analyses presented in the *Analysis Comparing Advective-Dispersive Transport Solution to Particle Tracking* AMR demonstrates that the FEHM particle tracking approach is conservative as compared to other techniques (DCPT and advective-dispersive). This is not discussed in the TSPA-SR document (see Sections 3.7.2 and 3.7.3).
- With regard to temporal variability, the basis supporting the assumption of modeling instantaneous changes from one flow condition to another is not apparent in the documentation. TSPA-SR (Section 3.2.3.1) simply states the approximation utilized, but does not discuss the basis or reference any supporting analyses.

**Table 13-1: Unsaturated Zone Radionuclide Transport**

<b>Model Purpose:</b> The purpose of the UZ transport model is to evaluate possible radionuclide transport from the potential repository horizon to the groundwater in the SZ. Both a process model and an abstracted model (for subsequent use in TSPA) are developed.				
<b>Summary</b>	<b>Source</b>	<b>Treatment</b>	<b>Basis</b>	<b>Impact</b>
<b>Conceptual Model Uncertainty</b>				
Conceptual model of UZ groundwater flow	Radionuclide transport in the UZ will be advective. As such, the conceptualization of groundwater flow in the UZ is a fundamental part of the conceptualization of radionuclide transport.	Utilized conceptualizations developed for the UZ flow model.	See companion report and table regarding UZ flow.	Characteristics of radionuclide transport in the UZ beneath the repository.
Conceptual models of radionuclide transport in the UZ.	Site characterization information, literature, field observations.	In general, the concepts related to UZ transport are fairly well certain (e.g., advection-dispersion, matrix diffusion, sorption, radioactive decay). The key uncertainties lie in developing representational models of these concepts and parameterization.	Observations	Characteristics of radionuclide transport in the UZ beneath the repository.
Colloid facilitated transport	Limited site and literature data as discussed in the <i>UZ Colloid Transport Model</i> AMR.	Develop conservative models - size exclusion and filtration. Both considered in the process model and only size exclusion considered in the abstracted model and TSPA.	Lack of data resulted in development of what is termed a conservative model. However, Section 7 of the UZ Colloid Model AMR states "the limitation [to representing colloid facilitated transport] is not having the data to support the implementation of the processes, which leads to assumptions made on top of assumptions, making it more difficult to defend the conservative approach taken in this analysis."	Transport characteristics for colloids (and radionuclides attached to them).
<b>Representational Model Uncertainty</b>				
Process Model - comparison of FRACL and EOS9nT module to analytic solution.	<i>Radionuclide Transport Models Under Ambient Conditions</i> , Section 6.4	Compared FRACL and EOS9nT with analytic results for a simplified 2-D problem. Results show that FRACL exactly reproduces the solution and EOS9nT reproduces the solution with appropriate grid size.	Model validation (perhaps more software verification).	Numerical modeling of radionuclide transport.

<p>Process Model - comparison of FEHM particle tracking (PT) with DCPT, advective-dispersive (AD), and discrete fracture network (DFN) techniques.</p>	<p><i>Particle Tracking Model and Abstraction of Transport Processes</i>, Section 6.4 compares the results of particle tracking to dual-permeability and discrete fracture benchmark simulations. <i>Analysis Comparing Advective-Dispersive Transport Solution to Particle Tracking</i> compares the FEHM particle tracking technique with both a dual continuum particle tracking approach (DCPT) and a fully coupled advective-dispersive code (T2R3D).</p>	<p>The results in the <i>Particle Tracking Model and Abstraction of Transport Processes</i> AMR indicate that for low diffusion, PT and DFN approaches yield similar results. It is claimed that DKM yields artificially early solute arrival times for systems with considerable fracture flow. For higher diffusion, solute arrival for PT is slower than arrival for DKM and DFN approaches. This felt to be due to the RTTF assumption inherent in the FEHM PT approach that solute that diffuses into the matrix becomes immobile until it diffuses back out (whereas in the other two approaches the solute moves within the matrix). This deviation is larger for sorbing solutes.</p> <p>The AMR entitled <i>Analysis Comparing Advective-Dispersive Transport Solution to Particle Tracking</i> compares the FEHM PT technique with both a DKM particle tracking approach (DCPT) and a fully coupled AD code (T2R3D). The results indicate that PT and AD approaches yield significantly different results, with particle tracking showing much earlier median transport times. The differences are also attributed to the RTTF matrix diffusion assumptions.</p>	<p>Apparent discrepancies between the particle tracking and fully-coupled advective dispersive techniques. On one hand, in the <i>Particle Tracking Model and Abstraction of Transport Processes</i> AMR, particle tracking results in slower median solute transport times. On the other hand, in the <i>Analysis Comparing Advective-Dispersive Transport Solution to Particle Tracking</i> AMR, particle tracking results in more rapid transport times. Both claim that the RTTF approach for modeling matrix diffusion is the source of the discrepancy. In the <i>Particle Tracking Model and Abstraction of Transport Processes</i> AMR, it is claimed that for the RTTF approach causes solute that diffuses into the matrix to remain stagnant whereas the advective-dispersive approach permits it to transport (in the matrix flow field), resulting in comparatively slower travel times for the RTTF approach (see page 68). In the <i>Analysis Comparing Advective-Dispersive Transport Solution to Particle Tracking</i> AMR, it is claimed that the RTTF approach tends to keep solute more associated with the fracture continuum, where faster velocities occur (see page 40).</p>	<p>Numerical modeling of radionuclide transport - representational model uncertainty. Claim in the <i>Analysis Comparing Advective-Dispersive Transport Solution to Particle Tracking</i> AMR that FEHM PT (with RTTF) is conservative, but more work is needed to reconcile differences.</p>
--	--	--	--	---

Process Model - comparison of FEHM PT with DCPT, AD, and DFN techniques.	See Above	See Above	A similar discrepancy was noted regarding initial arrival of solute (initial breakthrough). The <i>Particle Tracking Model and Abstraction of Transport Processes</i> AMR states that the early arrival of solute in the dual-permeability approach (as compared to particle tracking) is essentially erroneous, "because the fracture/matrix diffusion term is underestimated, and mass remains in the fracture to an unrealistic degree" (see page 68). However, in the <i>Analysis Comparing Advective-Dispersive Transport Solution to Particle Tracking</i> AMR, initial arrival is also earlier for the fully-coupled advective-dispersive model. This early breakthrough is not identified in that AMR as being erroneous. In fact, it is stated that "the diffusive mass flow between the fracture and matrix model in the T2R3D allows radionuclides to diffuse into the matrix, yielding much lower initial breakthrough times via the fractures" (see page 40).	Numerical modeling of radionuclide transport - representational model uncertainty. Claim in the <i>Analysis Comparing Advective-Dispersive Transport Solution to Particle Tracking</i> AMR that FEHM PT (with RTTF) is conservative, but more work is needed to reconcile differences.
Process Model - comparison of FEHM PT with DCPT, AD, and DFN techniques.	<i>Analysis Comparing Advective-Dispersive Transport Solution to Particle Tracking</i> compares the FEHM particle tracking technique with both a dual continuum particle tracking approach (DCPT) and a fully coupled advective-dispersive code (T2R3D).	Compares the FEHM PT technique with both a DKM particle tracking approach (DCPT) and a fully coupled AD code (T2R3D). The results indicate that PT and AD approaches yield significantly different results, with particle tracking showing much earlier median transport times. FEHM PT approach is identified as being conservative. The differences are also attributed to the RTTF matrix diffusion assumptions. Note discrepancy identified above.	FEHM PT is subsequently used in TSPA-SR, however it is not identified in that document as being a conservative method (see Sections 3.7.2 and 3.7.3).	Radionuclide transport rates in the UZ computed by the integrated TSPA model.
Number of particles to use in FEHM particle tracking approach	Numerical stability	The AMR entitled <i>Particle Tracking and Abstraction of Transport Properties</i> performs several benchmark calculations using the abstracted model, concluding that a sufficient number of particles must be used. This is best done by increasing the number of particles until the results no longer show a significant change from a simulation with fewer particles.	The <i>Analysis of Base-Case Particle Tracking Results of the Base-Case Flow Fields</i> AMR uses "nearly 100,000 particles over the repository region" (Section 4.3). However, neither TSPA-SR, nor the TSPA-SR Model (MDL-WIS-PA-000002, Section 6.3.6) state the number of particles used in TSPA simulations.	Accuracy of the numerical solution
<b>Parameter Uncertainty</b>				
Hydrologic properties	Development of the UZ flow model.	Hydrologic parameters determined during development of the UZ flow model. These parameters are used directly in the radionuclide transport models.	Consistency with the UZ flow model.	Characteristics of radionuclide transport in the UZ beneath the repository.

Numerical Grid	Development of the UZ flow model.	Numerical grid determined during development of the UZ flow model. Used directly in the radionuclide transport models.	Consistency with the UZ flow model.	Numerical modeling of UZ transport.
UZ Flow Fields - used by the abstracted model (FEHM particle tracking) when integrated into the TSPA model.	Output of the UZ flow model.	Process flow fields to make compatible with the FEHM software (see <i>Abstraction of Flow Fields for RIP</i> ), then utilize the flow fields directly in the FEHM particle tracker. Three flow fields provided for each climate (total of nine), one for each of three infiltration rate cases.	Consistency of FEHM particle tracking approach with results from the UZ flow model.	Characteristics of radionuclide transport in the UZ beneath the repository.
Sorption coefficients ( $K_d$ )	Sorption coefficients ( $K_d$ ) used in the abstracted model for TSPA are identified in Section 6.4.2 of the <i>Unsaturated Zone and Saturated Zone Transport Properties</i> AMR. Sorption coefficients are used in the process model are documented in the Radionuclide Transport Models Under Ambient Conditions AMR (accessible through a data tracking number - LB991220140160.019). Note - in both models, sorption in rock matrix only.	Probability distributions are used for the abstracted model - devitrified, vitric, and zeolitic tuffs (Table 2a of the AMR). Single values for sorption coefficients are used in the process model. These values differ from the mean values that are used in the abstracted model.	<p><u>Abstracted Model (FEHM Particle Tracker)</u></p> <p>Initial estimates of the distributions based on an expert elicitation held in 1993. The experts were familiar with sorption experiments that had been conducted by the Yucca Mountain Project prior to the time of the elicitation and with literature available at that time. Subsequent changes were made to the distribution parameters based on laboratory data obtained since the time of the elicitation. In particular, of the radionuclides considered in the TSPA model, the <math>K_d</math> ranges for all but Am, Th, and Pa have been modified to reflect more current data.</p> <p><u>Process Model</u></p> <p>Cited literature and Project data.</p>	Retardation of radionuclides in the rock matrix.

Matrix diffusion coefficients	Section 6.6.3 of the <i>Unsaturated Zone and Saturated Zone Transport Properties</i> AMR	Probability distributions are defined for anionic and cationic species that are based on reviews of literature and rock-beaker experimental results (tritiated water for cations, technetium as $\text{TCO}_4^-$ for anions). Further analysis of the rock-beaker experimental data indicates that application of the cationic diffusion coefficients is conservative for sorbing species.	Rock-beaker experiments and literature information. However, the rationale for selecting the beta probability distribution for the matrix diffusion coefficient (anionic and cationic species) and the bases for the selected distribution parameters are not provided (beyond what was stated above). In addition, it is not clear what sources of literature were used.  Inspection of the distribution parameters implies a broad range (minimum to maximum), application of the beta distribution results in a much narrower uncertainty range. However, for both anionic and cationic species, the range from the 1 <sup>st</sup> to the 99 <sup>th</sup> percentile is less than half an order of magnitude. Although no error analysis was presented regarding the experimental data, it is possible that the uncertainty in the diffusion coefficients inferred from this data is larger than a factor of five. The Busted Butte tests indicate that matrix diffusion coefficients measured in field tests are less than those measured in laboratory experiments, and generally decrease as tracer residence time increases (see Section 7 of the <i>Unsaturated Zone and Saturated Zone Transport Properties</i> AMR).	Degree of matrix diffusion, effecting rate of transport through the UZ.
Dispersivity	Several documents.	TSPA-SR uses a value of 20 meters over the approximately 300 meters of travel distance in the UZ for the abstracted model. The AMR entitled <i>Radionuclide Transport Models Under Ambient Conditions</i> (e.g., the process model) utilizes a value of 1 meter in the fractures and 0.1 meters in the matrix.	TSPA-SR cites consistency with a dispersivity versus scale correlation (approximately 10% of path length) and further states that prior analyses indicate that radionuclide transport in the UZ is insensitive to dispersivity over the range of 0 to 75 meters. The AMR entitled <i>Radionuclide Transport Models Under Ambient Conditions</i> (e.g., the process model) cites scientific judgement in the absence of available data.	Minimal impact expected. However, although radionuclide transport has been shown to be insensitive to variations in dispersivity, a clear link between the value chosen for use in TSPA and supporting AMRs does not exist. The lack of consistency between values used in TSPA and the process model (documented in the <i>Radionuclide Transport Models Under Ambient Conditions</i> AMR) also hampers transparency.

Colloid facilitated transport parameters	<p>For the abstracted model, documented in the <i>Uncertainty Distribution for Stochastic Parameters</i> AMR (primarily supports saturated zone transport modeling) and the <i>Particle Tracking Model and Abstraction of Transport Processes</i> AMR.</p> <p>For the process model, documented in the <i>Radionuclide Transport Models Under Ambient Conditions</i> AMR, size exclusion parameters were obtained from the <i>UZ Colloid Transport Model</i> AMR.</p>	<p>For the abstracted model, the <math>K_c</math> parameter distribution used in TSPA to model reversible colloid transport is identical to that used in the saturated zone. Constant parameters used in the size-exclusion models.</p> <p>For the process model, constant size exclusion parameters were used. However, it appears that the two process models developed in each AMR use different ranges of kinetic filtration parameters.</p>	Basis for $K_c$ parameter documented in the <i>Uncertainty Distribution for Stochastic Parameters</i> AMR (not provided here). Basis for size-exclusion factors is colloid size versus rock pore size.	Colloid facilitated transport rates. Sensitivity analyses conducted in the <i>UZ Colloid Transport</i> AMR demonstrate that size-exclusion effects play a significant role in the transport of colloids.
<b>Variability</b>				
Spatial Variability	UZ Flow and Transport Model	Spatial variability treated by using 3-D models that account for variability in hydrogeologic properties and groundwater velocities.	Basis for three-dimensional variability documented in the development of the UZ Flow Model.	Spatially varying radionuclide transport rates.
Temporal Variability	UZ Flow and Transport Model and TSPA-SR Model	Temporal variability due to climate change only. Modeled as being an instantaneous change from one flow condition to another. Flow in steady state under each flow condition.	Basis that modeling instantaneous changes from one flow condition to another is not apparent in the documentation. TSPA-SR (Section 3.2.3.1) simply states the approximation utilized, but does not discuss the basis or reference any supporting analyses.	Temporally varying radionuclide transport rates.
<b>Results</b>				
Process Model Results	<i>UZ Colloid Transport Model</i> and the <i>Radionuclide Transport Models Under Ambient Conditions</i> AMRs.	The <i>UZ Colloid Transport Model</i> AMR presents simulations of colloid-facilitated transport using a two-dimensional discrete fracture model. Sensitivity analyses using different assumptions about size exclusion and filtration are presented. The <i>Radionuclide Transport Models Under Ambient Conditions</i> AMR presents results of both two- and three-dimensional analyses using the process model. Several sensitivity analyses were conducted and documented.	Model developed in the AMR.	No direct impact to TSPA results. Colloid model implemented into abstracted model of UZ radionuclide transport, which is implemented in TSPA.

Abstracted Model Results	<p><i>Particle Tracking Model and Abstraction of Transport Processes, Analysis Comparing Advective-Dispersive Transport Solution to Particle Tracking, and the Analysis of Base-Case Particle Tracking Results of the Base-case Flow Fields</i> AMRs.</p>	<p>Results presented mostly for simplified one- and two-dimensional problems. The <i>Particle Tracking Model and Abstraction of Transport Processes</i> AMR presents results that compare the particle tracking technique to simple analytic solutions and to other numerical approaches. The AMR entitled <i>Analysis Comparing Advective-Dispersive Transport Solution to Particle Tracking</i> presents results that compare the particle tracking technique with both a dual continuum particle tracking approach (DCPT) and a fully coupled advective-dispersive code (T2R3D).</p> <p>The <i>Analysis of Base-Case Particle Tracking Results of the Base-Case Flow Fields</i> AMR presents results calculated using the three-dimensional abstracted model and the base case flow fields (determined from TOUGH2). A unit source of mass was released over the repository footprint and breakthrough curves are shown. Constant transport parameters (e.g., matrix diffusion, sorption coefficients) were used.</p>	Basis is the developed model.	Shows representative performance of the UZ for the abstracted model. This model is directly implemented into TSPA.
TSPA-SR Model Results	TSPA-SR document	<p>Results that fully couple the releases from the engineered barrier system with abstracted UZ transport model (including uncertainty in transport parameters) are shown in TSPA-SR (Section 4). An analysis using this fully coupled model to evaluate the sensitivity of the receptor dose to different matrix diffusion alternatives is also shown (Section 5.2.6).</p>	AMRs where abstracted models of UZ flow and transport are developed.	Impact is modeled UZ radionuclide transport within TSPA. Includes all uncertainties considered.

## 14.0 Saturated Zone Groundwater Flow Model

### 14.1 Model Purpose

The purpose of the SZ flow model analysis is to provide PA with a calibrated SZ site-scale flow model to be used for making radionuclide transport calculations. Input to the calibrated SZ site-scale flow model consists of the work developed in the AMRs described in the following section. These are the Hydrogeologic Framework Model, Water-Level Data Analysis, Recharge and Boundary Conditions, and Geochemical and Isotopic Constraints.

In general the SZ conceptual flow model processes for Yucca Mountain are fairly well understood. Data gaps exist in certain areas, but these gaps do not affect the understanding of the key conceptual processes that occur. Data gaps primarily exist in characterization of the alluvium and volcanic areas of the expected SZ flow path, which accounts for a significant portion of uncertainty in the SZ. Analyses and models used to develop the SZ site-scale flow model are more routine approaches than state-of-the-art.

### 14.2 Model Relations

The SZ site-scale model can be described as presented in Figure 14-1, Saturated Zone Flow and Transport Model Relation Diagram. Figure 14-1 shows a model relation diagram linking the input SZ flow AMRs to the site-scale flow model and the downstream transport components. Each supporting AMR to the site-scale model has input data where uncertainty is derived and propagated to the recipient downstream AMR. Three AMRs compose the primary input for the SZ flow model, while one is used as corroborative input. These AMRs are the Hydrogeologic Framework AMR, Water Level Data Analysis AMR, and the Recharge and Lateral Flow Boundary Conditions AMR. Listed below are descriptions of the SZ flow model input AMRs and downstream use.

- *Hydrogeologic Framework Model (HFM) AMR (ANL-NBS-HS-000033)* — The purpose of this AMR is to document the 3D hydrogeologic framework model (HFM). The HFM has been constructed specifically to support the fundamental geometric framework (hydrostratigraphic grid/mesh) used for the site-scale 3D ground-water flow model used to evaluate potential radionuclide transport through the SZ. The HFM is a geometric model that incorporates the features (conceptual models) expressed in geologic maps, borehole data, topographic information, cross sections, and the Geologic Framework Model (GFM).
- *Water-Level Data Analysis AMR (ANL-NBS-HS-000034)* — The Water-Level Data Analysis AMR documents water levels and an analysis of the water-level data collected to provide the SZ site-scale flow and transport model with a configuration of the potentiometric surface and target water-level data for model calibration. The analysis is designed to use existing water-level data and analysis results as the basis for estimating water-level altitudes and the potentiometric surface in the SZ site-scale model domain.

**SATURATED ZONE FLOW MODEL**

**SATURATED ZONE TRANSPORT MODEL**

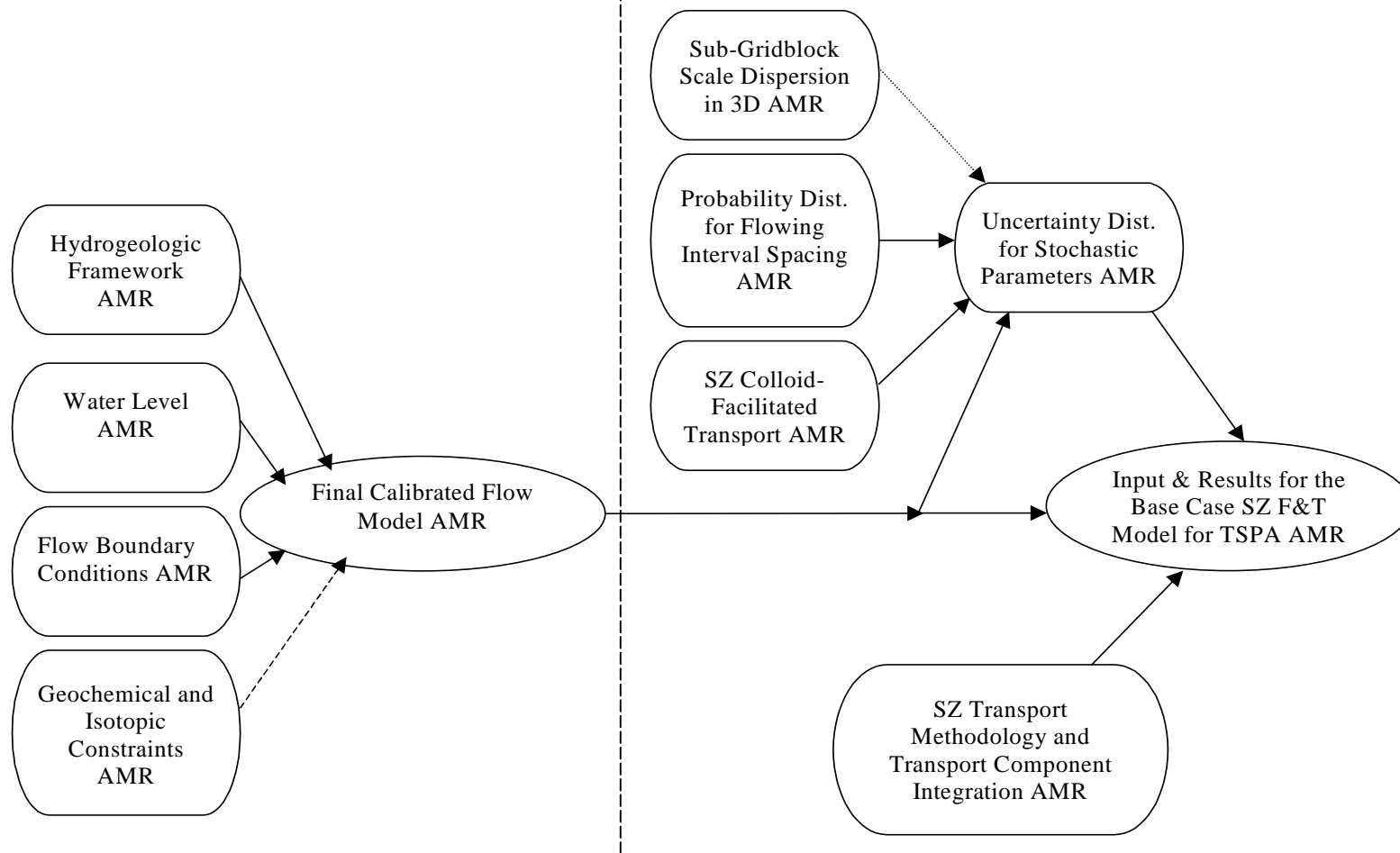


Figure 14-1: Saturated Zone Flow And Transport Model Relation Diagram

- *Recharge and Lateral Flow Boundary Conditions AMR (ANL-NBS-MD-000010)* — This AMR is an analysis that provides specified-flux boundary conditions to the SZ site-scale flow and transport model. This includes the compilation of data from the SZ regional-scale model, UZ site-scale model, and focused recharge along the Fortymile Wash channel.
- *Geochemical and Isotopic Constraints AMR (ANL-NBS-HS-000021)* — The purpose of this AMR is to provide an analysis of groundwater recharge rates, flow directions, and velocities, and mixing data. The analysis of hydrochemical and isotopic data is intended to provide a basis for evaluating the hydrologic system at Yucca Mountain independent of analyses based purely on hydraulic arguments. The AMR documents the use of geochemical and isotopic data to constrain rates and directions of groundwater flow near Yucca Mountain and the timing and magnitude of recharge in the Yucca Mountain vicinity.

### **14.3 SZ Flow Model Structure**

Figure 14-2, Saturated Zone Flow Model Structure Diagram, is a model structure diagram that maps the interplay between the conceptual model, parameters and inputs, representational model (FEHM), results, and TSPA abstraction components for the SZ Site-Scale Flow Model. The SZ flow model is a direct feed into the TSPA abstraction. The flow model is built upon a conceptual model with its mathematical representation and the model inputs. Results of the model are a calibrated flow model and sensitivity analyses for input to the TSPA abstraction AMR.

#### **A. Conceptual Model**

The general conceptual model for SZ flow at Yucca Mountain (described in more detail in the SZ PMR) at the site-scale characterizes groundwater flow in a southerly direction from recharge areas of higher precipitation at higher elevations north of Yucca Mountain toward the Amargosa Desert. Groundwater flow is through the volcanic aquifer, Tertiary volcanic rocks of the Alkali Flat-Furnace Creek groundwater basin, and then transitions to the valley fill/alluvium aquifer while flowing toward the Amargosa Desert. Recharge occurs from infiltration of precipitation and infiltration of flood flows from Fortymile Wash and its tributaries. In the southeastern part of the model area, considerable flows enter and exit the area in the lower carbonate aquifer system. This aquifer system is separated from the upper volcanic and alluvium system by confining strata. The lower carbonate system is believed to underlie much of the Alkali Flat-Furnace Creek groundwater basin. An upward vertical gradient exists between the lower carbonate aquifer and overlying volcanic and alluvial systems, due to a positive pressure head in the lower carbonate aquifer.

The flow field is considered isotropic lending to the general hydraulic gradient from north to south. Several faults are interpreted in the HFM as barriers to groundwater flow introducing large-scale heterogeneity. The Solitario Canyon Fault is one that exhibits barrier characteristics, causing a water table elevation differential across the fault of 45 m. More detailed flow field analysis indicates the flow from beneath Yucca Mountain trends from the west and converges with flow from the east at Fortymile Wash and turns southward toward the Amargosa Desert.

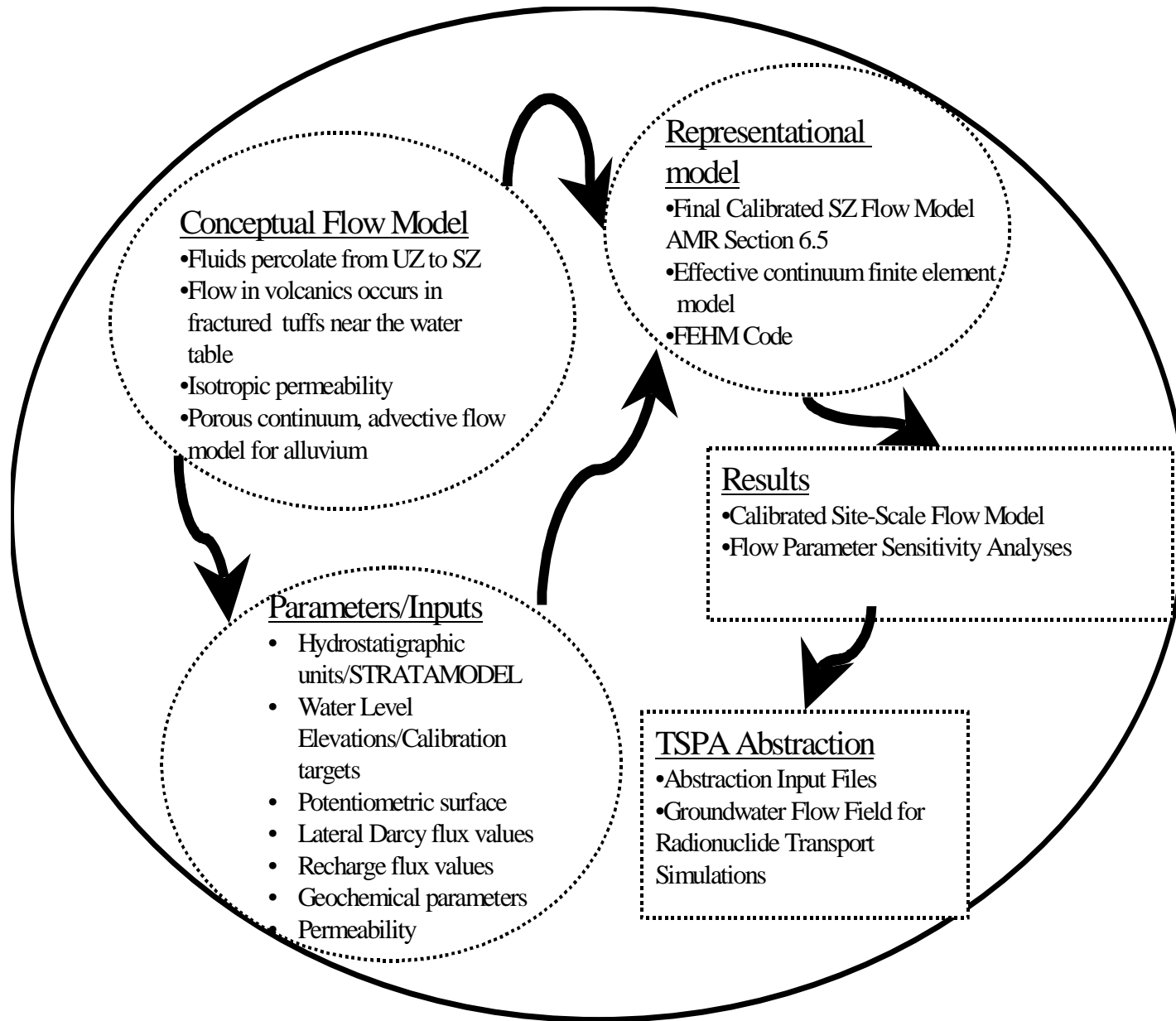


Figure 14-2: Saturated Zone Flow Model Structure Diagram

The flow path from the potential repository to the proposed compliance boundary begins in the volcanic tuffs and ends in the alluvium. Flow initially occurs within the highly fractured portions of the tuffs near the water table. Although matrix diffusion in the fractured volcanic rock is an important process in transport, it is negligible to groundwater flow. Low-permeability regions act as large-scale heterogeneities that give rise to large-scale macroscopic dispersion due to tortuous flow over a scale of hundreds of meters to kilometers. Flow transitions (alluvium uncertainty zone) from the volcanic aquifer to the alluvium aquifer where heterogeneous, advective porous processes occur. This transition from fracture flow representation in the volcanic rocks to a porous continuum representation in the alluvium reduces the calculated velocity significantly through increased cross sectional flow area and tortuosity.

## **B. Parameters and Input**

Model input in the form of analyses and parameters are captured in the individual AMRs for the site scale flow model. The model itself is captured in the *Calibration of the Site-Scale Flow Model AMR (MDL-NBS-HS-000011)*. The primary inputs to the model are the hydrostratigraphic units, water level data, flow field/potentiometric surface map, and boundary conditions. The basic skeleton of the flow model is derived from the HFM. In this AMR the geologic units are divided into hydrostratigraphic units based on similarities of hydraulic properties. A 3D geometric model is developed for the model domain that incorporates the features (conceptual models) expressed in geologic maps, borehole data, topographic information, cross sections, and the GFM on which it is based. When the HFM is constructed it is converted to a structural mesh using STRATAMODEL for direct input into FEHM. The HFM incorporates large-scale features that affect groundwater flow, such as the Solitario Canyon Fault.

The *Water-Level Data Analysis AMR (ANL-NBS-HS-000034)* produces a database of water table elevation and a potentiometric surface map for the model domain. The potentiometric surface map identifies the flow paths in the model domain, specifically the expected flow path from the potential repository to the biosphere. This map helps to constrain the flow model during calibration exercises. The SZ flow model uses 115 water level and head measurements for calibration targets.

Lateral boundary conditions for the site-scale flow model were derived from regional water and head data. The data are used to form fixed-head boundary conditions on the lateral sides of the model. Data were derived primarily from the Death Valley Regional Ground Water Flow Model (D'Agnese et al. 1997). Volumetric groundwater flow rates simulated by the regional flow model were extracted for lateral boundaries of the site-scale flow model. Recharge boundary conditions were obtained from distributed recharge taken from the regional-scale flow model, recharge below the area of the UZ flow model that coincides with the SZ flow model domain, and focused recharge along the Fortymile Wash channel. These boundary conditions are used as direct input for target calibration points of the flow simulation. Further information is located in the *Recharge and Lateral Flow Boundary Conditions AMR (ANL-NBS-HS-000010)*.

Geochemical parameters and permeability parameters were used in the model development, but only as corroborative data input. Permeabilities were derived from numerous sources in the area of the site-scale model. These include single-hole hydraulic tests, multiple hole hydraulic tests

(i.e., C-Wells), and evaluation of data from the NTS. Field derived permeability data were used to constrain the calibration adjustments made to the model. The data were used to guide the selection of bounds on the permissible range of permeabilities to be considered during the calibration and to check on the reasonableness of the final permeability estimates produced by the calibration. Further information regarding the permeability fields can be found in the *Calibration of the Site-Scale Flow Model AMR (MDL-NBS-HS-000011)*. Similarly, the geochemical parameters were used to compare hydrochemical data trends with the calculated particle pathways in the flow model analysis and to constrain rates and directions of groundwater flow near Yucca Mountain and the timing and magnitude of recharge in the Yucca Mountain vicinity. The numerical model for groundwater flow at Yucca Mountain was evaluated for consistency with the flow paths estimated from the hydrochemical data through particle tracking techniques inclusive of the FEHM code. Additional information regarding geochemical parameters can be found in the aforementioned calibrated flow model AMR and the *Geochemical and Isotopic Constraints AMR (ANL-NBS-HS-000021)*.

### **C. Representational Model**

The representational model for the calibrated site-scale flow model is the FEHM code (Zyvoloski et al. 1997). This model is discussed in more detail in the SZ PMR and the *Calibration of the Site-Scale Flow Model AMR (MDL-NBS-HS-000011)*. This code is used to obtain a numerical solution to the mathematical approach for groundwater flow. FEHM is a non-isothermal, multiphase flow and transport code that simulates the flow of water and air, and the transport of heat and solutes, in 2D and 3D saturated or partially saturated heterogeneous porous media. The code includes comprehensive reactive geochemistry and transport modules and a particle tracking capability. For the site-scale model, an equivalent continuum approach was used for fractured media and alluvium. Effective continuum methodology was selected because the gridblock size is large enough to average fracture and surrounding rock properties. This is assumed appropriate because the field tests of permeability include effects of fractures in the testing interval. It is also assumed that the features would have the same averaged permeability at the block size of the continuum (Table 14-1).

### **D. Results**

The output of the flow model process is a calibrated site-scale flow model and model parameter sensitivity analysis for use in TSPA abstraction (Figure 14-1 and Figure 14-2). The data feed to TSPA is abstraction input files and groundwater flow field model output files for radionuclide transport calculations. The *Calibration of the Site-Scale Flow Model AMR (MDL-NBS-HS-000011)* and the *Input and Results of the Base Case Saturated Zone Flow and Transport Model For TSPA AMR (ANL-NBS-HS-000030)* contain detailed information of the results and abstraction process.

## **14.4 Discussion of Uncertainty and Variability Treatment**

An evaluation of uncertainty and variability treatment in the AMRs was performed for this exercise. For each AMR, the uncertainties/variabilities were identified and an evaluation was made of the treatment that was performed for each AMR. Thorough treatment was considered to

be: identification, treatment, impact assessment, and clear presentation of the analysis and the propagation of uncertainty in the AMR. Table 14-1 is a synopsis of some of the uncertainties and variabilities identified in this exercise. The following is a discussion of the evaluation process and uncertainty/variability analysis trends within the AMR/model process.

Review of the AMRs associated with the SZ site-scale flow model indicates that the way uncertainties are addressed is very inconsistent between AMRs. In most cases all the AMRs make an attempt to identify the uncertainties, but the trend is that there is very little uncertainty analysis. Often an independent interpretation needs to be formulated during review of the document to extract this evaluation. It is also very evident that there lacks integration of uncertainty from AMR to AMR and how it is treated from the upstream AMR to the downstream, user AMR. Integration would be the transparent transfer of uncertainty treatment from one AMR to the downstream feed AMR, and the subsequent assessment of the uncertainty prior to use as input data.

### **A. Conceptual Models**

The conceptual model of flow for the SZ and associated uncertainties are not discussed in any of the associated AMRs. Rather, the conceptual model for flow is presented in the *Saturated Zone Flow and Transport Process Model Report (PMR)*, Section 3.2 and the components of conceptual flow are discussed in the AMRs. In section 3.2.5 of the PMR there is an elaborate discussion of uncertainty for specific components of the SZ conceptual flow model. The components are considered major elements where uncertainty is derived and provides an adequate assessment (Table 14-1). What the PMR does not effectively communicate is an evaluation of the general conceptual model versus alternatives proposed by others. The PMR presents as a summary of the other views, but does not discuss why these were not selected based on concrete evaluation, such as calibration of flow under alternative constraints, or supporting data to refute these alternative views.

The PMR summarizes a few parameter uncertainties in the model, but does not include all uncertain parameters, mathematical/numerical uncertainty/variability, and conceptual uncertainty/variability implicit in the AMRs. The PMR should be the place where all uncertainty and variability is summarized, but the analysis should be clearly evident in the AMRs and the propagation clearly traceable to the PMR, which is not always the case as presented in the following discussions.

### **B. Parameters and Input**

The representational model, FEHM code, incorporates the SZ flow AMRs, presented in Section 2.0, as input data (Figure 14-2). Three of these AMRs serve as the primary building blocks of the SZ Flow Model. These are:

- *Hydrogeologic Framework Model* AMR (ANL-NBS-HS-000033)
- *Water Level Data Analysis* AMR (ANL-NBS-HS-000034)

- *Recharge and Lateral Boundary Conditions for the Saturated Zone Site-Scale Flow and Transport Model AMR (ANL-NBS-MD-000010)*

These AMRs are the basic building blocks for input to the FEHM code geometric structure and boundary conditions. The lack of uncertainty analysis in these models tends to be carried forward into the representative model. For instance, the Flow Boundary Conditions AMR does not discuss uncertainty for any of the input from the UZ model. The recharge flux from the UZ can have significant uncertainty that is passed into the final calibrated flow model as a calibration target, thus introducing error in the flow model. The calibrated flow model does not provide a thorough uncertainty assessment of the flux and this untreated uncertainty is further propagated. The flow model then passes this compounded uncertainty to the TSPA abstraction AMR where further propagation occurs. In order to understand the cumulative effect of uncertainty propagation, each AMR must provide a thorough analysis and clearly present it for traceability from one AMR to the next. Each downstream AMR feed (data recipient) then must describe how the data is being used and the propagated impact of uncertainty.

In the AMR entitled *Hydrogeologic Framework Model AMR (ANL-NBS-HS-000033)*, most of the uncertainty and variability is due to limited data (spatial variability in stratigraphic picks, geological units simplified to hydrogeologic units, depth limited stratigraphic picks). The AMR discusses the adequacy of the available data representing the hydrogeologic structural conditions identifying the uncertainty, but does not explicitly discuss the treatment (Table 14-1). The analysis also does not clearly demonstrate the impact of the uncertainty on the overall conclusions of the AMR for use by the downstream AMR. The impact from the lack of analysis could be the misinterpretation of areal and vertical stratigraphy that is transposed to the downstream AMR (i.e., Final Calibrated Flow Model). As previously stated the greatest uncertainty and variability for his AMR is limited geologic data. Most boreholes are shallow leading to increased uncertainty with depth. Additionally, the number of boreholes to define extent of stratigraphy in the horizontal plane lends the AMR to a significant spatial variability. To overcome the lack of data the AMR uses practical methods of extrapolation and interpolation to estimate the vertical and horizontal extent of the stratigraphy. The uncertainty factor in this case is the distance between grid cells and known data points. As this distance increases, the uncertainty and variability increases. This is very apparent with respect to the definition of the alluvium/volcanic aquifer transition zone. This uncertainty is defined in the *Uncertainty Distribution for Stochastic Parameters AMR (ANL-NBS-MD-000011)*, where the distribution is used for transport calculations.

The AMR entitled *Recharge and Lateral Boundary Conditions for the Saturated Zone Site-Scale Flow and Transport Model AMR (ANL-NBS-MD-000010)* does not address uncertainty transparently. Input for this AMR consists of a compilation of data from the regional flow model, the unsaturated zone site-scale model (1997), and focused recharge data from Fortymile Wash. Each of these input sources inherently contains uncertainty, yet this AMR does not discuss the uncertainty associated with this input information. Within the AMR there are some

uncertainties (simplified conceptual representation) identified and treated through assumptions with no basis for the assumptions (Table 14-1). For example the AMR:

1. Assumes recharge components from input documents are sufficiently consistent for the purposes of the combined recharge model in the SZ site-scale flow.
2. Assumes three components of recharge from supporting documents provide a reasonable estimate of the magnitude and spatial pattern of recharge when combined.
3. Assumes that the integration of recharge flux extracted from the UZ model for use at the grid resolution of the SZ site-scale flow model is adequate to represent the recharge pattern in the area of the UZ model foot print.
4. Assumes recharge from Fortymile Wash represents the long-term recharge from this source.

All of the assumptions are simplifications needed to directly utilize the supporting input information/data without a thorough uncertainty analysis: identification, treatment, impact assessment, and clear presentation of the analysis and the propagation of uncertainty. The assumptions rely heavily upon the regional model (D'Agnesse et al 1997), which contains a significant degree of uncertainty. The regional model report does not discuss uncertainty, which makes evaluation of the uncertainty for input parameters to the site-scale model difficult. The site-scale model extracts lateral and recharge boundary conditions from the regional model. Due to differences in the grid scale between the two models, uncertainty and variability is introduced through direct transference of the boundary conditions (Table 14-1). Additionally, without data points to obtain water levels at the site-scale model domain boundary, it is difficult to verify the lateral flux values extracted for the site-scale model. A discussion of the uncertainty for boundary conditions is essential for downstream users to understand the quality of the data for input into the site-scale model. At a minimum the AMR should clearly present the input data uncertainty and integrate it with an output uncertainty analysis.

The AMR entitled *Water Level Data Analysis (ANL-NBS-HS-000034)* is an example of a thorough analysis of the data quality and the uncertainty and variability involved (parameter, conceptual) with using the data (Table 14-1). Most of the uncertainty is due to areas where the data are lacking and industry accepted practices of interpolation and extrapolation are used in data limited areas for grid generation. For example, a hybrid gridding technique in PETROSYS was used to construct a continuous grid or surface utilizing a set of data points in x, y, z, space. This method is a combination of the minimum curvature method and the first order least squares method. Because it was necessary to construct an estimated potentiometric surface with the available data points, gridding algorithms were used to extrapolate the potentiometric surface beyond the data points on all boundaries. This is an acceptable method, but uncertainties are introduced by the limited data set. The AMR does not evaluate the uncertainty and variability in the data sets and in the resulting potentiometric surface map. In a few cases the impact of individual parameter uncertainty or variability were not presented in the AMR (i.e., availability of water level data from sources, Section 5.1; mean water levels for period of interest, Section 5.1); however, the majority were. For instance, the AMR assumes averaged steady state water level altitudes for a period of time, not a specific year and represents conditions consistent with

the regional model. These water levels are used for calibration and to develop the potentiometric surface map that defines flow. An impact analysis of this assumption was not discussed in the AMR, but inherently the uncertainty in water level altitude in some areas may impact the understanding of flow paths.

The most exceptional case of uncertainty evaluation was presented in the AMR entitled *Geochemical and Isotopic Constraints AMR (ANL-NBS-HS-000021)* (Table 14-1). This AMR consisted of primarily simplifying assumptions that generated the uncertainty or variability. Each assumption was classified, associated with a method of treatment and basis, and generally provided an impact of the uncertainty/variability. Although some of the treatment methods might not be completely reasonable, it is easy to follow (traceable and transparent) within the AMR. Some areas that may need improvements are for example, the assumption regarding the annual deposition rate of chloride encompasses the present-day rate as well as the rates that prevailed when the sampled pore waters infiltrated below the soil zone (assumption 12). For this assumption there is a need to quantify the uncertainty in the deposition rate, and the resulting estimates of recharge obtained by the chlorine mass balance method. Another example is assumption 8 that states groundwater flow to Yucca Mountain from the areas directly north is minor. This assumption is not adequately discussed in the text. Flow direction in the Drill Hole Wash area is not discussed and the location is not shown in the AMR. Despite some of these issues, the structured approach the AMR used in dealing with assumptions made it easy to follow the uncertainty/variability analysis. Because this AMR is used more to corroborate the conceptual model for SZ flow and transport, the overall impact of the uncertainties and variabilities are not readily apparent, as the data are not used as input to the SZ flow model (FEHM Code).

### **C. Representational Model**

The AMRs previously discussed are used to develop the representational model, which is captured in the AMR entitled *Calibration of the Site-Scale Saturated Zone Flow Model AMR (ANL-NBS-HS-000011)*. The purpose of this AMR is to provide a calibrated site-scale SZ Flow Model for use in PA. The input for this AMR relies heavily on the output of the AMRs discussed above (Figure 14-1). As such, treated and untreated uncertainties in supporting AMRs are used inherently as direct input. This AMR does not evaluate the propagated uncertainty in the analysis and modeling of the site-scale flow. It does adequately identify uncertainty treated through assumptions made within the AMR; however, the analysis lacks an explicit discussion of uncertainty. For example, the assumptions regarding complicated water table configurations, fixed, constant head boundary conditions, and uncertainty in the vertical gradient, are not explicitly discussed with regard to treatment, basis, or impact of uncertainty. It does have a limited discussion on the analysis of weighted-residuals, but this does not explain how the weighting scheme applies to uncertainty in the model.

The numerical approach for the site-scale model is presented in the AMR and PMR. In particular, the AMR discusses the selection of using an effective continuum approach but does not explain why discrete fracture methodology or dual permeability was not used instead. It can only be assumed that this methodology was selected due to the lack of data to describe the fracture network in the detail needed for discrete fracture or dual permeability methods (Table

14-1). It can also be assumed that the effective continuum approach was selected due to its simplicity or computational efficiency, but the AMR does not adequately justify its use. The effective continuum approach is justified by the AMR as appropriate because the field tests of permeability include the effects of fractures in the testing intervals. This justification assumes scaling effects are not significant. The AMR does not discuss the uncertainties regarding scaling effects of field tests in relation to the use of effective continuum methods.

An adequate sensitivity analysis is presented in the AMR to bound parameters; however, the AMR does not evaluate alternative concepts. For example, the model is based on a horizontal isotropy. A calibration of the model to evaluate horizontal anisotropy is warranted to evaluate conceptual model uncertainty. Other alternative models, such as vertical extent of faults and thermal flow patterns, should also be evaluated to assure the current conceptual model is the best representation and to refute models presented by entities such as the State of Nevada and the NRC. Calibration of the model is executed through the adjustment of permeabilities in hydrogeologic units. The adjustment range of permeability for the calibrated model was constrained by data obtained from the site and areas in the vicinity of the site-scale model. For instance, permeability values were obtained from single well hydraulic tests, multi-well hydraulic tests (C-Wells), and from a database of permeabilities from the NTS. There exists a wide range of variability in the data sets, which puts to question the scaling effects of the tests. The AMR does not assess the variability or uncertainty in the permeability values. Areas where data are limited are given more uncertain weighting than more certain data areas during calibration and sensitivity analysis, but assessment of the uncertainty and variability beyond this does not occur.

The model does perform a comparative analysis of the simulated head and flux versus observed head and flux targets. This is an adequate means of addressing model error/uncertainty in comparison to the calibration targets. However, this method does not assess the propagation of the uncertainty from supporting model input. If the calibration targets are uncertain or in error, the model could also be equally uncertain. Because uncertainty in supporting AMRs was not always evaluated during both input and output stages of the AMRs, downstream users may propagate the uncertainty as is without adequate treatment.

#### **14.5 Uncertainty Propagation and Conclusions**

Uncertainty can be propagated in two ways throughout the modeling process. During development of each of the AMRs the uncertainty and variability should be assessed through sufficient identification, treatment and justification, impact assessment, and a clear, traceable, and transparent presentation of the analysis and the propagation of the uncertainty. This preferred process allows the downstream user to evaluate the input data for incorporation into downstream analysis and modeling processes, reducing input of inadequate data and reducing propagation of errors in the analysis. Another way uncertainty is propagated is failing to assess uncertainty and variability as described above at each step of the process, thus propagating cumulative error (uncertainty/variability) throughout the process, resulting in an end product that is not a realistic representation of the process being modeled.

The purpose of the flow model analysis is to provide PA with a calibrated SZ site-scale flow model to be used for calculating radionuclide transport calculations. The input data from this AMR to TSPA are parameter input files and flow field data (Figure 14-2). Each supporting AMR attempts to address uncertainty, but the overwhelming trend is that the analysis is incomplete and integration of uncertainty to downstream AMRs is not performed.

As described in the body of this paper for the SZ flow model component, the most critical uncertainties are associated with parameters and conceptual model alternatives. The majority resolution of the uncertainties in this model are bounding through sensitivity analysis, assumptions to capture the uncertainty, or doing nothing to evaluate the uncertainty. Calibration of the flow model utilizes the water level and boundary conditions as targets, while constraining parameter adjustment ranges with permeability data. The water level analysis AMR and the boundary conditions AMR uncertainties were not adequately evaluated, so the calibration propagates these untreated uncertainties into its analysis to be cumulatively passed onto the transport analysis in the form of the flow fields and calibrated input parameters. The geochemistry AMR is used to corroborate the conceptual model for the SZ flow and transport, but not used as direct input. Therefore, uncertainty in this AMR is not readily apparent in the flow model.

General incorporation of uncertainties from one AMR to the next without adequate uncertainty analysis can allow the incorporation of erroneous data resulting in non-representative modeling results. Throughout the AMRs it is not clear how uncertainty/variability was passed onto the downstream analysis due to the lack of documentation. It is clear in some AMRs that uncertainty was not treated at all and relied on downstream users to perform the assessment. In some cases incomplete uncertainty analysis was performed. Overwhelmingly, there is a complete lack of integration of uncertainty or at least documentation of integration between AMRs. This lack of integration is primary to the propagation of untreated uncertainty between AMRs, resulting in cumulative use of data that is potentially inaccurate.

**Table 14-1: Saturated Zone Flow Model**

<b>Model Purpose:</b> The purpose of the SZ Flow Model is to provide PA with a calibrated SZ site-scale flow model to be used for making radionuclide transport calculations.				
Summary	Source	Treatment	Basis	Impact
<b>Conceptual Model Uncertainty</b>				
<b>SZ Conceptual Flow Model</b>	SZ PMR (TDR-NBS-HS-000001) - Summarizes the selected SZ conceptual model with a focus on hydrogeologic framework, flow direction, and flow processes.	The SZ PMR does not treat uncertainties for the general conceptual model. The PMR has a limited discussion of uncertainty, but further analysis and discussion is deferred to the AMRs. Some of the AMRs contain an analysis of uncertainty for specific components of the overall SZ flow conceptual model. The PMR had an elaborate discussion of uncertainty for components of the conceptual model (SZ PMR Section 3.2.5). These are considered major conceptual uncertainties related to the conceptual model. The SZ PMR does present alternative views for the conceptual model, but does not present an analysis of why alternative views were not selected and why the chosen conceptual model was selected over other views.	The bases for components of the conceptual model are briefly described in the PMR with further analysis in the AMRs. For instance, the hydrogeologic framework is derived in the respective AMR from conceptual models in the form of cross-sections, geological maps, and borehole logs. The basis for the accepted conceptual model over alternative views is supported by peer review panels, NWTRB, ACNW, and other outside bodies, rather than internal analysis.	Based on the lack of data in some critical areas of the model domain, the most significant impact may be with regard to the direction of flow. The processes of flow in the different environments appear to be sufficiently understood.

Large Hydraulic Gradient	SZ PMR (TDR-NBS-HS-000001), Section 3.2.5	<p>The SZ expert elicitation panel narrowed theories of the large hydraulic gradient to two most credible hypotheses: the large hydraulic gradient is caused by flow through the upper volcanic confining unit or it is semi-perched water. The consensus of the panel slightly favored semi-perched water. The experts agreed that the issue was mainly one of technical credibility that the probability of any large transient change in the configuration of the large gradient is low, and long-term transient readjustment of gradients was of low probability. The question of whether perching of water is the cause of the large gradient was not fully resolved by the drilling of WT-24 (section 3.2.5)</p> <p>The SZ flow model treats the large hydraulic gradient area as a linear east-west barrier or zone of reduced permeability.</p>	Expert elicitation panel hypotheses and limited data from WT-24 drilling exercises (Section 3.2.5)	None Provided in the PMR other than the barrier diverts particles around the barrier to the east and the west (Section 3.2.5).
Perched Water-Matrix Flow-SZ Recharge	SZ PMR (TDR-NBS-HS-000001), Section 3.2.5	The basis of chlorine-36 and oxygen-18 data tentatively concludes that uncorrected carbon-14 ages approximate the true carbon-14 ages. The ages are generally between 7,000 and 11,000 years before present. In either case, these dates suggest that recharge episodes occurred several thousand years ago and that there is no evidence of a large amount of recharge under current climatic conditions (Section 3.2.5.2)	Chlorine-36 and Oxygen-18 analyses (Section 3.2.5.2)	No evidence of a large amount of recharge under current climatic conditions. Chemical data suggests SZ waters in the Yucca Mountain region infiltrated under somewhat colder conditions than perched waters within Yucca Mountain. Data also suggests that matrix flow is minimal due to the chemical resemblance of SZ water to perched water (Section 3.2.5.2)

<p>Horizontal Anisotropy - A conceptual model of horizontal anisotropy in the tuff aquifer is reasonable, given that flow in the tuff aquifer is believed to occur in a fracture network that exhibits a preferential north-south strike azimuth. Evaluation of the long-term pumping tests at the C-Wells complex supports the conclusion that large-scale horizontal anisotropy of aquifer permeability may occur in the SZ. There are important uncertainties, including differences in pumping test analysis methods, the fact that only a minimum number of observation wells were used, and additional uncertainty regarding the validity of assuming a homogeneous effective continuum over the scale of the c-wells test.</p>	<p>SZ PMR (TDR-NBS-HS-000001), Section 3.2.5</p>	<p>Take together the observations and inferences support an alternative conceptual model in which large-scale horizontal anisotropy of permeability, with higher permeability in a north-northeasterly direction, occurs in the volcanic units of the SZ to the southeast of the potential repository. <b>Sufficient uncertainty exists in this interpretation to warrant retention of the simpler, horizontal isotropic mode of permeability as the nominal conceptual model. Anisotropy is used in the TSPA calculations.</b></p>	<p>Sufficient uncertainty exists in the anisotropic interpretation to warrant retention of the simpler horizontal isotropic mode of permeability as the nominal conceptual model.</p>	<p>Uncertainty in the flow path.</p>
---	--	---	---	--------------------------------------

Climate Change	SZ PMR (TDR-NBS-HS-000001), Section 3.2.5	Future climate change is likely to change the SZ flow conditions. In particular the amount of precipitation is important because it largely determines the amount of infiltration and ultimately recharge to the SZ. The principle considerations of future climate are treated as follows: 1) Climate is cyclical, so past climates provide insight into potential future climates; 2) A relationship exists between the timing of long-term past climate change and the timing of changes in certain earth-orbital parameters, 3) Long-term earth-based climate-forcing functions, primarily tectonics, that operate on the million-year time scale have remained relatively unchanged during the last long earth climate cycle and will remain unchanged during the next 10,000 years. If changes due to climate-forcing functions are ignored, climate may be forecasted as cyclical with a period of ~400,000 years.	Climate proxies such as Owens Lake and Devils Hole	Change in the SZ flow conditions.
Changes in Water Table Elevation due to climate change	SZ PMR (TDR-NBS-HS-000001)	A higher water table is expected to result from future climate changes. Climate change is incorporated in TSPA.	Based on realizations of the regional flow model (D'Agnese et al. 1999).	An increase in elevation of the water table under Yucca Mountain is important because it decreases the UZ barrier between the potential repository and the SZ, and also because it may increase the hydraulic gradient resulting in shorter radionuclide transport in the SZ. An increase in the water table may also may change the direction of the transport flow path, although change in the flow path is unlikely (Section 3.2.6.1)

<p>Changes in Water Table Elevation due to disruptive events</p>	<p>SZ PMR (TDR-NBS-HS-000001)</p>	<p>Transient fluctuations on the order of a few decimeters have been observed in response to barometric variations, earth tide changes, and earthquakes. Modeling scenarios involving earthquakes or volcanic intrusions show that the maximum increase in the elevation of the water table resulting from these events is expected to be on the order of a few decimeters to 20 m (SZ PMR Section 3.2.6.1). A scenario (Ahola and Sagar 1992) involving a three-order magnitude increase in hydraulic conductivity in the area north and northeast of Yucca Mountain resulted in increase of up to 275 m in the water table below Yucca Mountain. Modeling of this scenario was not performed to show under what tectonic or volcanic conditions such an increase would occur (SZ PMR Section 3.2.6.1).</p>	<p>Based on realizations of the regional flow model (D'Agnese et al. 1999).</p>	<p>Change in the SZ flow conditions.</p>
--	-----------------------------------	--	---	--

<p>Continuous unsaturated conditions at Yucca Mountain during past epochs</p>	<p>SZ PMR (TDR-NBS-HS-000001)</p>	<p>Not all investigators are in agreement concerning the hypothesis of continuous unsaturated conditions at Yucca Mountain during past epochs. Szymansky (1989) postulated and modeled possible rises in the water table due to tectonic activity. Hill et al. (1995) suggests that upwelling of waters of elevated temperature into the potential repository is a possible source of calcite/opal deposits located at and near faults at Yucca Mountain. Possible scenarios in which the water table rises to saturate the potential repository have been excluded from consideration in TSPA analyses.</p> <p>The 3-D site scale flow model assumes confined conditions within the SZ. Changes in water level are modeled are modeled by increasing the hydraulic gradient and reducing the thickness of the UZ.</p>	<p>Stuckless et al. (1998) point out a number of errors and cite other sources of evidence to arrive at the contrary conclusion that the source of hypogene water in the inclusions is more likely infiltration through overlying soil and rock. The National Academy of Sciences also reviewed this issue and concluded that "none of the evidence cited as proof of groundwater upwelling in and around Yucca Mountain could reasonably be attributed to that process."</p>	<p>Change in the SZ flow conditions.</p>
<p>Changes in Groundwater Flux</p>	<p>SZ PMR (TDR-NBS-HS-000001)</p>	<p>Climate change in the TSPA-VA is modeled by increasing the groundwater flux along the transport path and an increase in solute flux is computed analytically from the increased groundwater flux. Effects of climate change on the transport of radionuclides in the SZ are incorporated in TSPA calculations by scaling the radionuclide mass breakthrough curves simulated for present climatic conditions and assumes a proportional scaling of groundwater flux in the entire SZ system in response to future wetter climatic conditions.</p>	<p>Estimates of the scaling factors for groundwater flux in the SZ under alternative climatic conditions are based on simulations using the regional scale SZ flow model (D'Agnese et al. 1999) and on results from the site-scale UZ flow model.</p>	<p>Change in the SZ flow conditions.</p>

Changes in Recharge and Discharge	SZ PMR (TDR-NBS-HS-000001)	Regional recharge and discharge estimates under present and glacial-transition climate conditions have been computed by the regional model (D'Agnese et al.).	Regional-scale SZ flow model (D'Agnese et al. 1997)	Change in the SZ flow conditions.
<b>Representational Model Uncertainty</b>				
FEHM was selected as the representational model for SZ Flow	<i>Calibration of the Site-Scale Saturated Zone Flow Model</i> AMR (ANL-NBS-HS-000011) - Provides a brief discussion of the numerical approach for the FEHM model. It also gives the rationale in selecting the FEHM code to represent the effective continuum input to build the model (i.e. boundary conditions, grid selection, framework)	An analysis of the numerical approach is presented in the AMR through a simplifying assumption of a steady state effective continuum approach (Section 5, Assumptions; Section 6.1, Methodology)	The basis for a steady state approach is such that the modern day flow system has had sufficient time to completely equilibrate to perturbations of climate over the past 15,000 years and that pumping from wells south of the model domain has had sufficient time to return to equilibrium conditions.  The assumption of effective continuum approach is justified because the model grid blocks are large enough to average the fracture effects and the model is steady state. Steady state conditions imply pressure equilibrium between the fractures and surrounding intact rock, excluding any local flow in a given gridblock, between fractures and surrounding rock.	No impact discussed in the AMR
The FEHM approach does not consider complicated water table configurations, making a simplifying assumption of a smoothly overlapping water table surface is adequate for the top layer of the model.	<i>Calibration of the Site-Scale Saturated Zone Flow Model</i> AMR (ANL-NBS-HS-000011), Section 5	No treatment in AMR other than making the assumption.	None provided in the AMR.	None provided in the AMR

<p>The site-scale flow model is constructed to represent the flow system as a confined aquifer.</p>	<p><i>Calibration of the Site-Scale Saturated Zone Flow Model</i> AMR (ANL-NBS-HS-000011), Section 5</p>	<p>A confined aquifer approach is used. The top model boundary is set as the observed water elevations. The approach still allows recharge to be modeled as spatially distributed source terms within the top layer.</p>	<p>Justified by the close match with the calibrated water levels from the site-scale SZ flow model. This approach solves a simplified, computationally more efficient numerical model.</p>	<p>The approach assumes no unsaturated zone and, therefore, solves a simplified and computationally more efficient numerical model. Because none of the fluid rock properties depend on head, no changes to the true solution occur other than forcing the bookkeeping coding in FEHM to assume fully saturated conditions. The negative side of this approach is that the top surface of the numerical model corresponds to the measured water-table surface and may be inconsistent with the model-derived water table surface (Section 6.1.3).</p>
<p>Uncertainty in the interpretation of infiltration onto the computational mesh to provide the surface flux boundary conditions.</p>	<p><i>Calibration of the Site-Scale Saturated Zone Flow Model</i> AMR (ANL-NBS-HS-000011), Section 5</p>	<p>Comparison of the infiltration map data and the recharge interpolation.</p>	<p>The interpolation procedure is designed to ensure that the local small-scale features of the infiltration map are represented in the boundary conditions and that the total flux is preserved (Section 6.2.3).</p>	<p>Comparison showed that the data are identical, thus preserving the recharge distribution.</p>
<p>Uncertainty in the use of effective continuum approach over dual permeability or discrete fracture methodologies.</p>	<p><i>Calibration of the Site-Scale Saturated Zone Flow Model</i> AMR (ANL-NBS-HS-000011), Section 6.1.1</p>	<p>Utilizes effective continuum approach and discusses other methodologies, but does not explain why other methods were not selected.</p>	<p>Selected effective continuum approach because the gridblock size is large enough to average fracture and surrounding rock properties. Appropriate because the field tests of permeability include the effects of fractures in the testing interval. This assumes that the features would have the same averaged permeability at the block size of the continuum.</p>	<p>Not discussed in the AMR.</p>

<b>Parameter Uncertainty</b>				
Uncertainty increases with depth and distance from the proposed repository, as data density decreases. The configuration of the unconformity between Tertiary and Paleozoic rocks is only defined by one borehole. The framework model grid is developed by picking data points that define the top of a hydrogeologic unit. Due to the lack of data with depth, these points often are interpolated and extrapolated.	<i>Hydrogeologic Framework Model for the Site-Scale Flow and Transport Model</i> AMR (ANL-NBS-HS-000033)	Evaluation of conceptual models and simplification of data (Section 6.4), testing (Section 6.5.3), model validation (Section 6.5.3), and visual inspection (Section 6.5.3). Additionally, the data picks used to develop the HFM are weighted based on the number of data points available for the specific unit for the extrapolation and interpolation (Section 6.3.4 and Table 6-1).	No basis is given other than simplification due to lack of data (Section 6.4)	Evaluation indicated the HFM closely approximates the input data and is more accurate where more data exists. Further evaluation of the uncertainty can not be performed without additional data and is deferred to calibration and sensitivity studies during development of the site-scale flow model.
The HFM assumes that the digital elevation model used to define the lateral extent of hydrogeologic units exposed at land surface provides a suitable degree of spatial resolution.	<i>Hydrogeologic Framework Model for the Site-Scale Flow and Transport Model</i> AMR (ANL-NBS-HS-000033)	Interpretation of the hydrogeologic units is constrained by the geologic map data.	Data in geologic maps, well logs, and other stratigraphic sources are used to justify.	Not addressed in the AMR.
Assumption that the results of the three components of recharge, derived through different methods, are sufficiently consistent for the purposes of the combined recharge model in the site-scale flow model.	<i>Recharge and Lateral Flow Boundary Conditions</i> AMR (ANL-NBS-MD-000010)	Not discussed in the AMR.	Justified by the observation that the total volumetric flow rate of recharge is a relatively small fraction of the total volumetric groundwater flow rate through the SZ.	Not discussed in the AMR.
Assumption for the distributed recharge from the regional model that the relatively coarse grid resolution of the regional model (1500 meters) is adequate for use at the higher resolution of the site-scale SZ flow model.	<i>Recharge and Lateral Flow Boundary Conditions</i> AMR (ANL-NBS-MD-000010)	Not discussed in the AMR.	The regional model is based on measurements of groundwater discharge and is consequently constrained by the water balance of the entire system. Relies totally on an uncertainty analysis at the regional model level.	Not discussed in the AMR.
Integration of recharge flux extracted from the UZ model for use at the grid resolution of the SZ site-scale flow model is adequate to represent the recharge pattern in the areas of the UZ model footprint.	<i>Recharge and Lateral Flow Boundary Conditions</i> AMR (ANL-NBS-MD-000010)	Not discussed in the AMR.	The relatively small total groundwater contribution from the UZ model relative to the distributed recharge model indicates this assumption is not of large consequence for the purpose of the site-scale model.	Not discussed in the AMR.

Estimates of recharge from Fortymile Wash are representative of the long-term recharge from this source.	<i>Recharge and Lateral Flow Boundary Conditions</i> AMR (ANL-NBS-MD-000010)	Not discussed in the AMR.	The relatively small total groundwater contribution from the focused recharge along Fortymile Wash relative to the distributed recharge model indicates this assumption is not of large consequence for the purpose of the site-scale model.	Not discussed in the AMR.
Average steady state water level altitudes are assumed, not levels for a specific year. The site-scale model represents conditions consistent with the regional model. Water levels used for calibration are used to develop the potentiometric surface map that defines flow. Some wells used in the analysis had little or no water level data available.	<i>Water-Level Data Analysis for the Saturated Zone Site-Scale Flow and Transport Model</i> AMR (ANL-NBS-HS-000034)	Available water level measurements were obtained from field data and databases [I.e., National Water Information Database (NWIS)]. All available water levels, with the exception of those anomalous data in Attachment I of the AMR were used. Areas of the potentiometric surface map without data points were inferred (Section 5.1). The AMR performs an analysis to identify the reliability of the measurements used.	Availability of data.	Not discussed in the AMR.
Composite water levels are used in the analysis due to lack of well completion data and limited wells with packed off intervals.	<i>Water-Level Data Analysis for the Saturated Zone Site-Scale Flow and Transport Model</i> AMR (ANL-NBS-HS-000034)	Average water level measurements for open boreholes or screens cross-cutting hydrostratigraphic units (Section 5.1).	Lack of available data on the specific well construction for certain wells to identify the interval measured combined with the lack of wells with specific screened intervals (Section 5.1).	The AMR states little impact on the potentiometric surface is expected from boreholes that are open at different depth intervals and to different hydrogeologic units (Section 6.1).
Large hydraulic gradient	<i>Water-Level Data Analysis for the Saturated Zone Site-Scale Flow and Transport Model</i> AMR (ANL-NBS-HS-000034)	The large hydraulic gradient north of the proposed repository is represented by water levels that are hundreds of meters higher than near the repository. The water levels may or may not represent the uppermost part of the SZ. An analysis was performed on the water levels in this area to see if they potentially represented perched water conditions. Professional judgement and specific criteria were used to make this determination (Section 6.1).	Professional judgement and evaluation of alternative conceptual models (Section 6.2).	The exclusion of data points where perched water conditions are suspected would result in modifications of the potentiometric surface map that correlates with the regional model potentiometric surface map. Limited hydraulic data preclude the determination that the water levels in these boreholes represent perched conditions (Section 6.2).

Possible perched water levels in wells USW G-2, USW G-1, UE-29 a#3, USW UZ-N91, UE-25 WT#18, and UE-25 WT#6.	<i>Water-Level Data Analysis for the Saturated Zone Site-Scale Flow and Transport Model</i> AMR (ANL-NBS-HS-000034)	Potential perched data were evaluated and flagged as "suspect perched" in the analysis. To prove perched-water conditions unequivocally requires demonstrating partial saturation beneath a suspected perched-water body (Section 6.1).	Professional judgement and selected criteria (Section 6.1).	Not discussed in the AMR.
Estimated range of annual deposition rates for chloride at Yucca Mountain encompasses the present-day rate as well as the rates that prevailed when the sampled pore waters infiltrated below the soil zone.	<i>Geochemical and Isotopic Constraints on Groundwater Flow Directions, Mixing, and Recharge at Yucca Mountain, Nevada</i> AMR (ANL-NBS-HS-000021)	The annual deposition rates for chloride are known and constant for present day conditions as well as over the long-term past. The calculations are taking into consideration the full range of chloride deposition.	Assumption is supported by several independent lines of evidence. First, the range of deposition rates assumed for Yucca Mountain encompasses the present day rates calculated for sites at Red Rock Canyon and Kawich Range, Nevada, which represent climates that are drier and wetter, respectively, than that prevailing at Yucca Mountain. The second line of evidence is the constancy of the <sup>36</sup> Cl/Cl ration throughout the Holocene, based on packrat midden data. Finally, the nearly uniform Cl concentrations in the perched water and SZ groundwaters beneath Yucca Mountain also support the assumption.	Affects conclusions in sections 7.2, 7.5, and 7.7.2.
Groundwater flow to Yucca Mountain from areas directly north of Yucca Mountain is minor, particularly in areas south of Drillhole Wash	<i>Geochemical and Isotopic Constraints on Groundwater Flow Directions, Mixing, and Recharge at Yucca Mountain, Nevada</i> AMR (ANL-NBS-HS-000021)	It is assumed that the southeast hydraulic gradient north of Drillhole Wash is controlled by the southeast trending faults and indicates that the flow to Yucca Mountain from areas directly north of Drillhole Wash is minor. This is further supported by major ions and isotopic data. In addition it is recommended to perform additional sampling at upgradient locations in order to further support this assumption. (Section 7.7.1)	The assumption is based on the southeastward direction of the hydraulic gradient north of Drillhole Wash, and the likelihood that northwest-southeast trending faults present in this area impart anisotropy that enhances flow along the trend of the faults (Section 7.7.1)	Affects conclusions in sections 7.2, 7.4, 7.6, and 7.7.1

Regional flow paths can be traced by linking areas with similar chemical and isotopic compositions in a downgradient direction.	<i>Geochemical and Isotopic Constraints on Groundwater Flow Directions, Mixing, and Recharge at Yucca Mountain, Nevada</i> AMR (ANL-NBS-HS-000021)	Assumes constancy of chemical composition with depth in the water table aquifer and ignore the possible chemical changes that may result from local recharge or vertical mixing between aquifers.	It is assumed that the two-dimensional nature of the analysis implicitly assumes the constancy of chemical composition with depth in the water table aquifer and ignores the possible chemical changes that may result from local recharge or vertical mixing between aquifers.	Affects conclusions in Section 7.1.
<b>Variability</b>				
Spatial Variability in stratigraphic picks-The HFM assumes interpolation and extrapolation of stratigraphy adequately represents the framework.	<i>Hydrogeologic Framework Model for the Site-Scale Flow and Transport Model</i> AMR (ANL-NBS-HS-000033)	Not discussed in the AMR	Standard geologic interpretation techniques used for analysis, interpretations, and representation of stratigraphic and structural features.	Not discusses in the AMR.
Availability of water level measurements	<i>Water-Level Data Analysis for the Saturated Zone Site-Scale Flow and Transport Model</i> AMR (ANL-NBS-HS-000034)	Averages spatial water levels for the time period of interest.	Availability of data for the time period of interest (Section 5.1).	Not discusses in the AMR.
Distribution of water level data	<i>Water-Level Data Analysis for the Saturated Zone Site-Scale Flow and Transport Model</i> AMR (ANL-NBS-HS-000034)	Development of different potentiometric surface maps to represent variable conceptual models and evaluation of each to determine which is most representative (Section 6.2).	Comparison of different possible representations (Section 6.2)	Limited impact as determined by the comparison of alternative potentiometric surface maps (Section 6.2).
Spatially varying (linear with depth) but temporally constant temperature field for the SZ flow model.	<i>Calibration of the Site-Scale Saturated Zone Flow Model</i> AMR (ANL-NBS-HS-000011)	Treated the temperature variability with a linear gradient with depth (Section 6.1.5).	Data in Sass et al. (1998) indicates the temperature gradients become more linear with depth (Section 6.1.5). This assumption adequately captures the general effects of groundwater viscosity with depth.	Not discusses in the AMR.

**Results**

<p>Uncertainty in the uniqueness of the calibrated model.</p>	<p><i>Calibration of the Site-Scale Saturated Zone Flow Model</i> AMR (ANL-NBS-HS-000011)</p>	<p>Calibration and sensitivity analyses</p>	<p>Standard operating modeling procedure. Criteria were used in the calibration process to constrain results within the bounds of field parameter results (Section 6.10)</p>	<p>Increased confidence in the results could be developed through incorporating transient and temperature analyses. Additionally, corroboration with modeling efforts and Hanford and INEEL would help build confidence (Section 6.10)</p>
---	---	---	--	--

INTENTIONALLY LEFT BLANK

## 15.0 Saturated Zone Radionuclide Transport Model

### 15.1 Model Purpose

The purpose of the SZ transport model analysis is to provide radionuclide transport simulation results from the SZ site-scale model for use in PA calculations. The final product is a set of radionuclide breakthrough curves 20 km from the repository. The breakthrough curves provide information on the radionuclide arrival times and mass of radionuclides delivered to the biosphere. A simplified one-dimensional radionuclide transport model for the purpose of simulating radionuclide decay chains in PA simulations is also produced for daughter product analysis.

The conceptual model for SZ transport is fairly well understood. The primary uncertainty is where there is a lack of data to support the understanding. For instance the location of the transition zone for transport from the volcanic rock to the alluvium is not sufficiently characterized and is represented as stochastic distribution. This aspect has a significant impact on the transport time to the accessible environment. Development of supporting models and data supporting the SZ radionuclide transport component do not utilize state-of-the-art technology that would introduce significant uncertainty. Like the SZ flow model component, the uncertainty is primarily focused around parameter uncertainty due primarily to limited data availability in the expected transport pathway.

### 15.2 Model Relations

The SZ site-scale transport model is presented in the right hand portion of Figure 15-1, Saturated Zone Flow and Transport Logic Diagram. Figure 15-1 is a model relation diagram linking the input SZ transport AMRs to the site-scale transport model component and TSPA feed. Each supporting AMR to the site-scale transport model has input where uncertainty is derived and propagated (treated and untreated) to recipient downstream AMRs. The transport model is captured in the *Inputs and Results for the Base Case Saturated Zone Flow and Transport Model for TSPA AMR (ANL-NBS-HS-000030)*. Three primary AMRs provide input to this AMR. These are the final calibrated flow model AMR, uncertainty distribution for stochastic parameters AMR, and the SZ transport methodology and transport component integration AMR. Three other AMRs are input to the stochastic parameters AMR. These are the sub-gridblock scale dispersion AMR, Probability distribution for flowing interval spacing AMR, and the *Saturated Zone colloid-facilitated transport* AMR. Listed below are descriptions of the SZ transport component AMRs and downstream use.

- *Sub-Gridblock Scale Dispersion AMR (ANL-NBS-HS-000022)* — This AMR documents a dispersion analysis for the purpose of providing estimates of the transverse and longitudinal dispersion that may occur at the sub-gridblock scale within the Tertiary volcanic rocks of the SZ site-scale model. Estimates of dispersivity from this analysis are described in the AMR as useable, directly or with modifications, in performance assessment calculations. Currently this AMR is used as corroborative data only in the transport model analysis (through the *Uncertainty Distribution for Stochastic Parameters* AMR).

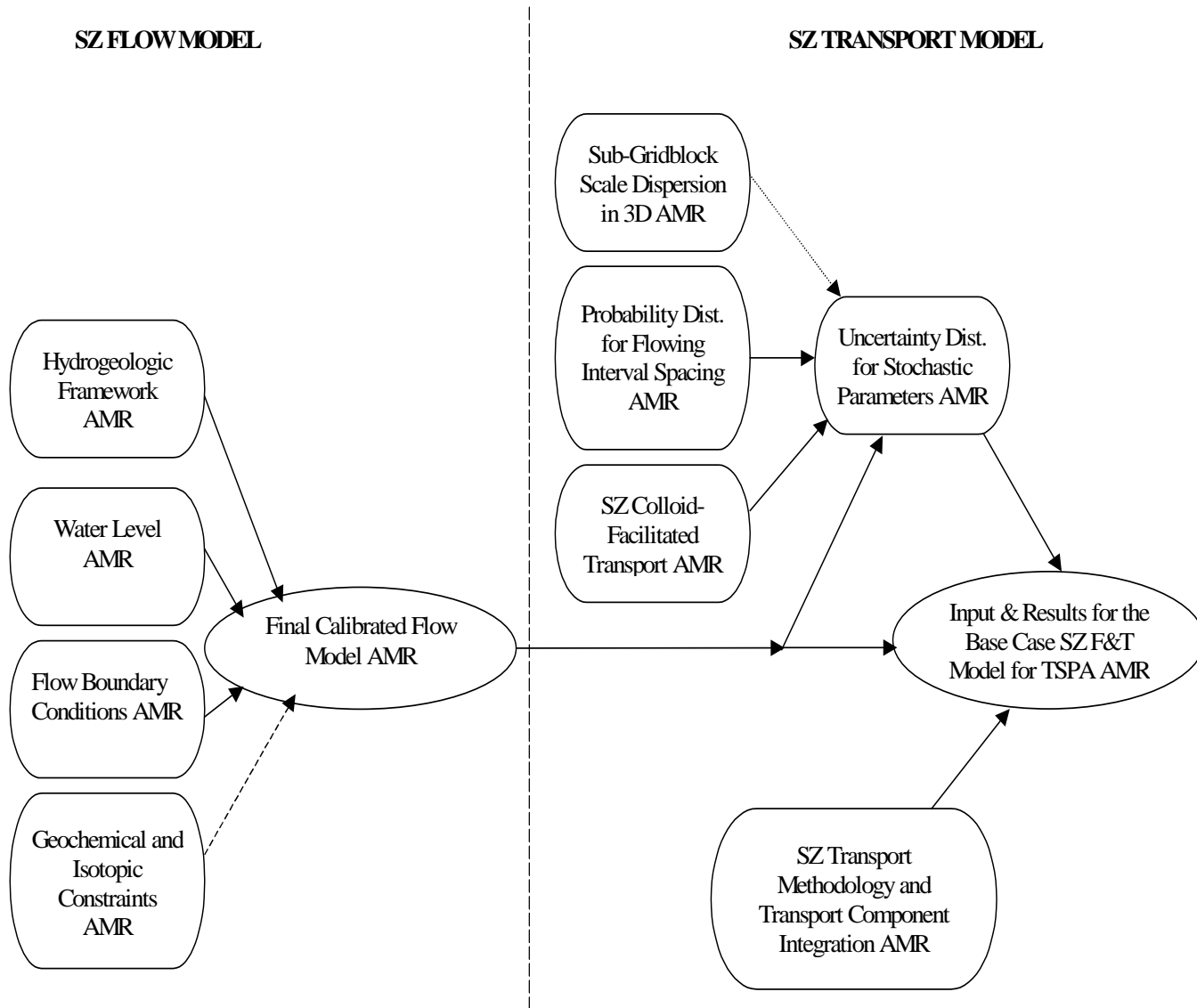


Figure 15-1: Saturated Zone Flow and Transport Logic Diagram

- *Saturated Zone Colloid-Facilitated Transport AMR (ANL-NBS-HS-000031)* — The purpose of this AMR is to provide retardation factors for colloids with irreversibly attached radionuclides in the SZ, between the point of entry from the unsaturated zone to the compliance point. Requirements and elements for the design of methodology to calculate colloid transport in the SZ are developed. The output from this AMR is an abstraction of colloid-facilitated transport parameters for use in the TSPA analyses (through the *Uncertainty Distribution for Stochastic Parameters AMR*).
- *Probability Distribution for Flowing Interval Spacing AMR (ANL-NBS-MD-000003)* — The purpose of this AMR is to present an analysis that develops a probability distribution for flowing interval spacing. The flowing interval spacing is a direct input into TSPA-SR (through the *Uncertainty Distribution for Stochastic Parameters AMR*).
- *Uncertainty Distribution for Stochastic Parameters AMR (ANL-NBS-MD-000011)* — This AMR determines the parameters that will be included as uncertain and also determines the constant parameters for use in the Site-Scale SZ Flow and Transport Model for TSPA-SR.
- *Saturated Zone Transport Methodology Component Integration AMR (MDL-NBS-HS-000010)* — This AMR establishes the requirements and elements for the design of a methodology to calculate radionuclide transport in the SZ at Yucca Mountain in support of TSPA. The purpose of the transport methodology and component analysis is to provide the numerical methods (particle tracker) for simulating radionuclide and model setup for transport in the SZ site-scale model.
- *Calibration of the Site-Scale Flow Model AMR (ANL-NBS-HS-000011)* — The purpose of the flow model analysis is to provide PA with a calibrated SZ site-scale flow model to be used for making radionuclide transport calculations.
- *Input and Results for the Base Case Saturated Zone Flow and Transport Model for TSPA AMR (ANL-NBS-HS-000030)* — This AMR is the basis for the SZ transport model. It provides a set of unit radionuclide breakthrough curves at the accessible environment (20 km from the repository). These breakthrough curves are computed from the 3D site scale SZ flow and transport model. They are used directly in TSPA through a convolution integral approach to determine radionuclide mass breakthrough at the receptor location based on the source term from the UZ into the water table. The convolution integral approach is discussed in this AMR. A one-dimensional model is also presented for direct inclusion into the TSPA model to compute radionuclide transport in the SZ for decay chain daughters (the linear convolution is incapable of modeling radionuclide decay chains).

### **15.3 Saturated Zone Transport Model Structure**

Figure 15-2, Saturated Zone Transport Model Diagram, is a model structure diagram that maps the interplay between the conceptual model, parameters and inputs, representational model (FEHM), results and TSPA abstraction components for the SZ site-scale transport model. Results of the SZ transport component are abstractions to TSPA in the form of breakthrough curves, a 1D model, and transient radionuclide flux at the SZ/biosphere interface.

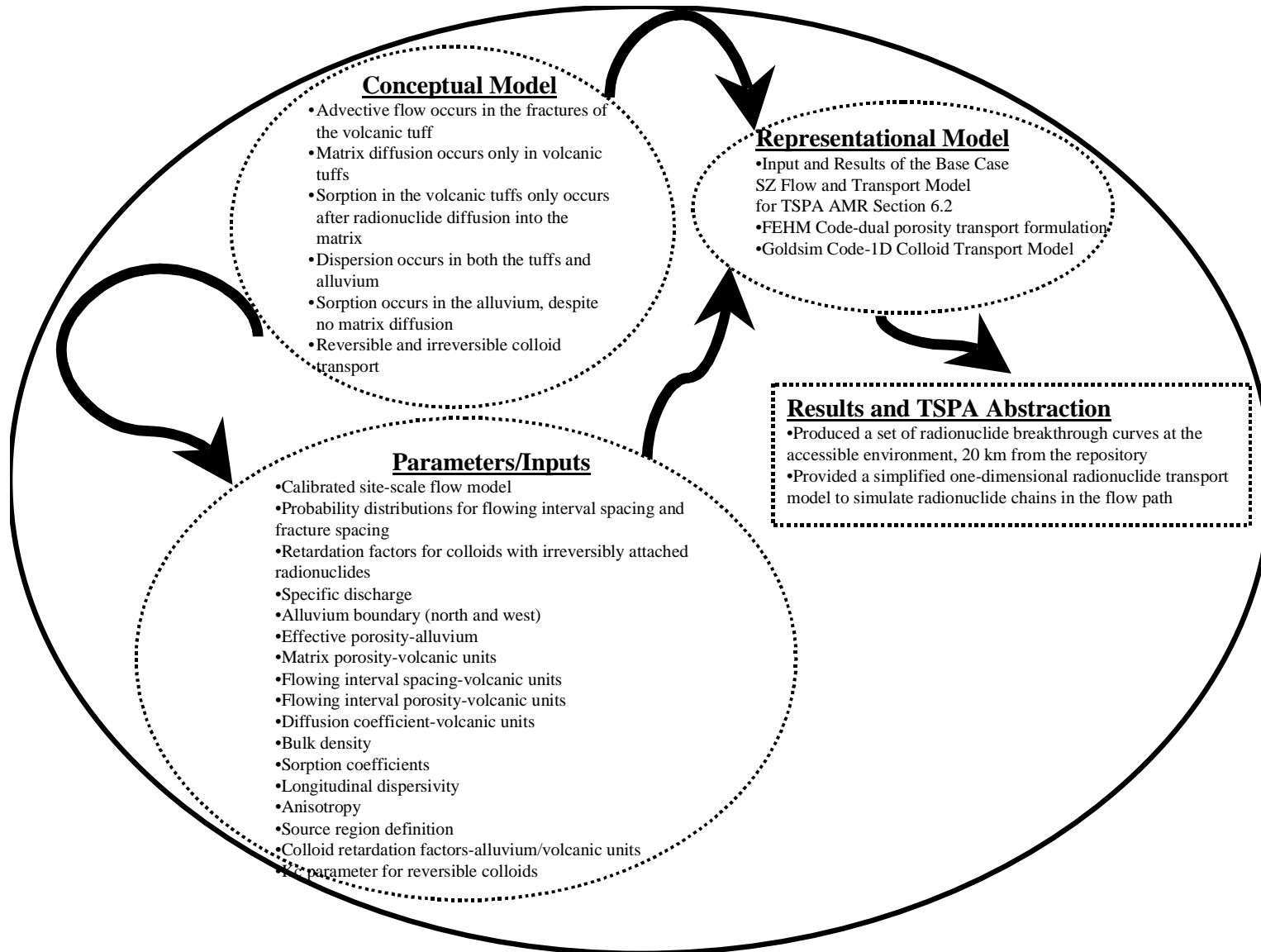


Figure 15-2: Saturated Zone Transport Model Diagram

## A. Conceptual Model

Conceptual model processes for SZ transport are presented in the SZ PMR. The conceptual model for transport is not the same for the alluvium as it is for the fractured volcanic tuff units (Figure 15-2). The pathway for radionuclide travel when it enters the SZ from the UZ is first through fractured volcanic tuff and then through alluvium where radionuclides may continue to travel toward the Amargosa Desert. Radionuclide transport occurs within the highly fractured portions of tuff near the water table. Flowing groundwater within the SZ is believed to be constrained to distinct intervals of fractured rock, with more intact regions having negligible flow. Assuming there is not a continuous zone of high permeability to the alluvium in the Amargosa Valley, low permeability zones will act as large-scale heterogeneities that will give rise to large-scale macroscopic dispersion. Transverse (horizontal and vertical) dispersion is expected to be small. Transport processes in the fractured tuffs consist of advection and matrix diffusion. Solutes travel preferentially along channels in which the apertures are largest. Sorption is possible in the fractured tuffs only after diffusion from the fractures into the matrix has occurred (diffusion is the only process to introduce radionuclides into the rock matrix). No sorption occurs in the fracture filling. Transport processes in the alluvium includes dispersion and sorption. The larger effective porosity in the alluvium, compared to the fractured volcanic units, allows slower velocities and sorption processes to take place more efficiently. As the alluvium thickens toward the Amargosa Valley, large-scale vertical dispersion increasingly takes place.

In addition to the advection-diffusion model for radionuclide transport, colloid facilitated transport of some radionuclides is possible. The conceptual model of colloid-facilitated transport of radionuclides in the SZ consists of two modes of transport. One mode involves radionuclides that are irreversibly sorbed onto or embedded in colloids. The second mode deals with radionuclides that are reversibly attached to colloids, such that at any time, radionuclides are partitioned between the aqueous and colloidal phases (linear sorption model).

## B. Parameters and Inputs

Transport model input in the form of analyses and parameters are captured in the individual component AMRs. Input parameters analysis for the transport model are presented in the AMR entitled *Uncertainty Distributions for Stochastic Parameters AMR (ANL-NBS-MD-000011)*. For each input parameter in this AMR it is determined if it will be included as an uncertain parameter or a constant parameter for the site-scale transport simulations. This AMR extracts analyses from four AMRs as presented in Figure 1 in addition to other sources of information. Flow properties are derived from the analysis and model activities associated with the site-scale flow model. Transport parameters are derived from model and analysis activities associated with the *Sub-Gridblock Scale Dispersion AMR (ANL-NBS-HS-000022)*, the *Saturated Zone Colloid-Facilitated Transport AMR (ANL-NBS-HS-000031)*, and the *Probability Distribution for Flowing Interval Spacing AMR (ANL-NBS-MD-000003)*.

Figure 15-2 presents the parameters/inputs that are the primary foundation for the SZ transport model. These parameters are developed in the AMRs presented in Figure 15-1. The AMR entitled *Uncertainty Distributions for Stochastic Parameters AMR (ANL-NBS-MD-000011)*

utilizes the supporting AMRs to develop an assessment of the parameters and to develop uncertainty distributions for parameters to which the model is sensitive. Sensitivity is due to the combination of the numerical importance of the parameter in the model and the uncertainty in the parameter value. Constant parameters are those that are not sensitive and can be sufficiently represented in this fashion. Because the stochastic uncertainty distributions are developed through an assessment of the supporting AMRs, it is important for the upstream AMRs to provide uncertainty assessments to pass on to the downstream analysis in this AMR. For instance, an effective evaluation of the uncertainty of alluvium boundary in the *Uncertainty Distributions for Stochastic Parameters AMR (ANL-NBS-MD-000011)* requires an effective assessment of this data uncertainty in the *Hydrogeologic Framework Model AMR (HFM) (ANL-NBS-HS-000033)* and subsequent *Calibration of the Site-Scale Flow Model AMR (ANL-NBS-HS-000011)*. The HFM AMR discusses the adequacy of the available data representing the hydrogeologic structural conditions and identifies the uncertainty, but does not explicitly discuss the treatment. Based on this it is difficult for the *Uncertainty Distributions for Stochastic Parameters AMR (ANL-NBS-MD-000011)* to be able to perform an effective downstream assessment of uncertainty due to the lack of a transparent assessment in the upstream AMR. It is therefore forced to make assumptions regarding the data uncertainty that may be perceived as resulting in non-conservative parameter distributions because of the lack of transparency in the uncertainty treatment.

### **C. Representational Model**

Representational model components are presented in Figure 15-2. The model methodology for the SZ transport is presented in the *Saturated Zone Transport Methodology and Transport Component Integration AMR (MDL-NBS-HS-000010)*. In this AMR the FEHM transport modules are derived and verified for incorporation into the FEHM flow model for transport simulation.

In order for the model to simulate radionuclide transport through the expected flow media, a particle tracking method in FEHM is employed to provide a solution to the advection-dispersion transport equation. This approach incorporates interrelated components of advection, dispersion, diffusion, and sorption. The particle tracking method alone accounts for advection, while a random-walk algorithm combined with the particle tracking method accounts for the dispersive component of the transport equation. To account for dual porosity transport (fracture-matrix interaction) and sorption, special modules included in the FEHM code are used.

The particle-tracking method incorporated into FEHM is based on placing particles at specific points in the flow field to represent a specified mass of solute. The particle-tracking method assumes a Lagrangian point of view, in which these particles move with the prevailing flow velocity. Based on the flow velocity field derived from the flow model, the trajectories for each particle are computed one at a time. Through a series of time steps, the particles are moved according to these computed trajectories. The dispersive component of the transport using the random-walk algorithm is based on the analogy between the mass transport equation and the Fokker-Plank equation of statistical physics. The dispersive displacement of each particle is computed using uniform random numbers, based on the dispersivity tensor and the porous flow velocity at the particle location. During each time step, the trajectory of each particle is

computed using the advective component of transport that is modified through a series of displacements due to the dispersion calculated for each particle.

Physiochemical processes of matrix diffusion and sorption are incorporated by the adaptation of the RTTF particle tracking method to the particle-tracking algorithm. In this method, adjustments to the travel time of a particle are made to account for the influence of sorption and matrix diffusion. In this process the particle is governed by a transfer function describing the probability of the particle spending a given length of time on that portion of its path. For cases of transport in the alluvium where matrix diffusion does not occur, the time delay is calculated deterministically by computing a retardation factor based of the sorption coefficients.

Test cases where the FEHM particle tracker results are compared with analytic solutions to demonstrate the validity of the approach. Although FEHM is capable of modeling radioactive decay and ingrowth, the ultimate use of results relies on linear convolution, which cannot model these processes. To simulate daughter product ingrowth by radioactive decay a simplified approach has been adopted utilizing a 1D model to derive radioactive daughter concentrations at the accessible environment. This process is simulated directly with the GoldSim software code in the TSPA model.

#### **D. Results**

The implementation of the SZ transport model results in products used in TSPA to calculate radionuclide mass flux and concentrations in the biosphere. Specifically, sets of radionuclide breakthrough curves are developed by the FEHM transport simulations. Individual radionuclide breakthrough curves are determined for a given sampling of uncertain SZ transport parameters. Multiple Monte Carlo sampling of uncertain parameters and subsequent execution of the SZ transport model results in a range of breakthrough curves for each radionuclide. This represents a library of breakthrough curves for all radionuclides of interest that captures the range of SZ transport characteristics for each radionuclide. This library of breakthrough curves is then accessed by the TSPA simulation tool (GoldSim) upon execution through the convolution integral approach.

Additionally, since the linear convolution approach cannot model decay product ingrowth, the 1D model itself is included directly into the TSPA model (along with the required parameters). Logic within the TSPA model ensures that the parameters used by the 1D model are consistent with those associated with a given parent radionuclide breakthrough curve.

#### **15.4 Discussion of Uncertainty and Variability Treatment**

An evaluation of uncertainty and variability treatment of the AMRs was performed to support development of this paper. For each AMR, the uncertainties/variabilities were identified and an evaluation was made of the treatment. Thorough treatment was considered to be identification, treatment, impact assessment, and clear presentation of the analysis and the propagation of uncertainty in the AMR.

Review of the AMRs associated with the SZ site-scale transport model indicates that the way uncertainties are addressed is very inconsistent between AMRs. In some instances it is difficult to ascertain the complete treatment of uncertainties. In some cases the information appears to be present, but it is in different sections of the AMR (data, assumptions, analysis), all depending on the way the author structured the approach.

Table 15-1 is a sampling of the uncertainties and variabilities identified in this exercise. The following is a discussion of the evaluation process and uncertainty/variability analysis trends within the AMR/model process.

## **A. Conceptual Models**

The overall conceptual model for transport in the SZ and associated uncertainties are not discussed in any of the supporting AMRs. The conceptual model for transport is presented in the *Saturated Zone Flow and Transport Process Model Report (PMR), Section 3.2*. Some of the various conceptual components of the total conceptual model are discussed in the AMRs. For example, in the AMR entitled *Probability Distribution for Flowing Interval Spacing AMR (ANL-NBS-MD-000003)*, correlation between flowing interval spacing and hydrogeologic units was evaluated (Table 1). This was done through a statistical analysis of percentage of flow in each flow interval, rock type and frequency of flowing intervals, and spacing of flowing intervals within each hydrogeologic unit. This evaluation determined there was little difference in the flowing interval characteristics by rock type of hydrogeologic units that had sufficient data to evaluate. The analysis assumes no correlation between flowing intervals and hydrogeologic units, primarily because of the lack of enough correlative data points for each hydrogeologic unit. The AMR stated the potential impact of this analysis is the misrepresentation of the hydrogeologic units, particularly for the Lithic and Calico Hills hydrogeologic units for which limited flowing interval data were available (SZ PMR, Section 6.4). This could impact the accuracy of modeled effects of matrix diffusion processes through these units in SZ transport models developed for performance assessment (Table 15-1).

For the AMR *Modeling Sub-Gridblock Scale Dispersion in Three Dimensional Heterogeneous Fractured Media, ANL-NBS-HS-000022*, two alternative conceptual models were evaluated for the radionuclide source geometry (Table 1). In this case the concept of planar source geometry was evaluated against point source geometry providing an analysis of plume spreading and the coupling of the unsaturated zone and the SZ. Overall this AMR adequately addressed the conceptual and mathematical uncertainties. Parameter uncertainty was also adequately addressed, but was not as significant in the fabric of the AMR.

In most cases alternative conceptual models were not evaluated. For example, in the *Saturated Zone Transport Methodology and Transport Component Integration AMR, ANL-NBS-HS-000010*, there are a number of conceptual model uncertainties not addressed (Table 15-1). The AMR addresses the algorithms used by the particle tracking code, but does not discuss how radionuclide decay and in-growth, colloidal enhanced transport, effects of nonlinear sorption, and effects of kinetic sorption, relate to the transport. The conceptual model case was not developed to support the algorithm. In the AMR entitled *Saturated Zone Colloid-Facilitated*

*Transport AMR (ANL-NBS-HS-000031)* there is no alternative conceptual model approach to the C-Wells interpretation for matrix diffusion.

## **B. Parameters**

Parameter uncertainty is the most critical of all uncertainties in the SZ model transport component, and treatment appears to be the strongest of all uncertainties. The AMR entitled *Uncertainty Distribution for Stochastic Parameters (ANL-NBS-MD-000011)* and the transport AMR entitled *Input and Results of the Base Case Saturated Zone Flow and Transport Model for TSPA (ANL-NBS-HS-000030)* clearly discusses the sources for uncertainty, how it was treated, and the basis is generally provided. As previously discussed, the AMR entitled *Uncertainty Distributions for Stochastic Parameters AMR (ANL-NBS-MD-000011)* utilizes the supporting AMRs to develop an assessment of the parameters and to develop uncertainty distributions for parameters to which the model is sensitive. Constant parameters are those that are not sensitive and can be sufficiently be represented in this fashion. Because the stochastic uncertainty distributions are developed through an assessment of the supporting AMRs, it is important for the upstream AMRs to provide uncertainty assessments to pass on to the downstream analysis in this AMR. The analysis resulted in the developments of stochastic parameter representations consisting of uniform distributions, truncated normal distributions, log-normal distributions, log-uniform distributions, exponential distributions, and cumulative distribution functions (Table 15-1).

As in the SZ Flow model the lack of data is the greatest source for uncertainty in the *Uncertainty Distribution for Stochastic Parameters (ANL-NBS-MD-000011)* AMR. For instance, there is limited information on horizontal anisotropy; therefore, a ratio arbitrarily developed by the NRC is used. The SZ flow model was not recalibrated using these anisotropy ratios nor were sensitivity studies conducted to evaluate the effects of anisotropy on the SZ flow system. Other examples in this AMR where limited data is the contributing factor for uncertainty are the western and northern alluvium boundary, effective porosity, flowing interval spacing, and porosity (Table 15-1). Due to the lack of data in certain scenarios, the parameter is bound by a fairly large uncertainty distribution.

## **C. Representational Model**

Discussions regarding mathematical model (representational model) (Figure 15-2) uncertainty are less transparent or non-existent. Certain aspects regarding model uncertainty are not addressed and left to other AMRs without a cross-reference provided (Table 15-1). For instance, in the AMR entitled *Saturated Zone Transport Methodology and Transport Component Integration (MDL-NBS-HS-000010)*, sensitivity to the hydrogeologic framework model, climate change, and hydrogeologic parameter uncertainty is deferred to the SZ PMR and associated AMRs. Uncertainty treatment in this AMR was deferred to other AMR sensitivity studies performed for the hydrogeologic framework, climate change, and parameters. In other words, this AMR relies on the uncertainties being subsumed through calibration and sensitivity studies in supporting AMRs, and does not make any attempt to evaluate uncertainties. Overall this AMR does not analyze uncertainty at all. Only a partial verification of the transport model methodology is addressed when comparing it to published solutions.

The results of the 1D model for decay daughters were compared to results obtained from the 3D particle tracker method and were shown to be appropriate.

The *Modeling Sub-Gridblock Scale Dispersion in Three-Dimensional Heterogeneous Fractured Media AMR (ANL-NBS-HS-000022)* is the only transport AMR that adequately discusses model uncertainty (Table 15-1). However, this AMR is not used as direct input and does not significantly affect the results of the TSPA abstraction. Rather, this AMR corroborates the dispersivity values selected for use that were based on an expert elicitation. AMRs that one would expect to see thorough mathematical model uncertainty analyses are *Probability Distribution for Flowing Interval Spacing AMR*, *Saturated Zone Colloid Facilitated Transport AMR*, and *Saturated Zone Transport Methodology and Transport Component Integration AMR*.

#### **D. Results**

Uncertainty evaluation in the *Uncertainty Distribution for Stochastic Parameters AMR (ANL-NBS-MD-000011)* and the transport AMR entitled *Input and Results of the Base Case Saturated Zone Flow and Transport Model for TSPA (ANL-NBS-HS-000030)* is satisfactorily addressed. The primary uncertainty is derived from upstream AMRs and is propagated into the computed library of breakthrough curves. The lack of uncertainty analysis regarding the SZ flow system results in no uncertainties regarding groundwater flow being carried into SZ transport results (except for specific discharge and horizontal anisotropy). In areas where there is insufficient data to support a constant parameter or narrow bound on the uncertainty, wide uncertainty ranges are used. In the case of developing a stochastic distribution of flowing interval porosity, the lower bound is developed using parallel plate theory models and the upper bound is developed using pump testing and tracer testing. The C-Wells testing complex results are the only data available for this analysis, which derives uncertainty and variability in results and scale effects.

#### **15.5 Uncertainty Propagation**

Limited uncertainty treatment was performed in all the SZ flow AMRs supporting the calibrated flow model. The calibrated flow model is in turn used to derive the flow field and input files for the SZ transport model and parameters for evaluation in the *Uncertainty Distribution for Stochastic Parameters AMR (ANL-NBS-MD-000011)*. Many assumptions used in this AMR result from the lack of uncertainty evaluation in supporting upstream AMRs, or in other words, assumptions are made to bound possible propagation of error to the downstream users. The *Uncertainty Distribution for Stochastic Parameters AMR (ANL-NBS-MD-000011)* sufficiently evaluated uncertainty with the data available to be used. However, because the upstream AMRs did not perform consecutive uncertainty evaluations building the flow and transport model throughout the process, the final downstream user (*Uncertainty Distribution for Stochastic Parameters (ANL-NBS-MD-000011)*) did not have any input for uncertainty evaluation and had to make assumptions regarding uncertainty related to the flow system (e.g., anisotropy, specific discharge, flow through alluvial materials). Although the impact is not readily apparent, it may have resulted in wide uncertainty ranges for stochastic distributions. These ranges then are passed onto the transport TSPA analysis, which may result in conservative or less than realistic results.

Uncertainty regarding radionuclide transport characteristics is propagated into TSPA through the use of convolution with the library of breakthrough curves and the 1-D model for radionuclide decay daughters. However, as discussed above, the range of breakthrough behavior is dominated solely by parameter uncertainty related to SZ transport.

## **15.6 Conclusions**

The purpose of the SZ transport model analysis is to provide radionuclide transport simulation results from the SZ site-scale model for use in PA calculations. The abstractions from this AMR to TSPA are a set of radionuclide breakthrough curves at the accessible environment, a simplified 1D-radionuclide transport model, and mass flux at the biosphere interface (Figure 15-2). Each AMR attempts to address uncertainty, but the overwhelming trend is that the analysis is incomplete and integration of uncertainty to downstream AMRs is not completely performed.

For the SZ transport model component, the most critical uncertainties are associated with parameters. Probability (stochastic) distributions or assumptions to capture the uncertainty primarily define the parameter uncertainties in this model. In some cases conservative values are assumed. The overall trend for the transport model appears to be that some of the uncertainties may be missing as information feeds to supporting AMRs and eventually into TSPA. Some uncertainties identified in the PMR or those that have not been explicitly identified have not been propagated into the TSPA model and documentation. In some cases that lack of uncertainty treatment has allowed the propagation of very uncertain parameters into the downstream AMRs (e.g., *Calibration of the Site-Scale Flow Model AMR, ANL-NBS-HS-000011, to Input and Results for the Base Case Saturated Zone Flow and Transport Model for TSPA AMR, ANL-NBS-HS-000030*).

**Table 15-1: Saturated Zone Transport Model**

<b>Model Purpose:</b> The purpose of the SZ Transport Model is to provide radionuclide transport simulation results for use in PA calculations.				
<b>Summary</b>	<b>Source</b>	<b>Treatment</b>	<b>Basis</b>	<b>Impact</b>
<b>Conceptual Model Uncertainty</b>				
SZ Conceptual Transport Model	<i>Saturated Zone</i> PMR (TDR-NBS-HS-000001) - Summarizes conceptual solute transport processes focusing on advection, matrix diffusion, sorption, and dispersion.	The SZ PMR does not treat conceptual transport model uncertainty. Conceptual solute transport processes are discussed and uncertainty treatment is deferred for treatment in the AMRs.		Potential impact on uncertainty in transport characteristics in the SZ (e.g., breakthrough)
Flowing Interval Spacing Conceptual Model	<i>Probability Distribution for Flowing Interval Spacing</i> AMR (ANL-NBS-MD-000003)	The AMR tests various conceptual models for correlations between flowing interval spacing and hydrogeologic units, flowing interval spacing from dip data and flow meter surveys, and rock type and frequency of flowing intervals.	Little difference was noted in the flowing interval characteristics by rock type or hydrogeologic unit for the units in which sufficient data existed. Flow meter survey graphs indicate the percentage of flow within an interval. Changes in slope of the graph represent changes in flow characteristics, which are defined as separate flow intervals.	Potential misrepresentation of the hydrogeologic units, particularly for the lithic and Calico Hills hydrogeologic units for which limited flowing interval spacing data were available (Section 6.4). This could impact the accuracy of modeled effects of matrix diffusion (unable to quantify degree) processes through these units in SZ transport models developed for performance assessment (PA).
Radionuclide source term geometry	<i>Sub-Gridblock Scale Dispersion in Three Dimensional Heterogeneous Fractured Media</i> AMR (ANL-NBS-HS-000022)	The AMR presents the conceptual model for the potential radionuclide plume within the UZ for the planar source geometry and the point source geometry. For the planar source geometry radionuclides enter the SZ in one of six different tubes from the UZ. For the point source geometry the potential radionuclide plume enters the SZ as a spatially compact source with all particles release points within a single numerical gridblock. (Note: AMR used as corroborative data only)	For the planar geometry, this was the current understanding of the UZ-SZ transport coupling. Representation of the permeability field as a heterogeneous system. This is the same concept used in the TSPA-VA. The point source assumption represents the most conservative case for coupling between the SZ and UZ in regards to estimates of plume spreading.	The planar source term geometry affects the distribution for the contaminant source plume entering the SZ. The Point source concept is the most conservative. Zones of high groundwater flux, and hence point source release locations, are positioned within high permeability features that channel flow paths resulting in less variation in travel times and therefore less dispersion.

Uniform flow and transport in equally spaced, parallel fractures	<i>Saturated Zone Transport Methodology and Transport Component Integration</i> AMR (MDL-NBS-HS-000010)	Uncertainty is not treated for a number of concepts such as: sizes of matrix blocks, geometry of matrix blocks, effects of heterogeneous fracture properties and/or discontinuous fractures, flow velocity, and non-uniform flow fields. The AMR recommends that sensitivity studies be carried out when applying the model rather than evaluate and treat uncertainties here also.	AMR states impracticality of acquiring more detailed data, necessity to aggregate properties due to computation grid size being much larger than block size.	Potential impact to breakthrough curves.
<b>Representational Model Uncertainty</b>				
Model sensitivity to hydrogeologic framework, climate change, and parameter uncertainty	<i>Saturated Zone Transport Methodology and Transport Component Integration</i> AMR (MDL-NBS-HS-000010)	Uncertainty in the transport methodology is deferred to other AMRs for treatment (namely SZ flow AMRs). Other AMRs do not perform the necessary uncertainty assessment, therefore indicating a lack of integration between AMRs.	Not discussed in AMR	Not discussed in AMR
Definition of the number of particles in the transport simulations	<i>Saturated Zone Transport Methodology and Transport Component Integration</i> AMR (MDL-NBS-HS-000010)	Not discussed in the AMR	Not discussed in AMR	Not discussed in AMR

<p>Uncertainty in the analytical solution used to describe numerical results of sub-gridblock scale dispersion.</p>	<p><i>Modeling Sub-Gridblock Scale Dispersion in Three-Dimensional Heterogeneous Fractured Media</i> AMR (ANL-NBS-HS-000022)</p>	<p>Assumed the solute plume can be described by a Gaussian distribution of concentration in three dimensions. Also invoked the Gaussian assumption for log transformed travel times for calculation of dispersivities. (Note: AMR used for corroborative data only)</p>	<p>By using a large number of particles (4000) the deviations from the Gaussian distribution are limited. Gaussian assumption for log transformed travel times made to use the log-transformed as a smoothing technique to decrease the effects of statistical outliers in the time or displacement distributions.</p>	<p>Gaussian assumption for concentrations required for the analytical solution does not agree with numerical results. At short travel distances the fracture permeability models create large spatial variability in groundwater flux across a plane normal to the flow direction. This created large variations in groundwater travel times at short distances resulting in high dispersivity and non-Gaussian behavior. As travel distances increase, the flow paths are channeled into higher permeability zones and the travel times become more homogeneous resulting in less dispersion and closer agreement between the numerical and analytical results.</p>
<p>Uncertainty in the background permeability model developed for the groundwater transport analyses</p>	<p><i>Modeling Sub-Gridblock Scale Dispersion in Three-Dimensional Heterogeneous Fractured Media</i> AMR (ANL-NBS-HS-000022)</p>	<p>Geostatistical simulation using an indicator approach to perform discrete nonparametric estimates of the true bimodal cumulative distributions functions for the flowing features and surrounding rock to simulate the anisotropic permeability field. Below the log permeability cutoff threshold, the permeability characteristics were assumed to be those of background permeability. (Note: AMR used for corroborative data only)</p>	<p>Post-processing checks using exponential variogram models to validate the fracture permeability model were used as a basis for the assumption. Comparison and statistical analysis of single well, double packer, and multi-well interference tests results and conceptual models (effective continuum approach, boundary conditions, source plume, fracture lengths, and orientation of the groundwater gradient) were evaluated. Cutoff values were calibrated by post-simulation audits of the permeability fields to verify flowing interval spacing in the simulation was similar to those observed in the field.</p>	<p>In the presence of large-scale high permeability features, the background fracture permeability has little effect on the transport results.</p>

Uncertainty in the enhanced permeability model developed for the analysis for high permeability features such as faults that were superimposed on the background permeability model.	<i>Modeling Sub-Gridblock Scale Dispersion in Three-Dimensional Heterogeneous Fractured Media</i> AMR (ANL-NBS-HS-000022)	Geostatistical simulation using an indicator approach was used to perform discrete nonparametric estimates of the true bimodal cumulative distribution functions for the flowing features and surrounding rock to simulate the anisotropic permeability field. Above the log cutoff threshold, permeability characteristics were assumed to be those of flowing features. Boolean simulation assuming gaussian distribution was used to place high permeability features as ellipses or disks with user specified radii at random locations within the model domain. Orientation of these features was modeled from a normal distribution with a mean orientation of 0 degrees and a standard deviation of 15 degrees. The Boolean simulation was constrained to comprise a total of 2 percent of the simulation domain. (Note: AMR used for corroborative data only)	Comparison and statistical analysis of single-well, double-packer and multi-well interference test results and conceptual models. Cutoff permeability value was calibrated by post-simulation audits of the permeability fields to verify flowing interval spacing in the simulation was similar to that observed in the field.	The results of the analyses show that large-scale, high-permeability features dominate the solute behavior.
<b>Parameter Uncertainty</b>				
Groundwater specific discharge	<i>Uncertainty Distribution for Stochastic Parameters</i> AMR (ANL-NBS-MD-000011), and Table 15 of the AMR. Saturated Zone Flow and Transport Expert Elicitation Project (MOL.199980825.008)	Utilize specific discharge distribution elicited from the expert panel-define medium case, high case (10 times medium case), and low case (medium divided by 10). Determine probabilities based on distribution.	Basis is entirely the expert elicitation results.	Groundwater velocities and radionuclide travel times in the SZ.
Alluvium Boundary	<i>Uncertainty Distribution for Stochastic Parameters</i> AMR (ANL-NBS-MD-000011) and Table 15 of the AMR	Define alluvium boundary uncertainty zone as a polygonal region with radionuclide transport properties representative of valley-fill aquifer hydrogeologic unit. Both northern and western boundaries vary uniformly from minimum to maximum.	Set bounds as follows: south-boreholes indicating alluvium at water table, north - boreholes with volcanic units at water table, west-where volcanic units outcrop.	Radionuclide transport pathways and travel times within the SZ.
Effective porosity of alluvium	<i>Uncertainty Distribution for Stochastic Parameters</i> AMR (ANL-NBS-MD-000011) and Table 15 of the AMR	Utilize information contained in Bedinger, et al., 1989 to develop a log-normal probability distribution for coarse grained basin fill unconsolidated sediments (section 6.3.2).	Assumption of Log-Normal distribution supported by Bedinger, et al., report, SZ expert elicitation, and S.N. Davis 1989 "Porosity and Permeability of Natural Materials:, TIC 246882. Argue that Bedinger information is from basin and range province, which Yucca Mountain is a part. Also compared to other information in section 6.3.2.	Groundwater velocities and radionuclide travel times in the SZ.

Total porosity of the alluvium	<i>Uncertainty Distribution for Stochastic Parameters</i> AMR (ANL-NBS-MD-000011) and Table 15 of the AMR	Use average of three points provided in Table 7 as constant	Lack of site-specific data.	Used to modify sorption coefficients only due to effective permeability approach taken (Section 6.3.2).
Flowing Interval Spacing	<i>Uncertainty Distribution for Stochastic Parameters</i> AMR (ANL-NBS-MD-000011) and Table 15 of the AMR	Flowing interval spacing is measured between midpoints of each flowing interval. Probability distribution documented in "Probability Distribution for Flowing Interval Spacing AMR (ANL-NBS-MD-000003)."	Limited borhole data. Justification is same as that provided in the AMR. 1) ALL boreholes used in the analysis deviate from vertical within normal drilling practice-assumption necessary to apply Terzaghi correction, 2) documented in boreholes flow meter survey reports. 3) analyses presented in Section 6.0 "Probability Distribution for Flowing Interval Spacing AMR (ANL-NBS-MD-000003)", 4) Dip data not associated with a particular flowing interval - not possible to examine correlation. Most likely correlation would be between steeply dipping features and the flowing intervals - lead to smaller flowing interval spacing and more matrix diffusion (conservative assumption).	Breakthrough characteristics
Effective Porosity of for All Non-Volcanic Units Which Are Assigned Constant Porosity	<i>Uncertainty Distribution for Stochastic Parameters</i> AMR (ANL-NBS-MD-000011) and Table 15 of the AMR	The SZ transport model requires values of effective porosity for all units, whether it is used or not - simply placeholders (Section 5.4, page 17). Several sources identified in Section 6.4.1, page 34.  For these units, effective porosity will vary from unit to unit, but is assigned a constant value within the unit. Table 8 lists values. (Section 6.4.2, page 34).	Values are only placeholders in the model. Attempt is made to give them meaningful values.	none

Matrix Porosity of Volcanic Units (Section 5.5, page 18 and Section 6.5, page 35).	<i>Uncertainty Distribution for Stochastic Parameters</i> AMR (ANL-NBS-MD-000011) and Table 15 of the AMR	Matrix porosity is treated as a constant parameter within each of nine hydrogeologic units contained in the model (volcanic). Section 6.5.2, page 35 provides analysis.	Used information from boreholes to determine constant values for use (Section 6.5.2, page 35). See Table 9 (page 36).	No impact since the model does not consider advective flow in the matrix of the fractured-volcanic units.
Flowing Interval Porosity (Section 5.7, page 19 and Section 6.7, page 37).	<i>Uncertainty Distribution for Stochastic Parameters</i> AMR (ANL-NBS-MD-000011) and Table 15 of the AMR	Estimate porosity assuming parallel plate fracture network - used to estimate lower bound of uncertainty range (Sections 6.7.2). Upper bound based on tracer tests (Section 6.7.4). Range is log-uniform: 0.00001 to 0.1.	Available data used to bound the uncertainty range - covers four orders-of-magnitude.	Directly impacts groundwater velocity. Impact on transport not clear - smaller porosity gives larger groundwater velocity, however more contact with matrix can enhance matrix diffusion.
Effective Diffusion Coefficient (Section 5.8, page 20 and Section 6.8, page 39)	<i>Uncertainty Distribution for Stochastic Parameters</i> AMR (ANL-NBS-MD-000011) and Table 15 of the AMR	Utilize theoretical analyses to demonstrate variability due to size, charge, and temperature. Then select Am as highest bound and Cs as lowest bound (for molecular diffusion). Then determine range of tortuosity based on testing at Yucca Mountain. Compute range of effective diffusion coefficient based on molecular diffusion coefficient and tortuosity. Then use order of magnitude range due to scale issues between lab tests and field scale. Range is $10^{-9}$ cm <sup>2</sup> /s to $10^{-6}$ cm <sup>2</sup> /s - applicable to all radionuclides, varies from realization to realization. (Section 6.8, page 39)	Uncertainty in future scenarios embodied in thermal, hydrogeological, and geochemical conditions.	Conservative approach to travel times
Bulk Density (Section 5.9, page 20 and Section 6.9, page 44).	<i>Uncertainty Distribution for Stochastic Parameters</i> AMR (ANL-NBS-MD-000011) and Table 15 of the AMR	Utilize constant values for all units as shown in Table 10, Section 6.9 (page 45).	It is stated that radionuclide transport is far more sensitive to flowing interval spacing and effective diffusion coefficient than bulk density (will affect retardation somewhat) - note: no reference to any sensitivity analyses to support assertion. (Section 5.9, page 20, Item 1). For alluvium, same density as was used in lab determination of alluvium Kd.	Impact of using an uncertainty range is likely to be minimal - impacts retardation only. Large distribution of Kd for several sorbing radionuclides will give uncertainty in retardation. In addition, fractured volcanic flowing interval parameters will dominate. In alluvium, uncertainty in Kd from measured data included uncertainty in density.

<p>Sorption Coefficients - for non-colloidal species only (Section 6.14, page 57).</p>	<p><i>Uncertainty Distribution for Stochastic Parameters</i> AMR (ANL-NBS-MD-000011) and Table 15 of the AMR</p>	<p>In the volcanics, only Np and U have a sorption coefficient assigned. All others non-sorbing (Section 6.10.1, page 48 - Table 11). For these, selected minimum range from rock type along pathway (Section 5.10, page 21, Item 2). In alluvium, Tc, I, U, Np all have sorption coefficients - based on laboratory batch-sorption tests (section 6.10.2, page 49 - Table 12.). For radionuclides associated with colloid facilitated transport, assign two probability distributions: one for moderately sorbing radionuclides (Cs, and Sr) - 0 to 50 ml/g and one for strongly sorbing radionuclides (Am, Pu, Pa, Th) - 0 to 100 ml/g. (Section 6.14, page 57.</p>	<p>Basis for non-colloid associated radionuclides is measured data and conservative assumptions made (e.g., use most conservative Kd in rock unit along pathway). Basis for colloid associated radionuclides is given as DTN:LA0003AM831341.001 only - no analysis or reduction of data discussed. (Section 6.14, page 57). In Section 5.14, (page 24, Item 4), it is stated that these distribution coefficients are less than solute and should give faster travel times.</p>	<p>Impact of uncertainty in Kd is minimal given transport times in SZ. SZ performance more by flow related parameters (ground water flux, anisotropy), and flowing interval model.</p>
<p>Longitudinal Dispersivity: SZ expert elicitation results used. Assumptions: 1) SZ expert elicitation results at 30 km applicable for 20 km, 2) Cannot distinguish dispersivities in volcanic and alluvial units. 3) correlate longitudinal and transverse dispersivity.</p>	<p><i>Uncertainty Distribution for Stochastic Parameters</i> AMR (ANL-NBS-MD-000011) and Table 15 of the AMR</p>	<p>Longitudinal dispersivity set as a probability distribution - normal distribution: <math>E(\log_{10}(m)) = 2.0</math>, <math>S.D.(\log_{10}(m)) = 0.75</math>. Horizontal transverse = longitudinal / 200. Vertical transverse = longitudinal / 2000. (Section 6.1.1, page 50).</p>	<p>Difficult to determine basis for the distribution chosen - it may link to "Modeling Sub Gridblock Scale Dispersion in Three-Dimensional Fractured Media," ANL-NBS-HS-000024, however this is difficult to see. The same is true for the correlations between longitudinal and transverse. Basis for assumptions (Section 5.11, page 21): 1) No justification for narrowing 30 km range given lack of site-specific data, 2) Gelhar (1993, p. 203), 3) analysis in Section 6.11 (it appears that the basis is "Modeling Sub Gridblock Scale Dispersion in Three-Dimensional Fractured Media," ANL-NBS-HS-000024.</p>	<p>Only impact of longitudinal dispersivity is on first arrival of radionuclides - thus only will impact receptor dose during transient behavior - once "steady state" is achieved, no impact (e.g., peak dose). No impact of transverse dispersivity given assumption of collecting all mass released at 20 km compliance point into receptor wells.</p>

<p>Horizontal Anisotropy: Determine parameters for an alternative flow model that accounts for anisotropy in the permeability field. Assumptions: 1) anisotropy represented by permeability tensor oriented in the north-south and east-west directions, 2) applicable to fractured-volcanics only, 3) alternative assigned equal probability as isotropic case. (Sections 5.12, page 22 and 6.12, page 51).</p>	<p><i>Uncertainty Distribution for Stochastic Parameters</i> AMR (ANL-NBS-MD-000011) and Table 15 of the AMR.</p> <p>Driving Source appears to be Winterle, et. al., "Review and Analysis of Hydraulic and Tracer Testing at the C-Wells Complex Near Yucca Mountain, Nevada," CNRWA - TIC: 246623.</p>	<p>Bound by setting anisotropy ratio to 5:1 - multiply horizontal permeability in north-south direction by 2.49 and divide in east-west direction by 2.49. (Section 6.12, page 51).</p>	<p>Appears that basis is Winterle, et. al., report - but not completely clear (Section 6.12, page 51). Basis for assumptions: 1) Winterle, et. al., reports, 2) volcanics are large portion of the flow path and would be area where anisotropy would have largest impact, 3) lack of information on relative validity of isotropic vs. anisotropic models. (Section 5.12, page 22).</p>	<p>Groundwater velocities and radionuclide travel times in the SZ.</p>
<p>Retardation of Radionuclides Irreversibly Sorbed on Colloids: This is a summary of the information contained in "Abstraction of Colloid-Facilitated Pu Transport Modeling for TSPA." ANL-NBS-HS-000031. (Section 5.13, page 23 and Section 6.13, page 52)</p>	<p><i>Uncertainty Distribution for Stochastic Parameters</i> AMR (ANL-NBS-MD-000011) and Table 15 of the AMR.</p> <p>"Abstraction of Colloid-Facilitated Pu Transport Modeling for TSPA." ANL-NBS-HS-000031</p>	<p>Use the probability distributions from "Abstraction of Colloid-Facilitated Pu Transport Modeling for TSPA." ANL-NBS-HS-000031. (Section 6.13, page 52).</p>	<p>Basis for treatment is "Abstraction of Colloid-Facilitated Pu Transport Modeling for TSPA." ANL-NBS-HS-000031</p>	<p>Transport characteristics of radionuclides irreversibly attached to colloids (Pu and daughters).</p>
<p>Retardation of Radionuclides Reversibly Sorbed on Colloids: The Kc Parameter. Assumptions: 1) Colloids with highest affinity for sorption used (Am waste form) - conservative, 2) maximum colloid concentration used (conservative). (Section 5.14, page 23, Items 1 and 2)</p>	<p>Driving Source is sorption of radionuclides onto Am waste form colloids - "Waste Form Colloid-Associated Concentration Limits: Abstraction and Summary," ANL-WIS-MD-000012.</p>	<p>Compute distribution of Kc based on equation <math>K_c = K_d * C_{coll}</math>. Kd is range from source referenced AMR. Ccoll is held constant at 0.003 mg/L per source AMR. Log-Normal distribution results (geometric mean = 3e-3, geometric standard deviation of 10). (Section 6.14, page 56).</p>	<p>It is stated that the two assumptions are conservative, hence the overall Kc value is expected to be conservative. (Section 5.14, page 23, Items 1 and 2)</p>	<p>Breakthrough characteristics of radionuclides reversibly sorbed onto colloids.</p>
<b>Variability</b>				
<p>Variations in the permeability testing results used as input for the groundwater transport analyses</p>	<p><i>Modeling Sub-Gridblock Scale Dispersion in Three-Dimensional Heterogeneous Fractured Media</i> AMR (ANL-NBS-HS-000022)</p>	<p>Incorporated the natural-log variance of the empirical cumulative distribution function for the data.</p>	<p>Statistical analysis of field data from single-well, double packer and multi-well interference test results. Cutoff value between background and feature permeability believed to realistically represent the observed data and create numerically stable solutions.</p>	<p>Treatment of the permeability input to the numerical model of heterogeneous and anisotropic permeability in the fractured volcanic rocks in the SZ, affects dispersivity analysis results.</p>

**Results**

Radionuclide release to the Biosphere: It is assumed that all radionuclide mass crossing the 20 km fence is captured by pumping wells in the hypothetical farming community.	<i>Input and Results of the Base Case Saturated Zone Flow and Transport Model for TSPA AMR (ANL-NBS-HS-000030)</i>	Assume entire mass flux of radionuclides is collected in receptor wells and uniformly distributed in total groundwater usage.	Justified as reasonable given large groundwater usage of the hypothetical community. Argued as conservative and bounding since all radionuclides are captured. In additional, draft regulations impose such an approach. (Section 6.2.4).	Assumption can directly influence the resultant does rate.
Radionuclide release to the Biosphere: It is assumed that the average concentration in the groundwater supply of the hypothetical community is an appropriate estimate of radionuclide dose	<i>Input and Results of the Base Case Saturated Zone Flow and Transport Model for TSPA AMR (ANL-NBS-HS-000030)</i>	Assume radionuclide concentration in receptor wells is evenly distributed.	Basis is that radionuclide concentrations in wells will be spatially variable, however biosphere transport processes will average out. In fact, basis is the critical group approach contained in 10 CFR 63.	Assumption can directly influence the resultant does rate.
Results	<i>Input and Results of the Base Case Saturated Zone Flow and Transport Model for TSPA AMR (ANL-NBS-HS-000030)</i>	Library of breakthrough curves to capture uncertainty - convolution integral.	All quantified uncertainty captured in results	SZ transport characteristics in TSPA-dose
Results	<i>Input and Results of the Base Case Saturated Zone Flow and Transport Model for TSPA AMR (ANL-NBS-HS-000030)</i>	Model plugged into TSPA with inputs same as those for 3D convolution integral.	Model decay daughters	Contribution to dose from daughter products.

## 16.0 Biosphere Model

### 16.1 Purpose of the Model and Intended Use

The purpose of the biosphere model is to develop BDCFs for subsequent use in TSPA analyses. A BDCF, as used in TSPA analyses, is simply a multiplier that converts a unit concentration of a radionuclide in a source (e.g., groundwater used for consumption or irrigation) to an annual radiation dose received by a human from that unit concentration. BDCFs are computed by modeling the transport of radionuclides through the various biosphere exposure pathways and the uptake of radionuclides by humans, resulting in a radiation dose. BDCFs are computed for the nominal and disruptive scenarios considered in TSPA in the form of probability distributions for a reasonable case and single values for a bounding case.

The approach for modeling the biosphere system in the vicinity of Yucca Mountain is similar to other modeling approaches taken to assess the level of risk associated with environmental contamination. All safety assessments of high-level nuclear waste repositories developed worldwide include biosphere models (some being generic models since specific sites have not been identified – Canada, Spain). Draft regulations<sup>1,2</sup> (and subsequent DOE guidance<sup>3</sup>) prescribe several aspects related to modeling the biosphere in the vicinity of Yucca Mountain. In addition, the approach for developing the Yucca Mountain biosphere model is consistent with similar approaches being pursued by the international scientific community (e.g., BIOMOVs II – Biosphere Model Validation Study, Phase II<sup>4</sup>), to the extent they apply to portions of the system not constrained by regulatory requirements and DOE guidance.

The development of a fully site-specific biosphere model at Yucca Mountain is not possible due to limited availability of site specific data. Where possible, the modeling effort has used site-specific and regional information. Literature information regarding biosphere modeling has been used to identify conceptual models and parameter inputs where site-specific or regional information is not available.

### 16.2 Model Relations

The *Biosphere* PMR (TDR-MGR-MD-000002) and its associated AMRs comprise the documentation of the biosphere model. The titles, document identification numbers, and objectives of these reports is discussed below:

---

<sup>1</sup> 64 FR 46976: Environmental Radiation Protection Standards for Yucca Mountain, Nevada; Proposed Rule 40 CFR 197. Readily Available.

<sup>2</sup> 64 FR 8640: Disposal of High-Level Radioactive Wastes in a Proposed Geologic Repository at Yucca Mountain, Nevada. Proposed Rule 10CFR63. Readily Available.

<sup>3</sup> Revised Interim Guidance Pending Issuance of New U.S. Nuclear Regulatory Commission (NRC) Regulations (Revision 01, July 22, 1999), for Yucca Mountain, Nevada. Letter from Dr. J.R. Dyer (DOE/YMSCO) to Dr. D.R. Wilkins (CRWMS M&O), September 3, 1999, OL&RC:SB-1714, with enclosure, "Interim Guidance Pending Issuance of New NRC Regulations for Yucca Mountain (Revision 01)." ACC: MOL.19990910.0079.

<sup>4</sup> BIOMOVs II 1996. *Development of a Reference Biospheres Methodology for Radioactive Waste Disposal*. Technical Report No. 6. Stockholm, Sweden: Swedish Radiation Protection Institute. TIC: 238329.

- *Biosphere PMR* (TDR-MGR-MD-000002) – Summarizes the information contained in the various AMRs. This report provides one of the sources of information regarding the conceptual model of the biosphere.
- *Evaluation of the Applicability of Biosphere-Related Features, Events, and Processes (FEP)* (ANL-MGR-MD0-000011) – Documents the screening of biosphere related FEPs and document the steps taken to validate the biosphere model in accordance with AP-3.10Q.
- *Identification of the Critical Group (Consumption of Locally Produced Food and Tap Water)* (ANL-MGR-MD-000005) – 1) develop screening groups using attributes of the potential behaviors and characteristics of the population surrounding Yucca Mountain from which a critical group can be identified; 2) identify a critical group consistent with DOE guidance; and 3) provide food and water consumption parameters and other characteristics of the critical group used in GENII-S calculations of BDCFs.
- *Groundwater Usage by the Proposed Farming Community* (ANL-NBS-MD-000006) – Quantify the annual volume of groundwater used by the farming community containing the critical group.
- *Input Parameter Values for External and Inhalation Radiation Exposure Analysis* (ANL-MGR-MD-000001) – Select and justify values for six external and inhalation exposure pathway input parameters used in GENII-S (mass loading, inhalation exposure time, chronic breathing rate, soil exposure time, home irrigation rate, duration of home irrigation)
- *Identification of Ingestion Exposure Parameters* (ANL-MGR-MD-000006) – Select and justify values of ingestion exposure pathway parameters used in GENII-S.
- *Environmental Transport Parameter Analysis* (ANL-MGR-MD-000007) – Develop or select values for environmental transport parameters for use in GENII-S.
- *Transfer Coefficient Analysis* (ANL-MGR-MD-000008) – Select values for transfer coefficients (including soil-to-plant transfer factors, animal feed transfer coefficients, and bioaccumulation factors for fresh water fish) for use in GENII-S.
- *Dose Conversion Factor Analysis: Evaluation of GENII-S Dose Assessment Methods* (ANL-MGR-MD-000002) – Verifies that doses calculated by GENII-S are consistent with those calculated using similar methods currently accepted by the scientific and engineering community in the field of radiation protection.
- *Evaluate Soil/Radionuclide Removal by Erosion and Leaching* (ANL-NBS-MD-000009) – Determine reasonable and conservative bounding estimates of annual surface soil removal representative of the major soils present in the vicinity of the projected reference critical group within Amargosa Valley.
- *Non-Disruptive Event Biosphere Dose Conversion Factors* (ANL-MGR-MD-000009) – Develop BDCFs for the nominal repository performance TSPA scenario. These BDCFs are also used in the igneous-eruption and human intrusion TSPA scenarios

- *Non-Disruptive Event Biosphere Dose Conversion Factor Sensitivity Analysis* (ANL-MGR-MD-000010) – Provide insights into which parameters and exposure pathways have the greatest impact on the BDCFs associated with the nominal scenario.
- *Disruptive Event Biosphere Dose Conversion Factor Analysis* (ANL-MGR-MD-000003) – Develops BDCFs for the disruptive event scenario where contamination is assumed to be dispersed by volcanic ash.
- *Disruptive Event Biosphere Dose Conversion Factor Sensitivity Analysis* (ANL-MGR-MD-000004) – Provide insights into which parameters and exposure pathways have the greatest impact on the BDCFs associated with the disruptive event scenario.
- *Distribution Fitting to the Stochastic BDCF Data* (ANL-NBS-MD-000008) – Derive statistical approximations (abstractions) to the nominal BDCF data.
- *Abstraction of BDCF Distributions for Irrigation Periods* (ANL-NBS-MD-000007) – Derive abstractions for the time evolution of the BDCFS due to radionuclide build-up effects in soil (includes build-up due to irrigation and loss due to soil erosion and leaching).

The AMRs can be divided into four categories: 1) definition of parameter input for GENII-S; 2) GENII-S modeling; 3) model validation; and 4) abstraction to TSPA. Figure 16-1, Biosphere Model Relations, shows how biosphere modeling information flows between the various AMRs.

Figure 16-1 was developed by reviewing the documented linkages between the AMRs. It should be noted that this information is not presented in any of the reports, including the Biosphere PMR and represents the reviewer's interpretation from the documentation as to how the various AMRs are linked. Of interest is the *Groundwater Usage by the Proposed Farming Community* (ANL-NBS-MD-000006) AMR which is linked to no other AMRs within the biosphere modeling area. Rather, this AMR provides input directly to the TSPA model.

### **16.3 Model Structure**

Figure 16-2, Biosphere Model Structure, depicts the various elements that comprise the biosphere model. Shown are those elements that comprise the conceptual and representational models, the various parameters needed, and the modeling results. Each is discussed in more detail below.

#### **A. Conceptual Model**

The overall conceptual model of the biosphere is summarized in the Biosphere PMR (Sections 3.1.4 and 3.1.5). The attributes of the biosphere model are based on a screening of FEPs associated with the biosphere. Two scenarios are considered.

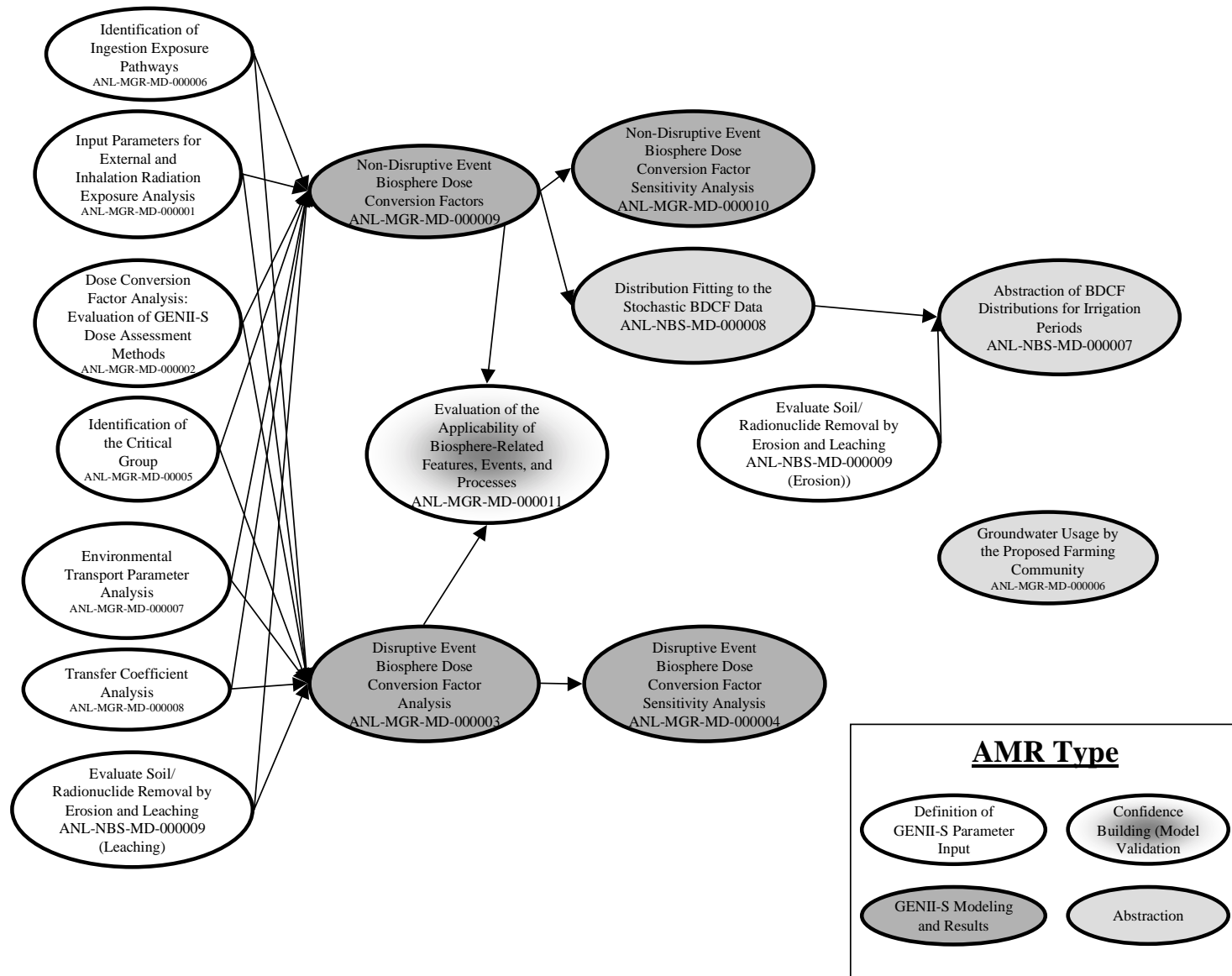


Figure 16-1: Biosphere Model Relations

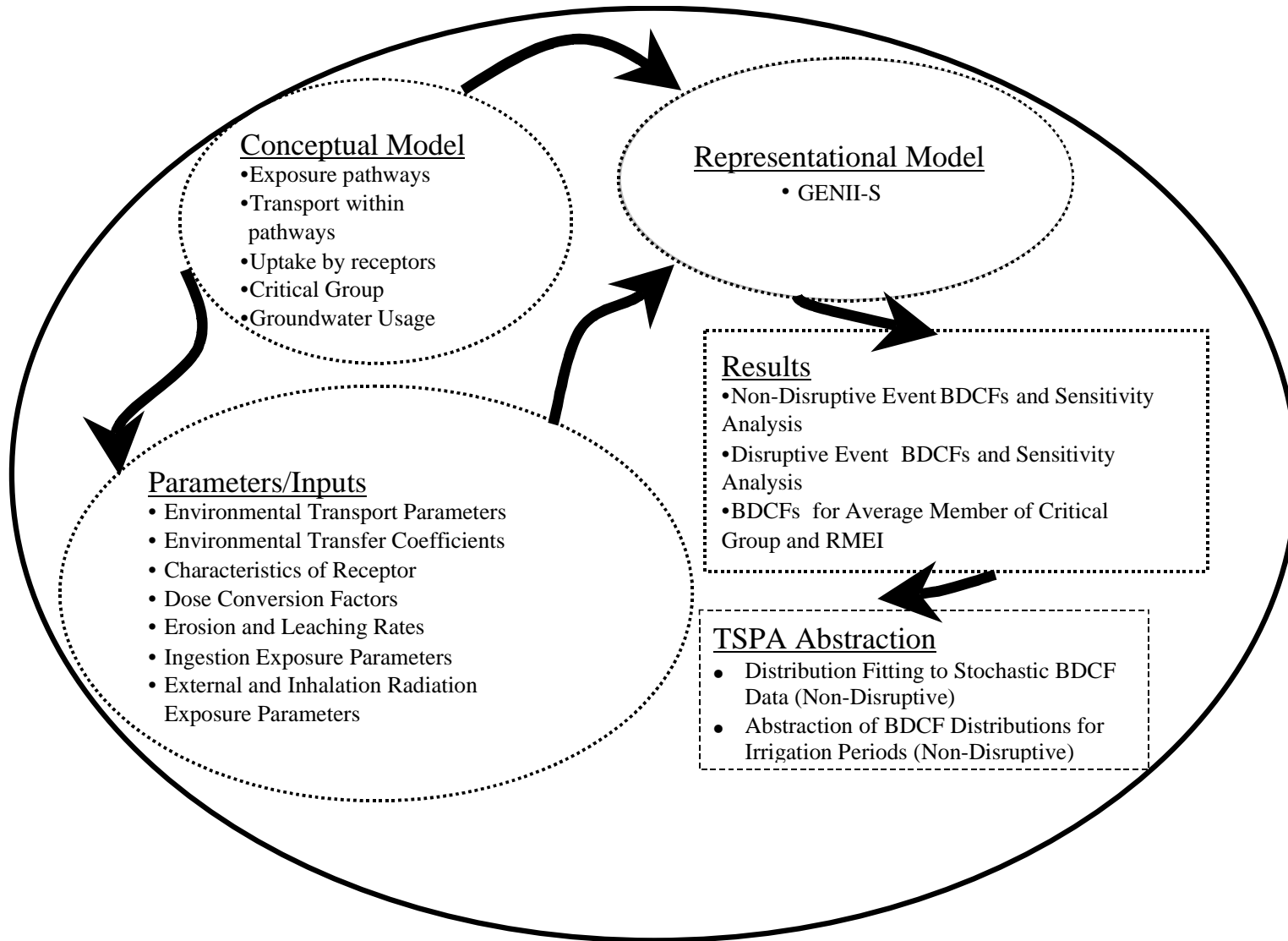


Figure 16-2 Biosphere Model Structure

The first exposure scenario is a groundwater contamination scenario where a receptor (farmer) is assumed to use contaminated groundwater for irrigation and consumption. This scenario is used to evaluate the radiological consequences of both undisturbed potential repository system performance as well as the consequences of selected disruptive processes and events. Contaminated groundwater used for irrigation causes contamination of soil and, subsequently, contamination of edible crops and animal feed. Contaminated animal feed results in contamination of animal food products (e.g., milk, meat, eggs). Contaminated soil may also be resuspended and deposited onto crops, adding to the contamination caused by irrigation. The second scenario considers the deposition of contaminated ash resulting from a volcanic eruption through the repository onto the ground surface.

Ingestion, inhalation, and external exposure are the exposure pathways considered in the conceptual model.

- The ingestion pathway includes drinking of contaminated water, consumption of locally produced crops that have been irrigated with contaminated groundwater, consumption of meat and dairy products from livestock that have been sustained on contaminated water and plants irrigated with contaminated water, and ingestion of contaminated soil. Specific ingestion exposure includes the following:
  - Consumption of contaminated tap water (nominal scenario only)
  - Consumption of locally produced and contaminated leafy vegetables, root vegetables, fruit, grain, meat (beef and pork), poultry, milk, eggs, fish
  - Inadvertent contaminated soil ingestion
- The primary inhalation pathway is through breathing of resuspended contaminated soil and volcanic ash during outdoor activities such as farming and recreation. This pathway includes expected inhalation of contaminated ash during and after a disruptive volcanic event.
- The external pathway occurs as a result of direct exposure to the radiation emitted by radioactive materials external to the body (e.g., those present in the soil or on the soil surface).

A key aspect of developing the biosphere conceptual model is defining the receptor. In the case of Yucca Mountain, the receptor is prescribed in draft regulations and incorporated into DOE guidance as the “average member of the critical group.” The AMR entitled *Identification of the Critical Group (Consumption of Locally Produced Food and Tap Water* provides the basis for identifying the critical group (consistent with DOE guidance) and identifying behaviors/ characteristics of the population in the vicinity of Yucca Mountain.

## **B. Representational Model**

The computer code GENII-S was chosen as the representational biosphere model. The rationale for choosing GENII-S is discussed in the Biosphere PMR, Section 3.2.1. A brief discussion of

some of the mathematics incorporated into GENII-S is provided in Section 3.2 and Appendix C of the *Biosphere PMR*. Validation of the GENII-S software is discussed in the AMR entitled *Evaluation of the Applicability of Biosphere-Related Features, Events, and Processes (FEP)*.

### **C. Parameters**

Contaminated groundwater is the primary potential source of radiation exposure as a result of disposing nuclear waste at Yucca Mountain. Thus, defining the manner in which groundwater may be used by the critical group is essential in modeling potential exposures. In this case as well, draft regulations and subsequent DOE guidance prescribe certain aspects related to groundwater usage. Based on this guidance, the *Groundwater Usage by the Proposed Farming Community* AMR utilizes the 1990 census data, the 1997 food consumption survey information, and 1997 water usage data published by the State of Nevada to develop a range of annual water usage for the critical group. Both parameter and scenario uncertainty are associated with the final parameter range. The AMR discusses the uncertainties involved and the assumptions (conservative) invoked to determine a probability distribution of water usage. This range is not used in any other biosphere AMRs and is input directly into the TSPA-SR model.

The objective of seven of the biosphere AMRs is to develop parameter inputs for use in the GENII-S code to calculate the BDCFs. These AMRs are:

- *Identification of the Critical Group (Consumption of Locally Produced Food and Tap Water)*
- *Input Parameter Values for External and Inhalation Radiation Exposure Analysis*
- *Identification of Ingestion Exposure Parameters*
- *Environmental Transport Parameter Analysis*
- *Transfer Coefficient Analysis*
- *Dose Conversion Factor Analysis: Evaluation of GENII-S Dose Assessment Methods*
- *Evaluate Soil/Radionuclide Removal by Erosion and Leaching*

These AMRs provide the bases for the selection of parameter values (both fixed value and probability distributions). Several of these AMRs provide parameter estimates for a reasonable case and for a bounding case. Although there are minor differences in the definitions, these AMRs appear to have generally used the same methodology in defining reasonable and bounding parameters. In general, the reasonable case is defined as being reasonably expected to occur based on characteristics of the critical group, DOE guidance, and information on the current population in Amargosa Valley. In some instances, conservatism is used in the definition of reasonable case parameters. In these cases, conservative is defined as a value or behavior that would result in a higher BDCF. In general, the selection of bounding parameters is based on extreme behaviors or conditions that would result in a higher BDCF.

Some of the input parameters used to define the reasonable case are represented as probability distributions, while others are represented by single values. The input parameters for the bounding case are represented as single values in all instances. The TSPA-SR biosphere model uses only the reasonable case parameters, of which 28 of almost 300 are represented by probability distributions.

#### **D. Results**

Two sets of AMRs document the integration of the information from supporting AMRs (discussed above) into inputs for GENII-S, the execution of the code, the results (BDCFs), and the results of sensitivity analyses. One set of AMRs documents the computation of BDCFs for the nominal scenario and one for the disruptive scenario. For the nominal scenario, the AMRs are *Non-Disruptive Event Biosphere Dose Conversion Factors* and *Non-Disruptive Event Biosphere Dose Conversion Factor Sensitivity Analysis*. For the disruptive scenario, the AMRs are *Disruptive Event Biosphere Dose Conversion Factor Analysis* and *Disruptive Event Biosphere Dose Conversion Factor Sensitivity Analysis*.

Within each of these sets, the first AMR summarizes the input information from the various source AMRs, documents the GENII-S execution, and reports the resultant BDCFs (distributions for the reasonable representation case and single values for the bounding case). For the reasonable case, the uncertainty in all parameters represented by probability distributions are propagated stochastically within the GENII-S software and result in probability distributions for the BDCFs. However, the critical group's consumption habits are single values, representative of the average member of the critical group determined in the *Identification of the Critical Group (Consumption of Locally Produced Food and Tap Water)* AMR. For the bounding case, all parameters are represented by single values (bounding) and a single GENII-S execution is conducted for each radionuclide.

The second AMR in each set presents a sensitivity/uncertainty analysis where regression techniques were used to identify which of the reasonable case input parameters represented by probability distributions contribute to the resulting BDCF probability distributions. In these analyses, the consumption habits were varied within the ranges identified in the *Identification of the Critical Group (Consumption of Locally Produced Food and Tap Water)* AMR.

Section 6.2 of the AMR entitled *Evaluation of the Applicability of Biosphere-Related Features, Events, and Processes (FEP)* is intended to validate the biosphere model in accordance with AP-3.10Q by 1) verifying that the GENII-S software is operating correctly and gives results consistent with the inputs; 2) demonstrating that the BDCFs produced using GENII-S and the biosphere model are reasonable when compared with results of other calculations and conceptual models<sup>5,6</sup>; and 3) conducting an independent review of the model by a technical expert. Section 3.2.3 of the *Biosphere* PMR also summarizes this information.

---

<sup>5</sup> LaPlante, P.A. and Poor, K. 1997. Information and Analyses to Support Selection of Critical Groups and Reference Biospheres for Yucca Mountain Exposure Scenarios. CNWRA 97-009. San Antonio, Texas: Center for Nuclear Waste Regulatory Analyses. TIC: 236454.

## **16.4 Discussion of Uncertainty/Variability Treatment**

An evaluation of uncertainty and variability treatment of the AMRs was performed for this exercise. For each AMR, the uncertainties/variabilities were identified and determined if a thorough treatment was performed. Thorough treatment was considered to be: identification, treatment, impact assessment, and clear presentation of the analysis and the propagation of uncertainty in the AMR. Table 1 is a synopsis of some of the uncertainties and variabilities identified in this exercise. The following is a discussion of the evaluation process and uncertainty/variability analysis trends within the AMR/model process.

### **A. Conceptual Model**

As discussed above, the conceptual model of the biosphere at Yucca Mountain is summarized in the Biosphere PMR (Sections 3.1.4 and 3.1.5). These sections focus primarily on the exposure pathways modeled and the basis for choosing these pathways (screening of features, events, and processes). Although clear on describing what pathways are being considered, the PMR does not provide detailed discussions of the conceptual models of radionuclide transport within these exposure pathways and the conceptual models for human uptake/fate. It also contains no discussion of conceptual model uncertainties. The conceptual models of radionuclide transport within the biosphere and human uptake/fate and the associated uncertainties are not discussed in any of the AMRs.

Section 3.5 of the Biosphere PMR states that no alternative conceptual models have been identified. It is further stated in this section that “the main reason for the absence of opposing views concerning alternative conceptual models is that the strategy for conceptualizing the biosphere model is consistent with similar activities being pursued by the international scientific community to the extent they apply to unconstrained portions [not constrained by regulatory requirements or DOE guidance] of the reference biosphere.”

Perhaps part of the reason for not discussing the overall conceptual model in detail (and its associated uncertainty) is the reliance on draft regulatory requirements and DOE guidance that prescribe certain aspects of the model, the use of techniques supported by the international scientific community (e.g., BIOMOV<sup>7</sup>) for the remaining portion of the model, and the use of the GENII-S software<sup>8</sup>. All are appropriately referenced and the PMR appears to be relying on these documents as the basis for the conceptual model.

---

<sup>6</sup> “Biosphere.” Chapter 9 of Total System Performance Assessment-Viability Assessment (TSPA-VA) Analyses Technical Basis Document. B00000000-01717-4301-00009 REV 01. Las Vegas, Nevada: CRWMS M&O. ACC: MOL.19981008.0009.

<sup>7</sup> BIOMOV<sup>II</sup> 1996. *Development of a Reference Biospheres Methodology for Radioactive Waste Disposal*. Technical Report No. 6. Stockholm, Sweden: Swedish Radiation Protection Institute. TIC: 238329.

<sup>8</sup> Napier, B.A.; Peloquin, R.A.; Strenge, D.L.; and Ramsdell, J.V. 1988 Conceptual Representation. Volume 1 of GENII: The Hanford Environmental Radiation Dosimetry Software System. PNL-6584. Richland, Washington: Pacific Northwest Laboratory. TIC: 206898.

## **B. Representational Model**

As discussed above, the biosphere PMR is the only source of information regarding the representational (mathematical) model GENII-S. The discussion in the PMR focuses primarily on the selection of the code as the appropriate computational tool for use (including the selection criteria and available codes). A discussion of the main mathematical models used in GENII-S is included in Appendix C of the PMR. References to the GENII-S documentation are provided for further discussion of the mathematical models within GENII-S. No discussion of the mathematical model uncertainties associated with GENII-S is provided in either the PMR or the AMRs.

## **C. Parameters**

The biosphere is a complex system with many parameters needed to mathematically simulate radionuclide transport within it and ultimate uptake by humans. Since modeling the biosphere has only recently become necessary by regulation, little site specific information exists to define model parameters. In several instances, regional information can be used. In other instances, it is necessary to utilize literature information, not necessarily specific to the Yucca Mountain region. The best available information was used to develop a complex biosphere model of the Yucca Mountain region.

As discussed above, the AMRs that develop input parameters for GENII-S define reasonable case and bounding case values or ranges. However, the TSPA-SR model uses BDCFs generated from the set of reasonable case input values. Because of this, the focus of the discussion that follows is on the reasonable case parameter definitions.

### **Data Source**

Again, one of the most critical sources of uncertainty in the biosphere model that does not appear to have been fully addressed in the AMRs is the use of non-site specific information as the bases for parameter selection. This source of uncertainty is clearly pointed out in two of the AMRs (e.g., *Transfer Coefficient Analysis* Section 4.1, *Environmental Transport Parameters Analysis* Section 4.1.1) that utilize only literature information. However, no discussion of the magnitude of the uncertainty, either qualitatively or quantitatively, is presented. Other AMRs use site-specific or regional data, where available in addition to non site-specific information.

For the *Transfer Coefficient Analysis* and *Environmental Transport Parameters Analysis* AMRs, all parameter values were obtained from literature and only some are specific to the Yucca Mountain environment. None of the selection criteria cited in AMRs where literature information is used to specify a reasonable parameter value (or distribution). It should be noted that the selection criteria do not cite conservatism in the choice of parameter values or ranges for the reasonable case. Specific examples include:

- *Environmental Transport Parameter Analysis* (Section 6):
  - Site-Specific data for a parameter value was used when this information was available

- If one parameter value appeared in more than half of the reviewed documents, it was considered that this generic value was agreed upon by the scientific community and represents the best available data. Thus, this value was selected for use.
- GENII-S default value was selected if available literature data were not consistent. It was considered that no single agreed-upon value was available to replace the default value.

In the case of this AMR, all parameters except one (crop resuspension factor) are represented by single point values chosen from literature with no assessment of uncertainty (beyond the determination of reasonable and bounding values). Thus, the impact of using non site specific information is not explicitly assessed.

- *Transfer Coefficient Analysis* (Section 6.1) (selection criteria in order of preference):
  - If one single value appears in at least half of the of the number of reviewed documents, this value is selected, because it is considered that this generic value is agreed upon by the scientific community.
  - If one value appears in at least half of the recent published documents (published after GENII, 1988), this new value is selected, because it is considered that it reflects recent studies.
  - If no single agreed value from available literature data meets the above two criteria, the values are ranked from lowest to highest with the middle rank selected from all available data.
  - GENII-S default value is selected when only very limited literature data are available.

In the case of this AMR, single values are chosen from literature to represent the best estimate of the soil-to-plant transfer factors, the animal feed transfer coefficient, and the fish bioaccumulation factor. In the case of the soil-to-plant transfer factor and the animal feed transfer coefficient, available literature information is used to define scale factors (log-uniform) distributions that “should cover the range in uncertainty for these parameters” (Section 6.2.5). In addition, bounding single values of the transfer factors are also determined, essentially at the extreme range defined by the reasonable case probability distributions. Sensitivity analyses (*Non-Disruptive Event Biosphere Dose Conversion Factor Sensitivity Analysis*) demonstrate that soil-to-plant transfer factors are not important for the nominal case (except for Tc-99). However, for the disruptive case, similar sensitivity analyses (*Disruptive Event Biosphere Dose Conversion Factor Sensitivity Analysis*) demonstrate that they are important. Again, the impact of using non site specific information is not explicitly assessed.

The *Identification of Ingestion Exposure Parameters* AMR defines several probability distributions for the various input parameters. Regional information is used primarily in the development of parameter values and ranges. The rationale for selecting some fixed values is that uncertainty in the parameter is not critical (storage times, Section 6.10) or the selected value is conservative (dietary fraction, Section 6.11). However, some of the fixed values are based on

calculations using limited site-specific and regional information. Examples include irrigation rates and grow times for beef and milk (alfalfa) and poultry and eggs (corn). Such values are likely to be uncertain, especially because of limitations in the available data. The current set of sensitivity analyses cannot determine the impact of such fixed values on the resultant BDCFs.

### **No Uncertainty Treatment**

The purpose of the AMR entitled *Dose Conversion Factor Analysis: Evaluation of GENII-S Dose Assessment Methods* is to demonstrate that the dose conversion factors (DCFs) for inhalation and ingestion exposure and the dose coefficients for external exposure that are used within GENII-S are conservative and appropriate for use. This is accomplished by comparing the GENII-S values with those contained in literature published roughly at the same time as GENII-S was developed. In the case of DCFs for ingestion and inhalation, it was demonstrated that the DCFs within GENII-S are comparable with literature information (ICRP-30, 1979; Federal Guidance Report No. 11, 1988; 10 CFR 20). It was also determined that the GENII-S dose coefficients for external exposure should be replaced with more recent EPA compilation (Federal Guidance Report No. 11, 1993). However, this AMR does not discuss the uncertainty associated with the DCFs or dose coefficients chosen, nor comparison with more recent values. These parameters are defined as single values (no uncertainty). It is expected that uncertainty in these parameters could result in significant uncertainty in the resultant BDCFs.

Although the DCFs and dose coefficients are likely to be prescribed by final regulations, the analysis still remains incomplete if a thorough uncertainty analysis to assess the potential impact is not conducted. Such an analysis could possibly help to quantify the overall uncertainty and degree of conservatism in the TSPA results that support the safety case.

The *Input Parameter Values for External and Inhalation Radiation Exposure Analysis* AMR provides probability distributions for four of the six GENII-S parameters needed to model external and internal radiation exposure. The bases for the selected parameter values or distribution ranges, primarily regional and site-specific information, are clearly provided. In one instance (chronic breathing rate), the decision to use a fixed value was predicated by the fact that GENII-S only allows for a fixed value of this parameter. For this case, a single value was selected from various values cited in literature (argued as being reasonably conservative). Thus, in this instance software limitations forced any uncertainty to be ignored.

### **Treatment of Variability**

In some instances within the *Input Parameter Values for External and Inhalation Radiation Exposure Analysis* AMR, it appears that the uncertainty range for the probability distributions is based on variability (temporal and spatial). Two examples are the mass loading parameter (Section 6.1) and the inhalation exposure time (Section 6.2). In the case of the mass loading factor, PM<sub>10</sub> data from YMP site 9 was used. Twenty-four hour measurements of particulate matter  $\leq 10 \mu\text{m}$  every six days from October 3, 1992 through December 30, 1997 were used to determine the uncertainty range. These measurements represent temporal variability in the parameter and not the uncertainty in the average value of the parameter over a given time period.

It is likely that the uncertainty range developed is larger than the uncertainty in the “true average” value of the mass loading factor over a given time period.

In the case of the inhalation exposure time, three lifestyle scenarios for the critical group were used to determine the uncertainty range (triangular distribution). Application of these scenarios results in variability in inhalation exposure time for random members within the critical group and not the uncertainty in the exposure time for the average member of the critical group. It is also likely that the uncertainty range developed is larger than the “true uncertainty” in the inhalation exposure time for the average member of the critical group. It should be noted that in the computation of the BDCFs in *Non-Disruptive Event Biosphere Dose Conversion Factors* AMR, a single value of this parameter was used (the mode of the triangular distribution). As such, no uncertainty in this parameter is carried forward into the calculation of BDCF distributions.

In several instances within the *Identification of Ingestion Exposure Parameters* AMR, it appears that the defined uncertainty range for the probability distributions is based on variability. Examples include the irrigation time, irrigation rate, crop yield, growing time, and the crop interception fraction for leafy vegetables. The uncertainty ranges for these parameters were based on calculations using different leafy vegetable crops (spinach, tomato, cucumber, peppers, lettuce, snap beans, peas, corn). The members of the critical group can be expected to grow a variety of leafy vegetable crops, with different individuals growing different crops and perhaps the same individual growing different crops over time. This represents variability within the critical group. The best estimate value of these parameters for the average member of the critical group would best be represented by the average of the calculated parameters (this value was computed). The ranges of the probability distributions are believed to be larger than the “real” uncertainty in these parameters for the average member of the critical group. For example, it is not anticipated that the entire critical group would grow only cucumbers (irrigation time of 2 months) or corn (irrigation time of 4.9 months) for the entire future. Although this example represents the extremes of the probability distribution, in general it is expected that for the average member of the critical group, over time, the “true” value of such parameters will tend to be more the average values cited in the AMR (with some associated uncertainty).

### **Correlation Between Parameters**

Any correlations between the various parameters are not discussed in the *Identification of Ingestion Exposure Parameters* AMR. For example, crop yield and irrigation rate may be correlated (e.g., increased irrigation may result in larger crop yield)? Are the crop intercept fraction, the irrigation rate, and the irrigation time similarly correlated? Such correlations may have an impact on the resultant BDCFs (namely, their uncertainty range).

### **Statistical Error in Data**

The basis for the determination of consumption habits in the *Identification of the Critical Group (Consumption of Locally Produced Food and Tap Water)* AMR is the food consumption survey, which has a documented error of  $\pm 5\%$  for the entire sample size. The error introduced by reducing the sample size towards the characteristics of the “resident” farmer is not assessed in

terms of its impact on the resultant parameter distributions beyond the following statement: “The survey data underlying the data presented in Table 3 are subject to error from a number of sources. However, tests done in regard to non-response bias as well as validity and reliability tests suggested that the survey data are valid and reliable and sufficient for biosphere modeling purposes” (Page 18). However, there will be some uncertainty associated with the sample mean for the resident farmer, likely greater than the  $\pm 5\%$  (e.g.,  $\sigma_{\text{sample mean}} = \sigma_{\text{sample}}/N^{1/2}$ ). Such a treatment could be used to define the uncertainty in the average member of the critical group’s consumption habits.

## **D. Results**

As discussed in Section III.D, the AMRs entitled *Non-Disruptive Event Biosphere Dose Conversion Factor Sensitivity Analysis* and *Disruptive Event Biosphere Dose Conversion Factor Sensitivity Analysis* present the sensitivity/uncertainty analysis. In these AMRs, regression analysis was used to identify which of the input parameters represented by probability distributions contribute to the variance in the resulting reasonable case BDCF distributions. The AMRs include no discussions regarding the impact of fixed parameters (this impact cannot be determined through regression analysis). Thus, it cannot be determined how any of these fixed parameters would affect the BDCFs, nor can the level of conservatism in the BDCFs be assessed. This is most important when the single value input parameters may not be conservative (e.g., environmental transport factors).

Further, recall that the consumption rates are fixed (at values representative of the average member of the critical group) for the purpose of computing BDCFs for TSPA use. However, the two sensitivity analysis AMRs consider them as uncertain and re-calculate the BDCFs for the purpose of conducting the sensitivity analyses. The subsequent results indicate that the variance in the consumption rates is significant in explaining the variance in the BDCF distributions. At issue is the fact that the sensitivity study does not fully explain the factors that dominate the variance in the BDCFs used in TSPA. The variance in the consumption habit parameters may be masking the importance of other uncertain parameters.

## **16.5 Uncertainty Propagation**

### **A. Process Models**

As discussed in Section III.D, two AMRs summarize the input information from the various source AMRs, document the GENII-S executions, and report the resultant BDCFs (distributions for the reasonable representation case and single values for the bounding case). One AMR (*Non-Disruptive Event Biosphere Dose Conversion Factors*) is for the nominal case and the other (*Disruptive Event Biosphere Dose Conversion Factor Analysis*) is for the disruptive case. No uncertainty evaluation is performed in these AMRs. In addition, although data tracking numbers are identified in the input data tables, a transparent connection to the source AMRs does not exist. Thus, it is extremely difficult to ascertain the source of the various input parameters within this AMR, including their uncertainty.

As stated above, the AMR entitled *Evaluation of the Applicability of Biosphere-Related Features, Events, and Processes (FEP)* is intended to validate the biosphere model in accordance with AP-3.10Q. While the AMR concludes (Section 7.1) that the model is “appropriate and adequate for the intended use,” it does not assess the conceptual and mathematical uncertainties associated with the model. In addition, it cannot be determined if the independent technical review thoroughly reviewed the conceptual and mathematical representations since the only source of this information is the PMR, which was written based on the information contained in the supporting AMRs (essentially after the fact).

How the results (consumption habit distributions) documented in the *Identification of the Critical Group (Consumption of Locally Produced Food and Tap Water)* AMR are used in subsequent analysis is not transparent. The AMR presents a range of consumption habits for the residential farmer (critical group) in Tables 4 and 5 and Figures 1-10. This range represents variability within the critical group; the mean values presented in Table 4 are more for the “average member of the critical group.” The reader is left with the impression that the entire range is passed on to GENII-S. Only in the input section of the *Non-Disruptive Event Dose Conversion Factors* AMR (Table 1) can the reader find that the average was used to determine the BDCFs with no supporting text stating such in either AMR.

## **B. Abstraction Models**

For the nominal case, there are two subsequent AMRs that develop the abstracted models for use in TSPA. These are the *Distribution Fitting to the Stochastic BDCF Data* and *Abstraction of BDCF Distributions for Irrigation Periods* AMRs. The *Distribution Fitting to the Stochastic BDCF Data* AMR uses the “realistic representation” information from *Non-Disruptive Event Biosphere Dose Conversion Factors* AMR and fits the data to various statistical distributions. The rationale for choosing the reasonable representation BDCFs over the bounding BDCFs for ultimate incorporation into TSPA is not provided.

The  $\chi^2$  test is used to check goodness of fit and determine final distribution parameters. No uncertainty is assessed within the AMR beyond stating that input data has associated uncertainties. The *Abstraction of BDCF Distributions for Irrigation Periods* AMR derives final abstractions for the time evolution of the BDCFs due to radionuclide build-up effects in soil (includes build-up due to irrigation and loss due to soil erosion and leaching). Neither of these AMRs explicitly treat uncertainty, beyond providing probability distributions for the BDCFs that are ultimately used within TSPA. In addition, the AMR does not discuss any correlation between the BDCFs. However, the TSPA-SR indicates that all BDCFs used are correlated to that of Np-237.

The BDCFs computed in the *Disruptive Event Biosphere Dose Conversion Factor Analysis* AMR are not used in TSPA. Rather, a different set of BDCFs is used, computed with a 1 cm ash thickness for a transitional period following a volcanic eruption (those computed in the AMR are for steady-state conditions with an ash thickness less than 0.1 cm). As such, traceability of input information and uncertainties for the disruptive event scenario from the AMRs into TSPA is non-

existent. This information is only traceable from the TSPA-SR document (Section 3.10.3.4) through a data tracking number<sup>9</sup>.

### **C. Use in TSPA**

TSPA-SR Section 3.9.2 provides a very brief discussion of uncertainty in the biosphere modeling effort. Essentially, it states that some parameters are represented as probability distributions and some are fixed single values. Those that are fixed are either well known or can be shown to be relatively unimportant to the biosphere modeling. It further states that in general, for both fixed and distributed parameters, the assessment philosophy is to use generally conservative assumptions to ensure that the results are unlikely to underestimate the corresponding BDCFs.

Review of the AMRs seems to contradict these statements. Many of the fixed value parameters are not well known and are based on very limited and at times non-site specific information. Only in a small number of cases have the analyses shown a fixed parameter to be unimportant (e.g., crop hold-up time). The only sensitivity analyses documented are for uncertain parameters—those represented by probability distributions. Although the statement that a certain parameter value is not important may be true, a robust demonstration that several of the fixed parameters are unimportant has yet to be performed. As stated above, the reasonable representation BDCFs are used. Many of the input parameters used in the calculation of the BDCFs are reasonable estimates with some that could be argued as conservative. Given this, it appears that it cannot be quantitatively demonstrated that the resultant BDCFs used by TSPA are indeed conservative.

---

<sup>9</sup> DTN: MO0006SPAPVE03.001 (contains input transmittal, preliminary scoping calculation and results). The objective of this input transmittal is to provide Performance Assessment Department with the sets of Biosphere Dose Conversion Factors for the different environmental conditions following volcanic eruption than those considered in the *Disruptive Events Biosphere Dose Conversion Factor Analysis Analysis/Model Report* (AMR)



**Table 16-1: Biosphere Model Uncertainty Treatment**

<b>Model Purpose:</b> The purpose of the Biosphere Model is to determine BDCF for subsequent use in TSPA analyses. A BDCF is a multiplier that converts a unit concentration of a contaminant in a source (e.g., pumping and using contaminated groundwater) to an annual radiation dose received by a human from than unit dose. BDCFs are computed for the nominal and disruptive scenario in the form of probability distributions for a reasonable case and single values for a bounding case.				
Summary	Source	Treatment	Basis	Impact
<b>Conceptual Model Uncertainty</b>				
Biosphere Pathways Conceptual Model	<i>Biosphere</i> PMR (TDR-MGR-MD-000002) – Summarizes the biosphere conceptual model, primarily focusing on exposure pathways with limited discussion of concepts invoked at more of a "sub-model" level.	No conceptual model uncertainty treated. No alternative conceptual models treated.	The biosphere conceptual model is argued as being based on the pathways that remain from screening of Features, Events, and Processes ( <i>Evaluation of the Applicability of Biosphere-Related Features, Events, and Processes (FEP) (ANL-MGR-MD0-000011)</i> ). Thus, it could be argued that no uncertainty exists regarding pathways to consider. However, what is not discussed are concepts regarding radionuclide transport along these pathways and ultimate uptake by humans. Concepts regarding transport within these pathways appears to be left to the documentation of the representational model (GENII-S) while concepts regarding human uptake and fate is treated through dose conversion factors (which are chosen from literature based on regulatory requirements). In summary, since conceptual model uncertainty is not discussed, no basis is provided.	Possible impacts on the uncertainty in the resulting BDCFs.
Definition of Critical Group - Identify the critical group within the population in the vicinity of Yucca Mountain consistent with draft regulatory and subsequent DOE guidance.	<i>Identification of the Critical Group (Consumption of Locally Produced Food and Tap Water) (ANL-MGR-MD-000005)</i> - Primary sources of information to define the critical group are the 1996 Food Consumption Survey and the 1990 census. Draft regulatory requirements (40 CFR 191 and 10 CFR 63) and subsequent DOE guidance constrain the definition of the critical group.	The results of the food consumption survey were evaluated to identify a sub-set of the total survey population that corresponds to the critical group as defined in draft regulatory requirements and subsequent DOE guidance. The average member of the critical group was defined as an individual with characteristics that correspond to a residential farmer as identified in the 1997 food consumption survey. No uncertainty in this conceptual approach was treated (nor necessary).	The basis for defining the critical group exists in draft regulatory requirements and subsequent DOE guidance. This guidance and the information sources cited were used to define the critical group, consistent with this guidance. Parameters regarding the critical group may be uncertain, but draft regulatory guidance aims to preclude speculation regarding the critical group, thus minimizing uncertainties regarding the definition of the critical group.	The definition of the critical group influences the characteristics of the receptor (e.g., consumption habits) which can affect the resulting BDCFs.

<p>Groundwater Usage - Quantifies the annual volume of groundwater used by the farming community. Inherent in this range are various concepts regarding water usage by the farming community.</p>	<p><i>Groundwater Usage by the Proposed Farming Community (ANL-NBS-MD-000006)</i> - Utilizes 1990 census data, 1997 food consumption survey, and water usage data. Draft regulatory requirements and subsequent DOE guidance also define the size of the farming community.</p>	<p>Both conceptual model and scenario uncertainty are ultimately subsumed into a final parameter range of annual groundwater usage. All possible scenarios are presented and a final range is chosen.</p>	<p>Selected range is argued as being both consistent with the definition of the farming community and conservative with respect to possible scenarios and/or conceptual models regarding groundwater usage.</p>	<p>The annual water usage by the critical group (farming community) has a direct impact on the dose, as given by the following formula: Dose = BDCF * Mass Flux out of Saturated Zone / Annual Well Withdrawal Rate.</p>
<b>Representational Model Uncertainty</b>				
<p>GENII-S was chosen as the representational model.</p>	<p><i>Biosphere PMR (TDR-MGR-MD-000002)</i> – Provides rationale for choosing GENII-S (Section 3.2.1) and a limited discussion of the mathematics incorporated in the software (Section 3.2 and Appendix C).</p>	<p>No representational model uncertainty discussed.</p>	<p>No basis discussed.</p>	<p>Possible impacts on the uncertainty in the resulting BDCFs.</p>
<b>Parameter Uncertainty</b>				
<p>Consumption Habits - Identifies food and water consumption habits of Critical Group.</p>	<p><i>Identification of the Critical Group (Consumption of Locally Produced Food and Tap Water) (ANL-MGR-MD-000005)</i> - Primary sources are 1997 Food Consumption Survey and 1990 census.</p>	<p>Food and water consumption information from the survey is used to identify a range of consumption rates for the critical group (variability). Average values, representative of average member of the critical group, from these range are then used in subsequent GENII-S calculations documented in <i>Non-Disruptive Event Biosphere Dose Conversion Factors (ANL-MGR-MD-000009)</i> and <i>Disruptive Event Biosphere Dose Conversion Factor Analysis (ANL-MGR-MD-000003)</i> AMRs. It should be noted that it is not until reviewing these AMRs was it found that the average values were used. A statistical error associated with the consumption survey was identified (5%) for the entire population. However, no error associated with the reduced sample size that represents the critical group was discussed. Such a statistical error would translate directly into an uncertainty in the consumption habits for the average member of the critical group.</p>	<p>No basis discussed.</p>	<p>Including uncertainty in the consumption habits of the average member of the critical group would likely affect the BDCF ranges subsequently used by TSPA. The BDCF ranges used by TSPA are computed using average consumption habits for the average member of the critical group. Additional sensitivity analyses where consumption habits were allowed to vary, documented in <i>Non-Disruptive Event Biosphere Dose Conversion Factor Sensitivity Analysis (ANL-MGR-MD-000010)</i> and <i>Disruptive Event Biosphere Dose Conversion Factor Sensitivity Analysis (ANL-MGR-MD-000004)</i>, show that the BDCFs can be affected strongly by consumption habit uncertainty.</p>

Ingestion Exposure Parameters	<i>Identification of Ingestion Exposure Parameters (ANL-MGR-MD-000006)</i> - Based primarily on limited regional information and some assumptions needed for calculations.	Utilized regional information and subsequent ancillary calculations to determine parameter ranges and fixed values. Both probability distributions and single values determined. See the variability discussion below regarding some of the probability distributions.  Correlations between input parameters has not been assessed (some parameters may be correlated, but are treated as independent in subsequent AMRs).	Assumptions regarding usage of source data argued as being reasonable or bounding. The basis for choosing some fixed values is that uncertainty in the parameter is not critical (e.g., storage fractions, Section 6.10) or the selected value is conservative (dietary fraction, Section 6.11). Some of the fixed values are based on calculations using limited site-specific or regional information (irrigation rates for beef (alfafa) and poultry and eggs (corn); grow times for poultry and eggs (corn) (See Tables 2 and 7). These parameters are likely to be uncertain especially because of limitations in available data (one primary source is Hogan, E. L. (ed.) 1988. Sunset Western Garden Book. Menlo Park, California: Lane Publishing Co. TIC: 243490. The parameters for other vegetables and fruit utilize the same sources of information, however uncertainty ranges are provided - see variability discussion below.	Possible impact on resulting BDCF (unknown). Sensitivity studies documented <i>Non-Disruptive Event Biosphere Dose Conversion Factor Sensitivity Analysis (ANL-MGR-MD-000010)</i> and <i>Disruptive Event Biosphere Dose Conversion Factor Sensitivity Analysis (ANL-MGR-MD-000004)</i> , show that the ingestion of leafy vegetables is one of the primary exposure pathways. However, these sensitivity analyses also indicate that the variance in the BDCF ranges is not strongly influenced by uncertainty in ingestion exposure parameters (except for the crop interception factor) - however, see the discussion below regarding these sensitivity analyses - in results. Correlations between parameters could also affect resultant BDCF distributions.
Inhalation/Direct Exposure Parameters	<i>Input Parameter Values for External and Inhalation Radiation Exposure Analysis (ANL-MGR-MD-000001)</i> – Primary source information is regional data (mass loading) and 1990 census information (inhalation exposure time).	Defines probability distributions and single point values for various GENII-S input parameters (see entry on variability below). Note that GENII-S is unable to handle uncertainty in some of these parameters (e.g., chronic breathing rate).	Probability distributions defined from regional information and literature - ranges felt to be bounding (see discussion on variability). Fixed values are deemed conservative.	See discussion below (variability). Fixed values may overestimate the resultant BDCFs - degree is not known (although likely to be small).

<p>Environmental Transport Parameters</p>	<p><i>Environmental Transport Parameter Analysis (ANL-MGR-MD-000007)</i>. Non site-specific literature information used as the basis for defining parameter ranges and fixed values. Literature sources include NRC Regulatory Guides, IAEA Safety and Technical Reports, NUREGs, EPRI and AECL documents. Only one parameter, total suspended particulate matter (TSP), which was used to calculate the resuspension factor, was site-specific.</p>	<p>Utilize selection criteria to determine probability distributions and fixed values. Criteria are:</p> <ol style="list-style-type: none"> <li>1) Site-Specific data for a parameter value was used whenever it was available.</li> <li>2) If one parameter value appeared in more than half of the reviewed documents, it was considered that this generic value was agreed upon by the scientific community and represents the best available data. Thus, this value was selected for use. Basis – considered that this generic value is agreed by scientific community.</li> <li>3) GENII-S default value was selected if available literature data were not consistent. It was considered that no single agreed upon value was available to replace the default value.</li> </ol> <p>All parameters except one (crop resuspension factor) are represented by single point values chosen from literature with no assessment of uncertainty (beyond the determination of reasonable and bounding values). Uncertainty associated with using non site specific information is not explicitly assessed.</p>	<p>None provided beyond criteria.</p>	<p>Potential impact on BDCFs, possibly increasing range in BDCF distributions had uncertainty been taken into account in GENII-S inputs. It is not possible to quantify the impact since sensitivity studies cannot reveal importance of fixed parameters (see discussion in Results below).</p>
---	--	--	---------------------------------------	--

Transfer Coefficients	<i>Transfer Coefficient Analysis (ANL-MGR-MD-000008)</i> - Primary input source is "summary articles and comprehensive does assessment reports that included selection of input parameters". Clearly identified as not site specific and generic - "uncertainty associated with selected parameters could be very large."	Used following criteria for selecting transfer coefficients since "range of food transfer coefficients is quite large for some food types and elements." In order of preference:  1) If one single value appears in more than half of the number of reviewed documents, this values is selected. Basis – considered that this generic value is agreed by scientific community. 2) If one value appears in at least two recent published documents (after GENII-S in 1988), new value is selected. Basis – reflects recent studies. 3) If no single agreed value from available literature meets the above two criteria, a middle value is selected from all available data. Basis – None. 4) GENII-S default value is selected when only very limited literature data are available. Basis – None.  Single reasonable and bounding case values provided. Literature information used to define probability distributions (scale factors in GENII-S) for three transfer factors (soil-plant, animal uptake).	Basis for criteria discussed in treatment. There is no discussion of the uncertainty associated with the transfer coefficients associated with each reference source.  Basis for scale factor is literature information. It is argued that these ranges "should cover the uncertainty of (soil-to-plant or animal food) transfer factors." (Sections 6.2.5 and 6.3.5).	Potential impact on BDCFs. Sensitivity studies documented Non-Disruptive Event Biosphere Dose Conversion Factor Sensitivity Analysis (ANL-MGR-MD-000010) and Disruptive Event Biosphere Dose Conversion Factor Sensitivity Analysis (ANL-MGR-MD-000004) show that the ingestion of leafy vegetables is one of the primary exposure pathways. These sensitivity analyses also indicate that the variance in the BDCF ranges is influenced transfer factors (primarily disruptive event BDCFs). However, there are some limitations in the sensitivity studies (see results section below).
Dose Conversion Factors for ingestion and inhalation, dose coefficients for external exposure	<i>Dose Conversion Factor Analysis: Evaluation of GENII-S Dose Assessment Methods (ANL-MGR-MD-000002)</i> – Compares the DCFs for internal and external exposure used in GENII-S with other widely-accepted sets of dose conversion factors for confirmation.	In the case of DCFs for ingestion and inhalation, it was demonstrated that the DCFs within GENII-S are comparable with literature information (ICRP-30, 1979; Federal Guidance Report No. 11, 1988; 10 CFR 20). It was also determined that the GENII-S dose coefficients for external exposure should be replaced with more recent EPA compilation (Federal Guidance Report No. 11, 1993).	Demonstration that values chosen are consistent with other values used.	AMR does not discuss the uncertainty associated with the DCFs or dose coefficients chosen, nor comparison with more recent values. DCFs and dose coefficients are likely to be prescribed by regulations. In this AMR, these parameters are defined as single values (no uncertainty). Uncertainty in these parameters could result in significant uncertainty in the resultant BDCFs.

Erosion and Leaching Parameters	<i>Evaluate Soil/Radionuclide Removal by Erosion and Leaching (ANL-NBS-MD-000009)</i> – Site specific and regional information used.	Deterministic input parameters used to compute reasonable and bounding estimates of soil erosion rates and leaching rates.	Uncertainties associated with the calculation are clearly identified and discussed (Section 6.3).	Single value of soil erosion and leaching rates propagated into BDCFs abstracted into TSPA. Incorporating uncertainty (into reasonable case) may broaden BDCF distributions. Not possible to quantify impact. Note that GENII-S cannot represent this model as a probability distribution.
<b>Variability</b>				
Consumption Habits - Identifies food and water consumption habits of Critical Group	<i>Identification of the Critical Group (Consumption of Locally Produced Food and Tap Water) (ANL-MGR-MD-000005)</i> - Primary sources are 1996 Food Consumption Survey and 1990 census.	Food and water consumption information from the survey is used to identify a range of consumption rates for the critical group (variability). As discussed above, average values, representative of average member of the critical group, from these range are then used in subsequent GENII-S calculations documented in <i>Non-Disruptive Event Biosphere Dose Conversion Factors (ANL-MGR-MD-000009)</i> and <i>Disruptive Event Biosphere Dose Conversion Factor Analysis (ANL-MGR-MD-000003)</i> AMRs. This is appropriate when analyzing the effects to the average member of the critical group (although some uncertainty in the parameters could be included).	The basis is that the objective of the biosphere modeling effort is to determine BDCF ranges for the average member of the critical group - using the entire consumption habit ranges in the Monte Carlo computation of BDCF ranges would be inappropriately treating variability as uncertainty. However, as discussed above, there is uncertainty in these "average" parameters resulting from the statistical sampling techniques employed in the survey.	See discussion above regarding inclusion of uncertainty in the "average" consumption habits on the resultant BDCF.

<p>Ingestion Exposure Parameters</p>	<p><i>Identification of Ingestion Exposure Parameters (ANL-MGR-MD-000006)</i> - Based primarily on limited regional information and some assumptions needed for calculations.</p>	<p>In several instances, parameters for several different vegetables are used to define an uncertainty range (probability distribution). Examples include the irrigation time, irrigation rate, yield, and grow time for leafy vegetables (Sections 6.4, 6.5, 6.7, 6.8). For these parameters, the single value (note - no uncertainty) for each type of vegetable is used to define an uncertainty range for leafy vegetables (see AMR sections and Table 7).</p>	<p>When more than one value was available, an uncertainty range was defined.</p>	<p>This approach translates variability into uncertainty. It is unlikely that the average member of the critical group will grow only one type of vegetable for the entire duration of the simulation (which is done when treating the variability as uncertainty). It is more likely that the over time, the "true" value of such parameters will tend to be more the average values cited in the AMR (with some associated uncertainty due to limitations in site-specific data). Translating variability into uncertainty could possibly impact the variance in the resulting BDCF distributions. Sensitivity studies documented Non-Disruptive Event Biosphere Dose Conversion Factor Sensitivity Analysis (ANL-MGR-MD-000010) and Disruptive Event Biosphere Dose Conversion Factor Sensitivity Analysis (ANL-MGR-MD-000004), show that the ingestion of leafy vegetables is one of the primary exposure pathways. However, these sensitivity analyses also indicate that the variance in the BDCF ranges is not strongly influenced by uncertainty in ingestion exposure parameters (except for the crop interception factor) - however, see the discussion below regarding these sensitivity analyses.</p>
--------------------------------------	---	--	--	---

<p>Inhalation/Direct Exposure Parameters - determination of uncertainty ranges for mass loading and inhalation exposure time based variability in measurements.</p>	<p><i>Input Parameter Values for External and Inhalation Radiation Exposure Analysis (ANL-MGR-MD-000001)</i> – Primary source information is regional data (mass loading) and 1990 census information (inhalation exposure time).</p>	<p>Mass loading - PM<sub>10</sub> data from YMP site 9 was used. Twenty-four hour measurements of particulate matter less than or equal to 10 microns every six days from October 3, 1992 through December 30, 1997 were used to determine the uncertainty range. PM<sub>10</sub> measurements represent temporal variability in the parameter and not the uncertainty in the average value of the parameter over a given time period. Inhalation exposure time - values calculated for three lifestyle scenarios for the critical group were determining the uncertainty range (triangular distribution). Application of three scenarios results in variability in inhalation exposure time for random members within the critical group and not the uncertainty in the exposure time for the average member of the critical group.</p>	<p>Mass Loading - utilized entire range of measured data to compute probability distribution. Inhalation exposure time - set distribution (triangular) based on range of calculated values, argued as being a reasonable, conservative distribution.</p>	<p>Mass loading - Uncertainty range developed is likely to be larger than the uncertainty in the “true average” value of the mass loading factor over a given time period. Inhalation exposure time - It is also likely that the uncertainty range developed is larger than the “true uncertainty” in the inhalation exposure time for the average member of the critical group. It should be noted that in the computation of the BDCFs in Non-Disruptive Event Biosphere Dose Conversion Factors (ANL-MGR-MD-000009) AMR, a single value of this parameter was used (the mode of the triangular distribution).</p>
				<p>As such, no uncertainty in this parameter is carried forward into the calculation of BDCF distributions. Overall affect may be to broaden BDCF ranges. The Non-Disruptive Event Biosphere Dose Conversion Factor Sensitivity Analysis (ANL-MGR-MD-000010) AMR concludes that the resultant BDCF distributions for the nominal scenario are not affected significantly by changes in the mass loading factor (as such it could be argued that the nominal BDCFs are not sensitive to the inhalation exposure time as well). The Disruptive Event Biosphere Dose Conversion Factor Sensitivity Analysis (ANL-MGR-MD-000004) AMR indicates that the disruptive scenario BDCFs may be sensitive to such parameters. In this scenario, it is possible that the BDCF uncertainty range may be somewhat broader than would be realized had average values been used.</p>

**Results**

Results discussion	<p><i>Non-Disruptive Event Biosphere Dose Conversion Factors (ANL-MGR-MD-000009) and Disruptive Event Biosphere Dose Conversion Factor Analysis (ANL-MGR-MD-000003)</i> - Documents analysis, source information is all supporting AMRs that define GENII-S parameters.</p>	<p>Integrates all information into GENII-S input, document execution and present BDCF results - distribution for reasonable case, single value for bounding case.</p>	<p>Basis is selection of GENII-S as appropriate representational tool and data input AMRs.</p>	<p>Computation of BDCFs for subsequent abstraction / use in TSPA. Note that any correlations between input parameters is not explicitly discussed.</p>
Sensitivity Analyses	<p><i>Non-Disruptive Event Biosphere Dose Conversion Factor Sensitivity Analysis (ANL-MGR-MD-000010) and Disruptive Event Biosphere Dose Conversion Factor Sensitivity Analysis (ANL-MGR-MD-000004)</i> - source information is all supporting AMRs that define GENII-S parameters.</p>	<p>Recompute BDCFs for reasonable case, allowing parameters related to consumption habits to vary (held fixed in computation of BDCFs for TSPA). Applied regression techniques to identify those input parameters that most affect variance in resultant BDCFs. Also identify those pathways that contribute most to overall BDCF.</p>	<p>None.</p>	<p>The AMRs include no discussions regarding the impact of fixed parameters (this cannot be accomplished through regression analysis). Thus, it cannot be determined how any of these fixed parameters would affect the BDCFs nor can the level of conservatism in the BDCFs be assessed. This is most important when the single value input parameters that may not be conservative (e.g., environmental transport factors).</p> <p>Consumption rates are fixed for the purpose of computing BDCFs for TSPA use. However, the two sensitivity analysis AMRs consider them as uncertain and re-calculate the BDCFs. The subsequent results indicate that the variance in the consumption rates is significant in explaining the variance in the BDCF distributions. At issue is the fact that the sensitivity study does not fully explain the factors that dominate the variance in the BDCFs used in TSPA. The variance in the consumption habit parameters may be masking the importance of other uncertain parameters.</p>

<p>Astraction</p>	<p><i>Distribution Fitting to the Stochastic BDCF Data (ANL-NBS-MD-000008) and Abstraction of BDCF Distributions for Irrigation Periods (ANL-NBS-MD-000007) – Source information used in final abstraction for TSPA are Non-Disruptive Event Biosphere Dose Conversion Factors (ANL-MGR-MD-000009) and Evaluate Soil/Radionuclide Removal by Erosion and Leaching (ANL-NBS-MD-000009).</i></p>	<p>The chi-square test is used to check goodness of fit and determine final distribution parameters. No uncertainty is assessed within the AMR beyond stating that input data has associated uncertainties. The Abstraction of BDCF Distributions for Irrigation Periods AMR derives final abstractions for the time evolution of the BDCFs due to radionuclide build-up effects in soil (includes build-up due to irrigation and loss due to soil erosion and leaching).</p>		<p>The treatment of uncertainty is not explicitly assessed, beyond providing probability distributions for the BDCFs that are ultimately used within TSPA. Correlations that may exist and could result in a direct impact on the uncertainty in the ultimate receptor dose are not discussed.</p>
-------------------	--	---	--	--

## 17.0 Integrated Site Model (ISM)

### 17.1 Purpose

The purpose of the ISM is to provide a common framework of stratigraphy, rock properties, and mineralogy for subsequent process and performance assessment modeling. The process models include groundwater flow and transport in the UZ and SZ, which in turn are used in the TSPA. The ISM also supports repository design activities.

The ISM is a set of static representations that provide 3D computer representations of site geology, selected hydrologic and rock properties, and mineralogical-characteristics data. The ISM is based on three component models: the GFM, the Rock Properties Model (RPM), and the Mineralogic Model (MM). Each model was developed using unique methodologies and inputs, and the determination of the modeled units for each of the components is dependent on the requirements of that component. Following a summary of the component models, the uncertainties and limitations of each of the models is addressed.

### 17.2 Model Component Relations

The ISM PMR (TDR-NBS-GS-000002) and the supporting AMRs comprise the documentation of the ISM. The purpose of the PMR and AMRs are as follows:

- *Integrated Site Model PMR* (TDR-NBS-GS-000002) – Summarizes the sources of data, methodologies used to construct the model components, and the modeling results, uncertainties, and limitations of each of the component models.
- *Geologic Framework Model* (MDL-NBS-GS-000002) – Documents the current version (Version 3.1) of the GFM (GFM3.1) with regard to data input, modeling methods, assumptions, uncertainties, limitations, validation of the model results, qualification status of the model, and the differences between Version 3.1 and previous versions. The GFM provides a three-dimensional representation of the stratigraphy and structural features within a model domain that extends vertically from land surface to the deep-lying Tertiary-Paleozoic unconformity and laterally over an area of approximately 65 square miles (170 square kilometers) that encompasses the layout of the potential repository. The GFM was constructed from geologic map and borehole data. The boundaries of the GFM were chosen to encompass the most widely distributed set of exploratory boreholes (the water table or WT series). Additional information used to construct GFM was taken from measured stratigraphic sections, and gravity and seismic profiles.
- *Rock Properties Model* (MDL-NBS-GS-000004) – Provides documentation of the latest version of the RPM 3.1 with regard to input data, model methods, assumptions, uncertainties, and limitations. The RPM is a 3D, discretized numerical representation of spatial variability and heterogeneity of a number of fundamental bulk and hydrologic material properties for the majority of rocks within the UZ at Yucca Mountain. The model volume includes four internally lithologically similar model units: the PTn, the TSw, the CHn, and the Prow Pass Tuff. For all four model units, the modeled parameters are matrix porosity, whole-rock bulk

density, and matrix saturated hydraulic conductivity. For the TSw model unit, additional material properties include lithophysical porosity and whole-rock thermal conductivity. The rock properties model is tied geometrically to the bounding surfaces of model units within the GFM 3.1.

- *Mineralogical Model* (MDL-NBS-GS-000003) – Documents the current version (MM3.0) of the MM with regard to data input, modeling methods, assumptions, uncertainties, limitations and validation of the model results. Version 3.0 of the MM was developed from mineralogical data obtained from borehole samples. It consists of matrix mineral abundances referenced to the stratigraphic framework defined in GFM3.1. The MM was constructed using the software STRATAMODEL. STRATAMODEL performs distance-weighted interpolations of borehole data within the stratigraphic units specified by the framework to produce a volumetric distribution of the mineralogic properties associated with each stratigraphic horizon. The MM provides the abundance and distribution of 10 minerals and mineral groups within 22 stratigraphic sequences in the Yucca Mountain area for intended use in transport modeling and repository design. The data inputs for the MM consist of stratigraphic surfaces from GFM3.1, quantitative XRD analyses of mineral abundances, and the potentiometric surface.

Figure 17-1, Integrated Site Model Relation Diagram, shows the interrelationships of the component models of the ISM and the downstream models and users. The ISM merges the detailed project stratigraphy into model stratigraphic units and properties, for direct input to the primary subsequent models and repository design, including the UZ and SZ groundwater flow and radionuclide transport models. The UZ/SZ models and repository design, in turn, are incorporated in the TSPA. Figure 17-2, Integrated Site Model Structure Diagram, depicts the various data inputs to the ISM for the component models. The result is the static 3D representation of site geologic, rock property, and mineralogical characteristics and their spatial variabilities. Intended applications of the ISM are to repository design and the UZ/SZ flow and transport models for use in TSPA.

### **17.3 Uncertainty Treatment in the ISM**

Sections 3.2, 3.3, and 3.4 of the ISM PMR contain summaries of the GFM, RPM, and MM treatments of model uncertainties, as well as discussions about alternative interpretations of the data and model validation. The following discussion is taken from the PMR and component AMRs.

#### **A. GFM**

The GFM is a description of the distributions of rock layers and faults in the subsurface of Yucca Mountain. The model was constructed as a volume model based on the additive application of individual geologic unit thicknesses. Isochores (unit thickness measured vertically) are the fundamental building blocks of the GFM; individual isochors are constructed primarily on the basis of borehole and surface geologic mapping data. Interpretative constraints consistent with known site geologic processes were applied to guide the shapes of the isochores.

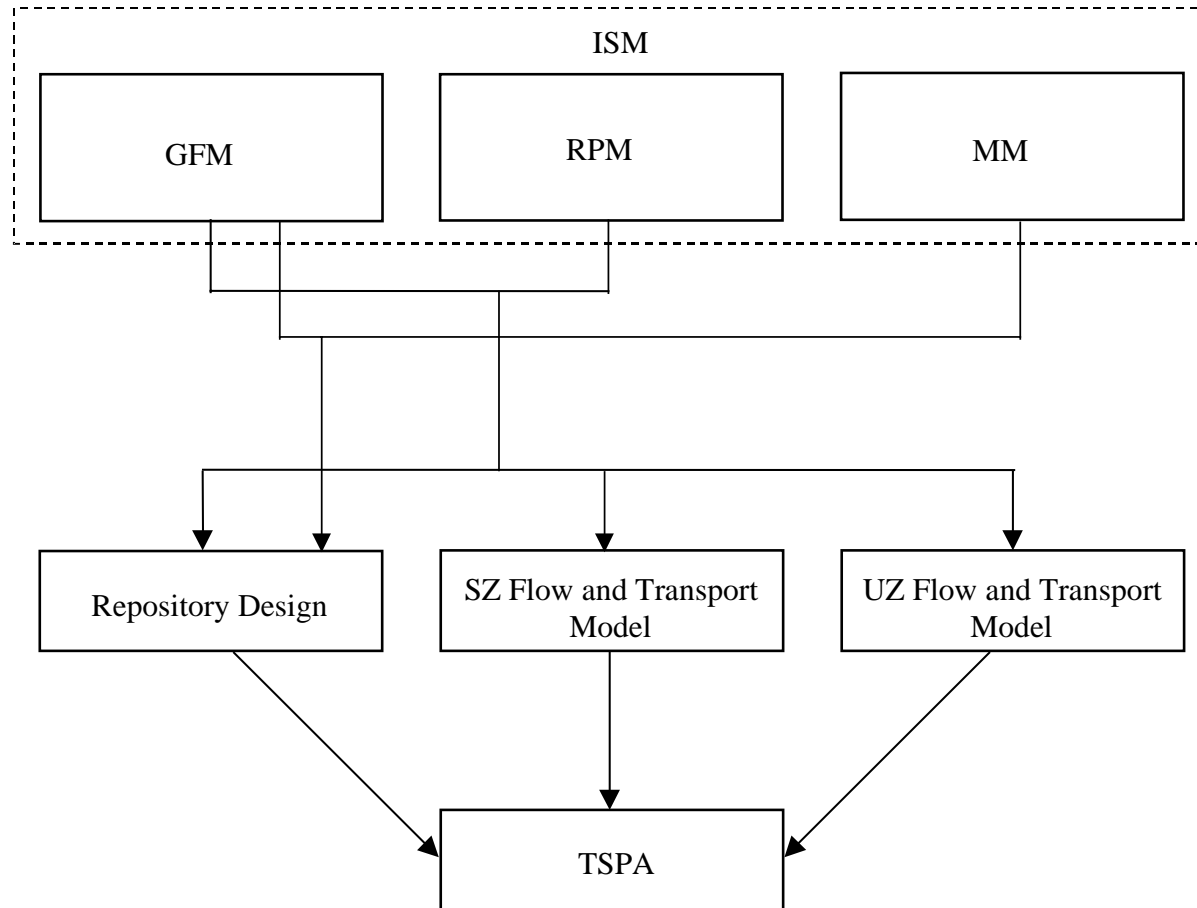


Figure 17-1: Integrated Site Model Relation Diagram

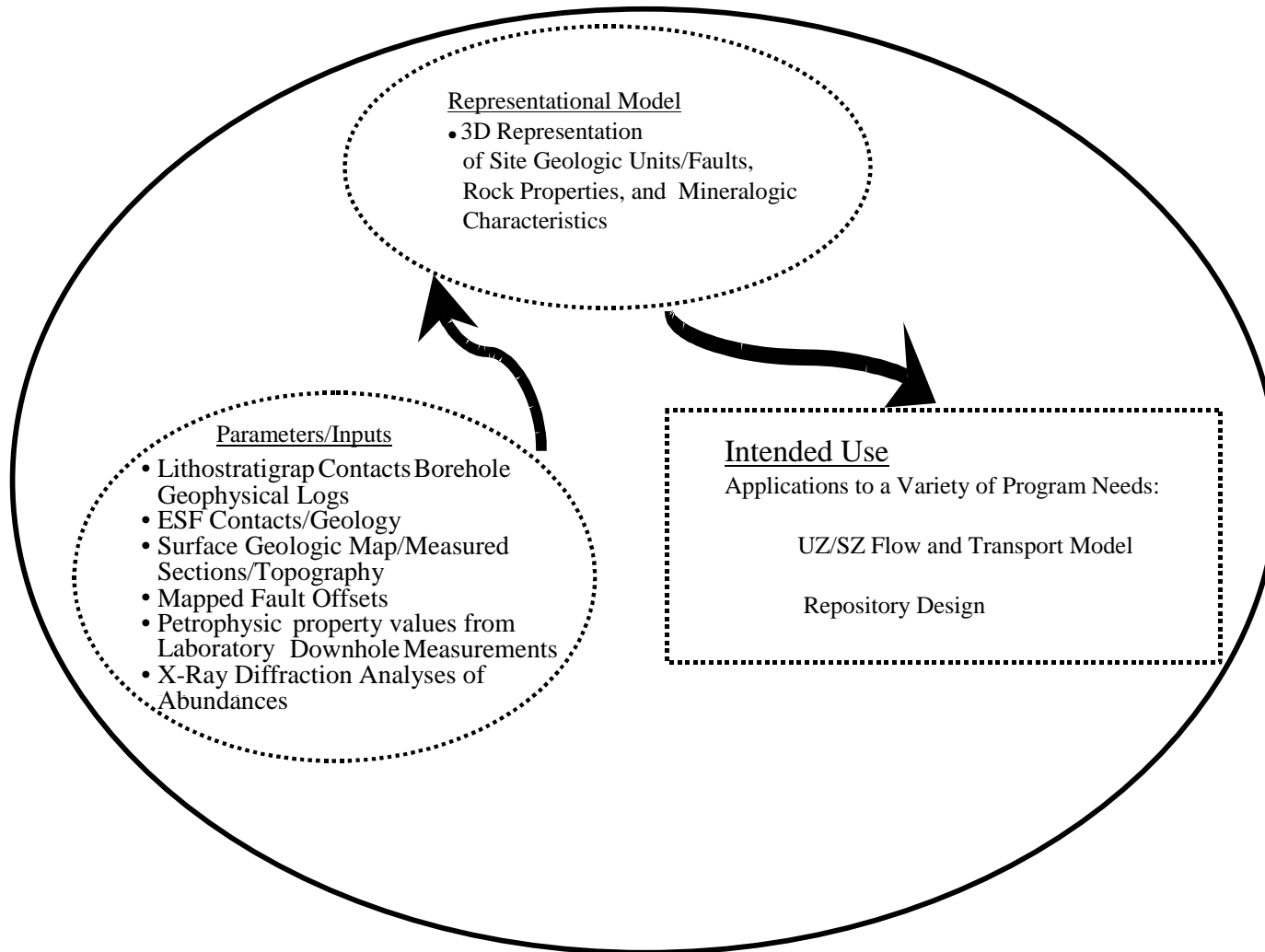


Figure 17-2: Integrated Site Model Structure Diagram

For GFM, uncertainty is an estimation of how closely the modeled contacts of rock units and structural features match their locations determined from boreholes and geologic maps. The primary factor affecting uncertainty in the GFM is distance from the data points. Because borehole data are restricted in depth, uncertainty increases with vertical distance below the boreholes and in horizontal distance away from them. In addition, interpretations regarding deeper rock units, which have fewer borehole penetrations, have more uncertainty associated with them than uncertainty associated with shallower rock units. Rock layers near the surface are constrained by data from geologic mapping.

Because of the faulting and tilting of the rock layers in much of the modeled area and the sparseness of data, geostatistical techniques were not used to estimate the uncertainty in the model. Instead, methods that examine the modeling process were used to determine the amount of uncertainty associated with gridding, contouring, interpreting, and interpolating. The details of these methods are provided in Section 6.5 and Attachment II of the *Geologic Framework Model (GFM3.1)* AMR.

The most uncertain areas in the model are its four corners and the volume deeper than the borehole penetrations. For locations between boreholes in the central part of the model (the constrained areas), model predictions are expected to fall within maximum vertical ranges (windows of uncertainty) as defined in Section 3.2.5 of the ISM PMR.

One of the principal areas of uncertainty is the depth to the Tertiary-Paleozoic unconformity. Only one borehole within the model area penetrated the unconformity (borehole p#1).

The GFM was validated by predicting the subsurface geology for two boreholes (SD-6 and WT-24) and the ECRB Cross-Block Drift. SD-6 and the Cross-Block Drift are located within relatively well constrained areas. WT-24, on the other hand, is located outside the area constrained by numerous boreholes. The predictions were made using GFM3.0, which was completed before the boreholes and the Cross-Block Drift. The results of the test were that the predictions for SD-6 and the Cross-Block Drift illustrated the predictive capability of the model and the model uncertainty in an area constrained by borehole data. Predictions for WT-24, while less accurate, were illustrative of model uncertainty in a less constrained area. GFM3.0 was subsequently updated to incorporate the new information from the boreholes and the Cross-Block Drift and was designated GFM3.1.

## **B. RPM**

The RPM is a description of the distributions of rock material properties, including matrix porosity, whole-rock bulk density, matrix-saturated hydraulic conductivity, lithophysal porosity, and whole-rock thermal conductivity for many of the stratigraphic units described in the GFM. A key assumption in the RPM is that there is a correlation between porosity and other rock properties, and that this correlation can be used to derive other input data using “porosity as a surrogate.” These derived data are bulk density, hydraulic conductivity, and thermal conductivity.

Geologic studies of the volcanogenic rocks at Yucca Mountain, and of similar deposits elsewhere in the world, indicate that the geologic processes responsible for deposition of these materials vary temporally and areally. For example, variations in cooling rates caused by local conditions affect the material properties in the resultant rocks. This spatial variation of geologic processes has produced spatial heterogeneity of material properties in all three dimensions. However, the spatial distribution of material properties within geologic layers is not simply random. Knowledge of rock property values at one location imposes limits on the values of those properties likely to exist at nearby locations.

Uncertainty associated with material properties is summarized in Section 3.3.3.4.2 of the ISM PMR and explained in detail in Section 6.6 of the *Rock Properties* AMR. An uncertainty model was generated for each material property-modeling unit combination by computing the node-by-node standard deviations for each set of 50 replicate models. The 50 replicate models are statistically indistinguishable models of porosity for each model unit and 50 replicate models for each one of the derivative properties (bulk density, matrix-saturated hydraulic conductivity, and thermal conductivity). Because there are few, if any, objective differences to distinguish the members of each suite of simulated property models, it follows logically that the variability among members of a suite represents an empirical estimate of the geologic uncertainty associated with each material property. Geologic uncertainty, in this context, is defined as the uncertainty that results from the inability to sample every point in a geologic system. This process produces uncertainty models that are themselves spatially heterogeneous. By theory and in practice, variability among simulations-and uncertainty, as defined by the standard deviation-is small in close proximity to measured values. Variability among simulations and uncertainty are high at great distances from measured data, or in the vicinity of conflicting measured values.

### **C. Mineralogic Model**

Uncertainties associated with the MM are discussed in Section 3.4.5 of the ISM PMR and Section 6.4 of the *MM* AMR. Some of the more significant observations relating to model uncertainty are:

- The basic mineralogic data for the 65.7 square mile area of the model come from 24 boreholes, most of which are confined to the central portion of the model.
- Scarce mineralogic data in the boundary regions of the model, particularly along the western boundary, impose limitations on the model resolution in these regions.
- The location of the transition from vitric to zeolitic in the Calico Hills Formation is uncertain.
- It is unclear whether the depth to zeolitization decreases rapidly and smoothly along a well-defined front, or whether the zeolitized zones are interfingering with vitric zones along a highly irregular front.
- Quantitative mineralogic data from several boreholes were obtained primarily from cuttings rather than cores. Drill cuttings have a tendency to average mineral abundance

over a finite depth range, and more consolidated rock fragments may be over-represented with respect to the softer, more friable rock fragments. The author notes that it is difficult to predict the magnitude of the potential error without obtaining additional mineralogic data.

The uncertainty treatment in the MM AMR is largely qualitative, based on the observations noted above about the weaknesses of the data set in different locations of the model volume. In Section 6.4.1 of the MM AMR there are discussions about possible methods to improve the MM. One of the approaches involves the development and refinement of a method of correlating the more abundant geophysical well-log data with mineralogic data, providing a means of constraining and improving the accuracy of the zeolite modeling throughout the exploratory block. Another improvement involves incorporating steeply dipping faults in STRATAMODEL.

MM model validation is described in Section 6.5 of the AMR. One criterion described in some detail involves comparing predicted mineral-abundance values for each of the ten mineral groups in the model with mineral-abundance values measured in boreholes. The model was tested for a unit having relatively uniform mineralogy (the middle nonlithophysal zone of the Topopah Spring tuff) and for a unit having distinctly varying mineralogy (the upper part of the Calico Hills Formation). Borehole data were used to construct the average, standard deviation, minimum, and maximum of the input data. For both units, the results were that the predicted values are within one standard deviation of the average values determined at adjacent boreholes.

#### **17.4 Conclusions**

The treatments of model uncertainty for both the GFM3.1 and RPM3.1 are well documented in the respective AMRs and summarized in the ISM PMR. Both treatments are rigorous and provide quantitative estimates of the uncertainties in the three-dimensional distribution of stratigraphic contacts and rock properties. In contrast, the uncertainty treatment for the MM3.0 is largely qualitative, based primarily on observations of the weaknesses in the existing data sets relative to the model volume.

**Table 17-1: Integrated Site Model**

<b>Model Purpose:</b> The purpose of the ISM is to provide a common framework of stratigraphy, rock properties, and mineralogy for input to the UZ and SZ flow and transport models and repository design.				
<b>Summary</b>	<b>Source</b>	<b>Treatment</b>	<b>Basis</b>	<b>Impact</b>
<b>Representational Model Uncertainty</b>				
Model construction <b>The basis for identification of the associated uncertainty is the appropriateness of the model construction approach.</b>	The methodology for constructing the ISM three-dimensional grid is described in Section 3.2.3.2 of the <i>Integrated Site Model</i> PMR.	The methodology for constructing the three-dimensional framework for the ISM included a combination of mathematical grid construction and the application of interpretative constraints in the form of augmenting contour segments. This approach allowed for interpretations based on geologic inferences to guide the gridding in areas where the data are sparse or where a grid generated by the modeling algorithm may be inconsistent with the conceptual geologic model.	The gridding method used is based on a <i>minimum tension</i> mathematical algorithm that calculates a surface passing through the input data. For every grid in the model, the minimum tension algorithm is constrained by field data (from boreholes, tunnels, measured sections, or the geologic map) and interpretive constraints in the form of contour segments.	Not discussed
<b>Parameter Uncertainty</b>				
GFM <b>The basis for identification is the appropriateness of the treatment.</b>	Uncertainties inherent in the GFM are discussed in Section 3.2.5 of the <i>Integrated Site Model</i> PMR and in Section 6.5 of the <i>Geologic Framework Model</i> AMR.	Faulting and tilting of rock layers in much of the model area and the sparseness of data dictated the use of methods that examine the modeling process to determine the amount of uncertainty associated with the gridding, contouring, interpreting, and interpolating.	Knowledge of the subsurface is defined by the number, areal distribution, and depth of penetration of boreholes and the volume of rock intersected by tunnels. For the modeled region at Yucca Mountain, approximately 1 percent of the subsurface volume (measured to the depth of the deepest borehole, 1830 meters below ground surface) is within 150 meters of a borehole or tunnel.	Section 6.5.1 of the <i>Geologic Framework Model</i> AMR discusses the uncertainties in the elevations of lithologic units resulting from the three-dimensional distribution of available data.

<p>RPM Appropriateness of treatment.</p>	<p>Uncertainties associated with the RPM are discussed in Section 3.3.3.4.2 of the <i>Integrated Site Model</i> PMR and in Section 6.6 of the <i>Rock Properties Model</i> AMR.</p>	<p>Section 6.6 of the RPM AMR includes detailed discussions of the treatment of uncertainty for this model. This section describes a number of limitations of both methodology and data that detract from the exactness or accuracy of the models generated by the analysis in the RPM AMR. The results of a stochastic uncertainty analysis is presented which attempts to quantify rigorously the geologic uncertainty that results from sparse data.</p>	<p>There are a number of factors affecting the analysis in the RPM that are best described as limitations of the data or the modeling process itself. These limitations include errors and biases in the sample data used in the analysis, the methodological use of porosity as a surrogate for other material properties, the combination of numerous lithostratigraphic units into four major modeling units, and the effect of geologic departures from the assumptions inherent in the use of the stratigraphic coordinate system adopted in the analysis.</p>	<p>The impact of "uncertainty" on the downstream usages of the RPM are well-described in Section 7.3 of the <i>Rock Properties Model</i> RPM.</p>
<p>MM <b>Lack of quantitative treatment is the basis for this component of the ISM.</b></p>	<p>Uncertainties associated with the MM are discussed in Section 3.4.5 of the <i>Integrated Site Model</i> PMR and in Section 6.4 of the <i>Mineralogical Model</i> AMR.</p>	<p>No quantitative treatment in the AMR.</p>	<p>Different reasons for uncertainty are (1) striking geographic differences in mineral abundances that relate to geologic processes, (2) borehole data not adequate for determining the precise location of the transition from vitric to zeolitic Calico Hills Formation, and (3) data obtained from cuttings rather than cores, where cuttings have a tendency to over-represent more consolidated rock samples.</p>	<p>Discussion of limitations of the MM in Section 6.4.1 of the AMR but no discussion of impact of uncertainties (particularly no quantitative estimates ) to downstream users.</p>

INTENTIONALLY LEFT BLANK

## 18.0 Summary, Conclusions, and Recommendations

The TSPA-SR integrates and analyses a very large array of types of technical information. The breadth, complexity, and interdependency of this information base presents the reviewer of the TSPA-SR with a formidable task. The YMP has developed a suite of documents that attempts to organize and present this information in a way that is transparent and understandable to the general technical community. These are difficult goals to achieve. Over the past decade a number of PAs have been conducted, by the YMP and others, but none have addressed as complex or broad range of information as the TSPA-SR.

This internal assessment was conducted by a team of YMP technical specialists who were generally not involved in the development of the documents. The primary objective of the assessment was to review and evaluate the uncertainty treatment in this suite of documents. There are clearly areas where the YMP can and should improve the treatment of uncertainty and how it is documented. This report includes recommendations on how to reach that goal for the TSPA-License Application. It is important to note that the current suite of documents includes some very good treatments of uncertainty, and these are identified in our conclusions to serve as examples for other areas of the YMP.

A number of conclusions and recommendations have been developed as a result of this document review. Several of our conclusions are similar to conclusions reached by recent reviews of PAs for other applications (NEA 1997, Andersson 1999). The review included summary descriptions of the discussions of uncertainty contained in the AMRs and PMRs, as well as descriptions of the actual treatment of uncertainty in the work that is reported in the documents. In addition to covering the uncertainty treatment documented in the AMR/PMR, this work also reviews the incorporation of spatial and temporal variability into the models. If these aspects are not incorporated explicitly into the process models, then they represent additional sources of uncertainty because the potential site is a spatially heterogeneous and evolving system.

In order to understand uncertainty treatment it is necessary to understand how the models are constructed, how data inputs are identified, and how parameter values are developed. These steps are an integral part of the scientific analysis that underlies the model development that supports the TSPA. There are potential uncertainties related to each of these steps, and potential uncertainties that are related to interdependencies between the steps. For these reasons, issues related to transparency and traceability are central to any analysis of uncertainty treatment. The issues related to transparency and traceability are even more important to analysis of uncertainty propagation through the TSPA hierarchy. Consequently, some of the conclusions and recommendations developed in this report address uncertainty treatment specifically and some address related issues of transparency and traceability.

The review of how uncertainty was addressed in the Rev. 00 documentation supporting the TSPA-SR involved a four-step process. 1) Initially a suite of process models was

identified and the relations of these models to the AMRs and to each other were determined. These relations are presented in the Model Relation Diagrams contained in the individual chapters of this report. 2) Next the internal structure of key models was developed. For each such model this involved the identification of the conceptual model(s) that describe the process, the parameters/inputs that support the model, the representational model that implements the conceptual model, and the model results for downstream use, particularly TSPA. This information is summarized on the Model Structure Diagrams that are included in each chapter of this report. 3) The identification and evaluation of uncertainty treatment and incorporation of variability, which is the main objective of this study, was summarized in uncertainty/variability tables that are organized around the elements of the Model Structure Diagrams. These tables are also included in the individual model chapters of this report. 4) The final step in the review involved evaluating the propagation of uncertainty through the suite of process models and into PA.

### **Summary of Observations Related to the Model Relation Diagrams**

The first step in understanding the technical basis for TSPA-SR, and the aspects related to that basis such as uncertainty treatment, is to understand the interrelations of the process models supporting the TSPA. The TSPA-SR document includes figures that illustrate the direct feeds to the TSPA, but similar figures for the underlying process models generally do not exist. Some of the PMRs contain very good figures, such as the UZ F&T, SZ F&T, WAPDEG, and Waste Form Degradation PMRs. Another basic problem for understanding the YMP's treatment of uncertainty is the difficulty in tracing information between AMRs. The primary problems are the use of input transmittals, via AP-3.14Q, *Transmittal of Input*, and the direct reference to Data Tracking Numbers without discussion of the data sources and selection. These activities are consistent with current YMP procedures. However, it is problematic for a reviewer since the reviewer may not have the complete understanding of past work and available information that is needed to evaluate the selection and use of input data. Effective implementation of AP-SIII.4Q, *Development, Review, Online Placement, and Maintenance of Individual Reference Information Base Data Items*, would go a long way toward improving this situation.

In some cases AMRs report models and analyses that are used only to support FEPs screening and do not support direct feeds to the TSPA. This is an important function because the YMP needs a firm basis for including or excluding a FEP from the TSPA nominal case. However, if it is not clear what the role is for a particular AMR it can be very confusing for the reader. The model relation diagrams provide a tool to illustrate these roles and improve transparency.

Another area where the model relation diagrams can improve transparency is the illustration of interrelations of models and submodels. In some cases models are developed for the sole purpose of developing feeds to other models that are themselves feeds to TSPA. The NFE area has good examples of this, where the ambient THC model is developed to provide input to the THC seepage model. A good example of submodels

being incorporated into a larger process model is the SZ Transport model. Submodels for dispersion and matrix diffusion are incorporated into the site-scale model for SZ Transport. These relations are important for transparency and the model relation diagrams provide a good vehicle to illustrate the relations.

### **Summary of Observations Related to the Model Structure Diagrams**

The model structure diagrams provide a tool for identifying the elements of a particular model. The categories of uncertainties provide a logical structure that allows the reader to identify what information is most important to the validity of the model results. The diagrams provide a framework for uncertainty identification and discussion.

Classification of the uncertainties allows for more systematic discussion and evaluation of the uncertainties and allows for the evaluation of the impacts of the uncertainties on the other parts of the model. As with any tool there are pros and cons associated with its use. The most important benefit is that the diagram provides a good way of organizing information about the model and presenting the information in a logical way to the reader. The biggest disadvantage of the tool is that use of the categories can lead to arbitrary distinctions in some cases.

Conceptual, representational, and parameter uncertainties are the categories used to develop the diagrams. There are a number of different ways that model elements could be categorized, as discussed in the introduction. The important question is, what is a useful way of presenting the information on the elements of the model? The structure chosen was found to be useful for understanding the models that support TSPA-SR. Development of the diagrams facilitated the transparency and understanding of the construction and implementation of the models.

In some cases, more or less arbitrary distinctions must be made when assigning items to the categories developed for the model structure diagrams. For example, the evaluation of the equivalent continuum and dual continuum representations could be categorized under either the representational or the conceptual category. The determination of some parameter values is based on how the process is conceptualized, such as for thermal conductivity or van Genuchten parameters.

### **Summary of Observations Related to the Uncertainty Review**

#### **Parameter Uncertainties**

Parameter uncertainty treatment is relatively straightforward. There are well established techniques for error analysis on data that are used to determine parameter values. There are a number of areas reviewed in which these techniques have been applied, and the parameter uncertainty treatment is robust. Excellent examples of parameter uncertainty treatment can be found in the *General Corrosion and Localized Corrosion of Waste Package Outer Barrier* and *General Corrosion and Localized Corrosion of the Drip Shield* AMRs. Disruptive events is another area where parameter uncertainty has received robust treatment and is well documented.

The treatment of parameter uncertainty in YMP technical documents could be improved by rigorous extension of a data distinction identified in AP-SIII.3Q, *Submittal and Incorporation of Data to the Technical Data Management System*. This procedure distinguishes between acquired data and developed data.

**Acquired Data**-Data that are obtained as a result of a data-gathering activity (QARD). Acquired Data may be procured or obtained from outside YMP sources or recorded as a result of a YMP field or laboratory data-gathering activity. YMP field or laboratory data recorded as raw data but converted to scientific or engineering terms is acquired data.

**Developed Data**-The results of reducing, analyzing, or interpreting data after data acquisition (QARD).

When these different types of data are used to establish parameter values, this distinction needs to be maintained. For parameters that are based on data that can be measured directly, at the appropriate scale, the uncertainty treatment could include discussions of measurement errors, representativeness, and related issues. These uncertainties should be adequately treated by the use of standard procedures, such as American Society for Testing and Materials procedures, or YMP technical procedures, and reference to those procedures should be all that is required in YMP documentation. Standard error analysis of measured parameter values is important to document and parameter distributions should be developed and analyzed whenever possible. Uncertainty treatment for “developed parameters,” based on developed data, is more complicated. These developed parameters have their values derived via some interpretive or analytical process involving scaling to appropriate dimensions, such as laboratory measurements of hydrologic properties, or conceptualization in terms of a model, such as incorporating lithophysal cavities into values for thermal conductivity. Error analysis of the values used for developed parameters is important, but it is also important to evaluate and discuss the uncertainties associated with the model and/or analysis bases for the parameter value. This is an area where it is particularly clear that transparency and traceability issues impact our understanding of uncertainty treatment. If the only uncertainty treatment is a statistical analysis of parameter values, the uncertainty that may impact the results because of way that the process is conceptualized is lost to view. This is not to say that the principal investigators are not aware of this source of uncertainty, but only that it is difficult for the reviewer to understand uncertainty treatment if this aspect is not specifically discussed in the documentation. The discussion of parameter uncertainty would be much more transparent if the distinction between measured and developed parameters was used systematically.

The treatment of parameter uncertainty is more complicated in the UZ modeling area because of the use of the inverse modeling approach to develop the full range of parameters needed for the site scale flow model. The data inputs and analysis technique is described well in the UZ AMRs and is reviewed in the chapter on UZ Flow Models.

Treatment of uncertainty in the WP degradation area is very good at the process model level, but is very complicated and unclear as it is propagated into WAPDEG.

There are a number of cases in the AMRs where parameter uncertainty is not characterized and a parameter value is chosen which is thought to be a bounding value. In some cases there is a clear explanation provided for the choice of the bounding value, but in many cases the explanation is less clear. The explanations could be improved by clearly identifying the logic for characterizing the representation as a bound. This logic could include a qualitative discussion or quantitative assessment of the potential impact of the choice. The logic could also include a discussion of data and/or models that are relevant to the bound. Neptunium solubility is a good example where a bounding value is chosen and justified, but there is no evaluation of the potential impact of the introduced uncertainty. Similarly, the sorption coefficient for all radionuclides in fractures is assumed to be zero. This is clearly bounding but the potential impact of this conservatism is not evaluated or discussed in sufficient detail. Seep flow rates, from the drift-scale seepage model, are increased 55 percent as an adjustment for drift degradation and rock bolts, which is considered to be bounding. These examples are generally explained well and justified on the basis of data, but the impacts are not evaluated. These are the types of issues that make it difficult for reviewers to understand and evaluate the process model and TSPA results. These types of issues also reduce transparency and traceability.

### **Representational Model Uncertainties**

In this report a number of things are included within the category of representational model. The mathematical formalism, such as Darcy's Law or Fick's Law, that is used to represent the natural processes; the numerical techniques such as finite element or finite difference that are employed to deliver a quantified output; and the representation of the process using the numerical technique, such as equivalent continuum or dual permeability are all considered within the category of representational model.

There are two different aspects of the uncertainties related to the representational model. One is the mathematical aspect that involves how well the model produces a quantitative result, and the other is the aspect of how well the model approximates the natural system. The mathematical aspect can be very straightforward. It may be as simple as determining if a computer program is calculating the correct answer for a diffusion equation. It may be more complicated, however, if the model involves submodels embedded within a larger model. The SZ transport model is an example of this situation, with models for matrix diffusion and dispersion embedded within the site-scale model. The *Saturated Zone Transport Methodology and Transport Component Integration* AMR presents the calculations that evaluate this aspect of the representational model and is an excellent example of how this issue should be addressed.

The AMRs supporting the NFE include a number of representational models, including models based on the NUFT and TOUGH2 codes. These models were evaluated using results from the in-situ thermal tests. The analysis found that there was essentially no

difference as long as the conceptual model selected for implementation and the model input parameters are the same. This is an excellent example of comparative evaluation alternative representational models using field data.

The AMRs supporting the UZ transport model include comparisons of FEHM dual-continuum PT, advection-dispersion equation representation, and DFN modeling techniques. Some differences between techniques are noted and associated uncertainties are discussed and evaluated. This is a good example of uncertainty treatment by analysis of alternative representational models in the absence of directly relevant field data.

The *Seepage Calibration Model* and *Seepage Testing Data* AMR includes an evaluation of two different representations of fracture flow for the seepage model. The AMR discusses a continuum representation for fracture flow and a DFN Model representation. The AMR concludes, “the DFNM has the advantage of being intuitively more appropriate for seepage predictions,” but goes on to conclude that the continuum approach is best for current use. A large part of the reason for using the continuum approach is the lack of appropriate data to support the DFN Model. This analysis is weaker than those discussed above, but it does help identify the data that would be required for a more thorough evaluation of the alternatives. The uncertainty treatment could be improved by adding a discussion, and potentially some quantitative analyses, of the potential impacts of these decisions about representational models on downstream users.

The examples described above are of cases where the YMP has done a superior job of evaluating uncertainty resulting from alternative representational models. In contrast, it is not clear from the documentation whether the representational model for infiltration has received similar analysis. WAPDEG is the representational model for WP degradation in the TSPA and there is no documentation that it has received the same kind of detailed evaluation. For the Biosphere, GENII-S is particularly opaque in this regard. These examples have been identified in this report to illustrate where uncertainty treatment needs improvement and to suggest positive examples to emulate.

### **Conceptual Model Uncertainties**

Uncertainty can be introduced into the PA if more than one alternative conceptual model is viable for a process, or if there is limited confidence in the validity of the available conceptual models. The UZ and SZ PMRs provide the best identification and discussion of conceptual models. In some cases alternative conceptual models are identified. However, neither the SZ nor the UZ PMR provides a thorough discussion of the rationale for the selection of conceptual models. In some cases it is stated that the most conservative representation is chosen; an example is the perched water model chosen for the UZ flow model.

Conceptual model uncertainty is one of the most difficult issues that the YMP is dealing with in the realm of uncertainty. The principal way of addressing this type of uncertainty is to develop and evaluate alternative models that constitute a spectrum of viable

conceptualizations. The analysis of stress corrosion cracking in the WP area is a good example of this approach. Two models for SCC are formulated and the most conservative is propagated forward for use with the TSPA. As another example, in the PSHA alternative tectonic models are developed and incorporated directly into the hazard analysis. PSHA and PVHA are the only examples identified among the models reviewed for which alternative conceptual models were incorporated directly into a probabilistic analysis.

Conceptual model uncertainty that results from limited confidence in the validity of available conceptual models is even more difficult to handle. An example of this situation is the model for passive film stability for alloy 22. This is an issue that is important for WP corrosion, and is an area of active research within the broader technical community. Another reason for limited confidence is the presence of data that are not easily explained by available conceptual models. The initial chlorine-36 results from the ESF created this type of situation and led to the implementation of new conceptual models for UZ flow. In general the YMP has addressed this issue by using conservative models to bound this type of uncertainty.

Several AMRs lack a discussion of conceptual models. This is partly because of the way that work is organized within a PMR area. For instance, the discussion of conceptual models for UZ flow are contained in a separate AMR, while in the SZ the conceptual model is discussed in the PMR and subcomponents are discussed in the AMRs.

### **Uncertainties in Results**

Clear discussion of uncertainties in AMR/model results is needed to ensure appropriate treatment of information in subsequent AMRs and ultimately in TSPA. For instance, probability distributions are identified for many of the inputs to the SZ flow model, but the impact of these uncertainties on the model outputs are not assessed. Without quantitative, or at least semi-quantitative, assessment of the integrated impact of model uncertainties on the result of the model, it is difficult to assess the actual confidence to place on the specific conclusions that are based on that model. Such quantification is also essential for the uncertainties to be passed to the next process model, incorporated into an abstraction, or implemented in the TSPA model.

### **Propagation Issues**

The propagation of uncertainty can be discussed for different levels of the modeling process. Uncertainties in input parameters to a model, or in the conceptual or representational aspects, can affect the uncertainty in the output results of that model. Uncertainty in the output of a model may affect the uncertainty in the output of a downstream process model or the TSPA. There are a number of texts that present quantitative approaches to the propagation of uncertainty (Bevington and Robinson 1992, Hahn and Shapiro 1967, Coleman and Steele 1999, ASME PTC 19.1 1998) and these should be used to the extent practical. The discussion of this uncertainty propagation is the weakest part of the YMP's uncertainty treatment. The UZ model development

includes choices as to which uncertainties are propagated forward (e.g. infiltration rate) and only a select few such uncertainties can be incorporated in the downstream models. However, the UZ PMR (Table 3.13-2) includes one of the best discussions of uncertainty propagation where there is specific identification of the types of uncertainty propagated from the individual process models to the TSPA, although this is still not a quantitative propagation.

NEA 1997 includes a discussion of uncertainty propagation issues and identifies deterministic approaches and probabilistic approaches. The PSHA and PVHA include the propagation of parameter uncertainties that are represented by probabilistic distributions through the analyses. In most cases, however, uncertainty propagation involves a more deterministic approach. For example, boundary conditions for high, medium and low infiltration are passed to the site scale model from the infiltration model. Parameter values for all parameters needed for the site scale model are developed for each boundary condition, or infiltration case, and reflect the propagation of uncertainty from the infiltration model. All of the uncertainty related to the UZ site scale flow model is propagated to subsequent models through the three sets of parameter values, developed for each climate scenario. The parameter values are passed to other models for further analysis, such as T-H calculations. Uncertainty is propagated, but not with a fully probabilistic representation, and choices have been made about the types of uncertainty that will be propagated.

## **Conclusions**

- The YMP could benefit from a systematic process for identifying, documenting, categorizing, evaluating, and quantifying uncertainties.
- The model baseline needs to be robust and controlled.
- A diagram indicating the connections among and between the process models, and the TSPA model itself, would improve understanding.
- Conceptual model, representational model, parameter/inputs and results provide categories that are effective for evaluating and discussing uncertainty treatment.
- Dividing the work discussed in AMRs into the categories identified above would clarify the presentation of uncertainty treatment.
- Treatment of parameter uncertainty is generally done well in YMP documents.
- Distinguishing between parameter values derived from acquired and developed data could improve parameter uncertainty treatment.
- Uncertainty discussion for developed parameters needs to include discussion of interpretive or analytic processes, or conceptualizations involved in the determination of parameter values.

- Systematic and detailed discussion of uncertainty treatment for developed parameters would help with many of the transparency and traceability issues associated with TSPA.
- Representational model uncertainty is addressed well in several YMP documents and these should serve as examples for others to follow.
- Conceptual model uncertainty is an area where the YMP could improve.
- The YMP could benefit from a consistent approach to the propagation of uncertainty through the TSPA model hierarchy.

## **Recommendations**

The following recommendations are offered for consideration to improve the YMP's treatment of uncertainty and the discussion of that treatment in its technical documents:

- Consider developing a systematic process for identifying, documenting, categorizing, evaluating, and quantifying uncertainties.

The YMP could be improved by a more comprehensive, rigorous approach to uncertainty treatment. The approach needs to be well thought out, with input from technical experts who will have to implement the approach. The approach also needs to be codified in YMP procedures. It would be useful to have criteria for different categories of uncertainty, for both process and system level models. AMRs should categorize each significant uncertainty within the model and discuss their treatment.

- Provide better discussions of the bases for determining parameter values and probability distributions.

In general AMRs contain very good discussions on the development and selection of numerical values and probability distributions used for parameter inputs to the models. There are many cases where very good statistical treatments of parameter value distributions are presented in the AMRs. Some discussions, however, are weaker. This is especially true in cases where bounding values are selected and in some instances where probability distributions are defined. Clearer criteria for adequacy of discussion of parameters in the appropriate procedures would help this situation.

- Distinguish between acquired and developed parameter values.

It would be best to develop a systematic way to classify parameters, based on what is measured and the analysis or interpretation involved in developing parameter values. This should also serve to elucidate the appropriate usage of developed parameters that have implicit models embedded in them. Systematic classification of parameters would allow for uncertainty treatment that was tailored to each class.

- Represent parameters in a fully probabilistic manner, if data are available and this representation is necessary.

To the extent possible, given the availability of data, uncertain parameters should be represented probabilistically. Statistical measure of “goodness of fit” should be provided for these distributions whenever practical. In cases where distributions are not developed, authors should clearly state why and discuss the impact.

- Provide more robust and consistent justification for parameter and model bounds.

If a bounding value is used for a parameter, or a bounding model is chosen, the basis for the selection needs to be clearly and fully discussed. The logic for characterizing the representation as a bound needs to be presented. The logic could include a qualitative discussion or quantitative assessment of the potential impact of the choice.

- Provide more than just Data Tracking Numbers as references.

In some cases data and other types of information are referenced to Data Tracking Numbers and have no other supporting reference documentation. There are a number of problems with this situation. First, a Data Tracking Number can have a wide variety of types of information or data and it is not always clear what part of the included information is being referenced. Second, a numerical value for a parameter may not be useful without accompanying explanatory information. The accompanying information may help constrain the use of the data or the applicability in a particular situation. Third, a Data Tracking Number may simply contain one piece of information in a larger string and the whole framework may be necessary to adequately understand the data that are needed. Providing the documentation containing the explanatory information or the additional context of the data should improve transparency and traceability.

- Develop a list of models that can serve as the structure for the model baseline.

There are a number of places in the documentation where confusion arises because the YMP does not use a consistent set of baseline models. In some cases it is hard to determine model feeds and whether models are used at all. There also seem to be areas where there is overlap between models. It should be recognized that establishing a set of models for baselining is not an easy task. There are areas where it is not clear whether the baseline should identify multiple models or simply modifications and alternate calculations using the same model. The baseline should include a diagram indicating the connections among and between the process models, and the TSPA model itself. Those connections should be defined by the information expected to be passed from one process model to another, or from one process model to its abstraction.

- Reevaluate the suite of AMRs that support the PMRs and the TSPA.

The AMR structure that supports the PMRs and TSPA, as it currently exists, lacks a systematic organization and rationale. Some AMRs include discussions of several models and some models are spread over several AMRs.

- Develop an overall conceptual model AMR for large, complex models. Improve conceptual model discussions within AMRs.

Conceptual model discussions are limited in several areas and spread through AMRs and PMRs. A concise conceptual model discussion, including its bases (multiple lines of evidence) and uncertainties is needed. For large, complex models, placing the conceptual model within a single AMR that other AMRs can reference would serve to elucidate the conceptual bases and the interrelations among the AMRs.

- Evaluate the effect of uncertainty in model inputs and in the models themselves on model outputs. Conduct detailed sensitivity studies at the process model level.

This will help with traceability and improve understanding of how uncertainties are propagated through the TSPA hierarchy. Consider adding a section to each AMR that quantitatively describes how critical uncertainties and assumptions effect the results. This will support high-level sensitivity analyses that identify importance at the “global” level. Detailed sensitivity studies at the process level will permit additional, more detailed importance analyses down to the lower level parameters. For example, future PA analyses may show that uncertainty in the global UZ flow system is important. Detailed process model sensitivities would show which critical uncertainties have the most influence on UZ flow. Additional sensitivity studies would also support the development of abstraction models in demonstrating that they appropriately capture important phenomena and uncertainties.

- Describe how uncertainties from upstream models have been incorporated into AMRs for downstream models.

This will also help with traceability and improve understanding of how uncertainties are propagated through the TSPA hierarchy. The discussion needs to be more than simply a citation of data source in Section 4 of the AMR. The documentation for the process models should clearly describe how the outputs of other process models have been used and how (and which) uncertainties in those results were incorporated and propagated.

- Re-establish the TSPA core team, as utilized in the development of the TSPA-VA to assist the process modelers.

This will improve communication and enhance transparency and traceability by integrating uncertainty treatment throughout the TSPA. This approach enjoyed good success during the development of TSPA-VA. System people in the PA organization can ensure that model outputs from one area fit with input needs for another and subsequently into TSPA.

- Provide better examples of what to characterize as a conceptual model.

The identification of what is a conceptual model and how it is described are issues that have received variable treatment in the YMP's documentation. There is room for interpretation and disagreement over the use of any term as high level as "conceptual model." The identification of examples in appropriate procedures will help the YMP use the term more consistently.

- Convene a workshop on conceptual model uncertainty.

The treatment of conceptual model uncertainty is clearly one of the most difficult issues that the YMP is facing regarding uncertainty. Convening a workshop and bringing in outside experts, including perhaps international experts, might lead to valuable discussion and exchange of ideas.

- Conduct reviews of down-stream AMRs by up-stream AMR authors.

AP-3.10Q, *Analyses and Models*, requires review of AMRs by affected groups; this forces down-stream review. Upstream review will ensure that information from up-stream AMRs is being used appropriately and will facilitate appropriate incorporation and propagation of uncertainties.

## 19.0 List of References

64 FR 46976: *Environmental Radiation Protection Standards for Yucca Mountain, Nevada*, Proposed Rule 40 CFR 197. Readily Available.

64 FR 8640: *Disposal of High-Level Radioactive Wastes in a Proposed Geologic Repository at Yucca Mountain, Nevada*, Proposed Rule 10 CFR 63. Readily Available.

ANL-EBS-HS-000003, Rev. 00, *Abstraction of NFE Drift Thermodynamic Environment and Percolation Flux*, E0130 TH Abs AMR, May 5, 2000, MOL.20000504.0296.

ANL-EBS-MD-000001, Rev. 00, *Environment on the Surfaces of the Drip Shield and Waste Package Outer Barrier*, March 27, 2000, MOL.20000328.0590.

ANL-EBS-MD-000002, Rev. 00, *Aging and Phase Stability of Waste Package Outer Barrier*, March 27, 2000, MOL.20000410.0407.

ANL-EBS-MD-000003, Rev. 00, *General Corrosion and Localized Corrosion of Waste Package Outer Barrier*, January 28, 2000, MOL.20000202.0172.

ANL-EBS-MD-000004, Rev. 00, *General Corrosion and Localized Corrosion of the Drip Shield*, March 27, 2000, MOL.20000329.1185.

ANL-EBS-MD-000005, Rev. 00, *Stress Corrosion Cracking of the Drip Shield, the Waste Package Outer Barrier and the Stainless Steel Structural Material*, April 28, 2000, MOL.20000504.0312.

ANL-EBS-MD-000006, Rev. 00, *Hydrogen Induced Cracking of Drip Shield*, March 27, 2000, MOL.200000329.1179.

ANL-EBS-MD-000007, Rev. 00, *Degradation of Stainless Structural Material*, March 27, 2000, MOL.200000329.1188.

ANL-EBS-MD-000011, Rev. 00, *Hydride-Related Degradation of SNF Cladding Under Repository Conditions*, March 27, 2000, MOL.20000319.0048.

ANL-EBS-MD-000012, Rev. 00, *Clad Degradation – Local Corrosion of Zirconium and its Alloys Under Repository Conditions*, April 5, 2000, MOL.20000405.0479.

ANL-EBS-MD-000013, Rev. 00, *Clad Degradation – Dry Unzipping*, May 3, 2000, MOL.20000503.0200.

ANL-EBS-MD-000014, Rev. 00, *Clad Degradation – Wet Unzipping*, April 28, 2000, MOL.20000502.0398.

ANL-EBS-MD-000015, Rev. 00, *CSNF Waste Form Degradation: Summary Abstraction*, January 20, 2000, MOL.20000121.0161.

ANL-EBS-MD-000016, Rev. 00, *Defense High Level Waste Glass Dissolution*, March 30, 2000, MOL.20000329.1183.

ANL-EBS-MD-000017, Rev. 00, *Pure Phase Solubility Limits – LANL*, May 8, 2000, MOL.20000504.0311.

ANL-EBS-MD-000019, Rev. 00, *Secondary Uranium-Phase Paragenesis and Incorporation of Radionuclides into Secondary Phases*, April 5, 2000, MOL.20000414.0644.

ANL-EBS-MD-000020, Rev. 00, *Colloid-Associated Radionuclide Concentration Limits: ANL*, March 28, 2000, MOL.20000329.1187.

ANL-EBS-MD-000023, Rev. 01, *Analysis of Mechanisms for Early Waste Package Failure*, February 25, 2000, MOL.200000223.0878.

ANL-EBS-MD-000026, Rev. 00 ICN 01, *In-Drift Thermal-Hydrological-Chemical Model*, E0065 IDTH AMR, July 27, 2000, MOL.20000802.0011.

ANL-EBS-MD-000027, Rev 00, *Drift Degradation Analysis*, E0080 DDA AMR, February 1, 2000, MOL.20000107.0328.

ANL-EBS-MD-000028, Rev 00, *Water Diversion Model*, E0085 Wdiv AMR, February 1, 2000, MOL.20000107.0329.

ANL-EBS-MD-000029, Rev 00, *Water Drainage Model*, E0070 Drn AMR, February 1, 2000, MOL.20000117.0216.

ANL-EBS-MD-000030, Rev 00, *Ventilation Model*, E0075 Vent AMR, February 1, 2000, MOL.20000107.0330.

ANL-EBS-MD-000031, Rev 01, *Invert Diffusion Properties Model*, E0000 InvD AMR, September 5, 2000, MOL.20000912.0208.

ANL-EBS-MD-000032, Rev 00 ICN 01, *Water Distribution and Removal Model*, E0090 WDR AMR, August 19, 2000, MOL.20000822.0006.

ANL-EBS-MD-000033, Rev 00 ICN 01, *Physical and Chemical Environment Model*, E0100 PCE AMR, August 1, 2000, MOL.20000807.0093.

ANL-EBS-MD-000034, Rev 00 ICN 01, *EBS Radionuclide Transport Model*, E0050 RnT AMR, July 27, 2000, MOL.20000727.0091.

ANL-EBS-MD-000035, Rev 00 ICN 01, *Engineered Barrier System Features, Events, and Processes and Degradation Modes Analysis*, E0015 Deg AMR, July 27, 2000, MOL.20000727.0092.

ANL-EBS-MD-000037, Rev. 00, *In-Package Chemistry Abstraction*, April 13, 2000, MOL.20000418.0818.

ANL-EBS-MD-000038, Rev 00, *In-Drift Microbial Communities*, E0040 Mic AMR, March 27, 2000, MOL.20000331.0661.

ANL-EBS-MD-000039, Rev 00, *Seepage/Backfill Interactions*, E0030 Sbac AMR, April 14, 2000, MOL.20000509.0243.

ANL-EBS-MD-000040, Rev 00, *In-Drift Gas Flux and Composition*, E0035 IDG AMR, May 23, 2000, MOL.20000523.0154.

ANL-EBS-MD-000041, Rev 00, *In-Drift Corrosion Products*, E0020 CorP AMR, December 15, 1999, MOL.20000106.0438.

ANL-EBS-MD-000042, Rev 00, *In-Drift Colloids and Concentrations*, E0045 IDCol AMR, May 5, 2000, MOL.20000509.0242.

ANL-EBS-MD-000043, Rev 00, *Seepage/Cement Interactions*, E0055 Cem AMR, March 16, 2000, MOL.20000317.0262.

ANL-EBS-MD-000044, Rev 00, *Seepage/Invert Interactions*, E0060 SI AMR, May 23, 2000, MOL.20000523.0156.

ANL-EBS-MD-000045, Rev 00, *In-Drift Precipitates/Salts Analysis*, E0105 P/S AMR, May 12, 2000, MOL.20000512.0062.

ANL-EBS-MD-000046, Rev 00, *Physical and Chemical Environment Abstraction Model*, E0010 PCE Abs AMR, May 23, 2000, MOL.20000523.0155.

ANL-EBS-MD-000048, Rev. 00, *Initial Cladding Condition*, May 23, 2000, MOL.20000523.0150.

ANL-EBS-MD-000049 Rev. 00, *Multiscale Thermohydrologic Model*, E0120 MSTHM AMR, June 9, 2000, MOL.20000609.0267.

ANL-EBS-MD-000050, Rev 00, *Summary of In-Package Chemistry for Waste Forms*, February 11, 2000, MOL.20000217.0217.

ANL-EBS-PA-000001, Rev. 00, *WAPDEG Analysis of Waste Package and Drip Shield Degradation*, May 26, 2000, MOL.20000526.0332.

ANL-EBS-PA-000002, Rev. 00, *FEPs Screening of Processes and Issues in Drip Shield and Waste Package Degradation*, May 26, 2000, MOL.20000526.0334.

ANL-EBS-PA-000003, Rev. 00, *Abstraction of Models for Pitting and Crevice Corrosion of Drip Shield and Waste Package Outer Barrier*, May 25, 2000, MOL.20000526.0327.

ANL-EBS-PA-000004, Rev. 00, *Abstraction of Models of Stress Corrosion Cracking of Drip Shield and Waste Package Outer Barrier and Hydrogen-Induced Corrosion of Drip Shield*, May 26, 2000, MOL.20000526.0326.

ANL-EBS-PA-000005, Rev. 00, *Abstraction of Models for Stainless Steel Structural Material Degradation*, May 25, 2000, MOL.20000526.0337.

ANL-MGR-MD-000001, Rev. 00, *Input Parameter Values for External and Inhalation Radiation Exposure Analysis*, April 17, 2000, MOL.19990923.0235.

ANL-MGR-MD-000002, Rev. 00, *Dose Conversion Factor Analysis: Evaluation of GENII-S Dose Assessment Methods*, October 13, 1999, MOL.19991207.0215.

ANL-MGR-MD-000003, Rev. 00, *Disruptive Event Biosphere Dose Conversion Factor Analysis*, December 28, 1999, MOL.20000303.0216.

ANL-MGR-MD-000004, Rev. 00, *Disruptive Event Biosphere Dose Conversion Factor Sensitivity Analysis*, April 6, 2000, MOL.20000418.0826.

ANL-MGR-MD-000005, Rev. 00, *Identification of the Critical Group (Consumption of Locally Produced Food and Tap Water)*, January 14, 2000, MOL.20000224.0399.

ANL-MGR-MD-000006, Rev. 00, *Identification of Ingestion Exposure Parameters*, December 2, 1999, MOL.20000216.0104.

ANL-MGR-MD-000007, Rev. 00, *Environmental Transport Parameter Analysis*, September 21, 1999, MOL.19991115.0238.

ANL-MGR-MD-000008, Rev. 00, *Transfer Coefficient Analysis*, September 28, 1999, MOL.19991115.0237.

ANL-MGR-MD-000009, Rev. 00, *Non-Disruptive Event Biosphere Dose Conversion Factors*, January 21, 2000, MOL.20000307.0383.

ANL-MGR-MD-000010, Rev. 00, *Non-Disruptive Event Biosphere Dose Conversion Factor Sensitivity Analysis*, April 6, 2000, MOL.20000420.0074.

ANL-MGR-MD-000011, Rev. 00, *Evaluation of the Applicability of Biosphere-Related Features, Events, and Processes (FEP)*, April 12, 2000, MOL.20000420.0075.

ANL-NBS-GS-000008, Rev. 00, *Future Climate Analysis*, RPC URN-0004.

ANL-NBS-HS-000001, Rev. 00, *Analysis Comparing Advective-Dispersive Transport Solution to Particle Tracking*, MOL.19990721.0518.

ANL-NBS-HS-000002, Rev. 00, *Analysis of Hydrologic Properties Data*, RPC URN-0055.

ANL-NBS-HS-000005, Rev. 00, *In Situ Field Testing of Processes*, MOL.20000504.0304.

ANL-NBS-HS-000015, Rev. 00, *Development of Numerical Grids for UZ Flow and Transport Modeling*, MOL.19990721.0517.

ANL-NBS-HS-000017, Rev. 00, *Analysis of Geochemical Data for the Unsaturated Zone*, RPC URN-0048.

ANL-NBS-HS-000019, Rev. 00, *Unsaturated Zone and Saturated Zone Transport Properties*, RPC URN-0038.

ANL-NBS-HS-000021, Rev. 00, *Geochemical and Isotopic Constraints on Groundwater Flow Directions, Mixing, and Recharge At Yucca Mountain, Nevada*, AMR, January 19, 2001, MOL.20010123.0120.

ANL-NBS-HS-000022, Rev. 00, *Modeling Sub-Gridlock Scale Dispersion in Three-Dimensional Heterogeneous Fractured Media*, AMR, October 23, 2000, MOL.20001107.0376.

ANL-NBS-HS-000023, Rev. 00, *Abstraction of Flow Fields for RIP*, MOL.20000127.0089.

ANL-NBS-HS-000024, Rev. 00, *Analysis of Base-Case Particle Tracking Results of the Base-Case Flow Fields*. MOL.20000207.0690.

ANL-NBS-HS-000026, Rev. 00, *Particle Tracking Model and Abstraction of Transport Processes*. MOL.20000502.0237.

ANL-NBS-HS-000026, Rev. 00, *UZ Colloid Transport Model*, RPC URN-0031.

ANL-NBS-HS-000027, Rev. 00, *Analysis of Infiltration Uncertainty*, MOL.20000525.0377.

ANL-NBS-HS-000029, Rev. 00, *Abstraction of Drift-Scale Coupled Processes*, CRWMS M&O, N0125 THC Abs AMR, March 31, 2000, MOL.20000525.0371.

ANL-NBS-HS-000030, Rev. 00, *Input and Results of the Base Case Saturated Zone Flow and Transport Model for TSPA*, AMR, May 26, 2000, MOL.20000526.0330.

ANL-NBS-HS-000031, Rev. 00, *Saturated Zone Colloid Facilitated Transport*, AMR, June 09, 2000, MOL.20000609.0266.

ANL-NBS-HS-000032, Rev. 00, *Simulation of Net Infiltration for Modern and Potential Future Climate State*, RPC URN-0006.

ANL-NBS-HS-000033, Rev. 00, *Hydrogeologic Framework Model for the Saturated-Zone Site-Scale Flow and Transport*, AMR, March 30, 2001, MOL.20010403.0147.

ANL-NBS-HS-000034, Rev. 00, *Water-Level Data Analysis for the Saturated Zone Site-Scale Flow and Transport*, AMR, March 30, 2001, MOL.20010405.0211.

ANL-NBS-MD-000003, Rev. 00, *Probability Distribution for Flowing Interval Spacing*, AMR, November 08, 2000, MOL.20001204.0034.

ANL-NBS-MD-000006, Rev. 00, *Groundwater Usage by the Proposed Farming Community*, February 24, 2000, MOL.20000407.0785.

ANL-NBS-MD-000007, Rev. 00, *Abstraction of BDCF Distributions for Irrigation Periods*, April 14, 2000, MOL.20000517.0257.

ANL-NBS-MD-000008, Rev. 00, *Distribution Fitting to the Stochastic BDCF Data*, April 14, 2000, MOL.20000517.0258.

ANL-NBS-MD-000009, Rev. 00, *Evaluate Soil/Radionuclide Removal by Erosion and Leaching*, February 24, 2000, MOL.20000310.0057.

ANL-NBS-MD-000010, Rev. 00, *Recharge and Lateral Groundwater Flow Boundary Conditions for the Saturated Zone Site - Scale Flow and Transport Model*, AMR, September 22, 1999, MOL.19991118.0188.

ANL-NBS-MD-000011, Rev. 00, *Uncertainty Distribution for Stochastic Parameters*, AMR, May 26, 2000, MOL.20000526.0328.

ANL-NBS-TH-000001 Rev. 00, *Thermal Tests Thermal-Hydrological Analyses/Model Report*, CRWMS M&O, N0000 TT TH AMR, April 13, 2000, MOL.19990721.0523.

ANL-NBS-TH-000001 Rev. 00/ICN 01, *Thermal Tests Thermal-Hydrological Analyses/Model Report*, CRWMS M&O, N0000 TT TH AMR, December 14, 2000, MOL.20010109.0004.

ANL-WIS-MD-000004, Rev. 00, *DSNF and Other Waste Form Degradation Abstraction*, February 22, 2000, MOL.20000223.0502.

ANL-WIS-MD-000006, Rev. 00, *Inventory Abstraction*, CRWMS M&O, F0015, April 3, 2000, MOL.20000414.0643.

ANL-WIS-MD-000007, Rev. 00, *Clad Degradation – Summary and Abstraction*, May 30, 2000, MOL.20000602.0055.

ANL-WIS-MD-000009, Rev. 00, *Miscellaneous Waste Form FEPs*, May 26, 2000, MOL.20000526.0339.

ANL-WIS-MD-000010, Rev. 00, *Summary of Dissolved Concentration Limits*, May 25, 2000, MOL.20000525.0372.

ANL-WIS-MD-000012, Rev. 00, *Waste Form Colloid-Associated Concentration Limits: Abstraction and Summary*, May 25, 2000, MOL.20000525.0397.

ANL-WIS-PA-000001, Rev. 00 ICN 01, *EBS Radionuclide Transport Abstraction*, E0095 RT Abs AMR, August 21, 2000, MOL.20000821.0358.

ANL-WIS-PA-000002, Rev. 00, *EBS FEPs/Degradation Modes Abstraction*, E0110 FEP AMR, May 25, 2000, MOL.20000525.0373.

ANL-WIS-PA-000002, Rev. 01, *EBS Features, Events, and Processes* (Note: There was a title change from Rev. 00 to Rev. 01 of this document.), E0110 FEPS AMR, February 15, 2001, MOL.20010312.0024.

B00000000-01717-2200-00099, Rev. 01, *Total System Performance Assessment-1993: An Evaluation of the Potential Yucca Mountain Repository*, 1994, NNA.19940406.0158.

B00000000-01717-2200-00136, Rev. 01, *Total System Performance Assessment-1995: An Evaluation of the Potential Yucca Mountain Repository*, 1995, MOL.19960724.0188.

B00000000-01717-4301-000[01-11], *Total System Performance Assessment-Viability Assessment (TSPA-VA) Analysis and Technical Basis Document*, 1998, MOL.19981008.00[01-11].

B00000000-01717-4301-00009, Rev. 01, *"Biosphere" Chapter 9 of Total System Performance Assessment-Viability Assessment (TSPA-VA) Analyses Technical Basis Document*, November 13, 1998, MOL.19981008.0009.

CAL-EBS-MD-000001, Rev. 00, *Breakage of Commercial Spent Nuclear Fuel Cladding by Mechanical Loading*, December 3, 1999, MOL.19991213.0237.

CAL-EBS-PA-000002, Rev. 00, *Calculation of General Corrosion Rate of Drip Shield and Waste Package Outer Barrier to Support WAPDEG Analyses*, March 16, 2000, MOL.20000319.0047.

CAL-EBS-PA-000003, Rev. 00, *Calculation of Probability and Size of Defect Flaws in Waste Package Closure Welds to Support WAPDEG Analysis*, March 29, 2000, MOL.20000424.0676.

CAL-MGR-MD-000001, Rev. 00, *Waste Packages and Source Terms for the Commercial 1999 Design Basis Waste Streams*, February 14, 2000, MOL.20000214.0479.

CAL-MGR-NU-000002, Rev. 01, *Source Terms for HLW Glass Containers*, August 15, 2000, MOL.20000823.0004.

CAL-MGR-NU-000003, Rev. 00, *Radionuclide Inventories for DOE SNF Waste Stream and Uranium/Thorium Carbide Fuels*, March 28, 2000, MOL.20000412.0764.

CAL-UDC-ME-000002, Rev. 00, *Thermal Evaluation of Breached 21-PWR Waste Packages*, December 8, 1999, MOL.20000120.0447.

CAL-WIS-MD-000002, Rev. 00, *Relative Contribution of Individual Radionuclides to Inhalation and Ingestion Dose*, December 15, 2000, MOL.20010103.0211.

CAL-WIS-MD-000003, Rev. 00, *Radioactive Decay and In-Growth Modeling Approximations for TSPA-SR*, December 15, 2000, MOL.20001226.0507.

CAL-WIS-MD-000004, Rev. 00, *Waste Package Radionuclide Inventory Approximations for TSPA-SR*, June 6, 2000, MOL.20000630.0247.

CAL-WIS-MD-000005, Rev. 00, *Relative Contribution of Individual Radionuclides to Inhalation and Ingestion Dose – One Million Years*, December 15, 2000, MOL.20010103.0209.

CAL-WIS-MD-000006, Rev. 00, *Per Canister Inventories for DOE SNF for TSPA-SR*, April 26, 2000, MOL.20000510.0155.

CAL-WIS-MD-000010, Rev. 00, *Stainless Steel in Waste Packages for TSPA-SR*, June 12, 2000, MOL.20000630.0249.

CRWMS M&O 1996, *Probabilistic Volcanic Hazard Analysis for Yucca Mountain, Nevada*, BA0000000-01717-2200-00082, Rev. 0, Las Vegas, Nevada: CRWMS M&O, MOL.19971201.0221.

CRWMS M&O 1997, *Unsaturated Zone Flow Model Expert Elicitation Project*, MOL.19971009.0582.

MDL-NBS-HS-000001, Rev. 00, *Drift-Scale Coupled Processes (DST & THC Seepage) Models*, CRWMS M&O, N0120 THC AMR, March 13, 2000, MOL.19990721.0523.

MDL-NBS-HS-000001, Rev. 01, *Drift-Scale Coupled Processes (DST & THC Seepage) Models*, CRWMS M&O, N0120 THC AMR, February 5, 2001, MOL.20010314.0003.

MDL-NBS-HS-000002, Rev. 00, *Seepage Model for PA Including Drift Collapse*, RPC URN-0023.

MDL-NBS-HS-000003, Rev 00, *Calibrated Properties Model*, MOL.19990721.0520.

MDL-NBS-HS-000004, Rev. 00, *Seepage Calibration Model and Seepage Testing Data*, 19990721.0521.

MDL-NBS-HS-000005, Rev. 00, *Abstraction of Drift Seepage*, MOL.200000322.0671.

MDL-NBS-HS-000005, Rev. 00, *Conceptual and Numerical Model of UZ Flow and Transport*, RPC URN-0036.

MDL-NBS-HS-000006, Rev. 00, *UZ Flow Model and Submodels*, MOL.19990721.0527.

MDL-NBS-HS-000007, Rev. 00, *Mountain-Scale UZ Thermal-Hydrological Model*, MOL.19990721.0528.

MDL-NBS-HS-000008, Rev. 00, *Radionuclide Transport Models Under Ambient Conditions*, RPC URN-0064.

MDL-NBS-HS-000010, Rev. 00, *Saturated Zone Transport Methodology and Transport Component Integration*, AMR, August 24, 2000, MOL.20000824.0513.

MDL-NBS-HS-000011, Rev. 00, *Calibration of the Site-Scale Saturated Zone Flow Model*, AMR, August 24, 2000, MOL.20000825.0122.

MDL-WIS-PA-000002, Rev. 00, *Total System Performance Assessment (TSPA) Model for Site Recommendation*, MOL.20001226.0003.

TDR-EBS-MD-000006, Rev. 00 ICN 01, *EBS Degradation, Flow and Transport*, EBS PMR, July 24, 2000, MOL.20000724.0479.

TDR-MGR-MD-000002, Rev. 00 ICN 01, *Biosphere Process Model Report*, May 25, 2000, MOL.20000620.0341.

TDR-WIS-MD-000002, Rev. 00 ICN 01, *Waste Package Degradation Process Model Report*, June 21, 2000, MOL.20000717.0005.

TDR-WIS-PA-000001, Rev. 00 ICN 01, *Total System Performance Assessment for the Site Recommendation*, December 11, 2000, MOL.20001220.0045.

TDR-WIS-MD-000001, Rev. 00 ICN 01, *Waste Form Degradation PMR*, July 13, 2000, MOL.20000713.0362.

Andersson, Johan, 1999, *SR 97-Data and Data Uncertainties: Swedish Nuclear Fuel and Waste Management Co.*, TIC: 246042.

ASME PTC 19.1-1998, *American National Standard: Supplement to ASME Performance Test Code, 19.1-1998, Test Uncertainty*, TIC: 249327.

ASTM D 5447-93, *Standard Guide for Application of a Ground-Water Flow Model to a Site-Specific Problem*, TIC: 249787.

Bevington, P.R. and Robinson, K.D., 1992, *Data Reduction and Error Analysis for the Physical Sciences*, Second Edition: McGraw-Hill, TIC: 243514.

BIOMOVS II, 1996, *Development of a Reference Biospheres Methodology for Radioactive Waste Disposal*, Technical Report No. 6. Stockholm, Sweden: Swedish Radiation Protection Institute, TIC: 238329.

Coleman, H.W. and Steele, W.G., 1999, *Experimentation and Uncertainty Analysis for Engineers*, New York, New York: John Wiley & Sons, TIC: 248936.

D'Agnese, F.A.; Faunt, C.C.; Turner, A.K.; and Hill, M.C., 1997, *Hydrogeological Evaluation and Numerical Simulation of the Death Valley Regional Ground-Water Flow System, Nevada and California*, Water Resources Investigation Report 96-4300, Denver, Colorado: U.S. Geological Survey, MOL.19980306.0253.

Flint, et.al., 1996, "*Conceptual and Numerical Model of Infiltration of the Yucca Mountain Area, Nevada*," DRAFT, MOL.19970409.0087.

Hahn, G.J. and Shapiro, S.S., 1967, *Statistical Models in Engineering*, New York, New York: John Wiley & Sons, TIC: 247729.

LaPlante, P.A. and Poor, K. 1997, *Information and Analyses to Support Selection of Critical Groups and Reference Biospheres for Yucca Mountain Exposure Scenarios*, CNWRA 97-009. San Antonio, Texas: Center for Nuclear Waste Regulatory Analyses, TIC: 236454.

Napier, B.A.; Peloquin, R.A.; Strenge, D.L.; and Ramsdell, J.V., 1988 Conceptual Representation, Volume 1 of GENII: *The Hanford Environmental Radiation Dosimetry Software System*, PNL-6584. Richland, Washington: Pacific Northwest Laboratory, TIC: 206898.

NEA, 1997, *Lessons Learnt From Ten Performance Assessments*, OECD Nuclear Energy Agency, Paris, TIC: 243964.

NEA, 1991, *Disposal of Radioactive Wastes: Review of Safety Assessment Methods*, OECD Nuclear Energy Agency, Paris, TIC: 226871.

Oelkers, E. H., 1996, *Chapter 3: Physical and Chemical Properties of Rocks and Fluids for Chemical Mass Transport Calculations*, in *Reviews in Mineralogy Volume 34, Reactive Transport in Porous Media*, Lichtner, P. C., Steefl, C. I., and Oelkers, E. H., Eds., Mineralogical Society of America, pp.131-191, TIC: 236866.

Revised Interim Guidance Pending Issuance of New U.S. Nuclear Regulatory Commission (NRC) Regulations (Revision 01, July 22, 1999), for Yucca Mountain, Nevada."Letter from Dr. J.R. Dyer (DOE/YMSCO) to Dr. D.R. Wilkins (CRWMS M&O), September 3, 1999, OL&RC:SB-1714, with enclosure, "Interim Guidance Pending Issuance of New NRC Regulations for Yucca Mountain (Revision 01)." MOL.19990910.0079.

Savard, C.S., 1998, *Estimated Ground-Water Recharge from Streamflow in Fortymile Wash Near Yucca Mountain, Nevada*, Water-Resources Investigations Report 97-4273, Denver, Colorado: U.S. Geological Survey, TIC 236848.

Standard Practice for Prediction of the Long-Term Behavior of Materials, Including Waste Forms, Used in Engineered Barrier Systems (EBS) For Geological Disposal of High-Level Radioactive Waste, ASTM C 1174-97, 1998, MOL.20000710.0227.

Tsang, Chin-Fu, November-December 1991, *The Modeling Process and Model Validation, Ground Water*, Volume 29, No. 6, pp. 825-831, TIC: 249788.

Wong, I. G. and Stepp, C. 1998, *Probabilistic Seismic Hazard Analyses for Fault Displacement and Vibratory Ground Motion at Yucca Mountain, Nevada*, Milestone SP32IM3, September 23, 1998, Three Volumes, Oakland, California: U.S. Geological Survey, MOL.19981207.0393.

INTENTIONALLY LEFT BLANK